Digitized by the Internet Archive
in 2023 with funding from
Kahle/Austin Foundation

https://archive.org/details/contributionsfro0011unse

UNIVERSITY OF ARIZONA
STEWARD OBSERVATORY
TUCSON, ARIZONA

Carnegie Institution of Washington

CONTRIBUTIONS

FROM THE

MOUNT WILSON OBSERVATORY

VOLUME XI

NOS. 228-254

WITH THIRTEEN PLATES

OCTOBER 1921—SEPTEMBER 1922

UNIVERSITY OF ARIZONA
LIBRARY

c28
v.11

CONTENTS

NO. PAGE

228. SPECTROPHOTOMETRIC METHODS FOR DETERMINING STELLAR LUMINOSITY. *Bertil Lindblad* 1

229. ON THE UPPER LIMIT OF DISTANCE TO WHICH THE ARRANGEMENT OF STARS IN SPACE CAN AT PRESENT BE DETERMINED WITH SOME CONFIDENCE. *J. C. Kapteyn and P. J. van Rhijn* . . 35

230. FIRST ATTEMPT AT A THEORY OF THE ARRANGEMENT AND MOTION OF THE SIDEREAL SYSTEM. *J. C. Kapteyn* 65

231. EFFECTIVE WAVE-LENGTHS OF 129 STARS WITHIN 0°.5 OF THE NORTH POLE AND OF THE Σ COMPANION OF POLARIS. *Ejnar Hertzsprung* 93

232. NOTE ON THE THICKNESS OF AIR REQUIRED TO PRODUCE THE ATMOSPHERIC ABSORPTION BANDS, A, *a*, AND B. *Arthur S. King* 103

233. ELECTRIC FURNACE EXPERIMENTS INVOLVING IONIZATION PHENOMENA. *Arthur S. King* 105

234. FURTHER EVIDENCE ON THE BRIGHTNESS OF THE STARS OF THE NORTH POLAR SEQUENCE. *Frederick H. Seares and Milton L. Humason* 117

235. REVISED MAGNITUDES FOR STARS NEAR THE NORTH POLE. *Frederick H. Seares* 131

236. NOTES ON IONIZATION IN THE SOLAR ATMOSPHERE. *Henry Norris Russell* 155

237. THE PHOTOGRAPHIC DETERMINATION OF STELLAR PARALLAXES WITH THE 60-INCH REFLECTOR. SIXTH SERIES. *Adriaan van Maanen* 161

238. THE VARIABLE DOUBLE STAR X OPHIUCHI. *C. H. Gingrich* . . 189

239. PARALLAXES OF STARS IN THE REGION OF B.D.+31°643. *C. H. Gingrich* 197

240. INTERFEROMETER OBSERVATIONS OF DOUBLE STARS. *Paul W. Merrill* 203

241. A GENERAL STUDY OF DIFFUSE GALACTIC NEBULAE. *Edwin Hubble* 217

242. INVESTIGATIONS ON PROPER MOTION. SEVENTH PAPER: INTERNAL MOTION IN THE SPIRAL NEBULA N.G.C. 2403. *Adriaan van Maanen* 255

CONTENTS

NO. PAGE

243. INVESTIGATIONS ON PROPER MOTION. EIGHTH PAPER: INTERNAL MOTION IN THE SPIRAL NEBULA M 94=N.G.C. 4736. *Adriaan van Maanen* 263

244. A SPECTROSCOPIC METHOD OF DETERMINING THE ABSOLUTE MAGNITUDES OF A-TYPE STARS AND THE PARALLAXES OF 544 STARS. *Walter S. Adams and Alfred H. Joy* 273

245. THE DISTRIBUTION OF THE VELOCITIES OF STARS OF SPECTRAL TYPES F TO M. *Gustaf Strömberg* 297

246. THE APPLICATION OF VACUUM THERMOCOUPLES TO PROBLEMS IN ASTROPHYSICS. *Edison Pettit and Seth B. Nicholson* . . 327

247. THE ELECTRIC FURNACE SPECTRUM OF IRON IN THE ULTRA-VIOLET, WITH SUPPLEMENTARY DATA FOR THE BLUE AND VIOLET. *Arthur S. King* 351

248. CHANGES IN THE SPECTROGRAPHIC ELEMENTS OF Y SAGITTARII. *John C. Duncan* 373

249. THE ABSENCE OF OXYGEN AND WATER-VAPOR LINES FROM THE SPECTRUM OF VENUS. *Charles E. St. John and Seth B. Nicholson* 377

250. THE SOURCE OF LUMINOSITY IN GALACTIC NEBULAE. *Edwin Hubble* 397

251. ORBITS OF THE SPECTROSCOPIC BINARIES LALANDE 13792 AND AOe 12584. *R. F. Sanford* 437

252. STELLAR SPECTRA OF CLASS S. I. GENERAL DESCRIPTION. *Paul W. Merrill*. 449

253. THE BEHAVIOR OF SPECTRAL LINES AT THE POSITIVE POLE OF THE METALLIC ARC. *Paul W. Merrill* 467

254. ORBIT OF THE ECLIPSING BINARY TW ANDROMEDAE. *Martha Betz Shapley* 475

LIST OF PLATES

FACING PAGE

NO.

I. Region of B.D.+31°643 Photographed with the 100-Inch Hooker Reflector 198

II. Globular Nebulae; (*a*) M 60, N.G.C. 4649; (*b*) M 87, N.G.C. 4486 221

III. Internal Motions in N.G.C. 2403 259

IV. Internal Motions in N.G.C. 4736 266

V. Types of Thermocouple Cells 328

VI. Photographic Records of Galvanometer Deflections Made by Stars of Various Spectral Types 344

VII. The Registering Microphotometer 346

VIII. Vacuum Electric Furnace 354

IX. Arc and Furnace Spectra of Iron in Violet and Blue . 368

X. Arc and Furnace Spectra of Iron 371

XI. Spectra of Venus and Sky 378

XII. One-prism Spectrograms of Stars of Class S: (*a*) R Andromedae; (*b*) R Geminorum; (*c*) S Ursae Majoris; (*d*) H.D. 35155 461

XIII. Spectrum of the Iron Arc 468

Contributions from the Mount Wilson Observatory, No. 228
Reprinted from the *Astrophysical Journal*, Vol. LV, pp. 85–118, 1922

SPECTROPHOTOMETRIC METHODS FOR DETERMINING STELLAR LUMINOSITY

By BERTIL LINDBLAD

ABSTRACT

Two spectrophotometric methods for determining absolute magnitudes.—(1) *Relative intensity of spectral regions on either side of λ 3907.* Using the 10-inch Cooke refractor with 6° objective prism, a series of images of decreasing density was obtained for each star on each plate, making each exposure 0.707 times the preceding, and from these images the exposure ratio ($E=t_2/t_1$) required to give the same density in the two adjacent spectral regions was determined for stars in well-known groups with common proper motions and hence common parallaxes—the Hyades, the Pleiades, the Ursa Major stream, and Praesepe—and also for some stars with known spectroscopic parallaxes, in all, 107 stars of types A and B and 74 stars of later types. The results show that, especially *for stars of type B8 to A3*, there is a definite correlation between E and M, the variation being such that even with the small dispersion here used the probable error of a determination of M for a star within this range of type and of absolute magnitude 0 to 4 is only $0^{M}4$. (2) *Relative intensity of cyanogen bands and adjacent spectral regions.* Using the same instrument and method as above, the relative density on either side of λ *3889* was determined from stars of known parallax, and since the band at λ 4216, though weak, is more favorable for the redder stars, the relative density in regions λλ 4144–4184 and λλ 4227–4272 was determined for 78 late-type stars. The absorption was found to be strongest *for the giants of types G5–K5* and much weaker for dwarfs; in fact all stars with $\log E>0.17$ are giants. Figures 3–5 show the variation of $\log E$ with M for various types.

Relation of spectra of A and B stars to absolute magnitude.—A study of some spectra made with the 60-inch showed that the increase in the density of the region λλ 3889–3907 with reference to λλ 3907–3935 is caused by a widening of the Hζ line and also of some arc lines of Fe and Si, which may be due to a greater density gradient in the outer layers of the less luminous stars of this type. α Cygni and the faint companion of o_2 Eridani represent extreme types.

Spectral type and luminosity of 137 faint stars of magnitudes 10 to 14, in Messier 11, Messier 13, and Selected Areas 63 and 64, were determined from 10 plates made with a small focal-plane spectrograph attached to the 60-inch. Dwarfs and giants were distinguished by applying the spectrophotometric results reported above.

Spectrophotometric parallax determinations.—The concordance of the results for $\log E$ as a function of M, as determined from the various groups of stars, indicates that the assumed parallaxes for the *Hyades, Pleiades, and Praesepe*, 0″023, 0″010, and 0″0072, respectively, are accurate to within 10 per cent. The value found for *Messier 11* is 0″00040.

Schwarzschild's constant p for Seed 23 plates was determined for images made with the 10-inch refractor and 6° prism and found to be equal to: $0.97-0.026\,(m-5)$, where m is apparent magnitude ranging from 4 to 8. X-ray developer was used.

I. A CRITERION OF ABSOLUTE LUMINOSITY FOR STARS OF SPECTRAL TYPE A

The faint companion of the star o_2 Eridani of apparent magnitude 9.5 and absolute magnitude $+10.3$ was found by Adams[1] to be of spectral type A0, and, intrinsically, is by far the faintest A-type star known. Some photographs of this object, taken with an objective prism on the 10-inch refractor and with a focal-plane spectrograph in conjunction with the 60-inch reflector, showed some peculiarities in the energy-distribution of the spectrum, when compared, for instance, with the spectrum of Sirius. The most conspicuous feature is the very strong widening of the wings of the hydrogen lines, connected with a decided weakening of the high-numbered members of the Balmer series. On the spectrograms of low dispersion taken here, Hη is the last hydrogen line to be identified with certainty. Seemingly as a consequence of this weakening of the extreme hydrogen lines, the photographs show a faint extension of the continuous spectrum much farther into the ultra-violet than is the case for an ordinary A-type star. A further difference between this star and Sirius was found in the distribution of energy between Hϵ and Hζ, apparently consisting in a considerable decrease of intensity in the region λ 3889–λ 3907 as compared with the region λ 3907–λ 3935. This phenomenon may be caused partly by the expansion of the wings of Hζ, but there was seemingly also some other cause; in particular, a widening of the silicon arc line λ 3905.6 was suspected. This line is well developed in the spectrum of Sirius, though probably it is to some extent a blend with an enhanced line of chromium. In order to see whether the last mentioned phenomenon might be a general criterion of intrinsic brightness for A-type stars, an investigation was begun on the Hyades which was later extended to include other groups of common proper motion.

---

[1] *Publications of the Astronomical Society of the Pacific*, **26**, 198, 1914.

The instrument used was the 10-inch Cooke refractor with an objective prism of 6°. The scale of the spectra thus obtained, about 340 A per mm in the region of the K line, is probably near the lower limit possible for a successful investigation of the effect. No widening of the spectra was undertaken. Satisfactory images of an A star of photographic magnitude 6.5 were thus obtained in one minute. Seed 23 plates were used, with X-ray developer. Owing to the steep color-curve of the objective for the extreme violet, only a small region of the spectrum can be in good focus for a given setting; that used corresponded to the interval λ 3889–λ 3920.

In order to measure the decrease of intensity at λ 3907 the following process was used. For each object a series of exposures was made on the same plate with exposure-times decreasing in the ratio $\sqrt{2}:1$. Each star thus produced a sequence of images of decreasing photographic density; that is, a scale of images which may be represented by the numbers 0, 1, 2, 3, etc., corresponding to the exposure-times t_0, t_1, t_2, t_3 . . . . , where $t_i:t_{i+1}=\sqrt{2}$. The density in the region λ 3895 to λ 3907 of a certain image, for instance, the first, was compared with that in the region λ 3907 to λ 3925 of the following images. The point in the scale of images for which the density in the second region equaled that of the first region in the reference image, was estimated by interpolation to a tenth of an interval. Suppose the exposure-time corresponding to this "scale-reading" to be t. The logarithm of the ratio $t_0:t$, denoted by $\log E$, is then a measure of the energy-fall in the spectrum near λ 3907. The successive images define a scale with intervals of logarithmic exposure-ratio equal to 0.15, and the "scale-reading" observed is therefore readily converted into $\log E$. As many estimations as possible were made from each series of images, starting with each of the spectra in succession as a reference image. The process is analogous to that used by Seares[1] in determining the color of a star by the method of exposure-ratios. Distorted images, as well as very dense or very weak images, have not been measured. Whenever possible, measurements were made with the plate in two opposite positions. In some of the measurements, especially of very bright stars, like Sirius, for which sufficiently short exposures could not be made with the accuracy necessary to form a reliable scale, the value of $\log E$ was estimated directly from the difference of density between the two regions in the same image. Apart from the influence of possible changes of gradation from one plate to another, the two methods, if checked against each other, should give equivalent results. This follows from Kron's[2] results for the law of photographic density as a function of intensity and exposure-time. If the gradation in a time-scale is constant, a difference in density obtained during the same exposure for two different light-sources will always correspond to the same ratio of exposure-times giving the same density, independently of the order of magnitude of the intensities, in this case, of the apparent magnitude of the star.

---

[1] *Proceedings of the National Academy of Sciences*, **2**, 521, 1916.

[2] *Publikationen des Astrophysikalischen Observatoriums zu Potsdam*, **22** (No. 67), 1913.

The wave-length λ 3907, separating the two regions, is easily identified with sufficient accuracy from its position relative to the lines Hζ, Hε, and K. The abrupt fall of intensity near this wave-length for low-luminosity A-type stars was confirmed by these observations and also on spectrograms of higher dispersion, as will be seen later. With the low dispersion used, the rapid change in intensity leaves the density fairly uniform in the two regions, λ 3895–λ 3907 and λ 3907–λ 3925. In fact, the success of the process depends on this circumstance. On the other hand, the smallness of the dispersion entails relatively large accidental errors, thus necessitating the use of a rather large number of images in order to get a reliable mean result.

Because of the juxtaposition of the two regions in the spectrum, it is evident that the influence of slight changes in the sensibility-curve of the plate, as well as of a variation in zenith-distance within reasonable limits from one object to another, will be negligible. The same will hold for a difference of gradation for the two regions. Further, if we use the law of density in Schwarzschild's form, $S=\phi\ (It^p)$, we may assume the value of p to be the same for the two regions. Suppose I_1 and I_2 to be the acting intensities for the first and second regions, respectively, and suppose S_1, t_1, S_2, t_2, to be corresponding values of density and exposure-time for the two regions. Then for equal densities we have $S_1=S_2$, and

$$I_1 t_1^p = I_2 t_2^p$$

$$\log\frac{I_2}{I_1} = p\log\frac{t_1}{t_2} = p\log E\,.$$

If we use the same kind of plates and the same developer, we have reason to assume p to be tolerably constant, though experience shows that large deviations may occur.

Since we may certainly disregard any difference in gradation for the two regions, there cannot, according to Kron's results, be any change of log E with the density of the images, a result which seems to be confirmed by the measures. This follows from the parallelism of the curves log It against log I for different degrees of density in Kron's diagrams. Two values of log I giving the same density will demand the same difference of log t for all values of the density. There may be, however, a slight change of log E with the absolute value of the acting intensity, that is, with the apparent magnitude of the star, due to the bending of the curves mentioned, corresponding to a change of the exponent p with the intensity.

The method described here admits a determination of Schwarzschild's constant p for a certain intensity, as soon as we have on a single plate the series of images of two different stars whose magnitudes are accurately known. The method of measurement is simply to interpolate the density of the successive images of one star into the scale defined by the images of the second star. In this way p has been determined from the relation $p=\frac{\Delta \log I}{\Delta \log t}$ for nearly all of the plates used here; in some cases p was determined for very different intensities on the same plate. The results seem to confirm Kron's conclusions. There is a decided decrease of p with the apparent magnitude. The mean from five plates is

$$\frac{\Delta p}{\Delta m}=-0.026\pm 0.002 \text{ (P.E.)},$$

for photographic magnitude 6.5.

Assuming a linear relation between p and m to hold for the variation of intensity met with in this investigation, we have as a mean for the first seventeen plates measured $p=0.97-0.026\,(m-5)$. Individual plates were assumed to differ from this equation by a constant ϵ, which in so far as possible was determined for each plate. The probable deviation in p from the formula for one plate, computed as a probable error for the seventeen plates mentioned, was found to be ± 0.03. A few Seed 23 plates of a later emulsion give, in the mean, lower values of p. One plate of the Pleiades was discarded by reason of an abnormally low value of p. The values of log E were reduced, as far as possible, to $p=0.97$. As a rule the corrections were small.

From stars measured on more than two plates it appears that the probable error of log E from a series of four measured images on a single plate is ± 0.025. The residuals of different plates indicate a probable systematic error of about ± 0.02. A considerable part of the probable error in log E for one plate must therefore be due to causes common to all the stars on the plate taken in the same exposure. For the greater part these are probably connected with irregularities in the images caused by imperfect guiding. From the foregoing discussion it seems unlikely that varying quality of the plates contributes appreciably. In computing the final values of log E, weights were therefore assigned equal to the number of images measured on the respective plates.

Attention was given first to members of well-known groups of stars with common proper motions, the Hyades, the Pleiades, the Ursa Major stream, and Praesepe, for which values of the parallaxes have been derived from the stream-motion or other plausible considerations. The large number of early-type stars in these clusters makes it much easier to establish the relation of spectral intensity to absolute magnitude than is the case for later types. Tables I–IV contain the results for stars of these groups; in addition, Table V gives results for some stars of types B5 to B9 of Kapteyn's groups in Orion and Scorpius, and for the two stars, α Cygni and Comp. o_2 Eridani, which may be considered as representing extreme limits for the luminosities of A-type stars.

For the Hyades the parallax used for computing the luminosities is that of Kapteyn-Küstner,[1] $\pi = 0\overset{\prime\prime}{.}023$. The Ursa Major stars are given according to Bottlinger.[2] Thirteen of the fifteen A-type stars which are certainly members of the group have been observed for this investigation. The absolute magnitudes of ϵ and ζ_1 Ursae Majoris, spectroscopic binaries with composite spectra of nearly equal intensities, have been increased by $+0\overset{\mathrm{M}}{.}75$ in order to reduce to the absolute magnitude of each component. For the Pleiades a list of probable members brighter than $9\overset{\mathrm{M}}{.}5$ photographic has kindly been communicated by Dr. Trumpler of the Lick Observatory. The value of the parallax adopted is Trumpler's[3] result, $\pi=0''.010$, derived by means of the orbital motion of ten visual binaries belonging to the group. Some stars of the list are not measurable on the plates because of overlapping images. The maximum exposures for the four plates used were 30 minutes, 10 minutes, 2 minutes, and 30 seconds, respectively. For the Praesepe cluster Kohlschütter's[1] value $\pi=0''.0072$ was adopted. This was derived by a comparison of the relations between apparent magnitude and spectrum for the early-type stars in the Hyades and Praesepe. This value is at least consistent since it gives for the four bright K stars of Praesepe a mean absolute magnitude nearly equal to that of the corresponding stars in the Hyades. For one of the Praesepe stars mentioned, B.D.+20°2166, Mr. Adams has kindly secured a spectrogram, from which he estimates the absolute

---

[1] *Publications of the Astronomical Laboratory at Groningen*, No. 23, 1909.

[2] *Astronomische Nachrichten*, **198**, 153, 1914.

[3] *Publications of the Astronomical Society of the Pacific*, **33**, 214, 1921.

TABLE I

HYADES, $\pi=0''.023$

Star		Vis. Mag.	Spectrum	log E	N	n	M_π	M_s	ΔM	Δ log E
Gron. 23	B.D.									
—	+15°632.....	3.62	F0	0.14	1	2	0.43			
—	18 640.....	3.63	G9	0.09	1	8	0.44			
28	15 612.....	3.86	G7	0.05	3	17	0.67			
79	17 712.....	3.93	G9	0.05	3	27	0.74			
224	15 631.....	4.04	G9	0.05	4	26	0.85			
143	17 719.....	4.24	A2	0.15	3	18	1.05	0.8	+0.3	−2
170	15 625.....	4.60	A5	0.17	4	27	1.41	1.1	+0.3	−2
315	14 720.....	4.75	A5	0.19	3	15	1.56			
107	17 714.....	4.84	A5	0.19	3	28	1.65			
385	15 666.....	4.85	A3	0.25	2	12	1.66	3.6	−1.9	+5
251	15 637.....	4.84	A5	0.22	2	9	1.65			
38	14 682.....	5.27	F0	0.19	3	23	2.08			
255	15 639.....	5.49	A5	0.20	3	16	2.30			
34	13 663.....	5.59	F0	0.19	3	13	2.40			
87	16 586.....	5.68	A2	0.22	3	18	2.49	1.9	+0.6	−2
245	15 636.....	5.70	F0	0.23	2	11	2.51			
64	13 668.....	5.76	A3	0.25	3	14	2.57	3.6	−1.0	+2
371	15 661.....	5.80	F0	0.19	2	10	2.61			
222	14 702.....	5.97	F0	0.19	3	10	2.78			
282	15 645.....	6.04	F0	0.17	3	16	2.85			
44	13 665.....	6.14	F2	0.11	3	12	2.85			
1	15 603.....	6.35	F5	0.15	2	6	3.16			
150	+15 621.....	6.39	F8	0.12	4	15	3.20			

---

[1] *Astronomische Nachrichten*, **211**, 289, 1920.

magnitude to be −0.4. A result of the same order is indicated by the strong absorption in the "cyanogen" bands shown by a spectrogram of the same star, taken by the writer with the Crossley reflector, which places the luminosity near that of β Geminorum ($M=+1.7$). The value $M=+0.69$ found with $\pi=0''.0072$ is in fairly good agreement with these results. The stars from Kapteyn's lists have been combined into groups having the same spectral type and nearly the same values of log E. The absolute magnitude was assumed to be the same within each group, and was calculated from the means of Kapteyn's values of the parallaxes.

TABLE II

URSA MAJOR STREAM

Star	Vis. Mag.	Spectrum	log E	N	n	M_π	M_s	ΔM	Δ log E
α Cor. Bor.	2.31	A0	0.12	2	19	0.37	0.4	0.0	0
ϵ Ursae Maj.	1.68	A0*p*	0.15	2	10	0.55	0.8	−0.2	+2
β Serpentis.	3.74	A2	0.13	2	13	0.56	0.5	+0.1	0
γ Ursae Maj.	2.54	A0	0.14	3	22	0.60	0.6	0.0	0
78 Virginis.	4.93	A2*p*	0.13	2	12	0.66	0.5	+0.2	−1
β Ursae Maj.	2.44	A2	0.15	3	11	0.80	0.8	0.0	0
α Canis Maj.	−1.58	A0	0.20	2	14	1.32	1.5	−0.2	−1
ζ_1 Ursae Maj.	2.40	A0*p*	0.20	2	8	1.44	1.5	−0.1	+1
76 Cygni.	6.05	A0	0.19	1	6	1.62	1.4	+0.2	−1
ξ Eridani.	5.23	A2	0.20	1	9	1.63	1.5	+0.1	0
δ Ursae Maj.	3.44	A2	0.21	4	29	1.71	1.7	0.0	0
g Ursae Maj.	4.02	A5	0.18	3	18	2.14	.....	......	......
ζ_2 Ursae Maj.	3.96	A0	0.23	1	4	2.25	2.2	0.0	0

The fourth column of the tables contains the final values of log E, corrected to $p=0.97$; the fifth and sixth give respectively the number of plates and the total number of images on which these values are based. The seventh column gives the absolute magnitude M_π, derived from apparent magnitude and parallax by the relation $M=m+5+5\log\pi$. The eighth column gives the absolute magnitude M_s, read by means of log E from the curves in Figure 1. The ninth and tenth columns give the residuals in M and log E from these curves.

The visual apparent magnitudes for the Hyades, the Ursa Major stars, and for Kapteyn's stars are from the Draper catalogue.

TABLE III

PLEIADES, $\pi=0''.010$

STAR		VIS. MAG.	SPECTRUM	LOG E	N	n	M_π	M_s	ΔM	Δ LOG E
Bessel	B.D.	Distance from Alcyone $\leqq 1°$								
η	+23°541	2.94	B5*p*	0.06	1	4	−2.06	.....	......	......
f	23 557	3.73	B8	0.06	2	8	−1.27	.....	......	......
b	23 507	3.76	B5*p*	0.11	3	12	−1.24	.....	......	......
c	23 516	3.93	B5	0.08	2	7	−1.07	.....	......	......
e	23 547	4.34	B5	0.09	2	11	−0.66	.....	......	......
d	23 522	4.28	B5	0.06	1	3	−0.72	.....	......	......
h	23 558	5.15	B8*p*	0.11	3	10	+0.15	0.2	0.0	+1
g	23 505	5.53	B5	0.11	1	4	0.53	0.2	+0.3	−2
28	22 563	5.54	B8	0.16	2	9	0.54	0.9	−0.4	+3
m	24 546	5.68	B8	0.09	2	11	0.68	.....	......	−5
k	24 553	5.83	B8	0.12	2	8	0.83	0.4	+0.4	−3
34	23 563	6.23	B8	0.19	3	12	1.23	1.4	−0.2	+1
32	23 561	6.66	B9	0.17	1	4	1.66	1.1	+0.6	−4
38	23 569	6.82	B9	0.24	3	15	1.82	2.5	−0.7	+3
12	24 562	6.88	B9	0.22	3	12	1.88	2.0	−0.1	0
24	23 540	6.93	B9	0.22	3	11	1.93	2.0	−0.1	+1
40	23 570	6.98	A0	0.23	3	17	1.98	2.2	−0.2	+1
29	23 553	6.99	A0	0.22	3	14	1.99	2.0	0.0	0
19	23 537	7.04	A0	0.24	3	16	2.04	2.5	−0.5	+2
22	23 538	7.19	B9	0.25	3	12	2.19	2.8	−0.6	+2
10	23 523	7.37	A0	0.24	3	15	2.37	2.5	−0.1	0
37	23 567	7.44	A0	0.22	3	13	2.44	2.0	+0.4	−2
39	24 578	7.46	A2	0.23	3	11	2.46	2.2	+0.3	−1
31	23 560	7.54	A0	0.28	1	3	2.54	3.6	−1.1	+4
20	24 566	7.68	A2	0.26	2	6	2.68	3.1	−0.4	+1
	24 540	7.79	A3	0.26	2	7	2.79	4.0	−1.2	+3
23	23 539	7.81	A2	0.24	2	5	2.81	2.5	+0.3	−1
7	23 517	7.87	A2	0.27	2	8	2.87	3.3	−0.4	+2
33	23 562	8.01	A2	0.23	2	5	3.01	2.2	+0.8	−3
1	23 510	8.06	A2	0.27	3	6	3.06	3.3	−0.2	+1
	23 496	8.07	A5	0.21	2	7	3.07	.....	......	......
	23 524	8.13	A2	0.29	2	7	3.13	3.9	−0.8	+3
30	23 559	8.14	A3	0.25	2	6	3.14	3.6	−0.5	+1
	23 504	8.22	A5	0.22	2	6	3.22	.....	......	......
	22 573	8.24	A3	0.23	2	6	3.24	2.6	+0.6	−1
	23 495	8.29	A5	0.19	2	9	3.29	.....	......	......
13	23 528	8.46	A5	0.24	2	5	3.46	.....	......	......
	23 508	8.51	A3	0.24	2	4	3.51	3.1	+0.4	−1
	22 565	8.53	A5	0.21	2	6	3.53	.....	......	......
	+24 563	8.59	A5	0.20	2	5	3.59	.....	......	......

TABLE III—*Continued*

STAR		VIS. MAG.	SPECTRUM	LOG E	N	n	M_π	M_s	ΔM	Δ LOG E
Bessel	B.D.	Distance from Alcyone 1° to 3°								
	+21°535....	6.0	B9	0.15	3	17	1.0	0.8	+0.2	−1
	22 523....	6.7	A0	0.17	3	18	1.7	1.1	+0.6	−4
	22 545....	6.9	A0	0.22	3	17	1.9	2.0	−0.1	+1
	22 572....	6.9	B9	0.22	3	16	1.9	2.0	−0.1	0
	24 527....	7.1	A0	0.21	3	18	2.1	1.7	+0.4	−2
	21 492 ...	7.4	A0	0.20	3	16	2.4	1.6	+0.8	−4
	24 537....	7.6	A3	0.23	3	14	2.6	2.6	0.0	0
	20 624....	7.7	A2	0.20	3	9	2.7	1.6	+1.1	−5
	22 569....	7.8	A2	0.29	3	13	2.8	3.9	−1.1	+4
	25 631....	7.8	A2	0.24	3	12	2.8	2.5	+0.3	−1
	22 544....	8.0	A2	0.22	3	10	3.0	2.0	+1.0	−4
	24 554....	8.2	A3	0.26	2	8	3.2	4.0	−0.8	+2
	24 568 ...	8.4	A3	0.21	2	8	3.4	1.9	+1.5	−4
	22 556....	8.5	A2	0.27	2	7	3.5	3.4	+0.1	−1
	21 530....	8.3	F0	0.13	2	6	3.3	.....	......	......
	24 528....	8.9	A5	0.22	2	4	3.9	.....	......	......
	+25 615....	8.9	A3	0.25	2	4	3.9	3.6	+0.3	−1

TABLE IV

PRAESEPE, $\pi = 0''.0072$

Star	Vis. Mag.	Spectrum	log E	N	n	M_π	M_s	ΔM	Δ log E
B.D.									
+20°2171.........	6.23	A2	0.17	2	14	0.52	1.1	−0.6	+4
20 2149.........	6.39	F0	0.15	2	10	0.68	.....	......	......
20 2166.........	6.40	G5	0.05	2	2	0.69	.....	......	......
20 2158.........	6.48	K0	0.08	2	5	0.77	.....	......	......
20 2159.........	6.48	A0	0.11	2	6	0.77	0.2	+0.6	−4
19 2069.........	6.54	F0	0.14	2	9	0.83	.....	......	......
19 2053.........	6.58	A5	0.13	2	13	0.87	.....	......	......
20 2175.........	6.60	A3	0.17	2	10	0.89	1.1	−0.2	+1
20 2172.........	6.77	A5	0.19	2	9	1.06	.....	......	......
20 2185.........	6.98	K0	0.10	2	3	1.37	.....	......	......
20 2143.........	7.09	F0	0.20	2	5	1.38	.....	......	......
20 2152.........	7.26	A0	0.16	2	8	1.55	0.9	+0.7	−4
20 2163.........	7.41	A0	0.24	1	4	1.70	2.5	−0.8	+3
20 2153.........	7.52	A0	0.18	2	6	1.81	1.2	+0.6	−3
19 2064.........	7.54	A3	0.17	2	7	1.83	1.1	+0.7	−4
20 2148.........	7.57	A3	0.21	2	6	1.86	1.9	+0.0	0
20 2132.........	7.72	A0	0.26	2	6	2.01	3.1	−1.1	+4
20 2165.........	7.74	A0	0.20	2	6	2.03	1.6	+0.4	−2
19 2078.........	7.77	A3	0.21	2	5	2.06	1.9	+0.2	−1
+19 2084.........	7.88	A5	0.20	2	6	2.17	.....	......	......

Those of the Pleiades are by Miss Parsons,[1] or by Müller and Kempf with the reduction −0.30 to the Harvard scale. For a few Pleiades stars Münch's photographic magnitudes have been used, reduced to the visual scale by means of color-indices inferred from the spectral type, which is not far from A0. The first part of Table III contains members of the group within 1°; the second, between 1° and 3° from Alcyone. For the latter stars the photographic magnitudes derived by Trumpler have been reduced to the visual scale in the same way as those by Münch. For Praesepe the photographic magnitudes by Kohlschütter on the Göttingen system were similarly reduced to visual magnitudes. The spectra are given according to Harvard with the exception that for Pleiades stars fainter than $7\overset{\mathrm{M}}{.}5$ the spectral types have been revised on the basis of the strength of the K line.

TABLE V

KAPTEYN STARS, COMP. o_2 ERIDANI, α CYGNI

Star	Vis. Mag.	Spectrum	log E	Mean	N	n	M_π	M_s	ΔM	$\Delta \log E$
Boss 4018	4.11	B9	0.11	......	1	7	....	....	.....	.....
1438	4.92	B9	0.10	......	2	12	....	....	.....	.....
1455	5.57	B9	0.11	0.12	3	19	0.01	0.4	−0.4	+2
1448	6.61	B9	0.16	......	3	11	....	....	.....	.....
Boss 1944	3.09	B8	0.08	......	1	5	....	....	.....	.....
4465	4.65	B8	0.08	......	1	5	....	....	.....	.....
2071	5.11	B8	0.08	......	1	5	....	....	.....	.....
4058	5.41	B8	0.07	0.08	1	5	−0.16	....	.....	.....
4006	5.61	B8	0.07	......	1	6	....	....	.....	.....
4573	5.79	B8	0.06	......	1	5	....	....	.....	.....
1788	5.88	B8	0.08	......	1	6	....	....	.....	.....
Boss 1262	3.68	B5	0.04	0.05	1	8	....	....	.....	.....
926	5.25	B5	0.06	......	1	7	−1.27	....	.....	.....
Comp. o_2 Eridani	9.5	B9	0.31	......	2	2	10.3	....	.....	.....
α Cygni	1.33	A2p	0.08	......	1	8	....	....	.....	.....

Table VI contains the results of measurements on later-type stars from the list of spectroscopic parallaxes by Adams, Joy, Strömberg, and Burwell, made in connection with an investigation of the "cyanogen" absorption beyond λ 3889. The means were taken for limited intervals of spectral type and absolute magnitude; N is the number of stars in each group. No correction was made for a variation of Schwarzschild's constant, and the measurements for the individual stars are not as accurate as for the A-type stars in the preceding tables. In fact, with the decrease in intensity of Hζ and the general strengthening of the metallic lines in later spectral types the region λ 3895–λ 3907 has no longer the same uniform appearance as for the early types. The results in the table show, however, that the effect still persists to some extent in the later types, in spite of the vanishing of Hζ.

---

[1] *Astrophysical Journal*, **47**, 38, 1918.

TABLE VI

MEAN RESULTS FOR STARS WITH DETERMINED SPECTROSCOPIC PARALLAXES

Spectral Range	Mean Type	N	Mean Abs. Mag.	Mean log E
F5*p*–G3*p*	G0*p*	4	−2.5	0.05
F4 –G8	G1	3	−1.7	0.04
A8 –F9	F4	3	0.3	0.09
F1 –G1	F7	15	3.9	0.15
G1 –K2	G8	12	0.9	0.05
G4 –K2	G9	6	5.7	0.16
K3 –Ma	K5	7	0.6	0.12
K3 –K7	K5	3	7.3	0.24

Figures 1 and 2 illustrate the result in the tables, log E being plotted against M_π, with different symbols for the different groups. α Cygni and Comp. o_2 Eridani are represented by arrows. The absolute magnitude of α Cygni can only be estimated qualitatively as very bright from exceedingly small proper motion. Comp. o_2 Eridani with $M=10.3$ falls below the margin of the diagram. Figure 1 gives the results for spectral types B5–A3; Figure 2 for types from A5 on. From B8 to A2 there is no certain evidence of a change in the curve; but the A3 curve for lower luminosities evidently falls below the B8–A2 curve, and forms a transition to the A5 curve in Figure 2. The degeneration of the curves for types A5–F is clearly a consequence of the decreasing intensity of Hζ with advancing type.

It is evident from these results that the increase of log E with decreasing luminosity can be used for determining absolute magnitudes for stars of spectral types B8–A3, but that the curves for later types cannot give very trustworthy results. The curves further show that for very bright stars log E approaches a limiting value representing a very smooth run of the energy-curve between Hζ and K, a consequence of the extreme narrowness of all absorption lines. This phenomenon seems to be more or less independent of type, α Cygni, A2*p*, falling in with the B5 stars of the Pleiades. The Cepheids and pseudo-Cepheids and the very bright F4–G8 stars in Table VI also fall near the same point of the diagram. The steepness of the curve for stars brighter than $M=0$ is such that only

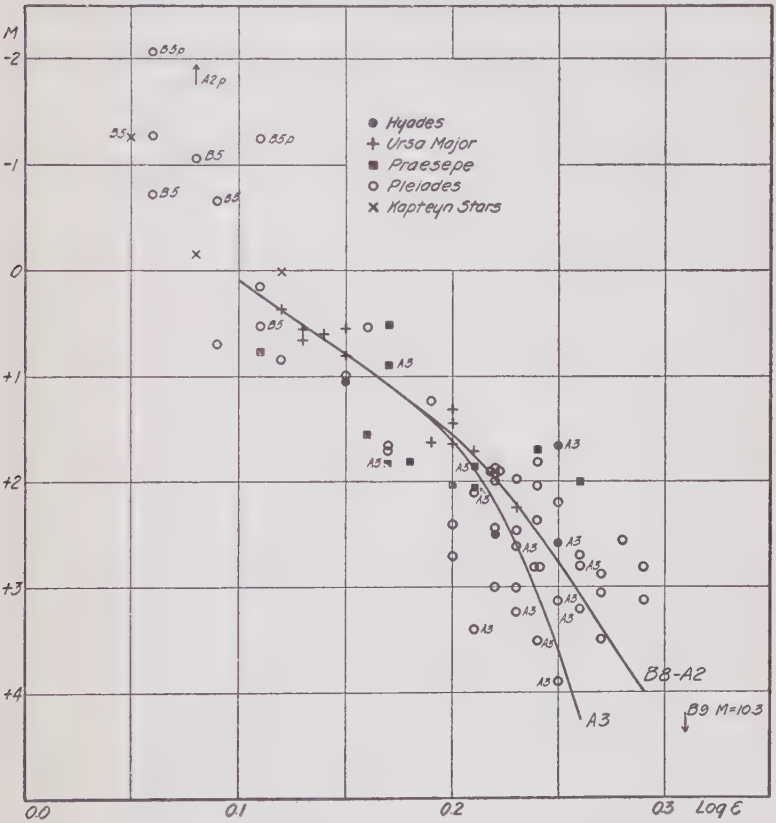

FIG. 1.—Logarithmic exposure-ratio for the regions λλ 3895–3907, 3907–3925, and absolute magnitude. Spectral types B5–A3.

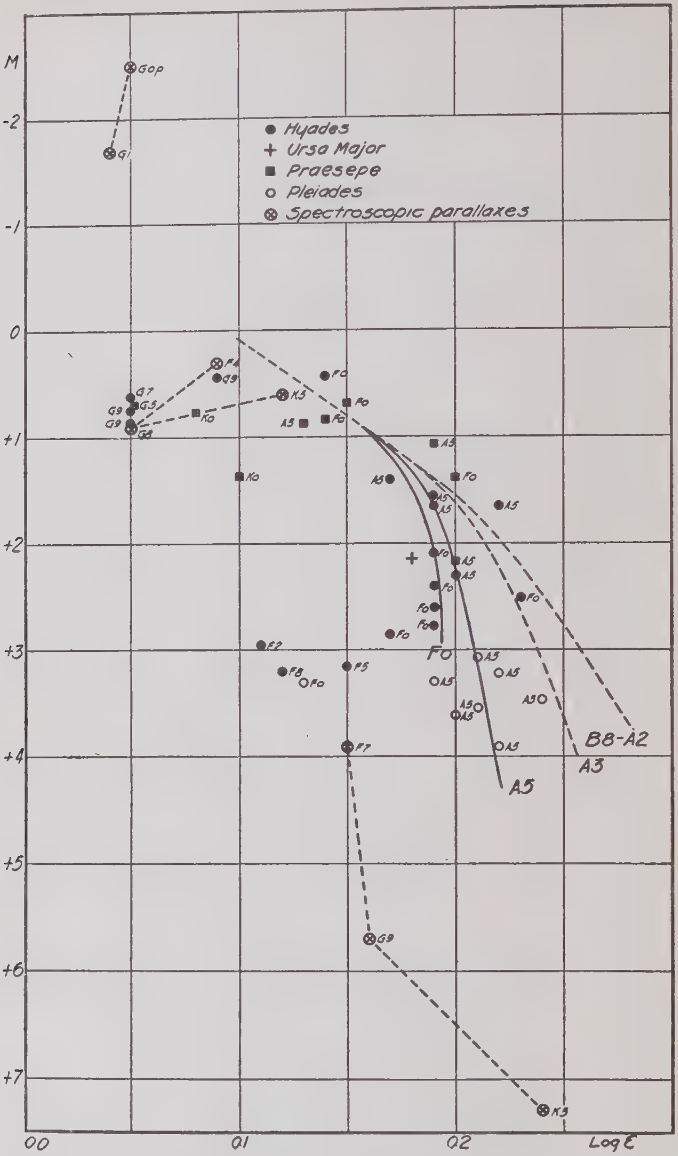

FIG. 2.—Logarithmic exposure-ratio for the regions λλ 3895–3907, 3907–3925, and absolute magnitude. Spectral types later than A5.

qualitative estimates of the luminosity can be made from values of log E less than 0.10.

To form the B8–A2 curve, means of log E for certain intervals of M were taken for both Ursa Major and Pleiades stars. Between $M=0$ and $M=+2$ the curve was drawn to represent the Ursa Major stars. A comparison with the eleven Pleiades stars in this region observed on three plates gave a systematic difference of +0.002 in log E, which is negligible. The remaining parts of the curves were then drawn in accordance with the results for the Pleiades, attention being given also to the Hyades and Praesepe stars in forming the A3 and A5 curves. The co-ordinates of the curves in Figure 1 then run as follows:

	B8–A2				
log E	0.10	0.15	0.20	0.25	0.28
M	+0.08	0.80	1.55	2.77	3.68
	A3				
log E	0.10	0.15	0.20	0.22	0.25
M	+0.08	0.80	1.62	2.20	3.60

The F0 curve in Figure 2 is drawn mainly from stars in the Hyades.

The absolute magnitudes, M_s, corresponding to log E have been read from these curves for all B8–A3 stars having log $E>0.10$; the two A5 stars in Figure 2 with log $E<0.18$ are included.

Errors in the assumed values of the parallaxes evidently combine with residual systematic errors in the measurements. From the discussion of systematic errors it seems that the reliability of any correction to the parallax that might result from the mean residuals for a group will probably depend more on the number of images measured for the individual stars than on the number of stars. The absolute magnitudes of the Ursa Major stars derived from stream-motion are probably but little affected by systematic errors. This likely is also true of the values of log E, because these stars were observed individually on a rather large number of different plates. As there seems to be no appreciable systematic difference between the Ursa Major stars and the Pleiades we may conclude that Trumpler's value of the parallax, $\pi = 0''.010$, is very good. With allowance for a possible systematic error of about 0.01 in log E the error may amount to about 10 per cent, or $\pm 0''.001$. For the Hyades and Praesepe we can determine the parallax which causes the systematic difference in log E to vanish. For the Hyades we find $\pi = 0''.023$, the value initially adopted; and for Praesepe, $\pi = 0''.0068$, differing by only $0''.0004$ from Kohlschütter's value. An uncertainty of 10 per cent is probably to be admitted for both these values. The Kapteyn stars of types B8 and B9 seem to agree with the curve as well as can be expected.

The residuals ΔM for the individual stars are seen to be very small for the Ursa Major stars, but are rather large for some of the A3 stars of low luminosity in the other groups. This is to be expected from the steepness of the curve. In all, the residuals for seventy-one stars give a probable deviation of $\pm 0^{M}.40$, which is comparable with the probable error of the spectroscopic method for late-type stars. With weights equal to the number of images, n, the probable deviation in log E from the curves is found to be ± 0.026 for a value based on four measured images. This value is to be compared with ± 0.025 previously derived from the residuals in log E from the mean for different plates. The latter value, it was concluded, was produced to a considerable extent by systematic errors common to a large number of stars in a certain group. In the new value, on the other hand, the systematic errors are combined with errors in the parallaxes, and may be partly eliminated in drawing the curves. The close agreement of the two results suggests, however, that the correlation between the energy distribution around λ 3907 and the absolute magnitude is close.

An investigation of spectra of higher dispersion for some selected A stars of different luminosities, photographed with a focal-plane spectrograph in the Newtonian focus of the 60-inch reflector, and with the Cassegrain spectrograph and an 18-inch camera, and also with a slitless quartz spectrograph used in conjunction with the Crossley reflector of the Lick Observatory, throws some light on the question of the physical cause of the effect investigated here. Undoubtedly the increase of log E with decreasing luminosity is to a considerable degree caused by a widening of the wings of the Hζ line, the extreme limits being represented by very bright stars such as α Cygni and α Leonis with narrow hydrogen lines and the very faint companion of o_2 Eridani, which has exceedingly wide lines. But there seems also to be evidence of another cause. It appears as though certain arc lines of iron and silicon in the region λ 3889–λ 3907 increase appreciably in width and intensity with decreasing luminosity. The lines suspected are λλ 3895.8, 3899.9, 3903.1, 3906.6 of iron, and λ 3905.6 of silicon. With the exception of λλ 3903.1 and 3905.6, these lines are classified by King[1] as belonging to Class IB. The exceptions are in classes II and III, respectively. A widening of these lines with decreasing luminosity seems to contribute perceptibly to the depression of the intensity in the region Hζ–λ 3907. There seems to be a similar effect, though much weaker, in the region λ 3914–λ 3923, including the two iron lines λλ 3920.4 and 3923.1 of Class IB. On the whole, in stellar spectra the region between λ 3907 and K is certainly affected by heavy arc lines to a much smaller degree than the region Hζ–λ 3907.

In some spectra of Sirius photographed by Nicholson with the Snow telescope, with a dispersion of 3 A per mm, the lines mentioned between λλ 3889 and 3907 are plainly visible, except the iron line λ 3906.6. The line λ 3905.6 is relatively strong, of about the same strength as the enhanced titanium lines λλ 3900.7 and 3913.7. We probably have here a blend of the silicon line with an enhanced line of chromium, but an indication that the blend is to a considerable part due to silicon may be found in the circumstance that the Kensington observers[2] state that it is somewhat weaker in the spectrum of ε Ursae Majoris than in the spectrum of Sirius, in spite of the fact that of thirty enhanced chromium lines all are found stronger in the former star, except one which is given as of the same intensity in both spectra. In the case of α Lyrae and α Coronae, which are stars of Ao type more luminous than Sirius, λ 3905.6 is still to be seen in the spectrograms taken with the Cassegrain spectrograph; of the iron lines only λ 3903.1 can be traced with certainty. On the other hand, in ζ_2 Ursae Majoris with $M=+2.25$, λ 3903.1 is strong, and λλ 3895.8 and 3899.9 are clearly visible; in the position of λ 3906.6 there is a very broad line seemingly including λ 3905.6 as a blend. The prominent arc lines of iron between Hζ and Hη are very broad and well marked, probably affecting to a perceptible extent the integrated intensity of the region between these two lines, at least from λ 3860 to Hη. To the red of λ 3907 no effects of similar importance for the variation of the integrated intensity of wide patches of the continuous spectrum can be seen, though the spectrum is evidently rich in lines. The K line, which indicates that the spectral type lies between A0 and A2, is weaker and sharper than in the spectrum of β Serpentis, type A2, $M=0.56$, in which the iron arc lines are faint. The visibility of the broad arc lines is therefore not likely to be interpreted as due to an increase in spectral type. In addition to these comparisons made with the Cassegrain spectrograph, the slitless spectrograms taken with the quartz spectrograph on the Crossley reflector, and the low dispersion slit spectra obtained with the 60-inch reflector, show an abrupt fall of intensity near λ 3907 for ζ_2 Ursae Majoris, as well as for Nos. 10, 20, and 31 of the Pleiades, types A0, A2, A0, $M=+2.37$, 2.68, 2.54, respectively, for No. 64 of the Hyades, A3, $M=+2.57$, and the Praesepe star B.D.+20°2165, A0, $M=+2.03$. The difference relative to the brighter Pleiades and Ursa Major stars is plainly recognizable. A very marked depression near λ 3906 is shown on a spectrogram of Comp. o_2 Eridani taken with the quartz spectrograph. From the appearance of the K line this star ought probably to be classified a little earlier than A0.

---

[1] *Mt. Wilson Contr.*, No. 66; *Astrophysical Journal*, **37**, 239, 1913; *Publications of the Astronomical Society of the Pacific*, **33**, 106, 1921.

[2] Solar Physics Committee, *Chemical Origin of Various Lines in Solar and Stellar Spectra*, p. 49, 1910.

The effect in question persists for later types, as shown by Table VI and is confirmed by results from spectra of other kinds. The energy-fall in a slitless spectrogram at λ 3907 is much more pronounced for a dwarf than for a giant. This fact confirms our results just derived, because the importance of the hydrogen line Hζ for the effect must be negligible in these types. On the other hand, the degeneration of the effect toward type F shows that Hζ probably causes a large part of the phenomenon in the A type.

The facts dealt with here are probably best understood from the standpoint of an increased density-gradient in the outer layers of a star of certain type with decreasing luminosity, which follows because the change in luminosity is in all probability due chiefly to a change of the mean density. For a layer of certain temperature the density will be appreciably greater in a star of low luminosity than in a more luminous one, a condition which may be thought to favor the strength and width of the arc and flame lines.

The eclipsing binaries offer an opportunity to derive a relation between the effect at λ 3907 and the mean density of the star. From some preliminary results obtained here it has been found that the energy-fall near λ 3907 is strong for RZ Cassiopeiae and RR Draconis, whose brighter components have especially high mean densities, and seems to be much smoother for the low-density stars examined. For RZ Cassiopeiae a value of M between +2 and +3 inferred from the spectrum is in fair agreement with Dugan's[1] results for the dimensions of the brighter component of this star.

II. THE "CYANOGEN" ABSORPTION IN SPECTRA OF TYPES G–M

Miss Maury[2] makes the statement in her classification of stellar spectra that the sudden decrease of general intensity in the spectrum from λ 3889 toward the ultra-violet found in types XIV and XV, as well as the degree of absorption in the regions λ 4055–λ 4078 and λ 4144–λ 4216, is developed to a different degree for different stars within these types. The variation of intensity in these regions is further thought to be correlated to some extent with the strength of the lines λλ 4215.7, 4227, and the compound line λ 4076.8–λ 4077.9. Kapteyn[3] showed that stars with heavy absorption in the violet and ultra-violet regions mentioned have on the average much smaller proper motions than stars with comparatively slight absorption. This result was thought by him to bear upon the problem of selective absorption in inter-stellar space. In more recent years, however, the influence of differences in the absolute magnitudes of the stars on the appearance of their spectra has been recognized, especially by Adams and Kohlschütter in the development of the spectroscopic method for deriving stellar parallaxes. In this method the lines λ 4216 and λ 4078 are two of the most important variable lines. That the energy-fall beyond λ 3889 is intimately connected with the spectroscopically determined absolute magnitude was found by the writer by using very short objective-grating spèctra.[1] The color-effect of the absolute magnitude was found to be much more strongly developed at the inner limit of the spectra in the "minimum wave-length" than in the "effective wave-length" measured by bisecting the images. It was then suspected that the effect could be due to an increase of absorption with stellar luminosity in the heavily winged lines of iron in the region λ 3870–λ 3890.

---

[1] *Contributions from the Princeton Observatory*, No. 4, 1916.

[2] *Harvard Annals*, **28**, 38, 1897.

[3] *Mt. Wilson Contr.*, No. 31; *Astrophysical Journal*, **29**, 46, 1909.

It has been found recently, however, that the effect is without doubt due to a variation in strength with stellar luminosity in the strong "cyanogen" band with its first head at λ 3883. On spectra of stars of different types and luminosities photographed with a slitless quartz spectrograph[2] on the Crossley reflector of the Lick Observatory three similarly behaving absorption regions were found to coincide with the three "cyanogen" bands with first heads at λλ 4216, 3883, and 3590. The band at λ 3883 is by far the strongest; the point most sensitive to changes in luminosity seems to be the region around and between the two heads at λ 3871 and λ 3883. Of the two other bands, that at λ 3590 seems to be somewhat stronger. The band at λ 4606 seems to be too faint to be identified with certainty.

The spectra of the following stars were photographed; the spectral types and absolute magnitudes are from the new list of spectroscopic parallaxes[3] by Adams and his collaborators.

---

[1] *Astrophysical Journal*, **49**, 289, 1919; *Upsala Universitets Årsskrift*, 1920.

[2] This instrument is described by W. H. Wright in the *Lick Observatory Bulletin*, **9**, 52, 1917.

[3] *Mt. Wilson Contr.*, No. 199; *Astrophysical Journal*, **53**, 13, 1921.

χ Leonis	F5,	0.8
39 Leonis	F8,	3.7
Lal 19896	G1,	4.5
Boss 2338	G3,	−1.0
Lal 21008	G6,	5.2
ε Virginis	G6,	0.0
ε Geminorum	G8,	−1.4
β Geminorum	G9,	1.7
θ_1 Tauri	G9,	1.4
o_2 Eridani	K1,	6.2
Cin. 1712	K3,	6.4
α Tauri	K4,	1.0
β Cancri	K4,	0.4
Lal 13284	K5,	7.1
Boss 2935	Ma,	10.5
Boss 1868	Ma,	−0.2
α Orionis	Ma,	−3.8

The development of the bands is at a maximum for giant stars of types between G5 and K5, and diminishes strongly toward the F and M types. In the dwarf stars of all types the bands are only faintly developed.

The absorption in the band at λ 3883 has been investigated here for stars of known spectroscopic parallax by means of the 6° objective prism on the 10-inch refractor. The method employed is analogous to that used for the A stars described in the first part of this paper. This investigation was carried out before the identification with the "cyanogen" band had been made. The two regions of the spectrum immediately adjacent to λ 3889 were compared in series of images taken with decreasing exposure-time to determine the exposure-ratio for equal photographic density in the two regions. The maximum effect seems to be in spectral types G8–K0, where the difference in exposure-ratio between average giants and dwarfs corresponds to nearly a magnitude. The effect decreases rapidly from G5 to G0. The Cepheids and pseudo-Cepheids have a somewhat peculiar position with even less contrast at λ3889 than dwarfs of the same spectral type. The smoothness of the spectrum around the Hζ line for these stars is probably due to the disappearance of the wings of the strong absorption lines following the advance of the spectrum toward Miss Maury's *c*-stage.

There is a very decided disadvantage, however, in the fact that the region in question is situated so far in the violet that for the redder stars the exposures must be made considerably longer. The band at λ 4216, though weaker, is much more favorable in this particular, and an investigation of it was therefore begun with the same instrumental arrangement. The region most strongly affected by this band lies between λλ 4144 and 4184.

This region of 40 A width, corresponding to about 0.09 mm on the plate, has been compared with that at λ 4227–λ 4272 as standard. The regions in question are easily identified with sufficient accuracy by estimating the distances from the G-band and the line λ 4227, which are conspicuous features of the spectra even with very low dispersion. For the dwarfs of types K5–M the intensity in the second region mentioned is probably somewhat modified by the wings of λ 4227 which produce an additional effect of luminosity on the exposure-ratio in the same direction as the effect of the "cyanogen" absorption in the first region. No special efforts were made to determine Schwarzschild's constant for the plates. The results obtained from the investigation of the A stars indicate that generally the changes in the constant are small and do not increase materially the probable error of the measured exposure-ratio, but that rather large changes may occur, especially from one emulsion to another. In this case several stars were measured on each plate, and systematic errors of large size ought to show in the residuals from the curves. The means of the residuals for the individual plates are found to be small, however.

As before, the plates used were Seed 23, size 8×10 inches, with X-ray developer. Images more than 3.6 inches from the center were excluded. The focus was set near λ 4200, and is tolerably constant over most of this area. Even within the adopted limit of distance, however, some images must be excluded by reason of distortion or bad focus, because the field has not exact symmetry of rotation with reference to the plate center.

A scheme for classifying the objective-prism spectra was developed by using types determined by Adams and his collaborators as standards. The classification is based on the appearance and relative strength of the hydrogen lines, the K line of calcium, the λ 4227 line of calcium, the titanium-oxide bands, and the general energy-distribution in the spectrum. Since the decrease of the hydrogen lines and the increase of λ 4227 with advancing spectral type proceed more rapidly in the dwarf series, while the increase of redness takes place faster in the giant series, and since λ 4227 has enormous strength in dwarfs of types K5–M, these characteristics

TABLE VII

Boss or Cin. No.	Harv. Vis. Mag.	Spectrum	*M*	log *E*	*n*	Spectrum Obj. Prism
3274	6.5	G8	0.4	0.25	6	G8*g*
3298	4.8	K3	0.6	0.27	8	K0*g*
3326	5.9	K0	4.2	0.16	4	K2
3344	6.5	G8	0.9	0.26	7	G8*g*
3362	4.9	Ma	−0.3	0.18	8	Ma*g*
C 1657	7.7	K2	6.4	0.14	4	K0*d*
3408	6.2	K4	0.5	0.25	4	K5*g*
3537	5.7	K3	0.4	0.25	4	K2*g*
3554	6.3	F9	4.3	0.12	6	G5*d*
4131	5.5	K2	1.1	0.27	5	K2*g*
4137	5.6	G2	4.7	0.12	7	G5*d*
4147	3.3	G6	0.0	0.19	5	G5*g*
4257	6.7	G8	4.7	0.13	7	K0*d*
4264	5.4	K5	0.8	0.24	7	K5*g*
4315	3.4	K2	0.6	0.26	5	K0*g*
4318	5.9	Ma	0.2	0.22	4	Ma*g*
4323	5.0	K5	0.2	0.29	5	K2*g*
4327	4.4	G2	−1.4	0.27	4	G5*g*
4342	7.9	K5	7.9	0.05	6	K5*d*
4370	5.3 5.3	K1 K2	6.3 6.3	0.12	7	K0*d*
4372	6.7	K4	7.3	0.08	5	K5*d*
4414	6.3	K1	1.3	0.24	3	K2*g*
4420	4.3	A9	1.6	0.12	4	F2
C 2322	7.9	K5	8.0	−0.02	4	K5*d*
Lal 31905	7.2	K2	2.1	0.25	4	K5*g*
4571	4.3 5.0	K0 K4	5.8 7.8	0.10	6	G8*d*
4580	4.7	G6	−0.1	0.27	6	G8*g*
4595	5.7	F4	2.8	0.12	6	F5
4618	6.1	G2	−0.3	0.20	6	G5*g*
4635	4.9	G5	−0.5	0.20	9	G0*g*
4638	3.4	G8	2.5	0.15	5	G8
A. G. Leip. 8449	7.6	K2	0.8	0.33	5	K2*g*
4660	5.7	G0	−0.8	0.22	9	G0*g*
C 2420	7.9	G5	5.5	0.11	5	G5*d*
C 2421	8.5	G9	5.2	0.10	6	G5*d*
A. G. Leip. 8507	8.9	G2	5.7	0.14	5	G5*d*
4678	5.4	G9	1.7	0.21	5	K0*g*
A. G. Leip. 8585	7.6	Ma	1.5	0.16	3	Ma*g*
4688	6.5	G8	2.8	0.22	3	K0*g*
4713	5.4	F0	1.6	0.11	6	A-F

TABLE VII—*Continued*

Boss or Cin. No.	Harv. Vis. Mag.	Spectrum	*M*	log *E*	*n*	Spectrum Obj. Prism
C 2456	8.8	Mb	10.7	−0.09	3	Mb*d*
4800	4.5	Mb	−1.2	0.15	8	Mb*g*
4817	5.4	F8	0.3	0.13	5	F8
4823	4.2	K1	1.0	0.28	11	K0*g*
C 2495	6.0	G4	3.7	0.10	10	G5*d*
4892	6.8	G4	5.5	0.13	3	G2*d*
4893	6.6	G6	5.7	0.12	3	G2*d*
4898	5.7	G8	−1.4	0.28	12	G8*g*
4910	6.3	G8	1.5	0.24	2	G5*g*
4912	4.5	K0	0.2	0.29	8	K2*g*
4920	6.0	F4	2.8	0.12	3	F8
4940	4.6	K4	0.5	0.26	4	K3*g*
4950	5.2	G8	5.1	0.13	5	G5*d*
5009	4.8	G9	5.8	0.09	6	G8*d*
5027	4.4	G8	0.0	0.22	6	G8*g*
5052	3.8	Ma	0.2	0.11	5	Ma*g*
5079	4.0	G2	0.7	0.13	6	G5*g*
5089	4.9	G9	0.8	0.18	5	G8*g*
5093	3.9	G8	3.9	0.13	5	G8
5098	5.8	G1*p*	−2.5	0.20	4	G5*pg*
5118	3.7	K6	0.5	0.25	6	K5*g*
5125	5.6	Mc	0.5	0.14	5	Mb*g*
5129	4.6	Mb	0.3	0.13	8	Mb*g*
C 2616	7.2	G8	5.6	0.13	2	G8*d*
5143	5.6	G8	0.0	0.27	2	K0*g*
5180	5.7	K2	5.9	0.13	6	K2*d*
5187	4.0	G9*p*	−2.0	0.23	4	G*pg*
5219	6.1	G2	5.2	0.06	3	G5*d*
5229	2.3	G0*p*	−3.0	0.24	5	G*pg*
C 2672	6.3	G8	6.2	0.12	4	G8*d*
5321	6.0	F5	3.6	0.13	2	F5
5346	3.6	G8	3.2	0.18	5	G8*g*
C 2707	8.6	Ma	9.4	−0.01	3	M*d*
C 2718	6.6	F7	3.9	0.10	9	F5
5420	6.2	G8	1.5	0.26	7	K0*g*
5431	3.9	K2*p*	−2.9	0.24	4	K*pg*
5433	5.6	K7	8.3	0.09	9	K5*d*
5434	6.3	K8	8.7	0.05	7	Ma*d*

alone will suffice in a great number of cases to determine the spectral type and to decide whether the star is a giant or a dwarf. From type G0 on, however, the degree of the "cyanogen" absorption must be taken into account, and the approximate luminosity will be obtained with the aid of log *E*. The spectra used are narrow and, in what concerns the visibility of the lines, are inferior to widened images; but this has been at least partly compensated by the large number of images with different intensities usually available. For spectral types G0–K0 both the hydrogen lines and λ 4227 are only faintly visible, but a fairly good discrimination between the stages G0, G5, and G8–K0 seems to be possible. Four Cepheids and pseudo-Cepheids among the stars observed were recognized as peculiar stars mainly by the abnormal strength of the hydrogen lines.

The results of the measurements and classifications are given in Table VII. The first four columns contain data from the list of spectroscopic parallaxes. The fifth column gives log *E*, the logarithmic exposure-ratio for equal intensities in the two regions λ 4144–λ 4184 and λ 4227–λ 4272, the former being situated in the densest part of the "cyanogen" band; *n* is the number of images used for determining log *E*. The last column gives the spectral type as determined from the objective-prism spectra, in most cases without knowledge of the more accurate values of the type in the third column. An added *g* or *d* indicates a giant or a dwarf, respectively. This estimation of luminosity is made mainly from the value of log *E* according to the curves in Figures 3 and 4, the value of the spectral type estimated from the objective-prism spectra being used as argument. The individual results given in the last column are therefore directly dependent only on the data secured from the low dispersion spectra. The good agreement between these results and the spectral type and absolute magnitude in the third and fourth columns seems to give promise of the usefulness of the method.

Figure 3 gives the relation between log *E* and the absolute magnitude for stars of types A9 to K2, Figure 4 for types K2–Mc. The curves drawn representing the different types have only provisional significance. Figure 5 gives log *E* as a function of the spectral type, different degrees of luminosity being represented by different notations. It is evident from these diagrams that the effect of the "cyanogen" band reaches a maximum near Type K2 and decreases toward G0 and M. The analogy between

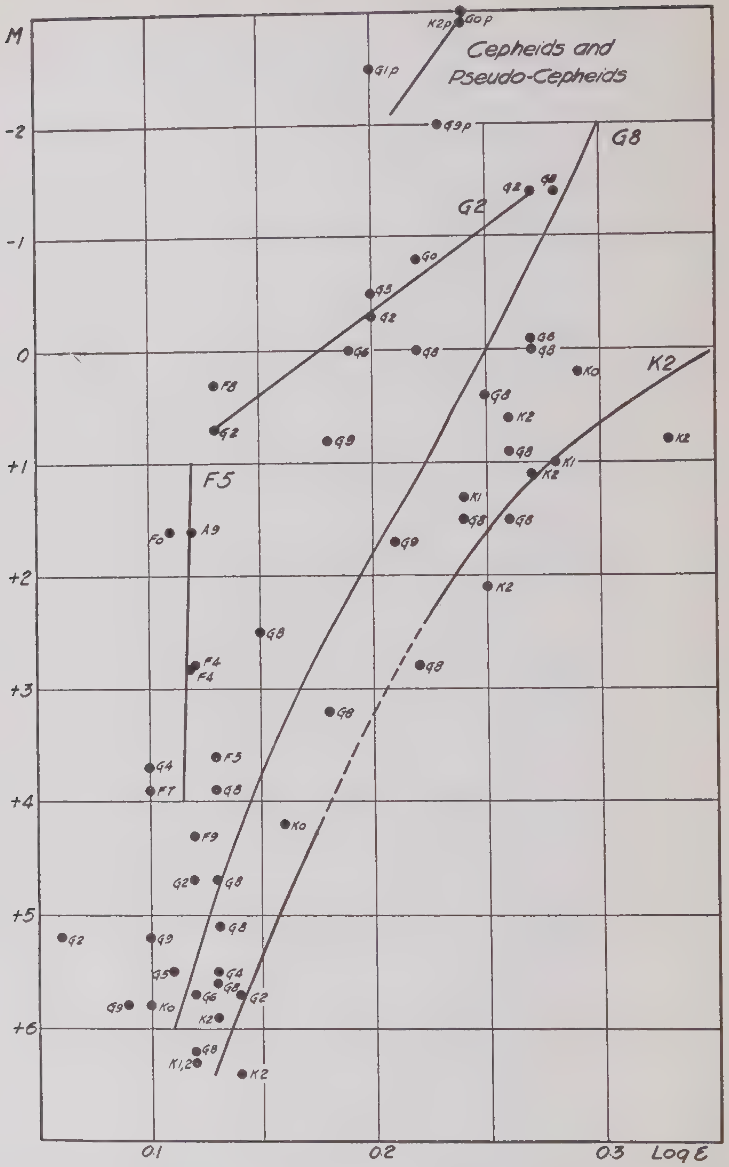

FIG. 3.—Logarithmic exposure-ratio for the regions λλ 4144–4184, 4227–4272, and absolute magnitude. Spectral types A9–K2.

Figure 5 and the diagram for the minimum wave-length of the grating-spectra[1] is very striking. The advantage of the present diagram, however, lies in the circumstance that the effect of the

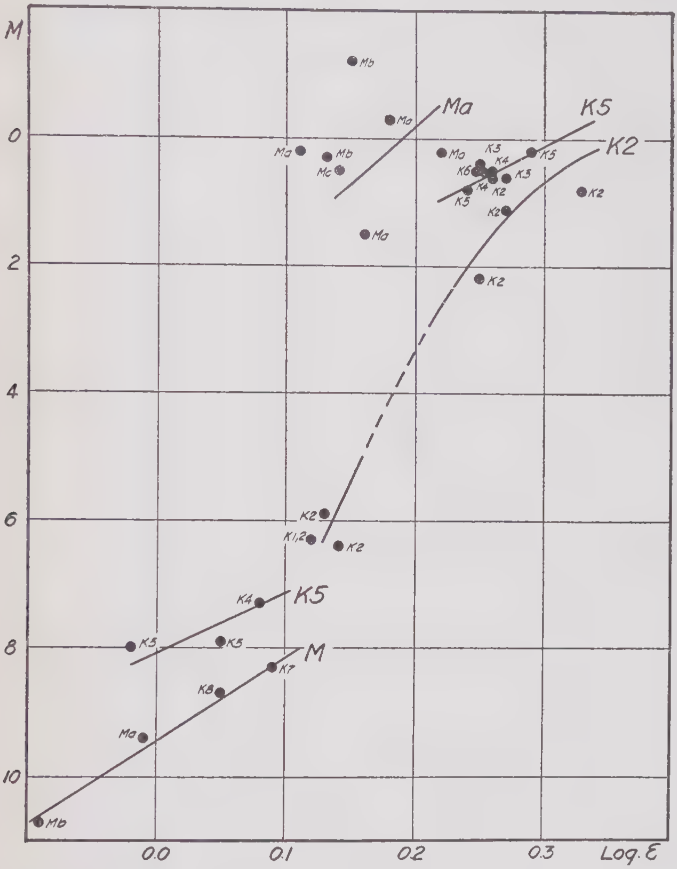

FIG. 4.—Logarithmic exposure-ratio for the regions λλ 4144–4184, 4227–4272, and absolute magnitude. Spectral types K2–Mc.

regular change in the energy-distribution in the spectrum due to the change of temperature in the spectral series has practically no effect on log E, owing to the closeness of the two compared regions. Except for the position of the Cepheids and pseudo-Cepheids the correspondence is nearly perfect between Figure 5 and a similarly arranged diagram for the absorption in the λ 3883 band. The variation in log E for the stronger ultra-violet band is, however, about 2.3 times as large as for the λ 4216 band. The increase of the effect from G8 to K2 probably explains the correlation of the absorption in the bands with the line λ 4227 found by Miss Maury in type XV.

---

[1] *Loc. cit.*

The rapid decrease of the effect toward G0, especially for stars with M between 0 and $+1$, is a disadvantage for a more accurate determination of luminosity. On the other hand, stars of this brightness, between types F0 and G2, seem to be very scarce. Most of the giants in this interval of spectral type given in the list of 1646 spectroscopic parallaxes, for example, are Cepheids or pseudo-Cepheids and of much higher luminosity.

The Cepheid variables and the pseudo-Cepheids seem to have an abnormally small absorption in the regions of the "cyanogen" bands; it is somewhat stronger, however, in the region of the λ 4216 band than in that of the λ 3883 band. In the case of the former band the stars still fall among the ordinary giants in the diagram in Figure 5, but in the case of the ultra-violet band, as mentioned before, they lie even below the dwarfs.

From K2 to M there is a general decrease of log E; the difference between giants and dwarfs is still well accentuated. The extent to which this difference is still due to "cyanogen" absorption in type M seems to be uncertain. For this type the line λ 4227, strong in the dwarfs, and the hydrogen lines, which are strong in the giants,[1] give a reliable criterion of the order of magnitude of the luminosity. The titanium-oxide bands characterizing type M are generally well developed in the objective-prism spectra. An observation of importance to be made from Figure 5 is that stars with log $E > 0.17$ are giants.

An application of the preceding principles to stars of faint apparent magnitudes in a few rich regions has been made with a small focal-plane spectrograph attached to the 60-inch reflector. The spectrograph has a 64° U.V. prism; the focal lengths of collimator and camera are about 6 inches. The dispersion gives 1.51

---

[1] See various papers by Adams and his associates on the spectroscopic method.

mm between Hγ and Hδ, and is 2.8 times that of the objective-prism spectra. The slit was removed, thus giving a field about $9' \times 9'$, of which about two-thirds is in good enough focus to be used. The objects investigated were the clusters M 11 and 13, and a few fields in Selected Areas Nos. 63 and 64 in the Cygnus region. A list of the photographs is given in Table VIII. Seed 30 plates were used, except for No. 33, which is Seed 23. All the plates were taken during good seeing, estimated about 5 and 6 on a scale of 10 in most cases. The last column gives for the Selected Area plates the number of the star in the Harvard Durchmusterung[1] which is nearest to the center of the field.

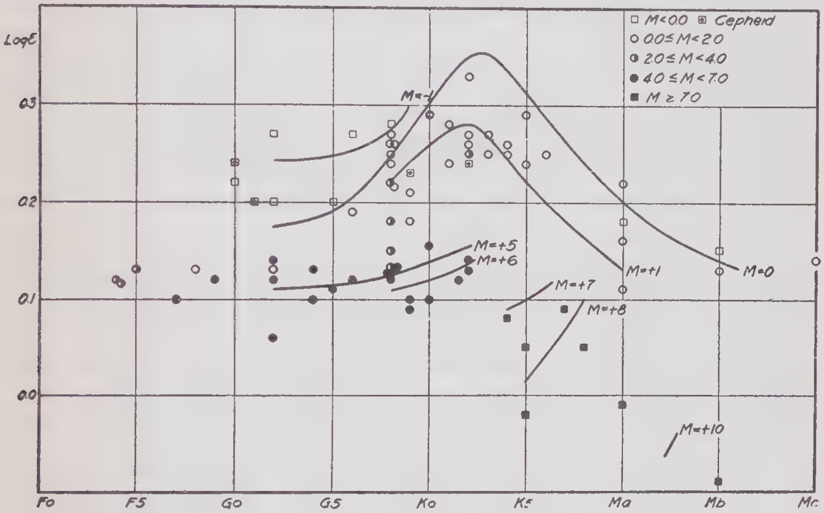

FIG. 5.—Logarithmic exposure-ratio for the regions λλ 4144–4184, 4227–4272, and spectral type.

Messier 11, R. A. $18^h 46^m$, Decl. $-6°23'$ (1900).—This well-known open cluster, situated in the bright galactic clouds in Scutum Sobieski, is very rich in stars, several hundred being brighter than the fourteenth magnitude. Magnitudes and colors for a large number of stars in the cluster have been determined by Shapley.[2]

---

[1] "Durchmusterung of Selected Areas," *Harvard Annals*, **101**, 1918.

[2] *Mt. Wilson Contr.*, No. 126; *Astrophysical Journal*, **45**, 164, 1917.

Table IX gives the results of the classification of spectra for eighty-five stars in the cluster. A great many stars which are sufficiently bright have their images superposed, thus making estimates of their spectral types impossible. For early types the classification is based on the strength of the K line relative to the hydrogen lines; for the late types the spectra have been compared with spectrograms of stars with known spectroscopic parallaxes, photographed with the same instrumental arrangement on the same kind of plates. The numbers are those of Stratonoff;[1] the photographic magnitudes are according to Shapley. The letter *d* after the spectral type means for an A-type star that the spectrum shows a marked energy-fall at λ 3907, thus indicating a relatively low luminosity ($M > 1.5$); for later types a *g* indicates giant characteristics, in this case strong "cyanogen" absorption in the region λ 4144–λ 4184.

TABLE VIII

List of Plates

Plate No.	Object	Date	Exposure-time	Harvard No.
33...........	Sel. Area 63	1921 May 10	$1^h 43^m$	527
35...........	Sel. Area 63	May 11	2 55	527
46...........	Messier 11	Aug. 2	30	....
47...........	Messier 11	Aug. 2	2 0	....
48...........	Messier 11	Aug. 2	5 1	....
49...........	Sel. Area 64	Aug. 2	4 0	666
50...........	Messier 13	Aug. 3	1 30	....
51...........	Sel. Area 64	Aug. 3	4 2	509
65...........	Sel. Area 64	Sept. 4	3 30	1029
75...........	Sel. Area 64	Sept. 5	4 37	454

The giants of types K0–K2 in Table IX have nearly the same apparent magnitude. The estimate $M = 0$ for their absolute magnitude seems to be fair, judging from the very marked "cyanogen" absorption in their spectra. The mean photographic magnitude of the four stars Nos. 252, 423, 666, 674, is 13.32. With a mean color-index somewhat exceeding unity, we find the modulus $M - m$ to be nearly equal to -12.

---

[1] *Publications de l'Observatoire de Tachkent*, No. 1, 1899.

The two brightest A stars in Table IX, Nos. 545 and 437, show sharp lines suggesting very high luminosity. With the value $M-m=-12$ their absolute magnitudes would be -2.8 and -0.5, respectively. The remaining A stars have fairly broad hydrogen lines. Between photographic magnitude 11.8 and 13.5 the energy-distribution around λ 3907 was found to be smooth, except for star No. 663; with the value of $M-m$ found above, those limits will correspond to $M=-0.2$ and $M=+1.5$. The faintest A stars in the tables show indications of a more abrupt fall of intensity at

TABLE IX

MESSIER 11

No.	Pg. Mag.	Spectral Type	No.	Pg. Mag.	Spectral Type	No.	Pg. Mag.	Spectral Type
193	....	A0	365	13.32	A0	571	13.16	A0
197	....	A2	366	13.02	A0	579	(Triple)	A0*d*
204	13.38	A0	375	12.54	A0	581	11.85	A0
214	13.48	A0	377	13.64	A0	583	13.84	A2*d*
221	13.07	A0	381	12.44	A0	590	13.04	(G8*g*)?
224	13.56	A0*d*	405	13.18	A0	592	14.22	A0*d*
227	12.06	A0	407	11.93	A0	597	12.78	A2
232	12.22	A0	423	13.46	K2*g*	598	13.02	G8*g*
236	13.07	A0	425	12.62	A2	599	12.40	A0
237	11.74	A0	426	13.21	A0*d*?	601	11.69	F?
245	12.15	A0	437	11.46	A0	616	13.89	A2*d*
252	13.08	K*g*	439	13.64	A0	617	13.25	A0
267	13.26	A0	460	12.97	A0	630	13.54	A0
273	13.00	A0	462	12.79	A0	631	12.46	A0
274	14.32	A2*d*?	464	13.94	A0	633	13.37	A0
280	13.01	G8*g*	468	13.91	A2*d*?	635	13.23	A0
285	13.08	A0	486	12.85	A0	647	12.66	A0
288	12.75	A3	487	12.39	A2	662	12.47	A0
297	12.44	A0	490	13.12	A0	663	11.90	A5*d*
307	14.20	A2*d*	491	12.33	A0	666	13.45	K0*g*
310	13.04	A0*d*?	494	12.32	A0	672	12.50	A0
322	13.46:	A0	511	....	G8*g*	674	13.28	K2*g*
325	13.04	A2	519	13.30	A0	704	....	A0*d*?
331	12.24	A0	525	12.08	A0	715	....	A0
336	12.08	A0	529	13.48	A0*d*?	762	....	K2*g*
341	12.42	A0	545	9.3:	A5	....	....	....
345	12.06	A0	548	12.23	A0	....	....	....
356	12.60	A0	552	14.20	A0*d*?	....	....	....
362	13.68	A0	568	13.31	A0	....	....	....
364	12.73	G8*g*	569	13.26	A0	....	....	....

λ 3907. For Nos. 224, 307, 592, 616, where this is most noticeable, we find for M the values of 1.6, 2.3, 2.2, 2.1, respectively, which are in good agreement with the results for the A stars in the first part of this paper. The A5 star, No. 663, photographic magnitude 11.90, is probably a relatively near star, superposed on the cluster. The spectra of the four faint A stars just mentioned are rather weak, and no definite conclusions can be drawn from these stars alone, but the indications are that the value $M-m=-12$ deserves a fair degree of confidence. Adopting this value we find for the parallax of the cluster $\pi=0''.00040$, corresponding to a distance of 2500 parsec or 8000 light-years. Shapley,[1] obtaining a value by an entirely different method, finds $\pi=0''.00014$. In view of the uncertainties affecting the two determinations the difference cannot be considered as by any means excessive.

Globular clusters.—On Plate No. 50 three of the brightest stars in the globular cluster Messier 13 are sufficiently well separated from other stars to permit an examination of their spectra. They are the Scheiner Nos. 47, 63, 127. Shapley[2] gives the photographic magnitudes 13.45, 13.70, 13.58, and the color-indices 1.41, 1.16, 1.42. With the parallax $=0''.000090$[3] the absolute magnitudes are -3.19, -2.69, -3.07, respectively. These stars seem to be of a spectral type not far from K0, but show a much smaller absorption in the region of the "cyanogen" band than the late-type stars in Messier 11. This agrees with the degree of luminosity found by Shapley, if the stars are pseudo-Cepheids; if they are ordinary giants we should estimate the absolute magnitude around $+1$. Low dispersion slit spectrograms of some stars in Messier 13 on a plate taken by Mr. Pease, and of stars in Messier 3 on a plate taken by Mr. Sanford, exposure-times 30^h and 20^h, respectively, seem rather to confirm the high degree of luminosity. The stars of earlier type on the first mentioned plate seem to have no appreciable change of intensity at λ 3907, and for the late-type stars on the latter plate, especially for the star von Zeipel No. 752, photographic magnitude 13.96, color-index 1.42, absolute magnitude according to

---

[1] *Proceedings of the National Academy of Sciences*, **5**, 344, 1919.

[2] *Mt. Wilson Contr.*, No. 116.

[3] Shapley, *Mt. Wilson Contr.*, No. 152; *Astrophysical Journal*, **48**, 154, 1918.

Shapley -3.18, the depression between λ 4100 and λ 4227 seems to be centered around Hδ and λ 4172 rather than in the "cyanogen" band, observations in favor of a classification in the pseudo-Cepheid type.

Selected Areas

No. 63, R.A. 19^h0^m, Decl.+30°0′, (1900)
No. 64, R.A. 19^h58^m, Decl.+30°0′.

TABLE X

Selected Areas 63 and 64

Harv. No.	Pg. Mag.	Spectral Type	Harv. No.	Pg. Mag.	Spectral Type	Harv. No.	Pg. Mag.	Spectral Type
Area 63			504....	14.5	A0	710...	12.87	A0
511....	13.20	K3*g*	524....	14.0	A2	719...	14.40	K2*g*
513....	12.61	G5*d*	535....	12.5	A0	726...	14.26	K2*g*
518....	9.61	A0	581....	12.5	B9	733...	11.70	A0
519....	10.50	A5	583....	12.0	A0	744...	13.06	F8
535....	12.43	G0*d*						
			603....	13.6	A2	748...	13.31	A0
539....	11.86	A5*d*	611....	13.8	F8	767...	12.10	G5*d*
546....	13.43	K2*g*	619....	14.6	A0	1005...	11.3	A0
			623....	14.2	A0	1007...	10.6	A0
Area 64			629....	13.7	A0	1017...	13.1	K0*g*
430....	14.6	A						
435....	13.2	K2*g*	646....	11.3	G8*g*	1020...	13.9	K2*g*
438....	13.8	F5*g*	661....	14.1	A0	1021...	13.6	B ?
442....	13.2	G8*d*	667....	14.18	K5*g*	1026...	10.9	F0
443....	14.0	F8*d*	668....	13.0	F8*d*	1027...	13.8	G0*d*
			671....	14.22	K0*g*	1028...	13.3	A0
445....	14.0	K5*g*						
448....	13.9	G5*d*	677....	13.31	A0	1104...	11.8	A2*d*
476....	13.5	G5*d*	680....	13.86	K0*g*			
479....	14.1	A0	682....	13.64	G5*d*			
486....	12.7	G5*d*	702....	13.81	K2*g*			
			706....	10.52	A2			

The results of classification for fifty-two stars in Selected Areas 63 and 64 are given in Table X. The numbers are according to the Harvard Durchmusterung. The photographic magnitudes for the central fields are according to unpublished Mount Wilson measures; for stars more distant from the center of the area the Harvard magnitudes have been reduced to the Mount Wilson system, and are given to only one decimal.

These two areas are situated in very rich galactic regions. There are eleven late-type stars classified as dwarfs in Table X, which as a group may be considered to be the nearest stars in the region. Of the remaining more distant stars twenty-eight are fainter than the thirteenth magnitude, twelve of which are found to be giants of types K0–K5, a remarkably high percentage. These late-type giants range in photographic magnitudes from 13.1 to 14.4, with a mean of 13.8. With a mean color-index of 1.2 and an absolute visual magnitude of 0.5 they should be at the same distance as M 11, about 4000 parsecs. If M 11 is associated with the galactic clouds in Scutum, the inference would be that these giant stars together with some of the A stars are members of the distant galactic cloud in Cygnus.

I wish to express my deep feeling of obligation to Director Hale for the opportunity to undertake this investigation during a stay of more than a year at the Observatory, and also to several members of the staff, especially Mr. Adams and Mr. Seares, for much valuable information and advice. I also wish to express my gratitude to Director Campbell for a month's stay at the Lick Observatory, and to Mr. Wright for his kind help and instruction in the work with the Crossley reflector.

Mount Wilson Observatory
October 1921

Contributions from the Mount Wilson Observatory, No. 229
Reprinted from the *Astrophysical Journal*, Vol. LV, pp. 242–271, 1922

ON THE UPPER LIMIT OF DISTANCE TO WHICH THE ARRANGEMENT OF STARS IN SPACE CAN AT PRESENT BE DETERMINED WITH SOME CONFIDENCE

By J. C. KAPTEYN[1] and P. J. VAN RHIJN

ABSTRACT

Distribution of stars in space.—Assuming no extinction of light in space and also symmetry around the galactic axis, the star density for any distance from the sun could be found for each galactic latitude if we knew both the *luminosity-curve*, $\phi(M)$, and the *apparent magnitude curve*, N_m, for each latitude. The necessary formulae are given and also tables of *values of the density as a function of distance and latitude*, based on assumed equations for these curves, both of the normal error type. Now $\phi(M)$ is known (see Table I*a*) for a range of 20 magnitudes which includes the maximum at $2^{M}693$; therefore extrapolation to larger magnitudes can introduce no important error. It is quite different in the case of N_m which has a maximum several magnitudes beyond the range for which the values are even approximately known. For instance, star counts have been made in the cloud between β and γ Cygni as far as visual magnitude 17.5, yet assuming an error-curve for N_m, the data do not give the constants accurately enough to determine whether the maximum, m_0, is at $25^{m}7$ or $29^{m}9$, the corresponding values for the total number of stars varying in the ratio of 1 to 6.5. If, however, N_m were known to $20^{m}5$, the probable error would be only one-third as great and might be reduced to perhaps one-ninth by using more extensive data. The value of the maximum m_0 has been found to decrease from about 27 for galactic latitude 0° to 18 for 80°, and therefore the equation for N_m can be more accurately determined by star counts at higher galactic latitudes. The *limits of distance to which the density can be determined* within 25 per cent when the values of N_m are known to visual magnitudes 14, 17, and 20, respectively, are found for various latitudes (Tables XII, XIII). We may expect complete values to $m=17$ in the near future and then fairly reliable densities can be determined, in the directions of latitudes 0° and 90°, to distances of 4000 and 1600 parsecs, respectively, that is, for the whole of the domain within which the density exceeds 1 per cent of that near the sun.

Star counts in cloud between β and γ Cygni, Selected Area 64, to $17^{m}5$.—Unpublished results of the Mount Wilson photometric survey and those in the Harvard Durchmusterung are tabulated and analyzed.

Comparison of Harvard and Mount Wilson photographic magnitude scales.—From the foregoing data, Mount Wilson minus Harvard is about $0^{m}26$.

The conclusions of the present paper must be considered only provisional, mainly for the two following reasons: (*a*) The extinction of light in space has been assumed to be inappreciable; (*b*) No use has been made of a recent substantial improvement in the average parallaxes of the more distant stars.

A more definitive solution now being made at the Laboratory of Groningen will duly take into account these two points. The progress of such a solution being necessarily very slow, the present provisional treatment was undertaken mainly for the purpose of finding the most promising lines for conducting the further treatment of the sidereal problem.

---

[1] Research Associate of the Mount Wilson Observatory.

The points which will be successively discussed are as follows:

I. If for any determined part of the sky we know *completely* (*a*) the luminosity-curve $y = \phi(M)$ and (*b*) N_m = the total number of stars of magnitude $m - 1/2$ to $m + 1/2$ *per ten thousand square degrees*, then we can find the star-density $\Delta(\rho)$ at any distance ρ. The solution is contained in *Mount Wilson Contribution*, No. 188, formula (13). The difficulty of the problem lies exclusively in the required completeness.

II. Half of the difficulty may be safely ignored, for it can be shown that at present and for a long, long while to come we may certainly adopt the form

$$\phi(M) = \frac{H}{\sqrt{\pi}} e^{-H^2(M-M_0)^2} = e^{p+qM+rM^2} \tag{1}$$

as representing the luminosity-curve completely, that is, for all values of M from $-\infty$ to $+\infty$.

We will here adopt the values of the constants p, q, r, given in *Contribution* No. 188, modified in accordance with the changes in definitions to be explained presently.

III. There thus remains only the difficulty due to our incomplete knowledge of N_m. We will show what limitation is thereby introduced in the solution mentioned in I, and we will further try to show how the limits can be extended by future countings of the fainter magnitudes.

In this inquiry, proceeding from the simple to the more difficult, we will consider three cases:

a) We will *assume* that the formula

$$N_m = \frac{h}{\sqrt{\pi}} e^{-h^2(m-m_0)^2} = 2e^{a+bm+cm^2} \tag{2}$$

holds not only for the magnitudes for which we have the necessary data but also for all fainter magnitudes.

b) We will drop the latter supposition, that is, in accordance with the results found thus far, we will adopt the error-curve (2) for the actually observed N_m, but will assume nothing about the fainter magnitudes which have as yet not been investigated.

TABLE I*a*

LUMINOSITY-CURVE

(Equation [5])

M	$\phi(M)$	$\log \phi(M)$		
+10	0.00229	7.359		
			470	
+ 9	.00675	7.829		70
			400	
+ 8	.0169	8.229		68
			332	
+ 7	.0365	8.561		69
			263	
+ 6	.0667	8.824		69
			194	
+ 5	.104	9.018		70
			124	
+ 4	.139	9.142		68
			056	
+ 3	.158	9.198		69
			013	
+ 2	.153	9.185		69
			082	
+ 1	.127	9.103		70
			152	
0	.0893	8.951		68
			220	
− 1	.0538	8.731		70
			290	
− 2	.0276	8.441		67
			357	
− 3	.0121	8.084		70
			427	
− 4	.00456	7.657		70
			497	
− 5	.00145	7.160		68
			565	
− 6	.000394	6.595		69
			634	
− 7	.0000914	5.961		69
			703	
− 8	.0000181	5.258		70
			773	
− 9	.00000305	4.485		69
			842	
−10	0.00000044	3.643		

$M=m+5 \log \pi$

c) We will consider the most general case, namely, that the actually observed values of N_m themselves are *not* distributed in an error-curve.

IV. Having thus found the limits within which a fairly reliable determination of the arrangement of stars in space can be made, we will introduce what we think must be considered a plausible supposition, by which these limits, at least for the lower galactic latitudes, can be somewhat farther extended.

TABLE I*b*

log Δ (ρ) (FORMULAE OF TABLE IV)

log ρ	Galactic Latitude				
	0°	30°	60°	90°	40°–90°
1.0	8.65−10	8.65−10	8.65−10	8.65−10	8.65−10
1.2	.65	.65	.65	.65	.65
1.4	.65	.65	.65	.65	.64
1.6	.65	.65	.65	.65	.61
1.8	.65	.65	.65	.65	.57
2.0	.65	.54	.50	.52	.49
2.2	.65	.46	.42	.45	.40
2.4	.65	.33	.25	.26	.25
2.6	.55	.16	.00	7.95	.03
2.8	.41	7.93	7.67	.51	7.73
3.0	.21	.64	.25	6.95	.32
3.2	7.97	.31	6.75	.27	6.85
3.4	.69	6.92	.15	5.46	.31
3.6	.35	.48	5.48	4.53	5.70
3.8	6.97	5.98	4.72	3.48	.01
4.0	.54	.44	3.88	2.30	4.24
4.2	.07	4.84	2.95	1.00	3.40
4.4	5.54	.19	1.93	....	2.48
4.6	4.97	3.49	0.84	....	1.49
4.8	2.35	2.73	....	....	0.42
5.0	3.68	1.92	....	....	....

Before entering on a discussion of these points it will be necessary to premise the following remarks:

a) Cluster observations by Shapley have fairly well proved the absence of any selective extinction of light in space, at least for distances like those considered in the present discussion. It does not follow that there is no appreciable general extinction of light, and the matter will be carefully considered in our definitive solution. Still, in view of Shapley's observations, we feel less hesitation in making the assumption of no appreciable extinction the basis of this provisional solution.

TABLE II

Distribution in Distance. Fractions of Total Number of Stars (W, Equation [12])

$\log \rho$	$m=8$	9	10	11	12	13	14	15	16	17	18	19	20
	Galactic Latitude = 0°												
$-\infty$ to 2.8	0.7779	0.6761	0.5596	0.4382	0.3224	0.2213	0.1409	0.0835	0.0458	0.0231	0.0107	0.0046	0.0018
2.8 to 3.0	.1223	.1590	.1886	.2037	.2002	.1804	.1478	.1107	.0753	.0470	.0268	.0138	.0065
3.0 to 3.2	.0640	.0972	.1344	.1689	.1950	.2048	.1961	.1708	.1366	.0994	.0658	.0400	.0220
3.2 to 3.4	.0256	.0456	.0734	.1085	.1456	.1781	.1994	.2040	.1900	.1610	.1252	.0886	.0570
3.4 to 3.6	.0080	.0164	.0309	.0531	.0833	.1197	.1568	.1864	.2026	.2016	.1825	.1505	.1131
3.6 to 3.8	.0018	.0046	.0100	.0202	.0370	.0617	.0942	.1316	.1670	.1931	.2041	.1975	.1737
3.8 to 4.0	.0003	.0009	.0026	.0058	.0125	.0244	.0439	.0711	.1053	.1428	.1764	.1982	.2038
4.0 to 4.2	.0001	.0002	.0004	.0013	.0032	.0075	.0156	.0296	.0513	.0811	.1166	.1538	.1850
4.2 to 4.4	.0000	.0000	.0001	.0003	.0007	.0017	.0042	.0095	.0192	.0353	.0596	.0916	.1286
4.4 to 4.6	....	....	.0000	.0000	.0001	.0004	.0009	.0023	.0055	.0118	.0233	.0417	.0686
4.6 to 4.8	....	....	....	....	.0000	.0000	.0002	.0004	.0012	.0031	.0070	.0147	.0283
4.8 to 5.0	....	....	....	....	....	....	.0000	.0001	.0002	.0006	.0017	.0040	.0090
5.0 to 5.2	....	....	....	....	....	....	....	.0000	.0000	.0001	.0003	.0009	.0021
5.2 to 5.4	....	....	....	....	....	....	....	....	....	.0000	.0000	.0001	.0004
5.4 to 5.6	....	....	....	....	....	....	....	....	....	....	....	.0000	.0001
	Galactic Latitude 40°–90°												
$-\infty$ to 2.8	0.9190	0.8696	0.8015	0.7161	0.6168	0.5079	0.4001	0.2979	0.2097	0.1397	0.0873	0.0513	0.0281
2.8 to 3.0	.0569	.0860	.1213	.1585	.1920	.2168	.2263	.2207	.1991	.1671	.1298	.0944	.0633
3.0 to 3.2	.0188	.0330	.0545	.0830	.1178	.1551	.1894	.2145	.2267	.2220	.2017	.1706	.1337
3.2 to 3.4	.0044	.0093	.0177	.0317	.0520	.0802	.1143	.1517	.1863	.2131	.2262	.2226	.2042
3.4 to 3.6	.0008	.0018	.0042	.0087	.0168	.0300	.0499	.0774	.1113	.1480	.1837	.2111	.2252
3.6 to 3.8	.0001	.0003	.0007	.0017	.0039	.0081	.0157	.0285	.0480	.0743	.1078	.1446	.1806
3.8 to 4.0	.0000	.0000	.0001	.0003	.0006	.0016	.0036	.0076	.0149	.0271	.0457	.0717	.1045
4.0 to 4.2	....	....	.0000	.0000	.0001	.0003	.0006	.0015	.0034	.0071	.0141	.0256	.0437
4.2 to 4.4	....	....	....	....	.0000	.0000	.0001	.0002	.0005	.0014	.0031	.0067	.0133
4.4 to 4.6	....	....	....	....	....	....	.0000	.0000	.0001	.0002	.0005	.0012	.0029
4.6 to 4.8	....	....	....	....	....	....	....	....	.0000	.0000	.0001	.0002	.0004
4.8 to 5.0	....	....	....	....	....	....	....	....	....	....	.0000	.0000	.0001

b) Up to the present, the luminosity-curve has expressed the number of stars of each magnitude contained in a specified volume of space in the neighborhood of the sun. It would certainly have been much more natural and convenient had it been given the form of a true frequency-curve, that is, one showing the fraction of all existing stars belonging to each absolute magnitude. This, of course, is not rigorously possible as long as our observations do not embrace all the stars, even the very faintest in existence. But since the luminosity-curve has been derived (in *Contribution* No. 188) over a range of more than twenty magnitudes and since its coincidence with a normal error-curve throughout this entire interval, which extends far beyond the maximum, is truly astonishing, it would seem very desirable to introduce the *assumption* that the best-fitting error-curve represents the luminosity-curve over its whole extent. In this way it becomes possible to define the luminosity function as a true frequency-curve.

TABLE III

Parameter	Galactic Latitude				
	0°	30°	60°	90°	40°–90°
h	−8.929	−8.292	−12.320	−17.418	−10.984
k	+5.705	+5.481	+ 9.320	+14.092	+ 8.120
l	−1.366	−1.508	− 2.441	− 3.542	− 2.171

Henceforth we will assume, therefore, that the luminosity-curve, over its whole extent, is perfectly representable by equation (1), which differs from formula (11) in *Contribution* No. 188, only in being divided by the factor $A = 0.0451$, the number of stars per cubic parsec in the neighborhood of the sun. If later on it should appear that this assumption deviates sensibly from the truth, the final results will still be unaffected. The ordinates of the curve will have only to be multiplied by a certain factor, while the densities will be divided by that same factor.

c) The parsec is again taken as a unit of distance, and in accordance with this definition the absolute magnitude of a star will equal its apparent magnitude as seen from a distance of one parsec.

d) Finally, the star-density $\Delta(\rho)$ now means the total number of stars from the brightest to the faintest in one cubic parsec.

Under these stipulations we have in (1), in accordance with *Contribution* No. 188,

$$H=0.2818, \qquad M_0=2.693 \tag{3}$$

$$p=-2.413^{1} \qquad q=+0.4278 \qquad r=-0.07944 \tag{4}$$

$$\log\phi(M)=-1.049+0.1858\,M-0.03450\,M^2 \tag{5}$$

$$M=m+5\log\pi=m-5\log\rho. \tag{6}$$

The numerical values of (5), that is, of the luminosity-curve according to the present definitions, have been tabulated in Table I*a*.

For convenience we give in Table III the values of the constants of *Contribution* No. 188, p. 13, changed to agree with our modified definitions, that is, with (4) instead of with the values previously given for p, q, r.

The values in Table III lead to the formulae in Table IV. These have been tabulated in Table I*b*.

TABLE IV

Gal. Lat.	Density and Distance		
0°................	$\log\Delta(\rho)=-3.878$	$+2.478\log\rho$	$-0.593\,(\log\rho)^2$
30°................	$=-3.602$	$+2.381$	-0.655
60°................	$=-5.351$	$+4.048$	-1.060
90°................	$=-7.565$	$+6.120$	-1.538
40°-90°...........	$=-4.770$	$+3.526$	-0.943

With these details premised we will now discuss the several points separately.

POINT I

As already mentioned, the solution of the problem involved in this case is contained in formula (13) of *Contribution* No. 188.[2] Modified in accordance with what precedes, this formula becomes:

$$N_m=3.046\int_0^\infty \rho^2\Delta(\rho)\phi(m-5\log\rho)d\rho. \tag{7}$$

---

[1] Differing from the corresponding value of p in *Contribution* No. 188, p. 15, by the amount $\frac{1}{\text{Mod.}}\log(0.0451)=3.099$.

[2] For this formula, in a slightly different form, see *Astronomical Journal*, **24**, 27 (No. 566), 1904.

From this equation it is at once clear that given N_m and $\phi(M)$ for *all* values of m and M, we can find $\Delta(\rho)$, and this constitutes in reality the solution of our problem. The derivation involves the solution of the integral equation (7). For the case in which $\phi(M)$ has really the form (1) and N_m the form (2), Schwarzschild has given an elegant solution, which, quoted already in *Contribution* No. 188, but modified in accordance with our present definitions, is contained in the following formulae:

$$\Delta(\rho)=e^{h+k\log\rho+l(\log\rho)^2} \qquad (8)$$

$$\left.\begin{aligned} l&=\frac{25cr}{r-c}\\ G^2&=-l-25r\\ R&=\frac{G^2(b-q)}{5r}\\ k&=5q-R-\frac{3}{\mu}\\ h&=a-p+\frac{\log G}{\mu}-\frac{R^2}{4G^2}-2.5203\\ \frac{3}{\mu}&=\frac{3}{\mathrm{Mod}}=6.9078. \end{aligned}\right\} \qquad (9)$$

Admitting that (8), which for brevity we will call the Schwarzschild formula, holds for all distances from $\rho=0$ to $\rho=\infty$, it is, of course, easy to determine all such quantities as those which follow (the area is always assumed to be 10,000 square degrees):

N_m = total number of stars of appt. mag. m
$(N_m)_0^\rho$ = the same within the distance ρ
N = total number of stars of all magnitudes together
N_ρ = the same within the distance ρ
M = median = distance within which lie one-half of all the stars
$W=(N_m)_0^\rho/N_m$
$Z=N_\rho/N$.

We find the formulae:

$$N_m=\frac{0.9696\pi\sqrt{\pi}}{\mu G}e^{G^2(\beta^2+\gamma)}=\frac{12.432}{G}e^{G^2(\beta^2+\gamma)} \qquad (10)$$

$$(N_m)_0^\rho=WN_m \qquad (11)$$

$$W=\frac{1}{\sqrt{\pi}}\int_{-\infty}^{G(\log\rho-\beta)}e^{-z^2}dz \tag{12}$$

$$2\beta G^2=-R-10rm \tag{13}$$

$$\gamma G^2=h+p+qm+rm^2 \tag{14}$$

$$N=\frac{12.433}{\sqrt{-l}}\,e^{h-\frac{\left(k+\frac{3}{\mu}\right)^2}{4l}}\qquad\left(\frac{3}{\mu}=6.9078\right). \tag{15}$$

As a check on the computations of h, k, l, N we have, expressed in terms of a, b, c,

$$N=\frac{\sqrt{\pi}}{\sqrt{-c}}\,e^{a-\frac{b^2}{4c}} \tag{16}$$

$$\log M=-\frac{k+\frac{3}{\mu}}{2l}\qquad\left(\frac{3}{\mu}=6.9078\right) \tag{17}$$

$$N_\rho=ZN \tag{18}$$

$$Z=\frac{1}{\sqrt{\pi}}\int_{-\infty}^{\sqrt{-l}(\log\rho-\log M)}e^{-z^2}dz. \tag{19}$$

Introducing the constants of Table III into (12), (13), and (14), we obtain

$$\left.\begin{array}{ll}\text{Gal. lat.}=0^\circ & \text{Gal. lat.}=40^\circ\text{ to }90^\circ\\ G=1.833 & G=2.039\\ \beta=1.560+0.1182m & \beta=1.550+0.0956m\end{array}\right\} \tag{20}$$

with the aid of which equation (12) gives at once an insight into the distribution in distance of the stars of each magnitude m. The results have been summarized for galactic latitudes 0° and for 40° to 90° in Table II. For the medians we find

$$\left.\begin{array}{lr}\text{Gal. lat. }0^\circ & M=39{,}000\text{ parsecs}\\ 40^\circ\text{ to }90^\circ & 2{,}900\text{ parsecs}\end{array}\right\} \tag{21}$$

Since the Schwarzschild formula does not hold for the smaller distances, results for these have been omitted from the table.

But the supposition that we know $\phi(M)$ and N_m completely, that is, for all values of M and m, is far from being justified. In the present state of science this incompleteness of our knowledge is very serious in the case of N_m, but of little account in the case of $\phi(M)$. The latter part of this statement constitutes the second point.

POINT II

The practical sufficiency of our knowledge of the luminosity-curve is due to the fact, already alluded to, that it has now been found for so large a range of magnitudes, viz., from the very brightest down to about absolute magnitude $M=+9$.

According to (6) a star of apparent magnitude m will be of absolute magnitude $+9$, when its distance is such that

$$\log \rho=\frac{m-9}{5}.$$

If, therefore, we write the equation (7) in the form

$$\frac{N_m}{3.046}=\int_{\log \rho=-\infty}^{\log \rho=\frac{m-9}{5}} \rho^2\Delta(\rho)\phi(m-5\log \rho)d\rho+\int_{\log \rho=\frac{m-9}{5}}^{\log \rho=+\infty} \rho^2\Delta(\rho)\phi(m-5\log \rho)d\rho \qquad (22)$$

the difficulty introduced by incomplete knowledge of the luminosity-curve lies exclusively in the first integral, for the second includes only stars brighter than $M=+9$, for which $\phi(M)$ is known. The difficulty cannot, therefore, be very serious because the first integral involves only stars relatively near the sun. In fact, as will be explained below, the values of $\Delta(\rho)$ within the limits of the first integral may be considered as completely known and its divergence from (8), though considerable, still unimportant for the present question, by a method wholly independent of (7) for all apparent magnitudes to $m=23$ (corresponding to the limit 2.8 for $\log \rho$). It will undoubtedly be a long time before we can expect useful data for N_m beyond $m=23$.

This being so, it is easy to show that there is an overwhelming probability that the first integral in (22) is entirely negligible, at least to the limit $m=23$. We first determine the value of this integral, denoted by V_m, on the supposition that for $M>+9$, $\phi(M)$ is still represented by (1). It is evident that V_m represents the number of stars of apparent magnitude m, absolutely fainter than $M=+9$.

We easily find

$$\frac{V_m}{N_m}=\frac{1}{\sqrt{\pi}}\int_{-\infty}^{P} e^{-z^2}dz \tag{23}$$

$$P=\frac{9r-\frac{1}{2}(b-q)-cm}{\sqrt{c-r}}\,. \tag{24}$$

The constants p, q, r are given by (4); a, b, c in *Contribution* No. 188, p. 13.

Table V, computed by the aid of (23), shows that, if the luminosity-curve (1) were correct over its *whole* length, the stars fainter than absolute magnitude +9 would not contribute to the total number N_{23} in the Milky Way more than 1 star in 16,000, or to those in galactic latitudes 40° to 90° more than 1 star in 300. For N_{22}, N_{21}, etc., the contribution is much smaller still.

TABLE V

VALUES OF V_m/N_m

m	Gal. Lat. 0°	Gal. Lat. 40°–90°
18	0.00000050	0.0000113
19	.00000143	.0000414
20	.00000392	.000139
21	.0000104	.00043
22	.0000262	.00121
23	.0000634	.0032
24	.000148	.0076
27	.00143	.0635
30	0.0095	.267

Therefore, even if beyond $M=+9$, the error-curve (1) should begin to fail very seriously to represent the true frequencies of the absolute magnitudes, it will still lead to values of N_m which will be practically correct to magnitude 23 and probably to even much fainter stars.

Suppose for instance that the frequencies, which up to $M=+9$ are represented with such astonishing closeness by the error-curve (1), should, beyond this magnitude, suddenly become tenfold the frequencies furnished by (1); even then the representation would be quite satisfactory for all values of N_m to $m=23$. Of course the overwhelming probability is that matters are really much more favorable. For we must surely expect that even if the true curve begins to diverge from (1), it will not suddenly show tenfold values. We should rather expect a deviation which for $M=+10$ is still small and only gradually increases, perhaps to very considerable amounts, as we approach fainter and fainter stars. If so, the divergence in the representation of N_m will undoubtedly be still much smaller.[1]

The conclusion from what precedes can only be: as long as observations do not extend beyond $m=23$, formula (7), in which $\phi(M)$ is given by (1), must be considered as valid. Should they ever reach stars fainter than $m=23$, a direct extension of the luminosity-curve beyond $M=+9$ may seem desirable. It is easy to see how this could be accomplished. We should require, however, more extensive data on the very faint stars having very considerable proper motions.

POINT III

It now remains to be seen what result for $\Delta(\rho)$ can be deduced from formula (7) with the aid of our *incomplete* data for the values of N_m. First consider the case:

III*a*. We *assume* the form (2) to hold for all magnitudes from the very brightest down to $m=\infty$, referring for less hypothetical considerations to III*b* and III*c*. The problem evidently is: given, $\phi(M)$ and N_m by the formulae (1) and (2) for all values of M and m; required, $\Delta(\rho)$ for all values of ρ.

The solution has been given above in equations (8) and (9). Although theoretically this solution leaves nothing to be desired, we find in most cases that, for moderately large values of ρ, it becomes practically illusory. The reason for this of course is that existing data do not furnish the values of the constants h, k, l, with sufficient precision.

---

[1] Perhaps this will not be granted, for of course it is not impossible, *mathematically*, that after $M=+9$, the frequencies instead of continuing to decrease, may begin to increase at such a tremendous rate that the preceding conclusion would no longer hold. Even this possibility must probably be denied. If after $M=+9$ the frequencies should increase at such a rate, the number of very faintly luminous stars near the sun, that is, apparently faint stars with very large proper motion would, I think, exceed what is reconcilable with the observations.

An example, which has a considerable interest of its own, will help to show the difficulty in its true light. As such, we will try to derive the arrangement in space of the stars in the star-cloud between β and γ Cygni. We choose this example because we happen to possess data for part of this region down to photographic magnitude 18.5 (=visual magnitude 17.33). The part in question is that covered by Selected Area (syst. plan) No. 64. The low limit of magnitude is reached by using unpublished results of the Mount Wilson photometric survey together with those in the Harvard Durchmusterung.[1] Simple countings gave the numbers in Tables VI and VII.

TABLE VI

HARVARD DURCHMUSTERUNG

Harv. Photographic Mag.		N'_m for $40' \times 40'$	Comp. by (25)	O−C
Limits	Mean			
8.00 to 8.99	8.5	1	2	− 1
9.00 to 9.99	9.5	7	7	0
10.00 to 10.99	10.5	21	19	+ 2
11.00 to 11.99	11.5	42	49	− 7
12.00 to 12.99	12.5	143	119	+24
13.00 to 13.99	13.5	227	269	−42
14.00 to +14.99	14.5	591	570	+21
Total		1032		

TABLE VII

MOUNT WILSON PHOTOMETRIC SURVEY

M.W. Photographic Mag.		N'_m for $15' \times 15'$	N'_m Reduced to $40' \times 40'$
Limits	Mean		
12.5 to 13.5	13.0	$20\frac{1}{2}$	146
13.5 to 14.5	14.0	$43\frac{1}{2}$	309
14.5 to 15.5	15.0	$97\frac{1}{2}$	693
15.5 to 16.5	16.0	$200\frac{1}{2}$	1426
16.5 to 17.5	17.0	$363\frac{1}{2}$	2584
17.5 to 18.5	18.0	$677\frac{1}{2}$	4817
Total		1403	

---

[1] *Harvard Annals*, 101.

These tables do not contain even approximately all the stars in the two catalogues. The faintest stars measured on the Harvard plates are 15.75 (phot.), those on the Mount Wilson plates 18.86 (phot.). Stars fainter than 14.99 and 18.50, respectively, were excluded because we cannot be sure that the catalogues are absolutely complete below these limits.

We have first of all to reduce the magnitudes to the same scale and to the same area. The latter reduction has already been made in the last column of Table VII. To find the scale difference the observed numbers N'_m in Table VI were represented by an equation of the form of (2). The result may be written

$$\log N'_m = 2.074 + 0.370(m-12.5) - 0.0145(m-12.5)^2. \tag{25}$$

The values computed by means of this formula are in the fourth column of Table VI; the fifth shows the residuals O−C, whose changes of sign are all that can be desired. With the aid of (25) the Harvard magnitudes were calculated for which the numbers N'_m become equal to the first three values of N'_m in Table VII, viz., 146, 309, 693. The results are 12.75, 13.68, and 14.78, whence we conclude:

	Mt. W.−Harv.
Harv. mag. 12.75 = Mt. W. mag. 13.0	$+0^{\mathrm{m}}.25$
Harv. mag. 13.68 = Mt. W. mag. 14.0	$+0.32$
Harv. mag. 14.78 = Mt. W. mag. 15.0	$+0.22$

There is no indication in the differences Mt.W.−Harv. of change with the magnitude, and we adopt

$$\text{mag. Mt. W.} - \text{mag. Harv.} = \text{Const.} = +0^{\mathrm{m}}.26. \tag{26}$$

By means of (26), the values in Table VII can now be reduced to the scale of Table VI.

A further reduction from the photographic to the visual scale is necessary because the luminosity-curve defined by (1) and (4) gives the frequencies for the visual magnitudes. For this we have used the corrections given in *Groningen Publications*, No. 27, p. 42. The first five columns of Table VIII show the complete reduction.

TABLE VIII

N'_m FOR 40′×40′

PHOTOGRAPHIC SCALE		VIS. SCALE HARV.	AMPL.	m H.S.	N'_m AMPL. 1. MAG.	COMPUTED		O−C	
Harv.	Mt. W.					(27)	(28)	(27)	(28)
8.00 to 8.99	....	7.64 to 8.61	0.97	8.125	1	2	3	− 1	− 2
9.00 to 9.99	....	8.62 to 9.57	.95	9.095	7	7	8	0	− 1
10.00 to 10.99	....	9.58 to 10.52	.94	10.05	22	22	22	0	0
11.00 to 11.99	....	10.53 to 11.47	.94	11.00	44	55	54	− 11	−10
12.00 to 12.99	....	11.48 to 12.41	.93	11.945	154	134	127	+ 20	+27
13.00 to 13.99	....	12.42 to 13.34	.92	12.88	247	296	281	− 49	−34
14.00 to 14.99	....	13.35 to 14.28	.93	13.815	635	629	598	+ 6	+37
....	12.5 to 13.5	11.71 to 12.67	.93	12.175	157	163	155	− 6	+ 2
....	13.5 to 14.5	12.64 to 13.58	.94	13.11	329	358	340	− 29	−11
....	14.5 to 15.5	13.58 to 14.51	.93	14.045	745	748	716	− 3	+29
....	15.5 to 16.5	14.51 to 15.45	.94	14.98	1517	1475	1439	+ 42	+78
....	16.5 to 17.5	15.45 to 16.39	.94	15.92	2749	(2751)	2793	(− 2)	−44
....	17.5 to 18.5	16.39 to 17.33	0.94	16.86	5124	(4835)	5176	(+289)	−52

The fifth and sixth columns give the observational data fully reduced for the present discussion. The numbers in the cloud were first compared with the corresponding numbers for the average Milky Way. It turned out at once that these numbers are all but perfectly proportional, the cloud having about 2.39 times the number for the average Milky Way. This is shown by the seventh column of the table which gives the carefully interpolated values for the Milky Way according to *Groningen Publication*, No. 27, reduced to an area of 40′×40′ and multiplied by 2.39. The agreement with the observed cloud numbers in the sixth column is as good as can be expected. The numbers in the Milky Way in *Groningen Publication*, No. 27, do not extend beyond magnitude 16. For these very faint magnitudes the table gives in parentheses the values furnished by

$$\log N'_m = -4.516 + 0.7242m - 0.0141m^2 \tag{27}$$

which best fits the numbers of *Groningen Publication*, No. 27, reduced to 40′×40′ and multiplied by 2.39.

On the assumption made in this paragraph, that the formula holds for *all* magnitudes, we conclude that at all distances the star-densities in the cloud are 2.39 times the corresponding densities in the average Milky Way.

Meanwhile we can represent the observed numbers quite as well by a formula somewhat different from (27); for instance, by

$$\log N'_m = -3.951 + 0.6334m - 0.0106m^2. \tag{28}$$

The representation by this formula is also shown in Table VIII.

By means of the constants in (27) and (28) and those of the luminosity-curve (5), we can at once pass from the distribution of the values N_m to that of the densities by means of formulae (8) and (9). We thus obtain

$$\begin{array}{lrr} & \text{Solution (27)} & \text{Solution (28)} \\ h\ldots\ldots\ldots\ldots & -8.060 & -3.488 \\ k\ldots\ldots\ldots\ldots & +5.719 & +2.678 \\ l\ldots\ldots\ldots\ldots & -1.375 & -0.882 \end{array} \tag{29}$$

The two solutions represent rather widely different arrangements in space. The best way of showing the difference in compact form will perhaps be to compute for both, by formulae (16) and (17),

N = total number of stars for a field of 40′×40′, and
M = median = distance below which lie just half of all the stars.

Introducing the values (29), we find,

	Solution (27)	Solution (28)	
M..........	39,000 parsecs	272,000 parsecs	(30)
N_0^∞.........	579,000 stars	3,700,000 stars	

Identical data thus lead to two solutions for the arrangement in space of the stars in the cloud. In the second, judging by the median values, the star-distances are 7 times those of the first solution. The total numbers[1] are as 1 to 6.5.

Evidently, therefore, the data at present available do not lead to a reliable determination of the real structure of the cloud. The reason clearly lies in the fact that the data of Table VIII are insufficient for a good determination of the constants for N_m in equation (2), and it is readily understood that it is mainly the uncertainty in the position of the maximum to which the failure of the solution is due.

In the notation of (2), this maximum lies at the magnitude

$$m_0 = -\frac{b}{2c} \qquad (31)$$

whence for

$$\left.\begin{array}{ll}\text{Solution (27)} & m_0 = 25.68 \\ \text{Solution (28)} & m_0 = 29.88\end{array}\right\} \qquad (32)$$

a difference of over 4 magnitudes!

We are thus led to consider the question as to how far the observed data must be extended in order to obtain a determination of $\Delta(\rho)$ which will satisfy moderate demands at least.

To answer this it will be necessary to determine: (*a*) how the precision of m_0 (prob. err. ρ_{m_0}) depends on the precision of the counts N_m; (*b*) how the precision of the median $\boldsymbol{M}$ depends on the precision of m_0.

---

[1] Since the total number of stars resulting from the two solutions differs enormously, it might seem worth trying to decide between them by measuring the total light of the cloud. To test the feasibility of such a plan I compared the values of the total light and found that the amounts involved in (27) and (28) are as 1.000 to 1.025. Practically, therefore, the idea is worthless, at least with the photometric means at present available.

As for (*a*): Consider first the somewhat easier question of what the accuracy of m_0 obtained from observed values of N_m will be for three favorably chosen, equidistant magnitudes

$$m_1-\sigma; \qquad m_1; \qquad m_1+\sigma. \tag{33}$$

For brevity call this the simplified problem. Since a rough estimate is all that is wanted, assume that the probable error of log N_m for these three magnitudes is constant and equal to r. When this simplified problem has been solved it will be easy to estimate roughly the accuracy obtainable by the use of all values of N_m.

In the Appendix is derived the formula which shows the relation between the probable errors ρ_{m_0} and r, namely,

$$\rho_{m_0}=\pm\frac{r\sqrt{2}}{4\sigma^2 c\mu}\sqrt{12(m_0-m_1)^2+\sigma^2}\,. \tag{34}$$

The value of r is readily determined by means of the deviations of the observed log N_m from a close-fitting curve. In the case of the star-cloud the number of observed stars brighter than 12 is rather small. This being the case, consider only the Mount Wilson observations in Table VIII, which show a better agreement *inter se* than the Harvard values. For the best-fitting curve I used a third solution, intermediate between (27) and (28), for which the constants are:

$$\begin{array}{lll} a=-10.019 & h=-6.038 & \\ b=+1.570 & k=+4.289 & \text{(area}=40'\times 40'\text{)} \\ c=-0.0294 & l=-1.165 & \\ m_0=26.73 & \text{Median } M=63{,}800 \text{ parsecs} & \end{array} \tag{35}$$

The value found for the probable error is $r=\pm 0.008$. Experience gained in other cases indicates that this value is accidentally low and that a better one would be

$$r=\pm 0.012. \tag{36}$$

For the fundamental magnitudes we choose the values (see Table VIII)

$$12.18, \qquad 14.52, \qquad 16.86, \tag{37}$$

then for the computation of ρ_{m_0} by (34)

$$\left.\begin{array}{ll} m_1 = 14.52 & \sigma = 2.34 \\ m_0 = 26.73 & c = -0.0294 \end{array}\right\} \qquad (38)$$

which lead to

$$\rho_{m_0} = \pm 2.6 \text{ mag.} \qquad (39)$$

Starting from solution (27) instead of (35), we find nearly the same result.

As for (*b*): We learn how the accuracy of the median M depends on that of m_0 by comparing the values of m_0 and M in the three solutions (27), (28), (35). Adding a fourth solution, we have altogether

$$\left.\begin{array}{llll} m_0 & & \log M & \\ \hline 25.68 & & 4.592 & \\ & 1.05 & & 0.213 \\ 26.73 & & 4.805 & \\ & 1.05 & & 0.203 \\ 27.78 & & 5.008 & \\ & 2.10 & & 0.426 \\ 29.88 & & 5.434 & \end{array}\right\} \qquad (40)$$

Evidently log M changes very nearly proportionally to m_0. In fact

$$\log M = -0.544 + 0.2\, m_0. \qquad (41)$$

Therefore

$$\rho_{\log M} = 0.2\, \rho_{m_0}; \qquad (42)$$

consequently, adopting the values (39),

$$\rho_{\log M} = \pm 0.520 \text{ (simplified problem).} \qquad (43)$$

It is now easy to see what can be gained by future extension of the counts to fainter magnitudes.

Table IX shows how the probable errors of both m_0 and log M change with increase in the limiting magnitude. In accordance with what precedes, we adopted ±2.6 as the probable error of m_0 in the case of the limiting magnitude 17.5, i.e., for limiting $N_m = 17.0$. The remaining probable errors were then computed by formulae (34) and (42). The results are summarized in Table IX.

Hence, if we were able to photograph the stars to magnitude 20.5 (visual scale), the probable error of log M in the simplified problem would be diminished to 0.176, which, roughly speaking, is equivalent to a probable error of about 42 per cent in the numerical value of M. I believe the error would be further lowered to less than 30 per cent, if the calculation of m_0 were based on all the available data for N_m instead of merely on those for the three fundamental magnitudes used for the simplified problem.

From an absolute point of view this precision may not seem to be very satisfactory. Still if it can be reached—and at present this is hardly subject to doubt—an enormous step in advance will have been made, for it means that the median parallax will have been determined with a probable error of about ±0″00001.

TABLE IX

PROBABLE ERROR OF m_0 AND LOG M (SIMPLIFIED PROBLEM)

Limiting Magnitude	Fund. Mags.			m_1	σ	m_0 Sol. (35)	ρ_{m_0}	$\rho_{\log M}$
17.5	12.0	14.5	17.0	14.5	2.5	26.73	2.60	0.520
18.5	12.0	15.0	18.0	15.0	3.0		1.73	.346
19.5	12.0	15.5	19.0	15.5	3.5		1.21	.242
20.5	12.0	16.0	20.0	16.0	4.0		0.88	.176
21.5	12.0	16.5	21.0	16.5	4.5		0.66	.132
22.5	12.0	17.0	22.0	17.0	5.0		0.51	0.102

Moreover, the accuracy can be greatly increased by taking several fields instead of but one.

The preceding considerations on the structure of one small region may of course be applied without change to the investigation of larger parts of the sky, for instance, to the Selected Areas for different zones of galactic latitude. The only difference is that we will obtain a much greater accuracy.

From the data of *Groningen Publication*, No. 27, Table V, we have found the values of m_0 for different galactic latitudes (β) entered in the second column of Table X. The other quantities in the table were obtained in the manner already explained.

In this table the probable errors are given, in the simplified problem, as they would be found for a single region containing the same number of stars as that in the case treated above. In conformity with (39), ρ_{m_0} for $\beta = 0$ and lim. mag. 17.5 was put at ±2.6. For the rest the computation was made with the aid of (34) and (42).

As was to be expected, the values of m_0 run somewhat irregularly. We therefore adopted the smoothed values of the third column, which, with the exception of that for $\beta = 20°$, represent the observations practically as well as those of the second column.

By using for each region all the material instead of the three values of N_m of the simplified problem, the probable error will be diminished. If further for each galactic latitude we take the greater part or all of the Selected Areas, the probable error will again be much reduced. Finally, a further important reduction can be made by taking into account the very extensive data for the brighter stars. In order to see more clearly what can be gained, some estimate must be made as to the effect of all these reducing causes. The matter certainly deserves careful study. We have not yet made such a study, but estimate provisionally that it should be easy to reduce the probable errors of Table X to one-third.[1]

TABLE X

PROBABLE ERROR IN SIMPLIFIED PROBLEM FOR A REGION 15′×15′

β	m_0	Adopted m_0	c	Lim. Mag. 17.5		Lim. Mag. 20.5	
				ρ_{m_0}	$\rho_{\log M}$	ρ_{m_0}	$\rho_{\log M}$
0°	26.7	26.7	−0.0294	±2.6	±0.52	±0.88	±0.176
20	27.2	25.6	− .0297	2.4	.48	.79	.158
40	23.1	22.9	− .0333	1.6	.32	.51	.102
60	19.1	19.9	− .0407	0.85	.17	.24	.048
80	18.2	17.9	−0.0486	±0.45	±0.09	±0.11	±0.022

For clearness we may express roughly the accuracy corresponding to this assumption in percentages of the whole. The results for the median M are thus found to be as given in Table XI.

Granting the suppositions made in III*a*, and that we are in possession of data for N_m to magnitude 20.5, we conclude that we can obtain what may be considered a good insight into the distribution of the stars in all galactic latitudes. With data to 17.5 alone (Mount Wilson Survey) this can be said only for the regions of high galactic latitude. Below latitude 40° the solution becomes rapidly less reliable.

---

[1] The comparison of the values m_0 in the second column of Table X with the smoothed values in the third leads at once to a precision of about this amount, notwithstanding the fact that the data of *Groningen Publication*, No. 27, extend but little beyond magnitude 14.5 visual.

Remark.—Meanwhile we need an extension of star-counts for regions near the galactic pole quite as much and probably more than for the lower latitudes, for just these observations of N_m in the higher latitudes will lead to a judgment on the general validity or non-validity of the analytical form (2). This follows because of the lower value of m_0 (Table X). Suppose for instance that we obtain counts to apparent magnitude 20.5. In high latitudes the curve for N_m will then become known considerably beyond the maximum, that is, for a very considerable fraction of the whole, and a fraction very much greater than that covered in the lower latitudes. In case formula (2) is confirmed for this large part of the curve in the region of the galactic pole, we will use the same analytical form with much greater confidence for the lower latitudes also.

TABLE XI

PROBABLE ERROR OF MEDIAN M IN PERCENTAGE OF ITS AMOUNT

Gal. Lat.	Limiting Magnitude	
	17.5	20.5
0°	41	13
20	38	12
40	25	8
60	13	4
80	7	1.5

III*b*. We know by observation that as far as magnitude 14 the values of N_m are well represented by (2); for the stars fainter than 14 we know nothing of the sort.[1] What results will it be possible to obtain from this knowledge?

Schwarzschild's solution, which is based on the supposition that *all* values of N_m fall on the curve (2), led to formula (8) which, but for the observation errors, would yield a knowledge of $\Delta(\rho)$ for *all* distances. This solution is not now generally applicable and we must look for another. Such a solution, based on quite different principles, which I will call solution K, has already been given in *Groningen Publication*, No. 11, and has also been applied in *Contribution* No. 188. It has there been carried through for galactic latitude 40° to 90°, and shows the very gratifying fact, which we had no right to expect beforehand, that, but for small distances (where Schwarzschild's solution is confessedly wrong) it agrees wonderfully well with the Schwarzschild solution. With the exception referred to, therefore, solution (7) represents all the data, those of *Contribution* No. 88 as well as the values of N_m in a way that leaves hardly anything to be desired.

---

[1] We take the limit $m=14$ because it represents what at present is really well known. The reasoning, of course, holds for any other limit.

Therefore, notwithstanding what has just been said, the Schwarzschild solution (8) must still be considered the most plausible to be obtained with the aid of the data at present available. This must be owing to the fact that further values of N_m, particularly those for the most influential magnitudes 15, 16 . . . . , do not deviate very much from the curve (2). Still this does not prove that formula (8) gives even an approximate solution for $\Delta(\rho)$ at very great distances. We see, for instance, from Table II, that according to (8) there are, in high galactic latitudes, hardly any stars beyond $\log \rho = 4.2$. As a consequence thereof, suppose that between $\log \rho = 4.0$ and $\log \rho = 4.2$, the density is a hundred fold the value given by (8); the total numbers of stars N_{14} will be changed by about 1 per cent only. For the brighter magnitudes the change would be still smaller. Evidently, therefore, nothing can be concluded from our data about the densities at such great distances. They may or may not agree with formula (8); we have no means of judging. The matter would be different if we had good counts (N_m) for very much fainter stars. The question thus presents itself: To what distance can the densities computed by (8) be accepted with some confidence? Or to be more precise: To what distance can we trust the values of $\Delta(\rho)$, found by (8), to be correct within 25 and 40 per cent, respectively, of their values?

In considering this question we will *assume* that what was found in *Contribution* No. 188 for galactic latitudes 40° to 90° will also be found for other galactic latitudes, viz., complete agreement of solution K with solution (8). It seems to me very probable that such will turn out to be the case. As solution K is independent of the values of N_m for $m > 14$ we may thus accept formula (8) for $\log \rho \leqq 2.8$[1] (excepting of course the small distances).

The question under consideration comes to this: How much can we change the densities (8) for $\log \rho > 2.8$, without spoiling the representation of the values of N_m to $m = 14$? Suppose that, for galactic latitudes 40° to 90°, we multiply the densities for

$\log \rho = 2.8$ to 3.0 by F_1,
$\log \rho = 3.0$ to 3.2 by F_2, etc.

Then the numbers in Table II (second part) for $\log \rho = 2.8$ to 3.0 will all be multiplied by F_1; those of the following line by F_2, etc.

The total number N_8 (see Table II) will thus be changed to

$$N_8(0.9190 + 0.0569F_1 + 0.0188F_2 + 0.0044F_3 + 0.0008F_4 + 0.0001F_5) \quad (44)$$

and, in order that the N_8 may still be represented, the sum must still equal N_8; or better, the expression in parentheses must equal 1.00. We also find similar expressions for magnitudes 9, 10, ... 14.

The question thus becomes: What is the smallest distance for which we can take for any one of the factors F, a value as high as 1.25 or as low as 0.75 (or, respectively, 1.40 and 0.60) without making it impossible to determine the remaining factors in such a way that the seven equations of condition are still bearably well satisfied. For "bearably well satisfied" we have used the condition that the range in the residuals should not exceed 10 per cent.

Suppose, therefore, having assumed the constant F for distance R to be 1.25, that we solve our equations of condition and obtain indeed a "bearable" set of residuals. Will this prove that for distance R a density deviating 25 per cent from (8) is admissible? By no means. For as a rule the values found for the other constants will be impossible or inadmissible because they lead to negative values of $\Delta(\rho)$ or to values running too wildly for the regularly increasing distances.

---

[1] In *Contribution* No. 188 this is the limit to which solution K extends.

In order to obtain an acceptable solution we must evidently introduce the condition that the values of F shall run smoothly for regularly increasing distances. This condition is pretty vague and introduces a certain degree of arbitrariness, but I think that there is really no serious objection to it. Moderate differences in the form of the curve will probably change the results little as long as we leave two or three constants indeterminate, to be found in a way best satisfying the conditions of the problem.

Before stating the form adopted for the factors F, consider the general course they must follow. From the value 1.00 for $\log \rho = 2.8$ they must either increase or decrease. Consider only the first case, because by satisfying this we more than satisfy the other. The initial increase cannot indefinitely continue because if all the factors are greater than 1.00, the total numbers N_m will all be increased. The values of N_m cannot well be represented, therefore, unless values of $F > 1.00$ are compensated by later factors < 1.00. The factors must therefore pass through a maximum, after which decrease sets in and they soon become 1.00. We assume that there is but one maximum. Consider now the various curves representing various hypotheses for the factors F. Take more curves for which the value of the maximum is respectively $F_{max} = 1.25$, $F_{max} = 1.30$, $F_{max} = 1.35$, ... and let R, R_1, R_2, ... be the values of the distance for which $F = 1.25$.

Then we think that generally

$$R < R_1 < R_2 \ldots .$$

That is, the factor $F = 1.25$ will be reached sooner by that curve for which $F = 1.25$ is a maximum.[1]

Since we wish to find the smallest distance at which F can become equal to 1.25, we consider only the latter case, that is, find the minimum distance, R, at which F can reach 1.25 as a maximal value, without being led to an "unbearable" representation of N_m.

This being premised, we now give the mathematical form adopted for F:

---

[1] We have not tried to find the demonstration. We have been content to verify its truth further on by means of the data in Table X.

$$\left.\begin{array}{l}\text{A. For the case, maximum factor}=1.25\\ \text{Before the maximum, } F=0.96+0.29\,e^{-h^2x^2}\\ \text{After the maximum, } F=1.25\,e^{-p^2x^2}\end{array}\right\} \qquad (45)$$

$$\left.\begin{array}{l}\text{B. For the case, maximum factor}=1.40\\ \text{Before the maximum, } F=0.96+0.44\,e^{-h^2x^2}\\ \text{After the maximum, } F=1.40\,e^{-p^2x^2}\end{array}\right\} \qquad (46)$$

in both of which

$$x=\log \rho-\log R. \qquad (47)$$

There remain, therefore, the three constants R, h, p, to be determined in such a way that R corresponds to the smallest distance for which the values of N_m can be represented with residuals not exceeding 10 per cent. This form for the factors F gives perfect smoothness throughout. It is that which a priori seems most plausible. Beyond the maximum, $\Delta(\rho)$ is evidently again represented by a form like (8), which represented the densities for the smaller distances with such perfection.

It does not, however, start at $\log \rho=2.8$ with the initial value 1.00, as premised. The reason is that the small discontinuity thus introduced at $\log \rho=2.8$ is of no real importance, while the representation of N_m is appreciably better.

Substituting the expressions for F into (44) and equating the result to the successive values of N_m we obtained a number of equations of condition.

In solving them we generally began by assuming two values for R, for each of which these equations were solved for h and p in such a way that practically the best possible representation of N_m(to $m=14$) was obtained. The range of the residuals was then found for both cases. The value of R for which the range is 10 per cent could then usually be found by interpolation. If not, the computation was repeated for a third value of R. In this way were found all the values entered in Table XII.

In all cases, with the exception of the third for $m=14$, the range of the residuals in N_m is nearly 10 per cent. In the exceptional case it is only 6.5 per cent. In fact, in this case, the knowledge of N_m to $m=14$ takes us little beyond what was reached by solution K.

From Table XII we may be pretty sure, now that we know N_m with some precision to $m=14$, that in the Milky Way there will be in the densities as computed by (8), no error of 25 per cent up to $\log \rho=3.1$ and no error of 40 per cent up to $\log \rho=3.2$. As soon as we have reliable knowledge of N_m to $m=20$ these limits will rise to $\log \rho=3.8$ and 4.0, respectively. We further learn from the table that by extending our knowledge of N_m from $m=14$ to $m=20$ we will extend the limits to which we can reliably determine the structure of the system:

TABLE XII

LIMITS OF RELIABILITY OF $\Delta(\rho)$ BY (8)

GAL. LAT.	N_m KNOWN TO $m=14$				GAL. LAT.	N_m KNOWN TO $m=20$			
	F_{max}	log R	h	p		F_{max}	log R	h	p
0°........	1.25	3.1	7.0	1.66	0°..........	1.25	3.8	4.0	1.66
0.........	1.40	3.2	6.0	2.70	0..........	1.40	4.0	3.7	3.6
40 to 90...	1.25	2.9	......	2.20	40 to 90....	1.25	3.4	4.0	2.05
40 to 90...	1.40	2.9	......	3.0	40 to 90....	1.40	3.5	4.0	3.73

$$\begin{array}{ll} \text{In the Milky Way} & \left.\begin{array}{l} 5.6 \text{ fold } (\log=0.75) \\ 3.5 \text{ fold } (\log=0.55) \end{array}\right\} \\ \text{In gal. lat. } 40^\circ \text{ to } 90^\circ & \end{array} \qquad (48)$$

In the case of the Mount Wilson Survey, which will yield N_m to $m=17$, the gain will be about half this amount.

III*c*. If finally, having extended the counts N_m to some higher magnitude, we find that the values of N_m no longer fit an error-curve like (2), then evidently formula (8) will no longer hold for the densities. In this case we must fall back on formula (7). We will thus find different values for the densities $\Delta(\rho)$. We may certainly expect, however, that, as long as these values do not deviate very widely indeed from the densities furnished by such a formula as (8), our considerations on the limits of reliability will still practically hold. For the present, therefore, we may safely rest content with the results just obtained.

POINT IV. EXTENSION OF THE LIMITS OF TABLE XII

There is, we think, reason to assume that the limits shown in Table XII give rather too unfavorable an impression of the real reliability. The reason is that the deviation, having once reached 25 (or 40) per cent, will grow no further, or at least not much further before it begins to diminish. This it will continue to do until it becomes *zero* and begins to increase again and, possibly, go on increasing indefinitely (on the other side). That is to say, beyond the limits assigned in Table XII the deviation from (8) for a certain time will still be mostly very moderate or small. Still much more important than this is a fact which will appear in a further publication, by one of us, in which a formula is derived theoretically which in the last analysis is an expression of the differential quotient $d\Delta(\rho)/d\rho$ as a function of ρ and $\Delta(\rho)$. The integration of this differential equation, if the equation could be accepted as definitely proved, would give $\Delta(\rho)$as a function of ρ for all distances. As it is, the equation is verified by observation as far as observation can fairly be relied on.

We thus have not only reliable values of $\Delta(\rho)$ up to the limits of Table XII, but also to these same limits, reliable values of $d\Delta(\rho)/d\rho$. This proves that we have a right to extend the use of the formula which yielded $\Delta(\rho)$ considerably beyond the limits of Table XII.

There is a third consideration which will enable us to extend the limits of Table XII with some probability of reliable results. In the publication just alluded to it will be shown that the equidensity surfaces are at least approximately similar ellipsoids. If we suppose that this form holds somewhat beyond the limits for which we have fair certainty, then the limits of Table XII will again be extended, at least for the lower galactic latitudes.

The three considerations (of which the second is the most important) together make us believe, that as soon as we have good data for N_m down to magnitude 17, which will be very shortly, we shall be able to find fairly reliable values of the $\Delta(\rho)$ for the entire region near the center for which $\Delta(\rho)$ exceeds one hundredth of the density near the sun, that is, for the whole of the space represented in Fig. 2, *Contribution* No. 188.

CONCLUDING REMARK

The conclusions arrived at in this paper may perhaps best be seen in their true bearing by comparing the limits within which we can find fairly reliable results for the structure of the stellar system by using different sets of data. Of course Table XIII claims no other merit than that of furnishing the means of a rough insight into what can be obtained at present or in the very near future.

TABLE XIII

LIMITS IN PARSECS WITHIN WHICH THE STRUCTURE OF THE STELLAR SYSTEM CAN BE FOUND

Method	Galactic Latitude		
	0°–20°	40°–90°	0°–90°
1. Direct parallax determination	....	....	50
2. Parallactic motion, now well known, to $m=10$	320	240	300
3. The same, to $m=13$	(830)	(610)	(720)
4. Parallactic motion, stars to $m=10$ and $\mu=0''.01$	400	320	360
5. The same together with N_m (the latter to $m=14$)	1600	800	1200
6. The same, N_m to $m=17$	(4000)	(1600)	(2800)
7. Extension according to Point IV, N_m to $m=14$	3000	1000	2000
8. The same, N_m to $m=17$	(8000)	1700	$\Delta=\Delta_0/100$

NOTES TO TABLE XIII

The limits in parentheses have not yet been reached but may be attained in two or three years.

1. The magnificent results lately obtained in direct parallax determinations by means of long-focus instruments show probable errors of the order of $0''.01$. Even if there were demonstrably no systematic errors left, a probable error of $0''.01$ would imply that we cannot derive from them the structure of the system beyond the limit of the table. Since the absence of systematic error cannot be claimed, the limit of the table is probably rather high.

2, 4. The table gives simply the mean distances corresponding to the mean parallaxes in *Groningen Publication*, No. 29, and in a paper not yet published.

3. Simple repetition of the parallax plates obtained at the Mount Wilson Observatory some five or more years after their first exposure, would give excellent values for the parallactic motion of the stars of magnitude 13. Similar repetition of the parallax work done in America on Boss stars by other observatories with long-focus instruments would also contribute to an important degree.

5, 6. From Table XII of the present paper.

7, 8. According to Point IV of present paper. In the last column of No. 8, $\Delta=\Delta_0/100$ means that for all latitudes the densities are fairly reliable for the whole of the space where the density is greater than 0.01 of that near the sun (compare Fig. 2, *Contribution* No. 188).

All the results will be greatly strengthened as soon as we know N_m to $m=20$. At the same time this will enable us to make good estimates for still greater distances.

APPENDIX

POINT III*a*. ON THE SIMPLIFIED PROBLEM

Given, r = probable error of each of the quantities $\log N_1$, $\log N_2$, $\log N_3$; required, ρ_{m_0} = probable error of the constant m_0.

By formulae (31) and (2) of the text

$$\log N_m=\mu a-2\mu m_0 cm+\mu cm^2 \qquad (\mu=\text{mod.}). \tag{a}$$

Hence

$$\left.\begin{aligned}\log N_1&=\mu a-2\mu m_0 c(m_1-\sigma)+\mu c(m_1-\sigma)^2\\ \log N_2&=\mu a-2\mu m_0 cm_1+\mu cm_1^2\\ \log N_3&=\mu a-2\mu m_0 c(m_1+\sigma)+\mu c(m_1+\sigma)^2\end{aligned}\right\} \tag{b}$$

from which for m_0

$$m_0-m_1=\frac{(H+1)\sigma}{2(H-1)} \tag{c}$$

in which

$$H=\frac{\log N_2-\log N_1}{\log N_3-\log N_2}. \tag{d}$$

Consequently

$$\rho_{m_0}=\frac{\sigma}{(H-1)^2}\rho_H \tag{e}$$

in which the probable error ρ_H must be found from (*d*). Since we assume

$$\text{Probable errors of } N_1,\ N_2, \text{ and } N_3 \text{ each}=r, \tag{f}$$

we obtain as in the text

$$\rho_{m_0}=\pm\frac{r\sqrt{2}}{4\sigma^2 c\mu}\sqrt{12(m_0-m_1)^2+\sigma^2}. \tag{g}$$

LEIDEN, HOLLAND
August 1921

Contributions from the Mount Wilson Observatory, No. 230
Reprinted from the *Astrophysical Journal*, Vol. LV, pp. 302–328, 1922

FIRST ATTEMPT AT A THEORY OF THE ARRANGEMENT AND MOTION OF THE SIDEREAL SYSTEM

By J. C. KAPTEYN[1]

ABSTRACT

First attempt at a general theory of the distribution of masses, forces, and velocities in the stellar system.—(1) *Distribution of stars.* Observations are fairly well represented, at least up to galactic lat. 70°, if we *assume that the equidensity surfaces are similar ellipsoids of revolution*, with axial ratio 5.1, and this enables us to compute quite readily (2) *the gravitational acceleration at various points due to such a system*, by summing up the effects of each of ten ellipsoidal shells, in terms of the acceleration due to the average star at a distance of a parsec. The *total number of stars* is taken as 47.4×10^9. (3) *Random and rotational velocities.* The nature of the equidensity surfaces is such that the stellar system cannot be in a steady state unless there is a general rotational motion around the galactic polar axis, in addition to a random motion analogous to the thermal agitation of a gas. In the neighborhood of the axis, however, there is no rotation, and the behavior is assumed to be like that of a gas at uniform temperature, but with a gravitational acceleration ($G\eta$) decreasing with the distance ρ. Therefore the density Δ is assumed to obey the barometric law: $G\eta=-\bar{u}^2(\delta\Delta/\delta\rho)/\Delta$; and taking the mean random velocity $\bar{u}$ as 10.3 km/sec., the author finds that (4) *the mean mass of the stars* decreases from 2.2 (sun = 1) for shell II to 1.4 for shell X (the outer shell), the average being close to 1.6, which is the value independently found for the average mass of both components of visual binaries. In the galactic plane the resultant acceleration—gravitational minus centrifugal—is again put equal to $-\bar{u}^2(\delta\Delta/\delta\rho)/\Delta$, $\bar{u}$ is taken to be constant and the average mass is assumed to decrease from shell to shell as in the direction of the pole. The angular velocities then come out such as to make the linear rotational velocities about constant and equal to 19.5 km/sec. beyond the third shell. If now we suppose that part of the stars are rotating one way and part the other, the relative velocity being 39 km/sec., we have a quantitative explanation of the phenomenon of star-streaming, where the relative velocity is also in the plane of the Milky Way and about 40 km/sec. It is incidentally suggested that when the theory is perfected it may be possible to determine *the amount of dark matter* from its gravitational effect. (5) The *chief defects of the theory* are: That the equidensity surfaces assumed do not agree with the actual surfaces, which tend to become spherical for the shorter distances; that the *position of the center of the system* is not the sun, as assumed, but is probably located at a point some 650 parsecs away in the direction galactic long. 77°, lat. −3°; that the average mass of the stars was assumed to be the same in all shells in deriving the formula for the variation of $G\eta$ with ρ on the basis of which the variation of average mass from shell to shell and the constancy of the rotational velocity were derived—hence either the assumption or the conclusions are wrong; and that no distinction has been made between stars of different types.

1. *Equidensity surfaces supposed to be similar ellipsoids.*—In *Mount Wilson Contribution* No. 188[2] a provisional derivation was given of the star-density in the stellar system. The question was there raised whether the inflection appearing near the pole in the

---

[1] Research Associate of the Mount Wilson Observatory.

[2] *Astrophysical Journal*, **52**, 23, 1920.

equidensity surfaces for small densities is real or not. I have since found that these inflections can be avoided without doing very serious violence to the results of observation. If this is done, the equidensity surfaces become approximately ellipsoids, and not only that, but the data can be represented without exceeding the possible limits of observation error, by assuming the equidensity surfaces to be *concentric, similar revolution ellipsoids, similarly situated.*

2. *Elements of the ellipsoids.*—Taking as unit of star-density that in the neighborhood of the sun, the adopted axes of the ellipsoids, which will be referred to as ellipsoids I, II, ... X and which correspond to the values (Δ being the density) $\log \Delta + 10 = 9.8, 9.6,$ . . . . 8.0, are as shown in Table I. The A-axis is directed toward the galactic Pole, the B-axis lies in the plane of the Milky Way.

TABLE I

EQUIDENSITY ELLIPSOIDS

Ellipsoid	Log Δ	*A*	*B*	*B/A*
		parsecs	parsecs	
I	9.80−10	118	602	5.102
II	9.60	198	1010	5.102
III	9.40	296	1510	5.102
IV	9.20	413	2106	5.102
V	9.00	553	2820	5.102
VI	8.80	717	3656	5.102
VII	8.60	902	4600	5.102
VIII	8.40	1114	5675	5.102
IX	8.20	1365	6960	5.102
X	8.00	1660	8465	5.102

For the Milky Way and for the direction toward the Pole this table yields densities which are fairly well represented, for $\rho > 150$ parsecs, by the formulae,

$$\log \Delta = -2.135 + 2.368 \log \rho - 0.593 (\log \rho)^2 \quad \text{(M.W.)}, \qquad (1)$$

$$\log \Delta = -5.356 + 4.890 \log \rho - 1.200 (\log \rho)^2 \quad \text{(Pole)}, \qquad (1a)$$

A section of the equidensity-ellipsoids through the sun (which has been assumed to be the center of the system) at right angles to the plane of the Milky Way is shown in Figure 1.

The agreement of the densities furnished by Table I with those of *Contribution* No. 188 is fairly good for all galactic latitudes up to 65° or 70°. For still higher latitudes it may perhaps still be called tolerable. At least the deviations hardly exceed what would be produced by an error of 0.1 mag. in the photometric scale for these regions.

In the present paper I have substituted these ellipsoids for the surfaces derived directly from observation in *Contribution* No. 188, *not* because I think they are nearer the truth, but simply because they are so enormously more convenient for further computation.

My aim in the present paper is simply to get hold of some approximate information about the real structure and motion of the system, and quantitative accuracy has been considered of secondary importance as long as we may hope that the main features are not affected. I trust that this hope will not be disappointed, notwithstanding the many defects—defects that will be duly pointed out—which still attach to the present treatment.

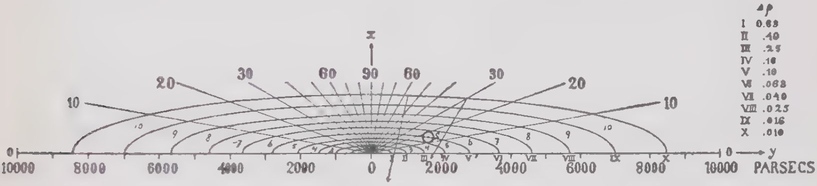

FIG. 1

3. *Advantage of the adoption of the ellipsoids.*—The form of the equidensity surfaces thus adopted has the advantage that it calls attention to the possibility of determining with some precision the gravitational attraction of the *whole* of the stellar system on any point inside ellipsoid X, while at the same time it renders the computation of that attraction a relatively easy matter.

In another paper[1] van Rhijn and I have tried to show that, as soon as we possess good counts of stars for each interval of magnitude down to apparent magnitude 17 (visual), we shall know with some tolerable approximation the density of the whole region covered by Figure 1, that is, of the whole extent of the stellar system for which the density exceeds one-hundredth of that in the neighborhood of the sun.

---

[1] *Mt. Wilson Contr.*, No. 229; *Astrophysical Journal*, **55**, 242, 1922.

In the near future such counts will be available. They will be furnished by the Mount Wilson "Catalogue of the Selected Areas" (from $\delta = -15°$ to $\delta = +90°$), the discussion of which is in the hands of Seares. A few provisional counts make it probable that this work will in the main confirm the elements used for Table I and Figure 1. I will assume, therefore, that even now the densities are sufficiently well known for the whole of ellipsoid X.

The advantage just alluded to is a consequence of the well-known property that the attraction of an ellipsoidal shell of constant density, bounded by two similar and similarly situated ellipsoids, on an internal point is *zero*. For it is evident by this property that, if in all that part of the system which lies outside ellipsoid X—for which part accurate data are still wanting—the arrangement in similar ellipsoids also holds, the attraction of this outside domain on a point inside ellipsoid X would be *zero*. And as the distribution of density inside ellipsoid X is known, the possibility of computing the attraction of the total system on a point inside of X becomes evident. If on the contrary the same arrangement does not hold outside ellipsoid X, it still seems highly probable a priori that any change in the form of the equidensity surfaces must be gradual, that is, the equidensity surfaces in the neighborhood of X will diverge little from similar ellipsoids, and the greater changes will begin to appear only at more considerable distances. For the consecutive shells, therefore, the attraction on an internal point will begin by being very small, both on account of the near approach to similarity of these shells and their small density and greater distance from the attracted point. For more distant shells the first circumstance will probably diminish in importance with increasing distance, while, on the contrary, the second becomes more and more important. On the whole, therefore, the attraction of all of that part of the system which lies outside X will be small, and its neglect will presumably not prevent us from obtaining fairly exact ideas about the total forces.

4. *Computation of the gravitational forces.*—In ellipsoid I, which for brevity I will call shell 1, and in each of the shells 2, 3, ... 10, between the surfaces of ellipsoids I, II, ... X, the density varies between limiting values which are in the ratio of 1 to 1.585.

In what follows I will assume for each shell a constant average density.

The computation of the gravitational forces has been carried through for:

(1) 10 points in galactic latitude 0° lying in the surfaces of ellipsoids I, II, ... X; these points have been designated by I, 0°; II, 0°; . . . . X, 0°.

(2) 5 points in galactic latitude 30°, situated on the surfaces II, IV, VI, VIII, X; denoted by II, 30°; IV, 30°; . . . . X, 30°.

(3) Similarly for the 5 points II, 57°1; IV, 57°1; . . . . X, 57°1. (57°1 = average latitude between 40° and 90°.)

(4) The 10 points I, 90°; II, 90°; . . . . X, 90°.

As a unit of attraction I have used the attraction on each other of two stars of average mass separated by a distance of 1 parsec.

I first computed the attraction of the full ellipsoids I, II, ... X on the points specified above, on the supposition that they are of a constant density such that every cubic parsec contains a single star. The formulae for this computation are given in the Appendix.

The attraction of the full ellipsoids having been found, simple subtraction gives the attraction of the separate shells 1, 2, ... 10, all supposed to have the density corresponding to one star per cubic parsec. The actual attraction of the shells was obtained by multiplying these results by the number of stars per cubic parsec contained in each shell. For the average densities, expressed in terms of the density in the neighborhood of the sun, I adopted the values corresponding to the logarithms 9.9, 9.7, 9.5, ... 8.1, each minus 10, multiplied by 0.0451, which according to *Contribution* No. 188 (12) is the number of stars per cubic parsec near the sun; this gives the numbers in Table II.

TABLE II

AVERAGE NUMBER OF STARS PER CUBIC PARSEC

Shell	No. Stars	Shell	No. Stars
1	0.0358	6	0.00358
2	.0226	7	.00226
3	.0143	8	.00143
4	.00900	9	.000900
5	0.00568	10	0.000568

Having found the separate attractions, the components of the total attractions parallel to the axes can at once be determined by noting that the attraction of any shell on an internal point is *zero*, and further, by neglecting the attraction of that part of the system outside of ellipsoid X on a point inside this ellipsoid. Instead of the components I have entered in Table III the total forces G and the angles that these forces make with the X-axis. These are of course found by the formulae

$$X=G\cos\phi \qquad Y=G\sin\phi. \tag{2}$$

In addition, I have given the values of $\phi-\psi$, ψ being the angle which the normal to the ellipsoid through the attracted point makes with the X-axis; ψ is determined by

$$\tan\psi=\frac{A^2}{B^2}\frac{\beta}{\alpha} \tag{2a}$$

The angle $\phi-\psi$ is of course the inclination of the direction of the force to the normal.

The interpretation of this table—of the first entry, for example—is: Attraction of the whole stellar system on a body in the point I, 0° is a force equal to the attraction of 33.19 stars of average mass at the distance of 1 parsec from that same body. This force makes an angle of 90° with the X-axis, and an angle of 0° with the normal to the equidensity ellipsoid through the attracted point.

5. *Analytical representation of G for galactic latitudes 0° and 90°.*—In trying to represent the force G by an analytical formula, I started from the consideration that, as the density is constant near the center, the attraction must be nearly proportional to the distance ρ for very small values of ρ; further, that for distances very great as compared with the dimensions of the stellar system, the attraction must be practically the same as it would be were the mass of the whole system concentrated in the center. For these latter distances, therefore, G must be proportional to $1/\rho^2$.

The following easily managed formula satisfies both conditions:

$$G=\frac{A\rho}{1+B\rho+C\rho^2+D\rho^3}. \tag{3}$$

TABLE III

Total Attractions of the Whole System

Attr. Point	Log Δ	Co-ordinates Attr. Point		G	φ	φ−ψ	Attr. Point	Log Δ	Co-ordinates Attr. Point		G	φ	φ−ψ
		α	β						α	β			
		parsecs	parsecs						parsecs	parsecs			
I, 0°......	9.80−10	0	602	33.19	90°	0°	I, 90°.....	9.80−10	118	0	40.06	0°	0°
II, 0	9.60	0	1010	37.76	90	0	II, 90	9.60	198	0	54.26	0	0
III, 0	9.40	0	1510	37.95	90	0	III, 90	9.40	296	0	62.45	0	0
IV, 0	9.20	0	2106	35.71	90	0	IV, 90	9.20	413	0	65.95	0	0
V, 0	9.00	0	2820	32.09	90	0	V, 90	9.00	553	0	66.12	0	0
VI, 0	8.80	0	3657	27.71	90	0	VI, 90	8.80	717	0	64.00	0	0
VII, 0	8.60	0	4600	23.67	90	0	VII, 90	8.60	902	0	60.63	0	0
VIII, 0	8.40	0	5675	20.12	90	0	VIII, 90	8.40	1114	0	56.41	0	0
IX, 0	8.20	0	6960	16.59	90	0	IX, 90	8.20	1365	0	51.56	0	0
X, 0	8.00	0	8465	13.53	90	0	X, 90	8.00	1660	0	46.52	0	0
II, 30°.....	9.60	187	325	52.34	18° 6′	14°18′	II, 57°.1....	9.60	196	127	53.99	6°54′	5°29′
IV, 30	9.20	391	677	59.26	22 6	18 18	IV, 57.1....	9.20	410	265	64.86	8 49	7 24
VI, 30	8.80	679	1176	53.97	25 8	21 20	VI, 57.1....	8.80	711	460	62.10	10 33	9 8
VIII, 30	8.40	1055	1827	44.64	28 2	24 14	VIII, 57.1....	8.40	1105	715	53.91	12 5	10 40
X, 30	8.00	1572	2723	34.46	30 54	27 6	X, 57.1....	8.00	1647	1066	43.85	13 42	12 17

In this formula A/D evidently equals the total number of stars, N, in the stellar system.

A rough estimate of this number can be made by assuming that formula (15) of *Contribution* No. 188, viz.,

$$N_m = e^{a+bm+cm^2}, \tag{4}$$

is true for all values of m. Integration over m gives

$$N = \frac{\sqrt{\pi}}{\sqrt{-c}} e^{a-\frac{b^2}{4c}}. \tag{5}$$

For the values of a, b, c best satisfying the numbers in *Groningen Publications*, No. 27, Table V, which gives the number of stars per square degree, I found the following:

Gal. Lat.	a	b	c	Number of Square Degrees
0° to ±20°	−10.564	+1.5985	−0.0276	14110
±20 to ±40	−10.539	+1.5468	−0.0288	12420
±40 to ±90	−10.815	+1.6592	−0.0414	14730

With these data, computing the total number of stars for each of the three zones, I obtained

Gal. Lat.	No. Stars
0° to ±20°	43.8×10^9
±20 to ±40	3.6×10^9
±40 to ±90	0.043×10^9

whence

$$\frac{A}{D} = N = 47.4 \times 10^9. \tag{6}$$

The remaining constants were so determined that (3) represents the values of G in Table III. I thus found

Gal. Lat. = 0°	Gal. Lat. = 90°
$A = 0.110$	$A = 0.376$
$B = 1.30 \times 10^{-3}$	$B = 1.83 \times 10^{-3}$
$C = 0.657 \times 10^{-6}$	$C = 3.40 \times 10^{-6}$
$D = 2.32 \times 10^{-12}$	$D = 7.93 \times 10^{-12}$

(7)

The representation of the tabular values is as follows:

ρ	Gal. Lat. = 0°			ρ	Gal. Lat. = 90°		
	G. Tab.	G. Form.	Tab. − Form		G. Tab.	G. Form.	Tab. − Form
500	30.0	30.2	−0.2	200	54.3	50.1	+4.2
1000	37.8	37.0	+0.8	500	66.2	68.0	−1.8
2000	36.0	35.0	+1.0	1000	58.5	60.3	−1.8
3000	31.7	30.2	+1.5	1500	49.1	49.4	−0.3
4000	26.0	26.0	0.0				
6000	19.0	19.9	−0.9				
8000	14.0	16.0	−2.0				

The agreement is not very good, but seems sufficient for our present purpose.

6. *Application of kinetic theory of gases.*—The results thus far obtained rest, it is true, on provisional data, which even now might be materially improved; they further depend on the supposition, not yet fully demonstrated, that, within the distances here considered, there is no appreciable extinction of light in space, but they are, nevertheless, I think, the legitimate outcome of our data.

For what follows I will now introduce some considerations borrowed from the kinetic theory of gases, the applicability of which to the stellar system might be considered doubtful. At all events I do not pretend to have demonstrated this applicability. The results which will be derived cannot lay claim to be demonstrably correct, but they seem to me to be so remarkable that, after a good deal of hesitation, I have resolved to publish them, in the hope that others, better versed in these matters, may furnish us with a more rigorous solution of the problem involved.

Even though it has been shown, in the main by unpublished investigations, that the peculiar motions[1] of the stars with some crude approximation are Maxwellian, the stellar system cannot be treated as a gas at rest; first, because of the existence of stream-motion; second, because of the form of the equidensity surfaces, which is certainly different from that of the equipotential surfaces of the gravitational force.

---

[1] Peculiar velocity is defined as the motion corrected for both the solar and stream-motion. The radial and transverse velocities agree in showing a certain excess of very large motions over the Maxwellian distribution. They are both represented satisfactorily by the sum of *two* Maxwellian distributions. A thorough separate treatment of all the spectral classes is still a great desideratum.

That they are different is proved by the fact, among others, that in general the forces are not normal to these surfaces. This is evident enough without further explanation. Moreover, it is clearly brought out by Table III, where the angle with the normal reaches values of more than 27°. Further it is well known that in a gas at rest under its own attraction, the equidensity surfaces are spherical.

The system cannot therefore be in a steady state unless it has a systematic motion. Since the discovery of the star-streams it is clear that such a motion really exists and that it is parallel to the plane of the Milky Way.

It seems rational, therefore, to assume that the system has a sort of rotational motion round the X-axis (see Fig. 1) which is directed toward the pole of the galaxy. The form of the equidensity surfaces found directly in *Contribution* No. 188 as well as that now adopted, strongly indicates some such motion.

This being assumed, the stars along the axis will still have no other motion than their peculiar motions, which, as was just mentioned, are Maxwellian, at least with some approximation. I venture to assume, therefore, that the stars in the immediate neighborhood of this axis are arranged as the molecules of a gas in a quiescent atmosphere.

If:

Δ be the star-density (number of stars per cubic parsec);
u one of the components of the peculiar velocity;
η the acceleration produced by the attraction of a star of average mass at a distance of one parsec, then on the above assumption

$$\overline{u^2}\frac{\delta\Delta}{\Delta} = -G\eta\delta\rho, \tag{8}$$

$\overline{u^2}$ being the average value of u^2.

The formula is analogous to that used for barometric determinations of altitude in an atmosphere of constant temperature throughout. On the other hand, we have found empirically formulae such as (1) and (1*a*) (see also *Contribution* No. 188, p. 13 [21]); in other words,

$$\log \Delta = -P + Q \log \rho - R(\log \rho)^3 \quad (\rho > \rho_0), \tag{9}$$

from which, by differentiation

$$\frac{\delta\Delta}{\Delta} = \frac{Q - 2R \log \rho}{\rho}\,\delta\rho. \tag{10}$$

Comparing the two expressions, (8) and (10), for $\delta\Delta/\Delta$

$$G\eta = -\overline{u^2}\left[\frac{Q - 2R \log \rho}{\rho}\right] \quad (\rho > \rho_0). \tag{11}$$

As the motions are supposed to be Maxwellian, the well-known formula used in the theory of least squares gives

$$\overline{u^2} = \frac{\pi}{2}(\overline{u})^2. \tag{12}$$

From observations of the radial velocities at the Lick Observatory, where no choice has been made on the basis of proper motion (*Lick Observatory Bulletin*, **6**, 126), I derived the value[1]

$$\overline{u} = 10.3 \text{ km/sec.} \tag{13}$$

or since

$$\left.\begin{array}{ll} 1 \text{ kilometer} & = 3.25 \times 10^{-14} \text{ parsecs} \\ 1 \text{ parsec} & = 3.08 \times 10^{13} \text{ kilometers} \end{array}\right. \tag{14}$$

I find, in the units parsec and second, here adopted,

$$\overline{u} = 3.35 \times 10^{-13} \tag{15}$$

$$\overline{u^2} = 1.763 \times 10^{-25} \tag{16}$$

so that (11) becomes

$$G\eta = -1.763 \times 10^{-25}\,\frac{Q - 2R \log \rho}{\rho} \quad (\rho > \rho_0) \tag{17}$$

Finally, for galactic latitude 90°, we obtain from equation (1*a*) the values:

$$Q = +4.890 \quad R = +1.200 \tag{18}$$

$$\eta = \frac{(-8.620 + 4.229 \log \rho) \times 10^{-25}}{G\rho} \quad (\rho > 150). \tag{19}$$

[1] There is a mistake in the derivation of this value. The true value is certainly somewhat lower. From considerations given below I have not deemed it necessary for the present paper to repeat the computations with an improved value of $\overline{u}$.

For small values of ρ, formula (9) does not hold. According to *Contribution* No. 188, and particularly according to *Contribution* No. 229, it represents the observations excellently for values of ρ well beyond the maximum (which in the present case lies near $\rho = 110$ parsecs). For values of ρ below the maximum the density is nearly constant. The differential-quotient $\delta\Delta/\delta\rho$ thus becomes very small and $\delta\Delta/\Delta\delta\rho$ very unreliable. In the present case it will probably be well not to rely on the formula below, say, 150 parsecs. This limit was adopted in (19).

I have computed the values of η from (19) both on the supposition that G has the values found directly in Table III and that it has the values yielded by formula (3). The former were adopted (Table IV).

TABLE IV

VALUES OF η AND $\overline{m}$

Point	ρ	η Form. (3)	η Adopted	$\overline{m}$ (Sun = 1)
	parsecs			
II, 90°	198	11.1×10^{-30}	10.2×10^{-30}	2.2
IV, 90	413	$8.9 \quad 10^{-30}$	$9.0 \quad 10^{-30}$	2.0
VI, 90	717	$7.3 \quad 10^{-30}$	$7.5 \quad 10^{-30}$	1.7
VIII, 90	1114	$6.6 \quad 10^{-30}$	$6.8 \quad 10^{-30}$	1.5
X, 90	1660	$6.5 \quad 10^{-30}$	$6.5 \quad 10^{-30}$	1.4

The quantity η is, as stated above, the acceleration per second, in parsecs, produced by the attraction of a star of average mass on a body at a distance of one parsec. The acceleration which the sun would produce, expressed in the same units, is

$$\text{Acceleration by sun} = 4.53 \times 10^{-30}. \tag{20}$$

This enables us to find the average mass $\overline{m}$ of a star expressed in the mass of the sun as a unit. The values of $\overline{m}$ thus found have been inserted in the last column of Table IV.

These values agree surprisingly well with what has been found by totally different considerations. In a recent paper[1] Jackson and Furner find for visual binary stars, as the best average

$$\frac{1}{\sqrt{m_1 + m_2}} = 0.855.$$

---

[1] *Monthly Notices*, 81, 4, 1920.

Consequently $m_1+m_2=1.60$, which agrees with Table IV if we suppose that the combined mass of the two components and not that of a single component is comparable with the mass of a single star, and especially if we further consider that there are theoretical grounds for expecting that the average mass will decrease for increasing distance.[1]

Remark. Dark matter. It is important to note that what has here been determined is the total mass within a definite volume, divided by the number of luminous stars. I will call this mass the average effective mass of the stars. It has been possible to include the luminous stars completely owing to the assumption that at present we know the luminosity-curve over so large a part of its course that further extrapolation seems allowable.

Now suppose that in a volume of space containing l luminous stars there be dark matter with an aggregate mass equal to Kl average luminous stars; then, evidently the effective mass equals $(l+K)\times$average mass of a luminous star.

We therefore have the means of estimating the mass of dark matter in the universe. As matters stand at present it appears at once that this mass cannot be excessive. If it were otherwise, the average mass as derived from binary stars would have been very much lower than what has been found for the effective mass.

7. *Angular velocities* (ω) *in the plane of the galaxy.*—Ignoring for an instant the fact that the stars in the Milky Way cannot be systematically at rest and treating the stars near this plane in the same way as those near the axis, I am led by a formula analogous to (17) to values of η which are not quite half those given in Table IV. I suppose that the difference must be wholly due to the centrifugal force induced by the rotational motions. In fact, I assume that the average mass is the same throughout the whole system, at least for points on the same equidensity surface.

If, therefore, ρ and ρ' represent the distances from the center, of two points on the same equidensity surface, the first in the direction of the Pole, the second in the Milky Way, for which points the total attractive forces of the system are respectively G and G', formula (11) gives

---

[1] Jeans, *Problems of Cosmogony and Stellar Dynamics* (1919), p. 239.

$$\text{For the Pole} \qquad G\eta = -\overline{u^2}\,\frac{Q-2R\log\rho}{\rho}, \tag{21}$$

$$\text{For the Milky Way} \quad G'\eta - \rho'\omega^2 = -\overline{u^2}\,\frac{Q'-2R'\log\rho'}{\rho'}, \tag{22}$$

where ω represents the angular velocity for the point in the Milky Way, and Q' and R' the constants of equation (9) for that same plane. The two equations determine η and ω. The equation for the latter is

$$\omega^2 = \frac{G'}{\rho'}\cdot\overline{u^2}\left[\frac{Q'-2R'\log\rho'}{G'\rho'} - \frac{Q-2R\log\rho}{G\rho}\right], \tag{23}$$

in which, for $\overline{u^2}$ see (16); for G' and G see Table V; and for Q and R see (18), and where finally, by comparing (9) and (1),

$$Q' = 2.368 \text{ and } R' = 0.593 \tag{24}$$

The maximum of Δ according to formula (9) lies, for the Milky Way at about $\rho = 100$, for the direction toward the Pole at $\rho = 110$. As has been mentioned, the formula ceases to be correct below these values. I assume, as before, that the limit of validity is $\rho = 150$.

8. *Angular velocity for stars not in the galaxy.*—For the regions not in galactic latitudes 0° or 90° I determine the angular velocity by the condition that the resultant of the attractive and centrifugal forces must be at right angles to the equidensity surfaces.

In order that the system may be in the steady state, I assume that the equidensity surfaces are at the same time equipotential surfaces for the resultant of the attractive and centrifugal forces. The above condition is implied in this assumption.

Since

X component of resultant acceleration $= -X\eta$,
Y component of resultant acceleration $= -Y\eta + \beta\omega^2$,

and since ψ is the angle between the normal and the X-axis, the equation for ω is

$$\beta\omega^2 - X\eta = -X\eta \tan\psi ,$$

which becomes slightly more convenient by writing

$$X=G\cos\phi \qquad Y=G\sin\phi .$$

Whence

$$\omega^2=\frac{G\eta}{\beta}\,\frac{\sin(\phi-\psi)}{\cos\psi}\,. \tag{25}$$

For the points in Table V, $\phi-\psi$ and ψ were taken from Table III. The computation was made with the aid of formulae (23) and (25).

TABLE V

VALUES OF ω^2

Point	ω^2	Point	ω^2	Point	ω^2
II, 0°.	0.1757×10^{-30}	II, 30°..	0.4066×10^{-30}	II, 57°.1..	0.4132×10^{-30}
IV, 0 .	$.0902 \quad 10^{-30}$	IV, 30 ..	$.2477 \quad 10^{-30}$	IV, 57.1..	.2835 10
VI, 0 .	$.03175 \quad 10^{-30}$	VI, 30 ..	$.1255 \quad 10^{-30}$	VI, 57.1..	.1606 10
VIII, 0 .	$.01237 \quad 10^{-30}$	VIII, 30 ..	$.0683 \quad 10^{-30}$	VIII, 57.1..	.0949 10
X, 0 .	$.00510 \quad 10^{-30}$	X, 30 ..	$.0376 \quad 10^{-30}$	X, 57.1..	.0568 10

For these same points I have furthermore computed the linear velocities in kilometers per second. They are in Table VI.

TABLE VI

LINEAR VELOCITIES

Point	β	$\beta\omega$	Point	α	β	$\beta\omega$	Point	α	β	$\beta\omega$
		km/sec.				km/sec.				km/sec.
II, 0°..	1010	13.0	II, 30°.	187	325	6.4	II, 57°.1	196	127	2.5
IV, 0 ..	2106	19.5	IV, 30.	391	677	10.4	IV, 57.1	410	265	4.4
VI, 0 ..	3657	20.1	VI, 30.	679	1176	12.8 (13.1)	VI, 57.1	711	460	5.7 (6.3)
VIII, 0 ..	5675	19.4	VIII, 30.	1055	1827	14.7 (15.7)	VIII, 57.1	1105	715	6.8 (9.1)
X, 0 ..	8465	18.6	X, 30.	1572	2733	16.3 (17.9)	X, 57.1	1647	1066	7.8 (11.1)

9. *Explanation of star-streaming.*—According to these numbers the angular velocity is not the same for the same distance β from the axis at different distances α from the plane of the Milky Way. Further on I will explain why the present solution must necessarily be a very crude one. For this reason I am not prepared to maintain the reality of this difference. On the contrary it seems very possible that a more definite solution will finally lead to the conclusion that all the points on a cylinder around the axis of the system move with the same velocity. In fact, if we base our solution on the equidensity surfaces as really derived from the observations,[1] instead

---

[1] *Mt. Wilson Contr.*, No. 188; *Astrophysical Journal*, **52**, 23, 1920.

of assuming similar ellipsoids, we approach at once much closer to this state of affairs. The numbers in parentheses in Table VI give rough estimates of $\beta\omega$ based on this supposition. In the absence of a more definite solution I will confine myself mainly to points in the plane of the Milky Way, the motions of which, except for small values of β, seem to be somewhat better determined.

The most striking feature brought out by these numbers is undoubtedly the fact that at distances from the axis exceeding 2000 parsecs the linear velocity of the stars is nearly constant, the average being 19.5 km/sec.; that is, the great bulk of the stars must have a motion of 19.5 km in a direction parallel to the plane of the Milky Way. Observation has already proved that there really exists a systematic motion of the stars, that it is exactly parallel to the plane of the Milky Way, and that the motion takes place in two exactly opposite directions, the two streams having a relative velocity of about

$$40 \text{ km/per sec.} \tag{26}$$

Since in the preceding theory the motion is introduced simply to explain certain centrifugal forces, it is at once evident that it supposes nothing about the direction in which the motion takes place. Nothing prevents us from assuming that part of the stars circulate one way, while the rest move in the opposite direction. The relative motion of the two groups will then evidently be

$$2\times 19.5 = 39 \text{ km/sec.} \tag{27}$$

The motion to which our theory leads, besides being in the same plane, has therefore practically the exact value which from observation is known to exist. In fact we are led in the most direct and natural way to a complete explanation of the phenomenon of star-streaming. The circumstance that observation led us to assume two rectilinear streams, whereas we here find the motion to be circular, is probably unimportant. It is of course infinitely probable that the sun must be at a certain distance from the center of the system. If we suppose it to be at the point S (see Fig. 1) then the star-streams are derived from the observed motions of stars within a volume whose dimensions are of the order of those of the sphere around S shown in the figure. As long as the radius of this sphere is small in comparison with the distance of S from the center, the curvature of the stream-lines must be inappreciable.

When we consider that the value (27) has been obtained by a study of the arrangement of stars in space, in which the proper motions play no other part than that of a criterion of distance, while the value (26) has been obtained by a study of the motions themselves, both radial and transverse, the close agreement of the two results seems very significant. It becomes more so through the fact that both theories yield a motion exactly parallel to the plane of the Milky Way. Further, if we take into account the fact that the present theory leads to a value for the average mass of the stars which is in close accordance with what has also been found from utterly different investigations, and if we add a final point, namely, the natural explanation of the different arrangement of the stars of different spectral types, we are led irresistibly to the following conclusion:

The theory here propounded, though it may require considerable modification on account of its defectiveness both as to observational basis and mathematical treatment is probably correct in its main features.

The last point mentioned, which is open to quantitative verification, requires further investigation, but even now promises to be no less significant than the others. It is referred to again in section 14 below.

10. *Accelerations including centrifugal effect.*—If with the aid of Table V we now add the acceleration due to the centrifugal forces to that produced by the attractive force, the resultant will be in the direction of the normal. We find the results in Table VII.

TABLE VII

ACCELERATION, INCLUDING EFFECT OF CENTRIFUGAL FORCE

Point	$G\eta$	Point	$G\eta$	Point	$G\eta$	Point	$G\eta$	$G_{\text{Pole}}/G_{\text{MW}}$
II, 0°	208×10^{-30}	II, 30°	508×10^{-30}	II, 57°.1	547×10^{-30}	II, 90°	553×10^{-30}	2.7
IV, 0	131 10^{-30}	IV, 30	495 10^{-30}	IV, 57.1	577 10^{-30}	IV, 90	593 10^{-30}	4.5
VI, 0	90 10^{-30}	VI, 30	367 10^{-30}	VI, 57.1	458 10^{-30}	VI, 90	480 10^{-30}	5.3
VIII, 0	65 10^{-30}	VIII, 30	268 10^{-30}	VIII, 57.1	359 10^{-30}	VIII, 90	384 10^{-30}	5.9
X, 0	48 10^{-30}	X, 30	193 10^{-30}	X, 57.1	277 10^{-30}	X, 90	302 10^{-30}	6.3
ψ	90°		3°49′		1°25′		0°	

11*a*. *Velocity of escape.*—Assuming formula (3) to be valid for all distances, I find for the velocity of escape of a star near the center of the system

$$\left.\begin{array}{ll}\text{In the Milky Way} & 104\text{ km/sec.}\\ \text{In the direction of Pole} & 98\text{ km/sec.}\end{array}\right\} \qquad (28)$$

As a matter of convenience I used for this computation the constant value

$$\eta = 7.5 \times 10^{-30} \qquad (29)$$

11*b*. *Velocity compared with circular velocity.*—The velocity of a star which moves in the plane of the Milky Way in a circular orbit is determined by the formula

$$V_c^2 = G\eta\beta. \qquad (30)$$

If for the point II, 0° we take $\eta = 10.2 \times 10^{-30}$, and for the others the value (29), we obtain the results in Table VIII. The linear velocities $\beta\omega$ are thus seen to be well below the critical velocity V_c.

TABLE VIII

LINEAR AND CIRCULAR VELOCITIES IN PLANE OF MILKY WAY

Point	β	G	$\beta\omega$ Table VI	V_c
			km/sec.	km/sec.
II, 0°	1010	37.76	13.0	19.2
IV, 0	2106	35.71	19.5	23.1
VI, 0	3656	27.71	20.1	26.8
VIII, 0	5675	20.12	19.4	28.5
X, 0	8465	13.53	18.6	28.5

12. *Defects of solution.*—The way in which the values ω have been determined has made the resultant of gravitational and centrifugal forces perpendicular to the equidensity surfaces. In order that the surfaces may be really equipotential there is, however, a second condition to be satisfied, viz., that for points on the same surface the total force shall be inversely as the distance of two consecutive surfaces. This condition is *not* satisfied. The difference is shown, in its most extreme form, in the last column of Table VII, which, for the points in the Milky Way and in the direction of the Pole, situated on the same ellipsoid, shows the quotient

$$\frac{\text{Force at Pole}}{\text{Force in Milky Way (including centrifugal force)}}. \qquad (31)$$

If the equidensity surfaces were really accurately represented by concentric similar ellipsoids, similarly situated, as assumed thus far, this quotient in every case would be 5.1. In reality this is far from being so.

There are certain facts indicating that actually the equidensity surfaces cannot be similar ellipsoids as hitherto supposed in this article. It is a well-known fact[1] that the stars of large proper motion show no concentration toward the Milky Way, but are distributed over the various galactic latitudes with very approximate uniformity. The meaning of this can hardly be other than that the equidensity surfaces for the smaller distances are spherical. The equipotential surfaces of the gravitational and centrifugal forces, in order to coincide with the equidensity surfaces, therefore must also be spherical for vanishing distances; hence the quotient (31) must approach 1.00. Now this is just what the values of the quotient given in Table VII do. The change in these values is therefore an encouragement toward an attempt at an improved theory rather than otherwise.

13. *Position of the sun relative to the center of the system.*—Before such an attempt can be made with any hope of success it will be necessary, however, to free the data from several imperfections. Foremost among these is the imperfection in the adopted position of the sun. The data used in what precedes rest on the assumption that the sun is at the center. It seems infinitely improbable that this should be the case. Our theory, crude though it necessarily must be, paves the way for overcoming this difficulty:

First, as seen from the sun, the center of the system must lie in a plane at right angles to the true stream-motion. Adopting for the vertex of the relative motion of the two streams $\alpha = 6^h 17^m$, $\delta = +11°9$, or gal. long. = 167°, gal. lat. = 0°, we find that the center, as seen from the sun, must lie in gal. long. 77° or 257°.

Second, nearly all astronomers who have dealt with the question, though from a very different point of view, agree in assuming for the center a *southerly* galactic latitude.[2]

---

[1] See for instance in *Verslag. Kon. Ak. v. Wetensch.*, Amsterdam, April, 1893, p. 137 (128).

[2] For instance, Struve, *Etudes d'Astronomie Stellaire*, pp. 61–62; Kapteyn, *Kon. Ak. Amsterd.*, April, 1893, p. 137; Hertzsprung, *Astronomische Nachrichten*, **196**, 207, 1914.

Third, Hertzsprung[1] from Cepheid variables finds the sun to be 38 parsecs north of the central plane of the Milky Way.

Fourth, the most difficult question probably will be that of the distance of the sun from the center. Still I think we can indicate a method which promises well.

For a first approximation, I start from the supposition, for want of a better one, that, even for the smaller distances, the *true* densities are as found in *Contribution* No. 188, which were derived on the basis of the erroneous assumption that the sun is the center. Further, for the moment, I will neglect the distance of the sun from the central plane of the Milky Way, which seems to be small.

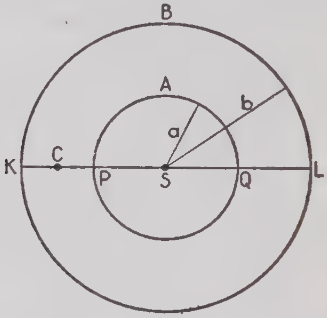

FIG. 2

In Figure 2, S represents the sun, C the center, and $CS=y$, the required distance. Let Δ_ρ represent the true star density at the distance ρ from the center. Now that we give up the erroneous supposition made in *Contribution* No. 188 and the present paper, we must consider the meaning of the densities given in Table VI of *Contribution* No. 188. What this table gives for a specified value of a (see Fig. 2) is in fact Δ', the average of the true densities at all points along the circumference PAQ around S with the radius a. This average will probably be not very different from the mean of the true densities at the points P and Q, and for the present, since our aim is only to arrive at a rough approximation, we will assume that it is exactly the case. Therefore, Δ being the true density,

$$\left.\begin{aligned}\Delta'_a&=\tfrac{1}{2}(\Delta_{y-a}+\Delta_{y+a})\text{ if }y<a\\ \Delta'_b&=\tfrac{1}{2}(\Delta_{b-y}+\Delta_{b+y})\text{ if }y>b\end{aligned}\right\}\qquad(32)$$

---

[1] *Ibid.*, p. 208.

If now, as a first approximation, we take as the true densities those obtained by formula (1) and assume in succession $y = 1500$, 1000, and 500 parsecs, we find values of Δ' corresponding to different values of a as given in Table IX.

Such a table then, or something like it, would have been obtained, instead of Table VI (lat. = 0°) of *Contribution* No. 188, if the center were actually at a distance y from the sun. Thus, if y were indeed 1500 parsecs, the considerations of *Contribution* No. 188 would have led to densities which, from distance *zero* up to distance somewhere near 1500 parsecs, would have increased. For $y = 1000$ we should still have found an initial increase, and even for $y = 500$ the same would have held. In this last case, however, the increase would have been so small that it might well have been overlooked owing to the errors of observation. Since in reality the observations lead to a regular decrease of the density throughout, I think we must conclude that y cannot have as high a value as 1500 or even 1000 parsecs. As an upper limit, we may take

TABLE IX

VALUES OF Δ'

a (Parsecs)	y in Parsecs		
	1500	1000	500
0	0.25	0.40	0.73
250	.26	.45	.865
500	.29	.49	.70
1000	.43	.59	.49
1500	.55	.43	.29
2000	.30	.245	.19
3000	.145	.115	.10
4000	.079	.062	.055
5000	0.044	0.039	0.035

$$y < 700 \text{ parsecs.} \tag{33}$$

We can also find a *lower* limit from the condition that the relative velocity of the two star-streams must not deviate greatly from the value of 40 km/sec. derived from observation.

In the neighborhood of the sun the linear rotatory motion of the system, that is, one-half the relative velocity of the star-streams, is $y\omega$.

If this velocity exceeded the circular velocity of a star at distance y from the center moving under the attraction of the whole system, the system certainly would not be in a steady state. Hence, on the assumption of a steady state,

$$y\omega < V_c, \tag{34}$$

or by formula (30)

$$y\omega < \sqrt{G\eta y}\,. \tag{35}$$

Assuming that inside ellipsoid II, η has everywhere the constant value 10.2×10^{-30}, we thus find, expressing results in kilometers, for

$y = 1000$ parsecs	$y\omega < 19.1$ km/sec.
700 parsecs	< 18.2 km/sec.
500 parsecs	< 16.5 km/sec.

If, therefore, we admit that $2y\omega$, the relative stream-velocity, cannot well be below 35 km/sec., we obtain as a lower limit

$$y > 600 \text{ parsecs} \tag{36}$$

The two limits (33) and (36) yield, as a first approximation,

$$y = 650 \text{ parsecs} \tag{37}$$

All these results agree fairly well in locating the center, as seen from the sun, at

$$\left.\begin{array}{lll} \text{Gal. long. } 77^\circ & \text{or} & \alpha = 23^h 10^m \\ \text{Gal. lat. } -3^\circ & & \delta = +57^\circ \\ \multicolumn{3}{l}{\text{Distance projected on galactic plane } = 650 \text{ parsecs}} \\ \multicolumn{3}{l}{\text{Distance projected at right angles to that plane } = 38 \text{ parsecs}} \end{array}\right\} \tag{38}$$

The principal remaining uncertainty is perhaps that for the galactic longitude, which instead of 77° might be 257°. Personally I am strongly in favor of adopting the former value, which is in good accordance with the investigations of Herschel, Struve, and myself already quoted. My own result[1] was

$$\alpha = 0^h, \quad \delta = +42^\circ.$$

The determination (38) lays claim to no accuracy. To improve it, it will be necessary to carry through a second, and perhaps a third and fourth, approximation, for the determination of the lower limit of y; besides, I think we may still improve or corroborate the values of the distance of the sun from the galactic plane.[1] Altogether, the location of the center would seem to be a laborious problem rather than one of great difficulty.

---

[1] *Verslag. Kon. Akad. Amsterdam*, January, 1893, p. 129.

There is, moreover, the possibility of a direct determination. Given sufficient data on numbers of stars and proper motions for the regions around galactic latitude 0° and longitudes 77° and 257°, there would be no difficulty in deriving separately the star-densities at different distances from the sun in these regions. If there is truth in the above theory, these densities must *increase* with the distance up to distance y, in the direction *toward* the center, whereas in the opposite direction they must decrease with increasing distance. The two solutions together must yield a rather crucial test of the whole theory.

14. *Further defects. Separate treatment of the different spectral types.*—There are several further defects in the solution of the present paper. I will enumerate those that occur to me:

a) In the investigation on which the present paper is based the average parallax, as a function of magnitude and proper motion, has been taken from *Groningen Publication*, No. 8. At the present moment we have already available, though not yet published, much improved values, especially for the very small proper motions.

b) The value of $\overline{u^2}$ is not the very best that could have been obtained.

c) The values of G in Table III have been computed on the supposition that the average mass of a star is independent of the distance, whereas later, in section 8, it was found that this is not the case.

d) In this same computation for G, it was further assumed that the attraction of the whole of the system outside ellipsoid X on an internal point is zero. Though reasons were given for admitting that this attraction is small, it may not be negligible. Since according to what precedes it is highly improbable that the equidensity surfaces within X, as well as without, are really similar ellipsoids, the whole computation for G will have to be revised in a more definitive treatment.

---

[1] Furthermore the distance of the center from the sun, as here found, is so small that, if special attention is given to the matter, it may not be hopeless to get evidence of the curvature of the stream-lines, particularly for the rather distant stars (faint stars having small proper motion).

e) The present solution is for all the stars together, that is, for a very heterogeneous collection of stars.

Only the last point is of fundamental importance, and I will devote a few lines to it. Just as in the higher, very attenuated parts of an atmosphere, where the molecular encounters become relatively rare and the different gases are, as it were, sorted out, so among the stars we must expect that the different spectral classes will show different arrangements in space, owing to the different values of $\overline{u^2}$ and η (mass) peculiar to these classes. The two cases are not identical, owing to the stream-motion in the stellar system, which is not supposed to exist in the atmosphere. Still there must be analogy. So, to take an extreme example, if there exists a class of stars for which $\overline{u^2}$ is zero, these stars, according to the present theory, would be confined exclusively to the central plane of the galaxy. For evidently a star not in that plane could not have pure stream-motion; that is, it could not move in a perfect circle around the axis and perpendicular to it, because the attractive force of the system on such a point does not lie in that plane. Therefore it would necessarily have a peculiar motion.

This simple consideration makes us understand at once the otherwise astonishing fact that the Wolf-Rayet stars lie with such close approximation in the central plane of the Milky Way. In the present theory this means simply that they can have no other than pure stream-motion (possibly with some peculiar motion *in* the plane of the Milky Way[1]). We thus realize that for the several classes of spectra there must be a very intimate connection between the values of $\overline{u^2}$ and η on the one hand, and the well-known differences in concentration toward the galaxy on the other.

Such considerations show that for the totality "all stars together" the value of $\overline{u^2}$ will doubtless change with the position in space and in particular with the distance of the stars from the plane of the Milky Way. The present investigation, therefore, suffers from the defect that this circumstance was neglected, $\overline{u^2}$ having been taken the same for the whole of the system. I think that this shows sufficiently the absolute necessity of treating the different spectral classes separately.

---

[1] It is noteworthy that, provided the peculiar motion *in* the Milky Way is also *zero* (as it must be when the Maxwellian distribution holds for this limiting case), the parallax of these stars becomes a pure function of the linear velocity, that is, of the quotient, radial velocity divided by sin λ, λ being the angular distance, star-apex.

For such a treatment the necessary data are not yet available, or at least not available in a satisfactory form. Fortunately, however, there exist at present instruments capable of dealing successfully with difficulties which, not so long ago, would have been insurmountable. With their aid we may hope to obtain material for several spectral classes separately, little or not at all inferior to what has already been obtained for the stars as a whole. I think that the determination of the spectral class for some 1000 stars of magnitudes 11 to 12, well distributed over the sky and for which the proper motion is either already sufficiently well known, or may be determined by taking a few additional photographic plates, will go far toward supplying us with what is so urgently wanted.

APPENDIX

Formulae for the computation of the attraction of a homogeneous revolution ellipsoid, of unit density (1 star per cubic parsec), on an exterior point.

Take the axis of revolution as X-axis and let the xy-plane contain the attracted point whose co-ordinates are α and β. Let A and B be the axes of the ellipsoid, the first coinciding with the axis of revolution, and let X and Y represent the components of the required attraction, Z being zero. Then from the well-known formulae,[1] if we put

$$\lambda^2=\left(\frac{B}{A}\right)^2-1 \tag{h}$$

$$K=\frac{2K}{\lambda^3}\left(\frac{B}{A}\right)^2 \tag{k}$$

$$p=\lambda\frac{A}{A'}, \tag{l}$$

---

[1] I have used the formulae as given by Duhamel, *Cours de mécanique*, V, 1, pp. 321 and 318.

where, if $\alpha=0$, A' is obtained from

$$A'=\sqrt{\beta^2-A^2\lambda^2} \tag{m}$$

and if $\beta=0$, from

$$A'=\alpha. \tag{n}$$

For other values of α and β we may write

$$E^2=\frac{\lambda^2}{2}-\frac{\alpha^2+\beta^2}{2A^2} \tag{o}$$

$$\eta=\lambda\frac{\alpha}{A} \tag{p}$$

$$\left(\frac{A'}{A}\right)^2=-E+\sqrt{E^2+\eta^2} \tag{q}$$

With these auxiliary quantities we find

$$X=-\alpha K\phi\ (p), \tag{r}$$

$$Y=-\beta K\omega\ (p), \tag{s}$$

in which $\phi(p)$ and $\omega(p)$, or rather their logarithms, have been tabulated in Table X by means of the formulae

$$\phi(p)=2[p-\text{arc tan } p] \tag{t}$$

$$\omega(p)=\text{arc tan } p-\frac{p}{1+p^2} \tag{u}$$

TABLE X

VALUES OF LOG ϕ (p) AND LOG ω (p) ACCORDING TO FORMULAE (t) AND (u)

p	Log ϕ	Log ω	p	Log ϕ	Log ω	p	Log ϕ	Log ω
0.000	$-\infty$	$-\infty$	0.05	5.920^{-10}	5.920^{-10}	0.5	8.861^{-10}	8.804^{-10}
1	0.824^{-10}	0.824^{-10}	6	6.157	6.156	0.6	9.076	8.997
2	1.727	1.727	7	6.358	6.357	0.7	9.252	9.149
3	2.255	2.255	8	6.531	6.530	0.8	9.399	9.272
4	2.630	2.630	9	6.685	6.682	0.9	9.524	9.372
5	2.921	2.921	10	6.821	6.819	1.0	9.633	9.455
6	3.158	3.158	11	6.945	6.942	1.1	9.728	9.525
7	3.359	3.359	12	7.058	7.054	1.2	9.812	9.585
8	3.533	3.533	13	7.161	7.157	1.3	9.886	9.635
9	3.687	3.687	14	7.257	7.252	1.4	9.954	9.679
10	3.824	3.824	15	7.346	7.341	1.5	0.015	9.717
11	3.948	3.948	16	7.430	7.423	1.6	0.070	9.750
12	4.061	4.061	17	7.508	7.500	1.7	0.121	9.780
13	4.166	4.166	18	7.581	7.573	1.8	0.168	9.806
14	4.262	4.262	19	7.651	7.642	1.9	0.211	9.828
15	4.352	4.352	20	7.717	7.707	2.0	0.252	9.850
16	4.436	4.436	21	7.779	7.768	2.1	0.289	9.869
17	4.515	4.515	22	7.839	7.827	2.2	0.325	9.885
18	4.590	4.590	23	7.896	7.882	2.3	0.358	9.900
19	4.660	4.660	24	7.950	7.935	2.4	0.389	9.914
20	4.727	4.727	25	8.002	7.986	2.5	0.418	9.927
21	4.790	4.790	26	8.052	8.035	2.6	0.446	9.939
22	4.851	4.851	27	8.100	8.081	2.7	0.472	9.950
23	4.909	4.909	28	8.146	8.126	2.8	0.497	9.960
24	4.964	4.964	29	8.190	8.169	2.9	0.521	9.969
25	5.018	5.017	30	8.233	8.210	3.0	0.544	9.977
26	5.069	5.068	31	8.274	8.250	3.1	0.566	9.985
27	5.118	5.118	32	8.314	8.288	3.2	0.587	9.993
28	5.165	5.165	33	8.352	8.325	3.3	0.607	0.000
29	5.211	5.211	34	8.390	8.361	3.4	0.626	0.006
30	5.255	5.255	35	8.426	8.396	3.5	0.645	0.012
31	5.298	5.297	36	8.461	8.429	3.6	0.663	0.018
32	5.339	5.339	37	8.495	8.461	3.7	0.680	0.023
33	5.379	5.379	38	8.528	8.493	3.8	0.697	0.028
34	5.418	5.418	39	8.560	8.523	3.9	0.713	0.033
35	5.456	5.455	40	8.591	8.552	4.0	0.728	0.038
36	5.492	5.492	41	8.621	8.581	4.1	0.743	0.042
37	5.528	5.528	42	8.651	8.609	4.2	0.758	0.046
38	5.563	5.563	43	8.680	8.635	4.3	0.772	0.050
39	5.597	5.596	44	8.707	8.662	4.4	0.786	0.054
40	5.630	5.629	45	8.735	8.687	4.5	0.799	0.057
41	5.662	5.661	46	8.761	8.712	4.6	0.812	0.060
42	5.693	5.693	47	8.787	8.736	4.7	0.825	0.064
43	5.724	5.723	48	8.813	8.759	4.8	0.837	0.067
44	5.754	5.753	49	8.837	8.782	4.9	0.849	0.070
45	5.783	5.782	0.50	8.861	8.804	5.0	0.861	0.072
46	5.812	5.811						
47	5.840	5.839						
48	5.867	5.866						
49	5.894	5.893						
0.050	5.920	5.920						

LEIDEN
September 1921

Contributions from the Mount Wilson Observatory, No. 231
Reprinted from the *Astrophysical Journal*, Vol. LV, pp. 370–379, 1922

EFFECTIVE WAVE-LENGTHS OF 129 STARS WITHIN $0\overset{\circ}{.}5$ OF THE NORTH POLE AND OF THE Σ COMPANION OF POLARIS

By EJNAR HERTZSPRUNG

ABSTRACT

Effective wave-lengths, color indices, and magnitudes of 129 stars within $0\overset{\circ}{.}5$ of the North Pole.—The results of measurements of about 500 images on 12 plates (Lumière Σ) taken in 1912 with the 60-inch reflector and a grating whose constant was 6 mm, are given in Table II. In determining the effective wave-length λ_{eff}, corrections were made (1) for diameters differing from the normal diameter 0.10 mm and (2) to reduce to zenith transmission. For each star the effective color index I_λ was obtained from λ_{eff} by use of the formula: $I_\lambda = 0.005(\lambda_{\text{eff}} - 4216 \text{ A}) = 19.721(\lambda_{\text{eff}} - 1.069 \text{ mm})$. The star, *Harvard Annals*, 48, No. 85, is probably wrongly included in the series of red stars of the North Polar Sequence. For the Σ *companion to Polaris*, I_λ was found equal to $+0.11 \pm 0.07$, which corresponds to a spectrum of type A0 to A5.

Relation between effective color-index and the color-index of Seares.—For 76 stars both I_λ and I_{MW} (the difference between photovisual and photographic magnitudes) were available for comparison. It was found that $I_\lambda = (0.90 \pm 0.05) I_{MW} - (0.10 \pm 0.05)$, a very satisfactory result.

Relation between photographic magnitude and diameter of image was found to be: $m = \text{Const.} - 34d + 35d^2$, for d between 0.05 and 0.30 mm.

During my stay at Mount Wilson in 1912 the plates of the North Polar region listed in Table I were taken with the 60-inch reflector for the determination of effective wave-lengths.[1] Lumière Σ plates were used. The focal length of the instrument is 7606 mm and the grating constant was exactly 6 mm.

The co-ordinates of the center of the field are given in the system of *Harvard Annals*, 48, 21, Table VI, sixteenth and seventeenth columns. The efficiency of each plate is indicated by the photographic magnitude of stars whose central image has a diameter of one-tenth of a millimeter. The total number of images measured is somewhat greater than that used in the present note because some stars showing only very faint images were finally rejected. The effective wave-lengths of hazy images were given half-weight. The mean weight-factor of a plate, which is given in the last column of Table I, may therefore be taken as a measure of the mean quality of the images. The quality 0.50 thus means that all images of the plate were given half-weight.

---

[1] Compare *Mt. Wilson Contr.*, Nos. 100, 101; *Astrophysical Journal*, 42, 92, 111, 1915.

TABLE I

Photographs of the North Pole

Plate No.	Date 1912	Aperture (inches)	Sidereal Time at Middle of Exposure	Exposure Time (min.)	Co-ordinates of Center of Field		Efficiency of Plate	Number of Images Measured	Quality of Images
					x	y			
4	July 19	60	$20^h\ 5^m$	60	−480″	+ 70″	$14^m.8$	32	0.64
5		40	22 23	95	−520	+ 30	14.6	108	.70
6		40	23 26	9.5	−510	+ 50	12.0	15	.83
10	July 20	40	21 1	9.5 3	−180 −350	+ 50	11.9 10.9	29	.83
11		40	22 36	95	−190	+ 50	14.6	112	.69
14	July 21	40	18 16	31.3	+ 10	+140	13.3	44	.50
15		40	19 15	30	− 40	+ 90	13.7	34	.56
16		40	19 53	10, 5 1, 0.3	−60, +20 +120, +190	+ 60	12.7, 11.7 10.7, 9.7	27	.52
17		60	21 48	60	−200	+ 30	14.9	23	.50
204	September 14	40	21 7	6	−120	− 10	11.6	14	.79
205		40	21 43	60	− 80	− 50	13.8	44	.56
206		40	22 29	19	− 60	− 70	12.7	29	0.83

The diameter of the field measured was 1150″ when the full aperture was used, and 2500″ when the mirror was diaphragmed down to 40 inches. The plates were measured and reduced at Potsdam. At the same time a series of plates of the Pleiades has been discussed, which afford 9972 effective wave-lengths. This last material has been used for a more thorough determination of the variation of the effective wave-length with the intensity of the image. The effective wave-lengths were measured in millimeters by moving the plateholder with a micrometer screw and reading to $\frac{1}{2}\ \mu$. The diameter of the central image of the star was taken as a measure of the intensity of the spectra of first order. As normal strength that shown when the diameter of the central image is 0.1 mm or 100 μ was chosen. For other diameters of the central image the following corrections to the normal diameter were found:

Diameter of central image $d=$	0.05	0.06	0.07	0.08	0.09	0.10 mm
Correction to $d=0.10$ mm	+13	+10	+7	+4	+2	+0 μ

0.11	0.12	0.13	0.14	0.15	0.16	0.17	0.18	0.19—0.24 mm
−2	−3	−4	−5	−6	−6	−7	−7	−7μ

No conspicuous difference in the corrections for stars of different effective wave-lengths was noted.

These corrections were also used in reducing the effective wave-lengths given in the present note. The correction required to reduce the effective wave-lengths to the zenith owing to selective extinction of light in the earth's atmosphere amounts to -23 A or $-6\ \mu$ for the North Polar region as seen from Mount Wilson.

To convert the effective wave-lengths expressed in millimeters into Angstrom units they must be multiplied by 3944.2. It will be more convenient for comparison with determinations of the difference between photographic and visual magnitudes, however, to transform the effective wave-length measured in mm directly into the equivalent values of color index.

I have found that a difference of 1^{M} in the color index in the system of I_H of the Göttingen Actinometry, Part B, corresponds nearly to a difference of 200 A in the effective wave-length. By adopting this and comparing the color indices I_H of stars occurring in the Göttingen Actinometry with their effective wave-lengths on other plates taken with the 60-inch reflector it was found that $I_H=0$ corresponds to an effective wave-length of 1.069 mm or 4216 A. Hence, indicating the color index calculated from the effective wave-length by I_λ, we have

$$I_\lambda=\tfrac{1}{200}(\lambda_{\mathrm{eff}}-4216\ \mathrm{A})=19.721(\lambda_{\mathrm{eff}}-1.069\ \mathrm{mm})$$

The accuracy of the effective wave-length varies with the intensity of the image. Different weights were therefore assigned to the effective wave-lengths, according to the diameter of the central image. These weights were decreased for images which were not of normal strength, because of the uncertainty of the reduction of the effective wave-length to $d=0.10$ mm, which may vary with the quality of the image. The following weights of I_λ were finally adopted for different values of the diameter d of the central image.

$d=$	0.05	0.06	0.07	0.08	0.09	0.10	0.11	0.12	0.13 mm
$1/\lambda_2(I_\lambda)=1/(\mathrm{m.e.})^2$	2	4	8	18	28	38	48	56	58

$d=$	0.14	0.15	0.16	0.17	0.18	0.19	0.20	0.21	0.22	0.23	0.24 mm
$1/\lambda_2(I_\lambda)=1/(\mathrm{m.e.})^2$	52	44	36	28	22	16	12	8	6	4	2

For example, for $d=0.19$ mm, the adopted weight is 16, corresponding to a mean error in the color index I_λ of $\pm\sqrt{1/16}=\pm 0.25$. As stated above, for bad (hazy) images these weights were divided by 2. In fact the North Polar plates here employed are perhaps the poorest I took at Mount Wilson.

The results are given in Table II. The first column contains the number of the star taken from the *Harvard Annals*, **48**, 21, Table VI, and the second, the number of the North Polar sequence. The third column gives the photographic magnitude as derived from my estimates of the diameter of the central image. These magnitudes, according to which the stars have been arranged in the table, are only approximate. No correction for distance from the center of the field has been applied. The scale of Seares[1] was taken as a standard. The following relation between magnitude and diameter d of the central image was found.

d=				0.04	0.05	0.06	0.07	0.08	0.09 mm
m+plate constant=				16.0	15.9	15.8	15.5	15.2	14.8
0.10	0.11	0.12	0.13	0.14	0.15	0.16	0.17	0.18	0.19 mm
14.6	14.3	14.0	13.8	13.6	13.3	13.1	12.9	12.7	12.5
0.20	0.21	0.22	0.23	0.24	0.25	0.26	0.27	0.28	0.29 mm
12.2	12.0	11.9	11.6	11.5	11.4	11.2	11.0	10.9	10.7

The fourth column contains the color index I_λ as derived from the effective wave-length, and the fifth column, its weight, i.e., the reciprocal square of the mean error. The sum of the weights of I_λ for all 129 stars is 10,281. The sixth column gives the number of images used, respectively, for the estimation of magnitude and for the determination of effective wage-length.

Of special interest is a comparison of I_λ with the color index of Seares[2] which is defined as the difference between the photographic and the photovisual magnitude

$$I_{MW}=m_{Pg}-m_{Pv}.$$

This comparison has been made in the following way. In Table II there are 77 stars for which both I_λ and I_{MW} have been deter-

---

[1] *Mount Wilson Contr.*, No. 97, Table IX; *Astrophysical Journal*, **41**, 206, 1915.

[2] *Loc. cit.*

TABLE II

Colors of the North Polar Stars

No.		m_{Pg}	I_λ	$p(I_\lambda)$	n_m, n_λ
H.A. 48	N.P.S.				
420	10	9.48	+ .03	66	8,5
356		10.37	− .03	30	3,2
101	13	10.59	+ .21	173	7,6
386	14	10.89	+ .35	240	12,10
184	7*r*	11.03	+ .93	293	12,10
350		11.09	+ .22	252	13,11
195	8*r*	11.10	+ .83	24	2,2
227	5*s*	11.23	+ .90	300	14,12
197	15	11.26	+ .17	271	12,11
419		11.40	+ .40	44	3,3
309		11.44	+ .27	144	8,7
75	6*s*	11.46	+ .65	255	12,11
62		11.57	+ .70	71	3,3
408	16	11.63	+ .15	209	9,8
282	17	11.85	+ .61	76	4,4
430		12.13	+ .71	57	3,3
67	9*r*	12.2	+1.28	6	1,1
320	18	12.32	+ .21	183	12,10
85	10*r*	12.62	+ .30	174	9,9
225	7*s*	12.66	+ .39	206	14,11
268	19	12.75	+ .25	194	10,9
494		12.83	+ .66	107	6,5
57		12.93	+ .43	124	9,8
302	20	12.94	+ .23	179	10,9
362		13.05	+ .54	158	8,7
219	11*r*	13.20	+1.11	201	10,9
427		13.24	+ .96	91	7,5
262		13.4	+ .56	32	2,2
234	23	13.44	+ .35	190	8,8
479		13.44	+ .51	88	5,5
489		13.45	+ .14	98	4,4
451		13.48	+ .45	83	5.5
292	22	13.52	+ .44	144	6,6
174		13.54	+ .52	105	5,5
248	21	13.57	+ .79	144	6,6
389		13.70	+ .60	116	5,5
151		13.79	+1.01	194	7,7
103		13.8	+ .81	58	1,1
436		13.82	+ .39	59	4,4
172		13.84	+1.21	144	5,4

TABLE II—*Continued*

No.		m_{Pg}	I_{λ}	$p(I_{\lambda})$	n_m, n_{λ}
H.A. 48	N.P.S.				
426		13.90	+ .32	95	4,4
25		14.0	+1.00	56	1,1
34		14.0	+ .05	28	1,1
300	12*r*	14.00	+1.17	149	5,5
279	24	14.04	+ .36	116	5,5
345		14.08	+1.50	141	5,5
90		14.12	+1.23	129	5,4
127		14.13	+ .66	168	6,4
243		14.15	+ .32	52	2,2
378		14.15	+1.07	116	4,3
146		14.17	+ .55	108	3,3
28		14.3	+ .15	24	1,1
33		14.3	+ .89	24	1,1
329		14.3	+ .88	115	4,4
134		14.33	+ .41	141	6,6
263	25	14.35	+ .30	117	6,6
319		14.38	+ .62	26	4,2
424		14.4	+ .39	48	2,1
131		14.43	+ .72	62	3,2
281		14.45	+ .38	80	4,4
332		14.45	+ .56	76	4,3
403		14.45	+ .22	67	2,2
142		14.47	+ .57	86	3,2
152		14.48	+ .67	162	6,4
176		14.48	+ .36	140	6,5
230		14.53	+ .78	90	3,3
401		14.53	+ .96	67	3,2
256		14.55	+ .75	142	4,4
191	8*s*	14.56	+ .66	148	5,4
13		14.6	+1.12	19	1,1
14		14.6	+1.08	38	1,1
327		14.6	+ .68	76	2,2
437		14.6	+1.10	19	1,1
439		14.6	+ .88	38	1,1
459		14.6	+1.30	19	1,1
480		14.6	+ .63	19	1,1
391		14.64	+ .52	64	5,3
265	9*s*	14.68	+ .86	128	4,4
154		14.7	+ .18	33	2,2
288	26	14.73	+ .85	66	3,3
60		14.8	+ .83	28	1,1
86		14.8	+ .38	28	2,2
105		14.8	+ .58	66	3,3
107		14.8	+1.36	28	2,2
111		14.8	+ .49	42	2,2

TABLE II—*Continued*

No.		m_{Pg}	I_λ	$p(I_\lambda)$	n_{m}, n_λ
H.A. 48	N.P.S.				
125		14.8	+ .57	61	3,3
175		14.8	+ .31	42	2,2
333		14.8	+1.06	28	1,1
336		14.8	+1.05	28	2,2
338		14.8	+ .83	42	2,2
342		14.8	+ .19	28	2,2
348		14.8	− .41	14	1,1
226		14.85	+ .51	94	4,4
74		14.9	+ .90	28	2,2
324	27	14.97	+ .80	56	3,3
192		14.98	+ .37	56	4,4
88		15.0	+ .66	23	2,2
130		15.0	+ .65	51	3,3
140		15.0	+1.06	65	3,3
283		15.0	+1.28	23	2,2
311		15.0	+ .14	37	2,2
159		15.08	+ .43	65	4,4
158		15.12	+ .63	55	4,4
190	28	15.15	+ .75	50	4,4
334		15.15	+ .80	18	2,2
132		15.2	+1.25	18	1,1
306		15.2	+ .53	18	2,2
341		15.2	+ .91	27	2,2
323	10*s*	15.27	+ .56	36	3,3
196		15.30	+ .65	36	4,4
139		15.35	+1.72	13	2,2
193		15.35	− .04	17	2,2
277		15.35	+ .62	13	2,2
254	11*s*	15.38	+ .65	35	4,4
215		15.40	+1.50	44	4,4
126		15.43	+1.04	8	3,2
165		15.45	+ .43	13	2,2
163		15.5	+ .76	4	1,1
201		15.5	+ .19	11	2,2
205		15.5	+ .76	8	1,1
218		15.5	+1.12	12	2,2
358		15.5	+1.09	9	2,1
339	13*s*	15.6	+ .81	6	3,2
365	12*s*	15.65	+ .94	10	2,2
295		15.7	+ .28	4	2,1
164		15.90	+1.25	2	4,1
368		15.9	+1.28	2	1,1
212	29	15.95	+ .21	2	2,1
186		16.1	+ .57	2	1,1

mined. Of these the star 439, for which the photographic magnitude of Seares and consequently I_{MW} is uncertain, was omitted. Among the other 76 stars there are 40 for which the weight of I_λ is less than 90. These and the star 101 have been combined into means of 2 or more stars as follows: 420 and 101 (combined weight of I_λ 239); 195 and 282 (100), 319, 424, and 403 (141); 142 and 401 (153); 391 and 154 (97); 288 and 125 (127); 336, 338, and 342 (98); 324 and 130 (107); 283, 311, and 159 (125); 158 and 190 (105); 334, 341, 323, and 139 (94); 254, 215, 126, 163, 205, 218, 358, 339, 365, 295, 164, 368, 212, and 186 (148). Thus 35 single and 12 combined objects were available. These 47 objects are

TABLE III

m_m	I_{MW}	I_λ	I_λ O−C	m_m	I_{MW}	I_λ	I_λ O−C
10.08	+ .13	+ .16	+ 9	13.63	+ .60	+ .36	− 7
10.76	+ .44	+ .35	+ 2	12.90	+1.78	+1.50	0
10.42	+1.04	+ .93	+ 5	13.83	+1.04	+ .66	−17
10.82	+ .37	+ .22	− 5	13.44	+1.40	+1.07	− 8
10.58	+1.03	+ .90	+ 3	14.04	+ .96	+ .55	−20
11.06	+ .33	+ .17	− 6	13.83	+ .98	+ .88	+11
11.06	+ .65	+ .65	+13	13.98	+ .89	+ .41	−28
11.42	+ .39	+ .15	−13	13.84	+ .48	+ .30	− 3
11.42	+ .69	+ .66	+11	14.09	+ .82	+ .35	−28
12.08	+ .38	+ .21	− 5	14.16	+ .80	+ .67	+ 6
12.36	+ .51	+ .39	+ 2	14.12	+ .90	+ .74	+ 4
12.48	+ .41	+ .25	− 3	14.26	+ .81	+ .75	+14
12.76	+ .51	+ .23	−14	14.14	+ .71	+ .66	+13
12.72	+ .82	+ .54	−11	14.38	+ .72	+ .40	−13
12.64	+1.16	+1.11	+16	14.30	+ .90	+ .86	+17
12.67	+1.20	+ .96	− 3	14.45	+ .84	+ .72	+ 8
13.35	+ .50	+ .35	0	14.38	+ .89	+ .71	+ 3
13.12	+ .63	+ .44	− 3	14.58	+ .70	+ .51	0
12.90	+ .85	+ .79	+12	14.68	+ .81	+ .73	+12
13.20	+ .74	+ .60	+ 3	14.68	+ .81	+ .50	−11
13.15	+1.14	+1.01	+ 8	14.87	+ .62	+ .69	+26
13.04	+1.61	+1.21	−14	14.74	+1.00	+ .87	+ 9
13.58	+ .50	+ .32	− 3	14.86	+1.21	+1.02	+ 6
13.15	+1.38	+1.17	+ 3				

given in Table III, arranged according to the photographic magnitudes of Table II. The first column of Table III contains the mean of the photovisual and photographic magnitudes of Seares, m_m, which is independent of their difference I_{MW}. The material of Table III was treated according to least squares with the following result:

$$I_\lambda - 0.632 = \underset{\pm 0.054}{0.895}(I_{MW} - 0.810) - \underset{\pm 0.014\ \text{(m.e.)}}{0.015}(m_m - 13.128)$$

or written in another way

$$I_\lambda - 0.632 = 0.888(m_{Pg} - 13.533) - 0.902(m_{Pv} - 12.723).$$

The differences O−C between the observed and calculated values of I_λ are given in the last column of Table III. These differences do not show any distinct run, the number of changes in sign being 25, where we should expect 23±3.4 (m.e.). The linear formulae therefore represent the observations sufficiently well.

From the first of these formulae it is seen that there is no sensible magnitude equation between I_λ and I_{MW}, as the coefficient of m_m practically does not exceed its mean error. This result is perhaps the most satisfactory one of the present note. As described above, special care was taken to avoid a magnitude error in the values of I_λ. Although an error of this kind does not appear in the differences $m_{Pg} - m_{Pv}$ this does not prove that the scales for m_{Pg} and m_{Pv} are necessarily correct; but they must be parallel.

To say the least the values of I_λ do not indicate any such inequality between the two scales of Seares.

To $m_m = 13.128$ and $I_\lambda = 0$ corresponds $I_{MW} = +0.10 \pm 0.05$ (m.e.), although we have both intended to reduce our scale of color index to the same zero point. As the small disagreement found is only about twice its mean error its reality is not beyond question.

The mean square of the difference O−C in Table III is $0.0141 = (\pm 0.12)^2$. As this square is the sum of the squares of the mean errors of I_λ and I_{MW} the accuracy indicated is about what could be expected.

Considering the individual stars, it may be observed that the star 85, for which $I_\lambda = +0.30 \pm 0.08$ (m.e.), seems to be wrongly included with the *r* series (No. 10*r*), as it does not appear to be of deep color. My photographic magnitude 12.62 gives in connection with the photovisual magnitude 12.03 of Seares: $I_{MW} = +0.41$, corresponding to $I_\lambda = +0.29$, thus confirming the value found directly.

On September 14, 1912, a plate (No. 207) was taken with several exposures of the Pole star in order to determine the effective wave-length of its Σ companion 18″3 distant. From six images was found $I_\lambda = +0.11$ with weight 188, or a mean error of ±0.073. This value of I_λ corresponds to a spectrum of A0 to A5 of the Harvard classification. Recently F. C. Leonard (*Publ. Astr. Soc. of the Pacific*, 33, 215, 1921) has found the spectrum of the companion to be of class F0.

Leiden
November 12, 1921

Contributions from the Mount Wilson Observatory, No. 232
Reprinted from the *Astrophysical Journal*, Vol. LV, pp. 411–412, 1922

NOTE ON THE THICKNESS OF AIR REQUIRED TO PRODUCE THE ATMOSPHERIC ABSORPTION BANDS, A, *a*, AND B

By ARTHUR S. KING

ABSTRACT

Thickness of air required to give the absorption bands A, a, and B.—On a plate stained with dicyanin, the A and B bands were obtained when the light from a tungsten lamp traversed minimum thicknesses of only 7 and 40 meters respectively; and though the air was hot and dry, the water band *a* at λ 7200 was obtained with absorption of 9.5 meters. To give the bands A and B visually respectively twelve and five times greater thicknesses of air are required.

In the course of experiments on absorption spectra in which the light from a 900-watt tungsten lamp passed through a heated graphite tube and thence to a 15-foot concave grating spectrograph, it was noted that the A band at λ 7600 frequently appeared on the spectrograms. This band is ascribed to the absorption of oxygen in the atmosphere. A test with the furnace cold showed that the absorption was due to the air at room temperature. The distance traversed by the beam through the air in the laboratory and in the spectrograph was about 12 meters. As this air-path is much shorter than that usually regarded as necessary to produce this band, other distances were tried in order to find, if possible, the minimum thickness required to give A, and also under what conditions the companion band B near λ 6900 could be obtained.

Placing the lamp as near the slit as could be conveniently arranged gave an air-path of 9.5 meters. The A band was still fairly strong and evidently would appear with a path considerably shorter. A surprising feature was that the water-vapor band *a* at λ 7200 could be detected at this distance. It was just at the limit of visibility on spectrograms having a favorable density of the continuous ground. As a part of the air-path was in the spectrograph pit, a determination of the humidity was not attempted; but the experiments were made on a particularly dry day, a hot wind blowing from the Mojave desert, so that the water-content of the air, both in the laboratory and in the ventilated pit, must have been very low.

Changing the air-path to 19 meters strengthened both A and *a*, but B was still invisible. The light was then passed the length of the laboratory to a plane mirror and back to the spectrograph, a distance of 39.4 meters. B now appeared, extremely faint, but the structure of both branches of the band could nevertheless be made out. Both A and *a* were strongly developed.

To find how small a layer of air would give A, it was necessary to use a shorter-focus spectrograph, and a 1-meter concave grating was tried. This involved a greatly reduced scale and, as the component lines of the atmospheric bands produced in this way are very fine, the matter of photographic resolution became important. Finally, by using a fine-grained film stained with dicyanin, the A band was detected with an air-path of seven meters.

These minimum distances of seven meters for A and approximately forty meters for B are much shorter than those given by Liveing and Dewar,[1] who extended the earlier observations of Egoroff and Janssen. Their tests, however, were visual, and the red-sensitive plate is certainly far more effective for the observations of A; while in the B region the plate probably still has an advantage over the eye in the detection of faint objects, on account of the possibility of adjusting contrast and the strength of the continuous ground.

Liveing and Dewar found that 7 atmospheres pressure in a steel tube 18 meters long rendered A visible, while 18 atmospheres were required to show B. The same tube filled with pure oxygen at atmospheric pressure showed A, while two atmospheres of oxygen were needed for B to appear. From this observation, A should be discernible through 90 meters of air. Egoroff[2] observed it through 80 meters of air, or nearly twelve times the amount found necessary in the writer's experiments by the photographic method.

MT. WILSON OBSERVATORY
November 1921

---

[1] *Proceedings of the Royal Society*, 46, 222, 1889.

[2] *Comptes Rendus*, 101, 1143, 1885.

Contributions from the Mount Wilson Observatory, No. 233
Reprinted from the *Astrophysical Journal*, Vol. LV, pp. 380–390, 1922

ELECTRIC FURNACE EXPERIMENTS INVOLVING IONIZATION PHENOMENA

By ARTHUR S. KING

ABSTRACT

Furnace temperature required to obtain the subordinate series lines of the alkali metals in absorption.—With the central plug at about 2600°C, the stronger lines of both the first and second subordinate series of K, Cs, and Rb were readily obtained, while for Na, less than 2350° was required. The lines observed for each metal are listed. The temperature of the absorbing vapor may be taken as about 400° less than that of the plug.

Furnace absorption spectrum of iron vapor above 2800°C.—Using lower temperatures, no absorption lines had previously been obtained longer than λ 5507, but with a plug temperature above 3200°, practically all the high temperature emission lines were obtained in absorption, up to the end of the range photographed, λ 6700.

Furnace spectra of Ca, Sr, and Ba vapors mixed with more easily ionized elements, K and Cs.—*Flame lines* are not affected, but the *intensity of enhanced lines* was found to be decreased for both absorption and emission spectra, when the easily ionized vapor of K (4.3 volts) or of Cs (3.8 volts) was added, the effect being very marked for Ca (6.1 volts), somewhat less for Sr (reduction to one-third) and small for Ba (5.2 volts), while adding Na (5.2 volts) to Ba vapor produced no change. Evidently the *quenching effect* depends upon the relative ease of ionization of the two vapors. Temperatures of 1800–1830° were used.

Furnace temperatures required to obtain certain flame lines in absorption and in emission.—The lines λ 4227 (*calcium*), λ 4607 (*strontium*), and λ 5535 (*barium*) were obtained in absorption (tungsten lamp source) but not in emission (exposure 2 hours) at temperatures of 1275°, 1200°, and 1400°C respectively. This lag of emission over absorption may be partly due to the wideness of the lines, and is not noticeable for sharp *iron* lines.

Relation of furnace observations to Saha's theory of spectra.—The foregoing results verify Saha's predictions that the subordinate series of the alkalies could be obtained in absorption if sufficiently hot vapor were used, and that a gas too cool to emit light should still be able to absorb the lines of the principal series; and the results with mixed gases are such as would be expected if flame and enhanced lines are associated with neutral and ionized atoms respectively, as Saha assumes.

This paper gives the results of some experiments which bear on certain features of the theory recently advanced in a series of papers by M. N. Saha,[1] concerning the part which ionization may have in the production of certain types of spectral lines. The points tested are (1) the possibility of obtaining in absorption the lines of the subordinate series of the alkali metals, and in general, the conditions necessary for any type of lines to appear in absorption, (2) the effect, on lines presumed to be due to the ionized atom, of mixtures with elements having lower ionization potentials, and (3) whether, under given conditions of the metallic vapor, a line appears in absorption at a lower temperature than it can be obtained in emission.

---

[1] *Philosophical Magazine*, **40**, 472, 809, 1920; **41**, 267, 1921; *Proceedings of the Royal Society*, A, **99**, 135, 1921

The tube-resistance furnace offers special possibilities for an investigation of this sort by reason of the close control of the temperature and pressure. Absorption spectra also are readily obtained, either by the use of a diaphragm within the tube or by passing white light through the tube from an external source.

The special means of excitation employed will be described under each heading. The furnace chamber was usually pumped out to about 8 mm of mercury. The spectrograms were all made with the bright first order of a 15-foot concave grating, giving a scale of 3.7 A per mm.

I. ABSORPTION SPECTRA OF SODIUM, POTASSIUM, CAESIUM, AND RUBIDIUM

In his discussion of absorption spectra,[1] Saha notes that for these elements only the lines of the principal series have been obtained in absorption, the experiments with sodium having been by Wood[2] and those with potassium, caesium, and rubidium by Bevan.[3] Saha's explanation of the failure of the subordinate series to appear is that the temperature of the absorbing vapor was not high enough. In view of the writer's recent study[4] of the production in absorption of lines belonging to various temperature classes, this explanation seemed reasonable. The subordinate series of lines certainly require, in emission spectra, a stronger excitation than the lines of the principal series, and they should appear in absorption when the temperature is high enough to furnish a fairly large number of atoms capable of emitting the subordinate series lines. However, it was worth while to test this in the specific case of the alkali metals.

Sodium.—A trial of the furnace with sodium, operated as usual to give emission spectra, yielded at 2250° C and without prolonged exposure the pair λλ 5683–88 of the first subordinate series, and two pairs, λλ 5149–54 and 6155–61 of the second subordinate series, in addition to the widely reversed D lines. This showed that the production of the required atomic orbits was well within the range of the furnace.

---

[1] *Philosophical Magazine*, **41**, 267, 1921.

[2] *Astrophysical Journal*, **29**, 97, 1909.

[3] *Proceedings of the Royal Society*, A, **83**, 421, 1910; **85**, 54, 1911.

[4] *Mt. Wilson Contr.*, No. 174; *Astrophysical Journal*, **51**, 13, 1920.

In order to obtain the absorption spectrum, a plug of graphite was placed near the middle of the furnace tube. The spectrograph was set to give, in addition to the pairs above mentioned, those at λλ 4979–83, 4748–52, 4665–68, the plate thus including three members each of the first and second subordinate series. A plug temperature of 2650°–2700° gave distinctly in absorption all six pairs. A temperature of 2350°, however, sufficed to show the three pairs of the first or diffuse series and the strongest pair of the second or sharp series at λλ 6155–61. The absence of the weaker sharp pairs was probably due to their extreme narrowness at low temperature in a vacuum source, so that the absorption lines were below the limit of photographic resolution. Aside from this feature, the sharp and diffuse series appeared in absorption with equal ease.

The temperature of the absorbing vapor was necessarily much below that of the plug, about 400° lower, according to the experiments previously reported,[1] which have since been confirmed so often that this value may be considered a constant of the special experimental arrangement employed. This means that near the end of the heated portion of the tube there is a layer of vapor sufficiently cooler than the plug to absorb radiation from the latter. The present experiments thus indicate that sodium vapor at 2000° C or higher, with a sufficiently hot background, will absorb the lines of the two subordinate series.

Potassium.—A trial with a plug temperature of 2700° gave in absorption the stronger lines of the subordinate series groups near λλ 5800 and 5340. These consist in each case of one pair belonging to the first and one to the second series.

Caesium.—The absorption spectrum with caesium chloride in the furnace was photographed from λ 5400 to λ 7000. All but the faintest of the arc lines in this region were obtained in absorption for a plug temperature of 2600°. The absorption spectrum showed nine lines of the first subordinate series and five weaker ones which Saunders,[1] by reason of the constant differences occurring among them, considers to belong to the second subordinate series. The two groups are as follows:

---

[1] *Loc. cit.*

I		II
5466	6011	5746
5503	6213	5839
5635	6724	6034
5664	6974	6355
5845		6587

Three lines, given by Saunders as λλ 5847.8, 6217.6, 6983.8, and classed by him as satellites of adjacent strong lines, are visible also in the absorption spectrum. In the arc the lines which presumably belong to the second series are very unsymmetrical toward the red, while the absorption furnace in vacuum gives for each of these a narrow line at the extreme violet side of the position of the arc line. Dissymmetries occurring among the lines of the first series are also eliminated by the furnace. When the furnace spectrum is more completely photographed, with proper standards, a revision of the wave-lengths can be made and the character of the second series definitely settled.

Rubidium.—For this element also, there was no difficulty in obtaining in absorption nearly all of the lines given by the arc. In the range λ 5100 to λ 6400, the following lines of the first and second subordinate series showed as absorption lines, only the fainter members of the second series being absent:

I		II
5151	5648	5654
5196	5724	6071
5260	6207	6160
5363	6299	
5432		

While not bearing so directly upon the ionization theory as the foregoing, a series of experiments with the iron spectrum in absorption may be mentioned. In the previous investigation,[2] when the furnace was heated in vacuum with the plug at about 2600° C, no iron lines were obtained in absorption to the red of λ 5507, an effect probably due, as was explained then, to the high-temperature character of the iron lines in the yellow and red. Later experiments have extended this limit. The furnace, operated at atmospheric pressure, had its tube thinned in the central region to permit very high temperatures of the plug and to give a strong gradient in the portion of the tube containing the iron vapor. Plug temperatures above 3200° C, the highest reading of the pyrometer employed, were thus obtained. The spectrum was photographed to λ 6700, and gave in absorption practically all of the lines shown in emission by the furnace at high temperature.

---

[1] *Astrophysical Journal*, **20**, 188, 1904.

[2] *Loc. cit.*

The conclusion from these results is that a sufficiently high temperature of the absorbing vapor, and proportionately higher temperature of the incandescent background, give in absorption all lines which the furnace can emit, and experience has shown these to include probably all lines not requiring conditions similar to those of the spark discharge.

This condition, which is an obvious consequence of the difference in excitation required to produce different groups of lines in the same spectrum, is enunciated by Saha to the effect that in order to reverse a given set of lines, it is not sufficient to send a beam of white light through a cooler layer of the vapor, but that "in the atoms present, there should be a fairly large number with orbits corresponding to the first term of the pulse of radiation to be absorbed. Thus in order that lines ($2p$–md) may be absorbed (as those of the subordinate series of the alkalis), we must have a sufficient number of atoms with ($2p$) orbits."[1]

2. EFFECT OF MIXTURES OF ELEMENTS HAVING DIFFERENT IONIZATION POTENTIALS

In the writer's studies of electric furnace spectra, it has been noted repeatedly that a mixture of substances may be vaporized without any suppression of the spectrum of one by reason of the presence of the others. In contrast with the arc containing such a mixture, each vapor appears to give its spectrum as if it were alone.

---

[1] *Op. cit.*, p. 277

No evidence against this view has been found as regards the great majority of the lines emitted by the furnace. These lines, according to the modern view, are emitted by various electron orbits of the "normal atom," that is, an atom which is not ionized through the removal of one or more electrons. The furnace is capable, however, of emitting, in general rather faintly, some of the enhanced lines, which are regarded as due to the ionized atom. For these lines, the degree of ionization is a determining factor, and this may be affected by conditions other than the temperature and pressure which are controlled in the furnace.

The calcium spectrum contains various series emitted by the normal atom, and also the enhanced lines H and K arising from the ionized atom. Designating the normal atom by Ca and the ionized atom and its lost electron by Ca^+ and e, respectively, Saha[1] states, "At a given temperature and concentration, a definite equilibrium will be established between the proportions of Ca, Ca^+, and e, as represented by the van't Hoff formula of reversible chemical action, $Ca \rightleftarrows Ca^+ + e$."

If then we add a large supply of electrons from some substance which becomes ionized more readily than calcium, fewer electrons from the calcium can exist in the free state, and the proportion of Ca^+ atoms becomes less, with a corresponding weakening of the H and K lines, relative to the lines of the normal atom. Since the ionizing potential of an element may be taken as the measure of its ionization under a given stimulus, a mixture of calcium with an element having a lower ionization, such as potassium, caesium, or rubidium, should alter the calcium ionization to an appreciable extent. A fairly crucial test of the basic assumptions of Saha's theory should thus be possible, and Dr. H. N. Russell has suggested to the writer that the control of conditions in the electric furnace affords an excellent means of applying the test. The following experiments were accordingly carried out for the spectra of calcium, strontium, and barium.

Calcium.—A temperature of about 1800° C was selected, which gives the H and K lines distinctly, and yet with intensities low enough to register easily any disturbance in the vapor producing them. The first experiments were with absorption spectra, which permit short exposures, during which there would be little change in the vapor within the tube. Instead of using a plugged tube, white light from a strong tungsten projection lamp was sent through the tube of the vacuum furnace. As the filament of the lamp was many hundred degrees hotter than the furnace tube, it could safely be assumed that the vapor in the highly heated portion produced the absorption, instead of that near the end as was evidently the case when a plug was used. The first mixture tried was calcium and potassium, whose ionization potentials are 6.08 and 4.32 volts, respectively. The absorption spectrum was first photographed with metallic calcium alone in the tube. The furnace was then recharged with a mixture of calcium and potassium chloride, and a second exposure made under the same conditions as the first. The quenching effect on the H and K lines was very distinct. With calcium alone, H and K appeared as absorption lines of moderate strength, comparable with some of the lines in the group of six near λ 4300 and in the series triplet λλ 4425–55. When calcium and potassium were vaporized together, scarcely a trace of H and K was to be seen, while the comparison lines due to the normal atom were practically unchanged. The nearly equal width of the strong flame line λ 4227 in the two exposures indicated that the density of calcium vapor was nearly the same in both cases. The experiment was repeated, the tube being wiped out before charging with the calcium alone, but the potassium was not entirely removed, as was shown by the presence of the violet potassium pair. H and K were thus somewhat weakened in the first exposure, but much more affected in the second with a large supply of potassium.

---

[1] *Proceedings of the Royal Society*, A, **99**, 139, 1921.

The comparison was repeated with a new tube and metallic potassium, instead of the chloride, for the second exposure. This eliminated a band structure in the H and K region which may have had some effect in the previous experiment. H and K were again much weakened with reference to the other calcium lines, though the narrower potassium lines showed that the metal did not give as effective a mass of vapor in the tube as was obtained with the chloride.

Experiments with emission spectra were next made, first with potassium chloride and then with caesium chloride, which were compared with calcium alone. The exposures were much longer, with resulting variations in the supply of vapor during the runs, but the effects observed for absorption were repeated, H and K being distinctly reduced in intensity when a mixture was used. As was to be expected, the effect of caesium, with an ionization potential of 3.81, appeared greater than that of potassium, but the effective quantities of the two may have been different, and at present it is desired to lay stress only on the general effect of a substance with lower ionizing potential.

Strontium.—The experiments with strontium were made first for the absorption spectrum with the chloride in the tube, at a temperature of 1860° C, then with a mixture of strontium chloride and potassium chloride. The enhanced lines λλ 4078 and 4216 were compared with the flame line λ 4607 and a group of strong furnace lines from λ 4722 to λ 4876, presumably due to the normal atom. As with calcium, the enhanced lines showed a decided effect from the mixture of potassium. λ 4078 was disturbed by a band spectrum, but λ 4216 was favorable for comparison, and relatively to the other lines, showed a reduction to not more than one-third of its former intensity. A repetition of the experiment, this time for the emission spectrum at 1830°, permitted both λ 4078 and λ 4216 to be observed. They were found to be weakened by the addition of potassium to approximately the same degree as in absorption. This tube was afterward used for the experiment with calcium alone and calcium with caesium in emission, mentioned in the preceding section. The stronger strontium lines persisted and the enhanced pair was much reduced by the addition of caesium.

Barium.—A series of experiments was made for the absorption spectrum of barium at λ 1830° C, using both barium chloride alone and also mixtures of either potassium chloride or caesium chloride. The enhanced lines λλ 4554 and 4934 were compared with λ 5535 and the strong furnace lines from λ 5778 to λ 6063. The effect on the enhanced lines was much smaller than with the corresponding lines of calcium and strontium, but a perceptible relative weakening of the enhanced pair followed the addition of both of the substances with lower ionizing potentials.

The ionization potential of barium is lower than that of strontium or calcium, being in fact halfway between potassium and calcium. This and the fact that the region occupied by the barium lines is not so favorable for the observation of absorption effects as the portion farther to the violet may be responsible in some measure for the smaller influence in the case of barium. A mixture with sodium vapor, whose ionization potential is almost exactly the same as that of barium, was tried and no effect whatever could be detected.

3. TEMPERATURES REQUIRED FOR THE INITIAL APPEARANCE OF A GIVEN LINE IN ABSORPTION AND IN EMISSION

It is desirable to extend the observations on this point much farther than has yet been possible, but the tests made on lines of a favorable type have given definite results, which will be reported here.

In his discussion of the radiation of the characteristic lines of the neutral atom,[1] Saha reasons that a mass of gas too cool to emit any light should still be able to absorb lines of the principal series. Further heating causes the atoms to progress toward ionization, and radiation will follow as a result of the mutual interchange of orbits. When the gas can emit the principal series rather strongly, it should absorb the lines of the subordinate series, a still higher temperature producing the latter series in emission.

The tests thus far made have been concerned with the question whether there is a temperature at which the principal series Ca λ 4227, Sr λ 4607, and Ba λ 5535 will appear in absorption and not in emission. The higher critical stage at which these lines are emitted and at which the subordinate series may show only in absorption has not yet been looked for.

The experimental arrangement provided a transition from absorption to emission conditions by simply turning off a 900-watt tungsten lamp, whose light was directed through the tube during the absorption exposure.

The exposures required for the absorption and the emission spectrograms were very different. For absorption one-half to one minute was sufficient to produce a continuous ground of the proper strength to show any absorption which was present. For the emission spectrum, it was a question of registering a very faint image, and a period of two hours was considered a fair time, in view of the power of the spectrograph, to show anything which the vapor could emit. Absorption spectra were photographed at the beginning and end of the emission run.

---

[1] *Proceedings of the Royal Society*, A, **99**, 140, 1921.

At 1275° C, λ 4227 of calcium appeared in absorption, 0.5 A in width, persisting as a well-defined absorption line at the close of a two-hour exposure for the emission spectrum, but the line failed to show in emission. At the same temperature, a very faint trace of λ 4607 of strontium could be seen as an emission line, but nothing whatever appeared in emission at 1200°, though at the latter temperature the absorption line λ 4607 was strong at the beginning and end of the period.

The barium line λ 5535 could be seen very faintly in emission at 1500°; but with the temperature held close to 1400°, at no time rising above 1440°, the line entirely disappeared. The absorption line was still strong at 1400°.

Some inherent difficulties must be recognized in tests of this sort. Lines such as the three just considered have, when plenty of the material is present, low photographic density and a considerable width, which features should make them appear in absorption under minimum excitation. The same characteristics retard their development through the threshold condition in emission. Lines which tend, when faint, to become very narrow, as is the case with the great bulk of furnace lines, hold up relatively better in emission than in absorption as the temperature becomes lower; since in absorption the very narrow line may disappear too soon by reason of failure of the spectrograph to produce the resolution of the continuous spectrum which enables an absorption line to be perceived. This fact, which with the narrow lines of the vacuum furnace would make the emission line in its early stages easier to see than the absorption line, may account for the fact that in the iron spectrum, emission and absorption spectra for the same temperature of the furnace are very nearly duplicates. While the series for iron are not known, the lines fall into definite temperature classes,[1] and the initial appearance of a line of certain type may be watched. An iron line in this sensitive state and with proportional exposures, shows as readily in emission at a given temperature as in absorption. This was tested through a range extending from the ultra-violet into the red. From the green into the red, it is somewhat easier, at a certain temperature, to be sure of the presence of a faint iron line in emission than in absorption. We may therefore say that the evidence thus far does not always favor the absorption method as a means of producing more numerous lines than are shown under equal excitation in emission, though the earlier appearance in absorption of principal series lines appears to take place in the spectra of calcium, strontium, and barium.

Mount Wilson Observatory
January 1922

---

[1] *Mt. Wilson Contr.*, No. 66; *Astrophysical Journal*, **37**, 239, 1913.

Contributions from the Mount Wilson Observatory, No. 234
Reprinted from the *Astrophysical Journal*, Vol. LVI, pp. 84–96, 1922

FURTHER EVIDENCE ON THE BRIGHTNESS OF THE STARS OF THE NORTH POLAR SEQUENCE

By FREDERICK H. SEARES AND MILTON L. HUMASON

ABSTRACT

Mount Wilson photographic and photo-visual scales of magnitude.—These scales were based wholly on plates made with the 60-inch reflector and as there was some question as to photographic magnitudes brighter than the tenth, and photo-visual magnitudes fainter than the eighth, *additional data* have recently been secured with the 10-inch Cooke refractor. Exposures both with and without a wire screen which absorbs 3.02 magnitudes were made on 54 plates. Taking the photographic magnitude of each star to be 0.19 C less for the 10-inch than for the 60-inch, where C is the color-index, and the photo-visual magnitude to be the same for both, the investigation reveals no appreciable error in the photographic scale and shows it to be homogeneous from the fourth to the fourteenth magnitude; and the slight correction of $+0^{\mathrm{M}}.05$ indicated for the photo-visual scale near the ninth magnitude is not confirmed by more reliable exposure-ratio results to be reported elsewhere. The original scales are therefore retained.

Revised magnitudes of stars of the Polar Sequence.—The plates also enable corrections to be given to the photographic magnitudes of 45 stars and to the photo-visual magnitudes of 28 stars. These average $\pm 0^{\mathrm{M}}.03$ and $\pm 0^{\mathrm{M}}.04$, respectively, for the two scales. The larger photographic corrections are in substantial agreement with those recently found at Greenwich by Jones.

The following pages summarize a recent investigation of the brightness of stars near the North Pole, undertaken in connection with the work of the International Commission on Stellar Magnitudes. Certain results of the earlier investigation[1] had not yet been fully confirmed by observations made elsewhere,[2] and, as the original measures had been wholly with the 60-inch reflector, it seemed desirable that additional data be secured with an entirely different instrument.

The question at issue related mainly to the photographic magnitudes of stars brighter than the tenth magnitude. From the tenth to the fifteenth or sixteenth magnitude there was evidence that the scale had been well determined; but between the sixth and tenth magnitudes there remained an unexplained difference of a quarter of a magnitude between the Harvard and Mount Wilson results.

---

[1] *Mt. Wilson Contr.*, No. 97; *Astrophysical Journal*, **41**, 206, 1915.

[2] Besides short series of measures by Parkhurst and Schwarzschild, King's results, *Harvard Annals*, **76**, No. 10, were in agreement with Mount Wilson. Jones's observations, *Monthly Notices*, **82**, 21, 1921, which are also in excellent agreement, appeared after the present investigation was begun.

Visual magnitudes of the stars of the Polar Sequence have been measured at the Harvard Observatory to the thirteenth magnitude. Besides these and the Mount Wilson photo-visual results published simultaneously with the photographic magnitudes in *Mt. Wilson Contribution* No. 97, there is no evidence bearing on the visual or photo-visual scale of the stars in the polar region fainter than the eighth magnitude. Further investigation of this scale was therefore also desirable.

The instrument used for the present investigation was the 10-inch Cooke refractor of 45 inches focal length, which represents a radical change in conditions as compared with the 60-inch reflector. Its relatively small aperture implies an entirely different relation between diffraction pattern and resulting photographic image of a star; its small focal length means minimized influence of atmospheric tremor; its large field results in small corrections for distance error (for a compact group of stars at least); while its large color equation presents an extreme example of the difference in the color-sensibility that may affect the instrumental equipment.

The reduced-intensity exposures were made with a wire screen absorbing about three magnitudes, placed in front of the objective. As usual, equal multiple exposures, arranged in a symmetrical sequence (for example: full aperture, screen, screen, full aperture), were made on each plate, the exposures for different plates ranging from 1 to 32 minutes in order that stars of widely differing brightness might be accurately measured.

The longer exposures for photographic brightness extend several magnitudes below the questionable portion of the scale. This greatly simplified the reductions; for since the photographic scale below the tenth magnitude may be accepted as reliable, the magnitudes in this region could be used to determine the absorption produced by the screen. Moreover, as will appear shortly, a series of photographs covering a wide range in exposure time affords a simple means of testing the homogeneity of the scale without actually calculating the magnitudes of individual stars. This calculation is eventually necessary, but it is convenient to see in advance if a divergence in scale is to be expected.

The photographs were taken and measured by Humason. For much of the calculation connected with their reduction we are greatly indebted to Miss Joyner. For the determination of the photographic scale 43 plates were available. The investigation of the photo-visual scale, which depends on only 11 plates, could be much abbreviated, since the results are supplemented by independent evidence obtained by combining the adopted photographic magnitudes with values of the color-indices derived by the method of exposure ratios. To restrict the labor as much as possible, only stars of the Polar Sequence were measured. Corrections for distance from the center of the plate were neglected, since the distances themselves are small. Only a few of the brighter stars are more than a degree or two from the Pole, and these were brought to the center of the plate by shifting the telescope before making the screen exposures.

The measurement of each photograph yielded two series of scale readings, one for full-aperture and one for screen exposure. These were first used to determine the screen constant and to test for homogeneity the scales of *Contribution* No. 97.

Since these scales refer to the color-system of the reflector, the individual magnitudes must be reduced to the system of the 10-inch refractor before they can be used with the latter instrument or compared with results obtained with it. The differences in the color-sensibility of different telescopes (together with the photographic plate) are of the same order as those in the visual color-perception of different observers. In careful work these instrumental peculiarities cannot be neglected, but in practice the data necessary for reduction to a normal system of color are usually lacking. It is not difficult to determine the relative color-equation of two instruments, but the second essential—the color of the star whose brightness is to be determined—is generally unknown, and the comparison of results obtained with different instruments then means little unless the relative color equations are small. In the present case, however, the colors of the stars are known.

The chief instrumental source of the color-equation lies in the violet and ultra-violet absorption occurring in the optical system. Since light of these colors plays little part in forming a photo-visual image, the relative color-equations for photo-visual magnitudes are much smaller than those for photographic, as long as the same brand of plate and the same filter are used. In the present instance we adopt provisionally for the reduction to the system of the 10-inch refractor[1]

$$m_{10}=m_{60}-0.19\,C \quad \text{(Photographic)} \qquad (1)$$

$$m_{10}=m_{60} \quad \text{(Photo-visual)} \qquad (2)$$

where m_{60} and C are magnitudes and color-indices given in *Contribution* No. 97. The resulting values of m_{10} are in the second column of Tables III and VI.

These magnitudes were plotted against the two series of scale readings (full-aperture and screen images, respectively) derived from each plate. In the ideal case of perfectly accurate magnitudes and no errors of observation, the plotted points would define two parallel curves, whose separations, measured parallel to the magnitude (ordinate) axis, would be equal to the value of the screen constant. Actually the behavior of the curves indicates the degree of homogeneity in the given scale. In the present case the photographic scale below the tenth magnitude is known to be substantially correct, and we should expect the curves in this region to be sensibly parallel. The screen constant is determined from this portion of the data.

Detailed results for the differences in the ordinates of the curves are given for individual plates in Tables I and II, omitting only those whose screen exposures show but one or two stars each. The first column indicates the ordinate (magnitude) of the full-aperture curve from which the distance between the curves was measured. The values of the separation for every half-magnitude are shown in the body of the tables in the form of deviations from an even three magnitudes. Thus the first value in Table I for plate 517, exposure 32 *m*, indicates a separation of 3.10 mag., measured

---

[1] Seares and Hubble, *Mt. Wilson Contr.*, No. 187; *Astrophysical Journal*, **52**, 8, 1920.

TABLE I

SCREEN CONSTANT, PHOTOGRAPHIC DATA

Mag.	32^m		16^m		8^m					4^m					2^m		
	517	525	508	509	479	493	494	495	496	478	489	490	491	492	477	485	486
9.0	....	....	....	....	+8	....	....	....	....	0	+2	−30	0	−15	0	−7	+8
9.5	....	....	+10	−5	+10	+23	+11	+20	+10	−2	0	−18	0	−8	−7	−4	+5
10.0	....	....	+6	−5	+10	+20	+10	+13	+7	+5	+2	−8	−3	−3	−4	−3	+2
10.5	....	....	+2	−5	+9	+16	+11	+8	+4	+12	+4	+3	0	0	−5	0	−3
11.0	....	+8	−1	−6	+10	+14	+14	+5	+1	+18	+4	+4	0	+3	−4	+5	−2
11.5	+10	+1	−5	−5	+10	+17	+20	+4	+6	+18	+2	+3	+6	+8	−1	0	−2
12.0	+4	−7	−5	−5	+10	+20	+20	+10	+10	+20	+5	0	+9	+13	+2	−4	−4
12.5	0	−16	−10	−1	+6	+17	+20	+14	+10	+16	+6	−4	+4	+14	+8	−5	−1
13.0	−2	−17	−9	−2	0	+10	+21	+16	+10	+4	+4	−4	+3	+9	....	−4	−1
13.5	−6	−16	−9	−4	0	+10	+4	+8	0	....	+3	+2	0	+2	....	....	....
14.0	+5	−8	−4	−7	−2	+10	+11	0	−2	....	....	....	....	....	....	....	....
14.5	+15	−4	0	−5	....	....	....	....	....	....	....	....	....	....	....	....	....
15.0	+20	−2	....	....	....	....	....	....	....	....	....	....	....	....	....	....	....
Mean	+6	−7	−2	−5	+7	+16	+14	+10	+6	+10	+3	−5	+2	+2	−1	−2	0
S.C.	−4	+9	+4	+7	−5	−14	−12	−8	−4	−8	−1	+7	0	0	+3	+4	+2

Mag.	2^m		1^m										No.	Mean(1)	Mean(2)
	487	488	476	481	482	483	484	510	511	512	513	514			
9.0	+4	0	0	+15	−18	−5	−12	+14	+22	−2	+5	+15	21	3.00	3.00
9.5	+3	0	+6	+11	−9	−2	−7	+14	+10	−3	+7	+13	27	3.03	3.02
10.0	+4	+1	+6	+7	0	0	−2	+9	−2	+2	+7	+18	27	3.04	3.02
10.5	+5	0	+6	+4	+1	+3	+2	+2	−11	−2	+9	+20	27	3.04	3.02
11.0	+8	−2	+4	0	0	+2	+2	+2	−11	−9	+4	+22	28	3.03	3.02
11.5	+10	−1	−4	−5	0	0	+2	+5	−13	−20	+2	+20	29	3.03	3.02
12.0	+13	+4	...	....	−2	0	+2	+4	−12	−23	−4	+22	27	3.04	3.03
12.5	+15	+10	...	....	....	+6	+2	....	....	....	....	....	21	3.05	3.04
13.0	+20	+15	...	....	....	...	....	....	....	....	....	....	18	3.04	3.02
13.5	....	....	...	....	....	...	....	....	....	....	....	....	13	3.00	2.98
14.0	....	....	...	....	....	...	....	....	....	....	....	....	9	3.00	2.97
14.5	....	....	...	....	....	...	....	....	....	....	....	....	4	3.02	3.05
15.0	....	....	...	....	....	...	....	....	....	....	....	....	2	3.09	3.12
Mean	+9	+3	+3	+5	−4	0	−1	+7	−2	−8	+4	+19	253	3.03	3.02
S.C	−7	−1	−1	−3	+6	+2	+3	−5	+4	+10	−2	−17	....	....	....

TABLE II

SCREEN CONSTANT, PHOTO-VISUAL DATA

Mag.	32^m			16^m				8^m				No.	Mean (1)	Mean (2)
	526	527	543	539	540	541	542	535	536	537	538			
9.0	+5	−11	−6	+6	−5	0	+4	−4	−14	+1	+2	11	2.98	2.98
9.5	+6	−15	−6	+4	0	+2	+6	−2	−4	0	+4	11	3.00	2.99
10.0	+5	−14	−9	+2	+7	+9	+4	+5	+7	0	+6	11	3.02	3.02
10.5	+5	−10	−14	+3	+10	+8	+4	+15	+13	+5	+10	11	3.04	3.04
11.0	+4	−5	−14	−1	+14	0	+8	+23	+20	+6	+7	11	3.06	3.05
11.5	+2	−1	−10	−6	+8	−6	+8	....	....	...	....	7	2.99	3.00
12.0	+2	0	0	...	....	...	...	....	....	...	....	3	3.01	3.06
12.5	+4	+2	+7	...	....	...	...	....	....	...	....	3	3.04	3.09
Mean	+4	−7	−6	+1	+6	+2	+6	+7	+4	+2	+6	68	3.02	3.02
S.C.	−2	+9	+8	+1	−4	0	−4	−5	−2	0	−4	....	....	....

from the point on the full-aperture curve whose ordinate is magnitude 11.5. For plate 508, on the other hand, the separation for the same ordinate is 2.95 mag.

Restricting our attention for the moment to the photographic scale (Table I), we note that the two values just given depend upon stars whose mean magnitudes are 11.5 and 8.5, respectively, those of the latter value having been reduced to an apparent brightness of 11.5 by the use of the screen. Were the magnitudes of these stars as given in *Contribution* No. 97 certainly dependable, the numbers 3.10 and 2.95 could be accepted at once as approximations for the screen constant. But since we assume the scale to be known only for stars fainter than magnitude 10, it follows that only values of the separation of the curves for ordinates 13.0 and fainter are available for the calculation of the constant.

We note, however, that the means of the quantities in each line of Table I, which are given in the last column but one under the heading "Mean (1)," are very nearly constant. There is no evidence of a progressive change, and this shows at once that the photographic scale of *Contribution* No. 97 is sensibly homogeneous, for, no matter what portion of this scale between the sixth and fifteenth magnitudes is used, we find appreciably the same value of the screen constant. Assuming the scale to be correct from the tenth magnitude downward, that between the sixth and tenth magnitudes must also be substantially correct. In the mean, the photographic data in Table I give the following result:

$$\left.\begin{array}{l}\text{Stars between mags. 6 and 10, } \Delta m=3.03 \text{ (207 values)}\\ \text{Stars between mags. 10 and 15, } \Delta m=3.02 \text{ (46 values)}\end{array}\right\} \qquad (3)$$

The value 3.02 mag. is therefore adopted for the screen constant. There is so little progressive change in the values of Mean (1) that the treatment of the photographic data reduces itself to a simple combination, arranged to diminish as much as possible the accidental errors in the individual magnitudes.

The agreement in the values of Mean (1) for the photo-visual results shown in Table II is nearly as satisfactory. The irregularities are a little larger and there seems to be a small progressive change, but the number of plates included in each mean is much smaller than in Table I. From all the data in Table II,

Stars between mags. 6 and 12.5, $\Delta m = 3.02$ (68 values) (4)

which is the same as the adopted constant found from the photographic data. We conclude, therefore, that the photo-visual scale is very nearly, if not quite, homogeneous; moreover, (4) shows that in the mean it is consistent with the photographic scale, and hence should be substantially correct. We shall examine the small progressive change in the values of Mean (1), Table II, in a later paragraph.

The individual values of Δm in both Tables I and II show the influence of appreciable systematic errors which are peculiar to a plate. The means for the separate plates shown at the bottom of the tables range from 2.92 to 3.19 (plates 512 and 514) and 2.93 to 3.07 (plates 527 and 535), respectively, with an average deviation of ±0.05 mag. This is only to be expected from observations which depend upon multiple exposures. Fluctuations in atmospheric conditions, the absorption of water vapor by the photographic film, and a variety of other factors combine to produce for each plate an effective value of the screen constant which differs more or less from the true value. The disturbance can be rendered accidental by increasing the number of plates, as in the present investigation, where its influence upon the adopted constant is very small.

The effect upon the magnitudes of individual stars will be more serious, however, unless special precautions are taken, for some of the stars appear on a few plates only. The difficulty can be avoided by reducing each plate with its effective constant; but we must first see whether this will modify the scale. This may be determined by applying to each value of Δm in each column the corresponding systematic correction in the last lines of Tables I and II, the corrections being the difference between 3.02 and the mean Δm for the plate in question. The horizontal means of the results thus found are given under the heading "Mean (2)," and represent what would have appeared under Mean (1), had the effective Δm for each plate been equal to 3.02. The revised values are sensibly the same as those of Mean (1), which shows that the scale will not be altered by reducing the individual plates with their effective constants. By so proceeding the errors in the individual magnitudes are appreciably diminished.

Since Table I gives no evidence of appreciable error in the photographic scale of *Contribution* No. 97, the determination of the magnitudes is a simple matter. It is only necessary to read from the full-aperture curves referred to above, with scale reading as argument, the magnitude of each star, subtracting the values of the effective constant from those interpolated with readings of images obtained with the screen. Since the effective constant cannot be determined when only one or two screen images appear, several photographs of bright stars were reduced with the mean constant 3.02 mag.

Each of the magnitudes thus found yields a correction to the corresponding magnitude given in *Contribution* No. 97. The results are summarized in Table III, which shows the mean correction derived from each group of plates, classified according to exposure time. The second column of the table gives the magnitude from *Contribution* No. 97, reduced to the color-system of the 10-inch refractor. The headings of the six following columns indicate the exposure and the number of plates in each group. The corrections in the body of the table are given separately for full-aperture (left-hand series) and screen exposures. The number of values included in each mean correction is usually the same as the number of plates in the group, except in the case of the 1-minute plates. For these the number varies from 1 to 24, with an average of 9. Individual corrections in excess of 0.3 mag., 4 in a total of 954, were rejected. The weighted means from all the data and the total numbers of values appear in the last two columns.

The corrections for stars 1, 4, 3*s*, and 1*r*, and for the faintest stars in the list are of relatively low weight. The largest among the corrections of high weight is −0.08 mag. The average deviation of a single magnitude is ±0.070 mag. The simple mean of the corrections based on five or more determinations is ±0.028 mag. The probable reality of the larger corrections is indicated by the agreement shown in Table IV with similar corrections found by

Jones,[1] the quantities in parentheses being the approximate relative weights within the respective series. There are only two cases of an actual difference in algebraic sign, which shows a close accordance between the recent Greenwich investigation and that reported here.

TABLE III

CORRECTIONS TO PHOTOGRAPHIC MAGNITUDES

Star	Pg. m_{10}	Exposure and Number of Plates						No.	Mean Corrn.
		32^m, 2	16^m, 2	8^m, 5	4^m, 5	2^m, 5	1^m, 24		
1	4.39	....	....	....	....	....	+ 7	4	+ 7
4	5.90	....	....	....	....	....	+14	4	+14
2s	6.43	....	....	+ 9	− 4	+ 4	− 2	25	+ 1
5	6.45	....	....	+ 6	−11	− 5	−10	20	− 5
3s	6.58	....	....	....	....	....	− 6	5	− 6
1r	6.32	....	....	....	....	....	+ 9	6	+ 9
6	7.10	....	+ 4	− 5	+ 1	+ 2	+14, 0	26	+ 2
7	7.43	....	− 8	− 5	+ 3	− 4	+ 8, + 4	36	+ 2
2r	7.64	....	+ 5	+ 3	+ 1	− 5	− 9, + 6	31	− 1
8	8.28	− 5	+10	+ 2	+10	0	+ 2, 0	34	+ 3
3r	8.69	0	+ 4	+ 5	+ 7	− 4	− 6, − 1	38	0
9	8.87	+10	+ 2	+ 3	+10, +14	+ 5, +10	+ 3, − 2	54	+ 5
10	9.11	+ 1	+ 8	0, +11	− 7, +10	− 4, + 6	− 2, − 4	57	+ 1
4r	9.04	− 6	−11	+11, − 5	+ 1	+ 3, + 2	+ 1, − 3	35	− 1
11	9.69	0	+ 9, − 6	+ 1, +10	− 3, − 1	+ 3, − 8	− 4	49	− 1
12	10.03	−14	+ 1, −10	− 5, 0	− 8, − 8	− 3	− 2	46	− 4
5r	9.85	−20	+ 8	0	+ 7, + 2	− 1, − 6	+ 3	30	+ 1
4s	10.17	−16	−10	+ 1, + 9	+ 5, 0	+ 3	+ 2	38	+ 1
13	10.50	−19	− 1, − 6	− 2, −10	− 1	+ 2	+ 7	35	− 1
6r	10.22	− 4	+ 2	+ 4, + 2	− 2, + 1	+ 2	− 1	38	0
14	10.90	− 4, − 8	−10, + 8	− 4, −22	− 3	−10	−11	37	− 8
7r	10.74	+12, + 7	+ 4, − 3	+ 7, − 3	− 1	+ 1	− 1	35	+ 1
5s	10.89	− 3	....	....	....	+12	−12	14	− 4
15	11.16	− 3, + 8	+ 6, + 2	+ 7	+ 8	+ 5	+ 8	33	+ 6
6s	11.26	−2	− 9	+ 1	+ 4	− 4	0	24	− 1
8r	11.25	+ 2, + 6	0, − 4	+ 5	+ 6	− 4	0	29	+ 2
16	11.55	− 9, 0	+ 1	0	− 2	− 3	0	22	− 2
17	11.76	0, +19	+ 5	+ 1	+ 2	+ 6	+ 1	29	+ 3
18	12.20	+11, +11	+ 9	0	− 4	+ 2	− 7	23	+ 1
19	12.61	0	+ 2	+ 1	− 1	− 2	....	18	0
20	12.92	+ 2	+ 4	− 4	0	− 9	....	16	− 2
21	13.17	− 3	− 2	− 1	+ 4	....	....	11	0
11r	13.00	....	− 4	+10	+11	....	....	7	+ 6
22	13.32	+18	− 4	+ 7	....	....	....	8	+ 7
23	13.50	+ 6	+12	+ 6	....	....	....	8	+ 7
12r	13.58	+ 2	....	....	....	....	....	2	+ 2
24	13.82	+ 7	− 2	− 1	....	....	....	7	0
25	13.99	+ 4	+ 5	....	....	....	....	4	+ 4
8s	14.36	−10	....	....	....	....	....	2	−10
26	14.47	−13	− 3	....	....	....	....	3	−10
9s	14.58	−16	....	....	....	....	....	2	−16
27	14.80	− 6	....	....	....	....	....	2	− 6
10s	15.14	+16	....	....	....	....	....	2	+16
11s	15.13	− 2	....	....	....	....	....	2	− 2

---

[1] *Loc. cit.*

For the seven red stars of high weight, *2r* to *8r* inclusive, there are two zero differences, four of 0.01 mag., and one of 0.02 mag. This confirms the reality of the large color equation of the 10-inch refractor for photographic magnitudes, and shows that the adopted coefficient in equation (1) is sensibly correct.

TABLE IV

COMPARISON WITH CORRECTIONS FOUND BY JONES

Star	Table III	Jones	Star	Table III	Jones
1*r*.........	+9(6)	+11(11)	5.........	−5(20)	+1(26)
14..........	−8(37)	−10(109)	12.........	−4(46)	0(113)
15..........	+6(33)	+ 5(96)	5*s*........	−4(14)	−6(108)
11*r*.........	+6(7)	+ 7(8)	8.........	+3(34)	+3(39)
3*s*.........	−6(5)	+ 1(9)	17.........	+3(29)	+2(56)
9..........	+5(54)	+10(33)	....	......	....

The corrections in the last column of Table III may be combined with the magnitudes in the second column to form weighted mean values referred to the system of the 10-inch refractor, or with the photographic magnitudes of *Contribution* No. 97, to obtain a revised system for the 60-inch reflector. Other data are available, however; and the final results, based on all the material which has been accumulated, are given in the following *Contribution* No. 235.

Turning now to the photo-visual magnitudes, consider first the small progressive change in the screen constant indicated by the last two columns of Table II. This suggests that the photo-visual scale requires a slight readjustment. The smoothed values of the constant are given in the second column of Table V, and it is readily seen that each of these would become equal to the adopted mean, were the original scale modified by the quantities shown in the third column of the table. Thus, since the first value of Δm depends upon the difference in brightness of stars whose mean magnitudes are 6.0 and 9.0, respectively, corrections of 0.00 and +0.05 at these two points of the scale would increase the observed value from 2.97 to 3.02. Again, the last value of Δm depends upon stars of mean magnitude 9.5 and 12.5. Corrections of +0.04 and +0.01, respectively, give the required reduction of 0.03 from 3.05 to the adopted mean. The maximum correction is +0.05 mag. in the vicinity of magnitude 9.

These results, however, scarcely justify a change in the original scale, for the divergence in question arises almost wholly from two of the eleven plates, Nos. 535 and 536, both of which show large differences in gradation between the full-aperture and the screen exposures (see Table II). There is, moreover, additional evidence. The colors of the stars near the Pole have been extensively observed by the method of exposure ratios, and since we now have reason to believe that the photographic scale for the brighter stars is reliable, it is clear that the photo-visual scale may be independently established by combining photographic magnitudes with color-indices derived from the exposure ratios. This material is discussed in *Contribution* No. 235, but the results are summarized in the last four columns of Table V, the significant quantities appearing under the heading "Corrn. (2)."

TABLE V

SCALE CORRECTIONS

Pv. Mag.	Δ*m*	Scale Corrn. (1)	Pv. Mag.	Scale Corrn. (2)	No. Stars	Rel. Weight
6.0	....	0	3.0	−3	2	3
6.5	....	+2	5.4	+3	4	4
7.0	....	+3	6.5	0	5	3
7.5	....	+4	8.0	−7	5	4
8.0	....	+4	9.5	−9	6	10
8.5	....	+5	10.4	−1	5	22
9.0	2.97	+5	11.1	−1	5	14
9.5	3.00	+4	12.4	+3	14	38
10.0	3.02	+3	13.5	+3	22	22
10.5	3.03	+3	14.3	+1	28	17
11.0	3.04	+2	15.4	−1	40	10
11.5	3.05	+2	16.2	+3	31	7
12.0	3.05	+2	16.9	−2	49	6
12.5	3.05	+1	....	....	....	....

With the exception of the values for 8.0 and 9.5 it will be noted that these corrections are small and in general accidental in character. Further, the two large corrections are opposite in sign to the values of Corrn. (1). In view of these results, which are of good weight, it appears that Corrn. (1) is of the order of the uncertainty affecting its determination, and may be disregarded. Nor does Corrn. (2) itself afford any certain basis for a change in the opposite direction. The exposure-ratio observations in these two groups are not well distributed, and most of the difference can be traced to three or four stars. A small systematic effect is certainly present, but as between the two series of magnitudes and the exposure ratios, its source cannot be located. The photo-visual scale of *Contribution* No. 97, as well as the photographic, is therefore adopted unchanged.

The problem of photo-visual magnitudes, provisionally at least, is therefore also one of diminishing the accidental errors of the original values in *Contribution* No. 97. Proceeding as for the photographic data, we find the results given in Table VI.

TABLE VI

PHOTO-VISUAL MAGNITUDES OF POLAR SEQUENCE STARS

Star	Pv. Mag. *Cont.* 97	Sums of Deviations +, −	No.	Corrn.	Star	Pv. Mag. *Cont.* 97	Sums of Deviations +, −	No.	Corrn.
2*s*	6.33	5,76	11	$-0\overset{\mathrm{M}}{.}06$	4*s*	9.83	35, 27	11	$+0\overset{\mathrm{M}}{.}01$
2*r*	6.35	8,73	11	− 6	7*r*	9.90	0,114	11	− 10
5	6.47	9,38	11	− 3	13	10.37	29, 17	11	+ 1
6	7.05	32,18	11	+ 1	8*r*	10.44	55, 11	11	+ 4
7	7.52	80, 7	10	+ 7	14	10.54	50, 0	11	+ 5
3*r*	7.56	36,12	11	+ 2	6*s*	10.73	0, 17	2	− 8
8	8.13	24,34	7	− 1	15	10.89	17, 30	11	− 1
4*r*	8.26	23,12	6	+ 2	16	11.23	24, 7	7	+ 2
5*r*	8.65	0,31	3	− 10	17	11.28	39, 0	7	+ 6
9	8.81	54,11	7	+ 6	18	11.89	11, 2	3	+ 3
10	9.07	19,46	12	− 2	11*r*	12.06	8, 0	2	+ 4
6*r*	9.21	81,22	13	+ 5	19	12.28	0, 39	3	− 13
11	9.53	69, 8	13	+ 5	21	12.48	16, 0	2	+ 8
12	9.80	7,82	11	−0.07	20	12.51	0, 30	2	−0.15

The magnitudes in the second column are taken directly from *Contribution* No. 97. The third column contains the sums of the positive and negative deviations for the 11 plates; the fourth column, the total number of values; and the fifth, the mean corrections to the magnitudes in the second column. Thus the first correction is $(+5-76)/11=-6$.

Neglecting three rejected corrections which exceed 0.3 mag., we find for the mean of the 231 remaining deviations ±0.065. The weighted algebraic mean of the final corrections for the red stars is less than 0.01 mag. This shows that for photo-visual magnitudes the color-systems of the 10-inch refractor and the 60-inch reflector are identical, and justifies the assumption expressed by equation (2).

As in the case of Table III, the corrections may be combined with the original magnitudes to form revised values. Those finally adopted, like the photographic results, also depend on data drawn from other sources and are given in *Contribution* No. 235.

In résumé, the investigation with the 10-inch refractor reveals no appreciable error in the photographic scale of *Contribution* No. 97 between the fourth and fourteenth magnitudes. The photovisual scale has been examined between magnitudes 6.3 and 12.5. A maximum correction of +0.05 mag. near the ninth magnitude is suggested, but independent data of higher weight do not confirm this result. The original scale is therefore adopted. The corrections to the magnitudes of *Contribution* No. 97 for accidental error (5 or more values) average ±0.03 and ±0.04 mag., respectively, for the two scales. The larger corrections for the photographic scale are in substantial agreement with those recently found at Greenwich by Jones.

Mount Wilson Observatory
February 1922

Contributions from the Mount Wilson Observatory, No. 235
Reprinted from the *Astrophysical Journal*, Vol. LVI, pp. 97–118, 1922

REVISED MAGNITUDES FOR STARS NEAR THE NORTH POLE

BY FREDERICK H. SEARES

ABSTRACT

Revised magnitudes and color-indices for stars near the North Pole.—Numerous comparisons with the polar standards have incidentally given extensive material for determining the errors affecting the standards themselves. The results for 55 stars (Table I) lead to revised magnitudes which are averaged with previously reported results obtained with the 60-inch reflector and the 10-inch Cooke refractor to give the adopted values listed in Table VIII. This table also gives the corresponding color-indices from magnitudes and from exposure-ratios for these and 37 other polar stars, all based on the color-system of the 60-inch reflector and the accessory equipment.

Exposure-ratio method of determining color-indices has been previously described. A discussion of the results of 177 exposures including stars of photo-visual magnitude ranging from 2 to 17.3, indicates that the average deviation of a single determination is ±0.12 magnitude, about half of which is due to the mean systematic error of the plate, and that in general the *probable error* is about 30 per cent less than in the case of a color-index derived by combining a photographic and a photo-visual magnitude. *Normal points for the calibration curve*, color-index as a function of log *E*, determined by observations on 216 stars, are given in Table IV and the adopted values in Table V.

Differential error between photo-visual and photographic scales of magnitude.—Although the exposure-ratio color scale is calibrated by measurements on stars of known color-index, systematic errors in the two magnitude scales upon which the color scale depends were eliminated by using stars with a wide range of magnitude. Hence the exposure-ratio scale is independent of the magnitude scales and may be used to test the differential error between them. The data (Table VII) show agreement to within $\pm 0^{\mathrm{M}}03$ from photo-visual magnitude 3 to 17, except for a few stars near magnitude 9 for which the mean difference is $0^{\mathrm{M}}09$.

The following pages bring together the results of several investigations bearing upon the magnitudes of stars near the North Pole. The basic determination of both photographic and photo-visual scales is that of *Mt. Wilson Contribution* No. 97,[1] which depends entirely upon observations with the 60-inch reflector. These results refer to the color-system of that instrument as used with the photographic plates[2] and a certain yellow filter habitually employed in photometric work at Mount Wilson.

To diminish the effect of accidental errors, the individual magnitudes of about fifty of the stars in *Contribution* No. 97 have been combined with a large amount of material obtained incidentally in connection with an entirely different investigation.

[1] *Astrophysical Journal*, **41**, 206, 1915.

[2] Seed's Gilt Edge, 27's and 30's, and Cramer's Instantaneous Isochromatic.

The revised magnitudes are on the scale and color-system of *Contribution* No. 97.

At various times during the last six years numerous measures of the colors of stars near the Pole have been made by the method of exposure ratios. The method must be calibrated upon stars of known color-index, but this can be accomplished in such a manner that systematic errors in the magnitude scales upon which the colors themselves depend do not enter into the calibration curve. Colors found from exposure ratios are thus essentially independent of the scale, and may therefore be used to test for differential error between photographic and photo-visual scales, since in the mean there should be no difference between the colors found by the two methods. A discussion of these data shows excellent agreement to the seventeenth photo-visual magnitude, except for a few stars near the ninth magnitude for which the mean difference is 0.09 mag.

Observations made at Greenwich, Harvard, and Potsdam confirm the substantial accuracy of the photographic scale of *Contribution* No. 97 to the sixteenth photographic magnitude.

A recent investigation made at Mount Wilson[1] with the 10-inch Cooke refractor affords further evidence on both the scales. The photographic scale is again confirmed. The photo-visual results are less reliable, but, considered in connection with the measures of colors, show that the scale of *Contribution* No. 97 must also be close to the truth.

These several investigations are combined to form a system of magnitudes embodying all the data bearing on standard polar stars thus far collected at Mount Wilson. The final results, which are on the color-system of the reflector and the accessory equipment mentioned above, represent the contribution of this observatory to the report of the International Commission on Stellar Magnitudes for 1922.

I. REVISION TO DIMINISH ACCIDENTAL ERROR

In determining the magnitudes of faint stars in the Selected Areas[2] it has been necessary to make a large number of comparisons, both photographic and photo-visual, with the polar standards of *Contribution* No. 97. Since the comparisons were intended only to establish the zero point of the magnitudes in the Selected Areas, and not the scale, the exposures were short, 2^m and 3^m, respectively. They afford, nevertheless, extensive material for the reduction of the accidental errors affecting the polar standards themselves.

---

[1] Seares and Humason, *Mt. Wilson Contr.*, No. 234; *Astrophysical Journal*, **56**, 84, 1922.

[2] See recent "Annual Reports of the Director of the Mount Wilson Observatory," *Year Book of the Carnegie Institution of Washington.*

We are here concerned only with exposures on the Pole of which there are two on each plate. As a part of the reduction, the scale readings for these had been plotted against the adopted standards in the usual manner. The deviations of individual stars from the smooth curves defined by the plotted points represent the combined influence of the accidental errors in the standards and the errors affecting individual plates. In the mean the latter are accidental, whereas the former enter systematically into the observed deviations from the curves and should be brought to light by forming the algebraic mean of a large number of such deviations.

Table I summarizes the results of this revision. The second, third, and fourth columns contain the mean systematic deviation for each star, obtained as just explained, and the number of values upon which each mean depends. The deviations are the corrections required by the magnitudes in *Contribution* No. 97 to bring them into agreement with the results of the polar comparisons. The fifth and sixth columns give the revised magnitudes. These are means of the values in *Contribution* No. 97 and those derived from the polar comparison plates, formed with weights equal to the respective numbers involved. The last two columns give the revised color-indices and the total numbers of individual observations for each star.

A few corrections are large and indicate cases of more or less serious discordance. Most of these are the result of low weight in one determination or the other.[1] For example, the photographic magnitude of star 439 given in *Contribution* No. 97 is clearly in error by a large amount and is rejected outright. Again, star 358 shows a difference of 0.47 mag. in the photo-visual magnitudes. Here both determinations are uncertain, and the adopted mean is

---

[1] Note that the numbers of values included in the means in *Contribution* No. 97 are equal to the differences in corresponding quantities in the fourth and last columns of Table I.

TABLE I

Magnitudes and Colors Derived with 60-Inch Reflector

Star	N.P.C.—*Contr.* 97			Revised Mags. and C.I.			
	Pg.	Pv.	No.	Pg.	Pv.	C.I.	No.
14	+ 5	+ 3	37, 9	11.00	10.55	0.45	94,27
16	− 8	− 4	21,13	11.59	11.21	0.38	64,29
19	+ 5	− 5	57,54	12.71	12.24	0.47	135,66
20	− 7	+ 2	69,60	12.99	12.53	0.46	155,72
22	+15	+ 6	27,25	13.47	12.84	0.63	72,36
23	− 2	−12	69,58	13.59	13.00	0.59	149,70
24	+ 1	− 3	44,34	13.93	13.31	0.62	115,46
25	+ 5	− 2	50,44	14.10	13.58	0.52	128,56
26	− 4	− 4	66,44	14.62	13.69	0.93	140,56
27	−10	−12	62,12	14.86	14.25	0.61	123,19
28	0	+ 4	28, 1	15.27	14.54	0.73	68, 8
31	0	....	17,..	16.41	15.62	0.79	62, 6
5s	+ 5	0	36, 3	11.11	10.06	1.05	96,31
7s	+10	− 8	44,45	12.65	12.04	0.61	114,57
8s	+10	− 3	29,10	14.53	13.77	0.76	79,22
9s	− 1	−14	68,41	14.74	13.74	1.00	134,53
10s	− 1	+25	22, 1	15.29	14.52	0.77	67, 8
11s	− 2	+ 1	52, 8	15.30	14.35	0.95	115,18
12s	+ 2	− 9	39, 2	15.34	14.67	0.67	100, 9
13s	− 5	....	22,..	15.52	14.54	0.98	65, 3
14s	+ 3	−15	26, 1	16.00	15.05	0.95	73, 8
15s	− 3	....	5,..	16.57	15.71	0.86	46, 5
16s	+ 4	....	1,..	16.86	15.50	1.36	37, 4
11r	+ 1	+ 1	43,41	13.22	12.07	1.15	122,53
12r	− 8	+ 1	69,59	13.81	12.47	1.34	151,71
125	−30	....	1,..	15.02	14.37	0.65	3, 5
127	− 4	....	2,..	14.34	13.31	1.03	8,11
130	−21	....	1,..	15.19	14.21	0.98	3, 9
134	−17	....	1,..	14.41	13.54	0.87	7,10
151	− 2	+18	3, 9	13.72	12.66	1.06	32,20
152	+12	− 3	3, 1	14.58	13.76	0.82	24,13
158	0	....	1,..	15.10	14.57	0.53	17, 5
176	+14	−13	5, 4	14.35	13.78	0.57	41,16
226	− 8	−21	25, 4	14.90	14.15	0.75	71,11
256	− 4	− 4	28, 8	14.66	13.84	0.82	78,19
277	+ 6	−15	49, 4	15.33	14.56	0.77	111,11
311	+ 4	− 5	42, 6	15.02	14.34	0.68	95,13
319	+ 9	+ 7	14,25	14.46	13.61	0.85	54,28
329	+10	+19	14,27	14.35	13.51	0.84	52,30
334	− 1	+ 3	51,14	15.20	14.44	0.76	121,21
338	+ 8	+ 6	5,10	14.73	13.84	0.89	33,13
341	− 6	+12	8,15	15.15	14.02	1.13	34,18
345	− 1	+ 5	36,35	13.79	12.05	1.74	94,46
350	+ 3	+14	26,11	11.02	10.71	0.31	72,23
358	+ 9	+47	9, 2	15.24	14.34	0.90	35, 4

TABLE I—*Continued*

Star	N.P.C.—*Contr.* 97			Revised Mags. and C.I.			
	Pg.	Pv.	No.	Pg.	Pv.	C.I.	No.
362.......	−12	− 5	67,61	13.08	12.27	0.81	153,73
378.......	− 2	+ 8	64,54	14.13	12.81	1.32	118,59
389.......	+ 8	+ 8	48,43	13.61	12.90	0.71	91,51
391.......	− 2	− 2	46,32	14.62	13.83	0.79	84,38
401.......	− 8	+10	25,33	14.50	13.70	0.80	61,36
403.......	− 4	+ 9	27,34	14.49	13.83	0.66	68,37
424.......	+ 2	+15	20,26	14.52	13.77	0.75	49,29
426.......	+ 7	+ 6	12,14	13.85	13.38	0.47	40,17
427.......	− 1	− 2	23,41	13.27	12.05	1.22	56,46
439.......	−51	....	21,..	14.78	13.49	1.29	21, 3

of little value. Occasionally, a difference is large, although numerous observations enter into each of the values combined to form the revision. Star 22 is an example, with a difference of 0.15 mag. The most plausible explanation is a small error in the distance correction. The star is at the edge of the useful field; the exposures for the polar comparison plates were always the same, while those for the original investigation were varied. Errors in distance correction tend to neutralize each other in the latter case because the photographic image varies in size from plate to plate, whereas there is no compensation in magnitudes derived from the comparison photographs. On this account the value from the polar comparisons has been given half weight. In general, however, the differences are as satisfactory as can be expected from results derived with a reflector of large focal ratio.

It should be noted that the revision concerns only the accidental errors affecting the original magnitudes. The reliability of the scales is a separate question, discussed partly in *Contribution* No. 234 and partly in the following sections of this paper.

2. COLORS OF POLAR STARS FROM EXPOSURE RATIOS

The method of exposure ratios for measuring a star's color has been described briefly in previous communications.[1] The term

---

[1] *Mt. Wilson Comm.*, Nos. 33, 38, 59; *Proc. Nat. Acad. Sci.*, **2**, 521, 1916; **3**, 29, 1917; **5**, 232, 1919. The second of these contains provisional results of the investigation discussed in this section.

"exposure ratio" is used to designate the logarithmic ratio of exposure times (symbol, log E) which produce blue and yellow images of the same size. This quantity can obviously be used as a measure of color.

Experience shows that for a given star the values of log E from plates of the same emulsion are nearly constant. The systematic differences in the means from groups of 5 or 6 plates each are usually negligible. Observations are now generally arranged in such a way as to check, if not actually determine, the zero point for each plate, but in the beginning a direct control, beyond that of accordance with other plates, was not ordinarily applied, the errors being minimized by multiplying the number of plates. In the case of bright stars, which must be observed individually, it is now customary to photograph several objects on the same plate, which greatly facilitates the reduction to a homogeneous system. In so far as possible, the same emulsion was used in all the earlier measures. When a change became necessary, the constant for reduction to a uniform system was carefully determined.

To translate values of log E into color-indices, which is an important step in giving them physical meaning, stars of known color-index must be measured. Inasmuch as the stars in the polar region are the basis of the Mount Wilson photometric system, they have been extensively observed for this purpose. The resulting data give not only the desired relation between color-index and log E, but also an independent determination of the colors of the individual stars. The exposures for the yellow images range from 8^s to 64^m, and results are now available for an interval of about 16 magnitudes, the lower limit being approximately 17 of the photo-visual scale. The details of interest in the present connection are as follows:

Series a.—About 150 plates; yellow exposures mostly 16^s and 32^s, on stars brighter than the eleventh magnitude, observed with images of standard size. A few plates of longer exposure extend the series to the thirteenth photo-visual magnitude.

Series b.—Nine plates with yellow exposures of 128^s. The faintest stars observed are of about the fourteenth magnitude.

Series c.—Three plates with yellow exposures of 8^m, three of 10^m, and two of 30^m. The limiting magnitudes range from 15.5 to 16.9.

Series d.—Nine plates with yellow exposures ranging from 8^s to 5^m. Only 17 stars between 9.0 and 12.5 were included, however, because the longer exposures were made with reduced apertures. This group of plates, along with several others included in the various series, was made under unusual conditions to test various details of the method which are of no interest in the present connection.

Series e.—Four plates, each including 10 to 15 stars brighter than the tenth magnitude, observed individually with yellow exposures of 8^s to 32^s and a standard size of image. In addition, observations with yellow exposures of from 32^s to 128^s were made at the beginning and end, to include stars between magnitudes 10.0 and 12.5. The results supplement and strengthen those of series *a*.

Series f.—Two plates with yellow exposures of 64^m each. The limiting magnitude is 17.3 photo-visual.

Lack of space prevents a detailed presentation of the reduction of these data, which has involved much time and several revisions as the results have accumulated. The discussion is therefore limited to a general statement of procedure, with extracts from the reduction sheets showing the accordance attained, supplemented by a collection of results, made particularly from the standpoint of their bearing on the magnitude scales.

The earlier observations were restricted to stars brighter than the eleventh photo-visual magnitude, because of the ease with which certain systematic errors could thereby be eliminated. It is well known that a photographic image produced by yellow light usually grows at a different rate from one produced by blue light; the value of log E therefore depends to some extent upon the size of the images from which it is derived. Differences in photographic gradation for light of different wave-lengths seem to depend upon a number of factors. In practice these are hard to control, and the most satisfactory results are obtained when the observations are arranged in such a way as to eliminate the disturbance or to permit its determination for each plate.

In the case of the preliminary measures this was accomplished by reducing all the stars to a standard intensity with the aid of screens and diaphragms and by using an essentially constant series of exposures throughout. Those for the yellow images were 16 and 32 seconds, although a few photographs with exposures ranging from 1 to 4 minutes were subsequently added. The latter gave results for bright stars already observed with short exposures, as well as for fainter stars, the overlap being sufficient to determine the zero-point and the correction to be applied for gradation. In practice the two corrections were combined. The differences in log *E* for stars within the overlapping region, when arranged in order of photo-visual magnitude, define a curve which could be extrapolated for an interval of one or two magnitudes without danger of serious error.

The discussion of the data of series *a* carried the results to the thirteenth magnitude. To extend them to still fainter stars, the procedure just described was applied in succession to the plates of series *b*, *c*, and *f* in the order of increasing exposure time. Series *d* and *e*, which control and strengthen the results of series *a*, were inserted and reduced in the order indicated by the series notation. The adopted values of C_e, the color-index derived from log *E*, and the number of determinations upon which each depends are given in the eighteenth and nineteenth columns of Table VIII, although results for a few stars, mostly of low weight, not included in the final collection of data, appear in Table VI.

The plates of series *f* show many faint stars for which individual results are not printed, although the means for groups of these stars appear in some of the statistical comparisons (see Table IV, for example).

The question as to how much the values of log *E* for faint stars have been affected by errors incident upon the extrapolation of the correction curve for gradation is important. The results for a single plate are systematically in error by small amounts at least; but for a series of plates these errors become accidental. An examination of the residuals for series *c*, in the interval 14.1 to 15.7, shows that the effect on the mean must be small. Although some of the plates of series *b* contribute results for two or three stars falling within the interval mentioned, the gradation curves for series *c* are in fact extrapolations from 13.7. The systematic deviations of individual plates from the mean, expressed in hundredths of a magnitude, are

Systematic deviation	− 9	− 1	− 8	+ 6	+ 8	+ 4	−5	+10
No. of stars	13	13	20	11	19	16	5	4

The average is ±0.064 mag., whence the probable value of the systematic error in the mean color-indices derived from log E for stars in this interval is of the order of ±0.02 mag. This could have been depressed to a still lower value by adding more plates, but the precision is sufficient for the present purpose.

As a further indication of accordance, it may be added that from the same data the average deviation for a single value of log E, including systematic errors, corresponds to ±0.118 mag. For stars in the interval between the tenth and thirteenth magnitudes, on the other hand, the agreement is as shown in Table II, which compares the mean results for each star as derived from series *a* to *e*. The table gives the deviations in log E in units of the third decimal and the number of values upon which each difference depends. There is here little evidence of residual systematic error; and since 0.010 in log E is equivalent, on the average, to 0.028 mag., the accidental deviations are also satisfactory. The combined effect of both types of error is indicated by the average of the 43 deviations based on 7, 8, or 9 observations each, whose value is ±0.013 in log E, or ±0.036 mag.

Finally, an examination of some of the bright stars in series *a*, which were observed individually with a standard size of image, throws light upon the fluctuations in the relative blue and yellow sensitiveness of different plates. Since for these stars no attempt was made to determine the zero-point correction for individual plates, the average deviations include the full effect of this error, combined with the accidental error of estimating the value of log E. Further, the mean log E usually depends upon two or even three different emulsions. The results have been referred to a standard emulsion, but the reduction constants are affected by an uncertainty which also enters into the average deviations.

The results for 15 of these stars which have been extensively observed are shown in Table III. The second and third columns give the number of plates and of emulsions used. In every case the observations extend over a period of more than a year, and many of the later measures were made with the original emulsion with which the observations were begun. There are small systematic differences affecting groups of plates of nearly the same date, but little evidence of actual changes in the color-properties of an emulsion with increasing age. The average deviations for a single plate in the fourth column show considerable fluctuation; their mean is ±0.106 mag. From other evidence it seems likely that this error is to be about equally divided between the neglected plate constants and the uncertainty in estimating the value of log *E*.

TABLE II

DEVIATIONS IN LOG *E* FOR DIFFERENT SERIES

Unit=0.001 in log *E;* No. of Values in Parentheses

STAR	PV. MAG.	SERIES				
		a	*b*	*c*	*d*	*e*
7r..........	9.90	− 5 (31)	−11 (9)	+25 (3)	+ 6 (9)	+30 (8)
5s..........	10.06	0 (35)	+ 5 (9)	0 (4)	− 2 (9)	+15 (7)
13..........	10.37	− 1 (14)	+18 (3)	....	....	....
8r..........	10.44	− 1 (15)	+10 (6)	+ 7 (5)	....	....
14..........	10.55	+ 6 (24)	+23 (9)	− 5 (7)	+16 (9)	−59 (6)
350..........	10.71	− 8 (24)	− 5 (7)	+11 (3)	+16 (9)	+26 (6)
6s..........	10.73	+10 (12)	+21 (8)	− 6 (6)	−23 (7)	....
15..........	10.89	+ 5 (15)	+23 (6)	−12 (6)	− 9 (9)	....
16..........	11.21	−32 (3)	− 1 (8)	+ 6 (8)	− 4 (9)	....
17..........	11.28	−28 (6)	− 3 (9)	+53 (6)	....	....
18..........	11.89	−16 (4)	− 1 (9)	+25 (8)	....	....
345..........	12.05	− 1 (11)	−10 (7)	−36 (2)	+52 (3)	+ 24 (4)
11r..........	12.07	− 3 (15)	+17 (9)	− 6 (8)	+17 (5)	− 9 (4)
427..........	12.05	−63 (1)	+ 6 (8)	+19 (8)	− 5 (5)	....
7s..........	12.04	+ 5 (18)	+11 (9)	+14 (7)	−30 (6)	+ 2 (6)
172..........	12.24	....	+42 (1)	+28 (2)	....	....
19..........	12.24	+20 (9)	− 9 (9)	− 9 (8)	+13 (5)	+ 7 (4)
362..........	12.27	+ 7 (19)	0 (9)	−27 (8)	+ 6 (5)	+43 (4)
12r..........	12.47	....	+22 (9)	−10 (8)	....	....
21..........	12.48	....	− 4 (6)	+13 (8)	....	....
20..........	12.53	+21 (18)	−23 (8)	−17 (8)	+42 (5)	−37 (4)
151..........	12.66	....	+37 (3)	− 9 (8)	....	....
378..........	12.81	+19 (16)	− 8 (6)	−24 (8)	....	....
22..........	12.85	....	0 (5)	+ 8 (8)	....	....
389..........	12.90	....	− 8 (7)	+18 (8)	....	....
23..........	13.00	+17 (13)	+ 8 (6)	−25 (8)	....	....

As mentioned above, it is now customary to determine the plate constant by comparison with standard fields, either directly or indirectly, which increases the precision appreciably. The results just discussed show, however, that even when the variations in color-sensitiveness from plate to plate are neglected, the exposure ratios lead to values of the color which are at least comparable in accuracy with those found by other methods of direct color-measurement. The errors given above are of the same order, for example, as those affecting individual magnitudes in the general run of photometric work. The uncertainty of a color-index derived by combining a photographic and a photo-visual magnitude should therefore be greater than that of a value from log *E* in the ratio of about 1.4 to 1. This is a fair statement of the advantage of the method of exposure ratios from the standpoint of precision.

TABLE III

Average Deviation in Color Index. Bright Stars

Star	No. Obs.	No. Em.	A.D.	Star	No. Obs.	No. Em.	A.D.
			mag.				mag.
10........	23	2	±0.135	7s.......	16	2	±0.124
13........	14	1	.092	1r.......	13	1	.119
14........	24	2	.084	3r.......	9	2	.093
15........	15	2	.097	7r.......	31	2	.099
20........	18	2	.105	8r.......	15	1	.072
1s.......	39	3	.097	10r.......	8	1	.138
5s.......	35	2	.111	11r.......	15	2	±0.155
6s.......	12	1	±0.062				

The calibration curve for the transformation of log *E* into color-index has been revised several times. The first approximation, which differs little from the adopted relation, was obtained from series *a* by first arranging the mean values of log *E* for each star in the order of increasing color-index as given in *Contribution* No. 97 and then forming the means of log *E* and of color-index for groups of stars within narrow limits of color. Accidental irregularities were eliminated by plotting the results and drawing a smooth curve. This curve represents the relation by means of which values of log *E* may be expressed in the customary form as color-indices.

Since most of the groups include stars scattered over a wide range in brightness, the errors in the photographic and photo-visual scales, which of course appear in the color-indices, are almost completely neutralized. In the present case, in which the scale errors are known to be small, their effect upon the mean relation between color-index and log E is negligible. Values of the color calculated from log E should therefore be free from errors in the scales, and when compared with the original color-indices arranged in order of increasing magnitude must bring to light any differential error in the scales themselves.

TABLE IV

NORMAL POINTS FOR RELATION BETWEEN COLOR-INDEX AND LOG E

C_m	log E	v	Pv. Interval	No. Stars
mag.		mag.		
0.04	9.040	+0.03	5.3– 8.8	8
0.26	.109	− 1	5.6–10.6	8
0.43	.186	+ 2	2.1–12.5	8
0.58	.229	− 1	11.3–15.2	10
0.67	.268	0	10.7–16.9	15
0.71	.319*	+ 10	15.5–16.8	15
0.81	.299	− 5	12.5–15.6	22
0.88	.367*	+ 7	15.5–17.0	15
0.99	.389	+ 2	8.3–16.3	18
0.99	.365*	− 4	14.8–17.0	15
1.06	.412*	+ 2	15.2–17.0	15
1.15	.410*	− 7	15.5–17.0	15
1.19	.444	− 1	9.2–16.0	17
1.23	.464*	+ 1	15.6–17.3	15
1.34	.485*	− 3	15.1–17.3	15
1.59	9.546	−0.08	5.1–12.0	5
Sum				216

* Supplementary faint stars from series *f*.

To obtain the last approximation for the reduction curve, the method just described was applied to the data from all the series as summarized in Tables VI and VIII, including the slight revisions of color-index given in Table I. The results are shown in Tables IV and V. The former gives the normal points and their representation by the adopted curve in Table V. Table IV also gives seven supplementary points based upon 105 faint stars between photo-visual magnitudes 14.8 and 17.3, which appear only on the two plates of long exposure in series *f*. Although of much lower weight, these points show substantially the same change in log E with color-index as the brighter stars. The average deviations of the two series of normal points in Table IV from the adopted curve are

±0.026 and ±0.049 mag., respectively. The average for the points in the first approximation, referred to the *final* curve, is ±0.028 mag. This approximation, it will be recalled, was based exclusively upon series *a*, which includes only stars brighter than the thirteenth magnitude. The large residual of −0.08 for the last point in Table IV arises mainly from the star 345, magnitude 12.05, which, in view of the numerous measures, is seriously discordant. (See Table VIII, last column.) No explanation suggests itself, except possibly systematic error in the estimates caused by the proximity of the brighter object, No. 350, magnitude 10.71.

TABLE V

Color-Index and Logarithm of Exposure Ratio

C.I.	log *E*	Diff. for 0.01 in log *E*	C.I.	log *E*	Diff. for 0.01 in log *E*
mag.		mag.	mag.		mag.
−0.2	8.940	0.026	0.8	9.315	0.028
0.0	9.015	.027	1.0	9.385	.030
+0.2	9.090	.027	1.2	9.450	.031
0.4	9.165	.027	1.4	9.513	.033
0.6	9.240	.027	1.6	9.573	.034
0.8	9.315	0.028	1.8	9.632	0.035

The absence of blue stars from the fainter objects is noteworthy, and confirmatory of earlier results. Among the supplementary stars from series *f* there is none with a color-index less than 0.6 mag.

From the ordinates of the adopted relation between color-index and log *E* given in Table V, it appears that the curve is nearly linear. The zero-point for log *E* is of course arbitrary. For comparison with the provisional relation between log *E* and spectral type given in Figure 1, *Mt. Wilson Communications*, No. 59,[1] a correction of −0.07 must be applied to the values of log *E* in Table V. This comparison leads to a result of importance, namely, the relation of the color-indices of the Mount Wilson photometric system to spectral type. Provisional values of the equivalents are listed in Table XII, *Contribution* No. 226. Detailed results and revised equivalents will be given in a later paper.

The data of Table V were used to calculate the color-indices for individual stars whose values, C_e, appear in Tables VI and

---

[1] *Proc. Nat. Acad. Sci.*, 5, 232, 1919.

VIII. Subtracted from the values of C_m found by comparing photographic and photo-visual magnitudes, these lead to the differences in the last column of the tables. These differences should be judged in connection with the number of separate determinations of the photographic and photo-visual magnitudes (sixteenth column, Table VIII) which enter into the observed color-indices, and of C_e (nineteenth column). Well-observed stars usually show a satisfactory agreement, although there are some unexpectedly large values. The case of No. 345 (12.05) has already been mentioned. No. 427 (also 12.05) should also show better agreement than it does. A similar difference for No. 172 (12.24), on the other hand, is not at all surprising, and this is also true of the four differences approximating 0.4 mag., all but one in Table VI. These latter results might have been rejected at once because of uncertainty, but they have been retained to show that

TABLE VI

OBSERVATIONS OF COLOR

(Stars not included in Table VIII, mostly of low weight)

No. *H.A.* 48	*Contr.* 97			EXPOSURE RATIOS		C_m-C_e
	Pg.	C_m	No.	C_e	No.	
126	15.58	0.93	2, 4	1.08	3	−15
139	15.30	1.34	2, 7	1.20	4	+14
142	14.60	0.89	2, 11	0.72	5	+17
143	16.35	0.84	7, 2	0.68	7	+16
146	14.52	0.96	2, 10	0.62	5	+34
154	14.95	0.59	8, 9	0.48	5	+11
159	15.20	0.70	16, 4	0.79	3	− 9
163	15.13	1.20	1, 3	0.82	3	+38
164	16.02	0.99	18, 5	0.86	3	+13
172	13.85	1.61	2, 1	1.38	4	+23
202	16.12	0.71	27, 4	0.78	3	− 7
205	15.97	0.89	11, 4	0.78	3	+11
214	15.39	0.73	9, 7	0.48	3	+25
215	15.47	1.78	10, 3	1.34	3	+44
218	15.47	1.36	17, 8	1.38	10	− 2
258	16.07	0.85	6, 4	0.64	3	+21
283	14.87	1.37	28, 3	1.24	4	+13
295	15.57	0.64	32, 5	0.66	8	− 2
301	16.23	0.66	26, 2	0.74	3	− 8
336	14.92	0.95	26, 5	0.77	5	+18
342	14.86	0.77	26, 3	0.64	5	+13
368	15.78	1.30	2, 3	1.21	3	+ 9

the values already published in *Contribution* No. 97 are open to suspicion. Superficially, one would expect a smaller difference for star 2 (5.28); its case is exceptional in that the values of log E for series a and e are discordant by about 0.4 mag., owing probably to an unfavorable combination of neglected plate constants. The persistent negative sign shown by the Polar Sequence stars near the fifteenth magnitude disappears when the differences for the *H.A.* 48 stars of the same brightness, in the latter part of Table VIII, are also taken into account. The systematic difference near the ninth magnitude is discussed in the following section.

TABLE VII

Comparison of Color-Indices from Magnitudes and from Exposure Ratios

Pv. Mag.	Series a			Series a–f		
	$C_m - C_e$	No. Stars	No. log E	$C_m - C_e$	No. Stars	No. log E
	mag.			mag.		
3.0........	+0.02	2	42	−0.03	2	46
5.4........	+ 3	4	21	+ 3	4	36
6.5........	0	5	14	0	5	34
8.0........	− 5	5	25	− 7	5	39
9.5........	− 8	6	65	− 9	6	103
10.4........	− 1	5	112	− 1	5	217
11.1........	+ 1	6	51	− 1	5	143
12.4........	+0.04	8	109	+ 3	14	379
13.5........	....	....	....	+ 3	22	216
14.3........	....	....	....	+ 1	28	167
15.4........	....	....	....	− 1	40	105
16.2........	....	....	....	+ 3	31	68
16.9........	....	....	....	−0.02	49	59
Sums...	....	41	439	....	216	1,612

3. CORRECTIONS TO PHOTO-VISUAL SCALE

It should be repeated that the two methods of deriving color-indices are independent, and that the values obtained from log E are essentially free from differential errors in the magnitude scales, as may be seen from the limits of brightness for the stars included in the normal points of Table IV (fourth column). The values of the differences $C_m - C_e$, when combined into means for groups of stars within narrow limits of magnitude, should therefore indicate the relative error in the scales. Since the photographic scale may

TABLE VIII

MEAN MAGNITUDES AND COLOR-INDICES

STAR	PHOTOGRAPHIC						PHOTO-VISUAL						ADOPTED MAGNITUDE			COLOR-INDEX			
	Contr. 97		10-Inch		N.P.C.		*Contr.* 97		10-Inch		N.P.C.		Pg.	Pv.	No.	C_m	C_e	No.	C_m-C_e
	Mag.	No.	Diff.	No.	Diff.	No.	Mag.	No.	Diff.	No.	Diff.	No.							
(1)	(2)	(3)	(4)	(5)	(6)	(7)	(8)	(9)	(10)	(11)	(12)	(13)	(14)	(15)	(16)	(17)	(18)	(19)	(20)
1s.....	2.54	40	.....	....	....	....	2.08	23	.....	....	....	....	2.54	2.08	40,23	+0.46	+0.51	39	− 5
1......	4.39	20	+ 7	4	....	....	4.37	9	.....	....	....	....	4.40	4.37	24, 9	0.03	−0.01	7	+ 4
2......	5.30	15	.....	....	....	....	5.28	11	.....	....	....	....	5.30	5.28	15,11	0.02	−0.18	7	+20
3......	5.83	22	.....	....	....	....	5.56	11	.....	....	....	....	5.83	5.56	22,11	0.27	+0.14	6	+13
4......	5.91	23	+14	4	....	....	5.84	9	.....	....	....	....	5.93	5.84	27, 9	+0.09	0.21	6	−12
5......	6.45	25	− 5	20	....	....	6.47	10	− 3	11	....	....	6.43	6.45	45,21	−0.02	0.02	8	− 4
2s.....	6.45	33	+ 1	25	....	....	6.33	10	− 6	11	....	....	6.45	6.30	58,21	+0.15	0.18	7	− 3
1r.....	6.61	27	+ 9	6	....	....	5.09	10	.....	....	....	....	6.63	5.09	33,10	1.54	1.54	17	0
3s.....	6.64	22	− 6	5	....	....	6.35	10	.....	....	....	....	6.63	6.35	27,10	0.28	0.23	4	+ 5
6......	7.11	16	+ 2	26	....	....	7.05	10	+ 1	11	....	....	7.12	7.06	42,21	+0.06	+0.05	7	+ 1
7......	7.41	26	+ 2	36	....	....	7.52	12	+ 7	10	....	....	7.42	7.55	62,22	−0.13	−0.16	7	+ 3
2r.....	7.94	22	− 1	31	....	....	6.35	12	− 6	11	....	....	7.93	6.32	53,23	+1.61	+1.55	8	+ 6
8......	8.32	36	+ 3	34	....	....	8.13	14	− 1	7	....	....	8.33	8.13	70,21	0.20	0.31	8	−11
9......	8.88	26	+ 5	54	....	....	8.81	12	+ 6	7	....	....	8.91	8.83	80,19	0.08	0.24	4	−16
3r.....	8.96	19	0	38	....	....	7.56	11	+ 2	11	....	....	8.96	7.57	57,22	1.39	1.43	13	− 4
10.....	9.12	21	+ 1	57	....	....	9.07	12	− 2	12	....	....	9.13	9.06	78,24	0.07	0.19	24	−12
4r.....	9.22	20	− 1	35	....	....	8.26	9	+ 2	6	....	....	9.21	8.27	55,15	0.94	1.10	7	−16
11.....	9.73	28	− 1	49	....	....	9.53	10	+ 5	13	....	....	9.72	9.56	77,23	0.16	0.26	3	−10
12.....	10.09	25	− 4	46	....	....	9.80	12	− 7	11	....	....	10.06	9.77	71,23	0.29	0.31	5	− 2
5r.....	10.13	24	+ 1	30	....	....	8.65	12	−10	3	....	....	10.14	8.63	54,15	1.51	....	....	.....
4s.....	10.25	19	+ 1	38	....	....	9.83	11	+ 1	11	....	....	10.26	9.83	57,22	0.43	0.52	2	− 9
6r.....	10.46	26	0	38	....	....	9.21	12	+ 5	13	....	....	10.46	9.24	64,25	1.22	1.24	7	− 2
13.....	10.53	19	− 1	35	....	....	10.37	16	+ 1	11	....	....	10.52	10.37	54,27	0.15	0.29	17	−14
7r.....	10.94	34	+ 1	35	....	....	9.90	28	−10	11	....	....	10.95	9.87	69,39	1.08	1.13	62	− 5
14.....	10.98	57	− 8	37	+ 5	37	10.54	18	+ 5	11	+ 3	9	10.97	10.56	131,38	0.41	0.48	57	− 7

5s.....	11.09	60	− 4	14	+ 5	36	10.06	28	.....	....	0	3	11.10	10.06	110,31	+1.04	+1.10	66	− 6
15.....	11.22	30	+ 6	33	....	....	10.89	10	− 1	11	....	....	11.25	10.88	63,21	0.37	0.37	37	0
6s.....	11.38	9	− 1	24	....	....	10.73	13	− 8	2	....	....	11.37	10.72	33,15	0.65	0.71	34	− 6
8r.....	11.44	32	+ 2	29	....	....	10.44	17	+ 4	11	....	....	11.45	10.46	61,28	0.99	0.97	26	+ 2
16.....	11.62	43	− 2	22	− 8	21	11.23	16	+ 2	7	− 4	13	11.60	11.22	86,36	0.38	0.35	30	+ 3
17.....	11.87	43	+ 3	29	....	....	11.28	13	+ 6	7	....	....	11.88	11.30	72,20	0.58	0.50	21	+ 8
18.....	12.27	49	+ 1	23	....	....	11.89	14	+ 3	3	....	....	12.27	11.90	72,17	0.37	0.40	21	− 3
10r.....	.....	....	.....	....	....	....	12.03	5	.....	....	....	....	.....	12.03	5	.....	.....	....	....
7s.....	12.61	70	.....	....	+10	44	12.10	12	.....	....	− 8	45	12.65	12.04	114,57	0.61	0.56	48	+ 5
19.....	12.69	78	0	18	+ 5	57	12.28	12	−13	3	− 5	54	12.71	12.24	153,69	0.47	0.44	37	+ 3
20.....	13.02	86	− 2	16	− 7	69	12.51	12	−15	2	+ 2	60	12.99	12.52	171,74	0.47	0.54	45	− 7
11r.....	13.22	79	+ 6	7	+ 1	43	12.06	12	+ 4	2	+ 1	41	13.23	12.07	129,55	1.16	1.10	43	+ 6
21.....	13.33	37	0	11	....	....	12.48	12	+ 8	2	....	....	13.33	12.49	48,14	0.84	0.69	16	+15
22.....	13.44	45	+ 7	8	+15	27	12.81	11	.....	....	+ 6	25	13.48	12.84	80,36	0.64	0.58	15	+ 6
23.....	13.60	80	+ 7	8	− 2	69	13.10	12	.....	....	−12	58	13.59	13.00	157,70	0.59	0.53	29	+ 6
12r.....	13.84	82	+ 2	2	− 8	69	12.46	12	.....	....	+ 1	59	13.80	12.47	153,71	1.33	1.30	19	+ 3
24.....	13.93	71	0	7	+ 1	44	13.33	12	.....	....	− 3	34	13.93	13.31	122,46	0.62	0.64	13	− 2
25.....	14.08	78	+ 4	4	+ 5	50	13.60	12	.....	....	− 2	44	14.10	13.58	132,56	0.52	0.62	14	−10
8s.....	14.49	50	−10	2	+10	29	13.78	12	.....	....	− 3	10	14.52	13.77	81,22	0.75	0.85	12	−10
26.....	14.64	74	−10	3	− 4	66	13.72	12	.....	....	− 4	44	14.62	13.69	143,56	0.93	1.06	13	−13
9s.....	14.75	66	−16	2	− 1	68	13.85	12	.....	....	−14	41	14.74	13.74	136,53	1.00	1.08	12	− 8
27.....	14.91	61	− 6	2	−10	62	14.33	7	.....	....	−12	12	14.86	14.25	125,19	0.61	0.69	10	− 8
28.....	15.27	40	.....	....	0	28	14.54	7	.....	....	+ 4	1	15.27	14.54	68, 8	0.73	0.92	5	−19
10s.....	15.29	45	+16	2	− 1	22	14.49	7	.....	....	+25	1	15.29	14.52	69, 8	0.77	0.92	7	−13
11s.....	15.31	63	− 2	2	− 2	52	14.35	10	.....	....	+ 1	8	15.30	14.35	117,18	0.95	0.97	10	− 2
12s.....	15.33	61	.....	....	+ 2	39	14.69	7	.....	....	− 9	2	15.34	14.67	100, 9	0.67	0.76	7	− 9
13s.....	15.54	43	.....	....	− 5	22	14.54	3	.....	....	....	....	15.52	14.54	65, 3	0.98	1.10	8	−12
29.....	15.82	40	.....	....	....	....	15.21	6	.....	....	....	....	15.82	15.21	40, 6	0.61	0.75	5	−14
14s.....	15.99	47	.....	....	+ 3	26	15.07	7	.....	....	−15	1	16.00	15.05	73, 8	0.95	1.21	7	−26
30.....	16.18	34	.....	....	....	....	15.44	5	.....	....	....	....	16.18	15.44	34, 5	0.74	0.74	5	0

TABLE VIII—*Continued*

Star	Photographic						Photo-visual						Adopted Magnitude			Color-Index			
	Contr. 97		10-Inch		N.P.C.		*Contr.* 97		10-Inch		N.P.C.		Pg.	Pv.	No.	C_m	C_e	No.	$C_m - C_e$
	Mag.	No.	Diff.	No.	Diff.	No.	Mag.	No.	Diff.	No.	Diff.	No.							
(1)	(2)	(3)	(4)	(5)	(6)	(7)	(8)	(9)	(10)	(11)	(12)	(13)	(14)	(15)	(16)	(17)	(18)	(19)	(20)
31.....	16.41	45	.....	....	0	17	15.62	6	.....	....	.....	....	16.41	15.62	62, 6	+0.79	+0.78	5	+ 1
15s.....	16.57	41	.....	....	− 3	5	15.71	5	.....	....	.....	....	16.57	15.71	46, 5	0.86	0.74	4	+12
32.....	16.76	33	.....	....	.....	....	15.58	3	.....	....	.....	....	16.76	15.58	33, 3	1.18	1.44	4	−26
16s.....	16.86	36	.....	....	+ 4	1	15.50	4	.....	....	.....	....	16.86	15.50	37, 4	1.36	1.45	4	− 9
33.....	17.06	32	.....	....	.....	....	15.97	3	.....	....	.....	....	17.06	15.97	32, 3	1.09	1.11	3	− 2
34.....	17.24	24	.....	....	.....	....	16.29	2	.....	....	.....	....	17.24	16.29	24, 2	0.95	1.10	3	−15
35.....	17.63	20	.....	....	.....	....	16.94	2	.....	....	.....	....	17.63	16.94	20, 2	0.69	0.80	3	−11
125.....	15.12	2	.....	....	−30	1	14.37	5	.....	....	.....	....	15.02	14.37	3, 5	0.65	0.65	5	0
127.....	14.35	6	.....	....	− 4	2	13.31	11	.....	....	.....	....	14.34	13.31	8, 11	1.03	0.89	12	+14
130.....	15.26	2	.....	....	−21	1	14.21	9	.....	....	.....	....	15.19	14.21	3, 9	0.98	0.60	3	+38
134.....	14.43	6	.....	....	−17	1	13.54	10	.....	....	.....	....	14.41	13.54	7, 10	0.87	.....	....	.....
151.....	13.72	29	.....	....	− 2	3	12.58	11	.....	....	+18	9	13.72	12.66	32, 20	1.06	1.14	13	− 8
152.....	14.56	21	.....	....	+12	3	13.76	12	.....	....	− 3	1	14.58	13.76	24, 13	0.82	0.68	12	+14
158.....	15.10	16	.....	....	0	1	14.57	5	.....	....	.....	....	15.10	14.57	17, 5	0.53	0.64	3	−11
176.....	14.33	36	.....	....	+14	5	13.81	12	.....	....	−13	4	14.35	13.78	41, 16	0.57	0.59	6	− 2
226.....	14.93	46	.....	....	− 8	25	14.23	7	.....	....	−21	4	14.90	14.15	71, 11	0.75	0.82	8	− 7
256.....	14.67	50	.....	....	− 4	28	13.86	11	.....	....	− 4	8	14.66	13.84	78, 19	0.82	0.92	10	−10
277.....	15.30	62	.....	....	+ 6	49	14.61	7	.....	....	−15	4	15.33	14.56	111, 11	0.77	0.72	9	+ 5
311.....	15.00	53	.....	....	+ 4	42	14.36	7	.....	....	− 5	6	15.02	14.34	95, 13	0.68	0.56	10	+12
319.....	14.44	40	.....	....	+ 9	14	13.55	3	.....	....	+ 7	25	14.46	13.61	54, 28	0.85	0.73	10	+12
329.....	14.32	38	.....	....	+10	14	13.34	3	.....	....	+19	27	14.35	13.51	52, 30	0.84	0.76	11	+ 8
334.....	15.20	70	.....	....	− 1	51	14.42	7	.....	....	+ 3	14	15.20	14.44	121, 21	0.76	0.86	9	−10
338.....	14.72	28	.....	....	+ 8	5	13.79	3	.....	....	+ 6	10	14.73	13.84	33, 13	0.89	0.82	8	+ 7
341.....	15.16	26	.....	....	− 6	8	13.92	3	.....	....	+12	15	15.15	14.02	34, 18	1.13	1.06	8	+ 7
345.....	13.79	58	.....	....	− 1	36	12.01	11	.....	....	+ 5	35	13.79	12.05	94, 46	1.74	1.50	29	+24

350.....	11.01	46	.....	....	+ 3	26	10.64	12	.....	....	+14	11	11.02	10.71	72,23	+0.31	+0.24	51	+ 7
358.....	15.22	26	.....	....	+ 9	9	14.11	2	.....	....	+47	2	15.24	14.34	35, 4	0.90	0.81	7	+ 9
362.....	13.13	86	.....	....	−12	67	12.31	12	.....	....	− 5	61	13.08	12.27	153,73	0.81	0.82	47	− 1
378.....	14.14	54	.....	....	− 2	64	12.74	5	.....	....	+ 8	54	14.13	12.81	118,59	1.32	1.33	32	− 1
389.....	13.57	43	.....	....	+ 8	48	12.83	8	.....	....	+ 8	43	13.61	12.90	91,51	0.71	0.62	17	+ 9
391.....	14.63	38	.....	....	− 2	46	13.85	6	.....	....	− 2	32	14.62	13.83	84,38	0.79	0.75	11	+ 4
401.....	14.53	36	.....	....	− 8	25	13.61	3	.....	....	+10	33	14.50	13.70	61,36	0.80	0.77	10	+ 3
403.....	14.51	41	.....	....	− 4	27	13.75	3	.....	....	+ 9	34	14.49	13.83	68,37	0.66	0.72	9	− 6
424.....	14.51	29	.....	....	+ 2	20	13.64	3	.....	....	+15	26	14.52	13.77	49,29	0.75	0.58	10	+17
426.....	13.83	28	.....	....	+ 7	12	13.33	3	.....	....	+ 6	14	13.85	13.38	40,17	0.47	0.55	10	− 8
427.....	13.27	33	.....	....	− 1	23	12.07	5	.....	....	−2	41	13.27	12.05	56,46	1.22	1.05	24	+17
439.....	(15.29)	1	.....	....	−51	21	13.49	3	.....	....	....	....	14.78	13.49	21, 3	1.29	1.39	10	−10

be accepted as substantially correct, it follows that the means may be regarded as corrections to the original photo-visual scale of *Contribution* No. 97.

Table VII shows the results found in this manner, both provisionally from series *a* and finally from the data in Tables VI and VIII supplemented by the faint stars appearing in series *f* alone. The means depend upon weights approximately proportional to the number of values of log E, unless C_m is much less reliable than usual. Technically, this is not the best method of procedure, but practically the final differences are little affected by the system of weighting or the grouping. It is noteworthy that the provisional corrections to the photo-visual scale given in the second column of Table VII, as far as they go, are in close agreement with those in the fifth column based upon much more extensive data.

With the exception of differences of −0.07 and −0.09 at magnitudes 8.0 and 9.5, the corrections are insignificant, and show that within very small limits of error the photographic and photo-visual scales of *Contribution* No. 97 are mutually consistent as far as the seventeenth photo-visual magnitude (about 18 photographic). The two discordant points indicate a small local systematic error, but its source cannot certainly be located.

The investigation with the 10-inch refractor[1] makes a negative correction to the photo-visual scale rather improbable. At the same time, the exposure-ratio observations are not very uniformly distributed, and some of them may be systematically affected by neglected plate constants. For the present it seems best to let the magnitude scales stand as they are, and to regard the results from exposure ratios as a check which establishes the mutual consistency of the scales within a few hundredths of a magnitude.

4. COLLECTION OF RESULTS. ADOPTED MAGNITUDES

The various results on the magnitudes and colors of stars near the Pole can now be brought together and combined into means. These results include: (*a*) the original determination in Table IX of *Contribution* No. 97, made with the 60-inch reflector; (*b*) the

[1] *Loc. cit.*

determination with the 10-inch Cooke refractor, in Tables III and VI of *Contribution* No. 234; (*c*) the revision for the reduction of accidental error, discussed in section 1 above; and (*d*) the values of the color-indices found from exposure ratios.

Assuming the photographic scale of (*a*) to be correct between magnitudes 10 and 15, (*b*) confirms the photographic scale of (*c*) between magnitudes 6 and 14, and the photo-visual scale between 6 and 12; (*d*) shows that the two scales are mutually consistent to the seventeenth photo-visual magnitude, with a maximum difference of 0.09 mag. at the ninth magnitude.

The essential details of the combination of these results are in Table VIII. The stars of the Polar Sequence, arranged in order of photographic magnitude, are given as far as Nos. 35 and 16*s*, where the revisions cease. The latter part of the table includes 30 additional stars in order of the *H.A.* 48 number.

The data in the first three and the eighth and ninth columns are copied directly from Table IX, *Contribution* No. 97. The results from (*b*) are in the fourth and fifth, and tenth and eleventh columns, and have been transcribed directly from the last two columns of Tables III and VI, respectively, of *Contribution* No. 234. Those from (*c*) are in the sixth and seventh, and twelfth and thirteenth columns, and have been taken from Table I above. The algebraic signs are such that when the differences are added algebraically to the magnitudes of *Contribution* No. 97 they give the results of the various revisions.

The final magnitudes are in the fourteenth and fifteenth columns. These are the means of the results in columns two to seven, and eight to thirteen, respectively, weighted according to numbers of values involved in each, excepting that the polar-comparison values for star 22 have received half the usual weight. Resulting color-indices, C_m, and the total numbers of observations are in the sixteenth and seventeenth columns. The results from exposure ratios in the eighteenth and nineteenth columns have already been discussed.

With the exception of the stars in Table IX of *Contribution* No. 97 not included in the revision, which stand as they are, Table VIII above summarizes all of the work done at Mount Wilson on the magnitudes and colors of stars near the Pole. The table itself gives little indication of the labor which lies behind it, the great burden of which in the measurement and reduction of the plates has fallen upon Miss Richmond and Miss Joyner of the Computing Division. I am deeply indebted to them for their part in an investigation which could not have been completed without generous assistance.

Mount Wilson Observatory
March 1922

COMPARISON STARS FOR NOVA PERSEI, NO. 2
A CORRECTION

Father Hagen has called my attention to an error in the identification of one of the comparison stars for Nova Persei, No. 2, whose magnitudes are given in *Mt. Wilson Contr.*, No. 192; *Astrophysical Journal*, **52**, 183, 1920. The star in question is No. 57 of his sequence. An uncertainty in the position and brightness was noted during the measurement of the photographs, but was overlooked when the MS was prepared several months later.

The confusion arose from the fact that the declination coordinates of stars 57 and 62 (+12.6 and +11.5, respectively) are interchanged in the Chart and Catalogue of Father Hagen. The star actually observed here is close to the catalogue position of No. 57, but is much fainter than that object. Neither No. 57 nor 62 has been measured on the Mount Wilson photographs; the former, in fact, is just outside the limit of distance from the center of the plate usually adopted. The visual magnitudes on the Mount Wilson scale are readily found, however, by reducing Father Hagen's values to that system. The results are

No. 57 12.7; No. 62 12.8

F. H. SEARES

Contributions from the Mount Wilson Observatory, No. 236
Reprinted from the *Astrophysical Journal*, Vol. LV, pp. 354–359, 1922

NOTES ON IONIZATION IN THE SOLAR ATMOSPHERE

By HENRY NORRIS RUSSELL[1]

ABSTRACT

Ionization in the solar atmosphere.—The effect of absorption of photospheric radiation by atoms in the sun's atmosphere should be to increase the degree of ionization, both directly, by shifting an electron into a position from which its removal is easier, and probably also indirectly, when enhanced lines are absorbed, by getting the ionized atoms into states in which they are less likely to combine with electrons. The effect should be relatively strong in the case of *barium* and weak or absent for *sodium*, and this may explain why Ba is more highly ionized in the sun than Na although their ionization potentials are the same. However, the abnormally high degree of ionization of *lithium* cannot be explained in this way and may be associated with the greater width of the spectral lines, due to the thermal agitation of so light an atom. In the case of *manganese* the behavior of the lines agrees well with what would be expected from its ionization potential alone.

Lines of barium and rubidium present in the solar spectrum.—Twenty-three Ba lines are more or less certainly present and are tabulated. All the strong lines arise from the ionized atom, but a few faint lines of the neutral atom are also probably included. Three enhanced lines of Rb are present though faint.

The following remarks may be regarded as extensions of the writer's recent paper, "The Theory of Ionization and the Sun-Spot Spectrum."[2] The ideas on which they are based grew largely out of conversations between the writer and Professors K. T. Compton, of Princeton, and F. A. Saunders, of Harvard, to both of whom he desires to acknowledge his indebtedness.

1. *Barium.*—The spectroscopic behavior of this element indicates that it is ionized to a much higher degree in the solar atmosphere, and even in the spots, than would be expected from its ionization potential, which is substantially identical with that of sodium.

The statement in the previous paper, that none of the lines of the neutral barium atom appear in the solar spectrum, is incorrect, for the second line of the principal series at λ 3071 is faintly present, although the first (at λ 5535) is absent or excessively faint, and

---

[1] Research Associate of the Mount Wilson Observatory.

[2] *Mt. Wilson Contr.*, No. 225; *Astrophysical Journal*, **55**, 119, 1922.

King[1] records that a number of lines belonging to the fundamental series of triplets,[2] which are very diffuse in the arc, but sharp in the vacuum furnace, are present in the sun, though very faint. Table I gives a list of all those barium lines which can be identified with tolerable certainty in the solar spectrum. The first three columns

TABLE I

LINES OF BARIUM IN THE SOLAR SPECTRUM

ARC SPECTRUM (KING)			SOLAR SPECTRUM (ROWLAND)				
I.A.	Int.	Class	λ	Origin	Int.	Δλ	Notes
3071.592	100 R	III	1.662	Ba	00	−0.044	(1)
3891.788	50	V	1.918	....	0	− .012	(2)
3995.633	30	III	5.769	Ba ?	000	− .010	(3)
4130.683	80	V	0.804	Ba	2	− .036	(2)
4166.027	20	V	6.161	Ba	0	− .018	(2)
4524.946	35	V	5.110	....	0	− .004	(4)
4554.038	1000 R	II	4.211	Ba	8	+ .003	(5)
4636.333	15 N	IV	6.501	....	0	− .007	....
4934.099	700 R	II	4.214 4.277	Ba	3 4	− .027	(5)
5267.013	20	IV ?	7.203	....	000	+ .005	....
5853.699	200	III	3.902	Ba ?	5	− .009	....
6141.760	600 R	III	1.938	Fe, Ba	7	− .032	....
6496.902	600 R	III	7.128	Fe	4	+0.013	(6)
	Doubtful Lines						
3993.395	80	II	3.616	Ba ?	00 N	+0.065	(3)
4132.444	20	I	2.560	Ba ?	0	− .041	....
4283.111	100	II	3.414	Ba ?	00 N	+ .141	....
4350.375	80	II	0.550	Ba ?	00 N	+ .012	....
4505.936	40	II	6.259	Ba ?	00 N	+ .156	....
4573.881	40	II	3.960	Ba ?	000	− .091	....
4899.970	35	IV ?	0.095	Ti, La	2	(− .055)	(4) (7)
6019.505	100	II	9.596	Ba ?	000	− .127	....
6110.808	300 R	II	1.005	....	0000	+ .064	....
6595.351	125	I	5.590	....	0000	+0.010	....

NOTES

1. Second member of the principal series of neutral atom 1s–3p.
2. Second member of diffuse series of enhanced lines 2P–4D.
3. Part of first member of fundamental series of neutral atom 3d–4f.
4. First pair of sharp series of enhanced lines 2P–3S.
5. First pair of principal series of enhanced lines 1S–2P.
6. Rowland gives this as an iron line: but the line in question is at 6496.462 (I.A.) according to Burns. The solar line is probably due to barium.
7. The barium line, if present, is masked.

---

[1] *Mt. Wilson Contr.*, No. 150; *Astrophysical Journal*, **48**, 13–34, 1918.

[2] Saunders, *Astrophysical Journal*, **51**, 25, 1920.

give the wave-length in I.A. from the measures of King or Schmitz, the intensity in the arc, and the temperature class; the next three, Rowland's wave-length, origin, and intensity; and the next, the difference $\Delta\lambda$ between Rowland's wave-length and the laboratory value after the application of St. John's value of the systematic correction.

All the high-temperature lines of King's classes IV and V, which are of intensity greater than 20 in the arc, appear in the solar spectrum, while numerous very strong low-temperature lines of classes I and II and intensities from 200 to 1000, are entirely absent. Most of the lines which are certainly present are well-known enhanced lines. The strong lines at 5853, 6141, and 6496 constitute, according to Saunders,[1] the first member of the diffuse series of enhanced lines, and are analogous to λλ 8662, 8542, 8498 of calcium, but reversed in order of wave-length. They are unaffected in the spot spectrum. The enhanced lines of the sharp series appear to be faintly present, and not absent, as stated earlier.

It appears, therefore, that neutral atoms of barium are probably present in the solar atmosphere, in a proportion which, though very small, is not insensible, as was stated in the preceding paper. The conclusion that barium is very highly ionized in the reversing layer, and even in spots, is confirmed by the re-examination of the data.

The conspicuous difference between its behavior and that of sodium remains to be explained. The solution of the puzzle probably lies in the fact that two ionizing agencies are certainly at work in the solar atmosphere—the temperature of the medium, and the radiation poured through it from the hotter photosphere below. Only the first is taken into consideration in the equations of Nernst and the theory of Saha, and, if it alone were active, there would be very strong reason to expect that the percentage of ionized atoms would be the same for the two elements. It is easy to see, however, that the second must create a difference of the sort which is observed.

Consider a barium atom which has just become ionized. Its first (or most easily removable) outer electron is lost; the second will be in the normal state of least energy content, denoted by 1S. In this condition it will immediately recombine with an electron which meets it under suitable conditions. But, if photospheric radiation (λλ 4934, 4554) falls upon it, it will absorb energy and the second electron will be lifted into one of the pair of positions 2P. If, after this, the charged atom meets a free electron, it is not so certain what will happen. It may be that it cannot recombine at all unless the second electron is in the normal position. If it can do so, the energy corresponding to the shifting of the second electron and the binding of the first one would have to be radiated. If this was done in a single quantum, the frequency would correspond to a "combination" between terms of the series of ordinary and enhanced lines, and such combinations have never been observed. Leaving aside the more delicate question whether the atom could emit two quanta at once from different electrons, it appears probable in any event that the $Ba+$ atom with its second electron in the 2P state would be *less likely* to recombine than one in the 1S state. Moreover, it will be decidedly easier to ionize a second time, for the energy required to remove the second electron is less (7.15 volts instead of 9.86, after absorption of λ 4554). There is also the probability to be considered that the absorption of a second quantum of radiation may raise the second electron to the state 3D, to which the considerations just urged will apply with even greater force.

---

[1] Unpublished.

The absorption of photospheric radiation by the ionized atoms of barium must therefore discourage recombination and encourage further ionization. Similar absorption by the neutral atoms will assist their ionization, so that, on the whole, the radiation must have a powerful ionizing influence.

For sodium, this influence must be very much smaller, and that for two reasons. In the first place, the enhanced lines of sodium, or at least the fundamental ones, lie in the extreme ultra-violet, beyond λ 377,[1] where the radiation of the photosphere is probably insensible, so that the sodium atom, once ionized, is not further disturbed by sunlight. Secondly, the principal lines of the neutral atom (the D lines) are very strong in the solar spectrum, with wings which indicate that they are absorbed to a great depth. Sodium atoms in the outer parts of the solar atmosphere are therefore exposed to a much enfeebled radiation of just those wavelengths which would be effective in aiding ionization.

---

[1] Millikan, *Proceedings of the National Academy of Sciences*, 7, 290, 1921.

For the corresponding lines of barium, on the contrary, the absorption is exceedingly small, and neutral atoms in the upper atmosphere are exposed to the full influence of the radiation.

When all these factors are considered, it is no longer surprising that barium is more highly ionized than sodium, in spite of the equality of their ionization potentials.

Whether the influence of radiation is competent to produce as great an effect as that which is observed can be determined only when a quantitative theory of its action has been developed. It may be noticed, however, that the 3D–2P lines of $Ba+$ are almost as strong in the solar spectrum as the pair 1S–2P, which indicates that a large fraction of all the singly ionized barium atoms in the reversing layer are in the states of "abnormally" large energy content.

The principle here sketched is evidently generally applicable. An element which has strong enhanced lines in the region where the continuous spectrum of the sun (or, for that matter, of any star) is strong, will behave as if it was relatively easier to ionize than one which does not possess such lines. The behavior of strontium, which resembles barium, but is less conspicuously "anomalous," is thus explained.

Most of the elements which are prominent in the solar spectrum possess such enhanced lines, with the exception of the alkali metals. The spectroscopic method suggested in the former paper should, therefore, give relatively high values for the ionization potentials of these metals, while it is probable that the errors for the other elements will be smaller. The alkaline earths, whose enhanced lines are very favorably situated, will probably come out with ionization potentials too low.

2. *Manganese.*—Saha[1] quotes the value 7.6 volts for the ionization potential, derived from unpublished studies by Catalan upon the series in its spectrum. This agrees satisfactorily with the spectroscopic evidence which puts its ionization potential rather more than halfway from Ca (6.1) to Zn (9.4).

---

[1] *Nature*, **107**, 683, 1921.

3. *Rubidium.*—Saunders[1] notes that the strongest of the enhanced lines given by Kayser[2] appear to be present, though faint, in the solar spectrum—the wave-lengths on Rowland's scale being given in Table II.

TABLE II

ENHANCED LINES OF RUBIDIUM

SPARK (EXNER AND HASCHEK)		SUN (ROWLAND)	
λ	Int.	λ	Int.
3940.62	20	Absent	....
4104.49	10	4104.459	00
4244.50	30	4244.500	00
4294.08	10	4294.077	000

The evidence for the presence of this metal in the sun is therefore strengthened. The principal enhanced lines lie probably in the far ultra-violet.

None of the stronger enhanced lines of the other alkali metals, as given in Kayser's *Handbuch*, appear to be present in Rowland's tables.

4. *Lithium.*—The absence of lithium lines from the solar spectrum, and their faintness in spots, still presents much difficulty. Lithium behaves almost exactly like rubidium, though its ionization potential is 5.37 volts, and that of the latter 4.16.

We cannot invoke any absorption of enhanced lines here, for none have even been discovered.[3] Compton suggests[4] that one factor in the problem is the small atomic weight. This will cause the mean atomic velocity of temperature agitation to be greater than for other elements (about three and one-half times that for rubidium), and thus broaden out all its lines, so that the atoms are able to take hold (so to speak) of a correspondingly greater range of wave-length in the photospheric radiation, and use it in assisting their ionization.

What other factors may enter remains for future discovery.

MT. WILSON OBSERVATORY
February 22, 1922

---

[1] Not previously published.

[2] *Handbuch der Spectroskopie*, 6, 350.

[3] Millikan, *op. cit.*, p. 292.

[4] Unpublished.

Contributions from the Mount Wilson Observatory, No. 237

THE PHOTOGRAPHIC DETERMINATION OF STELLAR PARALLAXES WITH THE 60-INCH REFLECTOR

SIXTH SERIES

By ADRIAAN VAN MAANEN

ABSTRACT

Trigonometric parallaxes determined with the 60-inch reflector.—(1) *The detailed measurements* of from 14 to 18 plates for each field are recorded *for 25 stars and nebulae:* Boss 1604, 1676, 2573, 3785, 4054, 4518, 4963, 5309, 5614, 5694, 5719, R Cancri, R Canum Venaticorum, Groombridge 3215, Lalande 29437, R Monocerotis, N.G.C. 1501, 1514, 6572, 7026, X and U Ophiuchi, Piazzi 23^h 267, R Trianguli and R Virginis. (2) *General discussion of the 164 parallaxes determined since 1913* by the author. The objects measured include 101 stars of known proper motion, chiefly of types F and M and of magnitudes 5 to 7; 15 stars of uncertain π (listed in Table VIII); 8 faint stars of large proper motion; 6 stars of types O and N; 12 variables; 2 novae; and 20 nebulae of which 16 are planetary (listed in Table IX). (3) *Systematic error in these parallaxes* is determined from eight comparisons with other data: (1) trigonometric; (2) spectroscopic results; (3) parallaxes from proper motion; (4) from absolute magnitude and velocity; (5) O, B, and N stars having very small parallaxes; (6) eclipsing and Cepheid; (7) long-period variables; (8) spiral nebulae. The final correction found is $-0''.0024 \pm 0''.0003$.

Variability of nebula R Monocerotis (N.G.C. 2261).—In view of the extremely small parallax found for this nebula, the large motions observed by Hubble are very remarkable and may perhaps be a question of illumination.

The present paper contains the results of twenty-five fields which have recently been measured for parallaxes. In general the work has been carried out in the same way as in the previously published series.[1] Only a few details need therefore be mentioned.

The fields of R Trianguli, R Monocerotis, R Virginis, R Canum Venaticorum, Boss 4518, Groombridge 3215, Boss 5309, Boss 5614, and Piazzi 23^h267 were measured with the Zeiss stereocomparator, the other fields with the new stereocomparator, which was described in an earlier paper.[2] For this instrument we find that 3260 estimated parts of the micrometer screw correspond to 1 mm $= 8''.227$ on the plates. We must accordingly multiply by 2.524 in order to reduce the measured quantities to thousandths of a second of arc. (For the Zeiss stereocomparator this factor is 1.629.)

The necessary data for each field are collected in the tables. On account of the high cost of printing these have been condensed, as compared with the analogous tables in the previous series. The present data for the individual fields consist of (1) The name of the object and its right ascension and declination for 1900. (2) A table containing in the first and second columns the dates of the morning and evening exposures which were combined in one pair; these dates are given in Greenwich mean time, with 1915.0 as zero-point. In the third and fourth columns the hour angles are given for the middle of the exposures; the fifth column gives the difference of the parallax factors; in the sixth column M, which is the value of $\Delta p\pi+\Delta m\mu_\alpha$ for each pair of plates, is given, and in the last the residuals v. (3) The normal equations, the results, and some remarks. (4) A second table for each field contains the data for the comparison stars used.

---

[1] *Mt. Wilson Contr.*, Nos. 111, 1916; 136, 1917; 158, 1918; 182, 1920; 204, 1921.

[2] *Ibid.*, No. 224, 1922.

TABLE I

Object	α 1900	δ 1900	Vis. Mag. Harvard	Mount Wilson Spectrum	Relative Parallax	μ_α	P.E.‡	No. of Exp.
R Trianguli	$2^h31^m0^s$	+33° 50′	Var.	Md	+0″.005	+0″.025	5,14	18
N.G.C. 1501	3 58 23	+60 39	13.0*	Pl. Neb.	+0.016	−0.020	3, 3	16
N.G.C. 1514	4 3 9	+30 31	8.0*	Pl. Neb.	+0.012	+0.008	9,15	16
Boss 1604	6 16 54	+22 34	3.19	Ma (G6)	+0.007	+0.051	5, 6	16
Boss 1676	6 29 40	+38 32	5.87	N	+0.003	+0.007	2, 3	16
R Monocerotis	6 33 44	+ 8 49	13.8*	Var. Neb.	−0.011	+0.006	3, 3	14
R Cancri	8 11 0	+12 2	Var.	Md	−0.001	+0.011	4, 6	16
Boss 2573	9 29 40	+36 16	5.48	K1	+0.066	−0.654	5, 6	16
R Virginis	12 33 26	+ 7 32	Var.	Md	+0.010	+0.014	4,12	16
R Can. Ven.	13 44 39	+40 2	Var.	Md	−0.010	−0.010	2, 6	14
Boss 3785	14 45 11	+38 13	5.98	F2	+0.041	−0.242	8, 8	16
Boss 4054	15 51 18	+43 26	5.54	Ma (G8)	+0.031	−0.051	3, 3	18
Lal. 29437	16 4 16	+ 6 40	6.02	K0	+0.026	+0.246	5,10	16
U Ophiuchi	17 11 27	+ 1 19	Var.	B8	+0.012	+0.043	8,18	16
Boss 4518	17 48 49	+40 0	6.06	F5†	+0.014	0.000	9, 9	18
N.G.C. 6572	18 7 14	+ 6 50	10.8*	Pl. Neb.	+0.003	+0.003	9, 9	16
X Ophiuchi	18 33 24	+ 8 44	Var.	Md	0.000	0.000	7,20	16
Boss 4963	19 21 45	+12 49	5.77	F†	+0.024	+0.005	8, 5	16
Groom. 3215	20 29 20	+41 33	7.04	K0	+0.050	−0.153	4, 6	18
Boss 5309	20 34 52	+29 59	5.86	K0	+0.011	−0.016	6, 8	16
N.G.C. 7026	21 2 55	+47 27	15.1*	Pl. Neb.	+0.011	+0.001	8, 4	16
Boss 5614	21 44 28	+60 14	5.64	K5	+0.019	−0.022	6, 4	16
Boss 5694	22 3 47	+58 21	6.31	G6	+0.015	−0.017	5, 2	18
Boss 5719	22 8 7	+58 55	5.19	Od†	+0.010	−0.004	4, 3	16
Pi. 23^h267	23 59 39	+34 6	6.23	G1	+0.009	+0.764	9, 9	16

* The magnitudes for the central stars of the nebulae are photographic, derived from counts of the number of stars of equal and brighter magnitude, and are based on Table IV of *Groningen Publications*, No. 27.

† Spectrum from *Harvard Annals*, 50.

‡ This column gives the probable errors of the parallax and of the proper motion in right ascension, respectively, expressed in thousandths of a second of arc as unit.

The plates for the three fields, Boss 3785, U Ophiuchi, and Boss 4963, were also measured by Dr. C. H. Gingrich, who has also assisted in securing the plates during his stay at the Observatory.

The fields of N.G.C. 1514, R Virginis, and Boss 4054 were so poor in stars that it was necessary to use comparison stars more than 10′ from the center. The first field has now been placed on the parallax program of the 100-inch reflector (42-foot focus), in the hope of securing a more reliable parallax for this beautiful object. On the plates of N.G.C. 6572 it was difficult to measure the central star of the planetary with great accuracy on account of the nebulosity near the star.

The results are collected in Table I, which is self-explanatory. The mean number of exposures is 16.2; the mean probable error of a final parallax, 0″.0056.

DISCUSSION OF SYSTEMATIC ERRORS

It has been my custom to discuss the Mount Wilson trigonometric parallaxes for systematic error after finishing each successive fifty fields. In the second and fourth series the conclusion was reached that such errors are small, but that the Mount Wilson parallaxes probably require a small negative correction. With the accumulation of material the possibility of deducing a systematic error is increasing rapidly; several new lines of thought can be followed, while some others which deserve relatively little weight may be abandoned.

After the completion of the present series several determinations of the systematic error were made, the results of which are discussed here.

a) The most obvious method is of course to compare the parallaxes with those derived by other observers for the same object. For 43 fields parallaxes have been published by other observers. The results of the comparison are collected in Table II.

For this purpose each observer was assigned the same weight as was used in *Contribution* No. 189 (page 7). The mean parallaxes and their weights are given in the second and fourth columns; the third column gives the abbreviation for the observer as follows: A, Allegheny; Ab, Abetti; B, Barnard; Be, Bergstrand; Bo, Bohlin; D, Dearborn; De, Delporte; F, Flint; Fr, Franz; G, Greenwich; H, Hasenstein; J, Jewdokimov; Jo, Jost; K, Kapteyn; Kos, Kostinsky; Ku, Küstner; M, McCormick; N, Newkirk; P, Philippot; Pe, Peter; R, Russell; S, Sproul; Y, Yale, Ye, Yerkes. The sixth column gives the differences $\pi_{\text{others}}-\pi_{\text{vM}}$; the last column gives the weights of these differences, determined by $w=\frac{\text{constant}}{\delta_1^2+\delta_2^2}$, where δ_1 is the probable error of the

TABLE II

Object	Weighted Mean of Other π's	Observers	Weight	π vM	π Others $-\pi$vM	Weight of Diff.
N.G.C. 224	+0″.027	Fr, B, Bo	0.5	+0″.006	+0″.021	0.2
Lalande 1966	+0.022	Y, Ye	1.5	+0.017	+0.005	1.0
Boss 373	+0.008	A	1.2	+0.036	−0.028	0.9
Boss 394	+0.107	Y, J	0.7	+0.120	−0.013	0.4
Boss 500	+0.005	A, Ye	2.2	+0.013	−0.008	1.4
Boss 592	+0.035	S	1.0	+0.010	+0.025	0.5
Boss 593	+0.039	S	1.0	+0.030	+0.009	0.5
Boss 654	+0.011	Ye, S	2.0	+0.029	−0.018	1.3
Nova Persei No. 2	+0.013	H, Y, Be, Kü	3.0	+0.009	+0.004	1.7
Lalande 6888	+0.026	Several*	4.2	+0.078	−0.052	1.0
Lalande 6889	+0.036	Several*	4.2	+0.083	−0.047	1.0
W.B. 4^h1189	+0.134	Y, F, S, M	2.7	+0.109	+0.025	1.5
Boss 1604	+0.026	A, M	2.2	+0.009	+0.017	1.4
R T Aurigae	+0.054	S	1.0	+0.008	+0.046	0.7
Boss 1846	−0.006	M	1.0	+0.010	−0.016	0.7
Boss 2378	0.000	M	1.0	+0.001	−0.001	0.7
Boss 2573	+0.119	Y, Jo, S, A	3.1	+0.068	+0.051	1.7
W Urs. Majoris	+0.013	Ye	1.0	+0.025	−0.012	0.7
Boss 3145	+0.004	F, K	0.8	−0.011	+0.015	0.5
Boss 3785	+0.013	A	1.2	+0.043	−0.030	1.5
Boss 3983	+0.052	G	1.2	+0.012	+0.040	1.0
Boss 3986	+0.041	G	1.2	+0.033	+0.008	1.0
Lalande 29437	+0.023	Y, A	1.7	+0.028	−0.005	1.2
U Ophiuchi	−0.006	Ye	1.0	+0.014	−0.020	0.7
Barnard's star	+0.540	D, Ye, M	3.0	+0.521	+0.019	1.7
Nova Aquilae, No. 3	+0.039	M, De, P	1.4	+0.021	+0.018	1.0
N.G.C. 6720	+0.015	N	1.5	+0.004	+0.011	1.0
Boss 4817	+0.003	A	1.2	+0.001	+0.002	0.9
17 Lyrae C	+0.129	Ye	1.0	+0.111	+0.018	0.7
Boss 4892	+0.039	Several†	4.0	+0.046	−0.007	1.0
Boss 4893	+0.041	Several†	4.0	+0.044	−0.003	1.0
B.D.+30°3639	−0.013	R	0.3	+0.007	−0.020	0.1
B.D.+35°4001	+0.010	K, D	1.3	+0.013	−0.003	0.9
B.D.+35°4013	+0.051	K, D	1.3	+0.004	+0.047	0.9
B.D.+36°3956	+0.091	K	0.3	−0.003	+0.094	0.1
Groom. 3215	+0.014	Y, Jo, A	2.1	+0.052	−0.038	1.5
Boss 5433	+0.307	Several‡	8.0	+0.327	−0.020	2.0
Boss 5434	+0.306	Several‡	8.0	+0.322	−0.016	2.0
Boss 5719	−0.015	Ye	1.0	+0.012	−0.027	0.7
Pi. 22^h214	+0.014	Y, Ye	1.5	+0.029	−0.015	1.0
Pi. 23^h164	−0.068	F, Y	0.8	+0.030	−0.098	0.3
Boss 6129	+0.086	A, M, Ye	3.2	+0.099	−0.013	1.7
Pi. 23^h267	+0.035	A, Y	1.7	+0.011	+0.024	1.2

* J, Ye, R, F, Y, M, D. † J, M, F, R, Ye, Y, Kos. ‡ Y, S, Ye, Ab, F, Pe, Jo, Y, R, A, M, K, Be, Kos.

mean parallax for the other observers and δ_2 the probable error of the Mount Wilson parallax. The weighted mean difference is

$$\pi_{\text{others}} - \pi_{\text{vM}} = -0\overset{''}{.}0015 \pm 0\overset{''}{.}0027$$

b) Strömberg[1] has recently published a new determination of the difference between the Mount Wilson spectroscopic and the trigonometric parallaxes; from 78 stars he finds

$$\pi_{Sp} - \pi_{\text{vM}} = -0\overset{''}{.}0030 \pm 0\overset{''}{.}0014$$

c) All the Mount Wilson trigonometric parallaxes of stars between spectral types B and Ma (excluding the companions of double stars) were compared with the system of mean trigonometric parallaxes, derived by van Maanen and Miss Wolfe in *Contribution*, No. 189. It may be recalled that this system is based on the mean parallax formula of the form

$$\bar{\pi} = ab^m \mu^c$$

where for each spectral type the constants a, b, and c were derived from the trigonometric parallaxes then available, viz., 901 stars with 1538 observations. It is doubtful if the material published since that time has introduced any considerable deviation from the system. The comparison includes 109 Mount Wilson parallaxes, with the result

$$\pi_{\text{system}} - \pi_{\text{vM}} = -0\overset{''}{.}0022 \pm 0\overset{''}{.}0007$$

d) A new series of determinations of the systematic correction is based on astrophysical data. In the first place we know that a relation exists between average absolute magnitude and average radial velocity of the stars of each type. The latest results along this line have been published by Adams, Strömberg, and Joy in *Contribution*, No. 210.[2] If now we select from among the stars for which parallaxes have been determined trigonometrically those which on account of their small cross-motions may be supposed to be of nearly the same absolute magnitude (nearly all the stars included in this investigation have the same apparent magnitude of about 6.0), we can derive corrections to the trigonometric parallaxes in the following simple way. Plot for each type M as abscissae against $\bar{\tau}$ as ordinates. For each type compute $\overline{M}$ and $\bar{\tau}$

---

[1] *Mt. Wilson Contr.*, No. 220; *Astrophysical Journal*, 55, 11, 1922.

[2] *Ibid.*, 54, 9, 1921.

from the trigonometric parallaxes and also the analogous values for $\pi_1=\pi-0''.0025$ and $\pi_2=\pi-0''.0050$, etc., and plot these values in the corresponding diagram. Both series of values will form nearly straight lines; from the intersection we can interpolate the values of the corrections which bring the observed parallaxes into the closest agreement with the values derived in *Contribution*, No. 210. The results are

Type F, $n=3$; Corr. $=-0''.0012\pm0''.0045$
G, $n=7$; $-0''.0022\pm0''.0031$
K, $n=11$; $-0''.0090\pm0''.0024$
M, $n=13$; $-0''.0006\pm0''.0022$

n being the number of stars.

e) For several objects the absolute magnitudes, and therefore the parallaxes, are now known with such accuracy that they are excellent for the derivation of the systematic errors in trigonometrically determined parallaxes. For instance, the Mount Wilson parallaxes contain four Wolf-Rayet stars, one B2 star and two N-type stars. For these different types we know the mean absolute magnitude from Gyllenberg's work[1] on the Wolf-Rayet stars and from Kapteyn's work on the B[2] and N stars.[3] The observed and computed data are collected in Table III.

TABLE III

Object	Mag.	Sp.	π_{vM}	π_c
B.D.+36°3956	7.9	O	−0″.003	+0″.0015
B.D.+35°4001	8.2	O	+0.013	+0.0013
B.D.+35°4013	8.0	O	+0.004	+0.0014
λ Cephei	5.6	O	+0.012	+0.0044
Boss 5083	5.5	B2	+0.009	+0.0066
Boss 1676	5.7	N	+0.005	+0.0021
Boss 3322	5.5	N	0.000	+0.0025
Means			+0″.0057	+0″.0028

From which

$$\pi_c-\pi_{vM}=-0''.0029\pm0''.0016$$

f) For eclipsing binaries and Cepheids, parallaxes have been calculated by Russell and Shapley. For the eclipsing binaries these are based on the elements of the eclipsing system and the surface brightness;[1] for the Cepheids, on the period-luminosity law.[2] In both cases the derived parallaxes are probably very close to the truth. In Table IV the comparison is given for six objects.

---

[1] *Arkiv för Matematik, Astronomi, och Fysik*, Band 11, No. 28, 1917.

[2] *Mt. Wilson Contr.*, No. 147; *Astrophysical Journal*, **47**, 104, 146, 255, 1918.

[3] *Ibid.*, **32**, 91, 1910.

TABLE IV

Object	Mag.	π_{vM}	π_c
SU Cassiopeiae................	6.1	+0″.010	+0″.0038
RX Aurigae..................	7.6	+0.001	+0.0006
RT Aurigae..................	5.3	+0.008	+0.0038
RR Lyrae....................	7.3	+0.008	+0.0030
W Ursae Majoris.............	8.6	+0.025	+0.0200
U Ophiuchi	6.3	+0.014	+0.0063
Means.......................	....	+0″.0110	+0″.0063

From which

$$_{\mathrm{vM}}=-0''.0047\pm0''.0016$$

g) For the long-period variables absolute magnitudes have been derived by Gyllenberg,[3] and recently by Strömberg in an unpublished work based on their peculiar motions and the radial velocities derived by Merrill. Gyllenberg's system has been reduced to the magnitudes of *Harvard Annals*, **57**; the mean absolute magnitude at maximum is then +0.2. Strömberg derived −0.3. I have assumed the mean M to be 0.0 at maximum. The comparison is given in Table V.

TABLE V

Object	Mag. (max)	π_{vM}	π_c
T Cassiopeiae................	7.7	+0″.029	+0″.0029
R Trianguli..................	6.2	+0.007	+0.0058
R Cancri.....................	6.6	+0.001	+0.0048
R Virginis...................	7.0	+0.012	+0.0040
R Can. Venaticorum..........	7.6	−0.008	+0.0030
X Ophiuchi...................	6.7	+0.002	+0.0046
Means........................	....	+0″.0071	+0″.0042

From which

$$\pi_c-\pi_{\mathrm{vM}}=-0''.0029\pm0''.0036$$

---

[1] *Ibid.*, **40**, 417, 1914.

[2] *Mt. Wilson Contr.*, No. 153; *Astrophysical Journal*, **48**, 279, 1918.

[3] *Arkiv för Matematik, Astronomi, och Fysik*, Band 14, No. 5, 1918.

h) Finally, we have the parallaxes of three spiral nebulae,

N.G.C. 224	$\pi_{vM} = +0''.006$
4051	+0.003
5194	+0.007

The real mean parallax of these objects most likely is less than +0".001. Assuming it to be +0".0005, we cannot be far from the truth. This gives

$$\pi_c - \pi_{vM} = -0''.0048 \pm 0''.0024$$

The results from this discussion are collected in Table VI.

TABLE VI

	n	Corr.	P.E.	Wt.
a From stars in common with other observers. .	43	−0".0015	±0".0027	0.1
b From spectroscopic parallaxes.	78	−0.0030	±0.0014	0.5
c From comparison with the system vM-Wolfe	109	−0.0022	±0.0007	2.0
d From $\overline{M}$ and $\overline{\tau}$ F stars.	3	−0.0012	±0.0045	0.1
G stars.	7	−0.0022	±0.0031	0.1
K stars.	11	−0.0090	±0.0024	0.2
M stars	13	−0.0006	±0.0022	0.2
e From stars of type O, B, and N.	7	−0.0029	±0.0016	0.4
f From short-period variables	6	−0.0047	±0.0016	0.4
g From long-period variables	6	−0.0029	±0.0036	0.1
h From spiral nebulae.	3	−0.0048	±0.0024	0.2
Weighted mean.	. . . . . .	−0".0029	±0".0003	. . . . . .

The weights in the last column have been taken in proportion to $1/r^2$; forming the unweighted mean, we obtain −0".0032.

In this discussion we have used +0".002 as the correction from relative to absolute parallax. By using the best values now available for the mean parallaxes of the comparison stars,[1] the reduction to absolute parallax becomes +0".0015, which would leave as a final correction to the Mount Wilson trigonometric parallaxes, −0".0024±0".0003.

Two conclusions drawn from this discussion may here be emphasized: First, the consistency of this result with the discussions previously published in *Contributions*, Nos. 136, 182, and 189; which illustrates how with relatively scanty material a fairly reliable systematic correction may be derived, and at the same time shows the constancy of the systematic error, even though no explanation of its existence is available. Second, the discussion shows that a few well-chosen objects give much more reliable results than a large number of stars observed in common with other observers. The weight of the correction derived from forty-three stars observed in common with others is smaller than that of most of the other determinations in Table VI. While in the present case this large probable error may be due to the fact that many of these stars were selected on account of the discordant values derived by other observers, yet it remains true that in any case half a dozen stars with small, well-known parallaxes, like the O-, N-, and early B-type stars, or half a dozen short-period variables will give a better result than two or three dozen stars observed in common with other observers.

---

[1] *Publications of the Astronomical Laboratory at Groningen*, No. 29, 1918.

DISCUSSION OF MOUNT WILSON TRIGONOMETRIC PARALLAXES

At this point a general discussion of the parallaxes thus far obtained seems appropriate. Since November, 1913, when the determination of trigonometric parallaxes was begun, two to six nights per month have been available for this work with the 60-inch reflector. During this time 150 fields, including 164 objects, have been measured. All the measures have been made by the author, except that Boss 3785, U Ophiuchi, and Boss 4963 were also measured by Dr. C. H. Gingrich. For the reductions I have had the help of Miss Davis, Miss Wolfe, and Mrs. Marsh, who have made all the necessary duplicate reductions. The 164 objects are discussed in groups as classified in Table VII.

1. The bulk of the material is for stars of known proper motion, magnitude, and spectrum. As the parallax work was originally undertaken in order to procure material which would aid in the determination of spectroscopic parallaxes, the stars selected are, as a whole, of types F to M, of magnitude 5 to 7, and proper motion $<0\overset{''}{.}5$. In 1913 there was little material available for these types, except for bright stars, or for those of large proper motion.

2. In the course of the work by Adams and his collaborators a number of stars were found for which the available trigonometric

parallaxes were very discordant. These were then placed on the trigonometric parallax program. The principal stars included for this purpose are collected in Table VIII, which gives in the first column the name of the object; in the second and third columns, the minimum and maximum trigonometric parallaxes, and in the fourth and fifth, the Mount Wilson trigonometric and spectroscopic parallaxes. Most of the large differences are due to the older meridian circle observations.

TABLE VII

1. Stars of known μ, mag., and spectrum	101
2. Stars of which the π by other observers is very uncertain	15
3. Faint stars of large proper motion	8
4. Stars of type O	4
5. Stars of type N	2
6. Short-period variables	6
7. Long-period variables	6
8. Novae	2
9. Planetary nebulae	16
10. Spiral nebulae	3
11. Variable nebulae	1
Total	164

TABLE VIII

Object	π Min.	π Max.	Mt. Wilson π	
			Trig.	Spec.
Lalande 1966	−0″.006	+0″.078	+0″.017	+0″.014
Piazzi $1^{h}159$	+0.058	+0.230	+0.120	+0.096
Lalande 6888	−0.132	+0.230	+0.078	+0.035
Lalande 6889	−0.132	+0.230	+0.083	+0.032
W.B. $4^{h}1189$	+0.112	+0.298	+0.109	+0.120
11 Leonis Minoris	−0.012	+0.225	+0.068	+0.096
Piazzi $11^{h}218$	−0.030	+0.062	−0.011	+0.023
6 Cygni A	−0.022	+0.100	+0.044	+0.066
6 Cygni B	−0.022	+0.100	+0.046	+0.055
Groombridge 3215	−0.012	+0.039	+0.052	+0.063
61 Cygni A	+0.218	+0.389	+0.327	+0.347
61 Cygni B	+0.218	+0.365	+0.322	+0.302
Piazzi $22^{h}214$	−0.022	+0.032	+0.029	+0.046
Piazzi $23^{h}164$	−0.082	−0.022	+0.030	+0.035
Piazzi $23^{h}267$	+0.008	+0.043	+0.011	+0.042

3. Among the faint stars with large proper motion are the following, whose motions were detected by the writer:

α 1900	δ 1900	Mag.	Sp.	π	μ
$0^h43^m52^s$	$+\ 4°55'$	12.3	Fo	$+0''.246$	$3''.01$
4 53 11	+39 13	13.2	....	+0.012	0.38
8 46 44	+28 42	14.1	....	+0.044	0.54

Three of the other faint stars are those near $\alpha = 2^h45^m$, $\delta = +22° 40'$, which were suspected of large proper motion by Puiseux, Burnham, and van Maanen. None of these has proved to have a considerable motion, but the one suspected by the writer has probably been given an erroneous declination in the *Carte du Ciel*.[1]

4. For three of the four Wolf-Rayet stars parallaxes had been derived by Kapteyn in *Groningen Publication*, No. 1. The mean parallax found was $+0''.049$, giving a mean absolute magnitude of +6.5, which seemed extremely low for stars of this type.

5 and 6. These stars seemed very appropriate for the determination of systematic errors in the trigonometric parallaxes.

7. A full discussion of five of the long-period variables was published in the issue of *Physica* for October, 1921.

8. The desirability of parallax determinations of novae is clear on account of the important rôle they play in the determination of the dimensions of the stellar universe. A serious objection to the reliability of their parallaxes arises from their seemingly great distances. Moreover, the practical difficulties in getting a series of plates while a nova is changing rapidly in brightness are considerable, especially if, as in the case of Nova Aquilae 1918 and possibly of Nova Cygni 1920, small rings of nebulosity are formed. For this reason it seems advisable to delay the determination of parallax until the magnitude has become faint and more or less constant. The objection to this procedure is that the star may become too faint for observation, but this will probably not exclude many objects.

9. The parallaxes of the sixteen planetary nebulae are collected in Table IX, together with the photographic magnitudes of the

---

[1] For full discussion of these stars see *Mt. Wilson Contr.*, No. 182, page 3, 1920.

central stars and their angular diameters, the last being taken from Curtis's list in *Publications of the Lick Observatory*, 13, 1918. The mean relative parallax is +0″.012; the mean absolute parallax, corrected for the systematic error derived above, is thus +0″.011, giving +7.5 for the mean absolute magnitude of the central stars. This value is of the same order as the absolute magnitude of the novae, after they have reached the Wolf-Rayet stage. On the other hand, the mean absolute magnitude of the Wolf-Rayet stars as derived by Gyllenberg[1] is −1.2. At first sight these magnitudes might appear to support the hypothesis that the planetary nebulae are old novae, which has recently gained considerable weight because of the appearance of nebular rings around Nova Persei 1901, Nova Aquilae 1918, and Nova Cygni 1920. The planetaries, however, are known to have high radial velocities, in the mean about 30 km/sec., while the novae have very small radial velocities. From the high radial velocities of the planetaries we might expect relatively large proper motions, and it is true that Wirtz[2] finds this to be the case; he has accordingly derived a mean parallax of

TABLE IX

Object	Phot. Mag.	Diameter	πRel.	μ_αvM	μ_αWirtz	V
N.G.C. 40.....	11.6	60″	+0″.003	−0″.012	....	−11
1501.....	13.0	56	+0.016	−0.020	+0″.152	+38
1514.....	8.0	120	+0.012	+0.008	....	....
2022.....	14.2	28	+0.008	+0.001	−0.015	− 1
2371-2 ...	13.5	60	+0.011	−0.004	....	+12
2392.....	10.0	47	+0.020	−0.006	−0.032	+73
6210.....	11.7	43	−0.003	+0.015	+0.055	−18
6543.....	11.3	22	+0.029	−0.013	0.000	−50
6572.....	10.8	16	+0.003	−0.055	+0.003	+10
6720.....	14.7	83	+0.002	+0.010	−0.059	+27
6804.....	13.4	63	+0.020	−0.004	−0.041	+ 4
B.D.+30°3639.....	10.2	5	+0.005	+0.024	....	−12
N.G.C. 6905.....	14.5	44	+0.013	−0.021	+0.006	+12
7008.....	12.8	86	+0.014	−0.022	....	−58
7026.....	15.1	25	+0.011	+0.001	....	−25
7662.....	12.9	32	+0.021	−0.003	−0.018	− 4
Means.....	12.3	....	+0″.012	0″.014	0″.038	24

---

[1] *Arkiv för Matematik, Astronomi, och Fysik,* Band 11, No. 28, 1917.

[2] *Astronomische Nachrichten,* **203,** 293, 1916.

0″.010 for twenty-nine gaseous nebulae, of which all but three or four are planetaries.

This agreement with the foregoing result seems at first sight to be extremely satisfactory. A comparison of the proper motions in right ascension leads, however, to a different conclusion. The motions in right ascension by van Maanen and Wirtz are given in the fifth and sixth columns of Table IX. It is granted that the proper motions, derived as a by-product of the parallaxes, are not very reliable; their probable errors, however, are in the mean only 0″.007. The enormous difference found, for instance, for N.G.C. 1501, 6210, 6572, 6720, 6804, can hardly be explained, unless by large errors in the motions used by Wirtz. If this is the case, and the small proper motions derived by the author are nearer the truth, then the smallness of these values is irreconcilable with the derived parallaxes. The problem is a puzzling one and cannot be settled by material at present available, and it seems unsafe, therefore, to draw any further conclusions based on the parallaxes, such as to size, mass, etc., although otherwise these might have been considered. It seems better to change the observing program from parallaxes of planetaries to their proper motions. For many fields, plates taken five or six years ago are available, and the intention is to duplicate these within the shortest possible time in order to derive more reliable motions. Should these, rather than the motions used by Wirtz, confirm our present proper motions, the parallaxes must be considerably smaller than those derived thus far. We must then admit a systematic error in the parallaxes of these objects quite out of proportion to those derived above.

That such exceptional errors for a system of objects with such different color indices are not at all impossible might be concluded from analogous results in the case of other series of parallaxes. For instance, in *Contribution* No. 189 it was shown that the Yerkes parallaxes have systematic errors which are practically independent of spectral type, except for the six M types, which may be excluded on account of the uncertainty of the system for the stars of extremely large proper motions. But during the investigation it was noticed that the Yerkes observations gave quite anomalous values for the stars of very early type. The material for these stars is collected in Table X.

TABLE X

Object	Mag.	π_{Yerkes}	π_c
ξ Persei	4.0	−0″005	+0″0091
Trapezium in Orion A	6.8	−0.009	+0.0025*
B	7.9	−0.021	+0.0015*
C	5.4	−0.016	+0.0048*
D	6.9	−0.018	+0.0024*
S Monoc.	4.7	−0.002	+0.0066*
B.D.+43°3571	7.5	+0.015	+0.0018
λ Cephei	5.6	−0.012	+0.0044
Means		−0″0085	+0″0040

* For these stars an even larger parallax, viz., 0″0057, was derived by Kapteyn, *Mt. Wilson Contributions*, No. 147, 1917.

From which

$$\pi_{\text{Yerkes}}-\pi_c=-0\overset{''}{.}0125\pm0\overset{''}{.}0029$$

while from one hundred and seventeen stars of types B–M we formerly found

$$\pi_{\text{Yerkes}}-\pi_c=-0\overset{''}{.}0036\pm0\overset{''}{.}0010$$

10. The spiral nebulae should be one of the best tests for the investigation of systematic errors, because it seems now fairly evident that their mean parallax must be between 0″000 and 0″001. The faintness of their central stars, their appearance, which is never quite stellar, and the scarcity of suitable comparison stars, due to their high galactic distribution, make it difficult, however, to derive parallaxes with the same accuracy as for other objects.

11. Fourteen exposures of the variable nebula N.G.C. 2261 = R Monocerotis, gave

$$\pi_{\text{rel.}}=-0\overset{''}{.}011\pm0\overset{''}{.}003$$

The nebulosity around the stellar part of this nebula, whose variability was discovered by Hubble, is not quite symmetrical, and extremely good seeing is necessary to secure reliable photographs. As the weather conditions for many of the fourteen exposures were such as to vitiate the results, six of the plates which are extremely good in quality were on this account measured again, giving:

$$\pi_{\text{rel.}} = -0''.007 \pm 0''.006$$

The negative parallax derived in both cases indicates that the real parallax must be small, probably less than $+0''.005$. This result is quite remarkable in relation to the motion (in one case reaching 20 to 30 seconds of arc annually) found by Hubble for some parts of the nebula.[1] Assuming as high a velocity as 1000 km/sec., this motion would still require a parallax of about $0''.100$, which is quite inconsistent with our present results. It seems necessary, therefore, to assume that the motions are a question of illumination, in which case we have to deal with the velocity of light. As we do not, however, know the orientation of the nebula, we can only conclude that the parallax must be small.

[1] *Astrophysical Journal*, **45**, 351, 1917.

R Trianguli $\alpha = 2^{h}31^{m}0^{s}$ $\delta = +33°50'$

Mor.	Ev.	t_1	t_2	Δp	M	v
5.645	5.931	−15°.5	−16°.7	+1.42	−12	−12
5.645	5.931	−11.5	− 6.7	+1.42	−20	−20
5.688	4.963	−11.2	− 6.2	+1.44	+ 2	−13
5.642	5.925	− 9.2	− 5.0	+1.40	+20	+20
5.645	4.958	− 7.0	− 2.0	+1.54	+25	+10
5.642	5.926	− 5.0	− 0.2	+1.40	+ 5	+ 5
5.694	4.958	− 3.5	+ 3.7	+1.40	+41	+26
5.645	5.043	− 2.7	+ 4.5	+1.80	− 8	−22
5.694	6.087	+ 2.7	+17.0	+1.70	+ 8	+ 9

$$+2.36\,\mu_a + 1.88\,\pi = +42$$
$$+1.88\,\mu_a + 20.49\,\pi = +88$$
$$\pi = +2.9 = +0''.005 \pm 0''.005$$
$$\mu_a = +15.5 = +0''.025 \pm 0''.014$$

No.	Br.	x	y	π
1.....	bf	+0′.8	+6′.6	+0″.014
2.....	f	+5.9	+2.1	−0.009
3.....	f	+2.2	−4.4	+0.015
4.....	bf	−0.1	−3.2	−0.011
5.....	bf	−5.8	−4.8	+0.005
6.....	bf	−3.7	+1.6	−0.009
7.....	f	−0.3	+2.5	−0.004

N.G.C. 1501 $\alpha = 3^{h}58^{m}23^{s}$ $\delta = +60°39'$

Mor.	Ev.	t_1	t_2	Δp	M	v
4.805	7.065	−15°.5	−13°.0	+1.40	+33	+ 6
6.740	7.062	− 8.5	− 9.2	+1.67	+ 9	− 5
6.819	7.059	− 9.2	− 8.0	+1.31	+14	+ 4
6.742	3.991	− 7.5	− 1.5	+1.36	−24	−11
5.762	4.073	− 7.0	− 2.7	+1.62	+ 8	+11
4.800	7.059	− 4.0	− 1.7	+1.42	+19	− 8
5.672	3.991	+ 0.2	+ 4.2	+1.29	− 9	− 3
6.740	4.068	+ 2.2	+ 7.5	+1.69	− 6	+ 4

$$+31.06\,\mu_a + 6.06\,\pi = -208$$
$$+6.06\,\mu_a + 17.48\,\pi = +64$$
$$\pi = +6.4 = +0''.016 \pm 0''.003$$
$$\mu_a = -7.9 = -0''.020 \pm 0''.003$$

No.	Br.	x	y	π
1.....	f	+0′.8	+2′.1	−0″.002
2.....	f	+0.8	+4.7	−0.003
3.....	f	+3.8	+2.9	−0.001
4.....	bf	−0.5	−6.0	−0.002
5.....	f	−2.6	−5.6	−0.002
6.....	f	−0.4	−1.5	+0.009
7.....	f	−2.1	+1.9	+0.004

N.G.C. 1514 $\alpha=4^h3^m0^s$ $\delta=+30°31'$

Mor.	Ev.	t_1	t_2	Δp	M	v
5.697	6.002	− 8.°2	−10.°0	+1.54	+ 8	+ 2
5.697	6.002	− 3.7	− 5.0	+1.54	+24	+18
4.797	4.065	− 1.7	− 0.7	+1.45	−10	−19
4.797	6.087	+ 3.7	+ 1.7	+1.52	−19	−22
4.803	3.994	+ 4.0	+ 3.5	+1.13	+ 2	− 6
4.800	4.065	+ 5.5	+ 4.0	+1.44	+42	+33
4.803	3.994	+ 8.2	+ 7.5	+1.13	− 2	−10
4.800	6.166	+12.5	+21.0	+1.56	+19	+16

$+6.10\,\mu_\alpha-1.07\,\pi=+14$

$-1.07\,\mu_\alpha+16.21\,\pi=+72$

$\pi=+4.6=+0''.012\pm0''.009$

$\mu_\alpha=+3.1=+0''.008\pm0''.015$

No.	Br.	x	y	π
1.....	bf	+ 8.′5	+7.′4	−0.″002
2.....	bf	+10.1	−4.1	−0.014
3.....	f	+ 4.1	−4.7	+0.017
4.....	bb	+ 0.3	−7.8	+0.012
5.....	f	− 3.8	−4.7	−0.014
6.....	bf	−10.8	+4.4	−0.010
7.....	f	− 6.7	+9.6	+0.010

Boss 1604 $\alpha=6^h16^m54^s$ $\delta=+22°34'$

Mor.	Ev.	t_1	t_2	Δp	M	v
4.882	5.122	−14.°2	−9.°0	+1.38	+12	+13
4.879	5.117	− 4.7	−7.0	+1.37	+ 7	+ 8
4.876	5.122	− 3.7	−4.7	+1.41	− 1	0
6.907	5.119	− 1.5	−4.7	+1.23	+37	+ 3
4.877	6.172	+ 0.2	−1.0	+1.57	−38	−17
6.819	5.117	+ 0.5	−3.0	+1.61	+43	+ 4
6.907	5.119	+ 3.0	−0.5	+1.23	+29	−11
6.819	6.172	+ 4.7	+3.2	+1.79	+21	+ 3

$+11.55\,\mu_\alpha+5.27\,\pi=+249$

$+5.27\,\mu_\alpha+17.04\,\pi=+155$

$\pi=+2.9=+0''.007\pm0''.005$

$\mu_\alpha=+20.2=+0''.051\pm0''.006$

No.	Br.	x	y	π
1.....	f	+2.′2	+3.′8	−0.″018
2.....	bf	+1.1	+0.3	+0.003
3.....	f	+1.4	0.0	+0.009
4.....	bf	+2.2	−1.1	+0.016
5.....	bf	+1.9	−4.5	−0.001
6.....	f	−1.9	−4.1	−0.007
7.....	f	−1.9	−0.3	−0.015
8.....	f	−4.9	+4.7	+0.013
9.....	f	−1.8	+1.5	−0.004

Boss 1676 $\alpha=6^h29^m40^s$ $\delta=+38°32'$

Mor.	Ev.	t_1	t_2	Δp	M	v
4.882	5.122	− 1°.0	− 0°.2	+1.38	−4	− 4
4.882	6.172	+ 2.7	+ 2.5	+1.56	+8	+10
4.877	6.087	+ 3.7	+ 5.0	+1.25	−8	− 5
6.907	5.122	+ 6.0	+ 5.7	+1.25	+7	+ 1
4.877	6.169	+ 8.0	+ 6.0	+1.58	−5	− 3
6.819	6.172	+ 8.5	+ 9.5	+1.80	+7	+ 3
6.907	6.169	+10.0	+10.0	+1.43	+2	− 1
6.819	6.087	+12.7	+10.5	+1.46	+2	− 1

$+9.54\,\mu_a-0.35\,\pi=+27$

$-0.35\,\mu_a+17.36\,\pi=+16$

$\pi=+1.0=+0''.003\pm0''.002$

$\mu_a=+2.9=+0''.007\pm0''.003$

No.	Br.	x	y	π
1.....	f	+0′.7	+1′.1	−0″.018
2.....	bf	+1.0	+5.1	+0.004
3.....	bf	+2.6	−0.5	+0.010
4.....	bf	+1.8	−3.6	−0.004
5.....	f	−0.5	−3.8	−0.007
6.....	bf	−1.4	−1.5	+0.018
7.....	bf	−4.1	+2.3	−0.001

R Monocerotis = N.G.C. 2261 $\alpha=6^h33^m44^s$ $\delta=+8°49'$

Mor.	Ev.	t_1	t_2	Δp	M	v
3.866.......	−6.087	−10°.5	− 9°.0	+1.29	− 7	+ 9
3.866.......	−6.087	− 6.0	− 3.5	+1.29	−33	−17
4.803.......	−5.119	− 1.5	+ 2.0	+1.65	− 2	+10
5.844.......	−3.098	+ 1.0	+ 4.2	+1.42	− 8	− 9
4.800.......	−5.119	+ 2.7	+ 7.2	+1.65	− 7	+ 5
4.803.......	−5.117	+ 3.0	+ 9.0	+1.64	−18	− 6
4.882.......	−3.095	+ 8.0	+11.5	+1.26	+ 5	+ 6

$+20.84\,\mu_a-\ 1.17\,\pi=+\ 85$

$-\ 1.17\,\mu_a+15.06\,\pi=-102$

$\pi=-6.5=-0''.011\pm0''.003$

$\mu_a=+3.7=+0''.006\pm0''.003$

No.	Br.	x	y	π
1.....	bf	+3′.6	+1′.8	−0″.015
2.....	bf	+3.4	+1.4	+0.014
3.....	ff	+2.3	−0.8	−0.009
4.....	f	+1.4	−2.1	+0.009
5.....	f	−0.5	−2.6	+0.007
6.....	f	−3.6	−2.2	−0.009
7.....	f	−4.3	+2.5	+0.003
8.....	bf	−2.5	+3.3	+0.001

R Cancri $\alpha = 8^h 11^m 0^s$ $\delta = +12^\circ 2'$

Mor.	Ev.	t_1	t_2	Δp	M	v
4.964	6.166	$-7^\circ.5$	$-6^\circ.0$	+1.18	− 7	− 2
4.964	5.199	− 3.5	− 1.5	+1.32	0	+ 1
5.932	6.166	+ 4.2	− 1.7	+1.32	− 4	− 3
6.907	5.199	+ 5.2	+ 4.5	+1.56	− 3	−10
5.932	5.207	+ 9.0	+ 6.2	+1.49	0	− 3
6.907	5.283	+ 9.7	+11.0	+1.77	+12	+ 5
5.926	5.207	+10.5	+11.7	+1.51	+18	+15
5.926	5.283	+14.7	+15.5	+1.69	− 3	− 6

$+8.62\,\mu_a + 6.75\,\pi = +35$
$+6.75\,\mu_a + 17.79\,\pi = +25$
$\pi = -0.2 = -0''.001 \pm 0''.004$
$\mu_a = +4.2 = +0''.011 \pm 0''.006$

No.	Br.	x	y	π
1.....	b	$+1'.2$	$+1'.0$	$+0''.001$
2.....	f	+4.5	+5.6	−0.002
3.....	bf	+6.5	−2.6	0.000
4.....	bf	+0.1	−4.7	+0.001
5.....	f	−5.2	−5.5	−0.001
6.....	bf	−5.1	+0.5	−0.003
7.....	f	−0.5	+5.9	+0.003

Boss 2573 $\alpha = 9^h 29^m 40^s$ $\delta = +36^\circ 16'$

Mor.	Ev.	t_1	t_2	Δp	M	v
3.994.......	−6.276	$-10^\circ.0$	$-4^\circ.0$	+1.47	+635	+ 3
4.964.......	−4.306	− 9.7	+ 1.0	+1.66	−130	− 6
3.994.......	−4.229	− 6.0	+ 2.5	+1.29	+101	+ 5
4.964.......	−4.229	− 4.5	+ 6.5	+1.41	−133	+19
6.005.......	−4.232	− 2.0	+10.2	+1.24	−424	+ 4
5.926.......	−6.331	+ 1.2	+11.0	+1.81	+133	−19
6.005.......	−6.333	+ 4.0	+14.2	+1.53	+130	+ 8
5.926	−4.232	+ 5.2	+14.5	+1.53	−407	− 7

$+12.57\,\mu_a + 2.03\,\pi = -3201$
$+2.03\,\mu_a + 18.07\,\pi = -50$
$\pi = +26.3 = +0''.066 \pm 0''.005$
$\mu_a = -258.9 = -0''.654 \pm 0''.006$

On 3.994−6.276 stars 2 and 6 were not measured.

No.	Br.	x	y	π
1.....	f	$+0'.7$	$+4'.3$	$-0''.011$
2.....	ff	+7.4	+3.6	−0.008
3.....	ff	+6.6	+1.8	+0.020
4.....	b	−1.5	−5.1	−0.022
5.....	f	−2.2	−1.2	+0.004
6.....	f	−7.1	−4.7	+0.017
7.....	bf	−3.2	+4.8	−0.002

R Virginis $\alpha=12^h33^m26^s$ $\delta=+7°32'$

Mor.	Ev.	h_1	h_2	Δp	M	v
5.117	5.398	$-3\overset{\circ}{.}7$	$-4\overset{\circ}{.}5$	+1.42	+14	+7
6.170	6.364	−1.7	+1.5	+1.04	+21	+17
6.003	5.371	−2.0	−0.5	+1.56	+17	+2
5.117	5.398	+0.5	+0.5	+1.42	+14	+7
5.044	5.374	+1.0	+2.5	+1.54	−7	−13
5.044	5.371	+6.5	+4.0	+1.53	−8	−14
6.167	5.374	+8.7	+7.0	+1.10	−5	−19
6.167	5.447	+15.0	+15.5	+1.32	+30	+16

$$+1.98\,\mu_\alpha+0.80\,\pi=+22$$
$$+0.80\,\mu_\alpha+15.21\,\pi=+100$$
$$\pi=+6.1=+0\overset{''}{.}010\pm0\overset{''}{.}004$$
$$\mu_\alpha=+8.6=+0\overset{''}{.}014\pm0\overset{''}{.}012$$

No.	Br.	x	y	π
1.....	f	$+3\overset{'}{.}4$	$+7\overset{'}{.}6$	$-0\overset{''}{.}012$
2.....	bf	+10.8	+0.4	+0.016
3.....	f	+0.1	−10.0	−0.017
4.....	bf	−4.9	−8.4	+0.015
5.....	bf	−5.1	+6.3	+0.015
6.....	ff	−1.5	+3.3	−0.017

R Canum Venaticorum $\alpha=13^h44^m39^s$ $\delta=+40°2'$

Mor.	Ev.	h_1	h_2	Δp	M	v
5.207	5.450	$+2\overset{\circ}{.}2$	$+3\overset{\circ}{.}2$	+1.27	−10	−4
5.117	5.398	+3.5	+7.2	+1.39	−6	+1
5.123	5.442	+12.7	+8.0	+1.56	−8	0
6.167	5.450	+9.5	+10.7	+1.44	−24	−10
6.170	5.398	+9.7	+14.0	+1.22	−1	+12
5.118	5.442	+10.2	+15.2	+1.57	−3	+5
6.170	5.447	+14.0	+16.5	+1.42	−15	−1

$$+1.97\,\mu_\alpha+1.31\,\pi=-21$$
$$+1.31\,\mu_\alpha+14.01\,\pi=-97$$
$$\pi=-6.3=-0\overset{''}{.}010\pm0\overset{''}{.}002$$
$$\mu_\alpha=-6.4=-0\overset{''}{.}010\pm0\overset{''}{.}006$$

No.	Br.	x	y	π
1.....	bf	$+1\overset{'}{.}1$	$+9\overset{'}{.}7$	$-0\overset{''}{.}014$
2.....	f	+3.4	+1.8	+0.001
3.....	f	+4.9	+1.5	+0.003
4.....	f	+6.0	+2.3	+0.007
5.....	bf	−3.3	−7.1	0.000
6.....	bf	−6.9	−4.9	−0.023
7.....	bf	−8.2	+0.3	+0.025

Boss 3785 $\alpha = 14^h 45^m 11^s$ $\delta = +38°13'$

Mor.	Ev.	t_1	t_2	Δp	M	v
4.145	2.451	−12°8	− 8°0	+1.50	−149	−11
4.145	3.418	− 8.2	− 3.5	+1.33	− 53	− 5
2.208	2.449	− 6.5	+ 1.0	+1.30	+ 72	+28
4.145	3.418	− 2.8	+ 0.5	+1.33	− 68	−20
2.208	2.449	− 2.0	+ 5.0	+1.30	+ 47	+ 3
6.167	2.449	+ 1.5	+10.8	+1.43	−321	+12
5.200	5.445	+ 6.8	+10.2	+1.31	+ 34	−11
5.200	5.450	+14.5	+11.8	+1.34	+ 52	+ 6

$+18.03\,\mu_\alpha + 8.52\,\pi = -1585$

$+8.52\,\mu_\alpha + 14.73\,\pi = -573$

$\pi = +16.4 = +0\overset{''}{.}041 \pm 0\overset{''}{.}008$

$\mu_\alpha = -95.7 = -0\overset{''}{.}242 \pm 0\overset{''}{.}008$

For this field Gingrich derived:

$\pi = +22.1 = +0\overset{''}{.}056 \pm 0\overset{''}{.}015$

$\mu_\alpha = -100.0 = -0\overset{''}{.}252 \pm 0\overset{''}{.}014$

No.	Br.	x	y	π
1.....	bf	+1′5	+5′2	−0″003
2.....	bf	+2.1	+8.8	−0.017
3.....	f	+2.5	−4.5	+0.002
4.....	f	+1.5	−8.2	+0.011
5.....	f	+1.2	−8.2	+0.006
6.....	b	−6.2	−5.9	−0.019
7.....	f	−4.7	+8.8	+0.025

Boss 4054 $\alpha = 15^h 51^m 18^s$ $\delta = +43°26'$

Mor.	Ev.	t_1	t_2	Δp	M	v
4.230	2.487	−13°2	−17°0	+1.38	−25	−7
4.145	2.490	−13.0	−15.0	+1.54	−13	+2
4.145	2.487	− 8.2	−12.0	+1.53	− 9	+6
4.230	2.490	− 7.7	−11.0	+1.39	−21	−3
2.282	2.490	− 5.0	− 5.7	+1.17	+25	+7
2.282	2.490	− 0.2	− 1.5	+1.17	+17	−1
2.208	2.528	+ 1.2	+ 2.0	+1.62	+19	−7
2.208	2.528	+ 6.0	+ 6.0	+1.62	+28	+2
2.285	1.483	+12.2	+11.5	+1.12	+ 2	+4

$+12.50\,\mu_\alpha + 9.28\,\pi = -140$

$+9.28\,\mu_\alpha + 17.77\,\pi = +29$

$\pi = +12.2 = +0\overset{''}{.}031 \pm 0\overset{''}{.}003$

$\mu_\alpha = -20.3 = -0\overset{''}{.}051 \pm 0\overset{''}{.}003$

On 4.145−2.490 and 4.145−2.487 stars 4 and 8 were not measured.

No.	Br.	x	y	π
1.....	f	+ 2′3	+ 1′4	+0″019
2.....	bf	+10.0	+ 8.2	−0.006
3.....	bf	+ 3.7	− 8.6	+0.001
4.....	f	+ 5.1	−11.2	−0.029
5.....	bf	− 1.0	−11.2	+0.027
6.....	bf	−11.0	+ 0.5	−0.024
7.....	f	− 6.5	+ 9.7	+0.012
8.....	f	− 4.0	+11.2	−0.003

Lalande 29437 $\alpha=16^h4^m18^s$ $\delta=+6°41'$

Mor.	Ev.	t_1	t_2	Δp	M	v
4.312	5.526	−10°5	−6°0	+1.21	−122	−16
5.319	5.529	− 8.0	−5.0	+1.18	+ 3	+11
6.282	5.532	− 4.0	−4.5	+1.37	+ 86	− 1
5.284	5.527	+ 2.2	−1.2	+1.34	0	+10
6.282	5.529	+ 1.5	−1.0	+1.36	+ 88	+ 1
6.329	5.532	+ 2.0	+0.5	+1.13	+ 90	0
5.284	5.524	− 1.5	+3.2	+1.33	− 2	+ 7
6.277	5.524	+11.0	+7.5	+1.36	+ 73	−15

$$+3.99\,\mu_a+\ 1.59\,\pi=+405$$
$$+1.59\,\mu_a+13.28\,\pi=+292$$
$$\pi=+10.4=+0''.026\pm0''.005$$
$$\mu_a=+97.4=+0''.246\pm0''.010$$

No.	Br.	x	y	π
1.....	f	+1'.5	+2'.2	+0''.008
2.....	f	+4.8	+5.1	+0.004
3.....	bf	+4.1	+0.5	+0.014
4.....	f	+1.8	−2.6	−0.034
5.....	f	+0.1	−6.0	+0.007
6.....	bf	−4.9	−4.0	+0.013
7.....	bf	−3.6	+0.8	−0.006
8.....	bf	−3.8	+4.7	−0.006

U Ophiuchi $\alpha=17^h11^m27^s$ $\delta=+1°19'$

Mor.	Ev.	t_1	t_2	Δp	M	v
6.364	6.572	−12°0	− 8°5	+1.18	+ 1	− 1
6.364	5.521	− 6.8	− 8.2	+0.93	+21	+ 3
6.277	5.521	+ 1.2	− 4.2	+1.32	+45	+26
6.329	6.572	+ 2.0	− 1.5	+1.36	− 2	− 5
6.331	6.575	+ 5.5	− 0.8	+1.36	− 2	− 5
6.329	6.580	+ 6.5	+ 3.8	+1.39	+ 7	+ 4
6.277	5.524	+ 6.8	+ 6.5	+1.33	+19	0
6.331	5.524	+10.0	+10.8	+1.11	− 7	−26

$$+2.71\,\mu_a+\ 2.40\,\pi=+\ 58$$
$$+2.40\,\mu_a+12.62\,\pi=+101$$
$$\pi=+\ 4.8=+0''.012\pm0''.008$$
$$\mu_a=+17.1=+0''.043\pm0''.018$$

For this field Gingrich derived:

$$\pi=+\ 1.3=+0''.003\pm0''.013$$
$$\mu_a=+42.4=+0''.107\pm0''.027$$

No.	Br.	x	y	π
1.....	f	+7'.3	+4'.4	+0''.001
2.....	bf	+5.1	−1.4	−0.008
3.....	bf	+4.4	−7.5	0.000
4.....	f	−4.3	−4.7	−0.003
5.....	f	−1.9	−0.4	+0.018
6.....	bf	−6.2	+2.7	−0.012
7.....	bf	−3.0	+3.6	+0.008
8.....	f	−0.5	+2.3	−0.006

Boss 4518 $\alpha=17^h48^m49^s$ $\delta=+40^\circ0'$

Mor.	Ev.	t_1	t_2	Δp	M	v
5.371	5.600	−17°5	−11°5	+1.29	− 5	−16
5.371	1.592	−13.2	−11.2	+1.26	+41	+31
4.307	1.592	− 5.5	− 5.0	+1.54	+55	+43
5.320	5.603	− 2.0	− 1.7	+1.54	−19	−32
4.307	5.644	− 1.5	− 0.2	+1.73	+41	+26
4.307	4.635	+ 3.0	+ 0.5	+1.70	− 3	−17
5.320	5.603	+ 4.5	+ 5.0	+1.54	+24	+11
5.374	1.562	+ 7.0	+ 8.5	+1.10	−15	−23
5.320	1.562	+10.7	+13.0	+1.35	−23	−33

$$+52.44\,\mu_a+14.20\,\pi=+107$$
$$+14.20\,\mu_a+19.27\,\pi=+158$$
$$\pi=+8.4=+0''.014\pm0''.009$$
$$\mu_a=-0.2=0''.000\pm0''.005$$

No.	Br.	x	y	π
1.....	f	+0′.4	+4′.0	+0″.020
2.....	bf	+2.9	+0.5	−0.004
3.....	bf	+5.4	−1.5	−0.005
4.....	b	−1.4	−3.8	+0.005
5.....	bf	−1.9	−3.0	+0.001
6.....	f	−3.0	+3.4	−0.017

N.G.C. 6572 $\alpha=18^h7^m14^s$ $\delta=+6^\circ50'$

Mor.	Ev.	t_1	t_2	Δp	M	v
5.399	6.575	−14°0	− 8°5	+1.04	+ 47	+21
5.399	6.580	−10.0	− 3.5	+1.07	+ 22	− 4
5.374	6.572	− 9.0	− 2.7	+1.15	+ 14	−13
5.374	6.575	− 2.5	− 2.5	+1.17	+ 26	− 1
6.329	2.616	− 1.5	+ 1.5	+1.55	−103	−25
5.371	2.575	+ 0.2	+ 5.2	+1.18	− 46	+13
6.329	2.616	+ 2.5	+ 6.0	+1.55	− 73	+ 5
5.371	2.575	+ 4.5	+10.5	+1.18	− 47	+12

$$+48.76\,\mu_a+12.79\,\pi=-1041$$
$$+12.79\,\mu_a+12.49\,\pi=-263$$
$$\pi=+1.1=+0''.003\pm0''.009$$
$$\mu_a=-21.6=-0''.055\pm0''.005$$

No.	Br.	x	y	π
1.....	bf	+2′.3	+3′.3	−0″.018
2.....	f	+2.7	−0.3	+0.009
3.....	b	+3.4	−1.6	−0.005
4.....	f	+1.5	−3.7	+0.002
5.....	bf	−2.7	−1.4	−0.013
6.....	b	−5.2	0.0	−0.002
7.....	f	−1.2	+1.0	+0.018
8.....	f	−0.1	+2.9	+0.007

X Ophiuchi $\alpha=18^h33^m24^s$ $\delta=+8°44'$

Mor.	Ev.	t_1	t_2	Δp	M	v
6.282	5.636	−15°.5	−13°.0	+1.72	−11	−11
6.282	5.638	−11.0	−13.0	+1.74	−18	−18
5.399	5.600	−10.5	−10.0	+1.17	− 9	− 9
6.364	5.638	− 6.5	− 7.7	+1.50	+13	+13
5.399	5.600	− 6.2	− 5.2	+1.17	+20	+20
6.332	5.603	− 3.2	+ 2.7	+1.46	+15	+15
5.371	5.641	+ 4.0	+ 8.0	+1.49	− 3	− 3
5.371	5.641	+ 8.0	+12.0	+1.49	0	0

$+2.09\,\mu_\alpha+\ 3.10\,\pi=0$

$+3.10\,\mu_\alpha+17.55\,\pi=0$

$\pi=0.0=0''.000\pm0''.007$

$\mu_\alpha=0.0=0''.000\pm0''.020$

On 5.399−5.600 star 9 was not measured

No.	Br.	x	y	π
1.....	bf	+0'.8	+0'.8	+0''.002
2.....	f	+2.9	+4.0	−0.017
3.....	bf	+4.0	0.0	+0.010
4.....	f	+3.2	−5.1	+0.010
5.....	f	−0.7	−3.4	−0.018
6.....	b	−5.4	−1.5	−0.002
7.....	b	−3.6	+1.2	+0.018
8.....	bf	−0.4	+3.4	+0.006
9.....	f	−0.7	+0.7	−0.011

Boss 4963 $\alpha=19^h21^m45^s$ $\delta=+12°49'$

Mor.	Ev.	t_1	t_2	Δp	M	v
5.442	6.657	−9°.5	−20°.0	+1.21	+31	+23
5.450	2.616	−9.2	− 7.0	+0.97	+19	+ 4
5.445	6.659	−8.0	− 5.5	+1.21	− 9	−17
5.450	4.632	−5.0	− 5.0	+1.05	+25	+13
5.442	2.616	−4.2	− 1.7	+1.01	+ 4	−12
5.448	6.659	−4.0	− 1.5	+1.19	0	− 8
5.445	4.632	−3.7	− 0.5	+1.08	+17	+ 5
5.448	5.693	0.0	+ 0.5	+1.32	+ 8	− 4

$+21.77\,\mu_\alpha+\ 2.65\,\pi=+\ 70$

$+\ 2.65\,\mu_\alpha+10.31\,\pi=+104$

$\pi=+9.5=+0''.024\pm0''.008$

$\mu_\alpha=+2.1=+0''.005\pm0''.005$

For this field Gingrich derived:

$\pi=+11.4=+0''.029\pm0''.011$

$\mu_\alpha=+\ 4.6=+0''.012\pm0''.007$

No.	Br.	x	y	π
1.....	bf	+1'.1	+1'.8	+0''.015
2.....	f	+1.9	+3.8	−0.019
3.....	bf	+5.2	+1.6	+0.005
4.....	f	+2.1	−3.0	−0.003
5.....	ff	−1.5	−5.2	−0.004
6.....	f	−1.8	−2.5	−0.001
7.....	b	−2.9	+1.1	+0.009
8.....	f	−2.9	+4.4	0.000

Groombridge 3215 $\alpha = 20^h 29^m 20^s$ $\delta = +41^\circ 33'$

Mor.	Ev.	t_1	t_2	Δp	M	v
5.522	5.693	−7°.2	−6°.5	+0.97	+ 47	+ 1
4.471	4.714	−7.0	−2.7	+1.32	+ 54	−10
5.522	5.693	−3.2	−2.5	+0.97	+ 56	+10
4.471	4.714	−2.7	+1.7	+1.32	+ 73	+ 9
4.468	3.679	−2.7	+2.5	+1.18	− 34	+ 4
4.468	3.785	+2.0	+2.5	+1.53	− 20	− 3
5.448	4.739	+3.0	+2.5	+1.51	− 24	− 4
5.451	3.785	+4.2	+6.5	+1.61	−122	−16
5.448	3.679	+6.5	+6.7	+1.27	−108	+19

$$+7.65\,\mu_a + 6.97\,\pi = -502$$
$$+6.97\,\mu_a + 15.57\,\pi = -173$$
$$\pi = +30.8 = +0''.050 \pm 0''.004$$
$$\mu_a = -93.7 = -0''.153 \pm 0''.006$$

No.	Br.	x	y	π
1.....	bf	+3′.6	+0′.7	+0″.005
2.....	b	+6.0	+3.0	+0.006
3.....	f	+4.8	−1.0	−0.001
4.....	b	+1.4	−7.3	−0.015
5.....	bf	−4.0	−2.7	+0.004
6.....	f	−5.4	−2.5	+0.013
7.....	bf	−3.3	+3.6	+0.016
8.....	f	−2.9	+5.1	−0.029

Boss 5309 $\alpha = 20^h 34^m 52^s$ $\delta = +29^\circ 59'$

Mor.	Ev.	t_1	t_2	Δp	M	v
5.451	5.690	− 7°.2	−11°.7	+1.31	−17	−28
5.451	5.690	− 3.0	− 7.0	+1.31	+17	+ 6
5.445	5.693	− 0.5	+ 1.2	+1.35	+34	+23
5.522	5.693	+ 2.0	+ 5.2	+0.97	+ 8	− 1
5.445	4.712	+ 3.5	+ 6.0	+1.42	+11	+ 5
5.522	3.676	+ 6.5	+ 8.0	+0.89	− 8	+ 4
4.504	3.673	+ 7.5	+10.2	+0.97	−11	−10
4.504	3.679	+12.5	+11.0	+1.00	− 7	− 6

$$+5.51\,\mu_a + 3.22\,\pi = -31$$
$$+3.22\,\mu_a + 10.95\,\pi = +45$$
$$\pi = +6.9 = +0''.011 \pm 0''.006$$
$$\mu_a = -9.7 = -0''.016 \pm 0''.008$$

No.	Br.	x	y	π
1.....	bf	+1′.4	+1′.9	+0″.008
2.....	b	+1.5	+1.4	0.000
3.....	bf	+2.7	+0.7	−0.008
4.....	bf	+2.6	−4.5	+0.002
5.....	bf	−0.3	−5.8	−0.005
6.....	bf	−3.3	+1.1	+0.013
7.....	f	−4.8	+5.8	−0.009

N.G.C. 7026 $\alpha=21^h2^m55^s$ $\delta=+47°27'$

Mor.	Ev.	t_1	t_2	Δp	M	v
6.496	6.736	−10°.2	−14°.0	+1.29	+13	+ 7
6.493	2.774	− 5.0	− 7.0	+1.43	+17	+ 9
6.496	4.709	− 3.5	− 2.0	+1.17	−10	−16
4.471	2.774	− 3.5	− 0.5	+1.53	+ 9	+ 1
6.493	2.777	+ 2.0	− 0.5	+1.44	− 5	−13
4.471	4.709	+ 3.2	+ 5.2	+1.29	+31	+25
3.504	6.736	+10.5	+ 5.7	+1.25	−12	−15
3.504	2.772	+17.5	+ 8.2	+1.37	+ 6	0

$$+44.73\,\mu_a+11.66\,\pi=+74$$
$$+11.66\,\mu_a+14.58\,\pi=+69$$
$$\pi\;=+4.3=+0''.011\pm0''.008$$
$$\mu_a=+0.5=+0''.001\pm0''.004$$

No.	Br.	x	y	π
1.....	f	+1′.5	+1′.9	−0″.001
2.....	bf	+1.9	+0.8	+0.011
3.....	f	+1.6	−1.1	−0.004
4.....	f	+1.2	−1.2	−0.003
5.....	f	−0.8	−2.1	+0.007
6.....	f	−1.6	−0.7	0.000
7.....	f	−3.7	+2.1	+0.002
8.....	f	−0.5	+0.7	−0.011

Boss 5614 $\alpha=21^h44^m28^s$ $\delta=+60°14'$

Mor.	Ev.	t_1	t_2	Δp	M	v
2.534	3.788	−14°.0	−11°.2	+1.31	+ 5	−28
2.534	4.712	−10.0	− 5.0	+0.98	+46	+ 6
5.522	5.761	− 5.5	− 7.0	+1.28	+44	+26
5.524	5.762	− 4.5	− 3.0	+1.26	+16	− 2
5.522	4.712	− 1.2	− 0.5	+1.05	+17	+16
5.524	3.745	− 0.5	+ 7.5	+1.19	−17	− 7
5.530	2.775	+ 5.7	+ 7.7	+1.29	−30	− 8
5.530	2.775	+ 9.7	+11.7	+1.29	−20	+ 2

$$+25.37\,\mu_a+\;5.66\,\pi=-274$$
$$+\;5.66\,\mu_a+11.75\,\pi=+\;61$$
$$\pi\;=+11.6=+0''.019\pm0''.006$$
$$\mu_a=-13.4=-0''.022\pm0''.004$$

No.	Br.	x	y	π
1.....	f	+1′.9	+4′.7	+0″.014
2.....	f	+3.7	+0.8	+0.015
3.....	bf	+2.2	−0.4	−0.007
4.....	f	+4.9	−1.2	−0.010
5.....	b	−3.8	−5.1	+0.008
6.....	bf	−1.6	−1.5	−0.006
7.....	ff	−4.9	−0.5	+0.005
8.....	f	−2.2	+3.0	−0.019

Boss 5694 $\alpha=22^h3^m47^s$ $\delta=+58°21'$

Mor.	Ev.	t_1	t_2	Δp	M	v
1.483	0.753	−12°0	−5°0	+1.38	+ 6	+ 3
5.530	5.764	− 8.2	−2.0	+1.25	+ 3	− 6
1.483	4.714	− 7.5	−2.0	+1.19	+21	− 8
6.490	0.753	− 7.0	−0.7	+1.35	−35	− 3
5.530	5.764	− 4.2	+2.2	+1.25	+17	+ 8
6.490	4.712	− 3.2	+1.0	+1.15	+15	+20
1.484	4.714	− 2.0	+2.2	+1.19	+27	− 2
6.490	0.750	+ 0.7	+2.0	+1.34	−45	−13
6.499	0.750	+ 0.5	+6.0	+1.31	−28	+ 4

$$+123.77\,\mu_a+17.71\,\pi=-749$$
$$+17.71\,\mu_a+14.52\,\pi=-37$$
$$\pi=+5.8=+0\overset{''}{.}015\pm0\overset{''}{.}005$$
$$\mu_a=-6.9=-0\overset{''}{.}017\pm0\overset{''}{.}002$$

On both pairs of plates 5.530–5.764 stars 2 and 6 were not measured.

No.	Br.	x	y	π
1.....	f	+6′3	+2′9	+0″022
2.....	f	+4.1	−2.9	−0.041
3.....	f	−1.1	−5.1	+0.008
4.....	bf	−3.8	−2.6	+0.029
5.....	f	−3.3	+2.1	−0.034
6.....	bf	−1.5	+3.7	−0.001
7.....	f	−0.3	+3.2	+0.006

Boss 5719 $\alpha=22^h8^m7^s$ $\delta=+58°55'$

Mor.	Ev.	t_1	t_2	Δp	M	v
6.499	3.785	−10°0	−11°5	+1.46	+17	+15
6.572	3.824	− 7.0	− 9.2	+1.24	− 1	− 2
6.499	3.824	− 6.0	− 4.0	+1.58	+ 1	− 1
6.493	6.818	− 4.2	− 5.5	+1.58	+ 3	− 3
6.496	6.736	− 3.2	− 3.2	+1.26	+ 3	− 2
4.504	6.818	− 1.5	− 1.2	+1.55	+16	+ 7
6.572	3.826	− 1.0	− 0.2	+1.25	− 8	− 9
6.496	6.736	+ 0.7	+ 1.0	+1.26	− 4	− 9

$$+35.20\,\mu_a+10.30\,\pi=-14$$
$$+10.30\,\mu_a+15.81\,\pi=+45$$
$$\pi=+3.8=+0\overset{''}{.}010\pm0\overset{''}{.}004$$
$$\mu_a=-1.5=-0\overset{''}{.}004\pm0\overset{''}{.}003$$

No.	Br.	x	y	π
1.....	bf	+2′5	+5′5	0″000
2.....	f	+4.8	+1.9	+0.002
3.....	bf	+4.0	−1.5	−0.014
4.....	f	+2.7	−4.1	+0.011
5.....	bf	−3.4	−4.3	−0.003
6.....	bf	−1.8	−2.7	+0.003
7.....	bf	−3.8	+1.1	−0.007
8.....	b	−4.9	+3.0	+0.008

Piazzi $23^{h}267$ $\alpha=23^{h}59^{m}39^{s}$ $\delta=+34^{\circ}6'$

Mor.	Ev.	t_1	t_2	Δp	M	v
5.601	5.843	−6°.7	−5°.2	+1.27	−83	+22
5.636	3.829	−4.2	−1.7	+1.04	+858	+4
5.601	5.843	−2.7	−1.5	+1.27	−81	+24
4.633	3.862	−1.7	0.0	+1.20	+313	−55
4.633	5.925	+3.0	+3.7	+1.39	−621	−20
4.581	5.925	+6.0	+8.2	+1.61	−617	−7
5.639	3.827	+6.2	+9.5	+1.02	+879	+25
5.639	3.827	+10.5	+13.5	+1.02	+850	−4

$$+14.06\,\mu_a+\ 1.92\,\pi=+6602$$
$$+\ 1.92\,\mu_a+12.34\,\pi=+\ 968$$
$$\pi=+\ \ 5.5=+0''.009\pm0''.009$$
$$\mu_a=+468.8=+0''.764\pm0''.009$$

On 4.633−5.925 stars 3 and 7 were not measured

No.	Br.	x	y	π
1.....	bf	+0′.7	+2′.5	−0″.004
2.....	f	+1.1	+4.9	−0.008
3.....	f	+3.8	−3.0	+0.002
4.....	f	+2.2	−4.7	+0.015
5.....	f	+2.1	−6.7	−0.001
6.....	f	−2.9	−2.6	−0.017
7.....	b	−5.6	+5.5	+0.018
8.....	bf	−1.8	+5.8	−0.006

I wish to express my acknowledgment to Messrs. W. P. Hoge and Milton Humason for their valuable aid in securing the plates, and to Mrs. Marsh, of the Computing Division, who has performed a large share of the necessary computations.

Mount Wilson Observatory
February 1922

Contributions from the Mount Wilson Observatory, No. 238
Reprinted from the *Astrophysical Journal*, Vol. LVI, pp. 132–138, 1922

THE VARIABLE DOUBLE STAR X OPHIUCHI

By C. H. GINGRICH

ABSTRACT

Variable double star X Ophiuchi.—From direct measurements by Hussey and later by Van Biesbroeck it is known that the two components of this interesting system are about $0''.22$ apart and were in a nearly north and south line in 1921, and that the north component is variable. During 1921 van Maanen made 16 plates to determine the parallax, which came out $0''.000 \pm 0''.007$. These plates have since been measured in declination to see whether any *displacement of the combined image* due to the variation in relative brightness of the components could be detected. With reference to exposures made near a maximum of the combined light, a mean displacement of about $0''.15$ to the south was found for a group of eight exposures made about midway between maximum and minimum. This result is in agreement with the previous conclusions mentioned above. On the plates measured there was no evidence of elongation of the image.

This interesting and rather exceptional object, whose position for 1900 is $\alpha = 18^h 33^m 24^s$, $\delta = +8^\circ 44'$, was first noted as variable by Espin in 1886. It is included in the list of variable stars in *Harvard Annals*, 55, 22, as star 183308, and is there assigned a range in magnitude from 6.5 to 9.0 in a period of 335 days. Its spectral classification is Md. Subsequent study of the variability of this star by Mr. Leon Campbell of the Harvard College Observatory based upon mean light curves extending over the interval from the year 1904 to the year 1921 indicates that the range is from magnitude 6.7 to 8.8 in a period of 337 days; $M - m =$ 189 days, $m - M = 148$ days.

Hussey in 1900 discovered that this object is a double star, the components being separated by $0''.22$ in position angle $195^\circ.2$. It appears as Hu 198 in the list of double stars published by him in the *Astronomical Journal*, **21**, 35 (No. 485), 1900.

Merrill, without realizing that the star was double, noticed that the spectrum of this object changed to such an extent from time to time as to suggest that there were two sources of light, and that at certain times the one predominated and at other times the other. Through correspondence with Van Biesbroeck, of the Yerkes Observatory, it was learned that in his program of remeasuring all the double stars discovered by Hussey his attention had been attracted to this object by its deep orange color, and that he was measuring the pair and observing the light variation for the purpose of determining which of the components was responsible for the variation of the pair or whether both components were variable. The mean results of six measures which he made in 1920 are

$$1920.668 \quad 171\overset{\circ}{.}1 \quad 0\overset{''}{.}218.$$

Later Van Biesbroeck furnished a light curve of the pair from estimates of magnitude extending from July, 1920, to October, 1921, covering more than one period of the variable, and showing the date of a maximum to be 1921, May 5. He also deduced the conclusion from estimates of relative brightness of the two components that the "north preceding star is the variable one."

In May, 1921, van Maanen completed a series of plates for determining the relative parallax of this object, and from them deduced the following result:

$$\pi = 0\overset{''}{.}000 \pm 0\overset{''}{.}007, \quad \mu_\alpha = 0\overset{''}{.}000 \pm 0\overset{''}{.}020.$$

Van Maanen and Merrill suggested that, since the image is undoubtedly displaced because of the relative change in brightness of the components, it would be desirable to measure the plates of the parallax series in order to discover the amount and direction of this displacement and thereby obtain an independent determination of the distance between the two, and also an indication as to which was varying.

Since the plates were taken within the period during which Van Biesbroeck made his measures, which show the stars to be nearly in a north and south line, it was immediately clear that the displacement due to variation in magnitude would be almost entirely in declination. Consequently the plates were arranged for measurement with the stereocomparator in the same pairs that van Maanen had used for the parallax measures, but were measured in declination instead of in right ascension as he had done. As the plates had been taken for maximum parallax displacement in right ascension they were of necessity extremely unfavorable to parallax determination in declination, but, as van Maanen had already shown the relative parallax to be very small, this feature was of no special importance for the present purpose.

It should perhaps be stated that on the plates measured there was no evidence of elongation of the image and that consequently the settings were made so as to bisect the image resulting from the combined light of the pair.

I used the light curve derived by Van Biesbroeck for obtaining the magnitude of the pair at the times when the several plates were taken and assumed the magnitude at minimum to be the magnitude of the invariable component, and by use of the formula

$$\log b_n = \log b_m - 4/10\,(n-m)$$

given in Young's *General Astronomy*, page 509, constructed the following table of values:

TABLE I

Plate No.	Date	Combined Mag.	Ratio of Light Intensity		Mag. Var.
			Var./Inv.	Inv./Comb.	
2675	1920, May 15	7.1	2.98	0.25	7.4
2699	25	7.0	3.37	.23	7.3
2802	Aug. 7	8.0	0.74	.58	8.9
2814	8	8.0	0.74	.58	8.9
2819	20	8.2	0.45	.69	9.5
2831	21	8.2	0.45	.69	9.5
2846	22	8.2	0.45	.69	9.5
3083	1921, Apr. 13	7.2	2.63	.28	7.6
3100	May 1	7.0	3.37	.23	7.3
3112	13	7.0	3.37	0.23	7.3

By using data determined by Campbell and by Van Biesbroeck it was found that the star was at maximum brightness on 1920, June 2, and 1921, May 5, and at minimum brightness on 1919, November 25; 1920, October 28; and 1921, September 30. The mean date of the first two plates, May 20, is only thirteen days before the maximum of June 2, and the mean date of the last three, April 29, is only seven days before the maximum of May 5.

The mean date of the remaining five plates, August 18, is seventy-one days before the minimum of October 28.

In the reductions of the measures the factors in the next to the last column in Table I were taken to represent the proportionate displacement of the image from the position of the variable star toward the position of the invariable one. It is probable that the displacement of the image of the combined light due to variation in one of the components does not take place rigorously according to the law implied in this method. However, in the absence of accurate knowledge at this point this assumption is the best which can be made as a working hypothesis.

At first that part of Van Biesbroeck's measured distance between the stars, namely $0\overset{''}{.}218$, indicated by the assumption just referred to, was applied to the measured quantities in a direction consistent with the conclusion that the north star is the variable one, and the residual quantities were used for determining parallax and proper motion in declination. However, because of the small parallax factors already referred to and because of the short interval of time involved, the probable errors of these determinations were so large as to make the values entirely unreliable and practically meaningless. Next an equation was formed for each pair of plates with the distance between the stars, as well as the parallax and proper motion, left as unknown. The same factors as before were used as coefficients of the unknown distance δ. A least-squares solution of these equations led to the following results:

$$\pi=-0\overset{''}{.}088\pm0\overset{''}{.}092;\quad \mu_\delta=-0\overset{''}{.}037\pm0\overset{''}{.}022;\quad \delta=0\overset{''}{.}348\pm0\overset{''}{.}025.$$

Inasmuch as this computed distance differs considerably from the distance measured directly, corrections based upon the computed distance were applied to the plate measures as before and a new determination of the parallax and proper motion made. The results were

$$\pi=-0\overset{''}{.}012\pm0\overset{''}{.}102;\quad \mu_\delta=-0\overset{''}{.}030\pm0\overset{''}{.}015.$$

These values of π and μ_δ are at least possible, but the probable errors make it unsafe to attach very much weight to them, especially in the case of the parallax value.

It was then decided to remeasure the plates by comparing each available exposure with a given exposure chosen as the standard, in order to detect the displacement from this standard position. The exposure on the plate numbered 3100 was chosen as standard because the date of the exposure, 1921, May 1, so nearly coincided with the date of the observed maximum, 1921, May 5. In all, fifteen exposures were compared with this standard, and equations formed, coefficients for π, μ_δ and δ (distance) determined by the same method as before being used. The following results were obtained:

$$\pi = +0.''002 \pm 0.''063;\ \mu_\delta = -0.''001 \pm 0.''012;\ \delta = -0.''385 \pm 0.''024.$$

The value of the parallax agrees well with that obtained by van Maanen by measuring these plates in right ascension, as already stated. Even though the time interval is short the probable error of the determined proper motion is small, and hence the value of μ_δ may be relied upon with some degree of confidence.

As for the value of the distance, the sign shows the displacement to be to the south of the standard position, and, since the standard exposure was made at a period of maximum, a time when the variable star was dominant, this fact furnishes independent confirmation of the conclusion by Van Biesbroeck that the north star is the variable one. The numerical value requires further consideration. The displacements obtained from the several plates are shown in Table II.

TABLE II

Plate Nos.	Displacement	Plate Nos.	Displacement
2675_1–3100	$-0.''015$	2831_1–3100	$-0.''154$
2675_2–3100	$-$ .035	2831_2–3100	$-$ .194
2699_1–3100	$+$ .039	2846_1–3100	$-$ .165
2699_2–3100	$+$ .003	2846_2–3100	$-$ .167
2802_1–3100	$-$ .126	3083_1–3100	$-$ .035
2802_2–3100	$-$ .115	3083_2–3100	$-$ .002
2814_1–3100	$-$ .168	3100–3100	.000
2819_1–3100	-0.190	3112–3100	-0.018

It has been shown that the relative parallax and proper motion of this object are very small, and their effect in displacing the image is therefore negligible. Hence the measured displacements may be considered as due to the relative change in magnitude alone. The mean displacement of the first four and the last four exposures, all of which were made very near to a period of maximum brightness, is −0″.008; the mean displacement of the remaining eight exposures, which were made within an interval of fifteen days, although seventy-one days before minimum, is −0″.160. There is therefore a measured displacement of −0″.152 in the interval from near maximum to seventy-one days before minimum. As the time during which this displacement took place is only one-half the interval from maximum to minimum, one might be led to conclude that a displacement of twice this amount would result from plates taken at minimum. As the distance between the stars obviously cannot be less than the measured displacement, this conclusion would indicate a distance fairly accordant with the computed value obtained above. Table I, however, would contradict such a conclusion in that it shows that on the mean date, August 18, of the second group of plates the invariable contributes more than twice as much light as the variable, instead of only an equal amount, as would seem to be required if the resultant image is to have a position midway between the extremes.

It seems, therefore, impossible to reach a definite conclusion because of uncertainty in two respects: first, the exact magnitude of the invariable star upon which depend the relative amounts of light contributed by the two components at the times of the exposures and, second, the effect of variable intensities upon the position of the resulting image. Both of these difficulties would vanish in a case in which we knew that the variable was entirely ineffective at minimum and completely dominated the formation of the image at maximum, and if we had one series of plates at maximum and another at minimum. The latter condition is not fulfilled in this instance, and it is probable that the former is not. The assumption of 8.6 as the magnitude of the invariable leads, as is seen in Table I, to the conclusion that the invariable star is responsible for one-fourth of the total light at maximum and for all of the light at minimum. It does not seem likely that the variable becomes so faint at minimum as to be entirely without any effect in the formation of the image at that time. Even though it may contribute a part of the light, it may, however, be such a small percentage as to be ineffective in displacing the measured center of gravity. In that case the computed value for the distance between the stars, 0.″385, would be too large. On the other hand the measured displacement, 0.″152, although apparently more than half the distance between the stars, is somewhat smaller than the distance. The true value for the distance would therefore lie between these two limits. A number of suppositions might be made which would lead from the foregoing conclusion to a value almost identical with the value obtained by Van Biesbroeck from direct measurement. We may therefore say, in conclusion, that this investigation shows without any doubt that the north star is the variable one, and if it does not confirm the value for the distance between the stars it most certainly does not contradict it. The writer expects to continue the study of this pair by securing plates at maximum and at minimum.

The suggestions by Mr. van Maanen and Mr. Merrill during this work were of great help and were thoroughly appreciated by the writer. Valuable assistance was rendered also by Mrs. Marsh, of the Computing Division, who checked the computations in the early part of the study.

Mount Wilson Observatory
May 1922

Contributions from the Mount Wilson Observatory, No. 239
Reprinted from the *Astrophysical Journal*, Vol. LVI, pp. 139–144, 1922

PARALLAXES OF STARS IN THE REGION OF B.D.+31°643

By C. H. GINGRICH

ABSTRACT

Diffuse, irregular nebula, and stars around B.D.+31°643.—*A photograph* made by Hubble with the 100-inch reflector is reproduced. From a series of plates taken by van Maanen with the 60-inch reflector, the *parallaxes and proper motions of 20 stars* with reference to six or seven among them which appear not to be related to the nebula, were determined. Five of these have *color-indices* from 0.74 to 0.95 in excess of normal and seem to be involved in the nebula. The mean of the parallaxes of these five stars is 0.″0095±0.″006. This is therefore taken to be the *parallax of the nebula*, equivalent to a distance of 350 light-years from the sun.

The star B.D.+31°643 is of special interest because it is apparently imbedded in the densest part of a diffuse, irregularly shaped nebula extending over the region surrounding this star. The photograph of this region published herewith is reproduced from a negative made by Mr. Hubble with the 100-inch Hooker telescope, November 9, 1920, and kindly loaned to me for this purpose. The exposure time of this negative was 180 minutes.

A series of plates of this same region, taken by Mr. van Maanen with the 60-inch reflector as a part of his regular parallax program, was begun in December, 1919, and finished in January, 1922. The stars which appear on the parallax plates are numbered on the photograph (Plate I), except the brightest star, whose image was too large for measurement. The one designated as π is the star B.D.+31°643. Mr. van Maanen gave me these plates to measure in order to find out whether, on the basis of the parallaxes, the stars could be classified in two groups, the one containing those stars which belong to the nebula and the other those which do not.

Another basis for a separation into such groups had already been suggested by Mr. Hubble, namely, a comparison of color-index with spectral type. He had noticed that in the case of certain of the stars the color-index was larger than would be accounted for by the spectral type, which led him to the conclusion that the excessive redness was due to the absorption of the blue light by surrounding nebulous matter.

In Table I the first column gives the numbers assigned to the stars on the parallax plates and corresponding to the numbering on Plate I; the second and third columns give, respectively, the distances of the various stars from the central star in right ascension and declination, in minutes of arc; the next five columns were supplied by Mr. Seares and Mr. Hubble from material now being prepared for publication by them; the last two columns give the final mean values of parallax and proper motion in right ascension, expressed in thousandths of a second of arc. These last quantities will be explained more fully later.

TABLE I

No.	x	y	Photo. Mag.	Spectrum	Observed Color-Index	Normal Color-Index	Color-Excess	π (Mean)	μ_a (Mean)
π	0′.0	0′.0	9.07	B6	+0.65	−0.14	0.79	− 8	− 14
1	−14.8	+7.7	....	.....	....	....	....	+ 67	− 56
2	− 9.0	+3.3	....	.....	....	....	....	− 17	− 34
3	− 7.6	0.0	11.81	.....	+ .59	....	....	+ 13	+ 25
4	− 5.5	−2.5	10.19	B8	+ .42	− .07	.49	+ 31	− 10
5	− 5.2	−2.7	10.31	B8	+ .48	− .07	.55	+ 28	− 15
6	− 3.2	−0.3	12.32	A2	+ .71	+ .07	.64	+ 8	+ 4
7	− 2.7	−2.2	12.08	F2	+ .65	+ .48	.17	+ 2	+ 10
8	− 2.2	+1.2	14.6±	.....	....	....	....	− 14	− 5
9	− 2.1	+0.4	12.14	A1	+ .82	+ .03	.79	+ 28	+ 22
10	− 0.7	+0.1	12.32	B9	+ .71	− .03	.74	+ 5	− 5
11	− 0.5	−3.4	11.42	B9	+ .92	− .03	.95	− 5	− 9
12	+ 0.3	+0.3	10.80	B9	+ .80	− .03	.83	+ 32	+ 75
13	+ 0.7	−3.0	14.5±	.....	....	....	....	− 44	− 85
14	+ 2.9	+5.8	14.8±	.....	....	....	....	+ 24	+115
15	+ 3.2	+7.1	14.3±	.....	....	....	....	+ 50	+ 75
16	+ 3.4	+9.5	11.99	A0	+ .96	.00	.96	+100	+210
17	+ 7.1	+0.7	14.0±	.....	....	....	....	0	+ 15
18	+ 7.1	−9.2	14.22	.....	+1.02	....	....	− 36	−162
19	+11.1	+7.5	9.40	K0	+1.53	+1.48	0.05	+ 34	+ 29

The plates were arranged in pairs and measured with the new stereocomparator of the Mount Wilson Observatory according to the method developed by van Maanen and fully described by him in *Mount Wilson Contribution* No. 111. For comparison stars those were chosen which, according to the color-index cri-

PLATE I

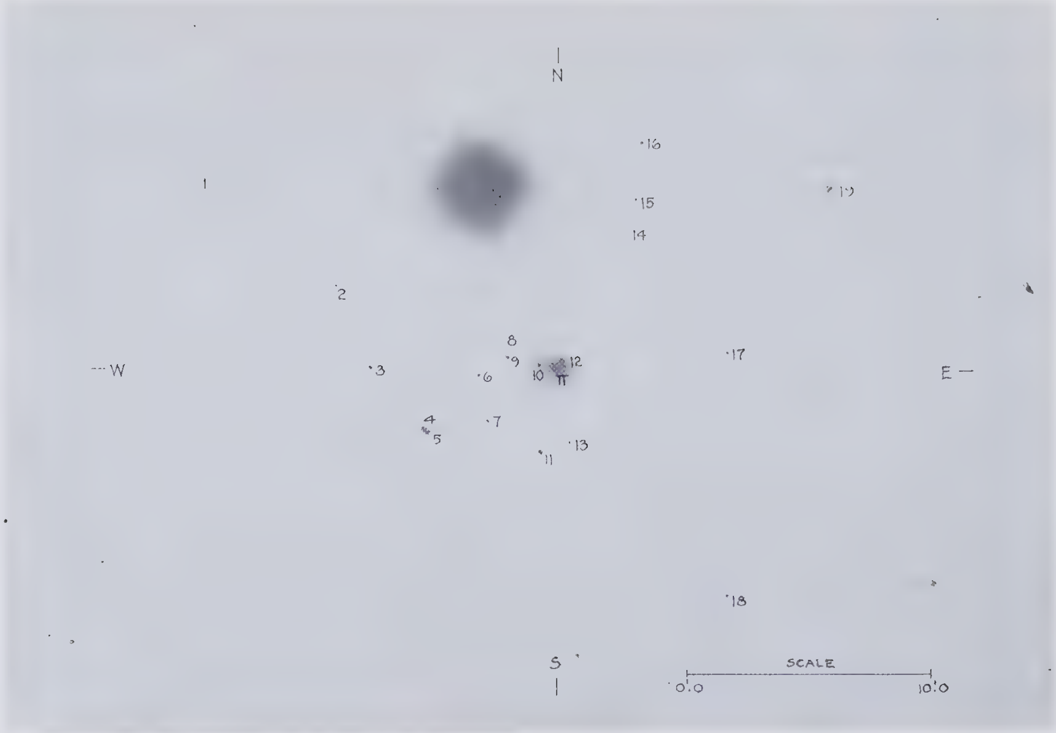

Region of B.D.+31°643 Photographed by Hubble with the 100-Inch Hooker Reflector, November 9, 1920

terion, had no connection with the nebula. As was to be expected, this selection resulted in having as comparison stars those situated at some distance from the nebula and consequently located at considerable distances from the center of the plate. It was accordingly advisable to use quadratic terms in the reductions. However, as the exclusion of the stars which may be connected with the nebula left only seven stars available for that purpose, the six plate constants could not be determined with great accuracy. Two other solutions were therefore made, omitting the quadratic terms. The number of comparison stars in the first solution was seven and in the later ones six and four, omitting those so far from the center as to show unsymmetrical images on some of the plates.

The fact that the number of comparison stars available was small is probably not a matter of mere accident. On the parallax plates certain regions are easily noticeable in which no stars appear. It therefore seems likely that the nebula so conspicuous in certain parts of the field extends faintly over perhaps the entire region of the parallax plates with the result that the light of the fainter stars is absorbed or scattered by it. This conclusion is confirmed on the basis of the total number of stars on the parallax plates. According to *Groningen Publications* No. 27, the total number of stars would indicate that the faintest stars appearing are of magnitude 12.3 approximately, whereas as a rule stars as faint as magnitude 13.7 appear on the plates. In other words we should normally expect to find more than three times as many stars on plates at the galactic latitude of this field as are actually found on these.

Moreover, as will be seen in Table II, no definite classification of the stars into nebulous and non-nebulous is possible on the basis of the parallaxes found.

The values of parallax and proper motion in right ascension for each of the stars from each of the three reductions are shown in Table II. The first values resulted from a solution including quadratic terms and using stars 1, 2, 3, 7, 17, 18, 19 as comparison stars; the second, not including quadratic terms and employing stars 2, 3, 7, 17, 18, 19 as comparison stars; the third is like the second except that only four comparison stars were used, 2, 3, 7, 17. The results are expressed in thousandths of a second of arc.

In order to determine the weights to be assigned to each of these sets of values the arithmetical means of the three were formed and the deviations from the means noted. These deviations indicated that weights 1, 1, 2 should be used. Adopting these weights the mean values of π and μ_a given in the last two columns of Table I were obtained. The mean probable error of all the parallaxes is ±0.″013 and of all the proper motions is ±0.″019. These values are unusually large because stars 1, 16, 18, and 11 are more than 10′ from the center, the limit usually set for parallax determinations, and hence not well suited for measurement. Excluding these stars from the computation, we find the mean probable error of the remainder of the parallaxes to be ±0.″009, and of the proper motions ±0.010.

TABLE II

SUMMARY OF π AND μ_a

	π_1	p.e.	μ_{a1}	p.e.	π_2	p.e.	μ_{a2}	p.e.	π_3	p.e.	μ_{a3}	p.e.
π..........	+ 36	8	− 2	12	− 22	7	+ 5	10	− 23	6	− 30	9
1..........	+ 11	3	+ 12	4	+ 57	31	−192	45	+100	19	− 21	28
2..........	− 24	5	− 30	8	− 25	11	− 75	16	− 10	3	− 16	4
3..........	− 7	3	+ 4	4	+ 24	7	+ 41	10	+ 18	5	+ 28	7
4..........	+ 26	9	− 18	14	+ 47	11	+ 38	16	+ 25	10	− 31	15
5..........	+ 25	2	− 20	3	+ 45	8	+ 37	12	+ 21	5	− 39	7
6..........	+ 40	9	+ 12	14	+ 2	11	+ 22	16	− 4	8	− 9	12
7..........	+ 26	5	+ 20	8	+ 7	9	+ 54	13	− 12	4	− 17	6
8..........	+ 33	11	+ 8	17	− 34	5	− 7	7	− 27	5	− 10	7
9..........	+ 70	11	+ 32	16	+ 13	8	+ 32	12	+ 14	6	+ 11	9
10..........	+ 50	21	+ 7	30	− 10	18	+ 12	26	− 10	20	− 19	29
11..........	+ 27	13	+ 17	19	+ 1	13	+ 51	19	− 24	8	− 52	12
12..........	+ 78	18	+ 88	26	+ 15	9	+ 91	13	+ 17	10	+ 61	15
13..........	− 10	11	− 58	16	− 40	10	− 31	15	− 64	12	−126	18
14..........	+107	33	+159	48	− 31	8	+ 51	12	+ 10	18	+125	26
15..........	+148	32	+138	46	− 16	8	− 13	12	+ 35	18	+ 88	26
16..........	+229	48	+319	71	+ 12	13	+ 75	19	+ 80	24	+224	35
17..........	− 1	1	+ 1	2	− 6	8	+ 48	12	+ 4	1	+ 5	1
18..........	− 5	1	− 5	2	− 6	7	− 51	10	− 66	45	−297	66
19..........	0	1	− 1	1	+ 5	4	− 18	6	+ 66	21	+ 68	31

A direct examination of the original negative from which the accompanying plate has been made would indicate that the stars numbered 1, 2, 3, 7, 14, 15, 17, 18, and 19 are not connected with the nebula; that those numbered 8, 13 are probably involved in it; and that those numbered π, 9, 10, 11, 12, 16 are apparently enmeshed in it. There is no nebulosity visible about the stars 4, 5, 6, but their color-indices are such as to lead one to suspect the presence of nebulous matter.

Selecting from Table I those stars which to all appearances are imbedded in the nebula, omitting the one numbered 16 because of uncertainty due to its distance from the center of the plate and from the other stars of the group, we have for the five stars, π, 9, 10, 11, 12, a mean relative parallax of +0.″0104. Two other stars, those numbered 3 and 6, have about the same parallax as the mean just found. The latter, as already stated, should probably be included among the five because of the evidence furnished by its color-index; as for the former, no evidence of connection with the nebula or with the group is indicated other than that of its parallax.

We are therefore led to the conclusion that the mean relative parallax of the five stars and hence the parallax of the nebula of which they almost certainly form a part is +0.″0104. By applying to this the correction of −0.″0009 derived by van Maanen[1] to reduce it to absolute parallax we find as the absolute parallax of the nebula +0.″0095. This value of the parallax indicates a distance from the sun of about 350 light-years.

The very bright star in the photograph is *o* Persei. Two determinations of the parallax of this star have been made: one at the Sproul Observatory, +0.″035; the other at the Allegheny Observatory, +0.″003. The mean of these shows a value not greatly at variance with the parallax found for the nebula.

The double star 4 and 5 is listed as number 1832 in Burnham's *General Catalogue* and is there assigned a separation of 11.″14 in position angle 128.°6. Measures extending from the year 1868 to the year 1903 show no change in either of these quantities.

The central star B.D.+31°643, designated on the plates used as π, is also a double star. It is numbered 1836 in Burnham's *General Catalogue* and consists of two stars of nearly the same brightness and only 0.″45 apart in 1880. Measures from the year 1891 to the year 1893 indicate a slight progressive increase in the distance. On the scale of our plates the two components combine to form a single symmetrical image.

---

[1] *Mt. Wilson Contr.*, No. 237.

This investigation would have been entirely impossible at this time had it not been for the series of plates taken by Mr. van Maanen, and in a sense therefore these results are due to him. Furthermore, his large experience in parallax work was heavily drawn upon throughout this work, and numerous constructive suggestions were cheerfully made by him.

The writer wishes also to express his hearty appreciation of the willing and generous co-operation of Mr. Seares and Mr. Hubble in the ways already indicated.

Mount Wilson Observatory
April 1922

Contributions from the Mount Wilson Observatory, No. 240
Reprinted from the *Astrophysical Journal*, Vol. LVI, pp. 40–52, 1922

INTERFEROMETER OBSERVATIONS OF DOUBLE STARS

By PAUL W. MERRILL

ABSTRACT

Interferometer observations of double stars.—(1) *Revised elements of the orbit of Capella* were obtained by combining the previously reported measurements of Anderson, slightly corrected, with observations made on ten nights from October 1920 to April 1921 using the rotating interferometer attached to the 100-inch telescope. The chief results are: $P=104.022$ days; $a=0''.05360$; $a_1+a_2=126.63\times10^6$ km; $\pi=0''.0632$; $m_1=4.2\odot$; $m_2=3.3\odot$. The average residuals are 1° for position angle and $0''.0007$ for separation. (2) κ *Ursae Majoris* was independently discovered as a double and was measured on five nights, March 1 to April 30, 1921. The separation decreased from $0''.0836$ to $0''.0772$, but the position angle changed only 2°. One component is brighter by perhaps half a magnitude. (3) ν^2 *Boötis* was found to be difficult to measure as the fringes behaved abnormally, so only a rough measurement was possible. The system may be complex. (4) *Search for new measurable double stars.* Some spectroscopic binaries, stars with composite spectra, variable stars, and some bright stars taken at random—in all 85 stars, of varying magnitude down to 5.7 (Table IV)—were examined for duplicity, but with the exception of six doubtful cases, δ Cancri, 10 Leonis Minoris, o Leonis, ϵ and f Ursae Majoris, and υ Sagittarii, no changes in fringe visibility with position angle of the interferometer were observed.

Tests by Michelson at the Yerkes and Mount Wilson observatories[1] showed that even in poor seeing interference fringes can be observed in star images with slit separations ranging from 40 to nearly 100 inches. Following these results in an attempt to make the interference method sufficiently accurate and convenient to justify its extended use in the measurement of double stars, Mr. Anderson devised a new type of stellar interferometer with which settings are made by rotating a pair of fixed slits. This instrument he applied with great success to the determination of the relative positions of the components of Capella.[2] His measures of distance, on five nights, ranged from $0''.0418$ to $0''.0505$, while the position angles were shown to be decreasing at a rate in keeping with a revolution period of 104 days. A double-star orbit was computed by him, using the spectroscopic elements previously determined at the Lick Observatory.

---

[1] *Mt. Wilson Contr.*, No. 184; *Astrophysical Journal*, **51**, 257, 1920.

[2] *Mt. Wilson Contr.*, No. 185; *Astrophysical Journal*, **51**, 263, 1920.

It is interesting to note that in 1900 J. Miller Barr called attention to the desirability of attempting the observation of Capella as a double star by interferometer methods.[1]

The present paper is a record of further applications of the rotating type of interferometer to known double stars, and to a search for new doubles of small angular separation. The 100-inch Hooker telescope was used in all the observations, and practically the same procedure as that described by Anderson was followed throughout.

The constants of the interferometer were redetermined independently. The factor which is used to reduce the actual separation of the slits to their corresponding separation in the Gauss plane was found by dividing the equivalent focal length of the telescope, 1606 inches, by 28.00 inches, the distance of the slits from the focus. The value thus obtained, 57.34, was checked by a direct determination. At the upper end of the telescope tube, on the struts supporting the secondary mirror, were placed two rectangular pieces of wood of the same shape as the slits, but with dimensions slightly smaller than those of the slits as projected in the Gauss plane. Thus, when the telescope was directed to a bright star, by removing the eye-piece and placing the eye at the focus, the blocks could be centered in the slits, leaving lines of light at the edges. The separation of the blocks, divided by the separation of the slits, gives the factor desired. This experiment yielded the value 57.2, which was thought to be a trifle small. The factor adopted for all the reductions was 57.3, which falls within the limits of uncertainty of both determinations.

CAPELLA

R.A. 1900 = $5^{h}9^{m}.3$; Dec. 1900 = $+45^{\circ}54'$; Mag. 0.2; Class G0.

Additional interference measures of Capella have been made by the writer on ten nights, and a revised orbit has been calculated.

As the series of observations was made during the winter months poor seeing was frequently experienced. Although the observing routine could usually be carried through in the regular way, on a few occasions the conditions became so bad that reliable settings could be made only by watching patiently and utilizing the best moments. The nights on which bad seeing prevents interferometer observations of Capella are quite rare. This is not true to the same extent of fainter stars.

---

[1] *Astrophysical Journal*, **11**, 248, 1900.

The new measures of Capella appear in Table I, in which the third column, with the heading Slits, gives the separation (in the Gauss plane) of the slits; the fourth column, η, contains the

TABLE I

Observations of Capella

Date	P.S.T.	Slits	η	θ	ρ	
1920 Oct. 5....	16h 15m	174.2 cm	46°.65	253°.9	474	
Nov. 3....	13 20	142.8	24.75	164.8	437	
	14 05	173.3	41.90	164.6	440	
	14 39	203.6	50.80	163.8	441	
1921 Jan. 14....	7 36	142.2	30.12	263.5	461	
	8 31	172.6	45.25	262.9	467	
	9 08	202.9	52.65	262.2	461	
	10 25	202.9	51.78	261.2	452	Weight ½
Jan. 31....	7 07	142.2	43.45	213.7	550	
	7 19	172.6	52.40	214.0	539	
	7 29	202.9	58.82	214.8	540	
	7 46	123.9	33.32	212.8	548	
Feb. 2....	7 18	172.6	52.67	209.8	542	
	7 52	142.2	43.30	208.6	548	
	8 55	202.9	58.07	207.9	529	Weight ½
Mar. 1....	6 52	172.6	36.95	106.0	411	
	7 10	202.9	47.00	105.6	410	
	7 23	232.8	53.25	106.2	407	
Mar. 2....	6 44	202.9	48.32	101.2	421	
	6 52	172.6	39.22	102.4	424	
	7 04	232.8	54.35	101.4	418	
Mar. 3....	6 52	172.6	39.27	98.1	425	
	7 08	202.9	48.10	97.8	419	
	7 23	232.8	54.05	98.4	415	
Mar. 31....	7 07	172.6	51.00	15.0	522	
	7 23	202.9	56.60	14.2	508	
	7 38	142.2	38.87	14.3	512	
Apr. 1....	7 16	142.2	37.50	11.4	503	
	7 35	172.6	48.65	11.4	498	
	7 55	202.9	56.32	11.7	504	

angle of projection for minimum fringe visibility;[1] the fifth column, θ, the position angle of the components; and the sixth column, ρ, their separation in units of one ten-thousandth of a second of arc, i.e., 474 = 0″.0474. The effective wave-length was taken to be 5500 A.

In Table II are collected the mean values for each night. The weights assigned depend principally on the number of complete individual observations. The total number of settings was increased during poor seeing in an attempt to give approximately standard accuracy to each complete observation. Since the factor 57.3 is somewhat smaller than that used by Anderson in the first observations, it was decided by mutual agreement between him and the writer that it would be better to change the original reductions. Hence the first five values of ρ in Table II are larger by 2.4 per cent than the corresponding figures in *Contribution* No. 185.

TABLE II

MEAN CO-ORDINATES OF COMPONENTS OF CAPELLA

G.M.T.	θ	O−C	ρ	O−C	Weight	
(1) 1919 Dec. 30.65	....	....	428	+3	⅓	Anderson
(2) 1920 Feb. 13.63	5.0	+2.2	469	−7	⅔	Anderson
(3) Feb. 14.65	1.0	+1.6	462	−6	1	Anderson
(4) Feb. 15.66	356.4	+0.5	454	−6	1	Anderson
(5) Mar. 15.63	242.0	+1.9	517	+10	⅔	Anderson
(6) Apr. 23.63	107.0	+0.4	....	....	⅓	Anderson
(7) Oct. 6.01	253.9	+2.6	474	−7	⅓	....
(8) Nov. 3.92	164.4	−1.6	439	−4	1	....
(9) 1921 Jan. 14.70	262.6	−0.1	461	+5	1	....
(10) Jan. 31.64	213.8	+0.6	544	+11	1	....
(11) Feb. 2.66	208.9	+1.1	542	+14	1	....
(12) Mar. 1.63	105.9	−0.9	409	−11	1	....
(13) Mar. 2.62	101.6	−1.1	421	−5	1	....
(14) Mar. 3.63	98.1	−0.4	420	−12	1	....
(15) Mar. 31.64	14.5	−1.0	514	+7	1	....
(16) Apr. 1.65	11.5	−1.0	502	+2	1	....

The orbital elements deduced by Anderson gave a fair representation of the additional observations but it was found possible to make some slight improvements.

---

[1] The out-of-step appearance of the fringes shown in Anderson's laboratory experiments (see illustration in *Mt. Wilson Contr.*, No. 185) was not observable. Accordingly the sensitive method of fringe bisection could not be used, but settings were made for the minima of visibility.

By comparing recent spectroscopic observations at Mount Wilson with those made at the Lick Observatory in 1900 Sanford[1] has found that the original figures for the period, 104.022 days, are very nearly correct. Accordingly this value has been used throughout the present computations.

Preliminary trials showed that the eccentricity is probably smaller than 0.016 as given by Reese. Hence it did not seem necessary to vary both T and ω. The date 2422596.79 was chosen for T by trial and retained thereafter. This corresponds to a periastron time 0.8 days later than that adopted by Anderson. Corrections to a and to Ω were then found by direct algebraic processes. Finally a least-squares solution was carried through for the elements ω, i, and e. This yielded very small corrections to the preliminary values.

The adopted elements follow:

$T=$ J.D. 2422596.79
$P=104.022$ days, angles decreasing.
$\omega=114^\circ\!.30$
$i=-41^\circ\!.08$
$\Omega=38^\circ\!.70$
$e=0.0086$
$a=0''\!.05360$

To these may be added the following quantities found by combining the foregoing elements with the spectroscopic results:

$a_1+a_2=126{,}630{,}000$ km $m_1=4.2\odot$
$\pi=0''\!.0632$ $m_2=3.3\odot$

The residuals from these elements are given in Table II. They are considerably larger than one might expect from the degree of accordance of the individual observations as shown by Table I. Moreover, observations made on successive nights exhibit a tendency toward similar residuals. This would seem to mean either that there are systematic errors in the observations, or that the best orbital elements have not been found, or that the orbit is not a true ellipse, or that there is present a combination of two or three of these causes.

---

[1] *Publications Astronomical Society of the Pacific*, 34, 178, 1922.

As to systematic errors it must be admitted there are possibilities of slight effects. For instance, no ready direct method was found of checking the position angle circle of the interferometer when attached to the telescope, so that the actual position angles of the slits may conceivably have differed by small amounts from the angles as read from the circle. Again, the condition of the telescope mirrors, the position of the struts supporting the secondary mirror, the settings of the compensator, the exact location of the focus, the condition and position of the observer's eyes, may have been responsible for small systematic errors. For the most refined results in an extensive investigation all these factors should receive attention.

In regard to the orbital elements it may be that a different set of values would give smaller residuals. Indeed it has been found by taking $T=2422563.76$, $\omega=0^\circ.0$, $e=0.01$, that the residuals in ρ are considerably reduced while the θ residuals are somewhat increased. With a circular orbit the representation is also very good. This indicates that as far as the interferometer observations are concerned the eccentricity and the time of periastron are practically indeterminate. As compared with the spectroscopic orbit this condition doubtless arises from the flexibility of the double star orbit due to the inclusion of the element representing the inclination of the orbit plane. By varying the orbital elements *arbitrarily* a better set of residuals than those in Table II could probably be found, but in view of the spectroscopic data there would apparently be no physical justification for such procedure and it has been thought better to retain the elements given on page 207 until future observations shed more light upon the situation.

One curious feature appears with several different trial sets of orbital elements, namely, that the early observations persist in giving positive residuals for θ (O−C). This may be due either to a systematic difference between Anderson's observations and the writer's, or to perturbations causing the position angle of the real node to decrease with time at the rate of about $2^\circ.4$ per year, or about $0^\circ.6$ in one orbital revolution. The physical interpretation and probability of such a perturbation may be a matter of interest to mathematical astronomers.

If, from the orbit adopted in this paper, we compute the position angles corresponding to the Greenwich observations[1] in 1900 (mean places), we find a fairly consistent set of residuals averaging +18°. Compared with the interferometer observations, this residual would be removed by a motion of the node of 0°9 per year in the same direction as that suggested by the residuals of the interference measures themselves.

Capella presents one of the very small number of cases in which a comparison of the visual and spectroscopic data leads to an accurate value of the parallax. The value found in the present investigation, 0″063, agrees well with the mean trigonometric determination, 0″067, and the spectroscopic value,[2] 0″076.

κ URSAE MAJORIS

R.A. 1900 = 8^h56^m8; Dec. 1900 = +47°33′; Mag. 3.7; Class A0.

On the night of March 1, 1921, Mr. Anderson and the writer were engaged in making some tests in connection with the stellar interferometer attached to the Hooker telescope, of a special apparatus[3] devised by the former to produce an artificial double star of known separation by means of which the constants used in the regular reductions might be checked. It consisted of a quartz plate two and a half millimeters thick, cut at 45° to the optic axis, which, when mounted in the converging beam, transformed a single star into a double star having a separation of 12 microns, which corresponds to 0″06 at the Cassegrain focus of the Hooker telescope. When the telescope was pointed toward κ Ursae Majoris and the observations were begun, anomalous results were obtained. Instead of the usual *four* minima in a complete revolution, a larger number appeared. We recognized that the behavior corresponded to that of a quadruple star and surmised that the star would be measurable as a double without the quartz plate. Proceeding at once to verify this by removing the quartz plate and making settings in the ordinary manner, we determined the position angle and separation to be 251°9 and 0″0836. It was not until a few days later that we learned that this star is a known double, A 1585, discovered by Aitken[1] in 1907 when its separation was about twice as great. This incident illustrates the fact that a close quadruple star can readily be detected by the interference method.

---

[1] *Monthly Notices, Royal Astronomical Society*, **61**, 72, 1901.

[2] *Mt. Wilson Contr.*, No. 199; *Astrophysical Journal*, **53**, 34, 1921.

[3] *Mt. Wilson Contr.*, No. 222; *Astrophysical Journal*, **55**, 48, 1922.

Subsequent interferometer measures made during March and April 1921 showed that the separation was decreasing at the rate of $0''.003$ per month, and the position angle by about one degree per month.

TABLE III

MEASURES OF κ URSAE MAJORIS

Date	Position Angle	Distance	
1907.83	$283^\circ.2$	$0''.21$	Aitken, micrometer
1909.33	281.4	0.25	Aitken, micrometer
1919.29	264.9	0.15	Aitken, micrometer
1921 Mar. 1	251.9	0.0836	
Mar. 2	252.5	0.0833	
Mar. 31	251.3	0.0801	
Apr. 1	250.7	0.0796	
Apr. 30	250.2	0.0772	

In good seeing the fringes are quite distinct even at minimum visibility, showing that the components are not equal. The magnitude difference is perhaps two or three times as great as in Capella, but probably does not much exceed one-half of a magnitude.

ν^2 BOÖTIS

R.A. 1900 = $15^h 28^m.2$; Dec. 1900 = $+41^\circ 14'$; Mag. 5.0; Class A2.

At the suggestion of Dr. Aitken the double star ν^2 Boötis, A 1634,[2] was placed upon the observing list. This close double of separation $0''.1$ or less had been found to be a difficult object to resolve with the Lick 36-inch refractor. His observations[3] indicate that the position angle has decreased from 237° in 1907 to about 213° in 1920.

Examination of this star with the interferometer showed that the visibility changed as the slits were rotated, but observations on different nights, and with different slit separations, did not yield the consistent results obtained with Capella and κ Ursae Majoris, and to be expected of any double star. The observations were rather difficult on account of the faintness of the image. The regular sized slits were employed although it might have been an advantage to use larger ones.

---

[1] *Lick Observatory Bulletin*, 4, 168, 1908.

[2] *Ibid.*

[3] Kindly communicated by letter.

On the night of June 18, 1921, immediately following rather unsuccessful attempts at measurement, this note was written:

> Seeing and visibility are good but settings on ν^2 Boötis seem almost impossible. Fringes are certainly visible in all position angles at 108.9, 142.2, 172.6, and 202.9 cm (slit separation). It is a question of *small* differences in visibility; these differences seem smaller tonight than previously. One must guard against the physiological factor that fringes appear more distinct when parallel to the line joining the eyes. This may cause some of the above readings to be illusory. However, I believe there are real variations in visibility. Perhaps the star is triple or complex. Sometimes there appear to be regions 20° to 30° wide of low visibility. There appear to be "shoulders" in the visibility curve; i.e., the visibility drops off on rotating 5°–10° but does not return at once on rotating further. Star is a puzzle so far. Perhaps a wide double with one star a close pair.

Mr. Humason also examined this star on the same evening, June 18, 1921, and thought the variations in visibility to be real.

If we assume the object to be a double star the most probable result deduced from all the settings appears to be $\theta = 192°$, $\rho = 0''.061$. This depends very largely on observations with a slit separation of 142.2 cm. The mean epoch was May 1921.

EXAMINATION OF STARS FOR DUPLICITY

A number of stars have been tested for evidences of duplicity by looking for variations in the visibility of the fringes as the slits were rotated. Slit separations up to 200 cm (80 inches) were used in nearly all cases. The stars in Table IV exhibited no appreciable variation of fringe visibility with position angle of the slits. If these stars are double, their components could not have been as much as $0''.03$ apart on the date of observation, provided their magnitudes are nearly equal. If the difference in magnitude is greater than 0.5, changes in visibility might escape detection unless the circumstances were especially favorable. The stars examined include spectroscopic binaries, stars with composite spectra, variable stars, and some bright stars taken at random.

TABLE IV

Stars Apparently Single

Star	Mag.	R.A. 1900	Star	Mag.	R.A. 1900
β Persei	var.	$3^{h}\ 1^{m}.7$	*d* Boötis	4.8	$14^{h}\ 5^{m}.8$
ζ Tauri	3.0	5 31.7	α Boötis	0.2	14 11.1
51 Aurigae	5.7	6 31.7	A Boötis	4.8	14 13.8
ψ^{5} Aurigae	5.3	6 39.5	θ Boötis	4.1	14 21.8
α Geminorum	2.0, 2.8	7 28.2	ρ Boötis	3.8	14 27.5
β Geminorum	1.2	7 39.2	ε Boötis	2.7, 5.1	14 40.6
40 Lyncis	3.3	9 15.0	109 Virginis	3.8	14.41.2
θ Urs. Maj	3.3	9 26.2	β Boötis	3.6	14 58.2
ε Leonis	3.1	9 40.2	δ Boötis	3.5	15 11.5
η Leonis	3.6	10 1.9	ι Draconis	3.5	15 22.7
α Leonis	1.3	10 3.0	β Cor. Bor	3.7	15 23.7
λ Urs. Maj	3.5	10 11.1	ν Boötis	5.2	15 27.3
ζ Leonis	3.6	10 11.1	α Cor. Bor	2.3	15 30.5
μ Urs. Maj	3.2	10 16.4	κ Serpentis	4.3	15 44.2
ρ Leonis	3.8	10 27.5	α Scorpii	1.2	16 23.3
46 Leo. Min	3.9	10 47.7	β Herculis	2.8	16 25.9
ψ Urs. Maj	3.2	11 4.0	α Herculis	3.5, 5.4	17 10.1
δ Leonis	2.6	11 8.8	δ Herculis	3.2	17 10.9
ξ Urs. Maj	4.4, 4.9	11 12.9	π Herculis	3.4	17 11.6
ν Urs. Maj	3.7	11 13.1	ο Herculis	3.8	18 3.6
χ Urs. Maj	3.8	11 40.8	*d* Serpentis	5.3	18 22.1
93 Leonis	4.5	11 42.8	α Lyrae	0.1	18 33.6
β Leonis	2.2	11 44.0	β Lyrae	Var.	18 46.4
β Virginis	3.8	11 45.5	113 Herculis	4.6	18 50.5
γ Urs. Maj	2.5	11 48.6	β Cygni	3.2, 5.4	19 26.7
δ Urs. Maj	3.4	12 10.5	δ Sagittae	3.8	19 42.9
γ Corvi	2.8	12 10.7	η Aquilae	Var.	19 47.4
η Virginis	4.0	12 14.8	31 Cygni	4.0	20 10.5
δ Corvi	3.1	12 24.7	32 Cygni	4.2	20 12.3
8 Can. Ven	4.3	12 29.0	β Capricorni	3.2	20 15.4
δ Virginis	3.7	12 50.6	47 Cygni	4.8	20 30.0
43 Com. Ber	4.3	13 7.2	α Equulei	4.1	21 10.8
20 Can. Ven	4.7	13 13.1	14 Pegasi	5.0	21 45.4
ζ Urs. Maj	2.4, 4.0	13 19.9	δ Cephei	Var.	22 25.4
17 Can. Ven	5.0	13 30.3	η Pegasi	3.1	22 38.3
τ Boötis	4.5	13 42.5	ο Androm	3.6	22 57.3
η Boötis	2.8	13 49.9			

NOTES

$7^{h}28^{m}.2$, α Geminorum, both components, 2.0, 2.8.
11 12.9, ξ Urs. Maj., both components, 4.4, 4.9.
13 19.9, ζ Urs. Maj., both components, 2.4, 4.0.
14 40.6, ε Boötis, both components, 2.7, 5.1.
17 10.1, α Herculis, both components, 3.5, 5.4.
18 22.1, *d* Serpentis, brighter component, 5.3.
19 26.9, β Cygni, both components, 3.2, 5.4.

Although the dates of observation, slit separations employed, the seeing, and notes on any apparent peculiarities were, of course, recorded in the observing book and will be made available to anyone interested in a particular star, these details do not seem worth publishing. For the most part the dates of observation lie between February 1 and June 17, 1921. Several stars observed by Anderson about a year earlier are included in Table IV. On a few nights Mr. Humason alternated with the writer in the examination of stars for duplicity.

Variations in visibility for *f* Ursae Majoris (R.A. 1900 = $9^h1^m.9$; Dec. 1900 = +52°0′; Mag. 4.5; Class A3p) were suspected on the night of April 30, 1921, but a complete set of minima as for a double star was not obtained and the variations were not definitely confirmed.

The following stars were also suspected of changes in visibility, but the reality of the changes is doubtful. They do, however, deserve careful re-examination, which it is hoped other observers will give them, as the double star work at the Mount Wilson Observatory has been discontinued.

	Mag.	R.A. 1900
δ Cancri	4.2	$8^h39^m.0$
10 Leo. Minor	4.6	9 28.1
o Leonis	3.8	9 35.8
ε Urs. Maj.	1.7	12 49.6
υ Sagittarii	4.6	19 16.0

In searching for doubles with the interferometer, poor and, in particular, variable seeing is a great disadvantage and renders conclusions uncertain. To illustrate this the following quotations from the observing record may be of interest.

γ Boötis	R.A. 1900 = $14^h28^m.1$; Dec. 1900 = +38°45′; Mag. 3.0; Class F.
1921 April 1	Seeing fair. "Several times suspected slight variations but cannot make any settings. Probably single."
June 16	Seeing poor. "Visibility very low on account of poor seeing. Fringes seen only by rare glimpses."
June 18	Seeing fair. "Round."

γ Lyrae	R.A. 1900 = $18^{h}55^{m}.2$; Dec. 1900 = +32°33′; Mag. 3.3; Class A.
1921 April 30	Seeing good but rather irregular. "Suspect slight variation but may not be real."
June 14	Seeing poor and variable. "Followed around at 142 cm with some suspicion as to variability (doubtless due to variable seeing). Followed partly around at 173 cm but seeing turned very poor and fringes disappeared."
June 17	Seeing poor. "About equally distinct in all position angles at 142 cm and 197 cm. Fairly well seen by waiting for best moments."

While complete disappearance of the fringes, as for a close double of equal components, would be noticed in any except the very worst seeing, small variations in visibility cannot be recognized with certainty in poor and irregular seeing. Thus the suspected doubles noted in preceding paragraphs may be spurious, while some of the stars in Table IV may prove to have small variations in visibility, due to unequal components, which were overlooked by the writer. The brighter the star the less the difficulty caused by the seeing.

GENERAL REMARKS

In the Mount Wilson interferometer the slits are separated by turning a divided head, the readings of which are calibrated in terms of the actual slit separation. For systematic double star observations it would probably be better to replace this design by a metal plate containing pairs of slits at several fixed separations so arranged that any pair could be easily moved to the center of the field, the others remaining covered. Time would be saved in observing and the possibility of errors in setting and reading the separations greatly reduced. The separations, moreover, would not be subject to change with time or with readjustment of the instrument, unless the distance of the plate from the focus were changed.

The accuracy of the results obtained by Anderson's method of rotating the apertures and the convenience with which it can be applied are so great as to make it probable that this method will become very important in the future of double star astronomy. The range in the separations and magnitude differences of the double stars to which it can be successfully applied is, of course, small, but the interferometer results would supplement the ordinary micrometer measures in a most desirable way, making it possible to follow some very close and especially interesting pairs with highly satisfactory precision. The new pairs discovered by the interferometer will not be numerous as compared to those now known through direct observations, but they are likely to be of very great individual importance.

The present investigation has been greatly facilitated by Mr. Anderson's kindness in placing his experience with the stellar interferometer in so far as possible at the disposal of the writer, and by considerable assistance in securing and recording the observations. This kindness is gratefully acknowledged, as well as that of Mr. Humason in aiding with the observations on several nights.

Mount Wilson Observatory
April 1922

Contributions from the Mount Wilson Observatory, No. 241
Reprinted from the *Astrophysical Journal*, Vol. LVI, pp. 162–199, 1922

A GENERAL STUDY OF DIFFUSE GALACTIC NEBULAE

By EDWIN HUBBLE

ABSTRACT

Suggested classification of nebulae.—Since the time of the Herschels, photography and spectroscopy have revolutionized the study of nebulae. The classification here suggested is based upon the fundamental differences between galactic and non-galactic nebulae. Galactic nebulae are subdivided into planetary and diffuse (luminous and dark), and non-galactic into spiral, elongated (spindle and ovate), globular, and irregular. The characteristics of each are discussed. The belief expressed by Curtis that all non-galactic nebulae are spirals is not justified by the facts.

Distribution of diffuse nebulae.—As shown in Figure 1 these nebulae are concentrated along two belts. One is the Milky Way and the other is approximately the belt of bright helium stars which defines the local cluster. Very few seem to occur in the vast regions between the Milky Way clouds and the local cluster.

Spectral characteristics of galactic nebulae and of associated stars.—(1) *Diffuse nebulae.* Some preliminary results, obtained with slitless spectrographs of various dispersions, are presented for sixty-two nebulae outside the Magellanic clouds, including the twenty-one whose spectra were previously known. They fall into two groups (Tables I and II): Group 1 contains thirty-three, giving predominantly continuous or absorption spectra; and Group 2, twenty-nine, giving predominantly emission spectra. The members of the "continuous" group have generally a smooth, cloudy structure and most of them are found in our local cluster, while those of the emission group are more likely to be filamentous and wispy and to lie in the Milky Way clouds. In the emission spectra the N_1 and N_2 lines are much weaker in comparison with $H\beta$ than in spectra of normal planetaries. (2) *Stars associated with diffuse nebulae* have been studied with slit spectrographs attached to the Mt. Wilson reflectors (Tables III and IV). Stars involved in nebulae having continuous spectra are nearly all of type B1 or later; but stars involved in emission nebulae nearly always have spectra earlier than B1, rarely showing any bright lines. (3) *Stars associated with planetary nebulae* show a corresponding relation. In fact, there is a steady progression in type from the Wolf-Rayet stars involved in small planetaries, through those involved in large planetaries, to the stars of types Oe5–B0 associated with extended diffuse nebulae of Group 1 and the stars of type B1 and later associated with diffuse nebulae of Group 2. A detailed discussion shows that, with the exception of the Cygnus loop and perhaps three other difficult or doubtful cases, each galactic nebula has associated with it one or more stars of a type conformable to its own spectral type. (4) This definite relation between the spectra of the nebulae and of the associated stars suggests that the *source of luminosity of the nebulae* is the radiation from those stars. According to this view, the nebulosity has no intrinsic luminosity but either is excited to emission by light from a star of earlier type or merely reflects light from a star of later type. From a consideration of the nebulosity around Rigel it appears that this luminosity may be excited at a distance of twenty light-years.

Nature of diffuse nebulosity.—From the foregoing results the nebulosity seems to consist of clouds of matter, molecules, dust, or perhaps larger particles, not hot enough to be self-luminous, but visible because of light excited by or reflected from involved or neighboring stars. Nebulae with continuous spectra seem usually more opaque than those giving emission spectra. Whether the association of such stars and nebulae is permanent or temporary is not yet known, but may be determined by studies of the radial velocities.

Uncatalogued nebulae.—Five are listed: Table I, Nos. 4, 5, 15, and 21; Table II, No. 15. The third is a bright cometary nebula with a thirteenth-magnitude star at the apex; $\alpha = 6^{h}3^{m}.1$; $\delta = +18^{\circ}42'$ (1920).

Radial velocities of five stars associated with galactic nebulae.—Results are given for stars associated with N.G.C. 1514, 6514, 6523, and 7635. Of these B.D. $-23^{\circ}13804$ and Boss 4560 are *binaries.*

CLASSIFICATION OF NEBULAE

The classification of nebulae from visual observations was of necessity based upon resolvability, brightness, size, and form. Thus Sir William Herschel distinguished between clusters and nebulae and devised, for the latter, three classes for brightness, a fourth for definite form, and a fifth for extra large size. It is true that he mentioned in his discussions the terms "milky nebulosity," "nebulous stars," and "stellar nebulae"; that his penetrating genius recognized the existence of nebulous fluid in the nebulous stars and probably in such milky nebulae as the great one in Orion, in contrast to the stellar nebulae or burred stars which he considered as distant clusters; that, in short, he did realize a distinction between planetaries and diffuse nebulae on the one hand and on the other the non-galactic nebulae; but throughout his researches he adhered strictly in catalogues and descriptions to the five classes: bright, faint, very faint, small with definite borders, and exceedingly large. This formal classification was elaborated by the simple system of abbreviation, still in general use, by which each object was described in considerable detail.

Sir John Herschel developed his father's system. His generation had discarded Sir William's idea of a nebulous fluid, as a direct result of the resolution of nebula after nebula by Lord Rosse's great mirrors. Even the Orion nebula, last stronghold of the nebulous fluid advocates, had been announced as resolved by the Parsonstown observers, and the central star in N.G.C. 1514, the great brightness of which as compared to the surrounding nebulosity had led Sir William to his belief in a nebulous fluid, was being explained not as a single star but as an exceptionally compact cluster of stars.

This state of affairs led Sir John Herschel[1] to avoid the discussion of physical distinctions among nebulae and to elaborate his father's formal classification in an ingenious manner. All nebulous objects were divided into regular and irregular, and the latter alone into nebulae and clusters, according to the difficulty of resolving them.

---

[1] *Cape Results* (1847), p. 137.

Regular nebulous objects were classified according to magnitude, brightness, roundness, condensation, and resolvability, with five degrees of each expressed by numbers. Thus a bright globular cluster would be 22322, meaning large, bright, round, condensed, and resolved. A small spindle might be classed as 43435, small, faint, elongated, considerably brighter center, irresolvable.

Irregular nebulae were classed as subregular, compact, branching, convoluted, cellular, fissured, and cometic, although Sir John remarks that these objects are so diverse that each one might well represent a separate class. Each subdivision was arranged in five orders of magnitude and brightness.

Here again is a tendency to distinguish between galactic and non-galactic objects, for the regular nebulae, although including the planetaries, for the most part make up the non-galactic nebulae, while the irregular are in general galactic nebulae.

This system of classification did not win a general acceptance because of its very elaboration and also because of the subsequent introduction of spectroscopy and photography. The new methods of research revolutionized the study of nebulae and the basis of nebular classification. Sir William Herschel's ideas were restored in part at least, for the existence of nebulous fluid in the form of gas or dust clouds in the planetaries and diffuse nebulae became a recognized fact. The old question of resolvability is now restricted to spirals and the kindred small non-galactic objects. There has slowly emerged a general recognition of the fundamental difference, hinted at by the Herschels, between planetaries and diffuse galactic nebulosities and the objects, spirals and others, that swarm in regions of high galactic latitude.

Curtis has expressed this new point of view by dividing nebulae into three classes—planetaries, diffuse, and spirals.[1] In explanation of the term "spiral" he states: "It is my belief that all the many thousands of nebulae not definitely to be classed as diffuse or planetaries are true spirals and that the very minute spirals appear as textureless discs or ovals solely because of their small (apparent) size."[1]

---

[1] *Adolfo Stahl Lectures* (1919), p. 98.

His argument for the truly spiral nature of all these non-galactic nebulae is this: "Were the great Nebula in Andromeda situated five hundred times as far away as at present, it would appear as a structureless oval $0'.2$ long, with very bright center, and not to be distinguished from the thousands of very small round or oval nebulae found wherever spirals are found. There is an unbroken progression from such minute objects up to the great Nebula in Andromeda itself. I see no reason to believe that these very small nebulae are of a different type from their larger neighbors."[2]

This argument is a daring extrapolation and is not justified by our present knowledge of nebular forms. Only a few hundred of the thousands of nebulae photographed show distinct traces of spiral arms. Objects of the most diverse forms, were they removed to the proper distances, would appear as faint "textureless discs or ovals" on the photographic plate. Curtis' extrapolation is not warranted unless all the larger objects examined show positive evidence in favor of, or at least no evidence against, a truly spiral structure.

Now the well-known irregular nebulae, N.G.C. 2366, 4214, and 4449, are unquestionably non-galactic and of considerable size, but by no stretch of the imagination, nor by any orientation, can these objects be termed true spirals. Yet many true spirals are recognized, which have diameters a tenth and less the diameters of these nebulae. It is possible of course to consider the irregular objects as rare exceptions to the general run of non-galactic nebulae.

Stronger evidence of non-spiral forms is found in a class of objects which may be termed globular nebulae. Some of the brighter examples of this type are M 49, 60, 84, 86, and 87, which average about two minutes of arc in diameter.[3] Repeated attempts with the 100-inch reflector under excellent observing conditions, using exposure times from one minute to nine hours, have failed to show any trace or suggestion of spiral structure in the objects mentioned. M 32, the smaller and brighter companion of the

---

[1] *Publications of the Lick Observatory*, 13, 12, 1918.

[2] *Loc. cit.*

[3] M 60 and M 87 are shown in Plate II.

PLATE II

North

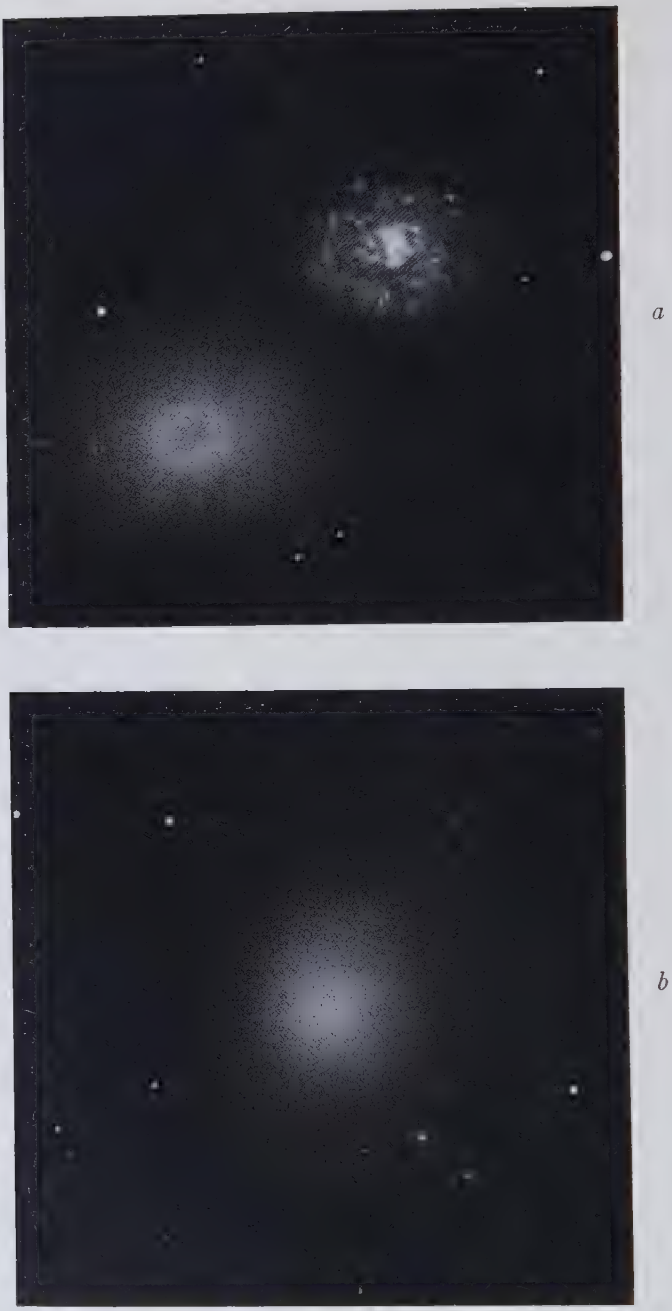

Globular Nebulae

a. M 60, N.G.C. 4649 Globular 1 mm = 4″.2
N.G.C. 4647 Spiral
b. M 87, N.G.C. 4486 1 mm = 5″.2

Photographed with the 100-inch Hooker reflector

Andromeda nebula, is a slightly elongated variant of the globular type which also fails to show spiral characteristics under the resolving power of the 100-inch reflector. A long list could be compiled of non-galactic nebulae with diameters over a minute of arc which show no indication of spiral structure under the highest resolving power available. The number is comparable to that of the known spirals. A progression in size of these globular objects can readily be formed running from diameters of over two minutes of arc down to the limits of photographic plates. Toward the lower end of the sequence they merge into the spirals so that the two types become completely indistinguishable (Plate II).

These globular nebulae may be considered as belonging to the same family as the spirals—distribution, velocities, spectra, non-stellar nuclei, and symmetry of form suggest as much—but there is no shadow of evidence for calling them spirals in fact.

Curtis' classification, however, is easily the most significant that has been proposed up to date, and with some modifications would be acceptable as a system the general use of which should be urged. There appears to be a fundamental distinction between galactic and non-galactic nebulae. This does not mean that the latter class must be considered as "outside" our galaxy, but that its members tend to avoid the galactic plane and to concentrate in high galactic latitudes. The distinction seems to be fundamental in a physical sense as well as in distribution. Galactic nebulae are in general associated with stars; even the dark nebulosities are detected by their obscuration of stars. Non-galactic nebulae show no effect on stellar distribution in their neighborhood and have no stars definitely associated with them save those occasional novae which have flared up in a few spirals. The distinction can also be traced in form, texture, velocity, and spectrum, with little if any overlap. In fact, one can say that in no case, except possibly the Magellanic clouds and the similar object N.G.C. 6822, is there any question, from its photographic appearance alone, as to the class to which an individual nebula belongs.

Once this major division is recognized, the subclasses of galactic nebulae follow directly. They are *planetaries* and *diffuse* nebulae. Diffuse nebulae can be divided into luminous and non-luminous or dark nebulae. More detailed classification of these groups will depend upon form, spectrum, and relation to stars, and can well be left to special investigators.

Subdivision of non-galactic nebulae is a much more difficult problem. At present and for many years to come their classification must rest solely upon the simple inspection of photographic images, and will be confused by the use of telescopes of widely differing scales and resolving powers. Whatever selection of types is made, longer exposures and higher resolving powers will surely cause a reclassification of many individual nebulae, although the true spiral once recognized as such will maintain its class with all more powerful instruments, and irregular and globular types are not usually subject to change. Only a very low percentage of nebulae, and these the smaller ones, which appear globular with 24-inch apertures, resolve themselves into spirals or reveal ansae with a 100-inch aperture.

Globular nebulae have already been mentioned. The few known *irregular* nebulae are chaotic forms with non-stellar nuclei and coarse granular texture, and with spectra and radial velocities similar to those of the spirals. Examples are N.G.C. 2366, 4214, and 4449. They are easily distinguished from diffuse nebulae by their non-stellar nuclei and their texture, although analogies have sometimes been drawn between these irregular nebulae and the Magellanic clouds.

The gap between *spirals* and *globular* types is filled with the *elongated* nebulae. There are two distinct varieties of these, the one probably spirals on edge and the other akin to globular nebulae. They may be termed, respectively, spindles and ovate. The former, with sharp nuclei and tapering ansae, are familiar to all observers. The latter deserve some further comment. Examples of the ovate type are M 32 and M 59. They are similar to the globular nebulae in all save their elongated forms. Both are to be described as large and bright, yet even the 100-inch under the finest observing conditions with both long and short exposures reveals no trace or suggestion of spirality in either nebula. Whatever their past or future, their present state is not that of true spirals within the limits set by our observational data.

Spindles and ovate types merge into one another with decreasing linear size of the images on the plates, and the resulting confusion detracts from the value of the distinction for small objects or small-scale photographs. As a matter of fact each system of classification that can be devised for non-galactic nebulae will favor a certain range of resolving powers. The present one favors the largest reflectors. It is a compromise between Curtis' generalization and Wolf's specialization.[1]

Some light on the validity of this classification, and a scale for standardizing results from instruments of various dimensions, for statistical purposes at least, can be derived from photographs of rich fields of nebulae made with telescopes of different apertures and equivalent focal ratios, and with one telescope and differing exposure times. Classification of the nebulae for each exposure will indicate the percentage of objects of each type which are changed from one type to another with increasing exposure and resolving power. Preliminary investigations along this line have already been made, apertures from 10 to 100 inches being used.

The classification proposed for general use, together with typical objects for each class, is as follows:

	Examples
I. Galactic nebulae	
1. Planetary	N.G.C. 7662
2. Diffuse	
a) Luminous	N.G.C. 1976
b) Dark	Barnard 86
II. Non-galactic nebulae	
1. Spiral	M 101 (N.G.C. 5457, 8)
2. Elongated	
a) Spindle	HV 24 (N.G.C. 4565)
b) Ovate	M 59 (N.G.C. 4621)
3. Globular	M 87 (N.G.C. 4486)
4. Irregular	N.G.C. 2366

DISTRIBUTION OF GALACTIC NEBULAE

The distribution, spectra, and radial velocities of planetaries are now well known, due largely to the investigations carried out at the Lick Observatory. Large planetaries are distributed more or less uniformly over the sky, while the small ones concentrate sharply along the Milky Way and are especially numerous between eighteen and twenty hours of right ascension. It is reasonable to suppose that the apparent diameters and nuclear magnitudes are rough indications of distance and that, when real distributions are determined, the vertical deviations from the galactic plane will prove to be relatively small. Radial velocities of ninety-six planetaries corrected for the solar motion average 30 km or about five times the average for B stars. Their spectra are almost purely emission, the continuous spectrum being entirely negligible except for the region on the more refrangible side of the head of the hydrogen series. The ratio of intensities between the N_1, N_2, and $H\beta$ images is 10:3:1, with few exceptions.

---

[1] Wolf's classification of non-galactic nebulae is to be found in *Publicationen des Astrophysicalischen Instituts Königstuhl-Heidelberg*, Band III, No. 5, 1909.

Much less is known concerning the diffuse galactic nebulae. Their distribution in the sky is certainly not a simple concentration along the galactic plane. Figure 1 represents the distribution in galactic co-ordinates of all objects of this class, excepting those between galactic longitudes 200° and 300° which are too far south to be observed from Mount Wilson. Two distinct belts are defined —the Milky Way, and a belt inclined at about 20° to the Milky Way. This latter belt has approximately the same nodal points as those of the bright helium stars, although the inclination is considerably greater than that usually given for the stars. The data are not sufficient to determine a value for the dip.

Such a distribution emphasizes the relation between diffuse nebulosity and early type stars. The high inclination of the nebular belt suggests that these objects are comparable in distance with the brightest of the B stars and for the most part lie on the inner side of the ring. There is some evidence that the diffuse nebulae are concentrated in the local cluster and in the Milky Way clouds, and that vast regions between the two are practically devoid of nebulae. If this were not the case, we should expect to find the gaps between the two belts more generally filled, and also a greater dispersion among the galactic nebulae. Perhaps the strongest point in favor of such a distribution is the absence of nebulae with large positive galactic latitudes between longitudes 80° and 200°. In all these 120 degrees of longitude only one diffuse nebula has a latitude greater than +2°. This object is B.D. +23°1301 at +3°.5, announced by Barnard as a nebulous star. The spectrum is B9, photo-visual magnitude 7.0, and hence it is probably relatively near. The greatest deviation from either plane is in the isolated group of dark and luminous nebulosity in Corona Australis, which includes the variable nebula, N.G.C. 6729. The distance of the group is of the order of one hundred parsecs,[1] so that it lies well within the local cluster, and its anomalous position in the sky must be due to perspective. The vertical distance from the galactic plane is about thirty parsecs.

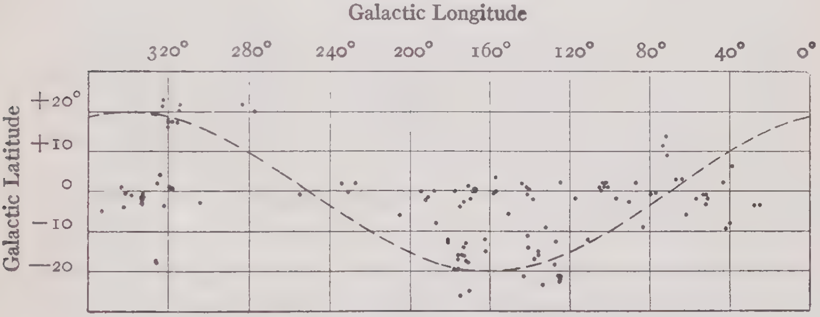

FIG. 1.—Distribution of diffuse nebulae in galactic co-ordinates

There is a decided tendency for diffuse nebulae to cluster. This is more pronounced among nebulae with predominantly continuous spectra than among those with emission spectra, and usually is accompanied by extensive dark nebulosity. Dark nebulae tend to follow the double distribution, although the scattering is greater and the gaps between the two belts are more generally filled than is the case with the luminous diffuse nebulae.

SPECTRA OF DIFFUSE NEBULOSITIES

Published results list emission spectra for thirteen diffuse nebulae as against continuous or absorption spectra for eight.[2]

---

[1] A distance of three hundred light-years is derived from the luminosity law applied to nebulous stars in the obscured areas, and from movements of luminosity in the nebula N.G.C. 6729 on the assumption that such movements have the velocity of light.

[2] This leaves out of consideration the nebulae in the Magellanic clouds.

This has somehow led to a presumption that an emission spectrum is a general characteristic of diffuse galactic nebulae.

Slit spectrograms of such faint objects will accumulate so slowly that it seems worth while to publish now some results from a preliminary survey with slitless spectrographs. Such instruments readily distinguish spectra which are predominantly emission from those predominantly continuous, although faint emission images on a strong continuous background cannot always be detected. Absorption lines are usually concealed in slitless spectra and the term "absorption spectrum" can be applied in general only to slit spectra. Several such spectra have been reported by Slipher and Pease, so that pure absorption spectra of diffuse nebulosities are as well established in fact as pure emission spectra. Indeed, they may be considered as better established, for it is more probable that all bright-line nebular spectra have some faint continuous background than that faint bright lines have been overlooked in absorption spectra of nebulae. The term "emission" will be used in discussing slitless spectra as an equivalent to "bright line" in slit spectra; the term "continuous," where neither bright nor dark lines can be seen; the term "absorption," where dark lines can actually be detected in either slit or slitless spectra. An unbroken series can readily be arranged from the slitless spectrograms, running from emission with no perceptible continuous spectrum to continuous with no emission. There is probably an uncertain number of objects listed as "continuous" in which faint emission images are present and not recognized, but in every case of previously known emission on a continuous background, the slitless spectra show unmistakable irregularities in distribution of density. In view of the uncertainty, however, the method adopted is to list the nebulae as giving predominantly continuous or predominantly emission spectra, and to call attention in notes to combinations of characteristics.

The various instruments employed in the survey are listed below and each is designated by a letter, by which it will be referred to in the course of this paper. It will be noticed that the range in the relation of scale to dispersion is sufficiently wide to accommodate itself to nebulae of all sizes. Seed 30 plates were used throughout, with exposures ranging from two to nineteen hours.

A. Focal-plane spectrograph with slit removed, attached to 60-inch reflector, primary focus. Collimator and camera lenses about 6-inch focus. Dispersion, Hβ to Hε = 5.0 mm.
B. 15° objective prism on 10-inch Cooke astrographic lens, focus 45 inches. Hβ to Hε = 5.3 mm.
C. 6° objective prism on 10-inch Cooke lens. Hβ to Hε = 1.8 mm.
D. 39° objective prism on 4-inch lens, 7-inch focus, Hβ to Hε = 4.1 mm.
E. 25° objective prism on 4-inch lens, 7-inch focus, Hβ to Hε = 2.5 mm.
F. 25° objective prism on kinematograph lens F/1.8, 3-inch focus. Hβ to Hε = 1.0 mm.

Results from the survey are collected in two tables, one comprising nebulae which give predominantly continuous, and the other, those which give predominantly emission spectra. Nebulae whose spectra were previously known are included for the sake of completeness and are starred to indicate this fact. One nebula has thus been included which is too far south to be observed from Mount Wilson—N.G.C. 3372, the nebulosity around η Carinae. The two lists should contain all diffuse galactic nebulae for which spectrographic data are available, excepting those in the Magellanic clouds. The tables give in the first column a list number; in the second, the catalogue designation of the nebula; the third and fourth columns give galactic longitudes and latitudes; the fifth column, a rough indication of size on a scale of 1 to 5, the numbers increasing with the size; the sixth column, the instruments employed; the seventh, remarks and references.

Table I contains thirty-three objects having continuous spectra, eight of which were previously known as such. Of the latter, four give pure absorption spectra—the Pleiades, M 78, ρ Ophiuchi, and N.G.C. 7023.[1] N.G.C. 1977 and the two variable nebulae, N.G.C. 2261 and 6729, give faint bright-line images as well, and one, N.G.C. 2245, is known only through an objective prism spectrogram.

---

[1] Slipher reports that in the spectrum of N.G.C. 7023, "Bright Hβ seems to be present but not so obviously emissive as in the star" (*Publications of the Astronomical Society of the Pacific*, **30**, 63, 1918). The involved star has bright reversed hydrogen lines. Hβ does not show on a spectrogram of the nebula made by Pease.

TABLE I

DIFFUSE NEBULAE WITH CONTINUOUS SPECTRA

No.	Object	Galactic		Size	Instrument	Remarks
		Longitude	Latitude			
1.....	N.G.C. 1333	126°	−21°0	2	C	
2.....	I.C. 348	128	−17.5	2	A, B, C,	Also listed as I.C. 1985. B.D. +31°643, involved
3.....	Pleiades*	134	−22.0	5	C	See Slipher, *Lowell Bull.*, No. 55, 1912
4.....	....	136	−15.5	2	B, C	Uncatalogued nebula, $\alpha=4^{h}14^{m}$; $\delta=+28°2'$ (1920)
5.....	....	141	−17.0	1	B, C	Uncatalogued nebula, $\alpha=4^{h}22^{m}.1$; $\delta=+24°32'$ (1920)
6.....	N.G.C. 1579	132	− 9.0	2	C	
7.....	I.C. 2087	141	−14.0	1	B, C	
8.....	N.G.C. 1788	171	−24.5	2	A, B, C,	
9.....	I.C. 2118	175	−26.0	5	B, D, E	Great nebulosity north preceding Rigel
10.....	N.G.C. 1977*	175	−19.0	3	B, C	Dark helium and bright hydrogen. See Slipher, *A.S.P.*, **31**, 22, 1919
11.....	2023	173	−16.5	1	A, B, C	Nebulosity around B.D. −2°1345
12.....	2068*	173	−14.0	2	B, D, E	See Slipher, *A.P.S.* **31**, 212, 1919
13.....	....	172	−13.0	5	B, D, E	$\alpha=5^{h}45^{m}.5$; $\delta=+1°$ (1920). Brightest portion of great "spiral" in Orion
14.....	2183	181	−11.0	1	A, B	
15.....	....	158	− 0.5	1	A, B	$\alpha=6^{h}3^{m}.1$; $\delta=+18°42'$ (1920). Comet nebula uncatalogued
16.....	I.C. 446	168	+ 0.5	1	B, C	Also listed as I.C. 2167
17.....	447	168	0.0	2	B, C	Also listed as I.C. 2169
18.....	N.G.C. 2245*	169	+ 0.5	1	B, C	See *Ap.J.*, **44**, 196, 191
19.....	2247	169	− 1.0	1	B	
20.....	2261*	171	+ 1.5	1	A, B, C	Faint emission on strong continuous spectrum. See *Lowell Bull.*, No. 81
21.....	....	193	− 1.5	1	B, C	Uncatalogued nebula about B.D. −12°1771
22.....	....	312	+17.0	3	B, F	Nebulosity about π Scorpii
23.....	I.C. 4592	322	+23.0	5	B, C, F	Nebulosity about ν Scorpii
24.....	4601	323	+21.0	2	B, C	Nebulosity about B.D. −19°4359 and B.D. −19°4361
25.....	4603	319	+17.0	4	B, C, F	Nebulosity about B.D. −24°12684
26.....	4604*	320	+18.0	4	B, C, F	Nebulosity about ρ Ophiuchi. See *Lowell Bull.*, No. 75, 1916
27.....	4605	320	+16.0	2	B, C, F	Nebulosity about 22 Scorpii
28.....	N.G.C. 6726, 7	327	−17.5	2	B, C	Nebulosity about B.D. −37°13023 and B.D. −37°13024
29.....	N.G.C. 6729*	327	−17.5	1	B, C	Faint emission on strong continuous spectrum. See *Lowell Bull.*, No. 81
30.....	6914	52	− 4.5	1	B, C	
31.....	7023*	72	+14.0	1	B, C	Slipher, *A.S.P.*, **30**, 63, 1918; Pease, *A.S.P.*, **27**, 240, 1915
32.....	7129	73	+ 9.0	1	A, B, C	
33.....	I.C. 5146	62	− 6.5	2	C	

NOTES

4. Photograph by Barnard, *Astrophysical Journal*, **25**, 219, 1907. This may be I.C. 359 whose position is given as 5^{m} preceding and 30′ south. No nebulosity is seen in that position.

5. In one of the dark lanes in Taurus.

7. In one of the dark lanes in Taurus. See Barnard, *Astrophysical Journal*, **25**, 218, 1906.

9. Faint extensions of this nebula stretch south and west to end in a faint obscuring cloud more than 35° from the galactic plane.

11. Wolf, *Astronomische Nachrichten*, **180**, 152, 1909, describes this as gaseous emission, but his observations undoubtedly apply to I.C. 434. See note on the latter nebula following Table II.

13. This is the brightest portion of the great loop encircling the belt and sword of Orion.

15. A bright uncatalogued nebula similar to N.G.C. 2245. A thirteenth-magnitude star is at the apex of the cometary form. It is surprising to find that so bright an object has been overlooked by observers.

21. Attention was called to this uncatalogued object in *Union Observatory Circular*, No. 7, 1911.

22. See Barnard's photograph in *Astrophysical Journal*, **23**, 144, 1906.

These nebulae show a decided tendency toward clustering, and can be divided as follows:

	Number
Taurus group	1– 7
Orion	8–14
Monoceros	15–21
Scorpius	22–27
Corona Australis	28–29
Cygnus	30–33

Their distribution in the sky, although affected by this grouping, is clearly not a simple concentration along the galactic plane.

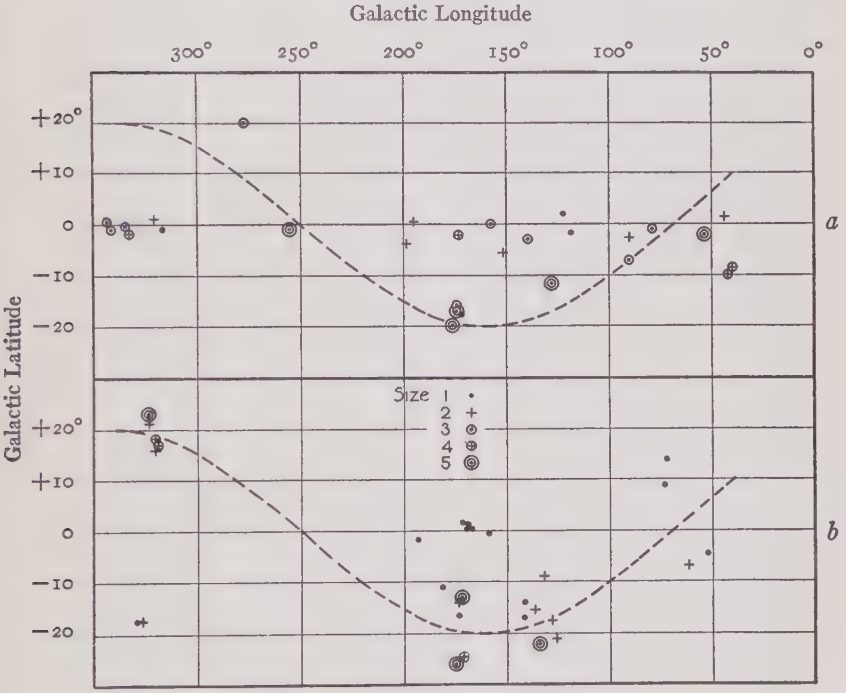

Fig. 2.—Distribution of diffuse nebulae

a. Nebulae with emission spectra

b. Nebulae with continuous spectra

In Figure 2 they are plotted in galactic co-ordinates, and it is at once evident that most of them favor the tilted plane of bright helium stars. The Monoceros group and the isolated pair in Corona Australis are the only exceptions. The latter, as has been mentioned, is relatively near; in fact, it is among our very nearest nebulous neighbors, and therefore can be properly assigned to the local cluster. The Monoceros group, on the other hand, may be truly galactic as judged by its position, the small size of its components, and the faintness of the stars involved.

Table II contains twenty-nine nebulae with emission spectra, thirteen of which were previously recognized as such. These objects show a greater preference for the galactic plane and less of a tendency to congregate into groups. They all lie close to the Milky Way, except the Cygnus nebula (N.G.C. 6960, 6992), N.G.C. 1499, 5128, and the Orion group. The largest objects in the galactic plane, however, fall at the nodal points of the belt of helium stars and might, from their position alone, be placed in either plane with equal reason. Starting from an assumption of double distribution, it is quite possible to divide the emission nebulae, assigning all five of the largest sizes, five out of thirteen of the graded sizes 4 and 3, and three out of eleven of the two smallest sizes, to the inclined plane. This distribution of sizes fits very well with the known fact that the local cluster of helium stars is nearer than the Milky Way clouds, and with the distribution in sizes of the "continuous" nebulae. Those assigned to the galactic plane have a very small dispersion and a mean galactic latitude of $-1\overset{\circ}{.}6$, which is exactly the latitude of the galactic circle as determined by Nort.[1] So close an agreement was of course unexpected, and lends some justification to the rather arbitrary division of nebulae between the two planes.

A study of the relative intensities of the monochromatic images in Table II leads to the interesting generalization that hydrogen in the extended nebulae as represented by $H\beta$ is much stronger compared to N_1 and N_2 than is the case in the planetaries. Wilson suggested this from the intensities in two extended nebulae, N.G.C. 1976 and 3372, and established the fact that emission nebulae in the Magellanic clouds occupy a position in this respect between the normal planetaries and the extended nebulae.

---

[1] *Recherches Astronomiques de l'Observatoire d'Utrecht*, 7, 1917.

TABLE II

DIFFUSE NEBULAE WITH EMISSION SPECTRA

No.	Object	Galactic		Size	Instrument	Remarks
		Longitude	Latitude			
1	N.G.C. 281	90°	− 7°0	3	B, C	One image, $N_1+N_2+H\beta$. Six hours with C much fainter than two hours' direct exposure
2	I.C. 59–63	90	− 2.5	2	B, C, D	Fan nebulae near γ Cass. D shows three images, $N_1+N_2+H\beta$(3), $H\gamma$(1), $H\delta$ (1)
3	N.G.C. 1491	118	− 1.5	1	C	Strong single image, $N_1+N_2+H\beta$
4	1499*	128	−11.5	5	B, C, D, E	Spectrum described in *A.S.P.*, **32**, 155, 1920. N_1+N_2 (2), $H\beta$ (2), 4686 (1), $H\gamma$ (2), $H\delta$ (1), $H\epsilon$ (1)
5	1624	122	+ 2.0	1	C	One image, $N_1+N_2+H\beta$
6	I.C. 405	139	− 3.0	3	C	Two images, $N_1+N_2+H\beta$ (2), $H\gamma$ (1). Faint continuous spectrum
7	N.G.C. 1952*	151	− 5.5	2	C	Four images, $N_1+N_2+H\beta$ (5), $H\gamma$ (2), $H\delta$ (0), 3727 (1). Strong continuous spectrum. See *L.O.B.*, **13**
8	I.C. 423	172	−17.5	1	B	Five images, N_1+N_2 (2), $H\beta$ (2), 4686 (1), 4363 (1), $H\gamma$ (2)
9	N.G.C. 1976*	176	−19.5	5	B, C, D, E	Orion nebula. See *L.O.B.*, **13**, and *A.S.P.*, **31**, 212, 1919
10	1982*	176	−19.0	2	B, C, D, E	Orion nebula. See *L.O.B.*, **13**, and *A.S.P.*, **31**, 212, 1919
11	I.C. 434*	174	−17.0	5	B	Bay nebula south of ζ Orionis. See Wolf, *A.N.*, **180**, 152. Five images, $H\beta$ (5), 4686 (2), $H\gamma$ (4), $H\delta$ (1), 3727 (2)
12	N.G.C. 2024	174	−16.0	3	B, D	N_1 (1), $H\beta$ (3), 4686 (2), $H\gamma$ (3), $H\delta$ (2), 3727 (2), faint continuous spectrum
13	2175	157	0.0	3	B, C	N_1 (1) $H\beta$ (3), $H\gamma$ (3)
14	2237	173	− 2.0	4	B, C, D	N_1+N_2 (2), $H\beta$ (1), $H\gamma$ (1)
15	....	198	− 4.0	2	C	One image, N_1+N_2
16	2359	194	+ 0.5	2	B, C	One image, N_1+N_2. Gaseous nature predicted from direct photographs by Pease, *Mt. Wilson Contr.*, No. 132
17	3372*	255	− 1.0	5	....	See *L.O..B*, **13**
18	5128	277	+20.0	3	C	$H\beta$ (2) 4686 (1), $H\gamma$ (2), $H\delta$ (1)
19	6302*	316	− 1.0	1	B	
20	6357	320	+ 1.0	2	C	One image, N_1+N_2
21	6514*	334	− 0.5	3	B, C	Trifid. See *L.O.B.*, **13**, N_1+N_2 (1), $H\beta$ (3), $H\gamma$ (2), $H\delta$ (1), 3727 (2)
22	6523*	333	− 0.5	4	B, C	M 8. See *L.O.B.*, **13**. N_1 (2), N_2 (1), $H\beta$ (4), 4363 (1), $H\gamma$ (3), $H\delta$ (1), $H\epsilon$ (1), $H\zeta$ (1), 3727 (2). Local variation to intensities
23	6611	343	+ 0.5	3	B	M 16. N_1+N_2 (1), $H\beta$ (3), $H\gamma$ (2). See *Mt. Wilson Contr.*, No. 177, p. 6
24	6618*	341	− 1.0	3	B	M 17. See *L.O.B.*, **13**, N_1 (4), N_2 (2), $H\beta$ (3), 4686 (0), 4361 (1), $H\gamma$ (3). Local variations
25	6888	43	+ 1.2	.....	B, C	$H\beta$ (2), $H\gamma$ (1), $H\delta$ (1), 3727 (2)
26	6960*	40	− 8.5	4	B	See Wolf, *A.N.*, **178**, 379; *ibid.*, **180**, 152
27	6992*	42	−10.0	4	B	See Wolf, *ibid.*, **178**, 152. Nos. 26 and 27, are really portions of one nebula—an enormous loop in Cygnus
28	7000*	53	− 1.0	5	B, C	Wolf, *Sitz. Heid. Akad. Wiss.*, **27**, 1, 1910
29	7635	79	− 1.0	3	A, B, C	$H\beta$ (5), $H\gamma$ (2), $H\delta$ (1), 3727 (4)

NOTES

Campbell and Moore were unable to see bright lines in N.G.C. 2024, 6992, and 7000. N.G.C. 6523, 6618, and 7635 each has at least one image of wave-length shorter than 3727.

7. The continuous spectrum in N.G.C. 1952 is so strong that the nebula might equally well be included in Table I.

11. I.C. 434. This is the remarkable Bay nebula stretching south from ζ Orionis, whose sharp edge on the following side is indented by a dark cloud billowing out from the obscured region bordering on the bright nebula. My plates give an emission spectrum which agrees with that described by Wolf in *Astro-*

nomische Nachrichten, **180**, 152, 1908, and ascribed by him to N.G.C. 2023. N.G.C. 2023, however, is a typical nebulous star, B.D. —2°1345, in the obscured region following I.C. 434. The nebulosity around it has a strong continuous or rather an absorption spectrum with no trace of emission. Furthermore, Wolf's remarks "sudlich von ζ Orionis—umittelbar nordlich von die grossen Bucht . . . ." clearly apply to I.C. 434. In view of these facts, I assume the nebula whose spectrum Wolf describes in *Astronomische Nachrichten*, **180**, 152, is really I.C. 434 and so list that nebula as one whose spectrum was previously known. N.G.C. 2023 is listed among those giving continuous spectra which were not previously known.

13. Continuous spectrum fairly strong. Emission spectrum checked by a slit spectrogram.

15. This is an uncatalogued nebula described by Knox Shaw in *Helwan Bulletin*, No. 15. Discovery announced in *Union Observatory Circular*, No. 7, 1911.

28. N.G.C. 7635, formerly known as a nebulous star, appears to be a large planetary immersed in diffuse nebulosity. The brightest portions of the non-planetary nebulosity give the emission spectrum described.

The normal ratio N_1, N_2, and $H\beta$ in the planetaries is 10:3:1. From the observations of Campbell and Moore and of Wilson, data can be gathered for extended nebulae as follows:[1]

	N_1	N_2	$H\beta$
N.G.C. 1976	10	3	5
3372	10	3	5
6514	3	1	10
6523	3	1	10
6618	10	3	5

Table II furnishes data of inferior accuracy, but strongly supporting those listed above.

	N_1+N_2	$H\beta$
N.G.C. 1499	1	2
I.C. 423	1	1
I.C. 434	0	5
N.G.C. 2024	1	3
2175	1	3
2237	2	1
5128	0	2
6611	1	3
6888	0	2
6960 6992	0	2
7000	0	2
7635	0	5

N.G.C. 1977 and 1982 are connected with N.G.C. 1976, the Orion nebula, and these, together with the outer region of the Orion nebula itself, show a decided weakening of the N_1 and N_2

---

[1] *Publications of the Lick Observatory*, 13.

lines, as compared to the 10:3:5 relation for the trapezium region. A spectrogram made at Mount Wilson with the slit east-west, just south of the B8 star B.D. $-5°1305$, $12'$ south and preceding the trapezium, shows Hβ ten times as strong as N_1 and apparently just stronger than λ 3727.[1] It is interesting to note that the nebulosity condensing about the star shows a pronounced strengthening of the continuous spectrum without affecting the emission lines.

N.G.C. 281, 1491, 1624, 2359, 6357, and I.C. 59, 63, and 405 show such faint overlapping images that they cannot be separated into components for the estimation of relative intensities.

In no case, excepting N.G.C. 1952, is Hβ less than half the intensity of N_1. In this exceptional case, as studied from a slit spectrogram by Sanford, the local variations and overlap of double lines interfere with estimation of relative intensities and the only statement which can be made is that Hβ and N_2 are of about the same order of intensity.

The significance of this generalization is not clear as yet. Of the six giant planetaries[2] only one, N.G.C. 7635, shows the stronger Hβ, and the same ratio holds for small planetaries out of the Magellanic clouds discussed by Campbell and Moore. The most striking examples of these latter, N.G.C. 40, I.C. 418, N.G.C. 4361, and B.D. $+30°3639$, are in no way exceptional in appearance or in their nuclear spectra. The nuclei, however, are unusually bright as compared with the general average.

Among the non-galactic nebulae showing emission lines, two described by Campbell, N.G.C. 1068 and 4151, seem to have the normal planetary ratio, 10:3:1 for N_1, N_2, and Hβ, while three others described by Pease and by Slipher, M 33, N.G.C. 4214 and 4449 show the relatively stronger Hβ.

Tables I and II more than double the number of known emission spectra, and quadruple that of known continuous spectra. The latter now outnumber the former for separately catalogued objects; but in view of the greater tendency to group among the nebulae with continuous spectra, it is preferable to regard the numbers as about equal. As emission nebulae are much more easily identified for a given surface-brightness because of the discontinuous distribution of light in their spectra, it seems a reasonable extrapolation to assume that continuous spectra are actually more numerous than emission among the diffuse galactic nebulae.

---

[1] "Apparently" in that an ordinary lens and a Seed 30 plate were used. Quartz or U.-V. glass and Seed 23 plates would show λ 3727 as much stronger than Hβ.

[2] The term "giant planetary" is used to describe those with diameter greater than $2'$. There are six such planetaries.

A study of direct photographs fails to give any necessary and sufficient criteria certain for predicting by inspection the nature of the spectrum of a given diffuse nebula. There are several general indications, but each has its exceptions. Filamentary and wispy nebulosity usually has an emission spectrum, as, for example, N.G.C. 1499, 1952, 1976, 2359, 6960, and 6992. This is not a necessary condition and is approximately satisfied in the "continuous" nebulosity about the Pleiades and 22 Scorpii; moreover N.G.C. 1952, the Crab nebula, has so strong a continuous background for its bright-line images that its spectrum could be classed as continuous almost as reasonably as emission. On the other hand, a smooth, cloudy structure is usually confined to "continuous" nebulosity, as in that about ν Scorpii and ρ Ophiuchi, but this again is approximated in the emission nebulae N.G.C. 2024 and the Trifid.

Nebulae with "continuous" spectra are usually associated with greater obscuration than are emission nebulae, although striking exceptions are found in Orion and N.G.C. 7000. It is of course a natural supposition that such vast bodies must be at least partly opaque, and that the "continuous" would be more so than the emission nebulae. Observation shows this to be the case. Obscuration is in fact a universal characteristic of diffuse galactic nebulae wherever the angular areas are large enough to warrant conclusions. The best direct evidence that I have found for transparency in any degree is presented by the helical nebula in Aquarius, N.G.C. 7293, the largest recognized planetary. Photographs made with the 100-inch reflector show three or four small non-galactic nebulae, including one spindle, within the luminous area of the planetary. The great size and galactic latitude of N.G.C. 7293 render it highly probable that the planetary is relatively near, at least nearer than the small nebulae, which, therefore, must be considered as shining through the planetary.

The brightest nebulae have emission spectra; the largest, continuous spectra. In general, however, the two classes mix pretty thoroughly when arranged in order either of size or of brightness. "Continuous" nebulae show a greater tendency to condense around stars, although most of the galactic nebulae have stars involved, and perhaps all have stars associated with them.

SPECTRAL TYPES OF STARS INVOLVED IN DIFFUSE NEBULOSITY

A study of the spectral types of such stars shows that those involved in "continuous" nebulae are of later types than those involved in emission nebulae. This conclusion is based on examination of slit spectrograms made with Cassegrain spectrographs on the 60-inch and 100-inch reflectors. One prism and an 18-inch camera were generally used, although for some of the faintest stars a 7-inch camera was necessary. Table III gives the types of stars involved in 29 of the "continuous" nebulae, which are designated by the list numbers of Table I.

Three cases are exceptional—the faint K8 star in No. 4, around which the nebulosity condenses so strongly and symmetrically that the star must be regarded as involved, and the nuclei of the two variable nebulae N.G.C. 2261 and 6729. V. M. Slipher reports the nuclear spectrum of N.G.C. 2261 as consisting of bright and dark lines agreeing closely with Nova Aurigae in its later stages. He suspected that the nucleus of N.G.C. 6729, R Coronae Australis, was similar, but three spectrograms made with the 100-inch reflector (7-inch camera) show a peculiar G-type spectrum with bright reversed hydrogen and enhanced iron lines. When these three cases are disregarded, the mean type of the other stars is about B4. None is earlier than B1.

There is a decided tendency toward uniformity of stellar type within the various groups. The Taurus group contains nothing earlier than B5. The Orion group is B2 and B3, with one exceptional B1 star in N.G.C. 1977, a nebula giving bright lines as well as a strong continuous spectrum. The stars in the Monoceros nebulae are B1 and B2, and those of the Scorpius group are B2 and B3 as in Orion, excepting the isolated case of I.C. 4601,

TABLE III

Stars Involved in Nebulae with Continuous Spectra

No.	Nebula	Pv. Mag. of Stars	Spectrum of Stars	
1	N.G.C. 1333	10.6	B8	
2	I.C. 348	8.4	B6	B.D. +31°643
		9.8–11.6	B8–A2	9 stars
3	Pleiades	....	B5	Maia and Merope
4	....	12.5	K8	Probably a dwarf
6	N.G.C. 1579	12.0–12.2	A0–B5	2 stars
8	1788	10.0–13.0	B8–B8	2 stars
10	1977	4.6	B1	Boss 1364
11	2023	7.8	B2	B.D. −2°1345
12	2068	10.4–10.8	B5–B8	B.D. +0°1177
14	2183	14.0	B3	
15	....	13.5	B1	
16	I.C. 446	11.3	B1	
17	447	8.1	B1	B.D. +10°1159
18	N.G.C. 2245	10.7	B1	Bright Hβ suspected
19	2247	8.8	B2p	Bright Hβ and Hγ
20	2261	Var.	Pec.	Approximates a nova spectrum
21	....	8.2	B1	B.D. −12°1771
22	....	3.1	B2	π Scorpii
23	I.C. 5592	4.2	B2	ν Scorpii
24	4601	7.1–8.4	B8–A0	4 stars
25	4603	7.8	B2	B.D. −24°12684
26	4604	5.2–5.9	B2–B3	2 components of ρ Ophiuchi
27	4605	4.9	B3	22 Scorpii
28	N.G.C. 6726, 7	7.2–9.4	B9–B9	2 stars
29	6729	Var.	Gp	R Coronae Australis. Resembles T Tauri
30	6914	9.3–9.9	B5–B5	B.D. +41°3731 and B.D. +41°3737
31	7023	7.2	B2p	Bright Hβ and Hγ
32	7129	10.2–12.4	B3–B8	3 stars
33	I.C. 5146	10.0	B1	B.D. +46°3474

NOTES

4. Nebulous star north following Barnard's nebula.

15. Nucleus of cometary nebula resembling N.G.C. 2245. It is not catalogued.

17. There is a group of six stars in this nebula, some of which are certainly not involved.

24. Boss 4150, visual mag. 6.2, G5 giant, is involved in nebulosity connected with No. 24.

28. B.D. −37°13017 and 13018, visual mag. 6.5 and 6.7, B5 and B6, are involved in connecting nebulosity.

29. R Coronae Australis has bright unsymmetrically reversed hydrogen and enhanced iron lines on an absorption spectrum that is approximately a G-type but which has contradictory characteristics. The spectrum resembles that of T Tauri except that it has no bright H and K.

in which are involved four stars, B8 to A0. The Corona Australis group really comprises two double stars in addition to R. The types are B5, B6, B8, and B9, R itself being, as mentioned above, a peculiar later type.

The Monoceros group comprises all the "continuous" nebulae which can be assigned to the galactic plane with any degree of certainty. This distinction is emphasized by the fact that they contain, as a group, the earliest types of involved stars. The only other B1 star (excepting the transitional case of N.G.C. 1977 mentioned above) is central in I.C. 5146, the Cave nebula in Cygnus. This object is so near a nodal point of the inclined plane that it can be placed in either belt with equal justification. These facts raise a question as to whether or not there may be a real difference in type between stars involved in nebulae belonging to the galactic plane as compared with those belonging to the local cluster. The various groups differ so much among themselves, however, that no great weight can be assigned to results from one of their number. Moreover, there seem to be some later-type stars in the cluster around S Monocerotis and possibly in I.C. 447.

The K8 star in No. 4 is not unique. Heretofore it has been thought that all stars involved in nebulosity are B-type or earlier. The following list, which does not include several known cases of A stars, some of which are of the α Cygni type, shows that this is not rigorously true.

1.	B.D. +31°597	K2 giant
2.	B.D. +28°645	F8±
3.	T Tauri	G peculiar with bright lines
4.	No. 4	K8 dwarf
5.	Boss 4150	G5 giant
6.	R Corona Australis	G peculiar with bright lines

These six objects have all been photographed directly with the 100-inch reflector and, in each case, the nebulosity condenses about the star so obviously that there can be little doubt that the stars are really involved. Some may be cases of stars and nebulosity meeting in the course of the peculiar motions through space, but others, notably T Tauri and R Coronae Australis, must surely be inherently associated with the nebulosity surrounding them. None of them, however, shows any indications of nebulosity condensing into stars.

Absorption spectra of diffuse nebulae are reported by Slipher and by Pease as agreeing with the spectra of the brightest involved stars, as well as could be determined with the small dispersions employed. In this connection it is of interest to mention the following nebulae with predominantly continuous or absorption spectra which have bright-line stars involved.

Nebula	Star
Pleiades	Bright Hα in several of the brighter stars
N.G.C. 2247	Bright line B1p
N.G.C. 7023	Bright line B2p
N.G.C. 2261	Approximately a Nova spectrum[1]
N.G.C. 6729	G peculiar with bright hydrogen and enhanced iron lines

The spectrum of the Pleiades nebulosity has not yet been examined in the Hα region. No slit spectrogram has been obtained of N.G.C. 2247, and the objective-prism spectra could easily obliterate faint emission images. N.G.C. 7023 and 6729 are suspected, N.G.C. 2261 is definitely proved by Slipher, to have spectra corresponding in detail to the spectra of the stars involved. There is thus no evidence against, and some in favor of, the assumption that nebular spectra that are predominantly "continuous" are the spectra of reflected starlight.

Table IV indicates types of stars involved in nebulae with emission spectra. N.G.C. 3372, the η Carinae nebulosity, is not included because its position is such that no investigation could be made here concerning the question as to which stars are involved and which are not. η Carinae itself is usually accepted as being so involved, and if this is true, it is the one example known of a peculiar bright-line star in emission nebulosity. The Draper *Catalogue* lists two Wolf-Rayet stars within the limits of N.G.C. 3372, but there again the question of their being involved, or simply aligned, requires special investigation that cannot be carried out at Mount Wilson.

---

[1] *Lowell Observatory Bulletin*, No. 81, 1918.

There are two probable cases of Wolf-Rayet stars associated with diffuse nebulae having emission spectra. These are N.G.C. 2359 and 6888. Photographs of both nebulae have been published by Pease.[1] N.G.C. 2359 shows a ring and tangential streak suggesting the present form of the nebula surrounding Nova Persei No. 2. An eleventh-magnitude Ob star is approximately central in the ring and hence presumably associated with the nebula. N.G.C. 6888 is a segment of an ellipse with the Ob star B.D. +37°3821 of magnitude 7.1 near the center of the ellipse. The photograph suggests a ring of nebulosity of non-uniform brightness, inclined to the line of sight. Both nebulae have some resemblance to the planetaries or to a transitional type between planetary and extended forms. Both the nebular forms and types of stellar spectra suggest the possibility that these two nebulae are remnants of former outbursts of novae.

TABLE IV

STARS INVOLVED IN NEBULAE WITH EMISSION SPECTRA

No.	Nebula	Pv. Mag. of Stars	Spectrum of Stars	
1	N.G.C. 281	8.6–10.2 10.3–11.6	Oe5 Bo	4 components of B.D. +55°191 3 stars
3	1491	10.6	Bo	
5	1624	13.0–14.0	Oe5	3 stars. Magnitudes estimated
6	I.C. 405	5.8	Bop	Boss 1249
9	N.G.C. 1976	5.4–7.9	Oe5–Bo	4 components of Trapesium
10	1982	6.8	B1p	Bond 734. 4686 strong for type
13	2175	7.5	Oe5	B.D. +20°1284
14	2237	7.4–8.2	Oe5	4 brightest stars of the cluster
16	2359	11.0	Od	Magnitude estimated
21	6514	7.8–8.5	Oe5–Bo	2 components of B.D. −23°338
22	6523	6.1–6.9	Oe5–Bo	2 brightest stars in M 8. B.D. −23°13814–16
23	6611	8.3–9.2	Oe5–Bo	3 brightest stars in M 16.

NOTE

21. B.D. −22°4510, pv. magnitude 7.25, A3p (α Cygni type) is central in the northern lobe of the trifid nebula, N.G.C. 6514. The excessive color-index of this star, +0.80 magnitudes, together with the pronounced general absorption of the nebulosity, suggests that the star is actually within the nebula.

γ Cassiopeiae is probably associated with the emission nebulae I.C. 59 and 63. The star is clearly not involved, but the fan-shaped masses of nebulosity pointing toward that star suggest an intimate association. If this is true, γ Cassiopeiae is the one known case of a bright-line B-star associated with emission nebulosity. The type is called Bo peculiar.[1] ζ Orionis can with equal justification be considered as associated with N.G.C. 2024. In fact, all the belt stars of Orion might be thought of as associated with emission nebulosity, for the faint cloud in which they are immersed brightens in the portion known as I.C. 434, the bay nebula south of ζ Orionis, sufficiently to permit its spectrum to be identified as emission. These stars are of the Bo type.

---

[1] *Mt. Wilson Contr.*, No. 186; *Astrophysical Journal*, **51**, 276, 1920.

Another feature of the table is the marked tendency of Oe5 stars to form clusters in emission nebulae. Examples are N.G.C. 281, 1624, 2237, and 6611. Definite data are restricted to the brighter members of these clusters, but small dispersion spectrograms suggest that the fainter members are of somewhat later types and that the brighter ones alone determine the spectrum of the nebulosity.

N.G.C. 6618 (M 17) has no stars obviously involved, but there are indications of a cluster on its southern border. Two of the brightest of these are B8 and two fainter ones are Bo. General indications from focal-plane slitless spectrograms are that the two stars mentioned are the only late B-type stars in the group. A reasonable conclusion is that the two B8 stars are merely aligned, and that the group of fainter stars, if they are connected with the nebula, are of the usual type—Bo. The B8 stars are B.D. $-16^\circ 4827$ and $-16^\circ 4828$.

The main features of Table IV are the close limitation of the stars within the types Oe5 and Bo—at least for the brighter stars in each nebula—and the relatively rare occurrence of bright lines. These are four probable cases of emission nebulae associated with bright-line stars, but in no case do the spectra of star and nebula agree. The fact is well established that in the case of emission nebulae, the nebular spectrum and the spectra of stars involved or associated do not agree. This recalls Wright's remarks on the rare agreement between nebular and nuclear spectra among the planetaries.

---

[1] B.D. $-10^\circ 1848$ may be another case, but the spectrum of the nebulosity is so confused on my plates that the statement cannot be made definitely. The star is Bop with bright hydrogen lines.

The progression in stellar type from gaseous to "continuous" nebulae seems to be definitely established. There is no overlap save in N.G.C. 1982, which shows marked transitional characteristics in its spectrum. The sequence is well illustrated in the Orion nebulae of which the spectra have been investigated by Slipher and by Campbell and Moore.

N.G.C. 1976 gives a typical nebular emission line and a weak continuous spectrum. The trapezium stars are of type Oe5 and B0.[1]

N.G.C. 1982 gives a transitional spectrum. It is predominantly emission, but has a very considerable continuous background which intensifies in a marked degree about the involved star Bond 734. This is a B1 star, with λ 4686 unusually strong for the type. It might be called an early B1.

N.G.C. 1977. The spectrum is predominantly continuous with bright hydrogen and dark helium lines. No nebulium can be seen. The involved star, Boss 1364, is of type B1.

N.G.C. 2023. The spectrum is continuous with dark hydrogen and helium lines, and that of the involved star, B.D. $-2^\circ 1345$, is B2.

N.G.C. 2068 (M 78). The spectrum is continuous with dark hydrogen and helium lines and was classed by Slipher as probably late B. The stars involved are classed as B3 and B5, but subject to a rather large uncertainty. My own plates tend to place the nebular spectrum as not later than B5.

N.G.C. 2237 in Monoceros might be placed at the head of this sequence as it gives a pure emission spectrum with no continuous background perceptible. The four brightest stars involved which have been investigated all show fine Oe5 spectra.

SPECTRA OF PLANETARY NUCLEI

The progression is so pronounced that it seemed advisable to investigate the possibility of extending it into the other type of galactic nebulae, the planetaries. Wright has shown that some planetary nuclei have bright lines or bands, and that others do not. Where emission does occur it is probably of the Wolf-Rayet type. He has not published results for any of the nuclei of giant planetaries, and, as these seem to have the closest affinity to extended nebulae, their spectra have been observed at Mount Wilson.

---

[1] It has been previously mentioned that "continuous" nebulosity condenses strongly about the B8 star B.D. $-5^\circ 1305$ in the outer region of N.G.C. 1976, while the emission lines of the nebula are not affected by the star.

As an arbitrary division, those planetaries whose mean diameter exceeds two minutes of arc are called giants. There are six such, all within reach in this latitude.

N.G.C. 246
1514
3587 (Owl)
N.G.C. 6853 (Dumbbell)
7293 (Helix)
7635

Two of them have central stars bright enough for the Cassegrain spectrograph with one prism and an 18-inch camera on the 100-inch reflector. These are N.G.C. 1514 and 7635, whose central stars are, respectively, B.D. +30°623, 9.4 photo-visual magnitude, and B.D. +60°2522, 8.7 photo-visual magnitude. Their spectra are similar and of a type not covered by the Harvard classification. They show no bright lines or bands. The following dark lines are present:

Hβ
Hγ
Hδ
4542[1]
4200[1]
4026[1]
4686 faint and hazy
4471 just perceptible

To these may be added λ 4481 in B.D. +30°623 nearly as strong as λ 4542, and in B.D. +60°2522, λ 4147 stronger than λ 4471, and H and K faint and sharp. With these exceptions, the spectra could be described as Od with the bright lines suppressed to the extent of a trace of absorption in λ 4686. Their position is intermediate between the Wolf-Rayet type and Oe5. Radial velocities for four plates of each are +35.4 km for B.D. +30°623 and −34.5 km for B.D. +60°2522.

A single slit spectrogram of the central star in N.G.C. 246 made with one prism and a 7-inch camera shows a spectrum similar to B.D. +60°2522, the central star in N.G.C. 7635. In all three objects, the line λ 4542 is the strongest except the hydrogen lines.

By way of comparison, a spectrogram of the nucleus of the smaller planetary I.C. 2149 was obtained, using one prism and an 18-inch camera on the 100-inch reflector. This nucleus is one for which Wright reported a continuous spectrum with no bright lines. An exposure of eight hours gave a legible spectrum in spite of very poor seeing conditions. The rather faint continuous spectrum of the nucleus holds up unusually well toward the violet, and is crossed by the bright lines of the nebula, so sharp and narrow that their source is unmistakable. Only three dark lines can be detected. $H\beta$ and $H\gamma$ are very faint and hazy and almost obliterated by the strong bright nebular lines superposed. The third dark line is λ 4542, exceedingly faint, but free from any nebular line. No trace of λ 4686, either bright or dark, can be seen. Thus the nuclear spectrum, freed from the bright lines due to the nebula, is rather similar to a weak spectrum of the three central stars discussed above.

---

[1] The lines λλ 4542, 4200, and 4026 are those discovered by E. C. Pickering in the spectrum of ζ Puppis, for which he employed the designation Hγ′, Hδ′, and Hε′, respectively.

Slitless spectra have been obtained for the nuclei of all six of the nebulae. The dispersion is small, about 5.0 mm from $H\beta$ to $H\epsilon$, and conclusions based on them are not as certain as one would wish. All six are essentially similar; at least no difference could be made out on the small-dispersion plates. No bright lines or bands are seen, and all show the well-known strength in the ultraviolet which Wright first reported. This similarity of slitless spectrograms, together with the results of a detailed study of three higher-dispersion spectra taken with a slit, permits the assumption that we have in these central stars a class of objects intermediate between stars involved in extended emission nebulae and in the smaller planetaries.

Wright himself published observations of only two planetaries with mean diameters greater than one minute of arc. These are N.G.C. 4361 and 6720. In both cases the nucleus gave a continuous spectrum with no bright lines. His fifteen nebulae whose nuclei show no bright lines have a mean diameter of about 30″ as against 20″ for the fifteen whose nuclei do show bright lines, probably of the Wolf-Rayet type.[1]

The evidence, as far as it goes, points to a progression in spectral type of central or involved stars from the small planetaries to the large ones, and this progression joins immediately on to that of the extended nebulae. The complete sequence of stars involved in galactic nebulae can be represented as follows:

---

[1] *Publications of the Lick Observatory*, 13, 252, 1918.

Small planetaries	Wolf-Rayet
Large planetaries	Intermediate between Wolf-Rayet and Oe5
Extended emission nebulae	Oe5 and B0
Extended "continuous" nebulae	B1 and later

The overlap is surprisingly small and for the most part confined to nebulae with unusual forms or spectra. No conclusions have been formed as to the end of the sequence, although it may be significant that the stars of latest type seem to favor faint nebulosity and pronounced obscuration. N.G.C. 2359 and 6888, on the assumption that the Ob stars are truly associated, fall out of place. In both cases, however, there is evidence of a ring structure that suggests a nova origin or at least an affinity with the planetary type.

ASSOCIATION OF GALACTIC NEBULOSITY WITH STARS

This intimate relation between spectral type of nebula and of involved stars raises a presumption that one is a consequence of the other. It seems more reasonable to place the active agency in the relatively dense and exceedingly hot stars than in the nebulosity, and this leads to the suggestion that nebulosity is made luminous by radiation of some sort from stars in certain physical states. The necessary conditions are confined to certain ranges in stellar spectral type and hence are possibly phenomena of effective temperature. The nebulous material itself must be in a physical state sensitive to the stellar radiation, and close enough for the density of radiation to be effective. The abrupt transition from emission to "continuous" nebulosity between stellar types B0 and B1 suggests a critical point in the spectral sequence or possibly effective temperature below which stellar radiation is incapable of exciting nebulous material to emission luminosity. From thence down the spectral sequence the luminosity gives a continuous spectrum and probably partakes more and more of the nature of reflected light.

A theory of nebular luminosity built on these lines meets a first obstacle in the necessity for locating stars conspicuously associated with each galactic nebula, of the required spectral type, and properly placed to energize the nebulosity. Planetaries offer no great difficulty. There is doubt in some cases as to whether the nuclei are truly stellar, but there is usually a condensed center which may well conceal a star or take the place of a star as a center of radiation. In several extended nebulae, however, there is a conspicuous absence of any obviously dominating star or group of stars. Such of those as give continuous spectra show pronounced obscuration in and surrounding the nebulosity, and offer the possibility that stars capable of playing the required rôle are present but entirely or partially obscured. Nos. 4, 5, 6, and 7 in Table I are examples.

Emission nebulosity exhibits much less general absorption, possibly because the matter is in a more highly dissociated state. Here the assumption of obscuration generally fails, and the radiation centers must be sought among the multitude of stars always found within, or near to, the nebulosity. Such stars need not be apparently bright, for the apparent surface luminosity of nebulae is independent of the distance. Furthermore, several of the giant planetaries, for instance, N.G.C. 3587, 6853, and 7293, have bright nebulosity with central stars of the thirteenth to the fourteenth magnitude. Such objects then as N.G.C. 1499 and the nebula in Cygnus, N.G.C. 6960 and 6992, might, with no great stretch of the imagination, be considered as receiving affective radiation from some of the neighboring stars, after the manner in which N.G.C. 2024 probably receives its energy from ζ Orionis.

These suggestions may be applied to the nebulae considered in this paper. Table I contains only six nebulae with continuous spectra, which have no stars obviously involved or conspicuous on direct photographs for location and brightness. They are Nos. 4, 5, 6, 7, 9, and 13. The first four fall in the Taurus group and lie in regions of complete obscuration. Involved stars would need to lie on the near side or very close to the nearer surface of the nebulae in order to be seen at all. In two of these four cases, Nos. 4 and 6, faint stars are present which are almost certainly dimmed by intervening nebulosity. It is possible and even reasonable to assume that bright stars may be involved or associated with all four of these objects, but partially or completely hidden by the obscuring clouds.

No. 9 is the nebulosity north of and preceding Rigel. The form of the nebula approximates an arc with Rigel at the center. Moreover, several fan-shaped details are present which in each case point toward that star. In short, the nebula shows a considerable degree of radial symmetry with Rigel as the point of convergence. The spectral type of Rigel, B8p, and the absolute magnitude, -5.5 according to Kapteyn, are significant. The nebulosity extends to a distance of $2\overset{\circ}{.}5$ from the star which, in terms of actual distance across the line of sight, is of the order of twenty light-years at the distance of Rigel. This seems an enormous distance over which to assume stellar radiation to be effective in illuminating nebulosity, but a comparison with the better-known Pleiades nebulosity indicates that the two cases are comparable, and Hertzsprung's[1] discussion of the Merope nebula lends considerable weight to the suggestion that reflected starlight can account for the whole of the nebular luminosity in that particular case. In terms of absolute magnitudes Rigel is about 4.7 magnitudes brighter than Merope and hence will have the same illuminating power at 8.7 times the actual distance of similar nebulosity from Merope; or since Rigel is about 1.5 times as distant as Merope from the earth, to an angular distance of about 5.8 times as seen from the earth. Nebulosity comparable in brightness to the nebulosity near Rigel exists nearer to Merope than to any other of the bright stars of the Pleiades, and it extends to a distance considerably more than 1/5.8 times its angular distance.

Inclusion of all the Pleiades stars will not entirely destroy the analogy. According to Trumpler's list of cluster stars, the equivalent brightness of the Pleiades cluster is of the order of magnitude 1.3 or about -3.7 absolute, and the center of the cluster is about $6'$ west of Alcyone. Rigel then is 1.8 magnitudes brighter than the entire cluster and would have equal illuminating powers on nebulosity at about 1.4 times the angular distance of equivalent nebulosity from the center of the cluster. The equivalent distance in the Pleiades cluster is about $100.'$ The actual nebulosity is rather sharply divided into bright inner clouds involving the more luminous stars and extending in parts to about $50'$ from the center, and very faint exterior clouds extending to 3° or 3°.5 from the center. The position of the nebulosity near Rigel would seem to fall between these extremes. This discussion disregards inclinations to the line of sight of the direction from star to nebulosity, and hence leaves an element of uncertainty in the conclusion. It does seem plausible, however, to regard the relation of Rigel to its neighboring nebulosity in the same category as the relation between stars and nebulosities in the Pleiades cluster.

---

[1] *Astronomische Nachrichten*, **195**, 449 (No. 4679), 1913.

No. 13, the great loop, sometimes called the spiral, around the belt and sword of Orion, offers difficulties of another sort. The belt stars and the general aggregation of fainter stars in the vicinity are sufficiently bright to account for the nebular luminosity on the same basis as in the case of Rigel and the Pleiades, but the continuous spectrum of the nebulosity does not fit the Bo spectral types of the brighter belt stars. These same stars appear to produce an emission type of illumination in nebulosity immediately adjacent to them, N.G.C. 2024, I.C. 434, etc.; yet if they truly do illuminate the more distant loop, it is with a different light altogether. It may be that the physical state of the loop nebulosity is different from that in the closer objects—that the physical state of all nebulosity depends upon distance from, and spectral type of, associated stars. Or, again, the ability of stellar radiation to produce emission luminosity may be restricted to certain limits of distance which in this case are exceeded.[1]

The facts seem definite—the nebulosity close to the belt stars gives emission spectra while that far away gives a continuous spectrum. Several nebulae giving continuous spectra, as, for example, N.G.C. 2023, are nearer to the belt than is the loop, but they lie on the near side of an obscuring cloud which seems to veil them from the influence of the belt stars and permits them to shine by the undisturbed action of their own involved stars. Slipher suggested that spectra of the Orion nebulosities change from emission to continuous or rather to absorption, as one proceeds outward from a center—probably the great nebula around

---

[1] The brightest portion of the loop is nearest the belt stars. The distance across the line of sight to the nearest belt star—ζ Orionis—is about forty light-years.

θ Orionis, and these new observations may be but another application of some law. However this may be, the loop in Orion, if it does receive its light from the group of stars that includes the belt, is the one known example of a nebula giving a predominantly continuous spectrum, having as the brightest stars associated with it those of a type earlier than B1.

The result of this examination is as follows: twenty-six out of thirty-three nebulae giving predominantly continuous spectra have prominent stars obviously involved in the nebulosity; in six of the remaining cases more or less plausible means can immediately be suggested to account for the absence of dominating stars within the nebulae; and in the last case, exceptional in many respects, there exists at least possible means of accounting for the nebular illumination as originating in stars.

The case of the emission nebulae is nearly as strong. Among those listed in Table II the following do not have early type stars actually within their borders:

Nos. 2, 4, 7, 8, 11, 12, 25 (26 and 27), 28.

No. 2, I.C. 59, 63—the fan-shaped nebulae near γ Cassiopeiae. That star is obviously associated with, although not involved in, the nebula. The very form of the nebulosity seems determined by radiation or repulsive action from the star which lies at a center of radial symmetry with respect to the fans. The spectral type of γ Cassiopeiae, Bop with bright lines, conforms to the rule previously established concerning the relation between stellar and nebular spectra.

No. 4, N.G.C. 1499—ξ Persei is the brightest neighboring star. The nebula lies on a rough arc, concave to ξ Persei, which can readily be considered as occupying the center of the arc. The star is of type Oe5 and hence conformable to the nebular spectrum. No other star in the vicinity brighter than ninth magnitude has a spectrum earlier than B3.

No. 25, N.G.C. 6888—a long segment of an ellipse, of which B.D. $+37°3821$ occupies the center. The stellar type is Ob, hence the star and nebula seem to resemble N.G.C. 2359. No other star in the neighborhood has a spectrum earlier than B5. The only brighter star near is of K-type.

These three cases offer positive evidence of association of star and nebulosity. In each, one definite external star appears to dominate the nebula, its position approximating a center of radial symmetry, its spectral type conforming to the established rule. No rival claimants can be found for any of the positions.

No. 12, N.G.C. 2024—ζ Orionis, Bo, a sort of super-giant with an absolute magnitude of -4.17 according to Kapteyn, is conveniently located to energize the nebula. Direct photographs give an instant impression that this star illuminates the nebula, although the details of nebulosity do not show such marked radial structure as is found in the three cases cited above.

No. 11, I.C. 434—the Bay nebula south of ζ Orionis. This seems part of a cloud involving the belt stars and σ Orionis. In this particular portion, both ζ and σ can be considered as sources of illumination, both from position and from spectral type.

No. 8, I.C. 423—a small loop between δ and ϵ Orionis, nearer the former. Both these stars from their spectral types can be considered as the energizing agents. Their positions bear no obvious relation to the figure of the nebula, but their distances are within reason unless greatly distorted by projection.

These three cases do not offer such definite evidence as the first three discussed. They pass from positive in No. 12 to suggestive in No. 8.

The last three cases, Nos. 7, 28, and 26 and 27, offer more serious difficulties. One indeed, 26 and 27, seems flatly to defy explanation on any observational basis.

No. 7, N.G.C. 1952, the Crab nebula, has two faint stars about centrally located. The brighter is of about 15.5 photographic magnitude and the other only slightly fainter. The nebular spectrum is strongly continuous with widely doubled bright lines. Curtis includes the nebula among the planetaries, although he calls it a doubtful classification. Exposure-ratio plates made at Mount Wilson indicate a decided negative color-index for the brighter star at least, and this, together with their approximately central position, permits the assumption that one or both are involved in or associated with the nebula. There are no bright stars in the neighborhood which can be considered as sources of energy, either from position or spectral type.

The question, then, is whether or not the faint central star or stars can dominate the nebula. The best answer is another analogy, this time with the Helical nebula in Aquarius, the giant planetary, N.G.C. 7293. This nebula has a diameter about three times that of the Crab and a central star about two magnitudes brighter. The relation between stellar magnitude and square of the radius are of the same order. If the Crab were at three times the distance of the Helical nebula the two objects would be comparable in size and brightness of their central stars. If the planetaries are energized by their central stars, then one may assume as a possibility that the same is true of the Crab nebula.

No. 28, N.G.C. 7000—the North America nebula. This object gives a considerable continuous spectrum with faint emission. Several stars from sixth to ninth apparent magnitude are involved, and heavy obscuration is evident around the borders, especially in the southern portion. The nebulosity is cloudy and devoid of filamentous detail. In a general way it recalls the appearance of the Trifid. The spectrum also has some resemblance to that of the Trifid, although this latter nebula has a stronger emission and a weaker continuous background. The stars involved in N.G.C. 7000 are all later than B1, and hence can account for only the continuous portion of the nebular spectrum.

Inspection of small-scale photographs of this nebula, for instance, those made by Barnard with the 6-inch Willard lens, suggests that α Cygni may be associated. The Trifid nebula offers a possible analogy, for in the north lobe of that object is a star of the same enhanced A-type as α Cygni. The star is B.D. $-22^\circ 4510$, photo-visual magnitude 7.2, with a spectrum remarkably similar to that of α Cygni. The star has a color-index of about 0.8 magnitude and hence is regarded as involved in the nebulosity. The Trifid nebula gives an emission spectrum on a continuous background. The emission portion can be attributed to the Oe5 star B.D. $-23^\circ 338$ in the southern lobe, but the lack of pronounced strengthening of continuous spectrum immediately contiguous to the star in the northern lobe suggests that the latter star may be responsible for part at least of the emission spectrum. The enhanced α Cygni type of stellar spectrum is so unique that unusual properties may be suggested for such stars without prejudice to the existing data. If the star, B.D. −22°4510, does produce some emission luminosity in the Trifid, then α Cygni can be considered a possible source of illumination in N.G.C. 7000.

α Cygni is some 5.5 magnitudes brighter than B.D. −22°4510; hence, if we assume the same absolute magnitude for both stars, α Cygni would have equal illuminating powers at about thirteen times the angular distance, or by figuring from the dimensions of the Trifid, to just under 2°. The nebulosity in N.G.C. 7000 actually does extend from 2°.5 to 3°.5 from α Cygni so that, disregarding inclinations to the line of sight, and remembering that nebulosity need not be similarly distributed in these objects, we can regard the distances in the two cases as roughly of the same order. It is necessary to emphasize that this discussion does not explain the luminosity of N.G.C. 7000, and that it does not even make out a strong case. The most that can be said is that a possibility is offered which derives some weight from analogy and which must receive some consideration before it can be definitely dismissed.

Nos. 26 and 27, N.G.C. 6960 and 6992, are portions of an enormous loop in Cygnus. This nebula apparently is the one absolute exception to the suggestion that all galactic nebulae have associated with them stars of spectral types conformable to the type of nebular spectrum. The spectrum of the loop in Cygnus appears to be almost purely emission, yet no stars earlier than B3 nor any stars of the enhanced α Cygni type can be located, which have any probable connection with the nebula. In fact no stars at all, brighter than 9.5 magnitude, can be suggested as associated with the nebulosity.

This discussion of emission nebulae indicates that seventeen out of the twenty-six objects in Table II have stars of conformable spectral types within and obviously associated with the nebulosity. Of the remaining nine objects, three give positive evidence of association with external stars, three suggest such association, two offer possibilities of association, and one seems flatly to contradict the idea of association.

Combining the results from Tables I and II there is one clear exception and three difficult or doubtful cases out of the sixty-two nebulae. Examination of an observing list of some one hundred and twenty-five extended galactic nebulae, all the known objects of this class north of -40° declination, shows no other exception and only one or two doubtful cases. The evidence then, with the single clear exception of the Cygnus loop, is very strongly in favor of the view that all galactic nebulae have associated with them stars of spectral types conformable to the types of the nebular spectra.

CONCLUSIONS

The general conclusion of this discussion is that all galactic nebulae are associated with stars and that the spectra of nebulae and associated stars have a definite relation. This suggests that galactic nebular luminosity has its source in stellar radiation. The phenomena are not simply those of reflected starlight, for in general the emission spectra of nebulae do not agree with the spectra of the associated stars. The reverse is true for diffuse nebulae with continuous spectra. In these cases the reflection theory appears to offer a reasonable explanation, or at least a working basis for further investigation. The mechanism of emission luminosity will probably find its explanation in the fact that it is always associated with the very hottest types of stars.

It is very doubtful whether or not a mass of diffuse nebulosity isolated in space and with no stars involved could hold together and at the same time shine by light generated by collisions of molecules. At temperatures corresponding to intensity-distribution or width of lines in nebular spectra, the average speeds of molecules would be so high compared to the velocities of escape that the nebulosities would probably dissipate rapidly. On the other hand, if molecular speeds were sufficiently small to admit of cohesion in the mass, the nebulosity would probably be too cold to radiate light. This argument suggests that diffuse nebulosity is not intrinsically luminous, but is rendered so by external causes. The only obvious external sources of energy are the stars actually involved in or neighboring to the nebulosity, and definite relations have now been found to exist between the radiations of such stars and nebulosity.

The resulting conception of diffuse galactic nebulae is that they are clouds of material (molecules, dust, or larger particles) illuminated by neighboring stars. The question as to whether the association is temporary or permanent can be answered by a comparison of radial velocities of stars and nebulae. Unfortunately the large majority of such stars are binaries which require a great deal of labor for determining the velocities of the systems. This is especially true of the Oe5 and B0 stars which are associated with the diffuse emission nebulae whose velocities are best determined.

The meager data available at present are indeterminant. Radial velocities are given by Campbell and Moore for six diffuse nebulae as follows:

N.G.C. 1976 (Orion)	+17.5 km
3372	+ 6.0
6514 (Trifid)	+11.0
6523 (M 8)	− 3.0
6618 (M 17)	+ 7.0

The brighter stars in N.G.C. 1976 are all binaries for which no velocities for the systems have been determined. The stars in N.G.C. 6618 are faint and no measures have been published as yet.

η Carinae, in N.G.C. 3372, gives for the hydrogen lines velocities differing from those of other emission lines. The mean of four spectrograms measured by Sanford[1] gives +33.8 km for hydrogen and −22.8 km for the other emission lines. It is just possible that the mean, +5.5 km, may have a significance when compared to the nebular velocity, +6.0 km.

The three brightest stars in N.G.C. 6514 have been observed at Mount Wilson. They are:

B.D. −22°4150, A3p	− 1.5 km, 3 plates
B.D. −23°13804 (brightest comp.), Oe5	− 4.7 km, 4 plates, range 26 km
B.D. −23°13804 (second brightest comp.), B1	+17.3 km, 3 plates, range 20 km
Mean	+ 2.9 km

The two brightest components of B.D. −23°13804 are undoubtedly binaries and the mean of the seven measures for the two, +6.3 km, is suggestive, but by no means conclusive, on the question of agreement between stellar and nebular velocities. B.D. − 22°4510 is definitely not in agreement. Its high color-excess[1] may mean that it is seen through the entire nebula.

---

[1] *Lick Observatory Bulletins*, **8**, 134, 1916.

One star in N.G.C. 6523 has been measured—Boss 4560, Oe5, magnitude 6.1. The spectrograms give a velocity of +12.6 km. As the range is 33 km, the star must be considered a binary.

Further data on this question are very desirable. A casual inspection of diffuse nebular structure and configurations of involved stars suggests that the association is for the most part temporary. This may be one fundamental distinction between diffuse nebulae and planetaries, for in the latter the central stars must be permanently associated with the surrounding nebulosity; otherwise their central positions could not in general be maintained.

MOUNT WILSON OBSERVATORY
May 1922

---

[1] The color-index is 0.8 magnitudes. See *Mt. Wilson Contr.*, No. 187, p. 15; *Astrophysical Journal*, **52**, 22, 1920.

Contributions from the Mount Wilson Observatory, No. 242
Reprinted from the *Astrophysical Journal*, Vol. LVI, pp. 200–207, 1922

INVESTIGATIONS ON PROPER MOTION

SEVENTH PAPER: INTERNAL MOTION IN THE SPIRAL NEBULA N.G.C. 2403

By ADRIAAN VAN MAANEN

ABSTRACT

Spiral nebula N.G.C. 2403.—Two pairs of plates covering eleven- and eight-year intervals, respectively, and all taken at the primary focus of the 60-inch reflector, were measured with the stereocomparator, and the motions of 76 points, presumably belonging to the nebula, were derived with respect to the mean motion of 24 comparison stars. The results for each point and star are shown by arrows on the accompanying *photograph*. *The proper motion of the nebula* as a whole comes out very small, namely, $\mu_\alpha = +0''.002$ and $\mu_\delta = 0''.000$. Taking the *inclination of the plane of the nebula* to the surface of the celestial sphere to be 48°, the *internal proper motions* in the plane of the nebula come out very similar to those found previously for M 33, 51, 81, and 101. The radial components are practically equal to the tangential components, both increasing with the distance from the center; the motions indicate an outward streaming along the spiral arms at a rate which increases from $0''.015$ per year at $1'.4$ to $0''.040$ at $8'.9$ (the average being $0''.019$), combined with an outward transverse motion of about $0''.007$ per year.

Proper motions of 24 comparison stars were also determined with a probable error of $\pm 0''.0038$ per year. All but one or two have velocities less than $0''.02$ per year.

In January, 1921, Mr. Duncan succeeded in securing with the 60-inch Mount Wilson reflector several plates of the spiral nebula N.G.C. 2403 with exposure times ranging from one hour to four hours. For this object Mr. Ritchey had already taken plates in 1910, 1916, and 1917, and Mr. Pease had taken a photograph in 1912. Of these plates four were selected for measurement, and combined into two pairs for which the observing details are given in Table I.

TABLE I

	Date	Observer	Exposure	Quality
1	1910 Feb. 7	Ritchey	1^h	g
	1921 Jan. 4	Duncan	1^h	fg
2	1912 Nov. 8	Pease	$3\frac{1}{2}^h$	g
	1921 Jan. 5	Duncan	4^h	fg

The nebula is described by Curtis[1] as "a bright, beautiful spiral 16′×10′. No nucleus apparent; many almost stellar condensations; of the general type of M 33." As the galactic latitude is not quite 30°, we have an abundance of stars which can be used for comparison purposes.

Seventy-six points, presumably belonging to the nebula, were measured, while for comparison purposes twenty-four stars from magnitude 13.5 to 17.0 were selected.

Both pairs of plates were measured with the new stereocomparator in four positions, with the direction east, west, north, and south successively coinciding with that of the increasing readings of the micròmeter screw. For each pair the two measures in right ascension and those in declination were combined into one series of displacements; these values, $M\alpha_1$, $M\alpha_2$, $M\delta_1$ and $M\delta_2$, were reduced to proper motions by equations of the form:

$$\left.\begin{aligned} M_\alpha &= a+bx+cy+dx^2+exy+fy^2+m_\alpha \\ M_\delta &= a^1+b^1x+c^1y+d^1x^2+e^1xy+f^1y^2+m_\delta, \end{aligned}\right\} \qquad (1)$$

in which a, b . . . . f^1 are the plate-constants, x and y the co-ordinates of the objects measured, and m_α and m_δ the proper motions, expressed in parts of the micrometer screw. In order to reduce these motions to annual proper motions, expressed in thousandths of a second of arc, the quantities m_α amd m_δ for the first pair of plates must be multiplied by 0.765, for the second pair by 1.022.

The plate-constants were derived by least-squares solutions from the sets of twenty-four equations of form (1) for the comparison stars. The constants thus found were substituted in the equations of conditions (1) of all the objects measured. The annual proper motions are given in the fourth, fifth, sixth, and seventh columns of Table II. The second and third columns of this table contain the co-ordinates in x and y, expressed in minutes of arc, with a precision sufficient for identification.

Weights 2 and 1 were assigned to the two pairs respectively; the mean motions thus derived for the nebular points include the motion of the nebula as a whole with respect to the 24 comparison

---

[1] *Lick Observatory Publications*, 13, 24, 1918.

TABLE II

Co-ordinates and Annual Displacements

No.	x	y	$\mu_{\alpha 1}$	$\mu_{\alpha 2}$	$\mu_{\delta 1}$	$\mu_{\delta 2}$
a	−6′.7	+0′.9	+0″.003	+0″.007	−0″.005	+0″.003
b	−4.8	+4.9	+ 4	+ 5	+ 21	− 7
c	−2.0	+5.2	+ 3	− 1	− 5	+ 16
d	−2.4	+3.6	− 6	+ 14	− 40	− 27
e	−2.8	+1.7	− 7	− 34	+ 3	− 6
f	−4.1	−0.3	− 4	− 6	+ 10	+ 11
g	−4.9	−1.5	+ 5	+ 6	+ 6	+ 17
h	−5.1	−4.3	+ 2	− 10	− 5	− 8
i	−3.2	−4.9	− 2	− 5	− 3	+ 8
j	−1.9	−4.4	− 6	+ 2	− 5	− 10
k	−1.6	−2.0	− 2	+ 2	+ 5	− 10
l	−2.4	−1.2	− 4	+ 11	− 3	− 13
m	−0.4	−2.1	+ 5	+ 16	+ 10	− 3
n	−0.5	−1.2	+ 14	+ 7	0	+ 6
o	+0.9	−1.8	+ 1	− 6	+ 11	− 5
p	+3.6	−5.0	+ 8	+ 19	+ 6	0
q	+4.5	−4.7	− 7	− 10	− 5	+ 2
r	+5.4	−2.5	− 3	− 3	− 7	+ 3
s	+5.9	−1.6	+ 2	− 13	− 1	+ 1
t	+4.5	+0.7	+ 5	− 9	− 10	− 3
u	+5.5	+2.4	− 2	+ 17	+ 5	− 9
v	+1.9	−0.2	− 5	− 8	− 1	+ 23
w	+3.8	+4.1	+ 1	+ 12	+ 5	− 5
x	+0.6	+5.7	− 2	− 13	+ 5	+ 14
1	−7.0	−0.3	− 20	− 42	+ 26	+ 2
2	−7.0	−0.6	− 36	− 36	+ 24	+ 29
3	−2.8	+2.8	+ 7	− 28	+ 17	+ 5
4	−2.8	+2.7	− 18	− 15	+ 13	− 19
5	−2.8	+2.6	+ 17	− 11	+ 18	+ 29
6	−2.7	+2.7	+ 8	+ 3	+ 32	+ 63
7	−2.5	+3.0	+ 5	+ 13	+ 18	+ 13
8	−3.6	+1.2	0	− 11	+ 27	+ 26
9	−3.2	+0.9	+ 2	− 4	+ 14	− 22
10	−2.9	+0.6	− 19	− 28	− 1	+ 6
11	−2.3	−2.3	− 19	− 13	+ 9	+ 7
12	−2.0	−0.8	− 2	− 16	+ 26	− 11
13	−1.9	−0.4	− 32	− 37	+ 18	+ 34
14	−1.7	−0.4	− 3	− 30	+ 7	+ 23
15	−1.4	+0.4	− 7	− 23	+ 15	− 5
16	−1.9	+0.8	− 8	− 32	+ 8	0
17	−1.6	+1.7	+ 11	+ 18	+ 28	− 10
18	−1.6	+1.8	+ 20	− 1	+ 42	+ 10
19	−1.4	+1.8	+ 22	− 3	+ 8	+ 22
20	−1.6	+2.6	+ 18	− 9	+ 28	+ 4
21	−1.7	+2.7	+ 6	+ 23	+ 22	+ 44
22	−1.2	+3.3	+ 19	+ 11	− 1	− 6
23	−0.1	+5.0	+ 8	+ 41	+ 17	+ 4
24	−0.6	+3.7	− 1	+ 19	+ 8	− 20
25	−0.4	+3.6	+ 8	− 19	+ 56	+ 8
26	−0.4	+1.8	+ 16	+ 26	+ 28	+ 7
27	−0.5	+1.5	0	+ 32	+ 4	+ 8
28	−0.2	+1.7	+ 14	+ 12	+ 12	− 30

TABLE II—*Continued*

No.	x	y	$\mu_{\alpha 1}$	$\mu_{\alpha 2}$	$\mu_{\delta 1}$	$\mu_{\delta 2}$
29	−0′.1	+1′.7	+0″.021	+0″.018	+0″.015	−0″.002
30	0.0	+1.7	+ 7	+ 39	+ 14	− 17
31	−0.3	+0.7	+ 5	+ 42	− 5	+ 6
32	−0.6	+0.8	− 15	− 32	+ 30	+ 8
33	−0.3	+0.4	+ 2	+ 22	+ 22	+ 6
34	−0.2	+0.3	+ 5	+ 17	+ 5	+ 24
35	−0.3	−0.1	− 4	+ 1	− 4	− 3
36	−0.3	−0.3	− 11	− 34	+ 2	− 21
37	−0.4	−0.5	− 18	− 24	− 3	− 40
38	−0.5	−0.9	− 6	− 13	+ 13	− 40
39	−0.7	−1.1	− 24	− 29	+ 20	− 20
40	−0.2	−1.0	+ 4	− 22	+ 1	− 29
41	−0.1	−1.2	− 5	− 22	+ 1	− 29
42	0.0	−1.2	+ 10	− 12	+ 10	− 30
43	−0.2	−1.8	− 5	− 28	+ 8	− 7
44	+1.3	−4.4	+ 4	− 16	− 8	− 21
45	+1.5	−3.5	+ 4	− 23	− 11	− 22
46	+1.3	−2.3	+ 5	− 10	− 3	− 31
47	+1.4	−2.3	− 23	+ 23	− 17	− 29
48	+2.0	−2.3	+ 16	− 30	+ 2	− 34
49	+2.1	−2.3	+ 11	+ 11	+ 1	− 10
50	+2.1	−2.2	+ 13	− 6	0	− 24
51	+2.0	−2.1	+ 4	+ 8	− 3	− 8
52	+1.5	−1.5	+ 29	− 8	− 13	− 30
53	+1.4	−1.5	+ 12	− 61	+ 7	+ 5
54	+0.9	−1.0	− 2	+ 5	− 2	− 39
55	+0.9	−0.7	+ 21	+ 4	− 5	− 19
56	+0.7	+0.4	+ 5	− 3	− 4	− 30
57	+0.6	+1.2	+ 18	+ 28	− 8	− 4
58	+1.1	+1.4	− 4	+ 9	− 15	− 38
59	+0.7	+3.7	+ 24	+ 18	+ 20	− 2
60	+0.6	+3.6	+ 28	+ 41	+ 29	− 21
61	+1.4	+0.5	+ 8	+ 16	+ 2	0
62	+1.5	+0.7	+ 17	+ 27	− 8	− 9
63	+2.1	+0.1	+ 20	− 8	− 13	− 17
64	+2.3	0.0	+ 36	− 4	− 19	− 35
65	+2.8	−0.4	+ 2	+ 31	− 1	− 21
66	+2.9	−0.5	+ 15	+ 23	− 16	− 30
67	+2.3	−0.7	+ 12	+ 30	− 3	− 72
68	+2.8	−2.4	+ 8	− 29	− 5	− 20
69	+2.7	−2.8	− 12	− 34	− 23	− 41
70	+2.9	−3.5	+ 10	− 35	+ 5	− 20
71	+2.4	−4.1	− 11	− 22	− 7	− 45
72	+2.5	−4.2	+ 2	− 12	− 8	− 61
73	+2.7	−4.1	− 3	− 23	0	− 9
74	+4.7	+2.7	+ 34	+ 31	− 10	− 16
75	+4.5	−2.3	+ 26	+ 24	0	− 46
76	+6.2	−1.8	+ 16	+ 24	− 35	− 15

stars as well as the internal motions of the individual points. To derive the motion of the nebula as a whole, the same process was followed as for the nebulae formerly discussed.[1]

---

[1] *Mt. Wilson Contr.*, No. 118, p. 9; *Astrophysical Journal*, 44, 218, 1916.

PLATE III

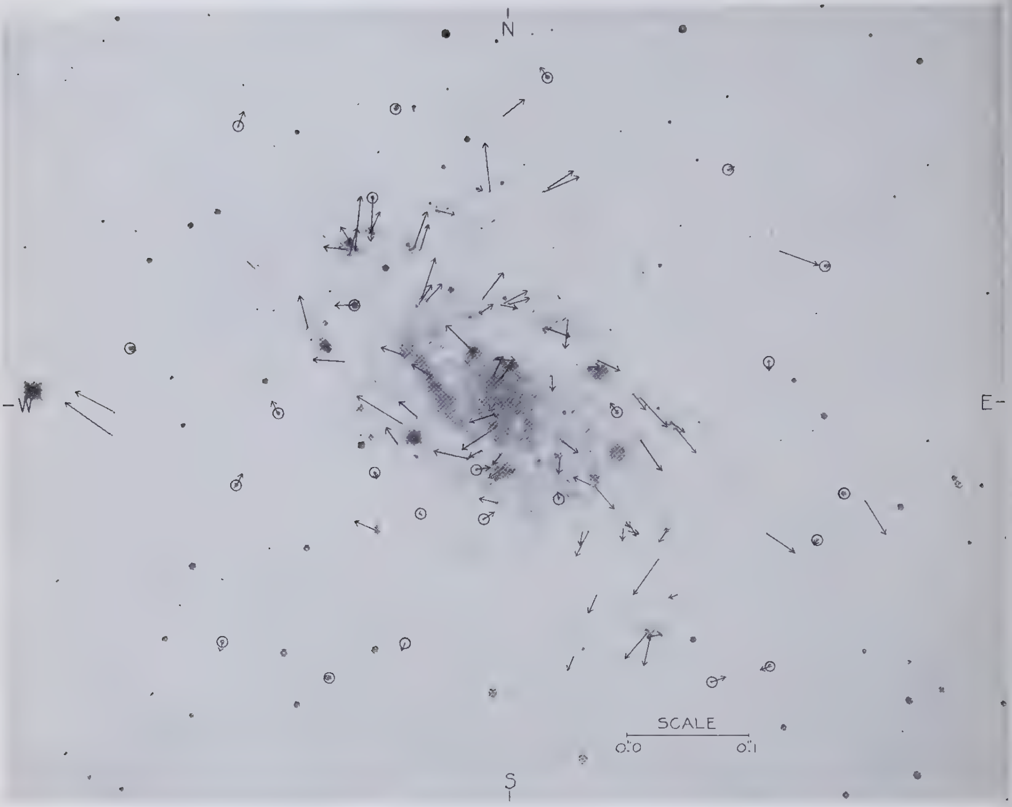

INTERNAL MOTIONS IN N.G.C. 2403

The arrows indicate the directions and magnitudes of the mean annual motions. Their scale (0″.1) is indicated on the illustration. The scale of the nebula is 1 mm = 8″.1. The comparison stars are inclosed in circles.

a) The mean for all of the 76 points gives:

$$\mu_\alpha = +0''.002 \qquad \mu_\delta = +0''.001.$$

b) If the points are divided into four groups, corresponding to the four quadrants, the means of the two groups in opposite quadrants should give a good agreement. We find:

$$\text{Means for I and III} \quad \begin{cases} \mu_\alpha = +0''.000^5 \\ \mu_\delta = -0''.001 \end{cases}$$

$$\text{Means for II and IV} \quad \begin{cases} \mu_\alpha = +0''.003^5 \\ \mu_\delta = +0''.000^5 \end{cases}$$

The four quadrants combined give:

$$\mu_\alpha = +0''.002 \qquad \mu_\delta = 0''.000.$$

c) In order to avoid points far from the center, which have an asymmetrical distribution, we may use only those within a radius of 4'.2. We find then:

$$\text{Means for I and III} \quad \begin{cases} \mu_\alpha = +0''.001 \\ \mu_\delta = -0''.002 \end{cases}$$

$$\text{Means for II and IV} \quad \begin{cases} \mu_\alpha = +0''.004 \\ \mu_\delta = +0''.001 \end{cases}$$

The four quadrants combined give:

$$\mu_\alpha = +0''.002^5 \qquad \mu_\delta = -0''.000^5.$$

Giving equal weights to each of the three methods used, we derive as the final motion of the nebula as a whole:

$$\mu_\alpha = +0''.002 \qquad \mu_\delta = 0''.000.$$

If now we subtract these quantities from the values μ_α and μ_δ for the nebular points, we obtain results which represent the internal motions and are given in the second and third columns of Table III and plotted in Plate III. The plate also shows the motions of the 24 comparison stars as given in Table II; these stars are surrounded by a circle. The scale of the motions is indicated in the lower right-hand corner. The arrows represent the motions in about 1300 years. The probable errors of the

TABLE III

ANNUAL INTERNAL MOTIONS

No.	μ_α	μ_δ	Rotational	Radial	Stream	Transverse
1	−0″.029	+0″.018	+0″.022	+0″.028	+0″.034	+0″.012
2	− 38	+ 26	+ 34	+ 32	+ 46	+ 8
3	− 7	+ 13	+ 6	+ 12	+ 8	+ 10
4	− 19	+ 2	− 16	+ 12	− 10	+ 18
5	+ 6	+ 22	+ 32	+ 10	+ 32	+ 6
6	+ 4	+ 42	+ 48	+ 30	+ 52	+ 20
7	+ 6	+ 16	+ 24	+ 10	+ 24	+ 6
8	− 6	+ 27	+ 30	+ 4	+ 30	+ 4
9	− 2	+ 2	+ 2	− 2	+ 2	− 2
10	− 24	+ 1	− 6	+ 30	− 2	+ 30
11	− 19	+ 8	+ 16	+ 8	+ 16	+ 8
12	− 9	+ 14	+ 16	− 2	+ 16	− 6
13	− 36	+ 23	+ 32	+ 28	+ 38	+ 20
14	− 14	+ 12	+ 16	+ 8	+ 18	+ 4
15	− 14	+ 8	+ 2	+ 16	+ 10	+ 14
16	− 18	+ 5	− 2	+ 18	+ 6	+ 16
17	+ 11	+ 15	+ 18	+ 6	+ 20	+ 2
18	+ 11	+ 31	+ 30	+ 20	+ 34	+ 16
19	+ 12	+ 13	+ 18	+ 4	+ 20	− 2
20	+ 7	+ 20	+ 20	+ 20	+ 26	+ 14
21	+ 10	+ 29	+ 32	+ 28	+ 38	+ 20
22	+ 14	− 3	+ 20	− 4	+ 18	− 6
23	+ 17	+ 13	+ 16	+ 24	+ 20	− 22
24	+ 4	− 1	+ 6	0	+ 6	0
25	− 3	+ 40	− 4	+ 50	+ 6	+ 50
26	+ 17	+ 21	+ 24	+ 32	+ 16	+ 36
27	+ 9	+ 5	+ 14	+ 8	+ 14	+ 10
28	+ 11	− 2	+ 14	+ 2	+ 14	+ 2
29	+ 18	+ 9	+ 18	+ 20	+ 16	+ 22
30	+ 16	+ 4	+ 14	+ 16	+ 14	+ 18
31	+ 15	− 1	+ 18	+ 2	+ 18	− 2
32	− 23	+ 23	− 8	+ 26	+ 8	+ 26
33	+ 7	+ 17	+ 14	+ 16	+ 22	+ 4
34	+ 7	+ 11	+ 10	+ 14	+ 14	+ 10
35	− 4	− 4	0	+ 8	0	+ 8
36	− 21	− 6	+ 16	+ 18	+ 24	+ 10
37	− 22	− 15	+ 16	+ 34	+ 24	+ 28
38	− 10	− 5	+ 6	+ 10	+ 12	+ 4
39	− 28	+ 7	+ 24	+ 14	+ 28	− 4
40	− 7	− 9	+ 6	+ 12	+ 12	+ 6
41	− 13	− 9	+ 16	+ 16	+ 22	+ 2
42	+ 1	− 3	− 2	+ 4	+ 2	+ 6
43	− 15	+ 3	+ 16	+ 2	+ 16	− 6
44	− 5	− 12	+ 10	+ 18	+ 18	+ 10
45	− 7	− 15	+ 16	+ 18	+ 24	+ 4
46	− 2	− 12	+ 8	+ 10	+ 12	+ 6
47	− 10	− 21	+ 24	+ 16	+ 30	+ 2
48	− 1	− 10	− 2	+ 8	+ 6	+ 6
49	+ 9	− 3	+ 8	+ 8	+ 12	0
50	+ 5	− 8	− 8	+ 8	− 4	+ 12
51	+ 3	− 5	+ 4	+ 10	+ 10	+ 6
52	+ 15	− 19	+ 2	+ 22	+ 18	+ 10

TABLE III—*Continued*

No.	μ_α	μ_δ	Rotational	Radial	Stream	Transverse
53	−0″.014	+0″.006	−0″.008	+0″.016	−0″.006	−0″.016
54	− 2	− 14	+ 16	+ 8	+ 16	− 8
55	+ 13	− 10	− 2	+ 16	+ 10	+ 12
56	0	− 13	+ 14	− 12	+ 10	− 16
57	+ 19	− 7	+ 22	+ 10	+ 22	+ 10
58	− 2	− 23	+ 14	− 30	+ 12	− 30
59	+ 20	+ 13	+ 18	+ 30	+ 24	+ 26
60	+ 30	+ 12	+ 28	+ 36	+ 32	+ 32
61	+ 9	+ 1	+ 4	+ 12	+ 6	+ 10
62	+ 18	− 8	+ 16	+ 16	+ 22	+ 10
63	+ 9	− 14	+ 14	+ 4	+ 14	− 4
64	+ 21	− 24	+ 26	+ 16	+ 30	− 2
65	+ 10	− 8	+ 6	+ 10	+ 12	+ 4
66	+ 16	− 21	+ 20	+ 14	+ 24	− 2
67	+ 16	− 26	+ 26	+ 18	+ 30	− 4
68	− 6	− 10	+ 16	+ 2	+ 14	− 6
69	− 21	− 29	+ 50	+ 10	+ 48	− 16
70	− 7	− 3	+ 12	0	+ 10	− 6
71	− 17	− 20	+ 36	+ 18	+ 40	− 2
72	− 5	− 26	+ 26	+ 24	+ 36	+ 6
73	− 12	− 3	+ 16	0	+ 14	− 8
74	+ 31	− 12	+ 26	+ 26	+ 30	+ 20
75	+ 23	− 15	− 4	+ 30	+ 26	+ 14
76	+ 17	− 28	+ 28	+ 20	+ 34	0

mean annual motions for the comparison stars are 0″.0036 in α and 0″.0039 in δ; for the nebular points, 0″.0071 in α and 0″.0082 in δ.

The plate indicates motions analogous to those found for M 101, 33, 51, and 81. They may be interpreted either as a rotation combined with a radial motion outward, or as a motion along the streamers outward. In order to investigate this it is necessary to take into account the inclination of the plane of the nebula to the tangential plane of the celestial sphere. It was estimated that the intersection of the two planes is in position angle 130° and that the inclination is about 48°. A diagram was constructed in which the foreshortening of the nebula was corrected; the motions in this diagram were then resolved into (*a*) rotational and radial components; (*b*) components along and perpendicular to the arms of the spiral (stream and transverse components). The results for the individual points derived from the diagram are in the last four columns of Table III, where the positive sign is used for motions in the direction north, east, south, west, and outward.

a) The mean rotational component is $+0''.015\pm0''.001$; the mean radial component, $+0''.014\pm0''.001$. There seems, however, to be a considerable increase of the motions with distance from the center; we have:

$r=1'.4$	$\mu_{\text{rot.}}=+0''.011$	$\mu_{\text{rad.}}=+0''.013$	$n=23$
3.1	+0.015	+0.011	37
5.1	+0.015	+0.019	11
7.3	+0.023	+0.023	3
8.9	+0.028	+0.030	2

The rotational components would correspond to hypothetical periods of from 50,000 to 120,000 years.

b) The mean stream component is $+0''.019\pm0''.001$, with a transverse component $+0''.007\pm0''.001$. With increasing distances from the center we find:

$r=1'.4$	$\mu_{\text{stream.}}=+0''.015$	$\mu_{\text{trans.}}=+0''.009$	$n=23$
3.1	+0.019	+0.004	37
5.1	+0.021	+0.012	11
7.3	+0.028	−0.001	3
8.9	+0.040	+0.010	2

The evidence is then, as in the cases of M 33, 51, 81, and 101, more in favor of a motion along the streamers of the spiral, combined with some radial motion outward, than of a rotational motion.

I wish to express my thanks to Messrs. Ritchey, Pease, and Duncan, who secured the plates used, and to Mrs. Marsh, of the Computing Division, for making all the necessary duplicate computations.

MOUNT WILSON OBSERVATORY
May 1922

Contributions from the Mount Wilson Observatory, No. 243
Reprinted from the *Astrophysical Journal*, Vol. LVI, pp. 208–216, 1922

INVESTIGATIONS ON PROPER MOTION

EIGHTH PAPER: INTERNAL MOTION IN THE SPIRAL NEBULA M 94=N.G.C. 4736

By ADRIAAN VAN MAANEN

ABSTRACT

Spiral nebula M 94 (N.G.C. 4736).—This beautiful object has a large nucleus surrounded by many closely packed whorls. Comparison of two plates taken in 1912 and 1921 by Pease and Duncan, respectively, gives an annual *proper motion* of the nebula with respect to 14 comparison stars, of $\mu_{\alpha}=-0''.014$, $\mu_{\delta}=0''.000$. The motions of 32 nebular points with reference to the nebula are shown on the *photograph*, Plate IV. The *internal motion* seems to be a stream motion of $0''.021$ outward along the arms of the spiral, combined with an outward transverse motion of about $0''.009$. The motion is analogous to that found for M 33, 51, 81 and 101 and for N.G.C. 2403.

Parallaxes of spiral nebulae.—A discussion of the methods of derivation leads to the conclusion that the three most reliable are: (1) Jeans's filament method, (2) comparison of proper motions and radial velocities, and (3) comparison of internal proper motions and spectroscopic velocities. These methods point to *parallaxes* of from $0''.0001$ to $0''.0010$ and indicate that the distances and sizes of the nebulae are considerably less than those required by the island universe theory.

Curtis[1] describes this nebula as "a beautiful object. From the very bright, large nucleus spring many bright, closely packed whorls, forming a bright inner oval $2'\times1'.5$ in p. a. about 110°. These inner whorls show many stellar condensations, whose sharpness and proximity to the nucleus would seem to make this one of the most favorable examples known for the investigation of motion in spirals. Fainter, closely packed, rather uniform outer whorls bring the nebula to a size of $5'\times3'.5$."

Three plates of this field were available for measurement, taken in 1912, 1916, and 1921. The first plate, secured by Pease, February 20, 1912, with an exposure of $3^{h}45^{m}$ was compared with the one taken by Duncan on January 5, 1921, with an exposure of $2^{h}10^{m}$. Fifteen stars of photographic magnitude 15.5 to 17.7 were selected for comparison purposes. One of these stars, *b*, was omitted in the reductions, as it showed a considerable proper motion; this star is a double having a companion of about the eighteenth magnitude at a distance of $\pm5''$ in $p=\pm355°$.

---

[1] *Lick Observatory Publications*, **13**, 33, 1918.

Thirty-two points presumably belonging to the nebula had measurable images on the plates; 19 of these belong to the inner whorls, while 13 are at greater distances from the center. Table I gives

TABLE I

Co-ordinates and Measured Annual Displacements

No.	x	y	μ_α	μ_δ
a	−4′.0	+5′.7	+0″.008	+0″.004
b	−4.8	+2.6	+ 59	− 118
c	−0.8	+3.0	0	− 14
d	−1.1	+2.7	− 12	− 6
e	−6.5	−1.8	− 10	− 3
f	−5.6	−2.9	+ 4	+ 5
g	−2.9	−2.7	+ 5	+ 8
h	−0.6	−3.3	+ 3	− 12
i	+1.6	−5.5	+ 8	− 3
j	+3.5	−4.5	− 18	+ 5
k	+8.2	−1.0	+ 1	+ 4
l	+2.8	−1.2	+ 12	+ 6
m	+6.6	+2.7	+ 8	− 20
n	+4.9	+4.7	− 3	+ 3
o	+3.0	+3.2	− 7	+ 26
1	−0.7	+0.6	+ 26	+ 9
2	−0.6	+0.6	+ 12	+ 3
3	−0.6	+0.4	− 34	+ 24
4	−0.6	+0.2	− 28	+ 28
5	−1.6	+0.4	− 49	+ 31
6	−1.9	−0.9	− 53	+ 11
7	−1.3	−0.9	− 70	+ 17
8	−0.9	−1.3	− 24	+ 20
9	−0.6	−1.5	− 50	− 6
10	−0.6	−0.1	− 26	+ 14
11	−0.1	−0.4	− 44	− 12
12	−0.2	−0.6	− 32	+ 4
13	+0.1	−0.5	− 19	− 3
14	0.0	−0.6	− 35	+ 18
15	+0.4	−0.5	− 41	− 21
16	+0.4	−0.6	− 34	− 28
17	+0.5	−0.8	− 24	− 30
18	+0.9	−0.6	+ 12	− 7
19	+0.8	−0.6	− 12	+ 9
20	+2.3	−1.1	− 3	− 30
21	+2.2	−0.8	− 7	− 8
22	+2.0	−0.6	− 10	+ 4
23	+0.9	+0.2	+ 3	+ 1
24	+0.7	+0.3	+ 24	− 19
25	+0.5	+0.5	− 7	− 12
26	+0.3	+0.6	+ 39	− 6
27	−0.1	+0.7	− 11	− 1
28	+1.0	+1.4	− 16	− 3
29	+0.7	+1.4	+ 16	+ 18
30	+3.0	+1.8	− 6	− 32
31	+2.0	+1.1	+ 31	− 6
32	0′.0	−1′.6	−0″.057	+0″.010

the positions and the annual motions in right-ascension and declination of the objects measured. The results were obtained in the same way as for the spirals discussed in earlier papers.[1]

The measures were as a whole rather difficult; the exposures were too long to prevent the points in the inner whorls from showing large images imbedded in much nebulosity; on the other hand the exposures were too short to give strong enough images of the points in the outer whorls.

As in all other cases previously discussed, the motions thus found are relative to the comparison stars. In order to derive the internal motions the results must be freed from the total motion of the nebula. We have therefore followed the same process as for M 101, 33, 51, 81, and N.G.C. 2403.

All 32 points give for the mean motion of the nebula:

$$\mu_\alpha = -0''.015 \qquad \mu_\delta = 0''.000.$$

Dividing the points according to the four quadrants, we have:

Means for I and III,

$$\mu_\alpha = -0''.016^5 \qquad \mu_\delta = +0''.000^5.$$

Means for II and IV,

$$\mu_\alpha = -0''.014^5 \qquad \mu = +0''.001.$$

The four quadrants combined give:

$$\mu_\alpha = -0''.015^5 \qquad \mu_\delta = +0''.001.$$

Using only the 19 points of the inner whorls, we find:

Means for I and III

$$\mu_\alpha = -0''.009^5 \qquad \mu_\delta = -0''.001^5.$$

Means for II and IV

$$\mu_\alpha = -0''.013^5 \qquad \mu_\delta = 0''.000.$$

---

[1] *Mt. Wilson Contr.*, No. 118; *Astrophysical Journal*, **44**, 210, 1916; *Mt. Wilson Contr.*, No. 213; *Astrophysical Journal*, **54**, 237, 1921; *Mt. Wilson Contr.*, No. 214; *Astrophysical Journal*, **54**, 347, 1921; *Mt. Wilson Contr.*, No. 242; *Astrophysical Journal*, **56**, 200, 1922.

The four quadrants combined give:

$$\mu_\alpha = -0''.011^5 \qquad \mu_\delta = -0''.001.$$

Giving equal weights to each of the three methods, we derive as the final motion of the nebula as a whole:

$$\mu_\alpha = -0''.014 \qquad \mu_\delta = 0''.000.$$

If now we subtract these quantities from the values μ_α and μ_δ for the nebular points, we obtain results which represent the internal motions. These are given in the second and third columns of Table II and plotted in Plate IV. The plate also shows the motions of the 15 stars as given in Table I; the stars are surrounded by

TABLE II

ANNUAL INTERNAL MOTIONS

No.	μ_α	μ_δ	Rotational	Radial	Stream	Transverse
1	+0″.040	+0″.009	+0″.033	−0″.026	+0″.037	−0″.020
2	+ 26	+ 3	+ 23	− 15	+ 23	− 14
3	− 20	+ 24	+ 10	+ 29	+ 19	+ 24
4	− 14	+ 28	+ 22	+ 22	+ 26	+ 13
5	− 35	+ 31	+ 24	+ 39	+ 27	+ 37
6	− 39	+ 11	+ 24	+ 31	+ 30	+ 26
7	− 56	+ 17	+ 43	+ 38	+ 47	+ 33
8	− 10	+ 20	+ 20	− 10	+ 17	− 14
9	− 36	− 6	+ 30	+ 19	+ 31	+ 17
10	− 12	+ 14	+ 15	+ 9	+ 16	+ 7
11	− 30	− 12	+ 19	+ 25	+ 25	+ 18
12	− 18	+ 4	+ 17	+ 3	+ 17	0
13	− 5	− 3	+ 4	+ 3	+ 3	+ 4
14	− 21	+ 18	+ 21	− 17	+ 21	− 17
15	− 27	− 21	+ 33	+ 6	+ 31	+ 12
16	− 20	− 28	+ 32	+ 11	+ 30	+ 15
17	− 10	− 30	+ 24	+ 20	+ 23	+ 21
18	+ 26	− 7	− 10	+ 26	− 13	+ 25
19	+ 2	+ 9	− 9	− 3	− 9	− 1
20	+ 11	− 30	+ 21	+ 24	+ 24	+ 21
21	+ 7	− 8	+ 5	+ 10	+ 8	+ 8
22	+ 4	+ 4	− 5	+ 3	− 4	+ 5
23	+ 17	+ 1	+ 5	+ 17	+ 6	+ 17
24	+ 38	− 19	+ 34	+ 27	+ 33	+ 28
25	+ 7	− 12	+ 13	− 7	+ 14	− 3
26	+ 53	− 6	+ 53	+ 12	+ 54	0
27	+ 3	− 1	+ 3	− 3	+ 3	− 2
28	− 2	− 3	0	− 4	− 1	− 4
29	+ 30	+ 18	+ 19	+ 29	+ 27	+ 20
30	+ 8	− 32	+ 31	− 12	+ 29	− 16
31	+ 45	− 6	+ 28	+ 37	+ 32	+ 33
32	−0″.043	+0″.010	+0″.042	−0″.010	+0″.041	−0″.012

PLATE IV

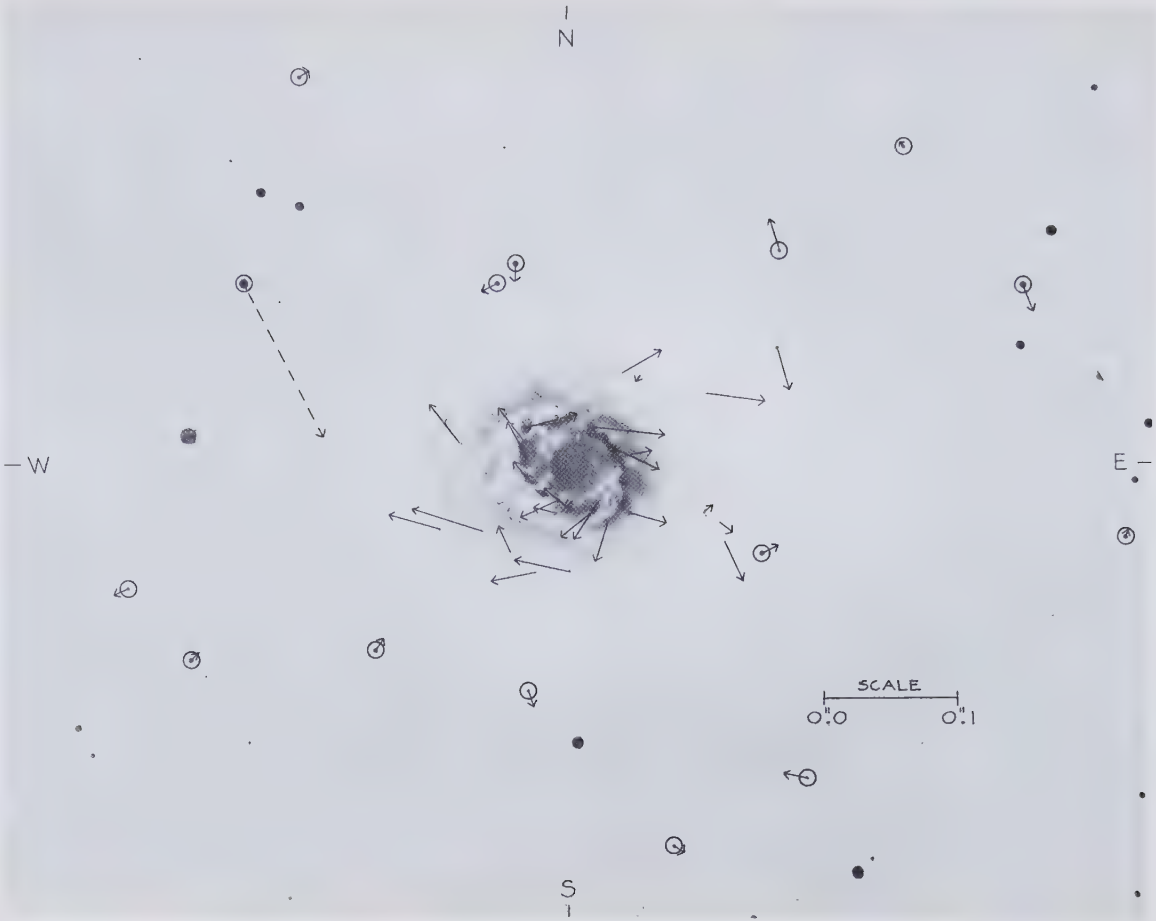

Internal Motions in N.G.C. 4736

The arrows indicate the directions and magnitudes of the annual motions. Their scale (0″.1) is indicated on the illustration. The scale of the nebula is 1 mm = 6″.7. The comparison stars are inclosed in circles.

circles; the motion of star *b*, which was excluded for comparison purposes on account of its considerable proper motion, is indicated by a broken line. The scale of the motions is indicated in the lower right-hand corner of the plate.

The internal motions were then resolved into: (*a*) rotational and radial components; (*b*) components along and at right angles to the spiral arms (stream and transverse components).

The results are given in the fourth, fifth, sixth, and seventh columns of Table II.

a) The mean rotational component is $+0\overset{''}{.}020 \pm 0\overset{''}{.}002$, the mean radial component, $+0\overset{''}{.}010 \pm 0\overset{''}{.}002$. For the points belonging to the inner whorls, with a mean distance from the center $r=0\overset{'}{.}7$, the values are

$$\mu_{\text{rot.}}=+0\overset{''}{.}018 \qquad \mu_{\text{rad.}}=+0\overset{''}{.}007.$$

For those in the outer whorls, ($r=2\overset{'}{.}0$) we have

$$\mu_{\text{rot.}}=+0\overset{''}{.}022 \qquad \mu_{\text{rad.}}=+0\overset{''}{.}015.$$

b) The mean stream component is $+0\overset{''}{.}021 \pm 0\overset{''}{.}002$, the mean transverse component, $+0\overset{''}{.}009 \pm 0\overset{''}{.}002$; the results for the inner and the outer whorl separately are:

Inner whorls $\mu_{\text{stream}}=+0\overset{''}{.}019$ $\mu_{\text{trans.}}=+0\overset{''}{.}007$.
Outer whorls $\mu_{\text{stream}}=+0\overset{''}{.}024$ $\mu_{\text{trans.}}=+0\overset{''}{.}012$.

Although in N.G.C. 4736 the whorls are so closely packed and so nearly circular that the difference between rotation and stream-motion is necessarily small, yet the latter seems to interpret the motions a little more satisfactorily than the former. Analogous results were found for the other spirals, except that the resemblance to stream-motion is considerably stronger in all cases. From the material now available it seems therefore necessary to give up the idea that the motions found represent a rotation. In my first paper on the internal motions in spirals[1] I computed from the rotatory components the possible masses for the spirals; this example has later been followed by Lundmark,[2] McLaughlin,[3] and others. Since now, however, it seems necessary to abandon the conception that we are dealing with rotation, we must at least for the present abstain from deriving conclusions as to the masses of the central bodies.

---

[1] *Mt. Wilson Contr.*, No. 118, 1916; *Astrophysical Journal*, **44**, 210, 1916.

[2] *Publications Society of the Pacific*, **34**, 113, 1922.

[3] *Popular Astronomy*, **30**, 294, 1922.

The problem of the distances of the spiral nebulae has been discussed by several astronomers during the last few years, principally by Curtis and Lundmark. In his exhaustive study, "The relations of the Globular Clusters and Spiral Nebulae to the Stellar System,"[1] Lundmark approaches the subject in not less than nine different ways. Some of these are based on the supposition that the spirals are comparable in size to the Milky Way system or to the Magellanic Clouds and thus start from assumptions which we are just trying to examine by deriving their distances. As examples we may quote Wolf's comparison of the caves in the Milky Way and in spiral nebulae and the hypothesis that the Magellanic Clouds are spiral nebulae. It is true that the large Magellanic Cloud resembles in appearance the nebula N.G.C. 4449, but then N.G.C. 4449 is far from a typical spiral. Curtis, for instance, describes this object as: "A very bright and interesting object, filling a space about $3'.5 \times 2'$. It is of exceedingly irregular structure, with many almost stellar condensations, and a bright nearly stellar nucleus. Of spiral type, as to nebulosity, but with very little evidence of spiral form."

Another derivation of the distances of spiral nebulae has been based on the appearance of novae in them. Assuming the absolute magnitudes of these novae to be the same as those in the Milky Way, a parallax can be derived. The assumption, however, that the novae in the Milky Way and those in the spirals have the same absolute magnitude is open to question. Of the 30 novae, more or less, which have been found in spirals, all but two (in N.G.C. 4321) appear in spirals showing a large amount of nebulosity. Attention has not before been called to this fact; why, for instance, has no nova ever been found in M 33, which resembles very much more Easton's structure of the Milky Way than does the Andromeda nebula? It is true that there exist a greater number of photographs of the Andromeda nebula; but of M 33 the Mount Wilson

---

[1] Dissertation, 1920. The work has been extended in several recent articles in the *Publications of the Astronomical Society of the Pacific.*

Observatory has available more than two dozen plates, all of which have been examined, principally by Messrs. Duncan and Humason, yet not a single nova has been found, while in the Andromeda nebula one in every two or three plates shows the image of a nova.

Of the other ways of determining the parallaxes of the spiral nebulae, the following may be mentioned.

a) The direct determinations seem to be unsatisfactory; the parallaxes derived by Barnard for the Andromeda nebula and by van Maanen for three spirals indicate that their parallaxes are smaller than the probable errors. This point might have been omitted if Bohlin[1] had not recently called attention to the large parallax derived by him for the Andromeda nebula, for which Barnard found $\pi = 0''.000$ and van Maanen $+0''.004$. Bohlin's measures are based on plates with the 6-inch Steinheil objective of the Stockholm Observatory, and it is well known from the researches of Kapteyn and others, that on plates taken with the smaller instruments, systematic errors of considerable size appear, especially if the hour-angles are large.

b) Star counts by Lundmark in the region of the Andromeda nebula show an increase of stars near the center; in M 33 there is no indication of an increase or a decrease in the number of stars as we approach the center of the plate. Lundmark concludes that these two spirals do not seem to absorb the light of stars as faint as magnitudes 16.5 and 15.7, respectively, and derives as a minimum parallax $0''.000360$ and $0''.000498$, respectively.

c) An ingenious method of determining the parallaxes of spiral nebulae was proposed by Jeans.[2] It is based on the conditions necessary for the breaking up of the line elements of the filaments thrown off by the nucleus. For M 101 Jeans thus derives a parallax of $0''.001$. Although no great stress should be laid on this figure, it gives an indication of the order of magnitude of the distances.

d) Curtis has derived the proper motions of many of the spirals for which plates had been taken at the Lick Observatory. In his later papers, he does not use these motions, on the supposition that they are not real motions but due to the accidental errors of the measures. Lately, however, Lundmark has derived the motions of several spiral nebulae from the positions given in several catalogues. Comparing his motions with those of Curtis, I find, after the necessary corrections for a systematic difference, that they agree in sign in 62 per cent of the cases. As, moreover, the twelve values derived by van Maanen show an agreement in sign with Curtis' values in not less than 75 per cent of the cases, we must come to the conclusion that Curtis' results are not altogether due to the influence of accidental errors. Another point shows this too; from the radial velocities we find a relation between the size of the spirals and their motion, the smaller spirals having the larger motions. The results are given in the second column of Table III, while the third column gives the number of objects included. As we find an analogous relation for the proper motions, which are given in the fourth column, we must conclude that these are at least partly real.

---

[1] *Jubiläums Nummer, Astronomische Nachrichten*, 1921.

[2] *Problems of Cosmogeny and Stellar Dynamics*, p. 217 (1919).

TABLE III

Diameter	V	n	$\bar{\mu}$	n^1
	km/sec.			
>10′	339	5	0″.031	6
5′–10′	474	9	0.032	10
<5′	826	10	0.041	13

If then we use Curtis' mean motion of 0″.033 for the 66 largest spirals, and compare this value with the mean radial velocity, we derive a mean parallax of 0″.0003. Dr. Lundmark, who has recently computed the apices and mean parallaxes derived from Curtis' and his own proper motions, kindly allows me to mention his result in advance of publication. Using 800 km/sec. for Campbell's K-term in the solution he finds:

Mean parallax from 67 motions derived by Curtis, 0″.00010
Mean parallax from 82 motions derived by Lundmark, 0″.00011

The value of K is as yet very uncertain; smaller values of K will give larger parallaxes, and vice versa.

e) Finally we may compare the internal motions found by van Maanen with those derived by spectroscopic means; these amount to a few hundred kilometers per second; the comparison yields parallaxes of a few ten-thousandths of a second of arc, giving for the diameters of the spirals quantities from 10 to 300 light years.

Of the methods mentioned above, those under *c*, *d*, and *e* probably deserve the most credit. This material does not seem to warrant the acceptance of the island-universe theory. It is of course possible that later results may contradict this statement; but it seems well to point out that the evidence based on the best material at present available does not indicate that the spiral nebulae are comparable with our Milky Way system.

Mount Wilson Observatory
June 9, 1922

Contributions from the Mount Wilson Observatory, No. 244
Reprinted from the *Astrophysical Journal*, Vol. LVI, pp. 242–264, 1922

A SPECTROSCOPIC METHOD OF DETERMINING THE ABSOLUTE MAGNITUDES OF A-TYPE STARS AND THE PARALLAXES OF 544 STARS

By WALTER S. ADAMS and ALFRED H. JOY

ABSTRACT

Spectroscopic method of determining the absolute magnitudes of A-type stars.—In order to ascertain whether a spectroscopic method could be applied to these stars, spectrograms were obtained of nearly all the A-type stars in the Taurus and Ursa Major groups, fifty-six in all, whose absolute magnitudes are accurately known. The stars were then grouped (*a*) according to spectral type and (*b*) according to whether the lines were diffuse or sharp. A good correlation between magnitude and spectrum was found, the magnitude being brighter the earlier the spectral type and also brighter for spectra with sharp lines. The study was then extended to include all A-type stars for which both the spectral type and parallax were known, and the same correlation was found (see Fig. 1), the average difference being only $\pm 0''.0077$ for eighty-two parallaxes determined by group motion, and $\pm 0''.0131$ for 104 trigonometric parallaxes. The accuracy of parallax determinations by this method for A-type stars is thus of the same order as for stars of later types, and the method is evidently capable of considerable further refinement. A-type stars having "c" characteristics, such as α Cygni, require separate treatment, which may perhaps be based on the intensities of the well-known enhanced lines λ 4481 and λ 4233.

Spectroscopic parallaxes of 544 stars of type B7 to F2, determined on the basis of the foregoing results, are given in Table VI. When grouped according to their proper motions, the mean parallax of each group is found to increase from $0''.011$ for $\mu < 0''.010$ to $0''.037$ for μ about $0''.2$ (Fig. 2). This correlation is a very satisfactory confirmation of the accuracy of the method.

The spectroscopic methods used in the determination of the absolute magnitudes of stars of the later spectral types cannot in general be applied to those of the A-type of spectrum. With some notable exceptions, such as α Cygni and stars of similar spectra and those in which certain lines like $\lambda\lambda$ 4077, 4216, and 4481 are especially strong, the stars of this type do not show the large variations in the intensities of the lines which appear in the later types. They do, however, show very great differences in the appearance of the lines, in some stars such as Sirius the lines being sharp and well defined, and in others such as Altair very diffuse and vague. The importance of this characteristic will appear in the course of the discussion.

With a view to studying the nature of the spectra of stars of this type with known absolute magnitudes, spectrograms were obtained of nearly all the stars of type A which belong to the Taurus and the Ursa Major groups. The absolute magnitudes of these stars are known with a high degree of accuracy from the motions of the groups, and for many of the stars of the latter group trigonometric parallaxes are also available. A considerable range in absolute magnitude as well as in spectral type is found among these stars, and they afford, accordingly, excellent material for such an investigation.

The first step in the study of these spectra, and as it proved the most important one, was an accurate classification of spectral type. Since the H and K lines of calcium, which form an important criterion in the classification of A stars by Miss Cannon and the other Harvard observers, are far to one side of the region of best definition on our spectrograms and do not appear at all on those taken with high dispersion, we have based our classification upon the intensities of the metallic arc lines showing in the stellar spectra. In this we were aided greatly by the use of the spectra of standard stars chosen from among those classified by Dr. Kohlschütter at this Observatory in the years 1912 to 1914. Spectra in which the helium lines do not appear and such prominent arc lines as λλ 4326 and 4384 are not present or are extremely faint are called A0. With increasing intensity of the arc lines the stars are classified as A1, A2, A3, etc. When the helium lines λλ 4026 and 4471 are just visible, the spectrum is classed as B9, and when λ 4471 and λ 4481 are equal, as B8. This system appears to be in good agreement with that of the Harvard observers and of Kohlschütter, a result which would naturally follow from the use of the standard types of the latter to check the results. A comparison of the spectral types as determined by Miss Cannon and by Kohlschütter has already been published by the Harvard College Observatory.[1]

In addition to the symbols indicating the spectral type, the letters "n" for nebulous and "s" for sharp have been appended to indicate the character of the spectral lines. Thus the spectrum of Sirius is A2s and that of Altair A2n. Stars like α Cygni have the "c" characteristics noted by the Harvard observers and are indicated by cA2s, for example. The lines are always exceptionally sharp and the letter "s" is scarcely necessary. These stars are few in number and do not enter into the present discussion, but a brief reference is made to them at a later point.

---

[1] *Annals of the Harvard College Observatory*, **56**.

If we separate the stars of the Taurus and Ursa Major groups into the successive spectral subdivisions obtained in this way, we find the results given in Table I. The absolute magnitudes are

TABLE I

Boss	*M*
A0n	
3117	+0.6
3190	1.7
3752	0.4
3961	0.3
4009	0.6
5573	1.7
A1n	
1024	+1.2
1034	1.8
1220	0.5
3480	2.1
A2n	
1033	+1.6
1143	2.2
2972	2.2
A3n	
1026	+1.3
1047	2.3
1051	2.8
1087	1.6
1194	1.6
A4n	
1027	+2.8
1067	1.9
1090	1.6
3382	2.7
A5n	
919	+3.0
1086	2.8
A6n	
1025	+3.2
1056	2.8
A7n	
892	+3.2
991	2.5
1022	2.1
1058	3.2
3360	2.8
A8n	
1004	+2.8
1007	2.4
1043	3.2
F0n	
935	+3.6
1040	2.9
A2s	
1732	+1.3
3363	−0.2
3474	+0.6
A3s	
1029	+1.3
2930	0.8
A4s	
553	+2.3
1046	0.7
3506	0.6
A6s	
1054	+2.1
A7s	
1092	+2.3
1122	1.9
3475	2.3
A8s	
1114	+2.6
1226	2.7
2813	3.3
5425	1.9
F1s	
961	+3.2
1013	3.0
1055	2.7
F2s	
1018	+2.8

those given by Rasmuson in his valuable memoir on moving clusters,[1] but a constant correction of +1.57 magnitudes has been applied to reduce to the unit of 10 parsecs instead of that of one siriometer as used by him. Six of the stars of the Ursa Major group are of type A0n and thus supplement in an important way those of the Taurus group which are of a more advanced type on the average.

---

[1] *Meddelanden från Lunds Astronomiska Observatorium*, Serie II, No. 26.

If these results are collected, we obtain the following mean absolute magnitudes for the various spectral subdivisions.

TABLE II

	M	No.		*M*	No.
A0n	+0.9	6	A2s	+0.6	3
A1n	1.4	4	A3s	1.0	2
A2n	2.0	3	A4s	1.2	3
A3n	1.9	5	A6s	2.1	1
A4n	2.2	4	A7s	2.2	3
A5n	2.9	2	A8s	2.7	4
A6n	3.0	2	F1s	3.0	3
A7n	2.8	5	F2s	2.8	1
A8n	2.8	3			
F0n	3.2	2			

Two conclusions may be drawn from an inspection of these results.

1. A definite progression is shown between absolute magnitude and spectral type, the stars of the more advanced types being the fainter. The change of absolute magnitude with type is most rapid among the earlier A stars and becomes comparatively slight in the later types.

2. The average absolute magnitude of the stars with sharp lines is in the case of the earlier A stars considerably brighter than that of the stars of the same types with diffuse lines. This difference becomes small for the later types.

The first of these results is in agreement with that found for the stars of the Taurus group in the case of the larger spectral divisions by Hertzsprung[1] and Kohlschütter,[2] who showed that for the successive spectral types A, F, G, and K the apparent magnitudes, and hence the absolute magnitudes for stars at the same distance, become progressively fainter. Without a more accurate knowledge of spectral type, however, it has not been possible hitherto to establish such a relationship for the subdivisions within the A type.

The second conclusion, that stars with sharp lines are brighter than stars of the same type with diffuse lines, is in accord with our knowledge of stars of the later types of spectrum. Thus the high luminosity of the Cepheid variables, the stars with the "c" characteristics of spectrum, and such objects as α Orionis and α Scorpii, is always found associated with narrow well-defined spectral lines. It is well known that the absorption spectrum of *o* Ceti changes from one with sharp lines at maximum of light to one with vague and diffuse lines near minimum. It seems altogether probable, as the measurement of stellar diameters has shown in a few cases, that the giant stars are large expanded bodies of gas of low density, a condition which favors the production of narrow lines, while the dwarf stars are smaller, more condensed bodies with atmospheres which show a much more rapid density gradient and so produce diffuse lines.

---

[1] *Astronomische Nachrichten*, **209**, 119, 1919.

[2] *Ibid.*, **211**, 297, 1920.

The results for the Taurus and Ursa Major groups proved to be of such interest that it seemed desirable to extend the investigation to include all the A-type stars for which reliable absolute magnitudes are available and for which photographs of spectra have been secured at Mount Wilson. The material used consists of 82 stars with absolute magnitudes derived from group motion and 104 stars with trigonometric parallaxes. Some of these are common to both lists so that the number of separate stars involved is 148. The absolute magnitudes of these stars have been taken from the lists of Rasmuson for the Taurus, Ursa Major, Perseus, Praesepe, and α Lyrae groups, and a few of his results have been included for other stars for which group motion seems to be clearly established. The trigonometric parallaxes are mainly from the Allegheny, McCormick, Mount Wilson, Sproul, Yale, and Yerkes observatories. These stars are all given in the general catalogue, Table VI of this article, with the corresponding trigonometric or group parallax, and so are not listed separately here. When an absolute magnitude has been derived both from group motion and from trigonometric parallax the arithmetical mean has been used.

All of these stars were classified independently by Adams and Joy, and in Table III are given the results for the two observers, collected according to spectral type and mean absolute magnitude.

TABLE III

	Adams		Joy			Adams		Joy	
	No.	*M*	No.	*M*		No.	*M*	No.	*M*
B9n	12	+0.6	5	+0.5	B9s	3	−0.1	4	0.0
A0n	16	0.9	28	1.0	A1s	4	+0.6	4	+0.6
A1n	15	1.3	5	0.7	A2s	10	0.9	9	0.7
A2n	12	2.0	11	1.9	A3s	8	1.4	4	1.6
A3n	11	1.9	3	1.6	A4s	2	1.7	4	2.1
A4n	13	2.1	7	2.2	A5s	4	2.0	3	1.4
A5n	7	2.3	14	2.3	A6s	4	2.0	3	0.5
A6n	6	2.6	10	2.3	A7s	2	2.9	2	2.3
A7n	3	3.0	4	2.2	A8s	4	2.3	3	2.8
A8n	2	2.8	9	2.6	A9s	1	3.8	1	3.0
A9n	3	2.7	1	3.6	F0s	......	....	6	2.5
F0n	......	....	2	2.9	F1s	4	2.0	1	3.0
F2n	1	3.6	......	....	F2s	2	3.4	2	2.4
F3n	......	....	2	3.0					

These results, although showing considerable variation in the number of stars of each subdivision as classified by the two observers, are in good agreement as regards the mean absolute magnitude for groups containing a fair number of stars. Most of the differences in classification represent variations of one or two subdivisions, as, for example, at A0n where several stars classified by Joy as of this type are called B9n by Adams.

TABLE IV

	Adams		Joy			Adams		Joy	
	No.	*M*	No.	*M*		No.	*M*	No.	*M*
B9n	12	+0.58	5	+0.5	B9s	3	−0.1	4	+0.1
A0n	16	0.87	33	0.92	A1s	4	+0.6	4	0.5
A1n	15	1.34	......	....	A2.5s	18	1.15	13	0.99
A2.5n	23	1.96	14	1.85	A4.5s	6	1.9	7	1.8
A4.5n	20	2.14	21	2.29	A7s	10	2.29	8	1.8
A6.5n	9	2.7	14	2.29	F1s	......	....	10	2.71
A8n	......	....	10	2.68	F2s	7	2.7	......	....
A9n	6	2.9	......	....					
F1n	......	....	4	2.9					

In order to facilitate the plotting of these quantities and partially to equalize the weights, the values have been further combined to form the mean results given in Table IV.

The curves plotted from these results are shown in Figure 1, and from these curves the values corresponding to each spectral subdivision have been determined as shown in Table V. Under O−C is given the difference between the values of the absolute magnitudes of Table III and those obtained from these curves. In other words, it shows to what extent the mean observed absolute magnitudes may be represented by a relationship based simply upon spectral type and the character of the spectral lines.

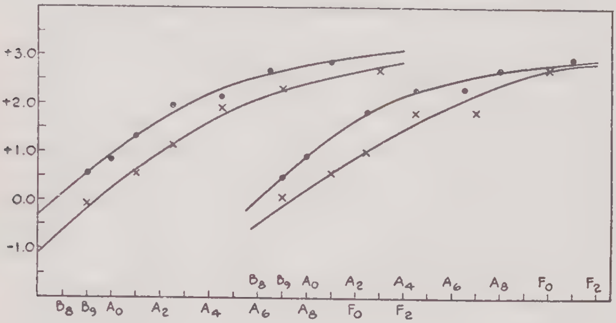

FIG. 1.—Curves showing the relationship between average absolute magnitude and spectral type for stars with parallaxes determined trigonometrically or from group motion. The points indicate groups of stars with diffuse (*n*) lines, the crosses sharp (*s*) lines. The curves on the left are for Adams, those on the right for Joy.

TABLE V

	ADAMS			JOY				ADAMS			JOY		
	M	O−C	No.	*M*	O−C	No.		*M*	O−C	No.	*M*	O−C	No.
B8n....	+0.2	......	.....	0.0	......	.....	B8s....	−0.7	......	.....	−0.5	......	.....
B9n....	0.6	0.0	12	+0.5	0.0	5	B9s....	−0.2	+0.1	3	−0.2	+0.2	4
A0n....	0.9	0.0	16	0.9	+0.1	28	A0s....	+0.2	......	.....	+0.2	......	.....
A1n....	1.3	0.0	15	1.3	−0.6	5	A1s....	0.6	0.0	4	0.5	+0.1	4
A2n....	1.7	+0.4	12	1.7	+0.2	11	A2s....	1.0	−0.1	10	0.8	−0.1	9
A3n....	2.0	−0.1	11	1.9	−0.3	3	A3s....	1.3	+0.1	8	1.2	+0.4	4
A4n....	2.2	−0.1	13	2.2	0.0	7	A4s....	1.7	0.0	2	1.5	+0.6	4
A5n....	2.3	0.0	7	2.3	0.0	14	A5s....	1.9	+0.1	4	1.7	−0.3	3
A6n....	2.5	+0.1	6	2.4	−0.1	10	A6s....	2.2	−0.2	4	2.0	−1.5	3
A7n....	2.7	+0.3	3	2.6	−0.4	4	A7s....	2.3	+0.6	2	2.2	+0.1	2
A8n....	2.8	0.0	2	2.7	−0.1	9	A8s....	2.4	−0.1	4	2.4	+0.4	3
A9n....	2.8	−0.1	3	2.7	+0.9	1	A9s....	2.5	+1.3	1	2.6	+0.4	1
F0n....	2.9	......	.....	2.8	+0.1	2	F0s....	2.6	......	.....	2.7	−0.2	6
F1n....	3.0	......	.....	2.8	......	.....	F1s....	2.7	−0.7	4	2.8	+0.2	1
F2n....	3.1	+0.5	1	2.9	+0.1	2	F2s....	2.8	+0.6	2	2.8	−0.4	2

This comparison shows clearly that the relationship between absolute magnitude and spectral type may be used to determine the mean absolute magnitudes of these groups of stars with a very satisfactory degree of accuracy. Since a large amount of the material consists of absolute magnitudes derived from the trigonometric parallaxes of stars which do not belong to recognized clusters, we may draw the important conclusion that this same relationship may be applied to A-type stars in general, as well as to such groups as those of Taurus and Ursa Major.

The vital question as to the application of this method to the case of individual stars is the next to be considered. If it can be so applied, it involves the conclusion that there is no dispersion in absolute magnitude among A-type stars which have very closely the same spectral type and the same spectral characteristics. This conclusion is perhaps not so radical as it appears at first, since the definition of spectral type and line-characteristics, if carried to extreme limits, might well serve to define the absolute magnitude of a star uniquely. Among stars of the M type, for example, the absolute magnitudes are determined by the relative intensities of certain pairs of lines. If these lines were used to define the spectral type, the latter could be used equally well to determine the absolute magnitude. With a few striking exceptions, such as the A-type companion of o^2 Eridani and some other stars to which reference will be made later, the A-type stars in general appear to be giant stars with no very wide dispersion in absolute magnitude. Within these limits, accordingly, it is quite conceivable that an accurate determination of the spectral characteristics might define the absolute magnitude.

The investigation of this question has been made in three ways:

1. Direct comparison with individual group parallaxes.
2. Direct comparison with individual trigonometric parallaxes.
3. Comparison of the average parallaxes and the average proper motion of 544 stars.

Since the results for the individual stars are all given in the catalogue appearing as Table VI, it seems unnecessary to repeat them here. The absolute magnitudes have all been determined by two independent observers and the parallaxes have then been combined. To illustrate: the spectral type of Boss 3474 (ζ^1 Ursae Majoris) as determined by Adams is A2s and by Joy A3s. Referring to Table V we find for these types the values +1.0 and +1.2 for the absolute magnitude. Combining with the apparent magnitude 2.4, we derive the parallaxes 0.″052 and 0.″057, or 0.″054 in the mean. Summarizing the results obtained in this way for 82 stars in Table VI with parallaxes derived from group motion, and 104 stars with trigonometric parallaxes, we secure the following comparison:

Group parallaxes: 82 stars; systematic difference, −0.″0014;
Average difference, ±0.″0077.

Trigonometric parallaxes: 104 stars; systematic difference, 0.″0000;
Average difference, ±0.″0131.

These results compare very favorably with those obtained in the case of the later-type stars where the average difference between spectroscopic and trigonometric parallaxes is ±0.″015.

The agreement with the group parallaxes could, of course, be improved by a very slight readjustment of our reduction curves, but it has seemed preferable not to assign too great weight to these stars, both on account of the uncertainty still outstanding in the parallax of the Taurus group and because they represent a special selection of stars, while the trigonometric parallaxes are more representative of stars in general.

It is of interest to call attention to the results for the three most prominent stars in the list, Sirius (Boss 1732), Vega (Boss 4722), and Altair (Boss 5062). All three have well-determined trigonometric parallaxes, and in addition Sirius and Vega belong to recognized stellar groups and their parallaxes have been derived from group motion. The spectral types of these stars have been determined as A2s, A1s, and A2n, which give absolute magnitudes of +0.9, +0.55, and +1.7, and parallaxes of 0.″316, 0.″123, and 0.″145, respectively. The trigonometric parallaxes are 0.″374, 0.″110, and 0.″205, which correspond to absolute magnitudes of +1.3, +0.3, and +2.5. The group motion gives a parallax of 0.″380 for Sirius and 0.″104 for Vega. The correction of +0.4 to the spectroscopic absolute magnitude of Sirius required to bring it into agreement with observation is not excessive, and a change of type from A2s to A3s would account for nearly the entire difference. In the case of Altair, the correction of +0.8 magnitude is larger than would be expected, but it may find its explanation in the well-known fact that the spectral lines in this star are extraordinarily diffuse. In such cases the absolute magnitude may prove to be fainter than that of stars with the usual "n" characteristics, and further refinement of the method may show that these stars require separate treatment.

This method of determining parallaxes has been applied to the 544 stars listed in Table VI. In order to condense the results the separate determinations of the absolute magnitudes and parallaxes by the two observers have been combined. As a result, this makes a slight apparent discrepancy in a few cases between the absolute magnitude and the corresponding parallax. Since all of the stars in Table VI are designated by their numbers in Boss's Catalogue, it has not seemed necessary to add their positions. The successive columns of Table VI, therefore, give the Boss number, the apparent visual magnitude on the Harvard system,[1] the proper motion according to Boss, the spectral types by Adams and Joy, respectively, the mean of the absolute magnitudes, and the mean of the corresponding parallaxes. The parallaxes as derived from group motion, the trigonometric parallaxes, and the sources for both are added in the last three columns. The following letters are used to indicate the principal authorities for the trigonometric parallaxes: A, Allegheny; F, Flint; M, McCormick; S, Sproul; W, Mount Wilson; Y, Yale; Ye, Yerkes.

The third test of the applicability of the method to A-type stars consists in a comparison between the average of the proper motions and the average of the parallaxes of the stars in Table VI. With the large number of stars available, this comparison should prove especially valuable. The stars have been divided into groups according to their proper motions, with the limits indicated. The

---

[1] In the case of visual binaries the values of m refer to the brighter component. In the case of spectroscopic binaries, however, owing to the uncertainty in the relative brightness of the components it has seemed to us preferable for the present to leave the magnitudes without correction.

TABLE VI

Boss	m	μ	Spectrum A.	Spectrum J.	M	Spect. π	Group π	Trig. π	Auth.
10	2.2	0″.213	A1n	A0n	1.1	0″.060	....	....	
43	4.4	0.052	A1n	A2n	1.5	0.026	....	....	
50	4.5	0.081	A0n	A1n	1.1	0.021	....	0″.017	A
52	6.0	0.028	B9s	B8n	−0.1	0.006	....	....	
66	6.6	0.015	B7n	B9n	0.2	0.005	....	....	
68	5.4	0.016	B9n	A0n	0.8	0.012	....	....	
91	5.2	0.039	A1n	A3n	1.5	0.020	....	....	
154	5.5	0.027	A2s	A3s	1.1	0.014	....	....	
159	5.4	0.022	B9s	A0n	0.4	0.010	....	....	
166	6.8	0.006	A2n	A1s	1.1	0.008	....	....	
169	5.4	0.014	B9s	A0s	0.0	0.008	....	....	
198	5.9	0.006	A3n	A1n	1.6	0.011	....	....	
223	5.9	0.024	A4s	A7s	2.0	0.016	....	....	
224	5.5	0.039	B9s	A0s	0.0	0.008	....	....	
247	5.7	0.018	B9n	B9n	0.6	0.010	....	....	
252	5.7	0.326	A8n	A8n	2.8	0.026	....	....	
257	4.5	0.010	B8s	B8s	−0.6	0.010	....	0.010	Ye
263	5.5	0.038	B9s	B9s	−0.2	0.007	0″.010	....	Perseus
284	5.8	0.028	A2sp	B9s	0.4	0.008	....	....	
289	6.7	0.008	A0n	A0n	0.9	0.007	....	....	
295	5.3	0.056	A1n	A2n	1.5	0.018	....	....	
314	2.8	0.306	A3n	A3n	2.0	0.068	....	....	
340	5.8	0.025	B9n	A0n	0.8	0.010	....	0.017	W
347	6.2	0.011	B9n	A0n	0.8	0.008	....	....	
379	5.4	0.053	B9s	B9s	−0.2	0.008	0.013	....	Perseus
425	5.0	0.010	B8s	B8s	−0.6	0.008	....	....	
446	4.7	0.061	A4s	A5n	2.0	0.029	....	0.020	S, Ye
449	4.1	0.045	A1n	A0n	1.1	0.025	....	....	
463 Ft.	5.2	0.042	A3n	A2n	1.8	0.022	....	....	
466	5.4	0.023	A2n	A1n	1.5	0.016	....	....	
469	5.4	0.072	B9n	A0n	0.8	0.012	....	0.009	A, F, S, Y
490	6.7	0.035	A0n	A1n	1.1	0.008	....	....	
508	5.3	0.035	A0n	A0n	0.9	0.013	....	....	
521	5.7	0.015	A0n	A0n	0.9	0.011	....	....	
522	5.1	0.058	A1n	B9n	0.9	0.014	....	....	
526	5.3	0.012	A3s	A1s	0.9	0.014	....	....	
536	5.9	0.128	A9s	F0s	2.6	0.023	....	....	
550	4.8	0.015	A3s	A4s	1.4	0.021	....	....	
551	4.9	0.027	B9n	B9n	0.6	0.014	....	....	
553	5.8	0.076	A4s	A3sp	1.4	0.014	0.020	....	Urs. Maj.
616	6.3	0.040	A2s	A3s	1.1	0.010	....	....	
622	3.7	0.210	A0n	A0n	0.9	0.027	....	0.049	A, M, Y, Ye
644	4.3	0.213	A4n	A5n	2.2	0.039	....	0.022	A
666	5.3	0.054	A0n	A1n	1.1	0.014	....	....	
674N	5.3	0.017	A3s	A2s	1.0	0.014	....	0.018	S
674S	5.6	0.017	A3s	A2s	1.0	0.012	....	....	
682	5.5	0.017	B9n	B9n	0.6	0.010	....	....	
686	5.9	0.014	A5s	A4s	1.7	0.014	....	....	
696	4.2	0.150	A0n	A3n	1.4	0.028	....	....	
699	5.8	0.006	A1s	A0s	0.4	0.008	....	....	
715	5.6	0.038	B9n	B9n	0.6	0.010	0.009	....	Perseus
719	5.6	0.019	B9n	A0n	0.8	0.010	....	....	
721	5.5	0.083	A3n	A6n	2.2	0.022	....	....	
727	6.8	0.018	A0n	A0n	0.9	0.007	....	....	
731	5.5	0.039	A2s	A2s	0.9	0.012	....	....	
757	5.0	0.058	A1n	A0n	1.1	0.016	....	....	
777	5.9	0.011	A1s	A0s	0.4	0.008	....	....	
791	5.0	0.033	A0n	A0n	0.9	0.015	....	....	
800	5.6	0.017	A1n	A2n	1.5	0.016	....	....	
801	5.1	0.021	B8n	B9n	0.4	0.011	....	....	
802	5.5	0.040	B8n	B9n	0.0	0.008	0.009	....	Perseus
833	5.6	0.032	B9n	A0n	0.8	0.010	0.008	....	Perseus
845	5.6	0.055	A4s	A5s	1.7	0.017	(0.013)	....	Perseus
849	5.7	0.020	A4s	A5n	2.0	0.018	....	....	
878	5.1	0.042	A1n	A1n	1.3	0.017	....	....	
892	6.0	0.147	A7n	A7n	2.6	0.022	0.028	....	Taurus
896	4.9	0.005	B9n	B9n	0.6	0.014	....	....	
898	5.3	0.039	B8n	B9n	0.4	0.010	0.009	....	Perseus
901 Ft.	6.3	0.034	A0n	A0n	0.9	0.008	....	0.005	M
919	5.8	0.141	A5n	A5n	2.3	0.020	0.028	....	Taurus

TABLE VI—*Continued*

BOSS	*m*	*μ*	SPECTRUM		*M*	SPECT. π	GROUP π	TRIG. π	AUTH.
			A.	J.					
935	5.5	0″.159	F2n	A9n	2.9	0″.030	0″.034	....	Taurus
961	5.7	0.143	F1s	F1s	2.8	0.026	0.032	....	Taurus
974	5.1	0.004	A1n	A0n	1.1	0.015	....	....	
989	4.8	0.066	A5s	A5s	1.8	0.025	....	....	
991	5.6	0.112	A8n	A6n	2.6	0.025	0.024	....	Taurus
997	5.4	0.064	A1s	A0s	0.4	0.010	....	....	
1004	5.6	0.121	A6n	F0n	2.6	0.026	0.028	....	Taurus
1007	5.3	0.116	A9n	A8n	2.8	0.031	0.027	....	Taurus
1012	5.3	0.043	A1n	A0n	1.1	0.014	....	....	
1013	5.8	0.118	F1s	F1s	2.8	0.024	0.028	....	Taurus
1018	5.7	0.114	F1s	F3s	2.8	0.026	0.027	....	Taurus
1022	4.8	0.124	A6n	A8s	2.4	0.034	0.029	....	Taurus
1023	5.8	0.029	A3n	A3n	2.0	0.017	....	....	
1024	5.2	0.072	A1n	A0n	1.1	0.016	0.019	0″.015	Urs. Maj., M
1025	6.0	0.123	A5n	A6n	2.4	0.018	(0.029)	....	Taurus
1026	4.4	0.112	A3s	A4n	1.8	0.030	0.025	....	Taurus
1027	5.4	0.132	A3n	A5n	2.1	0.022	0.030	....	Taurus
1029	4.2	0.109	A3s	A4s	1.4	0.028	0.026	....	Taurus
1033	4.4	0.123	A2n	A3n	1.8	0.030	0.028	....	Taurus
1034	4.6	0.118	A0n	A2n	1.3	0.022	0.028	....	Taurus
1040	5.7	0.118	A9n	F0n	2.8	0.026	0.027	....	Taurus
1043	6.0	0.111	A8n	A8n	2.8	0.022	0.027	....	Taurus
1046	3.6	0.107	A3s	A6s	1.6	0.042	0.026	....	Taurus
1047	5.1	0.111	A2n	A4n	2.0	0.024	0.028	....	Taurus
1051	5.7	0.106	A3n	A4n	2.1	0.019	(0.026)	....	Taurus
1054	4.8	0.116	A5s	A7s	2.0	0.028	0.029	....	Taurus
1055	5.5	0.110	F1s	F0s	2.7	0.027	0.028	....	Taurus
1056	5.5	0.110	A5n	A8n	2.5	0.025	0.028	....	Taurus
1058	6.0	0.109	A5n	A8n	2.5	0.020	0.028	....	Taurus
1061	6.1	0.007	A3s	A5s	1.5	0.012	....	....	
1064	5.9	0.029	A2s	B9s	0.4	0.008	....	....	
1067	4.8	0.104	A2n	A5n	2.0	0.028	0.027	....	Taurus
1069	5.8	0.028	A3s	A4s	1.4	0.014	....	....	
1076	4.4	0.066	A3s	A0s	0.8	0.019	....	....	
1086	5.8	0.094	A4n	A6n	2.3	0.020	0.025	....	Taurus
1087	4.3	0.104	A3n	A4n	2.1	0.036	0.028	....	Taurus
1088	5.3	0.067	A4s	A6n	2.0	0.022	....	....	
1089	5.2	0.074	A4s	A6s	1.8	0.020	....	....	
1090	4.9	0.084	A3n	A5n	2.2	0.028	0.023	....	Taurus
1092	5.6	0.082	A5s	A8s	2.2	0.020	0.023	....	Taurus
1093	5.7	0.053	B9n	A0n	0.8	0.010	(0.012)	....	Perseus
1095	5.0	0.046	A4s	A5s	1.7	0.022	....	....	
1097	5.4	0.027	B9n	A0n	0.8	0.012	....	....	
1099	5.7	0.061	A0n	A0n	0.9	0.011	0.016	....	Perseus
1103	5.2	0.067	A0n	A0n	0.9	0.014	0.016	....	Perseus
1106	7.2	0.047	A1n	A0n	1.1	0.006	....	−0.014	S
1114	5.4	0.098	A8s	A8n	2.6	0.027	0.029	....	Taurus
1118	5.7	0.052	A1n	A1n	1.3	0.013	....	....	
1122	5.4	0.066	A7s	A7s	2.2	0.024	(0.020)	....	Taurus
1143	5.1	0.091	A2n	A2n	1.7	0.021	0.026	....	Taurus
1146	5.6	0.013	A2n	A0s	1.0	0.012	....	....	
1150	5.6	0.007	A1n	A0n	1.1	0.012	....	....	
1155	5.8	0.010	A2s	A1s	0.8	0.010	....	....	
1161	4.4	0.012	A2s	A2s	0.9	0.020	....	....	
1163	4.7	0.145	A1n	A0n	1.1	0.019	....	....	
1165	5.7	0.024	B9n	B9s	0.2	0.008	....	....	
1177	5.6	0.067	A2s	A2n	1.4	0.014	....	....	
1182	6.0	0.013	F1s	F2s	2.8	0.022	....	0.002	W
1194	4.7	0.082	A3n	A4n	2.1	0.030	(0.024)	....	Taurus
1220	2.9	0.118	A1n	A2n	1.5	0.052	(0.033)	....	Urs. Maj
1226	5.4	0.074	A7s	F0s	2.5	0.026	0.029	....	Taurus
1248	6.2	0.016	A2s	A1s	0.8	0.008	....	....	
1272	6.5	0.019	A4n	A5s	2.0	0.012	....	....	
1275	5.7	0.003	A1n	A2s	1.0	0.011	....	....	
1281	4.7	0.020	B9s	B9n	0.2	0.012	....	....	
1293	5.9	0.015	B9n	B9s	0.2	0.008	....	....	
1310	5.7	0.019	B9s	B9s	−0.2	0.007	....	....	
1318	5.5	0.031	A0n	B9n	0.7	0.011	....	....	
1320	5.9	0.039	B9n	A0n	0.8	0.010	....	....	
1366 Ft.	7.3	0.005	B9s	B9n	0.2	0.004	....	....	

TABLE VI—*Continued*

BOSS	m	μ	SPECTRUM		M	SPECT. π	GROUP π	TRIG. π	AUTH.
			A.	J.					
1378.......	5.6	0″016	A7s	F0n	2.6	0″025	....	....	
1411.......	5.5	0.009	A2s	A2s	0.9	0.012	....	0″017	A
1423.......	5.7	0.059	A1n	A0n	1.1	0.012	....	....	
1424.......	5.5	0.010	F0s	F0s	2.6	0.026	....	....	
1427.......	6.4	0.007	A2n	A2n	1.7	0.011	....	....	
1433.......	6.0	0.024	A5s	A4s	1.7	0.014	....	....	
1453.......	4.9	0.014	A2s	A2n	1.4	0.020	....	....	
1478.......	2.8	0.047	A0np	A2np	1.5	0.055	0″025	0.035	Urs. Maj., F, J, M
1482.......	2.7	0.105	A1s	A1s	0.6	0.037	....	0.019	A
1568.......	5.3	0.021	B8n	B9s	0.0	0.009	....	....	
1572.......	5.4	0.017	B9s	B9s	−0.2	0.008	....	....	
1575.......	4.4	0.022	A2s	A4s	1.2	0.024	....	0.026	M
1588.......	6.2	0.006	A1n	A1n	1.3	0.010	....	....	
1607.......	5.5	0.021	A7s	A6s	2.2	0.022	....	....	
1646.	6.8	0.035	A2sp	A6sp	1.7	0.010	....	....	
1672.......	5.8	0.013	A1n	A0s	0.8	0.010	....	....	
1673.......	5.6	0.620	F2s	F3n	2.9	0.028	....	0.039	G, Y
1690.......	1.9	0.065	A2s	A2s	0.9	0.063	....	0.053	F, Ye
1716.......	5.3	0.015	A1n	A0n	1.1	0.014	....	....	
1732.......	−1.6	1.316	A2s	A2s	0.9	0.316	0.380	0.374	Urs. Maj., F, Gill, Ye
1751.......	5.7	0.023	B9s	B9s	−0.2	0.007	....	....	
1778.......	4.8	0.112	A4n	A5n	2.2	0.030	....	0.049	A
1880.......	5.8	0.011	B9n	A0n	0.8	0.010	....	....	
1886.......	3.6	0.068	A2n	A1n	1.5	0.038	....	0.038	A
1894.......	6.3	0.011	A9s	A8s	2.4	0.017	....	....	
1897.......	5.6	0.036	A6n	A6n	2.4	0.024	....	....	
1898.......	3.5	0.025	A3n	A6n	2.2	0.055	....	0.062	A, M
1903.......	7.4	0.048	A3n	A8n	2.4	0.010	....	0.009	A
1905.......	6.5	0.029	A0n	A0n	0.9	0.008	....	0.006	A
1930.......	5.3	0.028	A1n	A3n	1.6	0.018	....	....	
1952.......	4.2	0.236	A5s	A4s	1.7	0.032	....	0.055	A, Jo, M
1956.......	5.0	0.067	A1n	A3n	1.6	0.021	....	....	
1977.......	5.1	0.029	A0n	A0n	0.9	0.014	....	....	
1979 Br....	2.0	0.203	A2s	A3s	1.1	0.066	....	0.073	A, M, *et al.*
1984.......	5.8	0.016	B9n	A0n	0.8	0.010	....	....	
2045.......	5.3	0.027	B9n	A0n	0.8	0.012	....	....	
2051.......	5.1	0.017	A7n	A6n	2.6	0.031	....	....	
2054.......	6.2	0.020	A7n	A8n	2.7	0.020	....	....	
2078.......	5.0	0.047	A0n	A1n	1.1	0.016	....	....	
2121.......	6.2	0.017	A1n	A1n	1.3	0.010	....	....	
2122.......	5.9	0.011	A0n	A0n	0.9	0.010	....	....	
2178.......	6.4	0.017	A4s	A4n	2.0	0.012	....	....	
2185.......	5.5	0.005	A3n	A3n	2.0	0.019	....	....	
2237.......	4.0	0.071	A0n	A0n	0.9	0.024	....	....	
2240.......	6.3	0.011	A1n	A2n	1.5	0.011	....	....	
2241.......	6.3	0.011	A2n	A2n	1.7	0.012	....	....	
2246.......	5.4	0.070	A6s	A6s	2.1	0.022	....	....	
2287.......	5.6	0.027	A2s	A6s	1.5	0.016	....	....	
2295.......	4.2	0.074	B9n	A0n	0.8	0.020	....	....	
2305.......	6.7	0.036	A4n	A5n	2.2	0.013	0.011	....	Praesepe
2309.......	6.5	0.036	A2s	A2n	1.4	0.010	0.011	....	Praesepe
2311.......	6.3	0.036	A6n	A6n	2.4	0.017	0.011	....	Praesepe
2313.......	6.7	0.021	A4n	A7n	2.4	0.014	....	....	
2314.......	6.8	0.041	A6s	A6s	2.1	0.012	0.011	....	Praesepe
2328.......	5.7	0.011	A5s	A6n	2.2	0.020	....	....	
2343.......	6.0	0.005	A3n	A1n	1.6	0.016	....	....	
2353.......	5.7	0.098	A0n	A0n	0.9	0.011	....	....	
2357.......	5.2	0.046	B9n	A0n	0.8	0.013	....	....	
2381.......	5.7	0.045	A5n	A5s	2.0	0.018	....	....	
2400.......	5.2	0.062	A3s	A5n	1.8	0.022	....	....	
2404.......	3.1	0.502	A4n	A4n	2.2	0.066	....	0.090	Ab, F, Y
2407.......	4.3	0.054	A4s	A5s	1.7	0.030	....	....	
2417.......	5.8	0.007	A2n	A2n	1.7	0.015	....	....	
2423.......	5.7	0.004	A2n	A0n	1.3	0.014	....	....	
2424.......	3.7	0.073	B9n	A0n	0.8	0.026	....	....	
2429.......	6.3	0.008	A1n	A0n	1.1	0.009	....	....	
2443......	4.5	0.134	A8s	F0s	2.6	0.041	....	....	
2461.......	5.9	0.100	A3n	A4n	2.1	0.018	....	....	
2465.......	5.3	0.052	A1s	A2s	0.7	0.012	....	....	
2476.......	4.9	0.086	A1n	A0n	1.1	0.018	....	....	

TABLE VI—*Continued*

Boss	*m*	*μ*	Spectrum		*M*	Spect. *π*	Group *π*	Trig. *π*	Auth.
			A.	J.					
2479	3.8	0″338	A1n	A1n	1.3	0″032	....	0″017	A
2484	5.7	0.022	A1s	A3s	0.9	0.012	....	....	
2492	5.5	0.040	B9n	A0s	0.4	0.010	....	....	
2494	6.4	0.058	A2n	A5n	2.0	0.013	....	....	
2495	4.0	0.137	B9n	B9n	0.6	0.021	....	0.037	A, M
2540	3.8	0.117	A4n	A6n	2.3	0.050	....	0.033	A
2565	4.6	0.073	B9n	B9n	0.6	0.016	....	....	
2576	6.2	0.042	A1n	A1n	1.3	0.010	(0″011)	....	Praesepe
2584	5.2	0.020	A5n	A6n	2.4	0.026	....	....	
2598	6.1	0.029	A3n	A3n	2.0	0.014	....	....	
2632	3.9	0.330	A4n	A7n	2.4	0.050	....	....	
2634	6.0	0.049	F1s	F1s	2.8	0.022	(0.011)	....	Praesepe
2637	5.0	0.009	A1s	A3s	0.9	0.015	....	....	
2641	6.0	0.033	A3n	A4n	2.1	0.016	....	....	
2642	5.3	0.194	A5n	A7s	2.2	0.024	....	....	
2647	5.9	0.204	A1s	A1s	0.6	0.008	....	0.035	A, Ye
2650	5.8	0.076	A0n	B9n	0.8	0.010	....	....	
2692	4.5	0.054	A2n	A3n	1.8	0.028	....	....	
2698	1.3	0.247	B6n	B9n	0.4	0.064	....	0.033	Y
2712	6.1	0.021	A1n	A0n	1.1	0.010	....	....	
2724	5.4	0.074	B9n	B9n	0.6	0.010	....	....	
2726	5.7	0.090	A3n	A3n	2.0	0.018	0.022	....	*a* Lyrae
2737	5.8	0.065	A1n	A2n	1.5	0.014	....	....	
2744	6.7	0.001	A1n	A0n	1.1	0.008	....	....	
2745	5.6	0.130	A2n	A2n	1.7	0.017	....	....	
2756	5.8	0.027	A1n	A3n	1.6	0.015	....	....	
2768	4.8	0.107	F1s	A8s	2.6	0.036	....	....	
2773	5.8	0.102	A1n	A2n	1.5	0.014	....	....	
2777	5.9	0.014	A3s	A2s	1.0	0.011	....	....	
2787	5.9	0.011	A2s	A1s	0.8	0.009	....	....	
2788	5.2	0.052	A0n	A0n	0.9	0.014	....	....	
2797	5.5	0.048	B8n	B8n	0.1	0.008	....	....	
2798	5.8	0.015	A0n	A0n	0.9	0.010	....	....	
2802	4.8	0.141	A4n	A4n	2.2	0.030	....	0.028	A
2808	5.6	0.040	B9n	A0n	0.8	0.010	....	....	
2813	5.2	0.074	A8s	A8s	2.4	0.027	0.043	0.034	Urs. Maj., A
2819	6.3	0.050	F0s	F3s	2.8	0.020	....	....	
2839	6.9	0.013	B9n	A0n	0.8	0.006	....	....	
2853	5.3	0.289	A6n	F0s	2.6	0.028	....	0.023	A, Jo
2866	5.4	0.049	B9n	A0n	0.8	0.012	....	....	
2887	6.1	0.021	A3n	A3s	1.6	0.012	....	....	
2909	4.5	0.077	B9n	A0n	0.8	0.018	....	....	
2930	2.4	0.089	A3s	A2s	1.0	0.054	0.046	....	Urs. Maj.
2940	6.1	0.071	A3n	A2n	1.8	0.014	....	....	
2951	6.4	0.004	A3s	A2s	1.0	0.009	....	....	
2956	5.6	0.004	A3s	A2n	1.5	0.016	....	....	
2972	2.6	0.207	A2n	A2n	1.7	0.066	(0.085)	....	Urs. Maj.
2974	3.4	0.106	A2s	A2s	0.9	0.032	....	0.021	A
2987	4.8	0.102	A0n	A1s	0.7	0.016	....	....	
2990	4.1	0.095	B9s	B9s	−0.2	0.014	....	....	
3023	5.3	0.052	B9n	A0n	0.8	0.012	....	....	
3052	6.4	0.035	A1n	A3n	1.6	0.011	....	....	
3055	4.8	0.061	B9n	A0n	0.8	0.016	0.015	....	*a* Lyrae
3063	5.5	0.154	A4n	A3n	2.0	0.020	....	....	
3088	5.1	0.068	A1n	A2n	1.5	0.019	....	....	
3097	5.2	0.050	A1n	A0s	0.8	0.015	....	....	
3101	2.2	0.511	A2n	A2n	1.7	0.079	....	0.114	F, S, Y
3117	2.5	0.094	A0n	A0n	0.9	0.048	0.041	0.011	Urs. Maj., F, M
3120	6.5	0.009	A1n	A0n	1.1	0.008	....	....	
3123	5.5	0.025	A3s	A3s	1.2	0.014	....	....	
3143	5.1	0.323	A6s	A6s	2.1	0.025	....	0.013	A
3150	6.0	0.044	A7s	A7s	2.2	0.017	....	....	
3173	6.3	0.013	A1n	A1s	0.9	0.008	....	....	
3178	6.8	0.006	F1s	A8s	2.6	0.014	....	....	
3183	5.8	0.096	A7s	A8s	2.4	0.020	....	....	
3190	3.4	0.110	A0n	A0n	0.9	0.032	0.045	....	Urs. Maj.
3202	5.9	0.030	A1n	A2n	1.5	0.013	....	....	
3206	6.2	0.038	A8s	A8s	2.4	0.017	....	....	
3208	6.3	0.067	F0n	A6n	2.6	0.019	....	....	
3229	6.0	0.084	A6n	A5n	2.4	0.019	....	....	

TABLE VI—*Continued*

Boss	m	μ	Spectrum		M	Spect. π	Group π	Trig. π	Auth.
			A.	J.					
3231.......	5.1	0″.033	A3s	A2s	1.0	0″.016	....	....	
3256.......	3.1	0.251	B9n	A0n	0.8	0.034	....	0″.026	Ye
3257.......	5.7	0.060	A1n	A1n	1.3	0.013	....	....	
3266.......	5.4	0.020	A3s	A2s	1.0	0.014	....	....	
3276.......	6.1	0.023	A4s	A4s	1.6	0.012	....	....	
3277.......	5.4	0.084	B9n	B9n	0.6	0.010	....	....	
3284.......	6.7	0.019	A5s	A4s	1.7	0.010	....	....	
3290.......	5.9	0.040	A0n	A1n	1.1	0.011	....	....	
3309.......	4.9	0.135	B9n	B9n	0.6	0.014	....	....	
3310.......	5.5	0.078	B9n	B9n	0.6	0.010	....	....	
3323.......	5.2	0.112	A6n	A4n	2.4	0.027	....	....	
3329.......	6.0	0.054	A0n	A1n	1.1	0.010	....	....	
3332.......	5.8	0.022	A3n	A4n	2.1	0.018	....	....	
3334.......	6.4	0.068	A0n	A0n	0.9	0.008	....	....	
3337.......	5.6	0.051	A0n	B9n	0.7	0.010	....	....	
3338.......	6.2	0.055	A8s	A9n	2.5	0.018	....	....	
3339.......	5.8	0.095	A0n	A0n	0.9	0.010	....	....	
3343.......	5.9	0.101	A0n	A0n	0.9	0.010	....	....	
3360.......	6.3	0.067	A7n	A7n	2.6	0.018	0″.019	....	Urs. Maj.
3363.......	1.7	0.115	A2s	A2s	0.9	0.069	0.042	....	Urs. Maj.
3371.......	2.9	0.237	A1s	A1s	0.6	0.034	....	0.044	Ye
3382.......	4.9	0.101	A4n	A5n	2.2	0.030	0.036	0.031	Urs. Maj., A
3392.......	5.1	0.027	B9n	B9n	0.6	0.012	....	....	
3409.......	4.4	0.057	A2s	A2s	0.9	0.020	....	0.011	M
3428^1......	6.8	0.039	A1n	A1n	1.3	0.008	....	....	
3428^2......	7.2	0.039	A1n	A3n	1.6	0.008	....	....	
3462.......	5.9	0.080	A5s	A5s	1.8	0.015	....	....	
3474.......	2.4	0.130	A2s	A3s	1.1	0.054	0.044	0.049	Urs. Maj., F, M, Pe, Y
3475.......	4.0	0.136	A8s	A5s	2.0	0.052	0.046	0.022	Urs. Maj., M
3478.......	5.8	0.014	A3s	A2s	1.0	0.012	....	....	
3480.......	4.0	0.123	A1n	A0n	1.1	0.026	0.042	0.037	Urs. Maj., A, M
3506.......	4.9	0.052	A3s	A5s	1.5	0.021	0.014	0.028	Urs. Maj., M
3507.......	6.3	0.067	A1s	A2n	1.2	0.010	....	....	
3518.......	4.9	0.104	A1n	A2n	1.5	0.021	....	0.052	S
3526.......	6.3	0.112	A7n	A5n	2.5	0.018	....	0.015	A, M, S, Ye
3539.......	5.7	0.060	B9n	A0n	0.8	0.010	....	....	
3540.......	6.4	0.055	A0s	A1s	0.4	0.006	....	....	
3546.......	6.2	0.053	B9n	A0n	0.8	0.008	....	....	
3580.......	6.6	0.033	A2n	A2n	1.7	0.010	....	....	
3585.......	6.0	0.038	A1n	A3n	1.6	0.013	....	....	
3612.......	4.3	0.032	A1n	A0n	1.1	0.023	....	....	
3652.......	6.6	0.065	A9s	F2s	2.6	0.016	....	0.025	A
3653.......	5.6	0.044	A0n	B9n	0.7	0.010	....	....	
3654.......	4.6	0.067	A4n	A5n	2.2	0.034	....	0.025	A
3663.......	5.8	0.055	A5s	A5n	2.1	0.018	....	....	
3666.......	4.3	0.238	A1n	A0n	1.1	0.023	....	0.041	A
3669.......	5.7	0.070	A3s	A3s	1.2	0.013	....	....	
3684.......	6.0	0.030	A0n	A0n	0.9	0.010	....	....	
3692 Br....	5.1	0.072	B9n	A0n	0.8	0.014	....	0.017	S, Ye
3692 Ft....	7.4	0.072	F0s	F2n	2.8	0.012	....	0.020	S, Ye
3706.......	6.2	0.098	A2n	A2n	1.7	0.013	....	....	
3719.......	6.6	0.088	A2n	A2n	1.7	0.010	....	0.011	A
3722.......	3.0	0.182	A3n	A3n	2.0	0.062	....	....	
3729.......	4.5	0.228	F0s	F0s	2.6	0.043	....	....	
3743.......	5.5	0.027	A0n	A0n	0.9	0.012	....	....	
3752.......	4.4	0.061	A0n	A0n	0.9	0.020	(0.016)	....	Urs. Maj.
3756.......	5.8	0.026	B9n	B9n	0.6	0.009	....	....	
3766 Br....	5.2	0.238	A5n	A5n	2.3	0.026	....	....	
3771 Ft....	5.1	0.049	A2n	A2n	1.7	0.021	....	0.019	A
3787.......	2.9	0.131	F1n	F1n	2.9	0.100	....	....	
3788.......	5.7	0.024	B9n	B9n	0.6	0.010	....	....	
3814.......	4.6	0.192	A4n	A4n	2.2	0.033	....	....	
3820.......	6.4	0.029	A1n	A1n	1.3	0.010	....	....	
3866.......	4.7	0.061	B9n	B9n	0.6	0.014	....	....	
3868.......	6.0	0.068	A0n	A0n	0.9	0.010	....	....	
3875.......	6.3	0.029	B9s	B9s	−0.2	0.005	....	....	
3883.......	5.3	0.078	A0n	A0n	0.9	0.013	....	....	
3885.......	5.6	0.109	A1n	A3n	1.6	0.016	....	....	
3902.......	6.1	0.029	A5s	A4n	2.0	0.016	....	....	
3911.......	5.5	0.017	A2n	A1n	1.5	0.016	....	....	

TABLE VI—*Continued*

Boss	*m*	μ	Spectrum		*M*	Spect. π	Group π	Trig. π	Auth.
			A.	J.					
3915	5.4	0″.051	A0n	B9n	0.7	0″.012	....	....	
3918	6.1	0.077	A5n	A5n	2.3	0.017	....	....	
3940	3.7	0.190	F2s	F2s	2.8	0.066	....	....	
3946	6.1	0.016	B9n	B9n	0.6	0.008	....	....	
3960 Br.	4.2	0.068	A4n	A7n	2.4	0.044	....	0″.013	A, Ye
3960 Ft.	5.2	0.068	A5n	A6n	2.4	0.026	....	0.019	A, Ye
3961	2.3	0.158	A0n	A0n	0.9	0.052	0″.050	0.059	Urs. Maj., Corona, F, M
3985	5.8	0.162	A7n	A5n	2.5	0.022	....	....	
3993	5.3	0.044	A3np	A2s	1.4	0.018	....	....	
3998	4.0	0.105	A0n	A1n	1.1	0.026	....	0.021	A, S, Ye
4007	5.6	0.033	A2s	A0n	1.0	0.012	....	....	
4009	3.7	0.091	A1n	A0n	1.1	0.030	0.023	0.035	Urs. Maj., A, M
4016	3.6	0.092	A0s	B9n	0.4	0.022	....	....	
4021	5.1	0.070	A1n	A3n	1.6	0.020	....	....	
4022	5.8	0.010	A6s	A8s	2.3	0.020	....	....	
4026	3.8	0.136	A6s	A4s	1.8	0.042	....	0.035	A
4028	5.2	0.099	A0n	A0n	0.9	0.014	....	....	
4037	5.4	0.046	B7n	B6n	−0.6	0.007	(0.012)	....	Scorpius
4041	5.9	0.034	B9n	A0n	0.8	0.010	0.009	....	Scorpius
4070	5.6	0.034	A1s	A1s	0.6	0.010	....	....	
4072	5.0	0.193	A5n	A8n	2.5	0.032	....	....	
4080	4.9	0.045	A0s	A2n	1.0	0.017	....	....	
4097	5.6	0.065	B9n	A0n	0.8	0.010	....	....	
4119	4.9	0.027	A3s	A3s	1.2	0.018	....	....	
4120	5.5	0.041	A1n	A3n	1.6	0.016	....	....	
4122	5.9	0.014	A2s	A3s	1.1	0.010	....	....	
4146	5.7	0.028	A2n	A2n	1.7	0.016	....	....	
4155	4.8	0.042	A3s	A4s	1.4	0.021	0.011	....	Scorpius
4163	4.8	0.172	A5n	A7n	2.4	0.034	....	0.031	A
4165	3.8	0.062	A3n	A0n	1.4	0.035	....	0.017	A
4176	6.2	0.022	A1n	B9n	0.9	0.008	....	....	
4181	5.0	0.261	A6n	A8n	2.6	0.034	....	0.045	G
4182	4.5	0.079	A2s	A2s	0.9	0.019	....	....	
4184	5.5	0.026	A1n	A0n	1.1	0.013	....	....	
4203	4.0	0.097	A1n	A1n	1.3	0.029	....	0.000	A, M, S, Ye
4206	4.6	0.033	A2s	A5s	1.4	0.022	....	....	
4210	5.6	0.023	A1s	A1s	0.6	0.010	....	....	
4213	5.0	0.042	B9n	A0n	0.8	0.014	....	....	
4221	5.8	0.021	A1n	A2n	1.5	0.014	....	....	
4229	5.6	0.024	B9s	A0n	0.4	0.009	....	....	
4260	6.0	0.003	B9n	A0n	0.8	0.009	....	....	
4285	5.6	0.029	A2s	A0n	1.0	0.012	....	....	
4291	6.4	0.011	A0n	A1s	0.7	0.008	....	....	
4300	5.4	0.098	A5s	A6n	2.2	0.022	....	....	
4332	5.3	0.012	A3s	A3s	1.2	0.016	....	....	
4338	6.2	0.038	B9n	B9n	0.6	0.009	....	....	
4348 Br.	6.3	0.055	A1n	A3n	1.6	0.012	....	....	
4353	6.0	0.032	A0n	A2n	1.3	0.012	....	....	
4360	3.3	0.093	A3s	A1s	0.9	0.033	....	....	
4376	3.2	0.165	A0n	A0n	0.9	0.035	....	0.028	A, M
4391	4.8	0.066	A0n	A0n	0.9	0.017	....	....	
4395	4.4	0.036	A0n	A1n	1.1	0.022	....	....	
4402	5.1	0.018	B9n	B9s	0.2	0.011	....	....	
4418	5.7	0.044	A4s	A3s	1.4	0.014	....	....	
4419	4.5	0.038	B9n	B9s	0.2	0.014	....	−0.004	A
4420	4.3	0.132	A6s	A7s	2.2	0.038	....	....	
4430	5.8	0.015	A1n	A0n	1.1	0.012	....	0.014	Ye
4442	5.7	0.108	A0n	A3n	1.4	0.014	....	....	
4449	6.6	0.015	B9s	A1s	0.2	0.005	....	....	
4458	5.0	0.158	A5n	A6s	2.2	0.027	....	0.019	A, F
4459	2.1	0.262	A0n	B9n	0.7	0.052	0.046	0.062	Corona, F, M, Y, Y
4461	5.8	0.028	A5s	A8s	2.2	0.019	....	....	
4468	5.7	0.023	B9n	A0n	0.8	0.010	....	....	
4494	5.7	0.043	B9n	A0n	0.8	0.010	....	....	
4511	5.2	0.208	A1n	A0n	1.1	0.016	....	−0.001	A, Y
4514	6.4	0.009	A1sp	B9s	0.2	0.006	....	....	
4521	6.4	0.026	A0n	A2n	1.3	0.010	....	....	
4552	4.4	0.026	B9n	A0n	0.8	0.018	....	....	
4554	5.5	0.009	A9s	F2s	2.6	0.027	....	....	
4557	5.1	0.030	A1n	B9n	0.9	0.014	....	....	

TABLE VI—*Continued*

Boss	*m*	μ	Spectrum		*M*	Spect. π	Group π	Trig. π	Auth.
			A.	J.					
4581	3.7	0″.103	A5s	A5s	1.8	0″.042	....	0″.037	A
4592	5.2	0.027	A4s	A4s	1.6	0.019	....	....	
4640	6.5	0.010	B9n	A0n	0.8	0.008	....	....	
4643	5.5	0.057	A4s	A3s	1.4	0.016	....	....	
4669	5.7	0.034	A3s	A3s	1.2	0.013	....	....	
4685	5.2	0.035	B9n	A0n	0.8	0.013	....	....	
4702	5.4	0.007	B9s	B9s	−0.2	0.008	....	....	
4713	5.4	0.146	A5n	A8n	2.5	0.026	....	0.024	A
4719	5.8	0.026	A2s	A2s	0.9	0.010	....	....	
4722	0.1	0.346	A1s	A1s	0.6	0.123	0″.104	0.110	α Lyrae, F, J, Y, Ye
4748	6.0	0.057	A3n	A6n	2.2	0.018	....	0.000	Ye
4751 Br.	5.7	0.031	A3s	A6s	1.6	0.016	....	....	
4752	4.3	0.031	A5s	A8s	2.2	0.037	....	0.026	A
4754	5.9	0.022	A1n	A2n	1.5	0.013	....	0.030	A
4761	4.4	0.123	A2n	A5n	2.0	0.034	....	0.056	A
4777 Ft.	7.8	0.020	B8n	B8n	0.1	0.003	....	(−0.006)	Ye
4779	5.3	0.019	A0s	A1s	0.4	0.010	....	....	
4820	5.7	0.120	F2s	F2s	2.8	0.026	....	0.040	A, S
4821	5.8	0.002	B8n	B8n	0.1	0.007	....	....	
4824	3.3	0.008	B9sp	B9s	−0.2	0.020	....	0.012	M
4846	5.1	0.091	A2n	A4n	2.0	0.024	....	....	
4856	5.9	0.016	B9n	A0n	0.8	0.010	....	....	
4858	3.0	0.102	B9n	A0n	0.8	0.036	....	0.037	A, M
4866	5.7	0.056	A3s	A7s	1.8	0.016	....	....	
4867	5.5	0.098	A2n	A5n	2.0	0.020	....	....	
4899	5.6	0.044	A1n	A0n	1.1	0.012	....	....	
4914	5.1	0.011	A3n	A3s	1.6	0.020	....	0.011	A
4928	5.5	0.002	B9s	A0n	0.4	0.010	....	....	
4932	4.0	0.031	A4n	A7s	2.2	0.044	....	0.049	M
4947	6.0	0.019	A3s	A6s	1.6	0.014	....	....	
4953	3.4	0.265	A3n	A6n	2.2	0.058	....	0.057	A, M
4965	5.6	0.040	B9n	B9n	0.6	0.010	....	....	
4974	5.8	0.037	A0n	A0n	0.9	0.010	....	....	
4979	6.0	0.017	A0n	A0n	0.9	0.010	....	....	
4980	5.7	0.041	A0s	A0s	0.2	0.008	....	....	
4988	3.9	0.126	A1n	A0n	1.1	0.028	....	0.018	A, Ab
4998	4.9	0.004	B9n	B8n	0.3	0.012	....	....	
5007	5.9	0.006	B9np	A0n	0.8	0.009	....	....	
5024	5.4	0.032	A0s	A0s	0.2	0.009	....	....	
5042	6.1	0.017	A0s	B9s	0.0	0.006	....	....	
5048	3.0	0.065	A1n	A0n	1.1	0.042	....	0.055	S
5062	0.9	0.655	A2n	A2n	1.7	0.145	....	0.205	M, Y, Ye, *et al.*
5092	5.5	0.024	B9n	A2n	1.2	0.014	....	....	
5105	4.8	0.051	B9n	A0n	0.8	0.016	....	....	
5117	6.3	0.005	A1n	A0n	1.1	0.009	....	....	
5130	6.0	0.020	B9s	B9n	0.2	0.007	....	....	
5134	5.3	0.099	A6n	A6n	2.4	0.026	....	....	
5160	6.2	0.038	A0sp	A1n	0.8	0.008	....	....	
5171	3.4	0.032	B9s	B9s	−0.2	0.019	....	....	
5173	5.5	0.007	A1np	A0n	1.1	0.013	....	....	
5186	5.0	0.017	A0n	A0n	0.9	0.015	....	0.010	A, M
5188	5.0	0.094	A2n	A1n	1.5	0.020	....	....	
5211	5.5	0.046	A1n	A1n	1.3	0.014	....	....	
5220	6.1	0.022	A0n	A0n	0.9	0.009	....	....	
5224	5.4	0.018	B7n	B8n	−0.1	0.008	....	....	
5233	6.1	0.008	A0n	A0n	0.9	0.009	....	....	
5236	5.7	0.004	B7n	B8n	−0.1	0.007	....	....	
5244	5.0	0.026	A4n	A8n	2.4	0.031	....	0.024	M
5249	5.4	0.073	A1n	A0n	1.1	0.014	....	....	
5269	6.5	0.005	A1n	A0n	1.1	0.008	....	....	
5282	4.7	0.038	A1n	A4n	1.8	0.026	....	....	
5292	5.4	0.048	A2s	A2s	0.9	0.013	....	....	
5295	6.2	0.009	A0n	A0n	0.9	0.009	....	....	
5296	6.4	0.069	A3n	A5n	2.2	0.014	....	....	
5301	4.8	0.058	B9s	A1n	0.6	0.015	....	....	
5322	5.6	0.017	B8s	B9s	−0.4	0.006	....	....	
5337	3.8	0.044	A1n	A3n	1.6	0.037	....	0.023	M
5366	5.5	0.011	B9s	B9s	−0.2	0.007	....	....	
5371	4.8	0.051	A7n	F0s	2.7	0.038	....	0.010	M
5393	4.9	0.025	B9n	B9n	0.6	0.014	....	0.000	A

TABLE VI—*Continued*

Boss	m	μ	Spectrum		M	Spect. π	Group π	Trig. π	Auth.
			A.	J.					
5417	4.9	0″.060	A4s	A5s	1.7	0″.023	......	......	
5425	6.3	0.051	A8s	A8n	2.6	0.018	0″.013	......	Urs. Maj.
5443	4.8	0.169	A7s	A9s	2.4	0.034	......	0″.044	M
5465	5.4	0.015	B9s	B9s	−0.2	0.008	......	......	
5480	2.6	0.160	A2n	A0n	1.3	0.056	......	0.084	A, F, M
5491	5.1	0.054	A1s	A4s	1.0	0.016	......	......	
5498	5.7	0.124	A3n	A6n	2.2	0.020	......	......	
5511	5.5	0.206	A4n	A4n	2.2	0.022	0.052	0.037	α Lyrae, A, Jo
5525	5.4	0.018	B9n	B8n	0.3	0.010	......	......	
5532 Ft	8.0	0.012	A2n	A2n	1.7	0.005	......	(−0.011)	Ye
5548	6.0	0.008	B9n	A0n	0.8	0.009	......	......	
5550	6.3	0.026	A0n	A0n	0.9	0.008	......	......	
5555	5.3	0.100	A3n	A0n	1.4	0.018	......	......	
5558	5.8	0.117	A2n	A5n	2.0	0.018	......	......	
5573	6.0	0.052	A0n	A0n	0.9	0.010	0.013	0.010	Urs. Maj., M
5581	5.9	0.030	A2n	A4n	2.0	0.016	......	......	
5585	5.6	0.038	B9n	A2n	1.2	0.014	......	......	
5591	6.9	0.061	A5n	A8n	2.5	0.013	......	......	
5600	3.0	0.392	A3n	A5n	2.2	0.068	......	0.115	M
5626	6.5	0.001	B9n	A0s	0.4	0.006	......	......	
5639	6.0	0.009	B8s	B8n	−0.4	0.006	......	......	
5641	5.6	0.036	A0n	A0n	0.9	0.011	......	......	
5664	5.7	0.004	B7s	B6s	−1.2	0.004	......	......	
5667	5.5	0.007	B8n	B9n	0.4	0.010	......	......	
5669	5.6	0.039	B9n	A1n	1.0	0.012	......	......	
5709	4.4	0.026	A4n	F2n	2.6	0.043	......	0.005	A, M
5738	6.2	0.028	B8n	B9n	0.4	0.006	......	......	
5742	4.2	0.452	A6n	A6n	2.4	0.045	0.108	0.055	α Lyrae, A, M, S, Y, Ye
5780	6.2	0.004	A1n	A0n	1.1	0.009	......	......	
5803	4.9	0.030	A1s	B9s	0.2	0.012	......	......	
5818	5.5	0.014	A1n	A2n	1.5	0.016	......	......	
5847	6.1	0.019	A2s	A1s	0.8	0.009	......	......	
5848	5.2	0.019	A0n	A2n	1.3	0.017	......	......	
5858	4.8	0.036	A2s	A3s	1.1	0.018	......	......	
5879	5.7	0.037	A1n	A0s	0.8	0.010	......	......	
5904	3.5	0.052	A1n	A1n	1.3	0.036	......	......	
5967	5.3	0.024	B9n	B9n	0.6	0.011	......	......	
5969	5.6	0.015	A4s	A3s	1.6	0.015	......	......	
5973	5.2	0.017	A1n	A0n	1.1	0.016	......	......	
5996	5.9	0.012	A6s	A8s	2.3	0.019	......	......	
6011	6.2	0.017	A2s	A1s	0.8	0.008	......	......	
6020	6.5	0.233	A9n	F0s	2.8	0.018	......	0.016	W
6023	5.5	0.005	A2n	B9s	0.8	0.012	......	......	
6031	4.9	0.124	A3s	A3s	1.2	0.018	......	0.043	A
6063	5.5	0.042	A1n	B9n	0.9	0.012	......	......	
6075	5.3	0.016	B9n	B9n	0.6	0.011	......	......	
6113	5.8	0.027	A3n	A4s	1.8	0.016	......	......	
6128	5.4	0.033	A1n	A3n	1.6	0.018	......	......	
6133	6.2	0.013	A2s	A1s	0.8	0.008	......	......	
6139	6.1	0.014	A1s	A0s	0.4	0.008	......	......	
6166	5.7	0.007	A5s	A8s	2.2	0.016	......	......	
6168	6.1	0.013	B9s	B9s	−0.2	0.005	......	......	
6174	6.3	0.004	A4s	A3n	1.8	0.012	......	......	
6180	6.0	0.008	A2s	A1s	0.8	0.009	......	......	

results are given in Table VII and a curve drawn from them is shown in Figure 2.

Two results are given for the last group according as Boss 1732 (Sirius) is included or not. For statistical purposes it is, no doubt, better to omit it.

These values show an excellent degree of correlation between proper motion and parallax. The influence of occasional stars of small proper motion and large parallax, or large proper motion and small parallax, is not serious, because of the considerable number

TABLE VII

Limits of μ	No.	Av. μ	Av. π
<0″.010	49	0″.006	0″.011
0″.010 to 0″.019	83	0.015	0.012
0.020 to 0.029	72	0.025	0.014
0.030 to 0.039	56	0.035	0.014
0.040 to 0.049	39	0.044	0.016
0.050 to 0.069	74	0.059	0.019
0.070 to 0.099	55	0.084	0.020
0.100 to 0.149	68	0.118	0.029
0.150 to 0.250	30	0.196	0.037
>0″.250	18 17	0.430 0.378	0.071 0.057

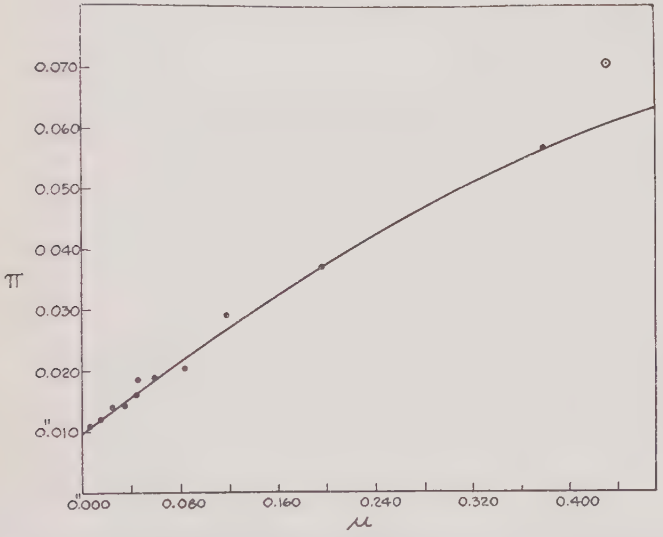

FIG. 2.—This curve shows the relationship between the average value of the proper motion and the average value of the spectroscopic parallax for the 544 stars of Table VI. The stars have been grouped according to the limits of proper motion given in Table VII. The point surrounded by a circle represents the value for the group of largest proper motion when Sirius is included; the neighboring point on the curve represents the same group when Sirius is omitted.

of stars in each group, the only important exception being that of Sirius. It is of interest to note that the curve would give an average parallax of 0″.009 for stars of zero proper motion, a result almost identical with that found by Strömberg[1] for stars of the later types of spectrum. Reference may also be made to the fact that the eighth group of stars, with proper motions between 0."100 and 0."149, while it includes most of the members of the Taurus moving cluster, also includes a large number of other stars. The parallax of 0."029 is in good agreement with that of Rasmuson for the Taurus cluster, thus indicating that the latter stars do not differ materially in distance from other A stars having the same amount of proper motion.

We have referred previously to α Cygni (Boss 5320) and some other stars with similar spectral characteristics. Most of these are listed as "c" stars by Miss Cannon and have sharp narrow lines with the enhanced lines remarkably strong and prominent. Those at λλ 4233 and 4481 are especially striking, and it seems probable from a brief examination already made that these lines vary definitely with absolute magnitude. At present, however, we have no results based upon trigonometric measures or other data from which to determine absolute magnitudes which may serve as standards of reduction for the spectroscopic intensities. There can be little question that α Cygni is extremely bright, its absolute magnitude probably being of the order of −4 or −5. In spectral characteristics, great luminosity, small proper motion, and low galactic latitude these stars are associated with the Cepheid variables and stars of similar spectra and appear to form a continuation of the Cepheid chain of giant stars. Table VIII gives the stars

TABLE VIII

Boss	Spectrum	μ	b
478	A2s	0."009	−3°
533	A1s	0.011	−3
534	A2s	0.005	−5
724	A2s	0.004	0
1268	A4s	0.016	−1
4503	A4s	0.015	−7
5320	A2s	0.001	+1
6111	A2s	0.010	0

---

[1] *Mt. Wilson Contr.*, No. 170.

of this type which we have found in our list. The galactic latitude is indicated by b.

The A-type companion of o^2 Eridani and probably the companion of Sirius appear to be cases of the rare phenomenon of A-type stars of very low luminosity. Three other stars of which we have spectrograms are much fainter than the vast majority of those of the A type. These are:

	m	Spectrum	μ	Trig. π	M
Lal. 5761	8.0	A2s	0''.90	0''.039	6.0
Lal. 28607	7.3	A2s	1.17	0.033	4.9
W. B. 23^h175	8.4	A2s	1.31	0.028	5.6

The last star is a double and the value of M refers to the combined magnitude.

The spectra of these stars are peculiar. The hydrogen lines are narrow and sharp, the metallic lines are very faint, and λ 4481 and λ 4233 are hardly visible. These latter lines, accordingly, show a behavior just the reverse of that in "c" stars like α Cygni. It is of interest to note that λ 4481 and λ 4233 are also very faint in the spectrum of the companion of o^2 Eridani.

Forty-five of the stars which appear in Table VI have been included in the list of 1646 stars[1] of the later spectral types for which absolute magnitudes derived by the spectroscopic method have been published. The latter values were obtained by an extrapolation of the reduction-curves for stars of the F type and have always been considered by us as subject to considerable uncertainty. A comparison of the results given in Table VI with those in the list of 1646 stars shows a mean difference of $0^M.5$, the absolute magnitudes in Table VI being the fainter. The difference is systematic although much of it is due to a small number of stars. We consider the parallaxes given in Table VI as superior to the earlier values and hope by means of these results to form a connection between the two systems which will render them consistent with one another.

[1] *Mt. Wilson Contr.*, No. 199; *Astrophysical Journal*, **53**, 13, 1921.

In conclusion, we may call attention to the agreement of the results of this investigation with those obtained by Lindblad[1] through a spectrophotometric study of the intensity of the continuous spectrum. Lindblad found that the region λ 3889–λ 3907, when compared with the adjacent region λ 3907–λ 3935, was relatively less intense in the spectrum of the intrinsically fainter stars. This effect he ascribed to the expansion of the wings of Hζ in such stars, as well as to the widening of certain of the arc lines of iron and silicon. In other words, the spectra of such stars are diffuse, and we obtain the same differentiation between the absolute magnitudes of stars with sharp and diffuse lines that has been found by other methods in the course of this investigation.

It is hardly necessary to state that the methods described in this communication can no doubt be greatly improved and refined. They appear capable, however, of yielding results of considerable value for the stars belonging to the largest of the spectral types. In addition, it seems probable that similar methods may be applied to the stars of the B type. It is well known from the work of several investigators that the stars of types B8 and B9 are considerably fainter intrinsically than those of the earlier divisions like B0 and B1. There is a strong probability, therefore, that a relationship between spectral type and absolute magnitude similar to that found for the A stars exists among those of type B.

SUMMARY

The principal results of this study may be summarized briefly.

1. A considerable number of A-type stars belonging to the Taurus and Ursa Major groups have been classified as accurately as possible into the subdivisions of this type and the spectra designated as nebulous or sharp according to the character of the lines.

2. From a comparison of the results a definite relationship between absolute magnitude and spectral type, as well as between absolute magnitude and the sharp or diffuse character of the lines, has been established.

---

[1] *Mt. Wilson Contr.*, No. 228; *Astrophysical Journal*, **55**, 85, 1922.

3. Through an extension to stars with parallaxes determined by trigonometric methods, it is found that the same relationships are valid for stars outside of the moving clusters.

4. When this method for the determination of absolute magnitudes is applied to individual stars, a degree of accuracy is found quite comparable with that for stars of the later spectral types.

5. A catalogue of the parallaxes of 544 stars derived in this way is given.

6. A comparison between the average of the proper motions and the average of the parallaxes of these stars shows a satisfactory degree of correlation between the two.

7. The stars such as α Cygni having the so-called "c" characteristics require separate treatment. It seems probable that the intensities of the well-known enhanced lines λ 4481 and λ 4233 may be used as criteria for the determination of the absolute magnitudes of such stars. The same lines may perhaps be used for intrinsically faint A-type stars, in which these lines are very weak.

MOUNT WILSON OBSERVATORY
May 1922

Contributions from the Mount Wilson Observatory, No. 245
Reprinted from the *Astrophysical Journal*, Vol. LVI, pp. 265–294, 1922

THE DISTRIBUTION OF THE VELOCITIES OF STARS OF SPECTRAL TYPES F TO M

By GUSTAF STRÖMBERG

ABSTRACT

Frequency-distribution of the velocity-vectors of stars of types F to M.—The three components of the velocities of about 1300 stars were computed from available data and referred to the galactic system of co-ordinates, assuming a solar motion of 20 km toward the apex $\alpha = 270^\circ$, $\delta = +30^\circ$. The frequency-distribution of the velocity-vectors in each of six groups, including, respectively, types A6–F9, F0–G5, G6–K1, K2–K9, Ma–Md, G0–M, and magnitudes 0–6, <3, <4, <4, <3, >3, was represented by a three-dimensional cosine-series with a large number of terms determined by harmonic analysis. From these results curves of equal frequency were drawn in the xy- and yz-planes (Figs. 1–6). It is evident from these that *giant stars* of types F to M form a single group or stream with an approximately ellipsoidal distribution, the shortest axis being nearly in the direction of the galactic pole. The elongation of the ellipsoid is greatest for the bright F stars and least for the late K and M stars, for which the distribution is nearly spherical. Among stars of spectral type F and magnitude 0 to 6 an additional stream was found moving nearly parallel with the Taurus group and including about one-fifth of the stars of this type. There is a marked asymmetry in the distribution of velocities, especially for the higher velocities. As a result, the most frequent velocity coincides neither with the mean velocity nor with the center of the velocity-ellipsoid, but has the values given in Table VII, being 13.4 km in the direction $\alpha = 86^\circ.2$, $\delta = -30^\circ.8$ (relative to the sun) for the giant stars. Another consequence of the asymmetry is that the constants of the ellipsoidal frequency-function depend somewhat on the method of computation on account of the difference in weighting the high velocities. The results of two methods are given (Tables IV, V, and VI). The *dwarf stars* also form a single group and show an ellipsoidal distribution of velocities, the most frequent velocity being 37.7 km in the direction $\alpha = 98^\circ.8$, $\delta = -17^\circ.4$ (relative to the sun).

Solar motion derived from the algebraic means of velocities of stars of types F to M is found to be dependent on the spectral types and absolute magnitudes of the group of stars used. Giant stars of later types give a somewhat higher declination of the apex ($+44^\circ$) than stars of earlier types ($+27^\circ$), while dwarf stars give $+30^\circ$. The velocity from giants comes out 18.8 km while dwarfs give 31.7 km; in fact, stars of high velocity give, in general, a higher solar motion than slower stars, which indicates that the high-velocity stars have a systematic motion in a direction opposite to the sun's motion.

The large number of spectroscopic parallaxes recently determined by Mr. Adams and his collaborators[1] has made it possible to compute the absolute motions in space of about 1300 stars for which the proper motions and radial velocities are determined. The fact that the errors of the spectroscopic parallaxes are proportional to the parallaxes themselves makes them in general better adapted to this purpose than the trigonometric parallaxes. A large number of radial velocities have been determined at the Mount Wilson Observatory during recent years, and I am greatly indebted to my colleagues engaged in this work for permission to use these, as well as the spectroscopic parallaxes, in advance of publication.

---

[1] *Mt. Wilson Contr.*, No. 199; *Astrophysical Journal*, **53**, 13, 1921.

The result of a study of the space-velocities, irrespective of their directions, was published in *Mount Wilson Contribution* No. 210; *Astrophysical Journal*, **54**, 9, 1921. Since it is well known that the frequency of velocity-vectors of a given size is quite different in different directions, a detailed study has been made of the general distribution of the three-dimensional velocities. In order to obtain the general character of this distribution, the possible dependency of the velocity-distribution upon position in space was neglected. The known dependency of velocity upon absolute magnitude and spectral type has been taken into account to some extent by grouping the stars according to spectral type and for each type dividing them into two groups of different absolute magnitudes.

COMPUTATION OF THE VELOCITY-COMPONENTS

The three co-ordinates of a star relative to the sun and referred to the equatorial system are

$$\Xi = D \cos \alpha \cos \delta\,; \quad \mathrm{H} = D \sin \alpha \cos \delta\,; \quad \mathrm{Z} = D \sin \delta\,,$$

where α and δ are the right ascension and declination of the star and D its distance from the sun in kilometers. Differentiating these equations with respect to the time, we obtain the three velocity-components in the equatorial system relative to the sun:

$$\left.\begin{aligned} \xi &= \frac{d\Xi}{dt} = V \cos \alpha \cos \delta - \frac{k}{\pi}(\mu_\alpha \sin \alpha \cos \delta + \mu_\delta \cos \alpha \sin \delta) \\ \eta &= \frac{d\mathrm{H}}{dt} = V \sin \alpha \cos \delta + \frac{k}{\pi}(\mu_\alpha \cos \alpha \cos \delta - \mu_\delta \sin \alpha \sin \delta) \\ \zeta &= \frac{d\mathrm{Z}}{dt} = V \sin \delta + \frac{k}{\pi}\mu_\delta \cos \delta \end{aligned}\right\} \qquad (1)$$

where V is the radial velocity relative to the sun, μ_α and μ_δ are the proper motions in right ascension and declination expressed in seconds of arc per year, π is the parallax, and k is the mean distance earth–sun in kilometers, divided by the number of seconds in a year. We have thus $k = 4.737$ km year/sec.

The proper motions have been taken from Boss's *Catalogue* and corrected according to the formula:[1]

$$\Delta\mu_{\alpha}^{s} = +0\overset{s}{.}00021 - 0\overset{s}{.}00015 \sin\alpha \tan\delta$$
$$\Delta\mu_{\delta}'' = -0\overset{''}{.}0023 \cos\alpha$$

For stars not in the Boss *Catalogue* the proper motions have in most cases been taken from the *Publications of the Cincinnati Observatory*, No. 18, Part IV, and in some cases, proper motions determined at Greenwich, and by Kapteyn, Roy, and others have been used. The radial velocities are from the lists published by the Lick, Mount Wilson, Yerkes, Cape, and other observatories, and in addition to these, use has been made of a large number of unpublished radial velocities determined at the Mount Wilson Observatory. The spectroscopic parallaxes have been used except in a few cases where the trigonometric parallaxes are large and well determined.

From this list of stars of known parallax, proper motion, and radial velocity, the following stars have been omitted: (1) the fainter components of binaries, the absolute magnitude used being that of the brighter component; (2) stars selected for observation on account of small proper motion, ninety-nine such stars being omitted; (3) spectroscopic binaries with large variation of the radial velocity for which the orbits are not determined. Many of the stars were of course selected for observation originally on account of large proper motion, but as this selection is mainly a selection of near and thus absolutely faint stars which have been treated separately, no omission is made for this reason. The inclusion of a large number of stars of large proper motion produces, however, an excess of stars of high speed among the giant stars.

SOLAR MOTION

If we form the means of the three velocity-components ξ, η, and ζ for a group of stars, we obtain the velocity of the "centroid" of this group of stars relative to the sun. The opposite vector is the velocity of the sun relative to this centroid. The polar co-ordinates of this vector are given by the equations:

---

[1] *Op. cit.*, p. xxviii.

$$\left.\begin{aligned} V_0 \cos A_0 \cos D_0 &= -\bar{\xi} \\ V_0 \sin A_0 \cos D_0 &= -\bar{\eta} \\ V_0 \sin D_0 &= -\bar{\zeta} \end{aligned}\right\} \qquad (2)$$

where A_0 and D_0 are the right ascension and declination of the sun's apex and V_0 is the solar velocity. Table I gives the results of this computation for different spectral types and absolute magnitudes. In this case all stars with a space-velocity higher than 100 km have been omitted.

TABLE I

Spectral Type	Absolute Magnitude	Number	A_0	D_0	V_0
A6 to F9	≤ 3.0	153	269°	+27°	21.2
	≥ 3.1	133	274	+35	23.4
G0 to G9	≤ 3.0	224	266	+32	19.9
	≥ 3.1	154	279	+23	40.2
K0 to K9	≤ 4.0	325	282	+43	18.3
	≥ 4.1	112	286	+31	33.1
M	<4.0	98	271	+44	16.2
	>6.0	16	354:	+68:	26.6:
A6 to M	Giants	800	272.7	+36.9	18.8
A6 to M	Dwarfs	415	280.8	+29.5	31.7

From Table I we see that for the giant stars the declination of the sun's apex shows a steady increase from +27° to +44°, which is in agreement with the results of several investigators who have determined its value from proper motions. This increase of the declination of the sun's apex with advancing spectral type was found by Dyson and Thackeray[1] to be especially pronounced among the faint stars in the zone +24° to +32°, and was attributed by them to an increase in the proportion of stars belonging to the second stream among stars of later types. That this explanation is in agreement with the results obtained in the present investigation will be seen later.

---

[1] *Monthly Notices of the Royal Astronomical Society*, **79**, 201, 1919.

Another conclusion to be drawn from Table I is that the dwarf stars apparently show a higher velocity for the sun than the giant stars. This result seems to explain the peculiar fact that the velocity of the sun as determined from the Mount Wilson radial velocities is somewhat larger than the original values of Campbell. The proportion of faint stars of large proper motion measured for radial velocity, most of which are dwarf stars, is fairly large among the stars observed at the Mount Wilson Observatory.

This increase in the velocity of the sun is especially marked if we group the stars according to space-velocity. This velocity, v, corrected for a standard solar motion of 20 km toward the point $\alpha=270^\circ$, $\delta=+30^\circ$, has been computed for each star according to the formula

$$v^2=\xi^2+(\eta-17.3)^2+(\zeta+10.0)^2.$$

Grouping the stars according to this space-velocity, v, and computing the solar motion for each group, we find a very great increase of the sun's motion with increasing space-velocity of the stars (Table II). This indicates that the stars of high velocity have a systematic motion opposite to the sun's motion, a result which was found by Adams and Joy[1] from a study of the space motion of thirty-seven stars of large radial velocity.

TABLE II

v	No.	$A_\odot$	$D_\odot$	$V_\odot$
km				km
0 to 60	1026	272°1	+29°5	20.6
60 to 100	210	295.4	+43.4	36.3
100 to 150	50	288.9	+38.6	75.7
>150	37	313.1	+53.8	209.1

DISTRIBUTION OF VELOCITIES

The solar motion is only one of a large number of characteristics which determine the general distribution of the velocities. To describe this distribution we may think of a certain number of stars starting at the same moment from a common origin with velocities equal and parallel to their velocities in space. After one second they will have spread out into a cluster, the mean density of which at a certain point is proportional to the probability that a star of this group has the velocity corresponding to the point in question. In studying this distribution two different types of frequency-functions have been used, viz., those based upon the two-drift theory of Kapteyn and the ellipsoidal theory of Schwarzschild. In order to make an inductive study of the distribution of the velocity-vectors without restricting ourselves to a special frequency-function, a more general type of function has to be used. One such function has been introduced by Charlier[1] for a "unitary statistical population" with three variables. The practical application of this function, however, requires the use of moments of high order, and this necessarily gives the stars of high velocity a much higher weight in the determination of the constants of the function than stars of low velocity. In the present case we are dealing with fairly small groups of stars and, on account of the selection of stars of large proper motion, too great a proportion of stars of high speed has probably been included. Hence it is especially important, at least when dealing with linear velocities, to use a function, the constants of which can be determined *directly* from the *numbers* of stars whose velocity-vectors lie between certain limits. To obtain the general character of the distribution of the velocities, we need, therefore, a general interpolation formula in three dimensions which can easily be integrated and whose constants can be determined simply from the integrated function. For this purpose use has been made of a three-dimensional cosine-series with the origin in the center of the limiting planes. Such a series can be written

---

[1] *Mt. Wilson Contr.*, No. 163; *Astrophysical Journal*, **49**, 179, 1919.

$$\left.\begin{aligned} F(xyz)=a_0&+a_{100}\sin\alpha+a_{010}\sin\beta+a_{001}\sin\gamma+a_{200}\cos 2\alpha+a_{110}\sin\alpha\sin\beta\\ &+a_{101}\sin\alpha\sin\gamma+a_{020}\cos 2\beta+a_{011}\sin\beta\sin\gamma+a_{002}\cos 2\gamma\\ &+a_{300}\sin 3\alpha+a_{210}\cos 2\alpha\sin\beta+a_{201}\cos 2\alpha\sin\gamma+a_{120}\sin\alpha\cos 2\beta\\ &+a_{111}\sin\alpha\sin\beta\sin\gamma+\ .\ .\ .\ .\ . \end{aligned}\right\}\qquad(3)$$

---

[1] *Meddelanden från Lunds Observatorium*, Serie II, No. 9, p. 79, 1913.

where

$$\alpha=\frac{x\pi}{2c_1}, \quad \beta=\frac{y\pi}{2c_2}, \quad \gamma=\frac{z\pi}{2c_3}.$$

The six limiting planes are $x=\pm c_1$, $y=\pm c_2$, $z=\pm c_3$. The three angles α, β, and γ vary between the limits $-\pi/2$ and $+\pi/2$. The only assumptions made in using this frequency-function are that the number of velocity-vectors terminating in a cube $dx\,dy\,dz$ varies continuously with x, y, and z, and that

$$\frac{dF}{dx}=0, \quad \frac{dF}{dy}=0, \quad \text{and} \quad \frac{dF}{dz}=0 \quad \text{for} \quad x=\pm c_1, \quad y=\pm c_2, \quad z=\pm c_3,$$

respectively.

The disadvantages of this function are that we must use a very large number of terms, and even then it may not be possible to represent the more rapid changes of the mean density of the velocity-cluster. The function is characterized by a large number of coefficients, and it is necessary to plot it graphically in order to gain an idea of its general character. It is, however, a convenient means for obtaining some information about the *actual* distribution of velocities, from which we can afterward decide what type of theoretical frequency-function can best be adopted.

The number of velocity-vectors of a group of stars terminating in a cube $dx\,dy\,dz$ is expressed by

$$F(xyz)\,dx\,dy\,dz\,.$$

Integrating this function between the limits x_1, x_2; y_1, y_2; z_1, z_2, we find

$$\left.\begin{aligned}\int_{x_1}^{x_2}\int_{y_1}^{y_2}\int_{z_1}^{z_2} F(xyz)dx\,dy\,dz=A(&A_0+A_{100}\sin\bar{\alpha}+A_{010}\sin\bar{\beta}+A_{001}\sin\bar{\gamma}\\ &+A_{200}\cos 2\bar{\alpha}+A_{110}\sin\bar{\alpha}\sin\bar{\beta}+A_{101}\sin\bar{\alpha}\sin\bar{\gamma}\\ &+A_{020}\cos 2\bar{\beta}+A_{011}\sin\bar{\beta}\sin\bar{\gamma}+A_{002}\cos 2\bar{\gamma}+A_{300}\sin 3\bar{\alpha}\\ &+A_{210}\cos 2\bar{\alpha}\sin\bar{\beta}+\;.\;.\;.\;.)\end{aligned}\right\}(4)$$

where

$$A=(x_2-x_1)(y_2-y_1)(z_2-z_1).$$

$$\bar{\alpha}=\tfrac{1}{2}(\alpha_1+\alpha_2)=\frac{\pi}{4c_1}(x_1+x_2)$$

$$\bar{\beta}=\tfrac{1}{2}(\beta_1+\beta_2)=\frac{\pi}{4c_2}(y_1+y_2)$$

$$\bar{\gamma}=\tfrac{1}{2}(\gamma_1+\gamma_2)=\frac{\pi}{4c_3}(z_1+z_2)$$

$$A_{lmn}=k_l k_m k_n a_{lmn}$$

$$k_l=\frac{\sin\frac{l\Delta\alpha}{2}}{\frac{l\Delta\alpha}{2}}\;;\quad \Delta\alpha=\alpha_2-\alpha_1=\frac{\pi}{2c_1}(x_2-x_1)$$

$$k_m=\frac{\sin\frac{m\Delta\beta}{2}}{\frac{m\Delta\beta}{2}}\;;\quad \Delta\beta=\beta_2-\beta_1=\frac{\pi}{2c_2}(y_2-y_1)$$

$$k_n=\frac{\sin\frac{n\Delta\gamma}{2}}{\frac{n\Delta\gamma}{2}}\;;\quad \Delta\gamma=\gamma_2-\gamma_1=\frac{\pi}{2c_3}(z_2-z_1)\,.$$

As the unit of volume, we have for convenience used 1000 km^3; thus we have to replace the A just given by

$$0.001(x_2-x_1)(y_2-y_1)(z_2-z_1).$$

Starting with a group of N stars of a certain range in spectral type and absolute magnitude, we can compute how many rectilinear velocity-components fall inside a parallelopiped inclosed by the planes $x=x_1$; $x=x_2$; $y=y_1$; $y=y_2$; $z=z_1$; $z=z_2$. If N is the total number of stars in the group and n is the number of velocity-vectors terminating inside this parallelopiped, we have equations of condition of the form

$$N\int_{x_1}^{x_2}\int_{y_1}^{y_2}\int_{z_1}^{z_2}F(xyz)dx\,dy\,dz=NA(A_0+A_{100}\sin\bar{\alpha}$$
$$+A_{010}\sin\bar{\beta}+\;.\;.\;.\;.)=n. \quad (5)$$

The computation of the constants of the series is very much facilitated by dividing the distances $-c_1$ to $+c_1$, $-c_2$ to $+c_2$, $-c_3$ to $+c_3$ into p_1, p_2, and p_3 equal parts, respectively, the p's being even numbers.

The solution of the equations of condition (5) is then simplified by the relationships

$$\left.\begin{aligned}
\Sigma \sin^2 \bar{\alpha} &= \Sigma \cos^2 2\bar{\alpha} = \Sigma \sin^2 3\bar{\alpha} = \Sigma \cos^2 4\bar{\alpha}, \text{ etc.} = \frac{p_1}{2} \\
\Sigma \sin^2 \bar{\beta} &= \Sigma \cos^2 2\bar{\beta} = \Sigma \sin^2 3\bar{\beta} = \Sigma \cos^2 4\bar{\beta}, \text{ etc.} = \frac{p_2}{2} \\
\Sigma \sin^2 \bar{\gamma} &= \Sigma \cos^2 2\bar{\gamma} = \Sigma \sin^2 3\bar{\gamma} = \Sigma \cos^2 4\bar{\gamma}, \text{ etc.} = \frac{p_3}{2}
\end{aligned}\right\} \qquad (6)$$

All the products in the least-squares solution vanish, and we have, for example,

$$NAA_0 = \frac{\Sigma n}{p_1 p_2 p_3}, \quad NAA_{100} = \frac{2\Sigma n \sin \bar{\alpha}}{p_1 p_2 p_3}, \quad NAA_{020} = \frac{2\Sigma n \cos 2\bar{\alpha}}{p_1 p_2 p_3},$$

$$NAA_{111} = \frac{8\Sigma n \sin \bar{\alpha} \sin \bar{\beta} \sin \bar{\gamma}}{p_1 p_2 p_3}, \quad NAA_{231} = \frac{8\Sigma n \cos 2\bar{\alpha} \sin 3\bar{\beta} \sin \bar{\gamma}}{p_1 p_2 p_3}.$$

When the coefficients A_{lmn} have been determined, the coefficients a_{lmn} are found from the equation

$$a_{lmn} = \frac{1}{k_l k_m k_n} A_{lmn}.$$

The total number of stars in the group has been reduced to 1000, and the series $F = a_0 + a_{100} \sin \alpha + a_{010} \sin \beta \ldots.$, gives us then the number of velocity-vectors terminating in a cube of 10 km on the edge, the center of which is in the point x, y, z.

The fact that the motions of the stars are related to the plane of the galaxy makes it convenient to use galactic co-ordinates instead of equatorial. In order to have the origin near the center of the distribution, we have corrected all velocities for a standard solar motion of 20 km toward the point $A_0 = 270^\circ$, $D_0 = +30^\circ$. The pole of the galaxy is supposed to have the position $\alpha = 190^\circ\!.6$, $\delta = +27^\circ\!.2$ (Kapteyn).

If x, y, and z denote the galactic co-ordinates, we have the following equations of transformation:

$$\left.\begin{aligned} x&=+0.185\,\xi-0.983\,\eta+17.0 \\ y&=+0.449\,\xi+0.084\,\eta+0.889\,\zeta+7.4 \\ z&=-0.874\,\xi-0.164\,\eta+0.457\,\zeta+7.4 \end{aligned}\right\} \qquad (7)$$

All constants derived from the frequency-functions are given in this system of co-ordinates. They can readily be converted into equatorial co-ordinates relative to the sun by aid of the equations

$$\left.\begin{aligned} \xi&=v\cos\alpha\cos\delta=+0.185x+0.449y-0.874z \\ \eta&=v\sin\alpha\cos\delta=-0.983x+0.084y-0.164z+17.3 \\ \zeta&=v\sin\delta\qquad\;\;=\qquad\quad +0.889y+0.457z-10.0 \end{aligned}\right\} \qquad (8)$$

In Table III are given some data for the six different groups for which the coefficients in the series have been computed. The first two of these groups are overlapping. All terms up to the sixth order have been computed and in some cases terms of an even higher order. The total number of stars is in all cases reduced to 1000, and the unit of volume is 1000 km³. The most frequent velocity corresponds to the point of highest density in the velocity-cluster, and such a point is inclosed by non-intersecting surfaces of equal density. The intersections of these equi-frequential surfaces with any plane are closed curves surrounding the point or points of highest density.

TABLE III

	GROUP					
	I	II	III	IV	V	VI
Spectrum	A6 to F9	F0 to G5	G6 to K1	K2 to K9	Ma to Md	G0 to M
Absolute magnitude	0.0 to 5.5	≤ 2.9	≤ 3.9	≤ 3.9	<3	≥ 3.0
c_1	40	40	60	60	60	160
c_2	30	30	60	60	60	160
c_3	30	30	60	60	60	160
Number of stars	278	197	252	220	115	343
Number within limits	174	148	231	205	108	340
Taurus stars omitted	9	4	5	0	0	0

In Figures 1 to 6 are shown the intersections of the surfaces of equal frequency with the *xy*-plane (galactic plane) and the *xz*-plane. The *x*-axis is directed toward the intersection of the galactic plane with the equator (in Aquila). The velocity of the sun in this system of co-ordinates has the components +17.0, +7.4, and +7.4 km, and is denoted by the symbol ⊙. The recognized members of the Taurus stream were omitted in the computation but are marked in the diagram by crosses. The dots in the diagrams represent the velocities of those stars whose velocity-components perpendicular to the plane of projection are small, the limits in Figures 1 and 2 being ± 10 km and in Figures 3 to 5, ± 20 km. For the dwarf stars in Figure 6 the projections in the *xy*- and *xz*-planes of the velocities of all the stars are given.

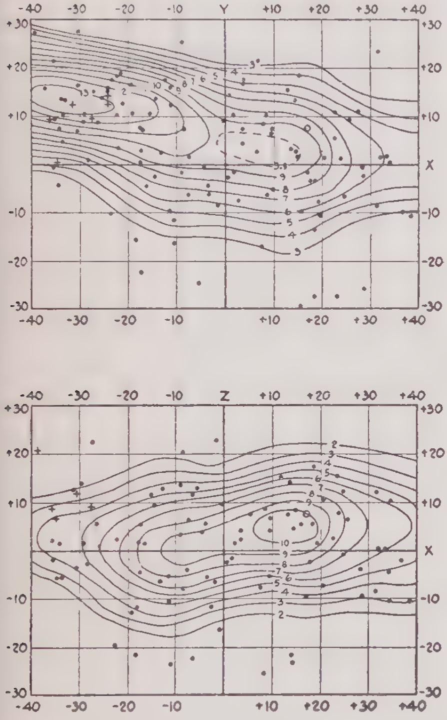

A6 to F9; M = 0.0 to 5.5

FIG. 1

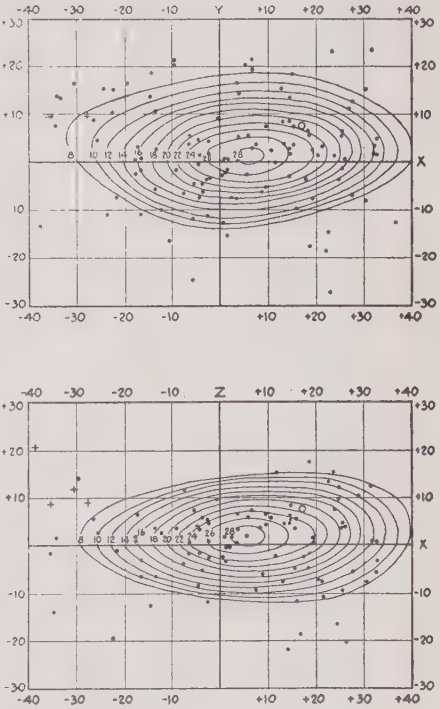

Fo to G5 M ≤ 2.9

FIG. 2

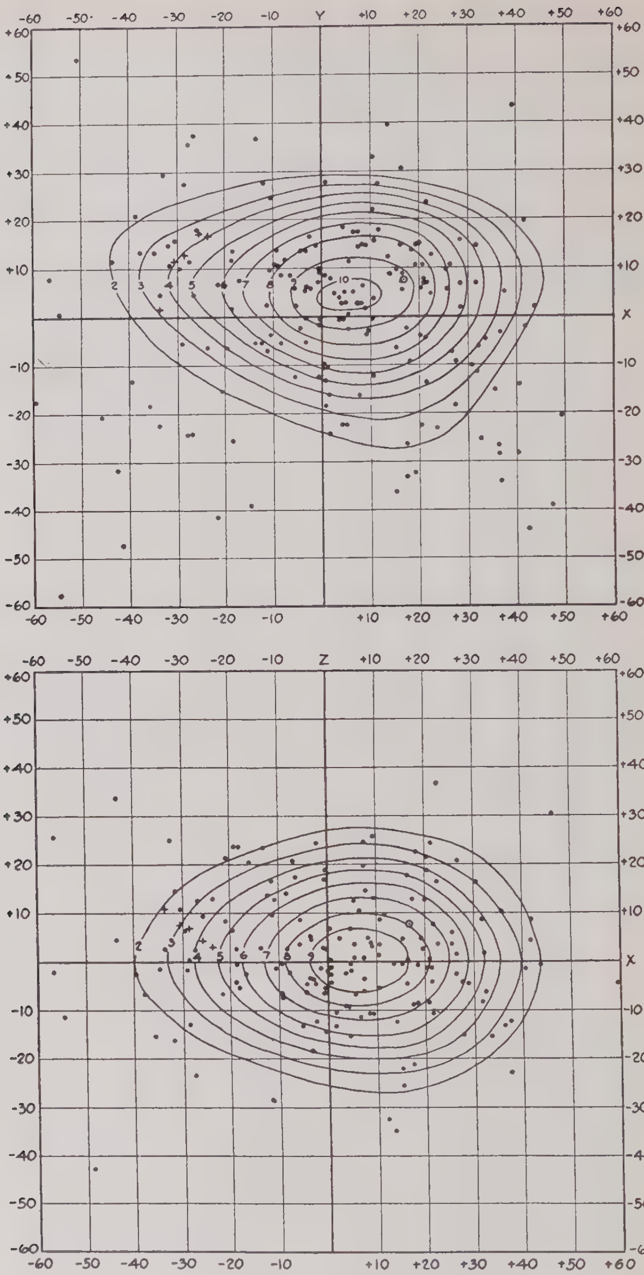

G6 to K1, M≦3.9

FIG. 3

A study of the diagrams in Figures 1 to 6 and the series upon which they are based leads to the following conclusions:

1. The giant stars of all types form a single "group" with an approximately ellipsoidal distribution, the longest and the intermediate axes in all cases lying very nearly in the galactic plane and coinciding approximately with the x- and y-axes. The shortest axis is nearly perpendicular to the galactic plane. The elongation of the ellipsoids is largest for the bright F stars and decreases for later types, the distribution being nearly spherical for the later K and the M stars.

2. The spread of the velocity-cluster increases with advancing spectral type and is much larger for the dwarf stars than for the giant stars.

3. The most frequent velocity does not coincide with the origin but lies for all the groups of giant stars in the first quadrant of the xy-plane and has the approximate values, $x=+5.8$, $y=+2.7$, $z=+1.7$ km. Relative to the sun this velocity is 13.4 km toward the point $\alpha=86°$, $\delta=-31°$.

4. If we exclude the very brightest F stars, many of which are Cepheid variables and stars of similar spectra, and take together stars of types A6 to F9, absolute magnitude 0 to 5.5, we find that these stars divide themselves into two streams. One of these coincides with the general group of giant stars, as can be seen from the agreement of its condensation point with that of the giant stars of other spectral types, while the other stream moves nearly parallel to the Taurus group. This latter stream comprises about 20 per cent of the ordinary stars of F type and its existence seems to indicate that a large number of stars of this spectral type in all regions of the sky are traveling with a velocity nearly identical with that of the Taurus group. Even among the brighter F stars, as well as among the G-type giants, the presence of members of this group is indicated by the protruding form of the equi-frequential surfaces in this region. This stream might be identified with Kapteyn's first drift, although the galactic latitude is not quite zero.

5. The dwarf stars, among which have been included stars of spectral types G0 to M of absolute magnitude fainter than 3.0, seem to form a group of their own as regards their motions. The

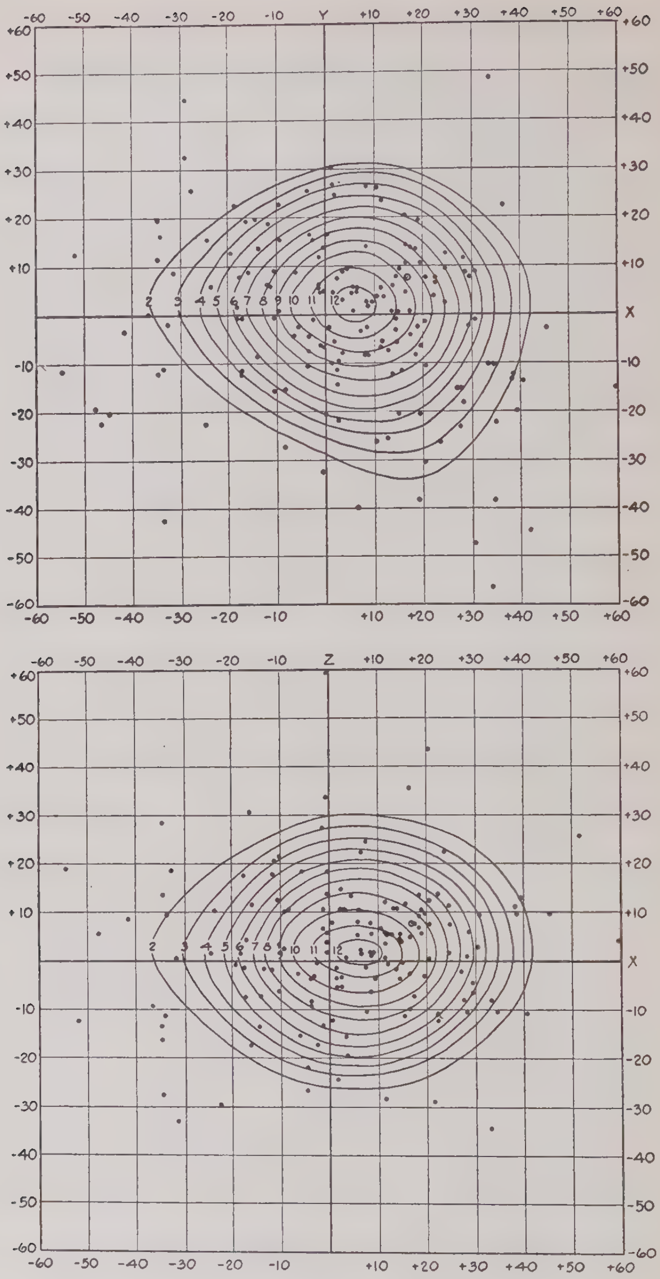

K2 to K9; $M \leqq 3.9$

FIG. 4

distribution of the velocities is ellipsoidal, with the major axis forming an angle of about 160° with the x-axis. The most frequent velocity is approximately $x=-19$, $y=-2$, $z=+1$ km, which nearly coincides with Kapteyn's first drift, while his second drift has been swallowed up by the ellipsoidal stream of giant stars.

6. There is a very marked asymmetry in the distribution of the velocities around the most frequent velocity-vector. The stars of high velocity show a tendency to avoid the first quadrant of the xy-plane. This produces a difference between the most frequent velocity and the mean velocity. The latter nearly coincides with the origin if the stars of very high speed are omitted, as was shown in the values for the solar motion given before. That this asymmetry is not due to any selection of stars of large proper motion moving opposite to the sun is shown by a study of the velocity-distribution of stars having very high speeds. In the diagram in Figure 7 are plotted the projections in the xy-plane of the velocities of the stars having space motions larger than 100 km relative to the origin. The effect of the selection of large proper motions relative to the sun instead of to our adopted origin is then insignificant, and we find that, whatever the spectral type or the absolute magnitude, if the velocity of a star is great there is an avoidance of the first quadrant of the xy-plane.[1] No star of speed higher than 100 km is moving in this direction, a result in agreement with that found by Adams and Joy[2] for stars of high radial velocity.

Different methods can be employed to obtain the constants of the frequency-functions. For all groups of stars except Group I we may use the ellipsoidal theory to represent approximately the distribution. We then disregard the asymmetry already alluded to and the excess of stars of high velocity which has been found to exist when a comparison is made with the distribution of velocities as given by Maxwell's law.[3] The first method was to use the

[1] Dr. Merrill has called my attention to the fact that this asymmetry in the motion of stars of high velocity is also indicated by the high value of the solar motion as derived from Md stars and bright-line nebulae. The former have a residual radial velocity of 31 km and give a velocity of the sun of 56 km (P. W. Merrill, *Popular Astronomy*, **29**, 637, 1921). The latter have a residual radial velocity of 30 km and give a velocity of the sun of 29 km (*Lick Observatory Publication*, **13**).

[2] *Loc. cit.*

[3] *Mt. Wilson Contr.*, No. 210; *Astrophysical Journal*, **54**, 9, 1921.

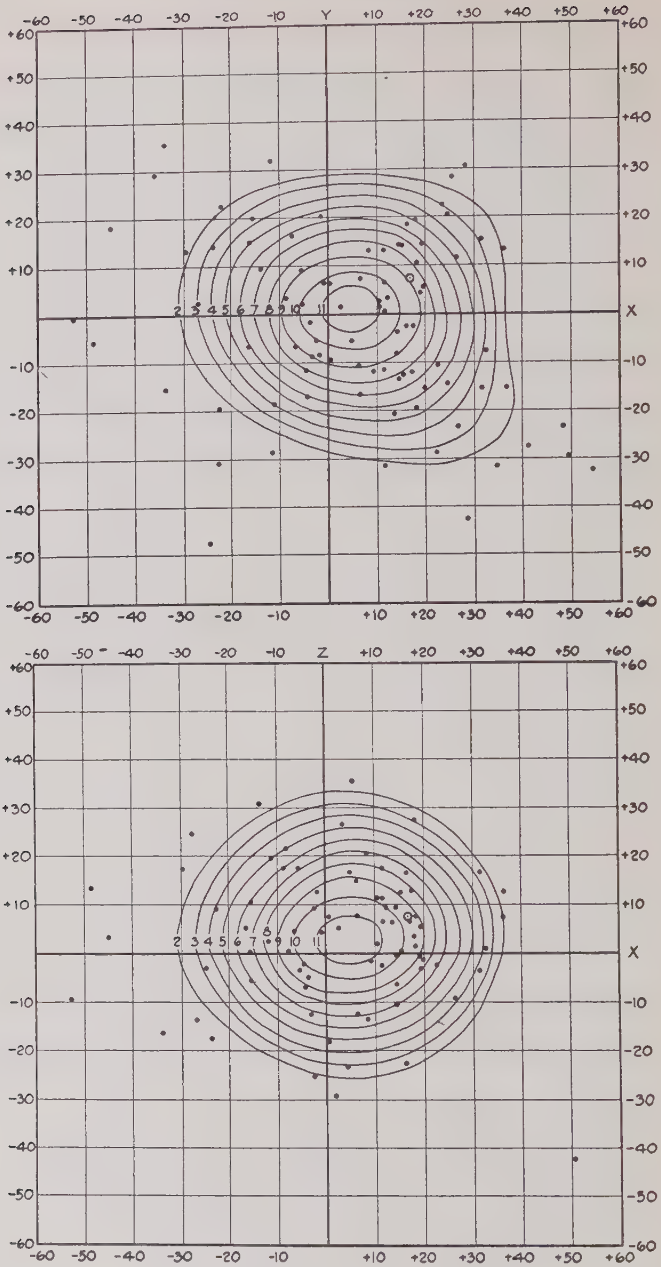

Ma to Md M< 2.0

FIG. 5

trigonometric series already determined, and from the coefficients to derive the moments of first and second order. We thus diminish to a large extent the effect of the higher velocities, although in a somewhat arbitrary way.

The values of $\bar{x}$, $\bar{y}$, $\bar{z}$, $\overline{x^2}$, $\overline{yx}$, etc., can be found from the relations

$$\left.\begin{aligned} k\overline{x^l y^m z^n} &= \int_{-c_1}^{c_1}\int_{-c_2}^{c_2}\int_{-c_3}^{c_3} x^l y^m z^n F(xyz)dx\,dy\,dz \\ k &= \int_{-c_1}^{c_1}\int_{-c_2}^{c_2}\int_{-c_3}^{c_3} F(xyz)dx\,dz\,dy \end{aligned}\right\} \tag{9}$$

From the trigonometric series we find

$$\left.\begin{aligned} a_{000}\frac{\pi^2}{4c_1}\bar{x} &= a_{100}-\frac{a_{300}}{9}+\frac{a_{500}}{25}+\ldots+(-1)^{\frac{n-1}{2}}\frac{a_{n00}}{n^2} \\ a_{000}\frac{\pi^2}{4c_2}\bar{y} &= a_{010}-\frac{a_{030}}{9}+\frac{a_{050}}{25}-\ldots+(-1)^{\frac{n-1}{2}}\frac{a_{0n0}}{n^2} \\ a_{000}\frac{\pi^2}{4c_3}\bar{z} &= a_{001}-\frac{a_{003}}{9}+\frac{a_{005}}{25}-\ldots+(-1)^{\frac{n-1}{2}}\frac{a_{00n}}{n^2} \\ \overline{x^2} &= \frac{c_1^2}{3}-\frac{8c_1^2}{a_{000}\pi^2}\left[\frac{a_{200}}{2^2}-\frac{a_{400}}{4^2}+\ldots+(-1)^{\frac{n}{2}+1}\frac{a_{n00}}{n^2}\right] \\ \overline{y^2} &= \frac{c_2^2}{3}-\frac{8c_2^2}{a_{000}\pi^2}\left[\frac{a_{020}}{2^2}-\frac{a_{040}}{4^2}+\ldots+(-1)^{\frac{n}{2}+1}\frac{a_{0n0}}{n^2}\right] \\ \overline{z^2} &= \frac{c_3^2}{3}-\frac{8c_3^2}{a_{000}\pi^2}\left[\frac{a_{002}}{2^2}-\frac{a_{004}}{4^2}+\ldots+(-1)^{\frac{n}{2}+1}\frac{a_{00n}}{n^2}\right] \\ \frac{a_{000}\pi^4}{16c_1c_2}\overline{xy} &= a_{110}-\frac{a_{310}}{9}-\frac{a_{130}}{9}+\frac{a_{510}}{25}+\frac{a_{330}}{81}+\frac{a_{150}}{25}+\ldots+(-1)^{\frac{m+n}{2}-1}\frac{a_{mn0}}{m^2n^2} \\ \frac{a_{000}\pi^4}{16c_1c_3}\overline{xz} &= a_{101}-\frac{a_{301}}{9}-\frac{a_{103}}{9}+\frac{a_{501}}{25}+\frac{a_{303}}{81}+\frac{a_{105}}{25}+\ldots+(-1)^{\frac{m+n}{2}-1}\frac{a_{m0n}}{m^2n^2} \\ \frac{a_{000}\pi^4}{16c_2c_3}\overline{yz} &= a_{011}-\frac{a_{031}}{9}-\frac{a_{033}}{9}+\frac{a_{051}}{25}+\frac{a_{033}}{81}+\frac{a_{015}}{25}+\ldots+(-1)^{\frac{m+n}{2}-1}\frac{a_{0mn}}{m^2n^2} \end{aligned}\right\} \tag{10}$$

From these moments we can determine the axes upon which we have to project the velocity-components in order to make the sum

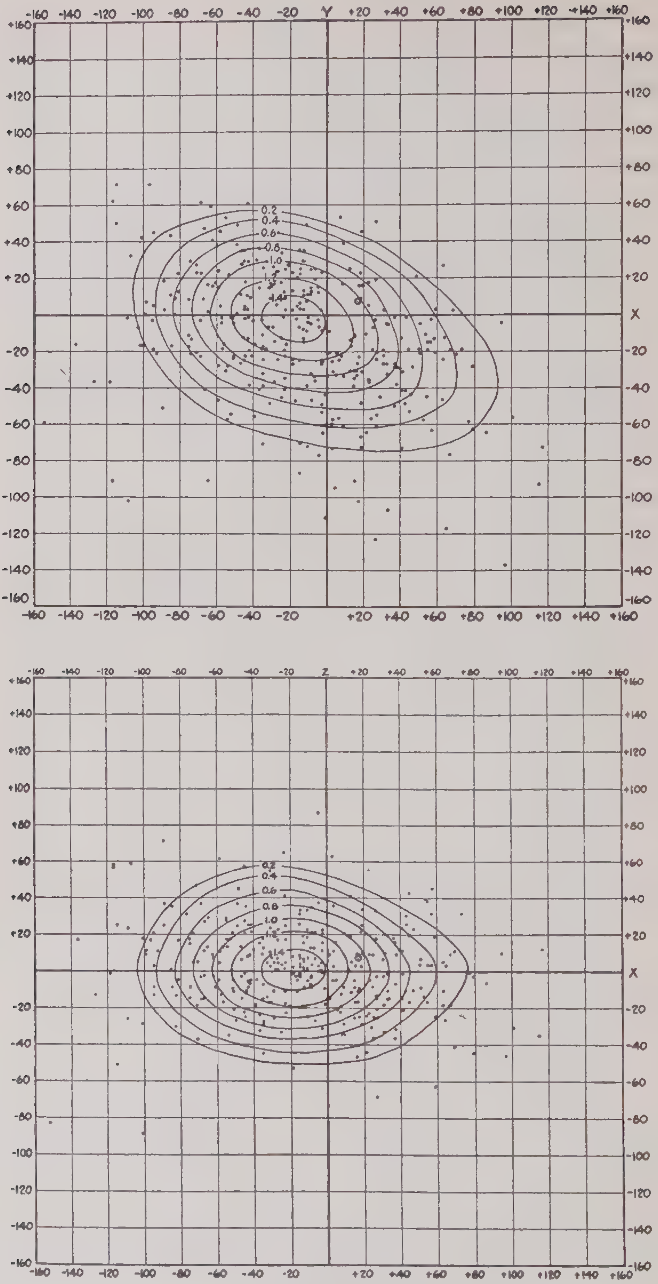

Go to Md : M ≧ 3.0

FIG. 6

of the squares of the projected velocities a maximum or a minimum. We thus obtain the principal axes of the velocity-ellipsoids, except for the effect of the stars outside the planes $\pm c_1$, $\pm c_2$, and $\pm c_3$, which have been omitted. We should expect in this case to find the length of the axes somewhat smaller than if they had been computed directly from all the velocity-components. On the other hand, the directions of the axes can be determined with higher accuracy than if the high-velocity stars had been included. In Table IV are given the co-ordinates of the centroid as computed from the trigonometric series. For comparison the co-ordinates of the centroid computed directly from the velocity-components are added, as well as the co-ordinates of the axes of the velocity-ellipsoids. All of these results are in galactic co-ordinates.

TABLE IV

Constants of Velocity-Ellipsoids as Computed from Moments and Referred to the Galactic Co-ordinate System

Group	Centroid from Trig. Series			Centroid from Velocity Comp. of Stars within Limits			Centroid from Velocity Comp. of All Stars		
	$\bar{x}$	$\bar{y}$	$\bar{z}$	$\bar{x}$	$\bar{y}$	$\bar{z}$	$\bar{x}$	$\bar{y}$	$\bar{z}$
	km	km	km	km	km	km	km	km	km
I	−2.9	+3.0	0.0	−4.3	+3.6	+0.3	−11.9	−14.8	+1.3
II	+3.3	+2.0	+0.1	+2.0	+2.0	+0.3	+1.4	−3.4	−2.2
III	+1.6	−0.1	+1.3	+0.6	+0.2	+1.5	−1.7	−2.4	+0.8
IV	+3.8	−2.5	+2.4	+4.2	−1.9	+2.0	+1.8	−5.4	0.0
V	+5.5	−2.2	+0.3	+5.7	−2.0	+0.5	+5.1	−5.7	+0.3
VI	−16.1	−12.4	+1.3	−15.3	−13.3	+0.9	−15.9	−16.9	+0.2

Group	Major Axis of Ellipsoid			Intermediate Axis of Ellipsoid			Minor Axis of Ellipsoid		
	L	*B*	*a*	*L*	*B*	*b*	*L*	*B*	*c*
			km			km			km
II	173°	−3	18.9	83°	+6°	13.5	238°	+83°	8.9
III	181	−2	25.2	92	+16	20.2	265	+74	15.6
IV	158	+10	21.8	65	+16	18.8	280	+71	11.1
V	147	+11	23.5	54	+14	19.1	275	+72	16.1
VI	153	+5	51.3	63	+5	32.3	285	+83	22.6

The moments, however, are affected to an unequal extent by small changes in the larger and smaller velocities, and furthermore we have arbitrarily omitted stars of high velocity. This effect may be quite appreciable since we have reason to expect an excess of stars of high velocity compared with ellipsoidal distribution, and the influence of the asymmetry of the distribution may not be eliminated properly. Accordingly another method has been used which gives the constants of the ellipsoidal distribution directly from the observed *number* of velocity-components of definite size. Starting from approximate values of the constants of the function, we can compute corrections to these values from the differences between the observed and the computed number of velocity-vectors terminating in different regions of space. In order to simplify conditions we have to start from axes of co-ordinates which nearly coincide with the principal axes of the velocity-ellipsoids. We assume the following form for the frequency-function:

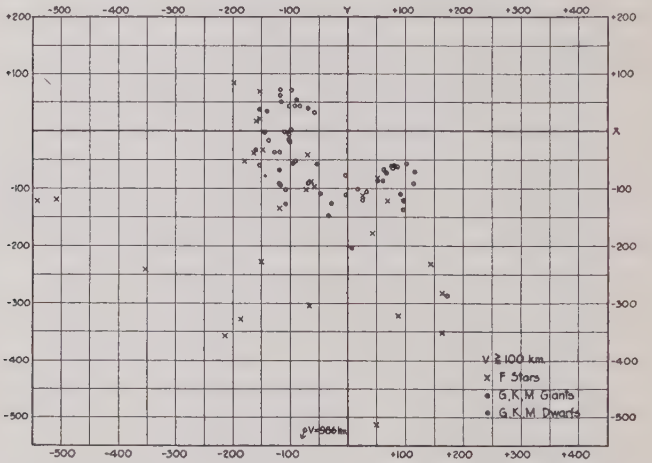

FIG. 7.—Projection on galactic plane of velocities of stars having speeds greater than 100 km per second.

$$F(x)dx\,dy\,dz = Ke^{-S}\,dx\,dy\,dz; \quad S = h_1^2\xi^2 + h_2^2\eta^2 + h_3^2\zeta^2 \,.$$

Integrating between infinite limits, we have for a total of 1000 stars

$$\int\!\!\int\!\!\int_{-\infty}^{+\infty} F(x)dx\,dy\,dz = K\frac{\pi^{3/2}}{h_1 h_2 h_3} = 1000$$

Thus

$$K=\frac{1000\, h_1 h_2 h_3}{\pi^{3/2}}.$$

The equation of the velocity-ellipsoid of Schwarzschild is then

$$\frac{\xi^2}{a^2}+\frac{\eta^2}{b^2}+\frac{\zeta^2}{c^2}=1=2S$$

and for the axes of the ellipsoid, in other words, the dispersion (mean square deviation) along the principal axes, we have

$$a=\frac{1}{\sqrt{2h_1}},\quad b=\frac{1}{\sqrt{2h_2}},\quad c=\frac{1}{\sqrt{2h_3}}.$$

We shall assume that the axes of the system of co-ordinates are approximately parallel to the principal axes of the ellipsoids. This assumption can be made in all cases except for the dwarf stars. For these a recomputation of the distribution has been made relative to another co-ordinate system turned through an angle of $-24°$ about the z-axis.

The co-ordinates ξ, η, ζ in the system of co-ordinates which corresponds to the principal axes of the ellipsoids and the center of which coincides with the center of the ellipsoids are connected with the co-ordinate system used previously by the equations

$$\left.\begin{aligned}\xi&=\alpha_1(x-x_0)+\alpha_2(y-y_0)+\alpha_3(z-z_0)\\ \eta&=\beta_1(x-x_0)+\beta_2(y-y_0)+\beta_3(z-z_0)\\ \gamma&=\gamma_1(x-x_0)+\gamma_2(y-y_0)+\gamma_3(z-z_0)\end{aligned}\right\}\qquad(11)$$

x_0, y_0, and z_0 here denote the co-ordinates of the center of the ellipsoid; α_1, α_2, and α_3, the direction cosines for the ξ-axis, etc.

Assuming approximate value of h_1, h_2, h_3, x_0, y_0, z_0 and $\alpha_1=\beta_2=\gamma_3=+1$; $\alpha_2=\alpha_3=\beta_1=\beta_3=\gamma_1=\gamma_2=0$, we can compute the number of velocity-vectors that terminate in a parallelopiped limited by the six planes x_1, x_2; y_1, y_2; z_1, z_2, as well as its derivatives with regard to the constants of the frequency-function. If n_c is this number, we have

$$n_c=K\int_{\xi_1}^{\xi_2}e^{-h_1^2\xi^2}\,d\xi\int_{\eta_1}^{\eta_2}e^{-h_2^2\eta^2}\,d\eta\int_{\zeta_1}^{\zeta_2}e^{-h_3^2\zeta^2}d\zeta$$

$$=125\,\Theta\,(\xi_1\xi_2)\,\Theta\,(\eta_1\eta_2)\,\Theta\,(\zeta_1\zeta_2)\qquad(12)$$

where

$$\Theta(\xi_1\xi_2)=\frac{2}{\sqrt{\pi}}\int_{h_1\xi_1}^{h_1\xi_2}e^{-t^2}dt\;;\quad\Theta(\eta_1\eta_2)=\frac{2}{\sqrt{\pi}}\int_{h_2\eta_1}^{h_2\eta_2}e^{-t^2}\,dt\;;$$

$$\Theta(\zeta_1\zeta_2)=\frac{2}{\sqrt{\pi}}\int_{h_3\zeta_1}^{h_3\zeta_2}e^{-t^2}dt\,.$$

The orientation of the ellipsoid can be determined by three independent quantities L_1, B_1, and B_2, of which L_1 and B_1 are the galactic longitude and latitude of the ξ-axis and B_2 the galactic latitude of the η-axis. These are all supposed to be fairly small quantities and correspond to small rotations about the z-, y-, and x-axis, respectively.

The equations of conditions then take the form

$$\left.\begin{aligned}&\frac{dn}{dh_1}\,\Delta h_1+\frac{dn}{dh_2}\,\Delta h_2+\frac{dn}{dh_3}\,\Delta h_3+\frac{dn}{dx_0}\,\Delta x_0+\frac{dn}{dy_0}\,\Delta y_0+\frac{dn}{dz_0}\,\Delta z_0\\&\qquad\qquad+\frac{dn}{dL_1}\,L_1+\frac{dn}{dB_1}\,B_1+\frac{dn}{dB_2}\,B_2+n_c\kappa=n_0-n_c\,.\end{aligned}\right\}\quad(13)$$

The observed number n_0 is reduced to a total of 1000 stars. Since we wish to determine the constants of the function from the distribution of velocities within a limited space, and do not wish to impose the condition that the number of stars of very high velocity is in exact agreement with the assumed distribution-law, we add the term $n_c\kappa$.

The expressions for the derivatives have been found to be the following:

$$\left.\begin{aligned}
\frac{dn}{dh_1}&=-\frac{250}{\sqrt{\pi}h_1}\Phi(\xi_1\xi_2)\Theta(\eta_1\eta_2)\Theta(\zeta_1\zeta_2)\\
\frac{dn}{dh_2}&=-\frac{250}{\sqrt{\pi}h_2}\Theta(\xi_1\xi_2)\Phi(\eta_1\eta_2)\Theta(\zeta_1\zeta_2)\\
\frac{dn}{dh_3}&=-\frac{250}{\sqrt{\pi}h_3}\Theta(\xi_1\xi_2)\Theta(\eta_1\eta_2)\Phi(\zeta_1\zeta_2)\\
\frac{dn}{dx_0}&=\frac{250h_1}{\sqrt{\pi}}\Psi(\xi_1\xi_2)\Theta(\eta_1\eta_2)\Theta(\zeta_1\zeta_2)\\
\frac{dn}{dy_0}&=\frac{250h_2}{\sqrt{\pi}}\Theta(\xi_1\xi_2)\Psi(\eta_1\eta_2)\Theta(\zeta_1\zeta_2)\\
\frac{dn}{dz_0}&=\frac{250h_3}{\sqrt{\pi}}\Theta(\xi_1\xi_2)\Theta(\eta_1\eta_2)\Psi(\zeta_1\zeta_2)\\
\frac{dn}{dL_1}&=\frac{250(h_2^2-h_1^2)}{\pi h_1h_2}\Psi(\xi_1\xi_2)\Psi(\eta_1\eta_2)\Theta(\zeta_1\zeta_2)\\
\frac{dn}{dB_1}&=\frac{250(h_3^2-h_1^2)}{\pi h_1h_3}\Psi(\xi_1\xi_2)\Theta(\eta_1\eta_2)\Psi(\zeta_1\zeta_2)\\
\frac{dn}{dB_2}&=\frac{250(h_3^2-h_2^2)}{\pi h_2h_3}\Theta(\xi_1\xi_2)\Psi(\eta_1\eta_2)\Psi(\zeta_1\zeta_2)\\
\Phi(\xi_1\xi_2)&=h_1\xi_1e^{-h_1^2\xi_1^2}-h_1\xi_2e^{-h_1^2\xi_2^2}\\
\Phi(\eta_1\eta_2)&=h_2\eta_1e^{-h_2^2\eta_1^2}-h_2\eta_2e^{-h_2^2\eta_2^2}\\
\Phi(\zeta_1\zeta_2)&=h_3\zeta_1e^{-h_3^2\zeta_1^2}-h_3\zeta_2e^{-h_3^2\zeta_2^2}\\
\Psi(\xi_1\xi_2)&=e^{-h_1^2\xi_1^2}-e^{-h_1^2\xi_2^2}\\
\Psi(\eta_1\eta_2)&=e^{-h_2^2\eta_1^2}-e^{-h_2^2\eta_2^2}\\
\Psi(\zeta_1\zeta_2)&=e^{-h_3^2\zeta_1^2}-e^{-h_3^2\zeta_2^2}
\end{aligned}\right\}\qquad(14)$$

where ξ_1, ξ_2, η_1, etc., are determined by equation (11). Using the products of the functions Θ, Φ, and Ψ as coefficients, we secure a homogeneous set of equations of condition.

The distribution of velocities for Group I cannot be represented even approximately by an ellipsoidal frequency-function. In this case the sum of one ellipsoidal and one spherical frequency-function has been used, viz.:

$$F(xyz)=\mu K_1 e^{-S}+(1-\mu)K_2 e^{-h^2[(x-x_0^{I})^2+(y-y_0^{I})^2+(z-z_0^{I})^2]}$$

$\mu/(1-\mu)$ is the relative proportion of stars belonging to ellipsoidal and to the spherical stream.

The new derivatives in this case are

$$\frac{dN_2}{dh}=-\frac{2N_2}{\sqrt{\pi}h}\left[\frac{\Phi(x_1^{I}x_2^{I})}{\Theta(x_1^{I}x_2^{I})}+\frac{\Phi(y_1^{I}y_2^{I})}{\Theta(y_1^{I}y_2^{I})}+\frac{\Phi(z_1^{I}z_2^{I})}{\Theta(z_1^{I}z_2^{I})}\right]$$

$$x_1^{I}=x-x_0^{I}, \quad y_1^{I}=y-y_0^{I}, \quad \text{etc.}$$

$$\frac{dn}{d\mu}=N_1-N_2, \quad n=n_c=\mu N_1+(1-\mu)N_2$$

$$\frac{dN_2}{dx_0^{I}}=\frac{250\,h}{\sqrt{\pi}}\Psi(x_1^{I}x_2^{I})\Theta(y_1^{I}y_2^{I})\Theta(z_1^{I}z_2^{I}), \text{ etc.}$$

We have then

$$\mu\left[\frac{dN_1}{dh_1}\Delta h_1+\frac{dN_1}{dh_2}\Delta h_2+\;\dots\;+\frac{dN_1}{dB_2}B_2\right]$$
$$+(1-\mu)\left[\frac{dN_2}{dh}\Delta h+\frac{dN_2}{dx_0^{I}}\Delta x_0^{I}+\frac{dN_2}{dy_0^{I}}\Delta y_0^{I}+\frac{dN_2}{dz_0^{I}}\Delta z_0^{I}\right]$$
$$+\frac{dn}{d\mu}\Delta\mu+\kappa n_c=n_0-n_c.$$

The results of this computation are given in Table V. The probable errors in each case are given below the corresponding numerical values. According to the usual convention, that direction of the major axis is given which most nearly corresponds to 180° of galactic longitude in order to be comparable with Kapteyn's first stream. The dispersion along the two shortest axes in several cases is so nearly the same that only the direction of the major axis can be well determined.

The elements of the spherical stream of Group I are found to be,

$$x_0 = -31.1 \pm 1.4 \text{ km}$$
$$y_0 = +14.5 \pm 1.1$$
$$z_0 = +\ 3.0 \pm 0.7$$
$$a = \frac{1}{\sqrt{2h}} = 8.1 \pm 0.5$$
$$1 - \mu = 0.185 \pm 0.028.$$

Relative to the sun and in the equatorial system of co-ordinates, this condensation-point has the co-ordinates

$$\alpha = 92\overset{\circ}{.}3\,, \qquad \delta = +4\overset{\circ}{.}9\,, \qquad v = 48.7 \text{ km}$$

Boss's value[1] for the convergent point of the Taurus group is

$$\alpha = 91\overset{\circ}{.}8\,, \qquad \delta = +6\overset{\circ}{.}9\,, \qquad v = 45.6 \text{ km}\,.$$

We can thus identify this stream, which is superimposed on the general ellipsoidal distribution, with the Taurus stream, although these stars are scattered all over the sky. The percentage of stars belonging to this general Taurus stream is, as appears from the value of $1-\mu$, 18.5 ± 2.8 per cent of the stars of spectral type A7 to F9 and absolute magnitude 0.0 to 5.5. If we include in this group the nine recognized members of the Taurus stream which were omitted in the analysis, we find that 22 per cent of the stars of this type and absolute magnitude belong to the general Taurus stream. The spread corresponding to a dispersion of 8.1 km is no doubt due in part to errors in the quantities involved, but may also be due in part to an inherent dispersion of the velocities. Attention may be called to the fact that the dispersion of the velocities of the members of the Taurus stream has necessarily been estimated too low hitherto because of the selection of stars whose velocities are very nearly parallel. Even among the stars of type G there are several which belong to this general Taurus stream. This may be

---

[1] L. Boss, *Astronomical Journal*, **26**, 31 (No. 604), 1908.

TABLE V

CONSTANTS OF THE VELOCITY-ELLIPSOIDS AS COMPUTED FROM DISTRIBUTION OF VELOCITY-VECTORS AND REFERRED TO THE GALACTIC CO-ORDINATE SYSTEM

Group	Center			Major Axis			Intermediate Axis			Minor Axis		
	x	*y*	*z*	*L*	*B*	*a*	*L*	*B*	*b*	*L*	*B*	*c*
	km	km	km			km			km			km
I.	+ 5.39 ± 1.30	+0.80 ±0.35	+0.06 ±0.55	173°6 ± 4.1	− 8°5 ± 3.0	22.86 ± 1.04	. . . .	. . . .	12.25 ± 0.36	. . . .	. . . .	11.68 ± 0.45
II. . . .	+ 5.49 ± 0.83	+1.52 ±0.65	+1.45 ±0.34	177.6 ± 3.4	− 0.1 ± 2.0	18.47 ± 1.13	87.6 ± 3.4	+ 9.1 ± 7.7	10.02 ± 0.43	+267.1 ± 3.4	+80.9 ± 7.7	7.92 ± 0.32
III. . .	+ 3.10 ± 1.02	−0.82 ±0.98	+0.68 ±0.53	181.0 ± 6.5	+ 4.1 ± 4.4	23.19 ± 0.87	. . . .	. . . .	16.49 ± 0.58	. . . .	. . . .	16.13 ± 0.69
IV. . . .	+ 3.30 ± 0.81	−1.03 ±0.87	+2.50 ±0.33	153 ± 12	+ 2 ± 5	19.86 ± 0.67	. . . .	. . . .	15.93 ± 0.50	. . . .	. . . .	14.55 ± 0.99
V.	+ 1.3 ± 2.1	−1.6 ±2.3	+5.5 ±1.3	142 ± 25	+27 ±22	18.8 ± 1.4	. . . .	. . . .	16.0 ± 1.4	. . . .	. . . .	15.2 ± 1.1
VI. . . .	−17.0 ± 2.7	−6.8 ±2.2	+1.2 ±1.3	148.7 ± 4.6	+ 7.3 ± 2.4	48.97 ± 1.07	58.7 ± 4.6	+37.0 ±11.5	26.94 ± 0.86	255.3 ± 4.6	+52.4 ±11.5	21.80 ± 0.90

seen from the form of the equi-frequential surfaces as well as from an inspection of the points in the diagram.

In Table VI are given the same quantities as in Table V but referred to the equatorial system of co-ordinates, the center of the ellipsoids being referred to the sun.

TABLE VI

CONSTANTS OF THE VELOCITY-ELLIPSOIDS AS COMPUTED FROM THE DISTRIBUTION OF VELOCITY-VECTORS REFERRED TO THE SUN AND TO THE EQUATORIAL CO-ORDINATE SYSTEM

GROUP	CENTER			MAJOR AXIS		INTERMEDIATE AXIS		MINOR AXIS	
	α	δ	v	α	δ	α	δ	α	δ
			km						
I	84°0	−37°7	15.2	90°2	+ 1°7	....	....	....	....
II	88.0	−34.0	14.2	95.5	+ 2.1	3.0	+71.7	190.1	+18.1
III	91.7	−36.7	17.5	104.8	+ 1.0	....	....	....	....
IV	98.7	−35.7	16.8	89.4	+24.8	....	....	....	....
V	109.6	−29.5	18.2	105.7	+44.0	....	....	....	....
VI	102.4	−24.6	37.4	92.4	+31.1	252.4	+61.8	181.6	− 9.4

If we take the vectors opposite to those given in columns 2–4 of Table VI, we have the velocity of the sun referred to the center of the velocity-ellipsoid. For the giant stars this velocity is appreciably smaller than the velocity of the sun computed from the mean velocity. This result is due to the asymmetry of the distribution of the velocities taken in combination with the different weights given different stars in the use of quantities of zero order (numbers) and of first order (means). If the solar motion is used for the purpose of computing parallaxes from parallactic motion, the velocity based upon the means of the components should be employed.

Another consequence of this asymmetry is that the most frequent velocity does not correspond either to the mean velocity or to the center of the ellipsoidal distribution. From the diagrams we can easily estimate this most frequent velocity by determining the points of highest density of the general frequency-function. In Table VII these values are given both in galactic rectilinear co-ordinates relative to our adopted origin, and in equatorial polar co-ordinates relative to the sun.

TABLE VII

Most Frequent Velocity-Vectors

Group	x	y	z	α	δ	v
	km	km	km			km
I	+ 9	+3	+5	100°	−33°	9.
II	+ 6.1	+1.1	+1.9	90.4	−36.6	13.7
III	+ 6.0	+4.9	+0.4	75.9	−24.6	13.2
IV	+ 5.8	+2.2	+2.0	88.6	−32.2	13.5
V	+ 4.7	+1.0	+3.4	97.9	−31.8	14.4
VI	−19.0	−2.0	+1.2	98.8	−17.4	37.7
Giants (II to V)	+ 5.8	+2.7	+1.7	86.2	−30.8	13.4

SUMMARY

The three components of the velocities of about 1300 stars of spectral types F to M have been computed from the proper motions, radial velocities, and parallaxes. The following are the principal results of the investigation:

1. The solar motion as derived from the algebraic means of the velocity-components is found to be dependent on the spectral types and absolute magnitudes of the stars to which it is referred. The giant stars of the later types give a somewhat higher declination of the sun's apex than the giant stars of earlier types. The dwarf stars give a much larger solar motion than the giant stars, and, in general, stars of high velocity give a larger motion than stars of low velocity.

The distribution of velocities of different groups of stars has been studied in different ways. The velocities are referred to the galactic system of stars and have been corrected for a standard solar velocity of 20 km toward the point $\alpha = 270°$, $\delta = +30°$.

In order to learn the nature of this distribution a very general type of frequency-function has been used, which in reality is an interpolation formula in three dimensions. The function is a three-dimensional cosine-series in which the coefficients are determined directly from the *number* of velocity-vectors within different limits. A very large number of terms has been determined by harmonic analysis, a synthesis has been made for the xy- and xz-planes, and curves of equal frequency have been drawn in these planes (Figs. 1–6 and Table III). From a study of these figures we can draw the following conclusions:

2. The giant stars of types F to M form a single group or "stream" with an approximately ellipsoidal distribution, the longest axis lying in the galactic plane and nearly coinciding with the x-axis, the line of intersection of the equator with the galactic plane. The shortest axis is nearly in the direction of the galactic pole. The elongation of the velocity-ellipsoid is largest for the bright F stars and smallest for the late K and M stars, for which the distribution is nearly spherical.

3. The most frequent velocity does not coincide with the origin, but for all groups of giant stars lies in the first quadrant of the xy-plane, and corresponds approximately to a velocity 13.4 km relative to the sun in the direction $\alpha=86\overset{\circ}{.}2$, $\delta=-30\overset{\circ}{.}8$. For the dwarf stars the most frequent velocity relative to the sun is 37.7 km in the direction $\alpha=98\overset{\circ}{.}8$, $\delta=-17\overset{\circ}{.}4$ (Table VII).

4. Among the stars of spectral types A7 to F9 and absolute magnitudes 0 to +6 there is in addition to the general group of giants another stream the motion of which coincides with that of the Taurus group. These stars are scattered all over the sky and comprise about 20 per cent of the stars of the above-mentioned spectral types and absolute magnitudes. Even among stars of somewhat later types there are stars belonging to this general Taurus group.

5. There is a marked asymmetry in the distribution of the velocities around the most frequent velocity-vector. Stars of high velocity show a tendency to avoid moving toward the first quadrant of the xy-plane. This asymmetry which is especially marked among the stars of very high velocity can be traced even among stars of ordinary velocity, thus producing a systematic difference between the most frequent velocity-vectors and the mean velocity.

6. Neglecting this asymmetry, the constants of the ellipsoidal frequency-function have been computed in two different ways: First, the method of moments was used, the moments being computed from the trigonometric series previously determined (Table IV). Second, the constants were determined from the distribution of velocities itself, approximate values for the constants being assumed and then corrected by values computed from the difference between the observed and the computed number of velocity-vectors

terminating in different parallelopipeds (Tables V and VI). The values computed in this way differ somewhat from those computed from the moments on account of the difference in weighting. The asymmetry in the distribution produces different values for the velocity of the sun, according as the latter is computed from the distribution of velocities itself, or from algebraic means. The first necessarily gives the smallest value for the sun's velocity, the latter the highest.

In the extensive computation involved in this investigation the author has received valuable help from the following members of the computing division: Mrs. Hannah M. Marsh, Miss Ada M. Brayton, and Miss Florence MacCreadie. Dr. Jean Paraskévopoulos of Athens and Professor D. T. Wilson of Cleveland also have taken part in the computations.

Mount Wilson Observatory
June 1922

Contributions from the Mount Wilson Observatory, No. 246
Reprinted from the *Astrophysical Journal*, Vol. LVI, pp. 295–317, 1922

THE APPLICATION OF VACUUM THERMOCOUPLES TO PROBLEMS IN ASTROPHYSICS

By EDISON PETTIT and SETH B. NICHOLSON

ABSTRACT

Sensitive vacuum thermocouples.—Construction of the couple and cells is described. The couples were made of metal strips about 3 mm long, $\frac{1}{10}$ mm wide and $\frac{1}{120}$ mm thick, each overlapping junction being fused to a blackened tin disk receiver, $\frac{1}{2}$ mm in diameter and $\frac{1}{100}$ mm thick, each couple weighing only about $\frac{1}{30}$ mg. The sensitivity with a high vacuum (10^{-4} mm) was found to be from two to eleven times the value at atmospheric pressure, depending on the couple. To maintain the vacuum, metallic calcium was used. With a sensitive galvanometer (5×10^{-10} amp./mm) the *temperature sensitivity* obtained was 8×10^{-5} deg./mm, in one case. The *efficiency*, however, was very low, only about 10^{-6} of the incident energy being transformed into electrical energy. An ideal heat engine would be a hundred and fifty times more efficient.

Stellar radiation measurements.—Method of application of the vacuum thermocouple is described. The cell was mounted on a plate adapted to the Newtonian double-slide plate-holder of the 100-inch telescope, and connected by wires to a D'Arsonval galvanometer in the basement where the deflections were recorded on a moving plate. *Photographic records of the deflections for Vega, Arcturus, α Herculis, and R Hydrae,* with and without a water absorption cell, are reproduced (Plate VI).

Applications of thermocouple to solar energy measurements already made are the registration (1) of spectral energy distribution, (2) of drift curves across the disk in various wave-lengths, and (3) of total radiation curves across sun-spots and faculae.

Self-registering microphotometer is described in which the photo-electric cell is replaced by a vacuum thermopile. A suitable optical system enables the light through a slit 9 mm long to be integrated so as to eliminate the grain effect in the spectrograms measured.

Transmission curve for water, 1 cm thick, is reproduced.

Optical system for sensitive galvanometer.—By placing a spectacle lens of 6 m focus at the galvanometer and observing the image with cross-hair and eyepiece, a power of 350 could be used and the scale read accurately to 0.1 mm at 8 m.

In 1895 Lebedew[1] found that a thermocouple of iron-constantan was more sensitive in a vacuum than at atmospheric pressure. Since that time the thermocouple has been used both in vacuum and at atmospheric pressure by a number of physicists, for the study of radiation problems. The vacuum thermocouple has been applied to the study of stellar radiation with marked success by Pfund, and more recently by Coblentz. Pfund employed couples of $95\text{Bi}+5\text{Sn}$ against $97\text{Bi}+3\text{Sb}$, and Coblentz employed Bi against $95\text{Bi}+5\text{Sn}$ and also Bi against Pt with success. The former[2] used charcoal heated by electric discharge, while the latter[1] employed metallic calcium, to maintain the vacuum.

---

[1] *Annalen der Physik*, 56, 12, 1895.

[2] *Allegheny Observatory Publications*, 3, 45, 1913.

FORM OF CELL EMPLOYED

In the present investigation we have used the three types of cell shown in Plate V. After considerable experimenting type 3 was adopted. The cell body and connecting tubes are made of Pyrex glass, the calcium tube *C* is of clear quartz, and the plug *P*, containing the platinum wires carrying the thermocouples, is of soda glass. The cell body *A* has an inside diameter of 42 mm and a wall 1.5 mm thick. The quartz tube *C* (14 mm inside diameter) is attached to the Pyrex tube by a ground joint and stop-cock grease, and sealed with red sealing wax. The metallic calcium is held in place by a wad of glass wool. The plug *P* carries three platinum wires to which two thermocouples are attached, at *T*. It is attached with a ground joint, sealed with stop-cock grease, and may be removed or replaced without destroying the thermocouples.

The cell *A* is fitted with two windows, W_1, W_2, of 10 mm clear aperture. The window W_1, which admits the radiation to the thermocouple, is closed with a quartz window 1.5 mm thick, the junction with the ground surface of the lip being made with stop-cock grease and protected by a rim of red sealing wax. In type 2 the window W_1 is of microscope cover-glass 0.12 mm thick. W_2 is closed with a piece of microscope slide-glass 1.28 mm thick. On looking through W_2 the thermocouple junction may be seen projected against the star image or other radiation entering W_1.

The advantages of this design of cell are as follows: (1) large bearing surfaces at the ground junctions of the plug and calcium tube; (2) a minimum exposure of contact surfaces at the windows; (3) couples may be withdrawn or replaced within the cell without danger of damage; (4) the blackened surfaces of the couples may be exposed to either window by simply rotating the plug, thus enabling the cell to be adapted to various apparatus.

PREPARATION OF THE THERMOCOUPLES

The choice of metals for the couples is dependent on a number of physical properties, which may be briefly enumerated as follows:

---

[1] *Bulletin Bureau of Standards*, **11**, 185, 1915.

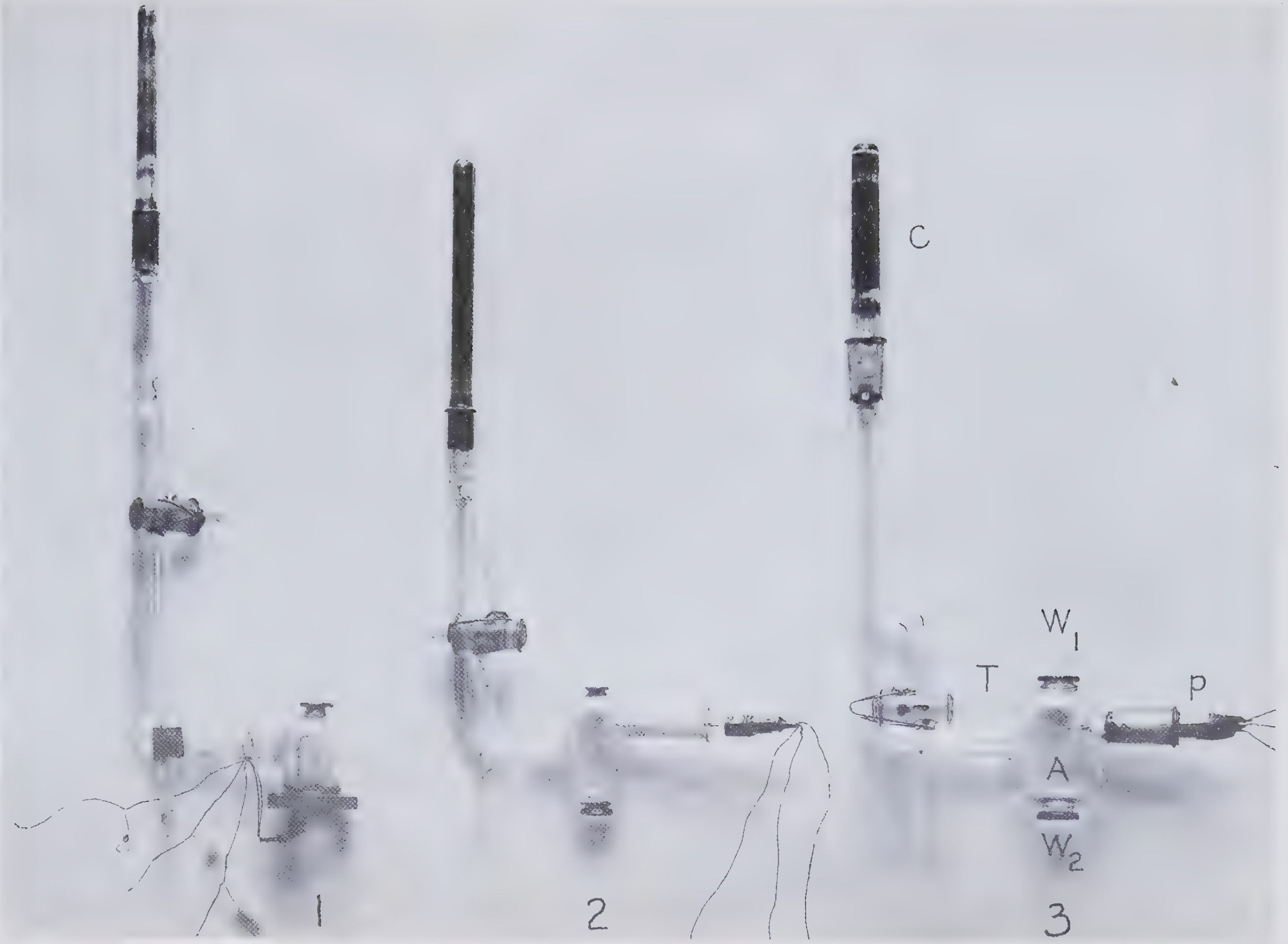

Types of Thermocouple Cells

(1) high electrical conductivity; (2) high thermoelectric power; (3) low heat conductivity; (4) low coefficient of brittleness; (5) approximately equal melting points; (6) low specific heat.

Of these six conditions (1) and (3) and also (2) and (4) are obviously antagonistic in nature. Generally the relative specific coefficients of thermal and electrical conductivity are nearly equal, and high thermoelectric power is associated with a crystalline structure making for great brittleness. There is a considerable range in the constants for some of the metals, especially those of more crystalline structure. This is due principally to two causes: differing conductivity and thermoelectric power in axial and equatorial directions, and impurities in the metal. Taking bismuth as an example, the thermoelectric power axially is $65 \times 10^{-6} V/\text{deg. C.}$, and equatorially $45 \times 10^{-6} V/\text{deg. C.}$ An impurity of $\frac{1}{3}$ of 1 per cent of tin will reduce the thermoelectric power to 0 relative to lead. The thermoelectric properties of alloys have been investigated by Mattheissen, Tait, Becquerel, Hutchins, and others, and it is found that most of the metals investigated are very sensitive to changes in the relative proportions of the alloy.

The current produced by the junction of a couple will depend on the thermoelectric power, p, the resistance, R, and the difference in temperature ΔT between the hot and the cold junction. The latter in turn depends on the specific heat of the junction, S; the mass, M; the quantity of heat, C, conducted away along the strips; the quantity C_1 conducted through the air; the quantity C_2 convected away; the quantity radiated, r; and the quantity incident on the junction, Q.

Then

$$I = \frac{kp}{SMR}[Q-(C_1+C_2+C+r)] \tag{1}$$

where I is the current and k is a constant depending on the units employed.

Obviously C_1, C_2 may be eliminated by placing the couple in a vacuum. Then r will depend only on the absolute temperature and C should be made as small as possible. In only a few cases, however, will this be of any advantage, since C and R are physically connected, and a decrease in C will correspondingly increase R.

The values of C and $1/R$ are both directly proportional to M, so that after a certain limit is reached, the only advantage in reducing M lies in the quickness of action of the couple in responding to changes in Q. Some advantage is gained, however, by placing at the junction of the two metals a thin plate of a third metal, functioning only as a receiver of the radiation and chosen so that the specific heat will be low. If the plate is very thin and M is small, then its conductivity is unimportant.

The thermoelectric power, p, is itself dependent on the absolute temperature at which the thermocouple is working. Generally this is high for low temperatures and decreases for the higher temperatures, passing through zero and reversing sign at the "temperature of inversion." Considerable advantage would be gained in operating the couple at the temperature, let us say, of liquid air, but the difficulties attending this modification of the apparatus have thus far prevented its successful application.

We have employed chiefly the following metals: Bi, 95Bi+5Sn, Pb, Sn, Pt, Au, Cu, 806Sb+696Cd, Ag, 97Bi+3Sb, Te. When the metals are easily fusible, the simplest method of producing fine flat strips suitable for thermocouples is that first proposed by Pfund. About 10 gm of the metals to be fused and alloyed are placed in a Rose's crucible and heated in a current of hydrogen, which prevents oxidation from destroying the ratios of the metals introduced. The molten metal is then dashed with all possible force perpendicularly on a large plate of window glass. The spattered metal is thus transformed into a spray of fine radiating wires. An abundant supply of strips 0.005 mm or more thick and 0.05 mm or more wide is thus obtained.

The operation of forming the junctions is carried out on a large sheet of plate glass. As one must everywhere avoid adhesion when working with such small masses, the glass is kept warm by laying it on the planed surface of a large iron casting which has previously been heated. A sheet of white paper lies between the glass and the casting.

Because of its low specific heat and melting point, tin or ordinary tinner's solder is chosen for the receivers. Shavings of the metal are rolled out into thin sheets; these are cut into narrow strips, which are cut into small pieces by means of a scalpel. The latter are fused with a bit of rosin by touching them with a loop of nichrome wire heated by a current of electricity. This immediately produces a minute sphere of the metal, which when pressed flat by a plate of glass produces a thin disk suitable for the receivers. By trial it is found that a sphere 0.15 mm in diameter can be pressed into a receiver 0.5 mm in diameter, which is almost as thin as can be handled. It is easy to find the length of strip necessary for these spheres, which can then be produced in quantity. After several dozens of them have been fused with a bit of rosin, the latter is dissolved away with amyl alcohol and the disks made as needed.

The operation of forming the couples, such as are shown in Figure 1, is carried out about as follows: The strips to be employed are removed from the glass plates carrying the spattered metals by means of a razor blade attached to a convenient handle. These strips are first examined under a microscope to detect any defects which might weaken them, and then laid so that the ends overlap. One of the prepared receivers is then laid over the junction without rosin or other soldering flux. A strip of mica 12×30×.02 mm, bent in the middle so as to keep the center raised 1 or 2 mm above the glass is then laid over the junction and held down with the finger and two 10-gm weights laid close on either side of the couple to keep the mica in contact with it. The welding together of the junction and receiver is accomplished by touching the mica directly above the receiver with the electrically heated loop of nichrome wire. The loop must be heated just below redness and only the briefest

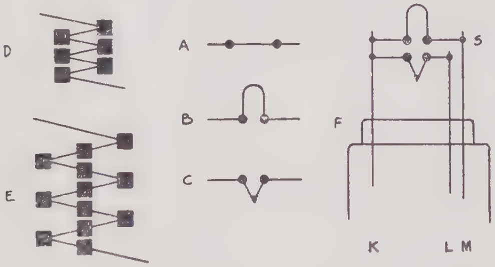

FIG. 1.—Types of thermopiles and thermocouples

possible contact made with the mica. Only one junction at a time is welded, otherwise one may adhere to the glass and the other to the mica, in which case it is impossible to remove the mica without destroying the couple.

The receivers are painted with a mixture of lampblack, two parts; platinum black, one part; turpentine, five parts; and alcohol, twenty parts. This paint, put on with a fine camel's hair brush, forms a black mat surface which will dry quickly.

In Figure 1 are shown five forms of thermocouple; *A*, *B*, and *C* are compensated junctions adapted to stellar observations, *D* and *E* are piles adapted to spectroscopic work, and *F* shows the method of mounting the couples on the platinum wires *K*, *L*, *M*. Forms *B* and *C* have been adopted for stellar observations, since the deflections may be doubled by shifting the junctions alternately on the star image as first applied by Pfund. In *B* the middle strip is folded into a U form in order to bring the junctions close together and leave a space between them, but for some of the more brittle metals which cannot be folded without breaking them, type *C* is used, where two short strips are welded together in V form. Type *D* is a pile which we have used on the registering microphotometer, and *E* is another type of pile first employed by Rubens[1] in 1898 for spectroscopic work at atmospheric pressure, and used more recently by Coblentz[2] in a vacuum.

The platinum wires *K*, *L*, *M* (Fig. 1, *F*) are flattened out on the free ends and solder is run over them on one side. After being washed in alcohol, the thermocouples are laid in place and small disks of solder, *S*, formed in the same manner as above described for the receivers, except that they are flattened out without first removing the rosin, are laid upon the ends of the couples where they cross the platinum wires at *S*. The solder on the platinum wires is then melted by touching it with the nichrome loop.

The masses of the couples so constructed are exceedingly small. The mass of the entire couple *A*, *B*, or *C* is approximately $\frac{1}{30}$ to $\frac{1}{40}$ mg, while the mass of the portion heated by the incident stellar radiation is only 0.012 mg. The metal strips forming the couple are each approximately 3 mm long and 0.008×0.10 mm in cross-section, and the receivers are $\frac{1}{2}$ mm in diameter by 0.009 mm thick. The resistance of course depends on the metals employed, but generally is 8 to 20 ohms.

---

[1] *Zeitschrift für Instrumentenkunde*, **18**, 65, 1898.

[2] *Scientific Papers, Bureau of Standards*, **17**, 188, 1921.

VACUUM EFFECTS

Lebedew[1] determined the law of sensitivity change with change in pressure for a constantan-platinum couple, and found that for the blackened couple the increase was 7.4 times and for the unblackened couple 34 times, for the highest vacuum attained, estimated less than 0.0001 mm. Pfund[2] found an increase of "six times," and Coblentz[3] a "four and one-half fold" increase. In the present investigation we have found increases of two to eleven fold for the vacuum effect.

The effect of the vacuum on the sensitivity does not appear to be the same for all thermocouples, even of the same construction and materials, though the effect of differing materials seems to be the most pronounced. Graphs of the galvanometer deflection against the pressure for three thermocouples are given in Figure 2. It will be seen that the vacuum has little effect upon the sensitivity until the region of 1 mm mercury pressure is reached. Then for the Ag-Te couple the entire increase takes place between 1 mm and 0.01 mm, while the Bi-Bi Sn couple shows an increase of 20 per cent between 0.01 mm and 0.0001 mm. From this it appears that the vacuum which must be maintained in order to keep the sensitivity constant depends on the metals employed in the thermocouple. Thus for Ag-Te couples a vacuum of 0.01 mm is sufficient; but for Bi-Bi Sn this vacuum would occur on a steep part of the curve and in order to insure constant sensitivity a vacuum of 0.0001 mm should be maintained.

A general explanation of the character of the curve is easily given. It is known that the thermal conductivity of a gas is independent of the pressure until the region of 1 mm is reached, when it begins to drop rapidly to zero as the mean free path of the molecules becomes comparable to the dimensions of the container.

[1] *Annalen der Physik*, **9**, 209, 1902.

[2] *Physikalische Zeitschrift*, **13**, 870, 1912.

[3] *Bulletin of the Bureau of Standards*, **11**, 636, 1915.

The thermal conductivity also depends on the nature of the gas; for hydrogen it is much greater than for any other. This should make a thermocouple less sensitive in this gas than in air, say. Figure 2 shows how this effect appears in the sensitivity curves when this gas is employed.

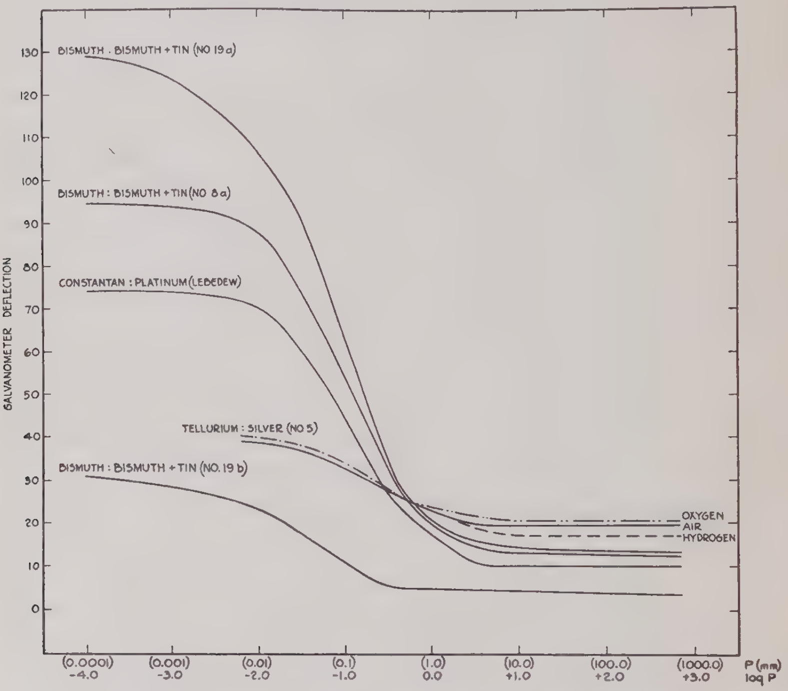

FIG. 2.—Variation of thermocouple sensitivity with pressure

The use of metallic calcium to maintain the vacuum has been studied by both Soddy[1] and Coblentz.[2] The calcium is heated while the pump is in operation to remove the hydrocarbon vapors. We have found it necessary to pump a considerable time to remove these gases completely. After the vacuum has been raised by the pump to a desired limit, it may thereafter be brought back to this point by merely heating the calcium tube to a low red heat with a small electric heater or lamp. After the lamp is removed the

[1] *Proceedings of the Royal Society*, A, 78, 429, 1907.

[2] *Op. cit.*, 11, 625, 1915.

absorption of the gases continues for about twenty minutes until the tube has cooled considerably.

Coblentz uses a discharge between two platinum terminals inserted in that part of the tube connecting the calcium tube to the thermocouple cell, to test the degree of evacuation obtained while heating the calcium. Since our cells are made of Pyrex glass, it was not feasible to use sealed-in electrodes for this purpose; outside electrodes were therefore substituted. It was found, however, that after the discharge passed, the sensitivity decreased to about 30 per cent to 50 per cent and remained at this level for some hours. On opening the stop-cock to the pump, which was maintained at about 0.001 mm pressure, the sensitivity immediately rose to normal again, and this could be repeated at will. Apparently the discharge did not produce a change in pressure, for none was detectable on opening the stop-cock to the gauge. On this account, the discharge test was discarded and tests of the sensitivity by use of a standard lamp were substituted. This is more satisfactory in another way, for it gives a quantitative test of the sensitivity which the discharge test does not give, and all that is necessary is to heat the calcium tube till the sensitivity rises to normal.

SOME PROPERTIES OF VACUUM THERMOCOUPLES

In thermocouples of these small dimensions some interesting properties were observed. Generally in a compensated couple, such as Figure 1 (*A*, *B*, *C*), the two junctions do not give the same deflections, i.e., the compensation is not exact. One case was observed in a couple of Bi-Bi Sn where the deflections for the two junctions were 125 mm and 25 mm and both in the same direction, the current flowing normally across the first junction and in reverse across the second. How this could occur we are unable to explain. As a rule, however, the compensation is so complete that, while observing star deflections, we can turn on all the lights in the dome, without disturbing the galvanometer. With this couple the Peltier effect was quite pronounced. When a deflection was observed with the first junction, the galvanometer mirror swung rapidly at first, then suddenly slowed down and crept up to maximum over 8 or 10 mm, but when a deflection was observed with the second junction the galvanometer mirror over-ran its maximum 2 or 3 mm and returned to normal deflection after one or two seconds.

The absorbing power of the black paint of course depends on the wave-lengths of the incident radiation, being somewhat greater for the shorter waves. Coblentz has found that the reflecting power of this paint is only about 2 per cent. Tests were made with both blackened and unblackened sides of the receivers turned to the window admitting the radiation. The ratio of deflections for the unblackened side to the blackened side was $\frac{1}{3}$ to $\frac{1}{4}$. It was thought that the sensitiveness of the couple might be increased by blackening, on both sides, the entire couple and strips except the receiver, but the effect was very slight. Several couples were repainted after testing, but this seemed to have little effect on the sensitivity.

The efficiency of a thermocouple is exceedingly low. An approximate value of this quantity may be obtained from data relating to the sensitivity tests of No. 19, for example. This efficiency is the ratio between the electrical energy produced and the quantity of the incident radiation, expressed in the same units. If W is the wattage of the lamp, D its distance from the couple, r the radius of the receiver of the thermocouple, R its resistance, i the galvanometer sensitivity in amperes, S the observed deflection, then the efficiency is

$$E=\frac{4R(DSi)^2}{Wr^2}\,. \tag{2}$$

Now for No. 19, $W=90$, $r=\frac{1}{4}$ mm, $R=20$ ohms, $D=3000$ mm, $S=125$ mm, $i=4.75\times10^{-10}$ amp./mm. Hence, $E=4.5\times10^{-7}$, i.e., only about half a millionth of the incident radiation actually produces deflection in the galvanometer. Of course we are assuming a uniform distribution of radiation about the lamp, and neglecting the heat convected away from it, as well as the absorption of the air through which the beam must pass. For a value of E so small, however, these quantities could hardly affect the order of the result.

We may approach the problem in another way. The receiver of the thermocouple will continue to increase in temperature until the heat lost and converted into electrical energy equals the amount being absorbed from the incident ray. The ratio of the heat converted into electrical energy to the total heat received is the desired value of E. As was seen in equation (1), since the thermocouple is in a vacuum, the only sources of lost heat are the quantity C, conducted away by the strips, and the quantity radiated, r.

In order to determine these values, let us assume the temperature at which the couple is working to be 20° C., and that a difference of 1° C. between the two junctions is produced by the incident radiation. Let us take couple No. 19 already cited. Since the area of the receiver is about $\frac{1}{5}\times 10^{-2}$ sq. cm, and since, as already seen, it radiates about $\frac{1}{3}$ as much from the unblackened as from the blackened side, then Stefan's law becomes

$$r=\tfrac{4}{3}\times\tfrac{1}{5}\times 10^{-2}\times 1.28\times 10^{-12}(T_1^4-T^4)\text{ cal./sec.}=$$
$$3.4\times 10^{-15}(T_1^4-T^4)\text{ cal./sec.}\quad(3)$$

and since $T_1=293$ and $T=292$, then

$$r=3.4\times 10^{-7}\text{ cal./sec.}$$

The amount conducted away varies directly as the cross-section of the metal strips A, and inversely with their length L, the constant of proportionality K being the amount conducted through one centimeter cube in one second per degree centigrade. This constant for bismuth is 0.02 cal./sec. Since there are two strips 3 mm long at each junction, one of which contains only 5 per cent tin, we may compute the heat conducted through one strip and call the total amount just double this. Hence the amount of heat conducted away is

$$C=\frac{2KA}{L}\text{ cal./sec.}=2\times 0.02\times 0.000008\times 3\text{ cal./sec.}$$
$$=9.6\times 10^{-7}\text{ cal./sec.}\quad(4)$$

Now the amount of heat, I, converted into electricity, expressed in cal./sec., varies directly with the square of the thermoelectric power p, the square of the difference in temperature ΔT, and the reciprocal of the resistance R, the constant of proportionality being the Joule equivalent, 0.24. Since $\Delta T = 1^\circ$ C., p = about 50×10^{-6} volts, and $R=20$ ohms, we have

$$I=\frac{0.24(p\Delta T)^2}{R}\text{ cal./sec.}=\frac{0.24\times(50\times10^{-6})^2}{20}\text{ cal./sec.}=3\times10^{-11}\text{ cal./sec.}$$

The efficiency then is

$$E=\frac{I}{r+C+I}=\frac{3\times10^{-11}\text{ cal./sec.}}{3.4\times10^{-7}+9.6\times10^{-7}+3\times10^{-11}\text{ cal./sec.}}\tag{5}$$

or

$$E=2.3\times10^{-5}.$$

These low values of the efficiency computed here are in part due to the small range in temperature over which the thermocouple works. From the principle of Carnot's Cycle it is known that the efficiency of the theoretically perfect heat engine is

$$E=\frac{T_1-T}{T_1}.\tag{6}$$

The efficiency of the thermocouple, then, considered as a converter of available heat, may be obtained by multiplying the values of E found in equations (2) and (5) by the reciprocal of equation (6). For equation (2) the value of T_1 is the room temperature at which the thermocouple was tested, which was 293° C. absolute. The difference in temperature (T_1-T) between the hot and cold junction for this thermocouple will be shown in equation (7) to be 16×10^{-5} deg. C. per mm deflection. Since in equation (2) the deflection was 125 mm, then $(T_1-T)=2\times10^{-2}$. The value then of $T_1/(T_1-T)$ is 1.5×10^4. Multiplying the value of E obtained in equation (2) by this coefficient, we obtain for the relative efficiency $E=6.7\times10^{-3}$. For the value of E in equation (5) $T_1=293$, $T=292$, which gives for the coefficient 2.93×10^2. Multiplying the value of E in equation (5) by this quantity we obtain for the relative efficiency $E=6.7\times10^{-3}$. It is, then, theoretically possible to construct a thermocouple one hundred and fifty times as sensitive as No. 19 considered here.

Ganot states that Clamond's thermoelectric battery of Fe-Sb Zn heated directly with coal gas under favorable conditions has an efficiency of $E=5\times10^{-3}$.

Some attempts to prevent the losses by radiation have been made by placing the couple at the center of curvature of a hemispherical mirror, the radiation being admitted through a hole in its center. We have not found it possible to apply this principle with the present apparatus since a slight displacement of the junction would render the mirror inactive. Again this would be effective on only one junction. The effect of a hemispherical mirror would be to reduce the losses by radiation to that emitted by the unblackened surface of the receiver, which is approximately one-fourth of the whole amount. Reducing the value of r in equation (5) to one-fourth of its value, we obtain a value for E which is just five-fourths its original value. Hence we may say that the effect of a hemispherical mirror is to increase the sensitivity one-fourth, assuming the mirror to reflect perfectly and the central hole to be of negligible area. In the case of the stellar thermocouples, Figure 1, B and C, the increase would be only one-eighth when the method of double deflections is used.

It is of interest to know the temperature sensitivity of the thermocouple. This may be determined from the current relations in the circuit.

Let us determine what change in temperature of the receiver will be required to give a deflection of 1 mm on the scale. If we let

$P=$ the potential produced in the circuit expressed in volts
$p=$ the thermoelectric power of the junction in volts
$i=$ the sensitivity of the galvanometer in amperes/mm
$R=$ the total resistance of the circuit
$\Delta t=$ the required change of temperature in deg. C.
$T=$ temperature of cold junction

then all the constants are known for any particular couple. Let us take No. 19 cited above. Here p normally should be about 150×10^{-6} V, but on account of the impurity of the bismuth, probably it is not greater than about 60×10^{-6} V. $i=4.75\times 10^{-10}$ amp., $R=20$ ohms. Then

$$\Delta t=\frac{P}{p}=\frac{iR}{p}=\frac{4.75\times 10^{-10}\times 20}{60\times 10^{-6}}=16\times 10^{-5}\text{ deg. C.} \tag{7}$$

and with a more sensitive galvanometer this figure could easily be pushed to one-millionth of a degree.

Since deflections of about 150 mm are employed ordinarily on recording apparatus, the difference in junction temperature must be approximately 2.4×10^{-2} deg. C. at maximum working deflection for the galvanometer employed. We may now form an estimate of the speed of action of the couple.

We may state the speed of action in terms of the time required for the heat to travel from the blackened face of the receiver to the junction on the rear side and reach a state of steady flow. The increase $\Delta t_2 = 2.4\times 10^{-2}$ deg. C. is that reached by the rear side of the receiver after the steady state is established. To determine the time required, it will be necessary to know the increase in temperature Δt_1 of the front (blackened) face also. This is given by

$$W = \frac{k(\Delta t_1 - \Delta t_2)}{u} \text{ or } (\Delta t_1 - \Delta t_2) = \frac{Wu}{k} \tag{8}$$

where W is the rate at which heat flows through unit cross-section, k is the conductivity, $\Delta t_1 - \Delta t_2$ is the difference of temperature between the two faces and u is the thickness of the receiver in cm. Now $W = (C_1 + R_1)/A$, where C_1 = heat conducted away along the two strips, R_1 = heat radiated from the rear face, and A is the area of the receiver in square centimeters.

Now taking couple No. 19 again as an example,

$$\begin{aligned} C_1 &= \Delta t_2 C \text{ [where } C \text{ is the value in eq. (4)]} \\ &= 2.4\times 10^{-2}\times 9.6\times 10^{-7} \text{ cal./sec.} = 2.3\times 10^{-8} \text{ cal./sec.} \end{aligned} \tag{9}$$

The amount radiated from the rear face is given by

$$R_1 = \tfrac{1}{3}\times\tfrac{1}{5}\times 10^{-2}\times 1.28\times 10^{-12}[(T+\Delta t_2)^4 - T^4]\,. \tag{10}$$

Let $T = 293°$ C. then

$$R_1 = \frac{1.28\times 10^{-14}}{15}\times 2.4\times 10^{6} = 2.0\times 10^{-9} \text{ cal./sec.;}$$

hence the total loss is 2.5×10^{-8} cal./sec. and the value of W is

$$W = 2.5\times 10^{-8}\times 5\times 10^{2} \text{ cal./sec.} = 1.25\times 10^{-5} \text{ cal./sec.} \tag{11}$$

and from equation (8)

$$\Delta t_1 - \Delta t_2 = \frac{1.25\times 10^{-5}\times 10^{-3}}{16\times 10^{-2}} = 7.8\times 10^{-8}\text{ deg. C.} \tag{12}$$

This is the stable condition and is reached only after an indefinite period of time. Since $\Delta t_1 - \Delta t_2$ is insignificant compared to the value of $\Delta t_2 = 2.4\times 10^{-2}$ deg. C., we may neglect it in the following computation. Let us inquire what time will be required for the rear face to reach a temperature 99 per cent of the steady state, i.e., the time required for the thermoelectric current to reach 99 per cent of its value under the influence of the incident radiation. We have Fourier's equation for the flow of heat

$$\frac{\Delta t_2}{\Delta t_1} = 99\times 10^{-2} = \frac{2}{\sqrt{\pi}}\int_{\frac{u}{2h\sqrt{t}}}^{\infty} e^{-\beta^2}d\beta \tag{13}$$

Since $u = 10^{-3}$ cm, $h^2 = 0.4$, this gives us

$$t = 6.2\times 10^{-3}\text{ sec.}$$

It follows then that the lag of the thermocouple is negligible when applied to recording apparatus. If we multiply the equation (10) by the factor 4, we obtain the total radiation from both faces of the receiver. This gives us 8×10^{-9} cal./sec. as the loss by radiation. This is only one-third the loss by conduction along the strips, which is 23×10^{-9} cal./sec. Hence the desirability of using substances of low heat conductivity for the strips.

APPLICATIONS TO THE ASTROPHYSICAL PROBLEMS

1. *Stellar radiation problems.*—To observe the total radiation from stars, the thermocouple is mounted on a plate provided with a low-power eyepiece and water cell which can be moved in front of the thermocouple or moved away by means of a lever on the face of the plate. The apparatus is adapted to the Newtonian double-slide plate holder of the 100-inch telescope. A four-wire cable 135 feet long connects the thermocouple with the galvanometer room in the basement of the dome. Two of these wires are used for the thermo-

couple circuit, and the other two connect the observer at the telescope with the observer at the galvanometer by telephone. The deflections are obtained by orienting the thermocouple so that the line connecting the two receivers is parallel to one of the guiding screws, and by shifting the receivers alternately upon the star image with a half-turn of this screw.

In order to test the fundamental sensitivity of the thermocouple during the observations, an electric lamp (100-watt "Peerless" mazda) is placed on a bracket in the Cassegrain plate holder. The light from this lamp is reflected from the Cassegrain flat to the Newtonian flat and is received by a small lens at the Newtonian plate holder and projected on the thermocouple. When not in use, the lens may be swung aside and the lamp turned off.

Two types of galvanometer have been employed, viz., Leeds and Northrup high sensitivity D'Arsonval No. 2285, and more recently the Coblentz-Thompson galvanometer of the same make. Of the D'Arsonval galvanometers, two of different electrical properties have been used. No. (1) has a period of 4.44 seconds, resistance of 9.1 ohms, and mirror sufficiently flat to use a scale at 8 m, which gives a sensitivity of 4.75×10^{-10} amp./mm. No. (2) has a period of 6.5 sec., resistance of 17.4 ohms, and sensitivity of 3.1×10^{-10} amp./mm with scale at 8 m.

This latter galvanometer had a mirror $\frac{5}{16}$ inch in diameter with very good figure when tested in the Pasadena laboratory, so good in fact that a scale could be read at 11 m. When the galvanometer was taken to Mount Wilson and set up in the 100-inch dome at a temperature of 34° F., the figure became so bad that a scale could scarcely be read at 1 m, and the projected image of a lamp filament at a distance of 4 m was a band 7 mm broad with sharp edges and dark center. On removing the galvanometer to Pasadena the figure was restored. The mirror was then detached and the beeswax which covered the entire back and was used as a cement to attach it to the moving coil was removed, and the mirror attached to the coil again by a bit of universal wax placed in the center of the back. This procedure effectually removed the annoying change in figure of the mirror, which has since performed admirably, although subjected to temperatures below freezing.

No. (1) was placed under a bell jar and subjected to variations in pressure. No change in sensitivity was observed, even when the pressure was reduced to 10^{-3} mm. At this pressure the period was reduced 4 per cent, while an enormous drift was introduced which could not be removed even by grounding various parts of the galvanometer.

Both visual and photographic methods have been employed to observe the galvanometer deflections. Visually two methods have been used. When the scale was at 8 m the highest power telescope it was found feasible to employ was approximately 45. But by placing a spectacle lens of 6 m focus directly in front of the galvanometer mirror and observing the image with an eyepiece with cross-hair in the field, a power of 350 could be employed advantageously, and the scale read with accuracy to tenths of a millimeter.

When visual observations are made, the drift of the galvanometer is difficult to allow for. This drift can be reduced to a minimum by inclosing the thermocouple cell in a wad of cotton wool, and surrounding the galvanometer by a double wall box, the space also being filled with cotton. With this arrangement the observed drift of the D'Arsonval galvanometer is at most only 1 or 2 mm per minute, and is often absent. By taking the observations at regular intervals, keeping the star on the receiver in the meantime, an approximate value of the drift may be obtained.

The method which we have adopted at Mount Wilson consists in recording photographically the deflections and drift. The photographic plate 7×17 inches, or 8×10 inches, is carried by a slide moving in cast-iron ways, which is driven by a screw so that the film is always in the focal plane of a cylindrical lens of semicircular cross-section, ½-inch aperture and 8 inches long, set with its axis at right angles to the motion of the plate. The image of a straight filament lamp, formed by the spectacle lens before the galvanometer mirror, is at right angles to the axis of the cylindrical lens. That portion, then, which the lens intercepts, will form a point image on the plate, which in turn registers the motion of the galvanometer. The plate is driven 2 cm a minute by a motor-driven gear from which a large range of speeds can be had.

Plate VI is a reproduction of photographic records of Vega (mag. 0.1), Arcturus (mag. 0.2), *α* Herculis (mag. 3.0), and R Hydrae (mag. 8.0), respectively, made with this apparatus on the same night and reduced to one half the original scale. The larger deflections, on the left, for each star were taken without a water cell, those on the right with a water cell 1 cm thick interposed in the beam. The increasing absorption of the water cell with the advance in spectral type is well shown, as is also the increase in total radiation for a given magnitude. The effects of poor seeing are well shown in the deflections for *α* Herculis without the water cell.

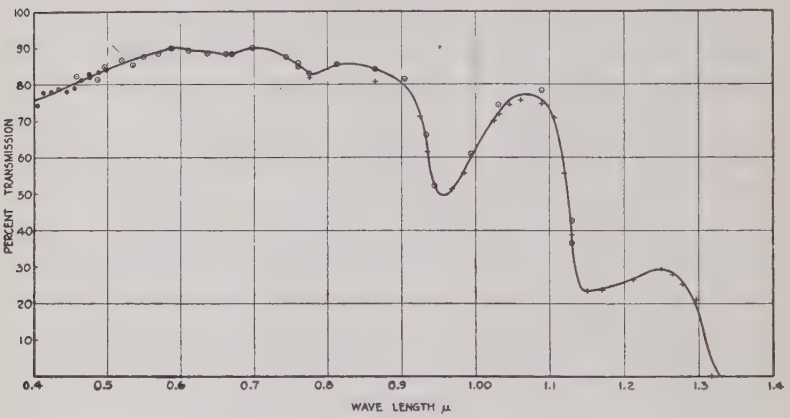

FIG. 3.—Transmission of a water cell 1 cm thick, having windows of microscope cover-glass 0.12 mm thick.

The water cell employed in these observations consists of a brass cylinder 1 cm long with microscope cover-glasses 0.12 mm thick cemented to the two ends. The transmission curve of this cell, filled with distilled water, as observed with the thermocouple in the Pasadena laboratory, is shown in Figure 3. From the curve it will be seen that very little energy is transmitted beyond 1.1 μ and none at all beyond 1.4 μ. It will also be noted that star deflections observed through the water cell cannot exceed 90 per cent of the deflections observed without it.

PLATE VI

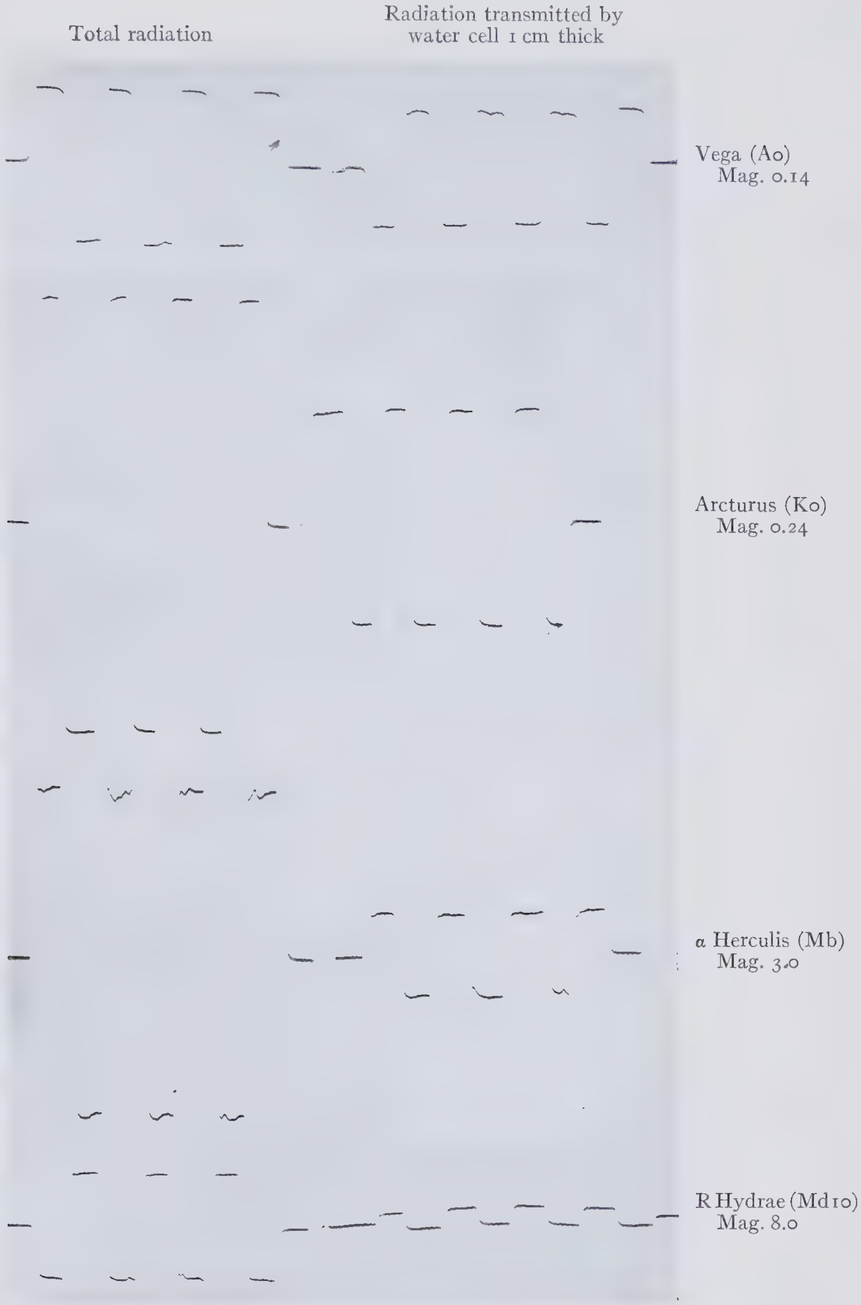

Photographic Records of Galvanometer Deflections Made by Stars of Various Spectral Types

2. *Solar applications.*—The problems to which we have thus far applied the thermocouple may be listed as follows: (1) registration of the spectral energy curve of the sun; (2) registration of drift curves across the disk in various wave-lengths; (3) energy relations across sun-spots and faculae.

The apparatus employed in these investigations consists of the photographic registering apparatus already described. For studying the energy relations across spots and faculae the apparatus is mounted on the head of the spectrograph of the 150-foot tower telescope. The thermocouple is contained in a wooden case carried horizontally by a screw-driven plate, which is connected by a back gear to the driving shaft of the photographic registering apparatus. A paper-covered metal shield, perforated with a needle point, is attached to the thermocouple case directly above one of the receivers in such a way that the needle hole can be adjusted by means of a screw so that the light from the solar image passing through it will fall on the receiver. An aperture in the side of the case, closed by a cork, enables the observer to effect this adjustment.

The spot is now brought by the slow motions of the coelostat in line with the pin hole, and the photographic registering apparatus set in motion. By means of the back gear, the ratio is so adjusted that the thermocouple is driven about 1 cm while the photographic plate travels 20 cm. The galvanometer, which is set on an arm of the spectrograph head, is connected to the photographic registering apparatus by means of an aluminum box 1 m long, which shuts out the light of the room from the cylindrical lens. By this apparatus the total radiation curve across the spot is obtained. By rotating the spectrograph head, curves may be obtained across the spot in any direction.

THE REGISTERING MICROPHOTOMETER

In 1912 Koch first introduced the principle of the registering microphotometer, using a photo-electric cell and string electrometer as the registering device. The curves were photographically registered on a falling plate controlled by clock work. In 1915 Stetson[1] modified the apparatus by substituting a thermopile and galvanometer for the photo-electric cell and electrometer, thus making the apparatus simpler and freer from the annoyances to which the photo-electric cell is subject. Stetson's apparatus was read visually and was not a self-recording apparatus. In 1921 Moll[1] applied the self-registering principle to the thermocouple, the negative and plate being driven by hand. In both Stetson's and Moll's apparatus the thermocouple operated at atmospheric pressure.

---

[1] *Astrophysical Journal*, **43**, 253, 1916.

The new registering microphotometer now in use at Mount Wilson was built in the Pasadena shop after designs by Mr. Babcock and set in operation in 1914. The photo-electric cell and string electrometer were employed by him as in Koch's apparatus. The modifications introduced by Babcock consisted in (1) moving the plate by a motor-driven screw, (2) providing for plates 15 cm × 100 cm, (3) introducing a gear shift between the moving microscope stage and plate screw so that a number of magnifications of motion between the negative and moving plate could be used, (4) use of a cylindrical lens in place of a slit before the moving plate, and (5) taking all light used in the apparatus from one Nernst filament. The modifications introduced by us consist in (1) replacing the photo-electric cell and electrometer by a vacuum thermopile and D'Arsonval galvanometer, (2) the use of both sunlight and a nitrogen-filled straight-filament lamp as sources of illumination, (3) adding a second microscope for setting purposes, (4) introducing an adjustable second slit before the thermopile, (5) projecting an illuminated slit upon the photographic film as in Moll's apparatus instead of limiting a large beam by means of a slit directly above the film as in Koch's machine, and (6) the introduction of parallel silvered plates into the barrel of the microscope to increase the field of the objective and the deflections of the galvanometer.

Plate VII shows the machine as it is now used, arranged for solar illumination. The whole instrument rests on a cast-iron bed-plate *AB*, 12 ft. long and 28 in. wide, which stands on a cement pier. The photographic registering device *C* and the traveling microscope stage *D* are connected by the shift-gear box *G* and driven by the motor *M*. The plate carrier *K* carries the plate *P* horizontally

---

[1] *Proceedings of the Physical Society of London*, 33, 207, 1921.

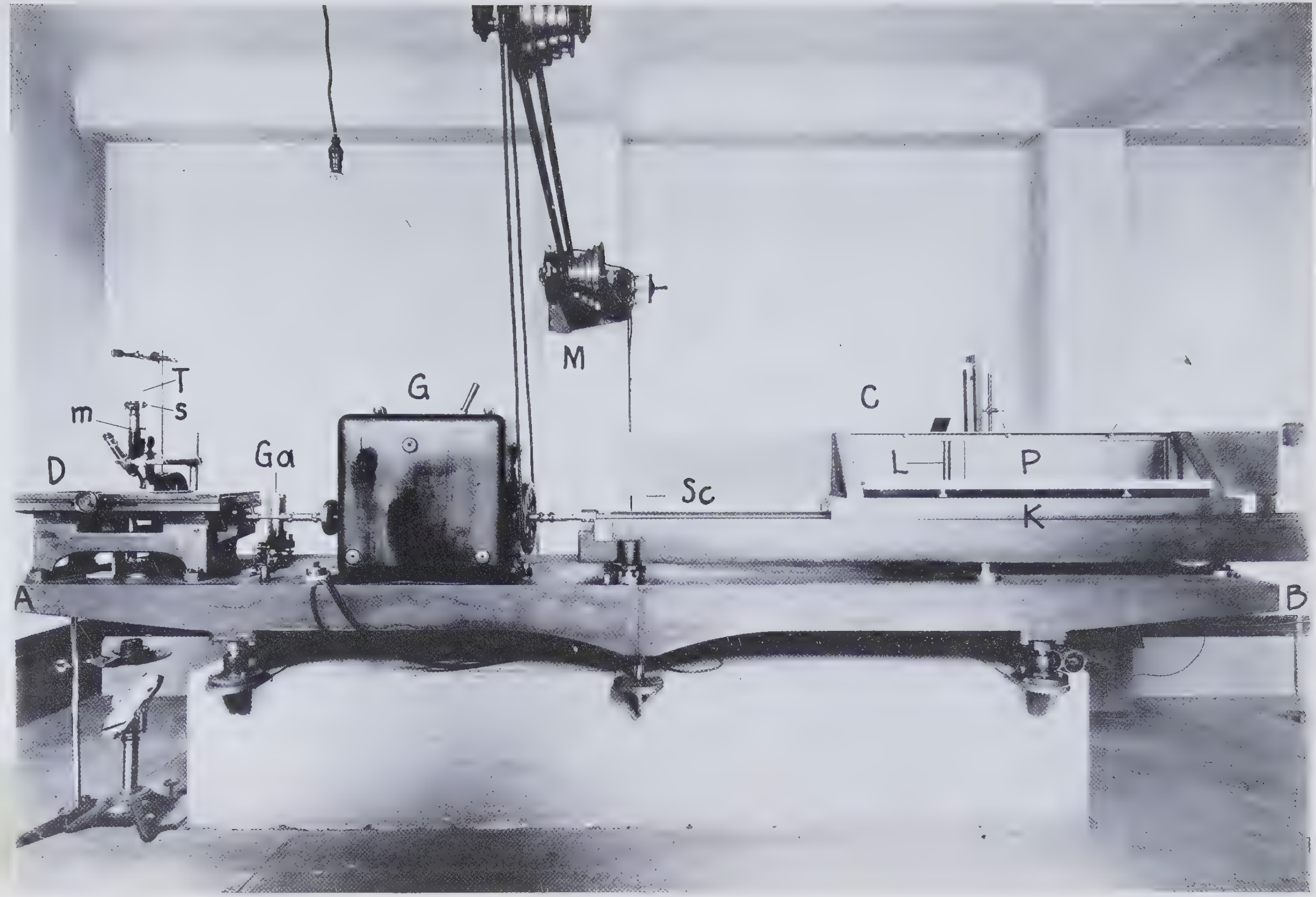

THE REGISTERING MICROPHOTOMETER

past the cylindrical lens *L*, and is moved by the long screw *Sc* of 2 mm pitch in the casting below. By means of two mirrors the image formed by the galvanometer mirror is made to play up and down along the cylindrical lens, and thus the curves are produced. The microscope stage *D* rests on four steel balls and is driven by a screw of 1 mm pitch connected to the gear box *G*, in the same direction as the photographic plate *P*. By means of the gear box *G* the ratio of speeds between *C* and *D* may be varied from two to fifty fold. The microscope *m* contains at its upper end an adjustable slit *S* above which the thermopile *T* is placed. Lead-wires from the thermopile are connected with the registering galvanometer *Ga* on the bed plate of the instrument. A motor is also provided to drive the machine at high speed so that the plate may be returned to starting position when several curves are being compared. In this way all the runs may be made in the same direction, thus eliminating the lag of the galvanometer due to its period.

In securing a curve representing the energy relations across a spectral line in a photograph, it is obvious that in order to avoid distortions of the curve it will be necessary to employ as narrow an element of the line as possible. This means, in effect, that the magnification of the microscope *m* should be large and that the second slit *S*, which limits the beam reaching the thermopile, should be narrow. There is, however, a limit to the width of the slit *S*, since too narrow a slit will introduce irregularities due to the clustering of silver grains in the film, or dust and defects in the film. With the present apparatus these irregularities begin to appear when the slit width is reduced to about 0.1 mm for the negatives employed. For very fine-grained plates this limit can of course be further reduced.

In order to remedy this defect it will be necessary to integrate over a greater length of line than is available with Koch's arrangement. The device adopted to facilitate this is shown in the diagram of the optical system now employed (Fig. 4). Artificial light or sunlight passes through a condenser and falls on a slit S_1, an image of which, formed by the objective O_1, is projected on the spectral line *L* of the negative on the moving microscope stage.

An image of this illuminated portion of the spectral line L is projected by the microscope objective O_2 on to the second slit S placed just in front of the thermopile T. By means of the two parallel mirrors M_1, M_2 the portions of the beam which would otherwise fall outside of the field are thrown back upon the thermopile and become effective. From tests it was found that the 40 mm objective employed had fair field over 10°, so that a spectral line 9 mm long could be employed. By adjusting the length of the slit S_1, or the distance from the mirrors M_1, M_2 to the objective O_2, the field may be limited to this value. The full lines indicate the path of the rays in the present arrangement, and the dotted lines the same for the arrangements of Koch and Moll.

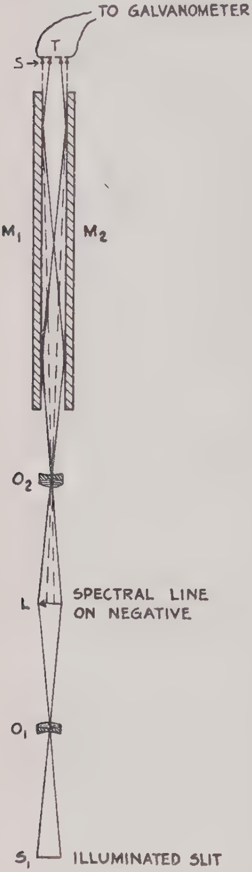

FIG. 4—Optical system of the registering microphotometer.

By adjusting the width of the first slit S_1, only that portion of the spectral line L is illuminated which is included in the image which passes through the second slit at S. This device employed by Moll reduces the scattering of the light in the film, but probably its greatest advantage is in eliminating the use of the first slit just above the moving plate at L, thus facilitating the adjustment of the negative.

When the thermocouple is employed to replace the photo-electric cell on the registering microphotometer, no means is available for compensating the apparatus against changes in the intensity of the illumination used. No mention of this is made in the descriptions of the apparatus employed by Stetson and Moll, who used storage batteries as a source of current for the illumination. While we cannot compensate the thermopile, we may, at the same time, however, register the variations in the illumination by projecting a portion of the beam incident on the first slit S_1, on a second thermopile and registering the fluctuations in intensity on the photographic plate by means of a second galvanometer of the same period as the one employed with the first thermopile T. The results of investigations with the apparatus and methods here described will appear in a future paper.

Mount Wilson Observatory
July 1922

Contributions from the Mount Wilson Observatory, No. 247
Reprinted from the *Astrophysical Journal*, Vol. LVI, pp. 318–339, 1922

THE ELECTRIC FURNACE SPECTRUM OF IRON IN THE ULTRA-VIOLET, WITH SUPPLEMENTARY DATA FOR THE BLUE AND VIOLET

BY ARTHUR S. KING

ABSTRACT

Electric furnace emission and absorption spectra of iron in the ultra-violet, for various temperatures from 1400° to 2600° C.—This paper supplements one published in 1913 on the iron furnace spectrum from λ 3884 to λ 7208. Furnace emission spectra extend into the ultra-violet only as far as the continuous spectrum of a black body at the same temperature. It has now been found, however, that by using a very hot source, such as a gas-filled tungsten lamp or a series of fine wires exploded by Anderson's method, absorption spectra corresponding to either low or high temperatures of the vapor may be obtained extending to λ 2298 or beyond. The relative intensities in absorption spectra are the same as in emission spectra of the same temperature. A large number of spectrograms have been made in the first and second orders of a 15-foot concave grating. Tables I–III contain the *temperature classification of 904 lines*, λ *2298 to* λ *3878*, and the relative intensities in the arc and in high, medium, and low temperature furnace spectra, either emission or absorption, upon which the classification is based. For iron, the low-temperature lines, classes I and II, are well developed at 1600°, the medium, class III, at 2000°, and the high-temperature lines, class IV, at 2300°. About sixty lines, of various classes, are relatively very weak in the arc; they are denoted by I A, II A, etc. A *revised classification of 262 lines*, λ *3884 to* λ *4531*, based on later spectrograms, is given in Table IV; and Table V contains a list of the most persistent low-temperature lines, the twenty-one from λ 3745 to λ 4482 emitted by the vapor at 1400°, as photographed by long exposure with a 1-meter concave grating. On Plate X a high-temperature absorption spectrum is shown between two arc spectra.

Discussion of the significance of the temperature classification of spectral lines.—Work with various metals indicates a parallelism between the successive temperature excitation stages and the radiation stages as the potential is increased in low-voltage vacuum arcs. For high boiling-point metals, the classification can perhaps be more readily made by the furnace method. To assist in the correlation of the two types of classification, elements which may have their spectra excited in either way should be carefully studied in both ways.

A paper on the electric furnace spectrum of iron from λ 3884 to λ 7208 was published by the writer[1] in 1913. The present paper begins at the violet limit of the former investigation and extends the study to λ 2298, which is as far as it has been possible to obtain lines by means of the furnace. Within this range, the lines given in tables of arc wave-lengths are covered with reasonable completeness, the missing lines generally being very faint in the arc or of the enhanced-line type, both of these classes requiring, as a rule, the stronger excitation of the electric discharge. As in other studies of furnace spectra, the purpose has been to show the changes in relative line intensity through various furnace temperatures and into the conditions of the arc, and from these data to classify the lines according to the temperatures at which they first appear and their rates of growth as the temperature rises.

---

[1] *Mt. Wilson Contr.*, No. 66; *Astrophysical Journal*, **37**, 239, 1913.

The temperature stages for this purpose must be selected for each element according to the observed changes in its spectrum, and it is desirable that at each stage there be a marked change from the spectrum at the stage below. For iron, the low-temperature spectrum was found to be well developed at 1600° C. and the plates for this group of lines were taken from 1600° to 1700°. For the medium temperature, at which another set of lines appears, about 2000° was used. The high-temperature spectrum develops at about 2300° and still higher temperature has little effect beyond increasing the reversals and giving general intensification. Nevertheless, temperatures of 2500° to 2600° were used for most of the high-temperature spectra, in order to obtain the full effect of the conditions corresponding to this stage.

The same methods of classification have been used as in previous studies, but an important new feature is the use which has been made of absorption spectra, obtained by methods described in recent papers,[1] and by others still more recently developed.

It was noted in the first paper on the iron spectrum, and has been many times confirmed for this and other spectra, that at a given temperature of the furnace the emission spectrum stops at a point in the ultra-violet somewhat short of the limit of the continuous spectrum given by a black body at the same temperature. A close approach to such a black body is easily obtained by placing a graphite plug in the central part of the tube and heating the furnace to the temperature previously used for the emission spectrum.

A limit is thus set to the wave-length range within which the furnace at a certain temperature can give emission lines, and if appearance at this temperature is the criterion indicating that lines belong to a certain class, all lines of shorter wave-length automatically go into a higher class. It is often the case, however, that the lines of shorter wave-length, when produced by the furnace at a higher temperature or in the arc, show no features that would distinguish them from those in the region given by the low-temperature furnace. This forced distinction, due to the fact that the furnace cannot emit beyond a certain point, was noted in the study of the spectra of calcium, strontium, barium, and magnesium.[1]

---

[1] *Mt. Wilson Contr.*, Nos. 174, 233; *Astrophysical Journal*, **51**, 13, 1920; **55**, 380, 1922.

In the present investigation, trials were made to see if iron vapor at low temperature would absorb radiation of shorter wave-length than it was able to emit. This proved to be the case. When a beam of white light from a very hot source was passed through the moderately heated furnace, iron absorption lines appeared as far in the ultra-violet as the solid body was able to build up a continuous spectrum; and by using successively hotter sources behind it, the furnace at 1600° C. gave absorption lines as far as λ 2298. The emission spectrum at this temperature ends at λ 3440, though this is due partly to the fact that for a considerable range below this, no low-temperature lines occur.

There seems to be no reason why ultra-violet absorption lines obtained in this way should not be classed as low-temperature lines. A stellar spectrum produced by sufficient difference of temperature between the body of the star and cool iron vapor surrounding it should show no difference (disregarding atmospheric absorption) between these lines and the low-temperature lines of the visible spectrum.

It has therefore been considered legitimate to use the absorption spectrum for a certain temperature stage as a means of extending the data beyond the point where the emission lines die out. This has resulted in a division of the tabulated lines into three sections. In Table I, from λ 2298 to λ 2808, the comparison is between the absorption spectra at high and low temperatures. Both of these extend to shorter wave-lengths than the corresponding emission spectra. At high temperature, however, it has been possible to force the emission spectrum to λ 2462. The relative intensities of emission and absorption lines with the furnace at high and low temperatures were so nearly the same as to justify printing only a single list. Table II includes data from λ 2813 to λ 3437. The high- and medium-temperature columns are for emission lines, but intensities of the low-temperature lines are to be obtained only from the absorption spectrum. Table III, for the range λ 3440 to λ 3788, makes use of emission spectra at the three temperature stages, though in compiling it constant reference was made to the reversibility of lines as shown by their strength in absorption spectra.

---

[1] *Mt. Wilson Contr.*, No. 150; *Astrophysical Journal*, **48**, 13, 1918.

EXPERIMENTAL METHOD

a) *Furnaces.*—Two electric furnaces have been employed. The first, in which the tube with its supports is inclosed in a strong cylindrical chamber, adapted for high pressure as well as vacuum, was used throughout the previous investigations. The other is for pressures not above the atmospheric limit, and consists of a heavy sheet-iron hood which is lowered upon a base-plate through which the connections for electric current and water pass to the supports of the furnace tube. These supports are hollow bronze blocks, water-cooled, and bored to hold cylindrical graphite bushings which make direct contact with the tube. The latter is of Acheson graphite, and various forms have been used in special experiments, but the size regularly employed has been of 13-mm bore, 19-mm outside diameter, and 30-cm length. The heated portion of the tube between the contact blocks is about 20 cm long. A tubular water jacket of cast iron, of 17.5 cm internal diameter, surrounds the furnace tube, so that no cooling of the outer inclosure is required. This furnace, and also the older one, were usually pumped out to a pressure of less than 1 cm of mercury, but numerous experiments were made at atmospheric pressure. An illustration of this furnace with the hood raised is shown in Plate VIII.

Iron in powdered form was placed in the heated portion of the tube. A preliminary heat was given at a temperature sufficient to melt the iron, which then stuck to the wall of the tube, probably forming a carbide. A supply of iron thus remained in place during the life of the tube, and no fresh charging was needed. The presence of air appeared to cause a more vigorous combination of the metal with the material of the tube.

PLATE VIII

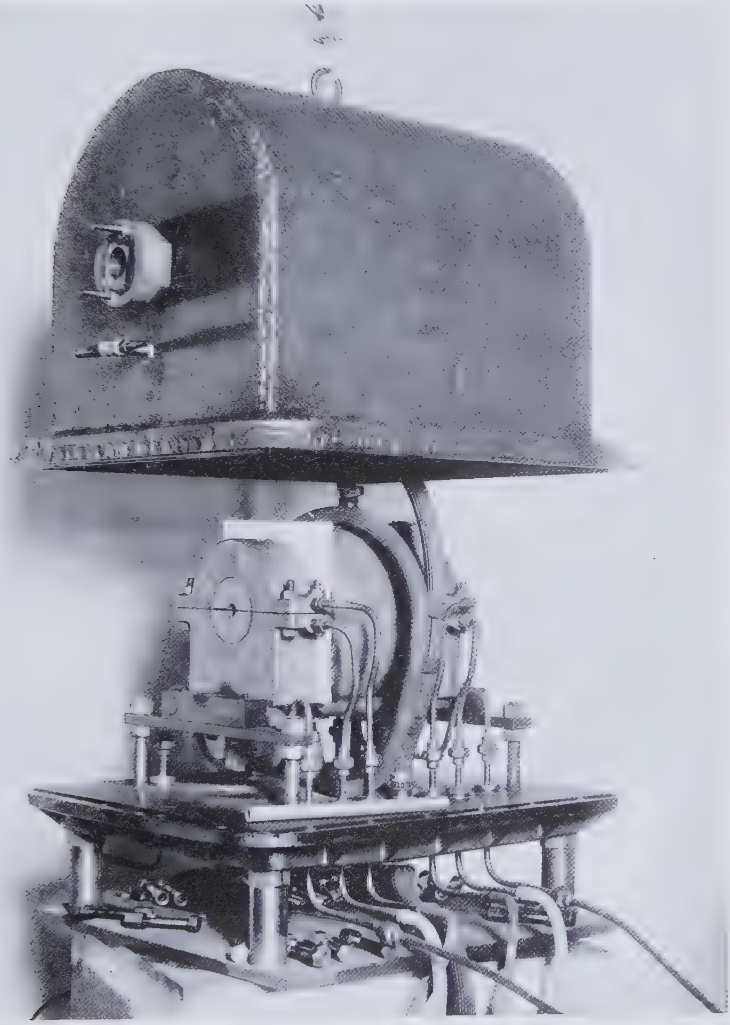

Vacuum Electric Furnace

Alternating current of from 10 to 30 volts was usually employed on the furnace tube; but in the later work, direct current from a 500-kw generator was often used. This was especially useful in experiments with the furnace at atmospheric pressure, as the temperature changes caused by the thinning tube could be compensated by a close control of the voltage.

b) *Production of absorption spectra.*—Three methods of obtaining absorption spectra were used during the investigation. A very useful method was to place a cylindrical plug of graphite near the center of the tube and observe the absorption produced by iron vapor in front of this plug. Very high black-body temperatures are obtainable in this way, the plug frequently being heated above 3200° C., the highest temperature readable on the pyrometer. With this arrangement, however, it is a question as to the temperature of the vapor which absorbs. As in previous work with this method, the spectrum indicated a difference of about 400° between the plug and the absorbing layer, which would mean that the relatively cool vapor near the end of the tube is effective, while the main mass of vapor in the tube is too hot to give the required gradient. This method, especially when the tube was made thinner near the middle, so that the plug was much hotter than the main length of the tube, gave good results for the high-temperature absorption spectrum. An absorption spectrogram for which the plug was held at a temperature of 3000° gave lines as far as λ 2447, the relative intensities showing no important difference from an emission spectrum at 2600°. In another test, the emission spectrum at 2400° was compared with absorption spectra for which the plug was held closely at 2400°, 2600°, and 2800°, respectively. The 2800° spectrum was identical in all essential features with the emission spectrum at 2400°. At low temperatures, however, it is desirable to know as accurately as possible the temperature of the absorbing vapor. For this purpose it is best to use an open tube, the temperature of whose wall can be closely measured, and pass through the tube a beam of light from a source so much hotter that the vapor in the main section of the tube can be safely assumed to be in a condition to absorb. This was arranged by placing a 900-watt gas-filled lamp, operating at 30 amperes, behind the furnace, and directing its beam through the tube. The rated temperature of the tungsten spiral in this lamp is 2900° C. To get the full benefit of the lamp in the ultra-violet region, a side tube closed by a quartz window was set in the bulb, which was then refilled with pure nitrogen.

A third method was to use as a source of continuous spectrum the light from exploding wires inclosed in a block of wood. This has been shown by Anderson[1] to give excellent absorption spectra of the material of the wire, extending far into the ultra-violet. Dr. Anderson kindly operated the explosion apparatus and the light was passed through the furnace heated at various temperatures. As it is necessary to use metals giving as few lines as possible in the region to be studied, wires of aluminium and of lead were tried. The latter was most nearly free from disturbing lines, both of the metal itself and of iron impurities, and a number of furnace absorption lines were added to the list obtainable by the other methods. The explosion method promises to be generally useful, the chief drawback, aside from the disturbing lines in the source, being the very large number of explosions required (on account of their almost infinitesimal duration) to build up a continuous spectrum with a high-dispersion spectrograph.

c) Photography of the spectrum.—The spectrograms for the various furnace temperatures were made as far as possible with the vertical concave-grating spectrograph of 15-foot radius. All of the photographs used for the final intensity estimates were made in this way, except when wire explosions were used as an absorption source, a 1-meter concave grating giving high intensity beyond λ 3000 then being employed. The second order of the 15-foot instrument, giving a scale of 1.86 A per millimeter, was used as far as λ 2800, while the first order was used for the shorter wave-lengths. Many spectrograms, especially for low-temperature spectra, were made with the 1-meter spectrograph and used for checking those of the higher dispersion. These were particularly useful in deciding whether certain lines can be brought out at a given temperature, since a long exposure with this instrument may be depended on to show lines which with higher dispersion are under-exposed.

---

[1] *Mt. Wilson Contr.*, No. 178; *Astrophysical Journal*, 51, 37, 1920.

EXPLANATION OF THE TABLES

Tables I, II, and III contain in the first column the wave-lengths of iron lines on the international system. These are for the most part according to the measurements of Burns,[1] rounded off to two decimal places, though in some cases values from the table of iron lines given by Kayser[2] have been used. Lines in the arc tables which are not given by the furnace even at high temperature are entered only when they offer a striking contrast with neighboring lines which in the arc are of equal intensity or even weaker, but which appear distinctly in the furnace. This rule is not followed closely in the region of wave-lengths shorter than λ 2500, where a large proportion of the strong arc lines are of polar type and are usually absent from the furnace spectrum.

The arc intensities in the tables are graded so that a large proportion of the lines are given values comparable with those for the high-temperature furnace. In the ultra-violet, the arc spectrum taken close to the poles is very different from that emitted by the central region, and it is the lines of the latter which in the main make up the furnace spectrum. The photographs for estimation of arc intensities were therefore made with the slit across the image of the arc and about midway between the poles. For the arc, as for the emission furnace, "r" and "R" refer to degrees of reversal, while a line of nebulous structure is denoted by "n."

In the gradation of furnace intensities, "tr" indicates that a trace is visible on a strongly exposed spectrogram, while a line distinctly outlined is given intensity "1." Lines of strength above 20 are likely to show some degree of reversal, and before this intensity is reached, the line has a softened appearance which may be mistaken for faintness. Some plates out of the large collection for each temperature stage usually showed the true condition of the line. The scale for absorption lines was made as closely comparable as possible with that for emission lines.

The "arc type," in the fifth column of Table I, refers to the relative strength of a line at the center and near the poles of the arc. Type "C" is strong in the center of the arc, while type "C–P"

---

[1] *Lick Observatory Bulletin*, **8**, 27 (No. 247), 1913.

[2] *Handbuch der Spektroscopie*, **6**, 896.

TABLE I

Temperature Classification of Iron Lines, λ 2298–λ 2808

λ (I.A.)	Arc Intensity	Furnace Intensities: High-Temp. Absorption	Furnace Intensities: Low-Temp. Absorption	Arc Type	Class	λ (I.A.)	Arc Intensity	Furnace Intensities: High-Temp. Absorption	Furnace Intensities: Low-Temp. Absorption	Arc Type	Class
2298.18	10r	4	2	C	II	2599.58	6	3	......	C–P	III
2299.25	2	1	......	C	III	2605.69	6	1	......	C–P	III
2303.57	3	2	1	C	II	2606.84	6	3	......	C–P	III
2309.00	2	1	......	C	III	2610.76	1	1	......	C	III
2313.12	2	1	......	C	III	2612.79	2	2	......	C	III
2320.37	2	1	......	C–P	III	2614.51	1	1	......	C	III
2354.88	3	2	1	C–P	II	2618.03	5	2	......	C–P	III
2368.60	10	1	......	C–P	III	2618.72	2	2	......	C	III
2373.74	15	2	1	C–P	II	2623.38	2	2	......	C	III
2382.04	20	2	1	C–P	II	2623.54	5	2	......	C–P	III
2438.19	2	1	......	C	III	2629.60*	2	2	......	C	III
2447.72*	4	4	?	C	II ?	2632.25	4	2	......	C–P	III
2453.48	5	1	......	C	III	2632.60	2	4	......	C	III A
2457.60	6	3	1	C–P	II	2635.82	8	4	......	C–P	III
2462.19	4	4	......	C	III	2636.49	1	1	......	C	III
2462.65	10r	12	3	C	II	2641.65	4	2	......	C	III
2465.16*	6	3	......	C–P	III	2644.01	8	3	......	C–P	III
2468.89	4	2	......	C–P	III	2645.43	1	2	......	C	III A
2472.37	5	2	......	C–P	III	2647.57	3	4	......	C	III
2472.90	12R	20	4	C	II	2651.72	2	1	......	C	III
2473.07	?			C	II	2656.15	3	tr	......	C	III
2476.67	3	2	......	C	III	2660.41	1	1	......	C	III
2479.48	6	10	2	C	III	2662.07	3	2	......	C	III
2479.78	20R			C	II	2666.41	2	1	......	C	III
2483.28	60R	40	10	C	II	2666.82	8	4	......	C–P	III
2483.54	10			C	II ?	2666.97	3			C	III
2484.19*	15R	8	2	C	II	2667.92	1	2	......	C	III A
2488.15	40R	30	8	C	II	2669.50*	2	......	......	C	IV
2489.76*	15r	8	2	C	II	2673.22	1	tr	......	C	III
2490.66	30R	20	4	C	II	2679.07	10	3	......	C–P	III
2491.16	20R	15	4	C	II	2680.46	2	1	......	C	III
2496.54	6	1	......	C–P	III	2689.22	8	3	......	C–P	III
2498.90	10	tr	......	P	IV	2689.84	2	tr	......	C	III
2501.14	20R	15	3	C	II	2690.07	2	2	......	C	III
2507.90	6	2	......	C–P	III	2695.04	1	tr	......	C	III
2510.84	15R	12	2	C	II	2697.03	2	tr	......	C	III
2512.37	5r	3	tr	C	III	2699.11	6	2	......	C–P	III
2518.11	12r	10	2	C	II	2706.02	4	tr	......	C	IV
2522.86	40R	30	5	C	II	2706.59	8	3	......	C–P	III
2524.29	8r	5	2	C	II	2708.58*	4	......	......	C	IV
2527.44	15r	12	3	C	II	2710.55	2	tr	......	C	III
2529.27	10r	8	tr	C	III	2711.66	4	2	......	C–P	III
2529.83	3	2	......	C	III	2714.88	1	tr	......	C	III
2530.70	3	2	......	C	III	2715.33	1	tr	......	C	III
2533.80	4	tr	......	C	IV	2717.79	2	1	......	C	III
2535.61	8r	6	......	C	III	2718.45*	6	?	......	C–P	III ?
2540.98	10R	10	1	C	III	2719.04	60R	60	10	C	II
2542.11	6	tr	......	C–P	IV	2719.43*	3	?	......	C	III ?
2543.93	6	tr	......	C–P	IV	2720.91	40r	40	6	C	II
2544.72	6	tr	......	C	IV	2723.58	15	15	3	C	II
2545.98	10r	10	1	C	III	2724.96*	10	3	......	C–P	III
2549.62	10r	10	1	C	III	2726.06	6	2	......	C–P	III
2552.63	2	2	......	C	III	2728.03	3	2	......	C	III
2556.87	1	1	......	C	III	2728.83	2	2	......	C	III
2576.70	4	2	......	C–P	III	2730.98	2	2	......	C	III
2582.31	6	1	......	C	III	2733.58	15	5	1	C	II
2584.54	8	3	......	C–P	III	2734.01	2	tr	......	C	III
2585.89*	20	1	......	P	IV	2734.27	2	tr	......	C	III
2588.01*	8	1	......	C	III	2735.48*	8	5	......	C–P	III
2594.05	1	1	......	C	III	2735.61*	8			C	III
2594.16	1			C	III	2737.31	20r	20	2	C	II

TABLE I—*Continued*

λ (I.A.)	Arc Intensity	Furnace Intensities		Arc Type	Class	λ (I.A.)	Arc Intensity	Furnace Intensities		Arc Type	Class
		High-Temp. Absorption	Low-Temp. Absorption					High-Temp. Absorption	Low-Temp. Absorption		
2742.02	2	1	......	C	III	2769.67	1	1	......	C	III
2742.26	20	30	5	C–P	III	2772.08	20	6	2	C–P	II
2742.41	30r			C	II	2772.11	1		......	C	III
2743.57	3	1	......	C–P	III	2773.23	2	tr	......	C	III
2744.07	10	8	2	C	II	2774.73*	3	2	......	C	III
2744.53	8	2	......	C–P	III	2778.08	3	5	......	C	III
2746.99*	20	2	......	P	III	2778.23	20			C–P	III
2750.15	25r	20	4	C	II	2778.85	3	3	......	C	III
2753.69	3	2	......	C	III	2780.70	1	tr	......	C	III
2754.03	3	2	......	C	III	2781.84	4	2	......	C	III
2754.43	2	1	......	C	III	2787.94	5	8	......	C–P	II
2756.33	20	10	6	C	I	2788.11	30		2	C	II
2757.32	10	3	......	C–P	III	2792.40	1	1	......	C	III
2759.82	4	2	......	C	III	2795.01	3	2	......	C	III
2761.79*	18	3	......	C–P	III	2797.78	15	3	......	C–P	III
2762.03	15	3	......	C–P	III	2799.15	1	tr	......	C	III
2763.11	4	2	......	C	III	2804.52	20	3	1	C–P	II
2764.33	3	1	......	C	III	2806.99	20	3	1	C–P	II
2766.91	2	2	......	C	III	2807.24	2	1	......	C	III
2767.52*	20	3	......	P	III	2808.33	2	1	......	C	III

2447.72	Probably present at low temperature close to Pb absorption line. Blends in arc with close polar line to red.
2465.16	Some strengthening at pole in arc. Possibly blend with polar line.
2484.19	Blend in arc with polar line to red.
2489.76	Blend in arc with polar line to red.
2585.89	Strong throughout arc, enhanced at poles.
2588.01	Blend in arc with polar line to red.
2629.60	Close blend in arc with polar line.
2669.50	Appears faintly in high-temperature emission spectrum.
2708.58	Appears faintly in high-temperature emission spectrum.
2718.45 2719.43	Blend in furnace with λ 2719.04.
2724.96	Blends in arc with polar line λ 2724.89.
2735.48–.61	Furnace line is chiefly λ 2735.61.
2746.99	Strong throughout arc, enhanced at poles.
2761.79	Slightly strengthened at poles.
2767.52	Much enhanced at pole.
2774.73	Blend in arc with polar line to violet.

indicates that the line is emitted with little change of intensity from center to pole. Polar lines, denoted by "P," are rarely visible in the furnace spectrum.

The classification of lines given in the last column of each table has been carried out in the same manner as in previous papers, except that class I B of the former paper on the iron spectrum is here replaced, as has been the case for the other metals studied, by class I.

Classes I and II are low-temperature lines, but those of class I maintain their strength at low temperature longer than do the lines of class II. These classes include practically all of the lines which

TABLE II

Temperature Classification of Iron Lines, λ 2813–λ 3437

λ (I.A.)	Arc Intensity	Furnace Intensities			Class
		High-Temp. Emission	Med.-Temp. Emission	Low-Temp. Absorption	
2813.29	30R	8	5	3	II
2815.51	3	2	......	......	IV
2817.51	6	5	2	......	III
2820.81	2	2	......	......	IV
2823.28	20	4	3	1	II
2825.56	20	6	3	2	II
2825.69	6	2	1	1	II
2827.89	5	3	2	......	III
2828.81	7	3	2	......	III
2832.43	25r	4	3	1	II
2835.46	6	4	4	4	I
2838.12	10	5	3	......	III
2840.42	6	4	2	2	II
2843.63	10	3	2	......	III
2843.97	20r	6	5	2	II
2845.60	8	6	3	......	III
2846.83	3	1	......	......	IV
2848.71	5	3	1	......	III
2851.80	15r	5	3	1	II
2858.90	5	3	2	1	II
2862.50	4	2	......	......	IV
2863.43	8	3	1	......	III
2863.87	8	6	3	3	I
2866.63	7	3	2	......	II
2867.31	3	1	......	......	IV
2867.57	3	1	......	......	IV
2868.44	3	1	......	......	IV
2869.31	10	6	6	6	I
2872.34	7	4	4	......	III
2874.18	10	8	6	6	I
2875.31*	5	3	......	......	IV
2877.30	8	4	2	......	III
2880.58	2	1	......	......	IV
2880.76*	5	......	......	......	V
2883.73*	4	......	......	......	V
2886.32	3	1	......	......	IV
2887.81*	5	......	......	......	V
2893.76	1	2	......	......	IV A
2893.88	2	1	......	......	IV
2894.51	10	3	1	......	III
2895.04	8	3	1	......	III
2899.42	8	3	......	......	IV
2901.38	5	4	......	......	IV
2901.92	5	2	......	......	IV
2907.52	5	......	......	......	V
2912.16	20r	12	10	8	I
2912.26	3	3	......	......	IV
2914.31	3	1	......	......	IV
2918.03	10	1	......	......	IV
2918.35	3	1	......	......	IV
2920.69	5	4	......	......	IV
2923.29	7	1	......	......	IV
2923.85	7	1	......	......	IV
2925.36	4	......	......	......	V
2925.90	4	3	......	......	IV
2926.58*	10	tr	......	......	V
2929.01	25r	15r	10	8	I
2929.12	6	4	......	......	IV
2929.62	2	1	......	......	IV
2936.90	60R	50r	20r	15	I
2937.81	10n	1	......	......	IV
2941.34	15r	15r	10	8	I
2944.40*	6	......	......	......	V
2945.07	3	1	......	......	IV
2947.66*	6	......	......	......	V
2947.88	60R	50R	20r	15	I
2948.44	4	1	......	......	IV
2949.21*	8	......	......	......	V
2950.25	20n	3	......	......	IV
2953.49	5	1	......	......	IV
2953.78*	5	......	......	......	V
2953.94	50R	35R	15r	10	II
2954.66	5	2	......	......	IV
2957.37	30R	25R	12r	8	II
2960.00	10	3	......	......	IV
2960.30	1	1	......	......	IV
2965.26	20	15r	10	6	II
2965.82	2	1	......	......	IV
2966.90	125R	100R	40R	20	II
2969.36	5	3	2	1	II
2969.48	10	6	4	4	I
2970.11	40R	30R	10r	10	I
2970.52*	4	......	......	......	V
2972.28	3	1	......	......	IV
2973.14	60R	50R	20r	15	I
2973.24	60R	50R	20r	15	I
2976.13	5	2	......	......	IV
2980.54	5	1	......	......	IV
2981.45	20r	15r	12	8	I
2981.86	6	4	......	......	IV
2983.57	125R	100R	30r	25	I
2984.83*	10	6	1	......	IV
2985.55	4	......	......	......	V
2986.46	3	5	5	1	III
2987.29	10	8	6	1	III
2988.47	2	3	......	......	IV
2990.39	6	4	......	......	IV
2991.65	5n	3	......	......	IV
2994.43* 2994.50*	100R	80R	40R	35	I
2996.39	5	2	......	......	IV
2999.52	30R	30R	12	5	II
3000.45	8	8	3	......	III
3000.95	100R	80R	30r	25	I
3002.65*	5	......	......	......	V
3003.03	10	10	6	tr	III
3005.31	3	1	......	......	IV
3007.15	8	8	3	......	III
3007.28	12r	10r	7	5	I
3008.14	60R	50R	20r	12	I
3009.10	5	3	......	......	IV
3009.58	25r	20r	10	3	II
3011.48	7	3	......	......	IV
3014.18	3	5	......	......	IV
3014.92	1	2	......	......	IV A
3015.93	4	1	......	......	IV
3016.18	12	8	8	tr	III
3017.63	15r	30R	15r	10	I A
3018.99	15r	12r	10	1	III
3020.50	100R	75R	30R	10	II
3020.64	200R	150R	80R	50	I
3021.08	150R	100R	40R	30	I
3024.04	15r	30R	15r	10	I A
3025.28	3	5	2	......	III
3025.64	15	8	1	......	IV
3025.85	50R	50R	25r	20	I

TABLE II—*Continued*

λ (I.A.)	Arc Intensity	Furnace Intensities			Class
		High-Temp. Emission	Med.-Temp. Emission	Low-Temp. Absorption	
3026.47	15	10	8	1	III
3029.24	3	3	......	......	IV
3030.15	15	8	1	......	IV
3031.22	12	6	......	......	IV
3031.64	15	10r	10	tr	III
3037.39	80R	60R	30r	20	I
3037.78	2	5	tr	......	IV A
3040.43	15	10	8	1	III
3041.64	10	6	1	......	IV
3041.75	15	10	8	......	III
3042.03	15	8r	8	......	III
3042.67	15	10r	8	......	III
3045.08	5	4	3	......	III
3047.61	100R	80R	40r	25	I
3053.07	5	2	......	......	IV
3055.27	12	6	2	......	III
3057.45	40R	20R	10r	5	II
3059.09	100R	80R	40r	25	I
3060.99	4	3	......	......	IV
3066.49	3	3	......	......	IV
3067.12	8	6	tr	......	IV
3067.25	30r	15r	8	4	II
3068.18	8	8	1	......	IV
3075.73	25r	15r	8	3	II
3078.02	4	8	1	......	IV A
3078.44	3	1	......	......	IV
3083.75	20	12	6	2	II
3091.58	20	12	6	2	II
3092.79*	2	2?	?	......	III ?
3093.81	3	6	......	......	IV A
3098.19	6	2	......	......	IV
3099.90	20	20	8	2	II
3099.97	15		8	2	II
3100.31	20	12	8	2	II
3100.67	20	15	8	2	II
3112.08	3	1	......	......	IV
3116.63	12	8	6	......	III
3117.63	1	3	1	......	III A
3119.50	6	4	......	......	IV
3120.44	6	3	......	......	IV
3125.66	15	10	7	......	III
3126.17	8n	1	......	......	IV
3128.88	1	1	......	......	IV
3129.33	5	5	tr	......	IV
3132.51	4n	......	......	......	V
3134.11*	10	8	5	......	III
3139.91	4n	......	......	......	V
3140.39	5n	......	......	......	V
3142.45	6	2	......	......	IV
3142.89	5	2	......	......	IV
3143.24	2	5	3	......	III A
3143.98	8	1	......	......	IV
3144.49	6n	1	......	......	IV
3151.34	10	2	......	......	IV
3153.21	5	3	......	......	IV
3154.51	2	1	......	......	IV
3155.29	2	1	......	......	IV
3156.27	5n	1	......	......	IV
3157.04	8	5	......	......	IV
3157.88	6	3	......	......	IV
3160.65	10	5	......	......	IV
3161.37	4	4	tr	......	IV
3161.95	8	4	tr	......	IV
3162.34	2n	1	......	......	IV
3165.01	3	1	......	......	IV
3165.86	4	2	......	......	IV
3166.44	6	3	......	......	IV
3168.86	2	1	......	......	IV
3171.35	5	1	......	......	IV
3171.66	2	1	......	......	IV
3172.07	2	1	......	......	IV
3175.45	12	6	tr	......	IV
3176.37	2	1	......	......	IV
3178.01	10	5	1	......	IV
3178.55	2	1	......	......	IV
3178.97	3	1	......	......	IV
3179.54	3	1	......	......	IV
3180.22	20	7	1	......	IV
3180.76	5	10	10	3	II A
3181.53	4	1	......	......	IV
3182.08	3	1	......	......	IV
3182.99	3	1	......	......	IV
3184.63	3	1	......	......	IV
3184.90	7	15r	8	7	I A
3186.75	3	......	......	......	V
3188.59	4	2	......	......	IV
3188.84	7	3	......	......	IV
3191.67	7	15r	10	10	I A
3192.81	8	5	tr	......	IV
3193.21	10	25r	10	10	I A
3193.31	8	5	......	......	IV
3194.42	3	1	......	......	IV
3196.09	2	1	......	......	IV
3196.15	2				IV
3196.94*	20	8	6	4	II
3199.53	15	8	6	3	II
3200.48	15	5	tr	......	IV
3200.79	2	6	4	tr	III A
3202.56	2	1	......	......	IV
3205.40	15	5	tr	......	IV
3207.09	2	1	......	......	IV
3208.48	4	1	......	......	IV
3209.33	6	2	......	......	IV
3210.25	8	4	......	......	IV
3210.83	10	4	tr	......	IV
3211.49	4	1	......	......	IV
3211.69	8	1	......	......	IV
3211.87	4	1	......	......	IV
3212.00	10	5	1	......	IV
3214.04*	20	8	2	......	III
3214.39	8	15r	8	8	I A
3215.94	12	5	1	......	IV
3217.39	10	5	tr	......	IV
3219.58	12	5	1	......	IV
3219.82	10	8	3	......	III
3221.94	2	1	......	......	IV
3222.07	20	6	4	......	III
3225.79	25	8	5	......	III
3226.73	2	5	2	......	III A
3227.07	3	1	......	......	IV
3227.76 3227.81	15	6	1	......	IV
3228.26	5	3	......	......	IV
3228.92	3	1	......	......	IV
3229.13	4	8	8	3	II A
3230.21	6	3	tr	......	IV
3230.98	10	5	tr	......	IV
3233.06	8	1	......	......	IV
3233.98	12	6	tr	......	IV
3234.62	7	15r	8	8	I A

TABLE II—*Continued*

λ (I.A.)	Arc Intensity	Furnace Intensities			Class
		High-Temp. Emission	Med.-Temp. Emission	Low-Temp. Absorption	
3236.23	8	20r	10	10	I A
3239.45	15	8	1	......	IV
3243.41	3	1	......	......	IV
3244.19	15	8	1	......	IV
3246.02	8	12	10	8	I
3246.49	3	1	......	......	IV
3246.97	6	3	......	......	IV
3247.30	3	1	......	......	IV
3248.22	10	5	......	......	IV
3249.20	3	1	......	......	IV
3250.63	4	2	......	......	IV
3251.24	8	1	......	......	IV
3252.93	4	1	......	......	IV
3253.61	4	1	......	......	IV
3254.37	10	2	......	......	IV
3257.24	2	1	......	......	IV
3257.60	8	4	tr	......	IV
3260.00	6	2	......	......	IV
3260.28	4	1	......	......	IV
3262.28	4	1	......	......	IV
3264.52	5	2	......	......	IV
3265.06	8	15r	10	8	I A
3265.63	15	6	2	......	III
3268.25	5	2	......	......	IV
3271.01	15	6	2	......	III
3276.48	4	2	......	......	IV
3278.74	4	1	......	......	IV
3280.27	8	2	......	......	IV
3284.60	5	3	......	......	IV
3286.03	2	1	......	......	IV
3286.76	20	8	4	......	III
3288.97	2	1	......	......	IV
3291.00	5	3	......	......	IV
3292.03	8	2	......	......	IV
3292.60	8	5	1	......	IV
3298.14	6	5	1	......	IV
3305.98	20	8	4	......	III
3306.36	20	8	4	......	III
3307.24	5	1	......	......	IV
3310.35	4	1	......	......	IV
3314.75	7	2	......	......	IV
3317.13	3	2	......	......	IV
3319.26	2	1	......	......	IV
3322.50	5n	1	......	......	IV
3323.74	7	3	......	......	IV
3324.54	4	2	......	......	IV
3325.47	4	2	......	......	IV
3328.87	5	1	......	......	IV
3331.62	3	1	......	......	IV
3335.78	4	1	......	......	IV
3337.67	6	3	......	......	IV
3339.20	2	1	......	......	IV
3340.57	6	4	......	......	IV
3341.91	5	10	10	......	III A
3342.23	5	2	......	......	IV
3342.30	4	......	......	......	V
3346.94	1	1	......	......	IV
3347.93	6	4	......	......	IV
3351.53	2	1	......	......	IV
3351.75	3	1	......	......	IV
3354.07	3	1	......	......	IV
3355.24	6	1	......	......	IV
3356.33	1	2	......	......	IV A
3356.41	3	2	......	......	IV
3359.50	2	5	2	......	III A
3366.79	5	1	......	......	IV
3366.87	5	2	......	......	IV
3369.57*	8	3?	2?	......	III
3370.79	10	6	tr	......	IV
3372.08	3	1	......	......	IV
3378.68	6	3	......	......	IV
3379.02	6	4	......	......	IV
3380.12	8	4	......	......	IV
3382.41	3	2	......	......	IV
3383.70	5	4	tr	......	IV
3383.99	8	6	1	......	IV
3387.41	2	1	......	......	IV
3389.75	2	1	......	......	IV
3392.02	2	tr	......	......	IV
3392.31	8	6	tr	......	IV
3392.66	15	9	3	......	III
3394.59	5	5	tr	......	IV
3396.98	4	8	5	......	III A
3397.64	2	4	1	......	III A
3399.34	15	8	2	......	III
3401.52	6	10	9	......	III
3402.26	5	2	......	......	IV
3404.30	3	7	3	......	III A
3404.36	6	5	1	......	IV
3406.45	3	1	......	......	IV
3406.81	6	5	1	......	IV
3407.47*	20	15	7	......	III
3410.18	3	tr	......	......	IV
3411.36	3	2	......	......	IV
3413.14	15	10	4	......	III
3415.54	4	4	......	......	IV
3417.85	12	7	2	......	III
3418.51	10	6	2	......	III
3422.50	3	1	......	......	IV
3422.67	7	5	1	......	IV
3424.29	10	8	2	......	III
3425.02	4	2	......	......	IV
3426.39*	5	10	6	......	III A
3426.65	5	6	tr	......	IV
3426.99	2	4	2	......	III A
3427.13	20	8	6	......	III
3428.20	8	6	2	......	III
3431.83	3	1	......	......	IV
3437.05	3	1	......	......	IV

2875.31 Blend in arc with polar line.
2880.76, 2883.73 Strong polar lines.
2887.81 Not a polar line, though absent in furnace.
2926.58, 2944.40, 2947.66, 2949.21, 2953.78, 2970.52 } Polar lines.
2984.83 Blend in arc with polar λ 2984.79.
2994.43–.50 λ 2994.43 is chief part of blend, which shows in furnace as a reversed line with violet side strongest.
3002.65 Polar line.
3092.79 Blend with strong Al line.
3134.11 Blend Ni, but arc and furnace lines chiefly Fe.
3196.94 Blend Ni on red side.
3214.04 Apparently a close double with components of equal strength.
3369.57 Blend Ni. Probable intensity of Ni line subtracted.
3407.47 Probably double.
3426.39 Double with faint violet component.

TABLE III

Temperature Classification of Iron Lines, λ 3441–λ 3878

λ (I.A.)	Arc Intensity	Furnace Intensities (Emission)			Class
		High Temp.	Med. Temp.	Low Temp.	
3440.61	150R	125R	125R	125r	I
3440.99	75R	75R	75r	60	I
3442.36	5	4	tr	......	IV
3442.68	3	8	5	......	III A
3443.88	50r	50R	50r	50	I
3445.16	20	8	4	......	III
3447.28	8	6	1	......	IV
3450.33	10	7	1	......	IV
3451.62	2	1	......	......	IV
3451.92	10	7	1	......	IV
3452.28	10	12	8	1	III
3458.31	4	2	......	......	IV
3459.92	4	1	......	......	IV
3462.35	2	1	......	......	IV
3463.31	2	2	......	......	IV
3465.86	60r	60R	60r	50	I
3466.50	3	6	4	......	III A
3468.85	4	2	......	......	IV
3469.83	2	1	......	......	IV
3471.27	5	3	......	......	IV
3471.34	6	5	......	......	IV
3475.45	70r	75R	75r	60	I
3475.65	6	6	tr	......	IV
3476.71	40	40R	40	40	I
3483.01	3	6	5	tr	III A
3485.34	7	6	tr	......	IV
3489.67	4	2	......	......	IV
3490.58	100r	100R	75r	75	I
3495.29	8	4	......	......	IV
3497.11	10	10	2	......	III
3497.84	40	40R	40r	40	I
3500.57	2	2	......	......	IV
3504.87	2	2	......	......	IV
3505.07	2	1	......	......	IV
3506.50	6	4	......	......	IV
3508.49*	5	3	......	......	IV
3513.82	30	25R	20	10	II
3516.41	5	1	......	......	IV
3521.26*	25	20R	20	10	II
3521.84	2	4	......	......	IV A
3524.08	3	3	......	......	IV
3524.24	4	6	tr	......	IV
3526.02	1	1	......	......	IV
3526.07	20	30R	30r	30	I
3526.17	15	15r	10	6	II
3526.38	4	3	......	......	IV
3526.47	4	5	tr	......	IV
3526.67	5	4	......	......	IV
3527.80	4	4	......	......	IV
3529.82	6	8	3	......	III
3530.38	2	2	......	......	IV
3533.00	5	4	......	......	IV
3533.20	10	7	......	......	IV
3536.55	15	10	1	......	IV
3537.50	1	1	......	......	IV
3537.73	3	3	......	......	IV
3537.89	4	4	......	......	IV
3540.13	3	3	......	......	IV
3540.71	3	8	6	......	III A
3541.09	15	10	1	......	IV
3542.08	15	10	1	......	IV
3542.24	1	1	......	......	IV
3545.64	5	4	......	......	IV
3549.87	4	4	1	......	III
3552.11	1	1	......	......	IV
3552.84	3	2	......	......	IV
3553.74	6	2	......	......	IV
3554.12	4	12	10	1	III A
3554.52	2	2	......	......	IV
3554.92	40	15	3	......	III
3556.88	7	10	tr	......	IV
3558.52*	30	30R	20	10	II
3559.51	2	1	......	......	IV
3560.71	5	1	......	......	IV
3565.38	60r	60R	60r	50	II
3565.58	3	2	......	......	IV
3567.05	2	1	......	......	IV
3568.98	4	2	......	......	IV
3570.10	100R	100R	100r	75	I
3570.24	20	10	4	......	III
3571.23	2	4	......	......	IV A
3572.00	6	5	......	......	IV
3573.40	2	tr	......	......	IV
3573.84*	3 }	4	......	......	{ IV
3573.89*	4 }				{ IV
3575.25	2	1	......	......	IV
3575.38	4	4	2	......	III
3575.98	2	1	......	......	IV
3576.76	2	1	......	......	IV
3581.20	250R	200R	150R	150r	I
3581.65	1	1	......	......	IV
3582.20	5	2	......	......	IV
3583.32	2	1	......	......	IV
3584.66	8	7	1	......	IV
3584.79	1	1	......	......	IV
3584.96	4	2	......	......	IV
3585.32*	30	30R	15	10	II
3585.71*	20	20R	15	8	II
3586.12	10	6	......	......	IV
3586.99*	30	25R	18	12	II
3587.25	2	1	......	......	IV
3587.42	2	1	......	......	IV
3587.75	3	2	......	......	IV
3588.62	3	3	......	......	IV
3588.92	2	1	......	......	IV
3589.11	8	12r	12	2	III
3589.45	3	2	......	......	IV
3594.63	8	6	tr	......	IV
3595.29	2	1	......	......	IV
3596.20	1	1	......	......	IV
3597.05	3n	1	......	......	IV
3598.71	1	2	......	......	IV A
3599.63	3	tr	......	......	IV
3602.10	1	3	......	......	IV A
3602.46	2	1	......	......	IV
3602.54	3	2	......	......	IV
3603.20	10	7	1	......	IV
3603.82	1	1	......	......	IV
3605.45*	15	12	tr	......	IV
3606.68	20	10	4	......	III
3608.15	3	2	......	......	IV
3608.86	100r	80R	60r	60	I
3610.15	20	9	2	......	III
3610.71	2	1	......	......	IV
3612.08	8	3	......	......	IV
3612.94	1	4	......	......	IV A
3614.56	2n	tr	......	......	IV
3616.58	3n	tr	......	......	IV
3617.32	2	tr	......	......	IV
3617.79	12	6	tr	......	IV

TABLE III—*Continued*

λ (I.A.)	Arc Intensity	Furnace Intensities (Emission)			Class
		High Temp.	Med. Temp.	Low Temp.	
3618.39	2	2	......	......	IV
3618.77	125R	100R	80r	80	I
3621.46	15	8	1	......	IV
3622.01	12	7	1	......	IV
3623.19	8	7	1	......	IV
3623.45	1	1	......	......	IV
3623.78	2	1	......	......	IV
3625.15	6	3	......	......	IV
3628.09	1	1	......	......	IV
3630.35	4	2	......	......	IV
3631.09	7	4	tr	......	IV
3631.46	125R	100R	75r	75	I
3632.04	10	5	......	......	IV
3632.55	3	1	......	......	IV
3632.98	3	2	......	......	IV
3633.84	1	tr	......	......	IV
3634.34	6n	1	......	......	IV
3634.68	4n	tr	......	......	IV
3635.19	2	6	1	......	IV A
3636.19	2	3	......	......	IV
3636.65	1	tr	......	......	IV
3636.99	2	1	......	......	IV
3637.25	1	1	......	......	IV
3637.86	3n	tr	......	......	IV
3638.30	12	7	tr	......	IV
3640.39	15	10	1	......	IV
3643.62	2	1	......	......	IV
3643.72	1	1	......	......	IV
3645.09	2	1	......	......	IV
3645.49	1	1	......	......	IV
3645.83	6	2	......	......	IV
3647.43	3	1	......	......	IV
3647.85	100R	100R	75r	75	I
3649.31*	5	20r	25	20	I A
3649.51	12	10	1	......	IV
3650.03	4	2	......	......	IV
3650.28	5	5	1	......	IV
3651.47	20	12	2	......	IV
3653.76	1	1	......	......	IV
3655.47	4	2	......	......	IV
3656.23	3n	tr	......	......	IV
3657.14	1	tr	......	......	IV
3657.89	1	1	......	......	IV
3659.52	8	6	1	......	IV
3663.46	1	1	......	......	IV
3664.56	2	1	......	......	IV
3666.24	1	tr	......	......	IV
3667.28	3n	1	......	......	IV
3668.00	1	tr	......	......	IV
3669.16	3	tr	......	......	IV
3669.53	10	8	1	......	IV
3670.04	3	2	......	......	IV
3670.09	3	2	......	......	IV
3670.81	1	1	......	......	IV
3672.69	1	1	......	......	IV
3674.77	2	1	......	......	IV
3676.31	6	6	tr	......	IV
3677.31	2	tr	......	......	IV
3677.63	12	9	1	......	IV
3678.86	3	3	......	......	IV
3679.92	40r	100R	80r	80	I A
3680.69	2n	tr	......	......	IV
3680.80	1	tr	......	......	IV
3681.77	1	tr	......	......	IV
3682.24	20	8	tr	......	IV
3683.06*	10	20r	20	20	I A
3684.11	15	8	1	......	IV
3686.00	15n	7	1	......	IV
3686.26	2	2	......	......	IV
3687.10	2	3	......	......	IV
3687.46	40r	40R	40	30	I
3687.66	4	3	1	......	III
3689.46	12	6	1	......	IV
3690.73	4	1	......	......	IV
3693.02	1	tr	......	......	IV
3694.00	20	8	1	......	IV
3695.05	8	4	......	......	IV
3697.44	6n	3	......	......	IV
3698.61	2	1	......	......	IV
3699.14	1	tr	......	......	IV
3701.08	20	9	1	......	IV
3702.03	3	2	......	......	IV
3702.49	1	2	......	......	IV A
3703.56*	5	?	?	......	IV ?
3703.70	3	1	......	......	IV
3703.82	3	1	......	......	IV
3704.46	10	4	tr	......	IV
3705.57	100r	100R	80r	80	I
3707.05	8	3	......	......	IV
3707.83	20	20r	20	20	I
3707.92	8	10	5	......	III
3709.25	75r	40R	30	15	II
3711.23	3	2	......	......	IV
3711.41	2	tr	......	......	IV
3715.92	4	4	tr	......	IV
3716.45	12	6	tr	......	IV
3718.41	3	2	......	......	IV
3719.94	250R	300R	300R	300r	I
3721.28	2	2	......	......	IV
3721.40	1	1	......	......	IV
3721.51	2	1	......	......	IV
3722.57	50r	100R	80r	80	I A
3724.38	8	8	2	......	III
3726.92	6	4	tr	......	IV
3727.10	4	2	tr	......	IV
3727.62	50r	40R	30	20	II
3727.81	3	2	......	......	IV
3728.67	1	1	......	......	IV
3730.39	3	2	......	......	IV
3730.95	2	1	......	......	IV
3731.37	2	1	......	......	IV
3732.40	10	10	6	1	III
3733.32	40r	80R	60r	60	I A
3734.87	300r	150R	100R	100r	II
3735.33	6	4	......	......	IV
3737.14	150R	200R	200R	200r	I
3738.31	10	4	......	......	IV
3739.11	1	1	......	......	IV
3739.32	1	1	......	......	IV
3739.54	3	2	......	......	IV
3740.26	3	2	......	......	IV
3742.62	4	3	......	......	IV
3743.36	20	40R	25	20	II A
3743.47*	6	?	?	......	IV ?
3744.10	4	3	......	......	IV
3745.56	100R	150R	150R	150r	I
3745.90	40r	80R	80r	75r	I A
3746.48	1	1	......	......	IV
3746.93	6	4	......	......	IV
3748.26	60R	125R	100r	100r	I A
3748.49*	7	?	?	......	IV ?
3748.96	5	3	......	......	IV
3749.49	200R	125R	80r	50	II
3753.61*	8	5?	3?	......	III

TABLE III—*Continued*

λ (I.A.)	Arc Intensity	Furnace Intensities (Emission)			Class
		High Temp.	Med. Temp.	Low Temp.	
3754.50	1	1	......	......	IV
3756.07	1	2	......	......	IV A
3756.94	4	1	......	......	IV
3757.46	1	tr	......	......	IV
3758.23	150R	125R	75r	40	II
3760.05	8	6	3	......	III
3760.53	6	5	2	......	III
3761.41	1	1	......	......	IV
3763.79	100r	80R	50	30	II
3765.54	20	6	1	......	IV
3766.67	1	tr	......	......	IV
3767.19	80r	60R	40	25	II
3768.03	3	3	tr	......	IV
3770.00	4	1	......	......	IV
3770.31 3770.41	3	1	......	......	IV IV
3773.69	1	tr	......	......	IV
3774.83	5	4	tr	......	IV
3776.46	6	5	tr	......	IV
3777.45	2	1	......	......	IV
3778.52	4	tr	......	......	IV
3779.42	3	1	......	......	IV
3779.50	2	1	......	......	IV
3781.19	2	3	tr	......	IV
3782.46	1	tr	......	......	IV
3785.95	6	4	tr	......	IV
3786.18*	4	1	......	......	IV
3786.68	8	8	8	2	III
3787.88	50	30R	20	20	II
3789.18	3	1	......	......	IV
3790.09	12	10	10	6	II
3790.76	1	2	tr	......	IV A
3792.16	2	2	......	......	IV
3792.83	1	1	......	......	IV
3793.35	1	1	......	......	IV
3793.87	1	1	......	......	IV
3794.34	8	4	1	......	III
3795.00	60	40R	30	25	II
3797.52	12	4	1	......	III
3798.51	40	30R	20	20	II
3799.55	50	40R	20	20	II
3801.68	3	2	......	......	IV
3801.81	1	tr	......	......	IV
3805.35	12	5	tr	......	IV
3806.22	2	tr	......	......	IV
3806.70	10	4	1	......	III
3807.54*	7	8?	3?	......	III
3808.73	4	3	......	......	IV
3810.76	2	tr	......	......	IV
3811.89	2	tr	......	......	IV
3812.97	40	25R	20	20	II
3813.06*	5?	?	......	......	IV
3813.64	2	1	......	......	IV
3813.89	2	......	......	......	V
3814.53	5	10	8	2	III A
3815.84	100r	50R	30	20	II
3816.34	4	5	1	......	IV
3817.64	3n	1	......	......	IV
3820.43	250R	200R	200R	60	II
3821.18	10	4	tr	......	IV
3821.84	3	2	......	......	IV
3824.08	1	1	......	......	IV
3824.31*	2	?	......	......	IV ?
3824.44	50r	100R	100r	100r	I A
3825.89	200R	125R	80r	40	II
3826.84	1	1	......	......	IV
3827.57	1	1	......	......	IV
3827.83	75r	50R	30	20	II
3829.46	1	1	......	......	IV
3830.76	1	1	......	......	IV
3830.87	1	1	......	......	IV
3833.31	5	5	1	......	IV
3834.23	100r	80R	60	30	II
3836.34	4	2	......	......	IV
3837.14	1	1	......	......	IV
3839.26	7	3	......	......	IV
3840.44	80r	60R	40	25	II
3841.05	80r	25r	25	15	II
3843.26	8	4	tr	......	IV
3846.41	2	tr	......	......	IV
3846.81	8	2	......	......	IV
3849.97	40	40r	30	25	II
3850.82	12	15r	20	10	II
3852.58	6	6	1	......	IV
3856.37	50r	100R	100r	100	I A
3859.22	10	6	2	......	III
3859.91	300R	250R	200R	200r	I
3861.34	2	1	......	......	IV
3863.75	2	1	......	......	IV
3865.53	30	40r	25	20	II
3867.22	7	4	......	......	IV
3867.93	1	tr	......	......	IV
3869.56 3869.59	3	2	......	......	IV IV
3871.75	4	3	......	......	IV
3872.51	60	60R	35	20	II
3872.92	1	tr	......	......	IV
3873.77	8	8	1	......	IV
3876.04	4	15	12	1	III
3878.02	60	60R	40	20	II
3878.58	100r	100R	100r	75r	II

3508.49 Probably double.
3573.84–.89 Blend in furnace. Violet component appears strongest.
3521.26
3558.52
3585.32–.71
3586.99
} Become very faint at 1600°.
3605.45 Blend Cr on violet side.
3649.31 Between Classes I and II. Weak at 1600°.
3583.06 Blend V on red side.
3703.56 Blend V.
3743.47 Blend with preceding line.
3748.49 Blend with preceding line.
3753.61 Blend V. Probable intensity of V line subtracted.
3786.18 Probably double.
3807.54 May be partly V.
3813.06 Blend with preceding line.
3824.31 Blend with following line.

reverse readily in the furnace or in the arc with moderate current. The distinction between the two classes will be considered further in the discussion. Lines of class III are absent or at least very faint at low temperature, and first appear distinctly at medium temperature. There is much variety among these lines, but a large proportion show a rapid increase in intensity through the high-temperature stage and under the conditions of the arc. Class IV lines require strong excitation and usually appear only at high temperature, though perhaps faintly at medium temperature. Most of the fainter arc lines belong in this class, but many lines of intensity 10 or higher in the arc require the high-temperature furnace for their appearance. Class V lines appear in the arc but are absent from the furnace. Lines of this character are listed in Tables I–III only when they show considerable strength in the arc. Their number is relatively few, since polar lines are seldom included, and, except for these, class V is made up chiefly of very faint arc lines.

"A" after the class number denotes that the line is relatively weak in the arc. The selection depends to some extent on the average intensity adopted for arc and furnace spectra. In the tables, a line whose arc intensity is not more than half of that for the high-temperature furnace is placed in this division.

An asterisk after the wave-length refers to a note at the end of the tables.

REVISED CLASSIFICATION OF BLUE AND VIOLET IRON LINES

Table IV contains 262 lines, from λ 3884 to λ 4531, which are within the range covered by the former paper. A revision of the classification seemed desirable to make this portion of the spectrum uniform with the ultra-violet region treated in the present paper. This is chiefly on account of the change in the temperature steps, 1600°–1700° now being used for the low temperature stage instead of 1800°–1900°. Twenty-six lines not in the former list are included in Table IV, and ninety lines have their classes changed. About half of the changes are from class V to class IV, due to improved high-temperature spectrograms, which show distinctly many faint lines not obtained before with the furnace. Of the remaining changes, a few are due to errors incident to the first attempt at a

TABLE IV

Classification of Iron Lines, λ 3884–λ 4531

λ	Class	λ	Class	λ	Class	λ	Class
3884.37	IV	3971.33	III	4143.42	III	4267.83	IV
3885.51	III	3973.66	V	4143.87	I	4268.75	IV
3886.29	I	3976.62	IV	4147.68	III	4271.17	III
3887.05	I	3977.75	III	4149.37	V	4271.76	II
3888.52	II	3981.78	III	4152.18	II A	4282.41	III
3888.83	IV	3983.96	III	4153.92	IV	4285.45	IV
3890.84	IV	3985.39	IV	4154.50	III	4291.47	I A
3891.93	V	3986.18	IV	4154.82	IV	4294.13	II
3893.40	IV	3989.86	V	4156.81	III	4298.04	IV
3893.92	IV	3990.38	V	4157.81	IV	4299.25	III
3894.01	III	3994.12	V	4158.81	V	4305.46	IV
3895.66	I	3995.99	IV	4170.91	IV	4307.91	II
3897.45	IV	3997.40	III	4172.13	IV	4309.38	IV
3897.89	IV	3998.06	III	4172.75	II A	4315.09	III
3898.01	II	4001.67	III	4173.32	IV	4325.77	II
3899.03	IV	4005.25	II	4173.93	II A	4337.05	II
3899.71	I	4006.31	IV	4174.92	II A	4351.55	IV
3900.52	V	4006.63	IV	4175.64	III	4352.74	III
3902.95	II	4007.27	IV	4176.57	IV	4358.51	IV
3903.90	IV	4009.72	III	4177.60	II A	4367.58	IV
3906.48	I	4014.54	III	4181.76	III	4367.91	III A
3907.47	III	4017.15	III	4182.39	IV	4369.78	III
3907.94	IV	4021.87	III	4184.89	III	4375.93	I
3909.67	V	4024.75	V	4187.05	III	4383.55	II
3909.83	III	4030.51	IV	4187.81	III	4387.90	IV
3910.85	IV	4032.64	III	4191.45	III	4388.42	IV
3913.64	III	4043.90	IV	4195.34	IV	4389.25	II A
3916.74	IV	4044.62	IV	4196.22	IV	4390.96	IV
3917.19	II	4045.82	II	4198.31	III	4404.75	II
3918.42	IV	4058.23	IV	4199.10	III	4415.13	II
3918.65	IV	4058.77	IV	4199.97	I A	4422.57	III
3920.26	I	4062.45	III	4202.03	I	4427.31	I
3922.92	I	4063.60	II	4203.99	III	4430.20	IV
3925.65	IV	4066.98	III	4206.70	I A	4430.62	III
3925.95	IV	4067.28	III	4207.13	IV	4433.22	IV
3927.93	I	4067.99	III	4208.61	V	4435.15	II A
3930.30	I	4070.78	III	4210.36	III	4439.89	IV
3932.64	IV	4071.75	II	4213.65	IV	4442.35	III
3933.61	IV	4074.79	IV	4215.42	IV	4442.84	IV
3935.82	III	4076.64	IV	4216.19	I	4443.20	III
3937 33	IV	4078.36	IV	4217.56	IV	4445.43	I A
3940.89	II	4079.25	IV	4219.36	IV	4447.14	IV
3942.45	IV	4079.85	IV	4220.34	IV	4447.73	III
3943.35	IV	4080.23	IV	4222.23	III	4454.39	III
3944.90	IV	4083.78	IV	4224.17	IV	4459.13	III
3945.12	IV	4084.51	IV	4224.51	IV	4461.66	I
3947.00	IV	4085.01	IV	4225.46	IV	4462.01	IV
3947.54	IV	4085.31	IV	4225.96	IV	4464.77	IV
3948.11	IV	4095.98	IV	4226.43	IV	4466.56	II
3948.78	IV	4098.19	IV	4227.45	III	4469.39	IV
3949.96	III	4100.75	II A	4229.75	III	4476.02	III
3951.17	IV	4104.14	V	4232.72	IA	4479.61	IV
3952.61	IV	4107.50	III	4233.61	III	4480.14	IV
3953.16	IV	4109.81	IV ?	4235.95	III	4482.18 4482.26	I
3955.37	IV	4114.45	IV	4237.16	III A	4484.24	IV
3956.46	IV	4118.56	IV	4238.04	IV	4485.67	IV
3956.68	III	4120.21	IV	4238.83	IV	4488.92	IV
3957.04	IV	4121.81	IV	4239.85	III	4489.74	I A
3963.12	V	4122.52	IV	4245.26	III	4490.09	IV
3964.52	V	4126.19	IV	4247.44	III	4494.57	III
3966.07	III	4127.62	IV	4248.22	IV	4525.15	IV
3966.63	IV	4132.06	II	4250.13	III	4528.62	II
3967.43	IV	4132.91	III	4250.79	II	4531.16	II
3967.97	IV	4134.68	IV	4258.39	I A		
3969.26	II	4137.00	IV	4260.49	III		
3970.39	IV	4139.94	II A	4266.97	IV		

classification of this kind, but most of the alterations result from the new low-temperature stage. A line may retain at 1800°–1900° an intensity sufficient to place it in class I if this were the low temperature selected; but a temperature drop of 200° may weaken it so that it clearly belongs in class II, possibly verging on class III. Naturally some lines still strong at 1600° may weaken rapidly below this, and the most pronounced low-temperature lines reduce to the small number in Table V (see p. 370) emitted at 1400°. The 1600°–1700° stage emits, however, a set of lines retaining fair intensity under as weak excitation as is ordinarily usable for the iron spectrum in the laboratory, and the high-temperature lines have had an opportunity to drop out in the range below 2000°.

As the gradation of intensities for the lines included in Table IV is shown in the 1913 paper, it was considered sufficient in this revision to print the classes only. Beyond λ 4600 into the red, the later photographs confirm the earlier so closely as to classes that it seems unnecessary to go over the ground.

Table IV is supplemented by a reproduction of this region in Plate IX. Three furnace spectra for temperatures of 2600°, 2000°, and 1650°, respectively, are given with a strong arc spectrum, the latter just sufficing to show some of the more pronounced lines of the sort which are relatively stronger in the furnace than in the arc. The strong lines emitted in the furnace and not in the iron arc are due chiefly to titanium and vanadium. λ 4227 of calcium is strong in the medium- and low-temperature spectra.

DISCUSSION OF RESULTS

a) *Distinctive features of classes I, II, and III.*—The difference between classes I and II is not as decided in the ultra-violet as in the visible region and for many purposes the two classes may perhaps be considered together as the low-temperature group. In segregating the lines in this paper, the absorption spectrum at low temperature has been of much service. It was considered that lines appearing in absorption at a temperature as low as 1600° were at least in class II, and those which maintained their intensity to the greatest extent were placed in class I. In the portion covered by the low-temperature emission spectrum, as far as λ 3440, the

PLATE IX

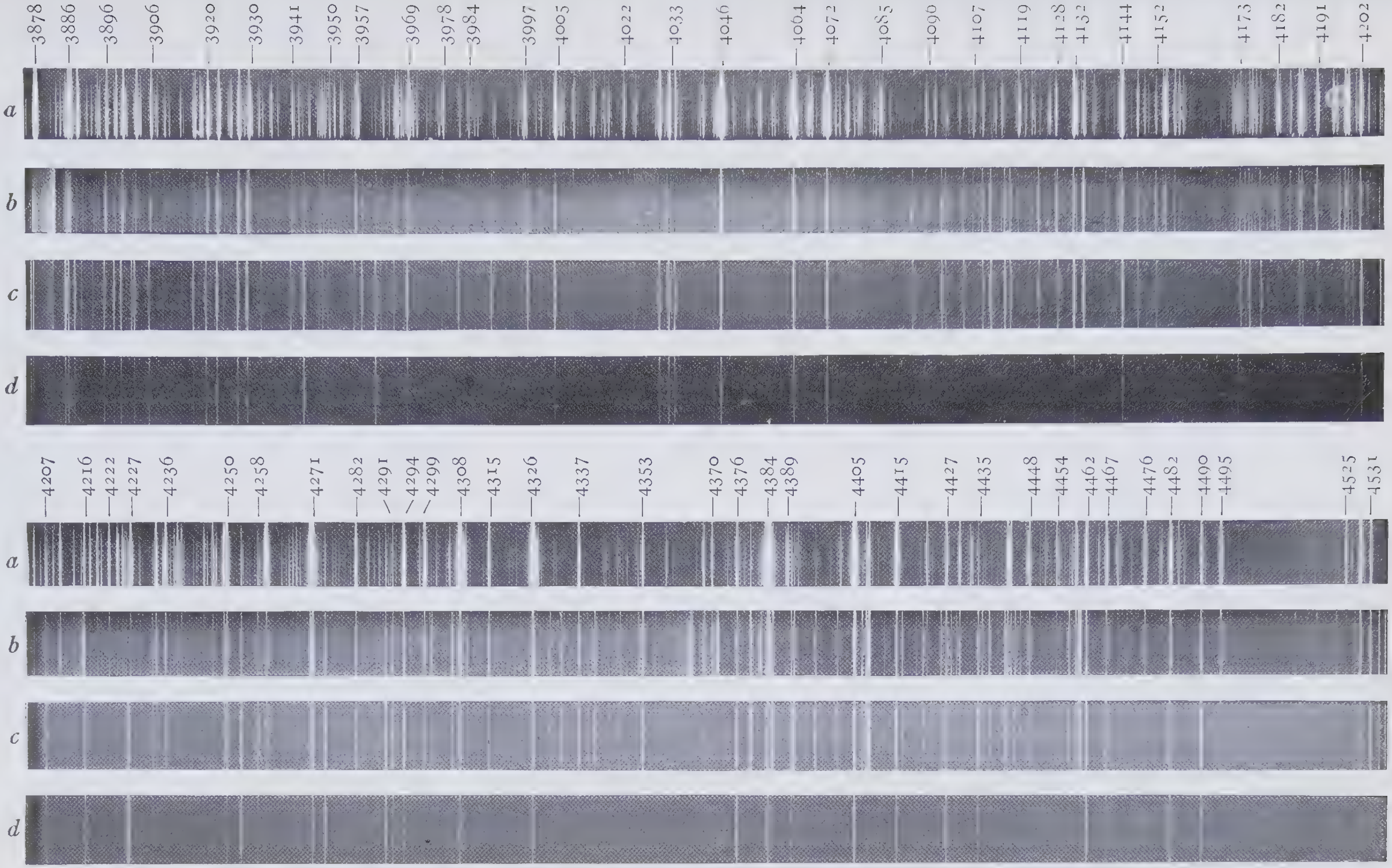

Arc and Furnace Spectra of Iron in Violet and Blue

a Arc spectrum; *b*, *c*, *d* Furnace spectra at 2600°, 2000°, 1650° C., respectively

appearance of the lines both in emission and absorption was considered. The experiments of Hemsalech[1] with the flame spectrum of iron showed that, of the stronger lines, a portion are emitted with relatively high intensity in the outer mantle of the flame, while others require the stronger excitation found on the boundary of the cone. The lines of these two classes correspond closely, in the region common to both investigations, with classes I and II, respectively, of the furnace lines. The susceptibility to reversal in either the high-temperature furnace or the arc often distinguishes between these two classes. Of two emission lines having approximately the same width, one may show a wider reversal. In a low-temperature absorption spectrum it will be distinctly the stronger line. This indication that the line maintains its strength in the lower-temperature absorbing vapor distinguishes the class I line. The contrast between λ 3734.87 and λ 3737.14 illustrates this point. The first, having in the arc much greater brightness in proportion to its width, is given the higher intensity. In the low-temperature furnace, the second is much the stronger. In the visible region, the quartet of class I lines λλ 3920–3930 contrasts in the same way with the class II triplets having stronger lines at λ 4045 and λ 4384.

Class III lines, by reason of their absence from low-temperature vapors, do not show reversal in the furnace emission spectrum, and in the absorption spectrum, when the furnace is hot enough to absorb these wave-lengths, their weakness in comparison with lines of classes I and II is very pronounced. The rapid development of class III lines is the chief cause of the very different appearance of the low- and high-temperature spectra; while in the arc, the fact that the class III lines are often among the strongest in the spectrum and classes IV and V have become prominent makes the arc spectrum of iron very different from that of the furnace.

b) Lines appearing at 1400° C.—It may be of interest to record a list of the most persistent low-temperature lines of iron. By means of long exposure with a 1-meter concave grating spectrograph, the emission lines listed in Table V were obtained. The furnace temperature was held close to 1400° C. The film was of the Eastman portrait variety, showing little sensitiveness beyond the blue. The twenty-one lines which appear are all pronounced members of class I, except that a bare trace is visible of λ 4384, the strongest of the class II lines. The absence of the triplets to which λ 4384 and λ 4046 belong is one of the striking features of this very low-temperature emission. λ 4376 is under these conditions the strongest line of the spectrum.

---

[1] *Philosophical Magazine*, **33**, 1, 1917.

TABLE V

PERSISTENT LOW-TEMPERATURE LINES OF IRON

λ	Intensity	λ	Intensity
3745.56	1	3920.26	8
3820.43	1	3922.92	8
3824.44	2	3927.94	8
3825.89	1	3930.30	8
3856.37	4	4216.18	2
3859.91	4	4375.93	10
3878.58	5	4383.55	tr
3886.29	6	4427.31	8
3895.65	5	4461.65	4
3899.70	5	4482.18	2
3906.47	2		

c) *Lines relatively weaker in arc than in furnace.*—In all of the furnace spectra thus far studied, attention has been drawn to this type. Such a line may be extremely weak in the arc and still strong in the furnace. The type may be found in any temperature class and its occurrence points to a difference, as yet obscure, between the arc and furnace excitations. These lines, designated by "A" after the class number, may reverse at high temperature, in which case they remain strong at low temperature and belong in class I A. Those which do not reverse are of two types. The type prevailing in the ultra-violet usually comes under class III A, becoming very faint at low temperature. The other type consists of I A lines, which are narrow at all temperatures, but remain strong at low temperature. These appear to be confined to the visible region, where λλ 4200, 4258, 4291, 5225, 5247, 5250.2, 5255 may be noted as conspicuous examples.

d) *Relation to arc types.*—It has been noted that lines appearing in the furnace spectrum are likely, in the arc spectrum, to show strongest in the region of the arc away from the poles. It was

PLATE X

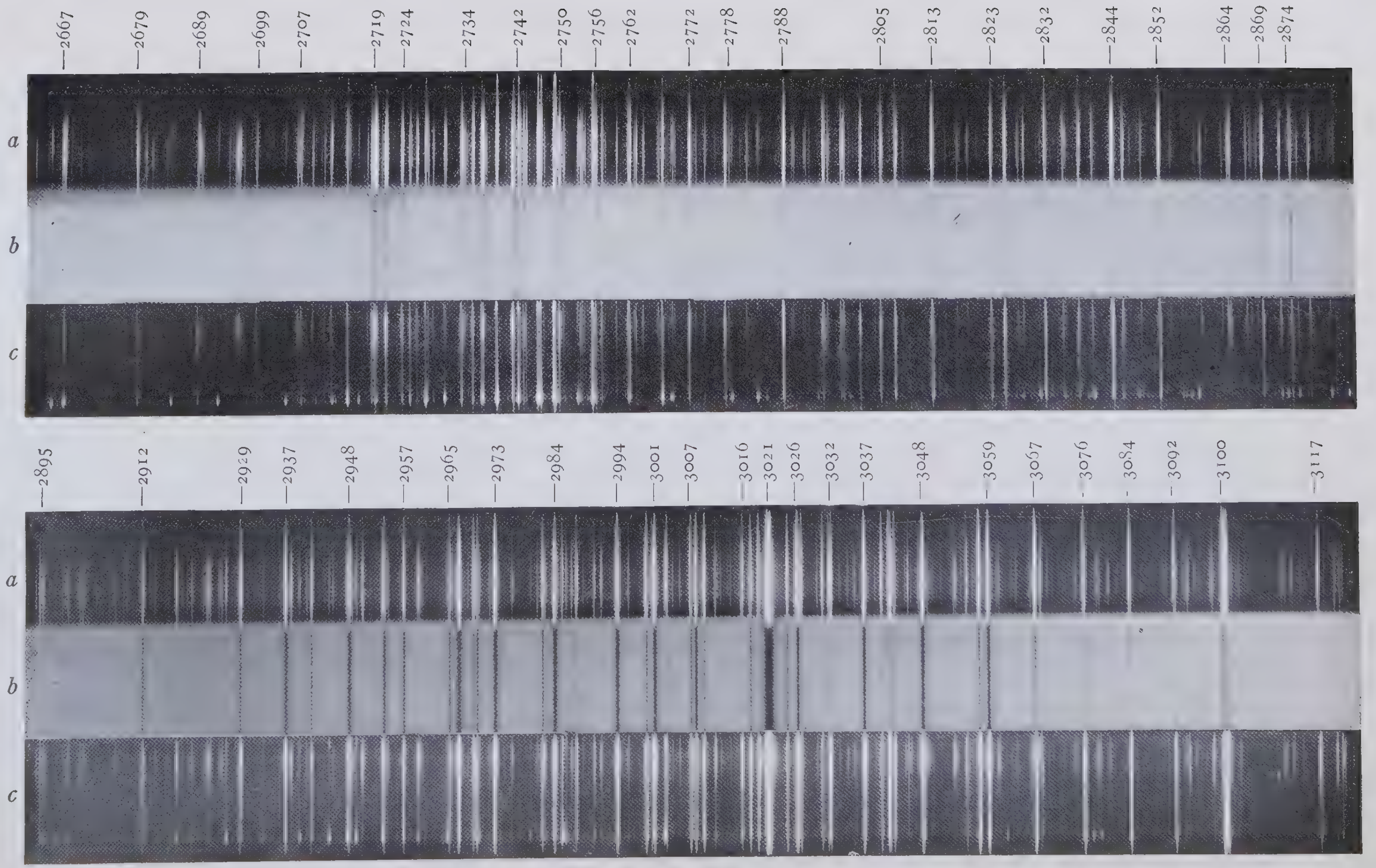

Arc and Furnace Spectra of Iron

possible to photograph the spectral region below λ 2800, covered in Table I, so as to show this change from center to pole, as the astigmatism of the concave grating is small for this part of the spectrum. Plate X reproduces a section of this region, a high-temperature furnace absorption spectrum being placed between two arc spectra, the upper being the integrated spectrum of the central and polar vapors, and the lower taken with the axis of the arc along the slit. In the upper strip it may be seen that some lines relatively faint in the arc, such as λ2750 and λ2756 are distinct in the furnace, being radiated chiefly by the vapors away from the pole, while the adjacent strong lines λ2749 and λ2755, with major emission at the poles, are absent in the furnace. Strong furnace lines are wide and frequently reversed in the hood of vapor above the center of a vertical arc, and fade rapidly toward the lower pole, where polar conditions are more concentrated. Lines of the intermediate type, designated in Table I as "C–P," of about the same strength from center to pole, are usually present in the furnace, but relatively weaker than lines which are more closely confined to the center.

d) Probable relation to ionization phenomena.—The trend of recent investigations has been to show a parallelism between the excitation stages given by different temperatures and those produced by various voltages in studies of ionization potentials. As no work has been done with iron vapor as to the effect of different voltages, nothing definite can be said for this spectrum, but for metals which have been studied in both ways, there has as yet been no contradiction of the view that the two modes of excitation result, at corresponding points, in the same radiative processes. In other words, temperatures can be selected to bring out successive groups of lines in the same way that various voltages may be used, as in the recent work of Foote, Meggers, and Mohler.[1] On account of the high vaporization point of substances such as iron, the classification of many spectra can be carried out best by the furnace method, but the close connection of the critical voltages with the quantum theory, in the results obtained by the voltage method, makes desirable a study of the correspondence for those elements which may have their spectra excited in either way. The short extension into the ultra-violet of the furnace spectrum has prevented the observation of many important low-temperature lines as long as emission spectra only were employed. The methods here described for the production of the low-temperature absorption spectrum of iron can be applied with other elements to the grouping of their lines at various temperatures through the range from perhaps λ 2300 into the infra-red.

---

[1] *Philosophical Magazine*, **42**, 1002, 1921; *Astrophysical Journal*, **55**, 145, 1922.

Mount Wilson Observatory
August 1922

Contributions from the Mount Wilson Observatory, No. 248
Reprinted from the *Astrophysical Journal*, Vol. LVI, pp. 340–343, 1922

CHANGES IN THE SPECTROGRAPHIC ELEMENTS OF Y SAGITTARII[1]

BY JOHN C. DUNCAN

ABSTRACT

Changes in the spectrographic elements of Y Sagittarii.—A velocity curve of this Cepheid variable, derived from 17 single-prism spectrograms made at Mount Wilson and three triple-prism spectrograms made at Mount Hamilton in 1921, is compared with the curve derived from 26 single-prism spectrograms made at Mount Hamilton in 1908 (Fig. 1). Elliptic elements for both years are given. The velocity of the system is found to have changed from +3.6 to −5.9 km/sec., while the eccentricity in 1921 appears to be double its value in 1908. Other elements also seem to have changed, but less markedly.

Y Sagittarii is a well-known variable star of the δ Cephei class. The variability of its brightness was discovered by Sawyer in 1886, and that of its radial velocity by Curtiss in 1904. A preliminary velocity curve and elliptic elements, derived from observations made with the single-prism spectrograph of the Lick Observatory in 1908, were published by me in 1909.[2] Last winter my attention was called by Mr. Joy to the fact that observations made at Mount Wilson in 1918 gave a velocity some twenty kilometers below that shown by my curve of 1908, and I then undertook a new determination of the curve.

The star was placed by Mr. Adams on the observing list of the 60-inch and 100-inch reflectors, and in the spring and summer of 1921 seventeen one-prism spectrograms were secured. An approximate curve derived from these observations showed unmistakably a velocity of the system several kilometers less than that of 1908. This difference seemed too great to be due to the use of different spectrographs and methods of measurement, but that question was nevertheless referred to Director Campbell, who very kindly had three plates made with the three-prism spectrograph and measured at the Lick Observatory, the dates of the plates corresponding to salient points of the curve. These plates agree very well with the Mount Wilson plates, and in the final determination of the elements were given additional weight on account of their high dispersion. Data concerning the 1921 plates, and also three plates made at Mount Wilson in 1918 and one in 1919, are given in Table I. Plates with numbers preceded by γ were made with the 60-inch telescope; by C, with the 100-inch. The phase (days since maximum brightness) is computed from the elements of Hellerich.[1]

---

[1] Read at the Swarthmore meeting of the American Astronomical Society December, 1921.

[2] *Lick Observatory Bulletin*, 5, 82, 1909.

TABLE I

Plate	Date, G.M.T.	J.D. 2420000+	Phase	Vel.	O−C	Wt.
γ 7145	1918 July $19^d 19^h 22^m$	1794.807	3.912	0.0	−12.1	.....
γ 7157	July 21 17 27	1796.727	0.059	−23.0	+ 0.1	.....
γ 7206	Aug. 17 16 20	1823.681	3.919	+ 2.2	−10.0	.....
γ 8710	1919 Sept. 13 15 00	2215.625	3.281	− 3.3	− 7.3	.....
γ 10002	1921 Mar. 17 01 10	2766.048	5.244	− 9.8	− 1.6	1
γ 10011	Mar. 18 01 05	2767.045	0.468	−28.4	− 5.9	1
C 952	Mar. 20 00 42	2769.029	2.452	− 0.9	+ 4.3	1
γ 10088	Apr. 17 00 19	2797.013	1.569	−10.0	+ 3.8	1
γ 10127	Apr. 25 23 26	2805.976	4.759	+18.7	+ 3.4	1
γ 10136	Apr. 27 23 53	2807.995	1.005	−19.9	− 1.2	1
γ 10165	May 25 19 57	2835.831	5.748	−14.4	+ 8.1	1
γ 10166	May 25 20 45	2835.865	5.782	−15.5	+ 7.3	1
γ 10178	May 26 22 28	2836.936	1.079	−25.9	− 7.8	1
γ 10204	June 15 22 07	2856.922	3.745	+ 9.3	− 0.6	1
γ 10207	June 16 21 11	2857.883	4.706	+19.8	+ 3.4	1
γ 10216	June 19 21 30	2860.896	1.946	−10.0	+ 0.2	1
γ 10221	June 20 19 45	2861.823	2.873	− 3.9	− 3.2	1
γ 10233	June 22 21 09	2863.881	4.931	0.0	− 9.1	1
C 1174	July 24 19 42	2895.821	2.232	−10.4	− 2.9	1
Lick	July 26 18 43	2897.780	4.191	+15.0	− 0.7	3
C 1185	July 26 18 54	2897.787	4.198	+11.0	− 4.8	1
γ 10337	July 26 19 07	2897.797	4.208	+12.8	− 3.1	1
Lick	Aug. 14 17 13	2916.717	0.035	−21.5	+ 1.4	3
Lick	Aug. 16 17 06	2918.712	2.030	− 8.6	+ 0.8	2

The velocity is in each case the mean result of measures by two or more observers. The residuals O−C are taken from the 1921 velocity curve shown in Figure 1.

Although the binary hypothesis of Cepheid variation is not universally accepted, the usual elliptic elements seem still to be the best means for numerically representing the observed variations in radial velocity; and I accordingly give these elements, leaving their interpretation on the pulsation and other hypotheses to the reader. Corrections to the preliminary elements of 1908 (except the period) were computed by least squares. These corrections were in every case smaller than their probable errors. The period found from photometric observations by Hellerich was adopted. A least-squares solution was made for the elements of 1921, using the seventeen plates made at Mount Wilson and the three made at Mount Hamilton. The results are shown in Table II.

---

[1] Inaugural Dissertation, Berlin, 1913.

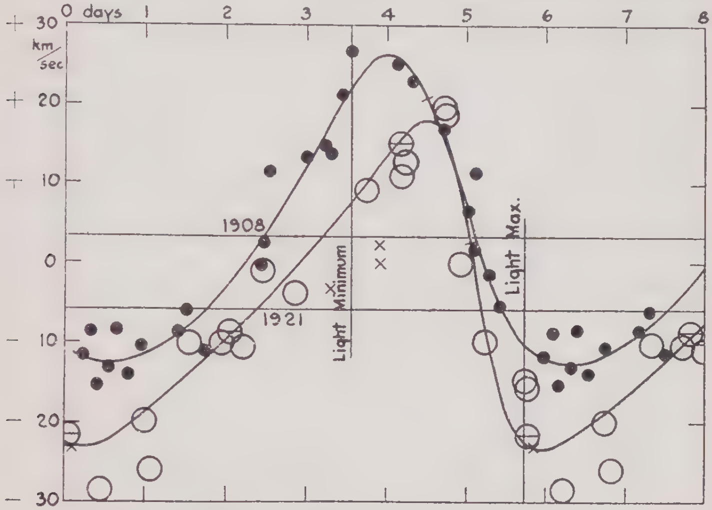

FIG. 1.—Velocity curves of Y Sagittarii, 1908 and 1921

TABLE II

	1908	1921	Difference
P	....	5.773268 days (Hellerich)	....
K	19.3± 0.8 km/sec.	20.6±0.8 km/sec.	+ 1.3± 1.2 km/sec.
γ	+3.6± 1.2 km/sec.	−5.9±1.5 km/sec.	− 9.6± 1.9 km/sec.
ω	43°0±13°8	74°5±6°2	+31°5±15°1
e	0.21± 0.04	0.42±0.04	+0.21± 0.06
T	4.51± 0.21	5.05±0.08	+0.54± 0.22
$a \sin i$	1 500 000 km	1 354 000 km	−146 000 km
$\frac{m_1^3 \sin^3 i}{(m+m_1)^2}$	0.004⊙	0.003⊙	....
ϵ	±2.4 km/sec.	±3.1 km/sec.	....

The time T of periastron passage is counted in days from the time of light-maximum. The interval from light-maximum to velocity-minimum was 0.64 days in 1908 and 0.19 days in 1921; the interval from light-minimum to velocity-maximum was 0.27 and 0.72, respectively—the former interval having diminished and the latter increased, each by 0.45 days. The observations, and the velocity curves representing the above elements, are plotted in Figure 1. The Lick observations of 1908 are indicated by filled circles; those of 1921 by barred rings; the Mount Wilson observations of 1921 by plain rings; and those of 1918 and 1919 by crosses.

The most important changes found are those in the velocity of the system and in the eccentricity, which are so large as to leave little doubt of their reality. From the large negative residuals of the observations made near light-minimum in 1918 and 1919, one might infer that the curve has differed more from its position of 1908 at some intermediate epoch than in 1921. It seems evident that the star will repay further observation.

WHITIN OBSERVATORY
WELLESLEY, MASSACHUSETTS
February 1922

Contributions from the Mount Wilson Observatory, No. 249
Reprinted from the *Astrophysical Journal*, Vol. LVI, pp. 380–399, 1922

THE ABSENCE OF OXYGEN AND WATER-VAPOR LINES FROM THE SPECTRUM OF VENUS

By CHARLES E. ST. JOHN and SETH B. NICHOLSON

ABSTRACT

Absence of oxygen and water-vapor lines from the spectrum of Venus.—It has been generally assumed that the atmosphere of Venus is like our own, containing both oxygen and water vapor, but the spectroscopic evidence for this assumption is very doubtful. Recently spectrograms have been made with the Snow telescope and the Littrow grating spectrograph at times when the relative velocity of Venus and the earth was sufficient to separate completely corresponding lines produced by the two atmospheres. Special attention was given to the lines of water vapor near λ 5900 and to the bands α and B due to oxygen. No trace of any line due to the planet's atmosphere was observed. It is estimated that in the path traversed by the solar light through Venus' atmosphere there must be less than the equivalent of one meter of oxygen, less than one-thousandth of that in our atmosphere, and less than one millimeter of precipitable water vapor.

Atmosphere of Venus.—Various observational facts and theories concerning this atmosphere are discussed. Although the new data prove that there is no appreciable amount of oxygen or water vapor above the visual surface of Venus, nothing is definitely known about the elevation of this surface above the presumably solid surface of the planet, or whether this reflecting layer is composed of cirro-strati, of haze, or of clouds of dust produced by violent atmospheric circulation.

It has been generally assumed in the literature on planetary atmospheres that the atmosphere of Venus is similar to our own; in particular, that oxygen and water vapor are present. Secchi,[1] 1868, noted in the spectrum of Venus a nebulous band on the red side of the D line and also one to the violet, the δ of Brewster. He observed these with Venus at a high altitude and when the air was so dry that he assumed that they were not of telluric origin. Huggins[2] had previously, 1863, studied the spectrum of Venus, Mars, Jupiter, and Saturn. Of Venus he says:

> The light of Venus gives a spectrum of great beauty. The line D was seen double, B, C, and numerous solar lines to a little beyond G, were distinctly visible; and the principal of these were measured and found to agree with corresponding lines in the solar spectrum. Lines other than these, and in the position in which the stronger atmospheric lines present themselves, were carefully looked for, but no satisfactory evidence of any such lines has been obtained.

---

[1] *Spettri e Protuberanze*, p. 24, 1869.

[2] *Philosophical Transactions of the Royal Society*, 154, 422, 1864.

The basis of the assumption permeating the literature on planetary atmospheres is found in the observations of Vogel.[1] Of his observations on the oxygen band at λ 6275 and the water-vapor bands at λλ 5945 and 5925 he says:

> Die Venus stand bei den Beobachtungen so hoch, dass man nicht annehmen kann, dass unser Atmosphäre einen merklichen Einfluss auf das Venusspectrum ausgeübt habe, die Linien oder Streifen sind daher entschieden dem Venusspectrum eigen und deuten auf die absorbirende Wirkung einer Atmosphäre.

Scheiner[2] in his review of the question sums up as follows:

> There seems to be no doubt that the telluric lines appear stronger in the less refrangible portions of the spectrum of the planet than in the solar spectrum. There can therefore be no doubt that the atmosphere of Venus exerts an absorption similar to that of our own, and hence the nature of the two atmospheres must be similar. . . . . We may safely assume that the clouds of Venus consist of condensed aqueous vapor, thus again resembling those of the earth.

Arrhenius[3] is still more specific and states that:

> The humidity (on Venus) is probably about six times the average of that on the earth or three times that in the Congo where the average temperature is 26° C. The atmosphere of Venus holds about as much water vapor 5 km *above* the surface as does the atmosphere of the earth *at* the surface. We must therefore conclude that everything on Venus is dripping wet. The vegetative processes are greatly accelerated by the high temperature. Therefore the life time of organisms is probably short.

The fallibility of these older visual observations, in which conclusions are drawn from estimates of the relative intensities of integrated groups of lines in the spectrum of Venus and of the moon or sky, is shown by comparing Vogel's observations in the green region with our spectrograms of Venus and the sky. Vogel notes, among others, groups at λ 5216 and λ 5251 as strengthened in the spectra of Venus, and Scheiner accepts the observations as definite proof of the similarity of the atmosphere of Venus and the earth. Arrhenius' conception of supertropical moisture and luxuriance of vegetation is founded likewise on these older observations. These groups are resolved on the Mount Wilson spectrogram, Plate XI, and our

---

[1] *Untersuchungen über die Spectra der Planeten*, pp. 10–16, 1874.

[2] *Astronomical Spectroscopy*, pp. 197–198, 1894.

[3] *The Destinies of the Stars*, pp. 250–251, 1918.

PLATE XI

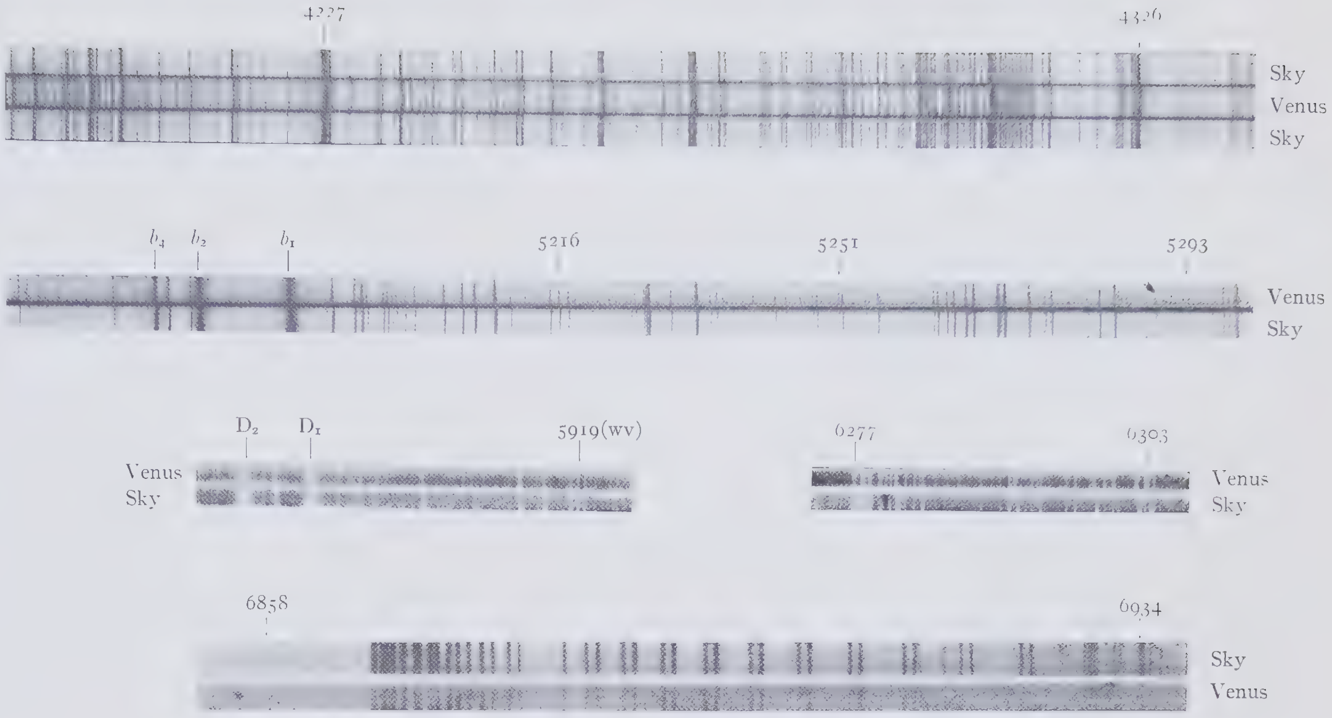

Spectra of Venus and Sky

examination shows no strengthened lines in the spectrum of Venus. The lines of both groups are identified as iron lines of intensity 2 and 3 on the Rowland scale. The degree of dependence that can be placed upon the Mount Wilson spectrograms may be inferred from observations at λ 5293 of some lines which are marked Awv? and 00 intensity in the Rowland table. These were clearly displaced in the spectrum of Venus, with no lines visible in the undisplaced positions. An examination of juxtaposed spectra of the east and west limbs of the sun confirms this evidence that the lines are entirely solar and not atmospheric.

These older visual observations depended on estimating the relative intensities of integrated groups of lines in the spectra of Venus and skylight. Lowell[1] suggested measuring the position of the oxygen and water-vapor lines to see whether they were affected by the Doppler shift, and V. M. Slipher obtained spectrograms of Mars and the moon and of Venus and the sky with a dispersion of 50 A per mm at 6100 A.[2] Of the spectrograms of Mars, Lowell says:

> The results at first seemed significant. To the writer's eye the shift of the solar lines under the microscope was perceptible though slight and in the shift the *a* band seemed to share. The lines of water vapor near D though present in both spectra were not strong enough to make much deduction possible.

Of Venus he says,

> Here again eye estimates by the writer subscribed to a shift in the *a* band, the water vapor lines, very faint, concurring; . . . . As regarded differences in density, none was perceptible between either the Martian and the lunar or the solar and Venusian, either in the oxygen *a* band or the water vapor lines near D. Water vapor is probably non-existent on the illuminated side of Venus and extremely scarce on Mars. As for oxygen the results above show that the spectroscopic method is hardly a delicate enough one in this respect to decide the question.

And Slipher remarks:

> Examination and measurement of them led to the same uncertain results as in the case of those of Mars. Although this attempt has failed to detect aqueous vapor in Mars and Venus, the conclusion should not be drawn that it

---

[1] *Lowell Observatory Bulletin*, No. 17, 1905.

[2] Campbell and Albrecht in observations on Mars quite independently applied the Doppler-Fizeau method to a planetary atmosphere. *Lick Observatory Bulletin*, **6**, 11 (No. 180), 1910.

does not exist in their atmospheres, nor that it will always remain impossible to discover it spectrographically.

This brief account reviews the spectroscopic evidence upon which the current views in respect to the constitution of the atmosphere of Venus were founded when we began our observations in March, 1921, and indicates the extreme detail reached in their interpretation. At the Berkeley meeting of the Astronomical Society of the Pacific in August, 1921, when we reported our results, Dr. Slipher also reported results of his recent observations in which he used relative intensity as a criterion, and obtained similar negative results.

INSTRUMENTAL METHODS

The spectrograms were obtained with the Snow telescope and the Littrow grating-spectrograph.[1] To Professor Wood we are greatly indebted for the loan of a large grating very bright in the first order. It was ruled by Anderson and has a surface of 95×170 mm. The dispersion in the first order of the 18-foot spectrograph is 3 A per millimeter. For the a band and the 5900 region the plates were Seed 23's, sensitized to red light by pinacyanol. Ilford Special Rapid panchromatic plates, hypersensitized with ammonia, were used for the B band, λ 6867.

The wave-lengths of eight water-vapor lines near D and of seven oxygen lines in the a band were measured on five spectrograms of Venus and on three of the sky, using I.A. wave-lengths of solar lines, corrected for motions, for standards of reference. On three of the spectrograms of Venus the wave-lengths of the water and oxygen lines were referred also to iron arc lines; the spectrum of the arc was put on intermittently during the long exposures on Venus. On a fourth spectrogram of the sky they were referred to the lines of a simultaneously exposed iron arc. The wave-lengths thus found were compared with the wave-lengths of the same telluric lines, obtained under much higher dispersion, given in Table I.

From the variation among the differences, Rowland *minus* International (R−I in Table I), the relatively low accuracy of measurement of water-vapor and oxygen lines is apparent, even on spectrograms with a scale of 0.72 A per millimeter. For the oxygen line λ 6278, which is double on the Mount Wilson plates, the mean wave-length of the two components is used for the comparison with the Rowland value. In such a series of measurements as is presented in this paper, where the scale is 3 A per millimeter, a precision in the final means greater than 0.005 A is hardly to be expected. The results of the measurements are shown in the eighth column of Table II under Δλ, the Δλ being the difference between the observed wave-lengths and those of Table I.

---

[1] *Mt. Wilson Contr.*, No. 208; *Astrophysical Journal*, 54, 381–382, 1921.

TABLE I

WAVE-LENGTHS OF THE COMPARISON LINES

Water Vapor* I.A.	R−I	Oxygen† I.A.	R−I
5885.982	+0.211	6278.106	+0.197
87.227	0.218	81.186	0.201
87.665	0.215	81.963	0.201
5909.001	0.212	92.171	0.202
19.058	0.218	92.967	0.203
19.646	0.214	95.186	0.203
24.276	0.214	95.968	+0.202
32.097	+0.219		

* *Mt. Wilson Contr.*, No. 223; *Astrophysical Journal*, 55, 36, 1922.

† Unpublished results by St. John and Babcock.

Because of the dearth of reference lines, a different method of measurement was adopted for the oxygen lines in the B band, λ 6867. The positions of nineteen oxygen lines in the spectra of Venus were compared with their positions in the spectra of the sky taken under similar spectrographic conditions. The scale readings of the solar lines on the spectrograms of the planet were corrected for the relative velocity of Venus and the earth. The average difference between these adjusted scale readings and those of the same lines on the sky spectrograms was then applied to all lines, thus bringing the readings of the solar lines into mean agreement on the two spectrograms. In the absence of absorption by oxygen in the atmosphere of Venus, the oxygen lines should now have the same scale readings in the two spectra; on the other hand, the presence of absorption should register as a displaced component of the oxygen lines, broadening or doubling them, according to the relative velocity. Spectrograms were taken with Venus east and west of the sun, the range in velocity corresponding to a Doppler

TABLE II

OBSERVATIONAL DATA

Plate	Subject	1921	P.S.T.	z sec z	Velocity E−V	Doppler Shift	Δλ	Lines Meas.	Refer. Lines	Phase
					km	A	A			
V 274....	Venus	Feb. 24	5^h36^m–9^h00^m	67° 2.56	−12.87	−0.254 −0.270	+0.015 −0.010	water vapor α, oxygen	arc sun	98°.0
275....	Sky	Feb. 25	4 30	76° 4.13	....	....	+0.003 −0.001	water vapor α, oxygen	sun	....
276....	Venus	Feb. 25	5 40 –9 00	68° 2.67	−12.84	−0.253 −0.269	+0.014 −0.004	water vapor α, oxygen	arc sun	98°.7
277....	Sky	Feb. 27	4 58	81° 6.39	....	....	−0.006 +0.001	water vapor α, oxygen	sun	....
278....	Venus	Feb. 27	5 37 –9 00	68° 2.67	−12.79	−0.252 −0.268	−0.012 −0.015	water vapor α, oxygen	arc sun	100°.3
279....	Sky	Feb. 28	3 49	68° 2.67	....	....	−0.009 −0.013	water vapor α, oxygen	arc	....
280....	Sky	Feb. 28	4 10	71° 3.07	....	....	−0.014 −0.021	water vapor α, oxygen	sun	....
282....	Venus	Feb. 28	7 20 –9 05	76° 4.13	−12.76	−0.252 −0.268	−0.005 −0.006	water vapor α, oxygen	sun	101°.1
285....	Venus	Mar. 1	7 19 –9 00	76° 4.13	−12.73	−0.267	−0.005	α, oxygen	sun	101°.8
289....	Venus	Mar. 3	6 16 –9 00	69° 2.79	−12.69	−0.249	+0.026	water vapor	sun	103°.4
301....	Venus	Mar. 24	5 55 –8 35	70° 2.92	−10.99	−0.252	+0.013†	B, oxygen	sun	125°.1
303....	Venus	Mar. 27	5 45 –8 38	71° 3.07	−10.38	−0.238	0.000	B, oxygen	sun	129°.0
359....	Venus	Aug. 13	15 0 –23 0*	31° 1.17	+12.44	+0.286	−0.002	B, oxygen	sun	67°.1

* Exposure interrupted; total 7^h10^m.

† Weight $\frac{1}{3}$

shift of 0.538 A. The results of the comparison are given in the eighth column of Table II, where the Δλ for these plates is the difference Venus *minus* sky.

OXYGEN

Five spectrograms of Venus were taken in the region of the α band when the relative velocity of Venus and the earth was −12.8 km, the corresponding Doppler shift being 0.268 A to the violet, an amount sufficient to separate completely the terrestrial components from those of Venus. Although some solar lines of intensity 000 are faintly visible on these spectrograms, no lines are observable where they should appear if produced by oxygen in Venus' atmosphere. The measured wave-lengths of the oxygen lines present on the spectrograms of Venus and the sky and the magnitude of their deviations from the wave-lengths of Table I show, moreover, that the oxygen lines produced by the earth's atmosphere in the spectrum of the planet are not measurably shifted by blending with lines originating in the atmosphere of Venus and wide enough to overlap those of terrestrial origin.

The B band is producible by a much smaller quantity of oxygen than the α band and therefore furnishes a more sensitive test. King has recently shown that 39.4 m of air at 72 cm pressure, equivalent to 8 m of oxygen, give the lines of the B band faintly.[1] His solar spectrograms indicate that the lines of the B band produced by 39.4 m of air are comparable in intensity with solar lines of intensity 00 on the Rowland scale. On the spectrograms of Venus in this region lines of intensity 1 have about the same visibility as the limiting lines on King's spectrograms. To obtain an estimate of the length of an oxygen column which would produce the lines of the B band with an intensity of 1, we have made use of a valuable paper by Jewell[2] on the variation of the intensity of water-vapor lines with the quantity of water vapor traversed and of the change in intensity of the oxygen line λ 6287.953 with zenith distance. Jewell determined the intensities of Fraunhofer lines—000 to 6— in terms of the Fe line λ 5930.406. Graphs from these data show that the intensity intervals from 000 to 6 are roughly equal, and that the intensity of the water-vapor line λ 5919.860 is strictly proportional to the amount of water vapor traversed (Figs. 1, 2). A similar proportionality is shown to hold for the oxygen line λ 6287.953 and is assumed to hold for the oxygen lines of the B band. The interval from 00 to 1 is approximately 0.16 of the intensity of the Fe line λ 5930. This is equivalent to an increase in the length of path of 16 per cent. Hence the lines of the B band would probably appear on the spectrogram of Venus if the absorbing column contained the equivalent of 9.2 m of oxygen under ordinary conditions of pressure.

---

[1] *Mt. Wilson Contr.*, No. 232; *Astrophysical Journal*, **55**, 411, 1922.

[2] *Astrophysical Journal*, **4**, 324, 1896.

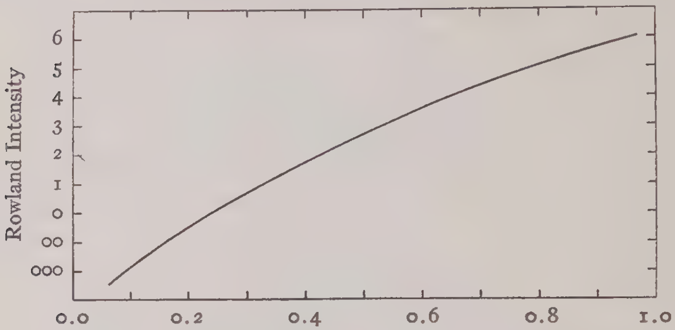

Fig. 1.—Rowland intensities in terms of λ 5930 taken as unity

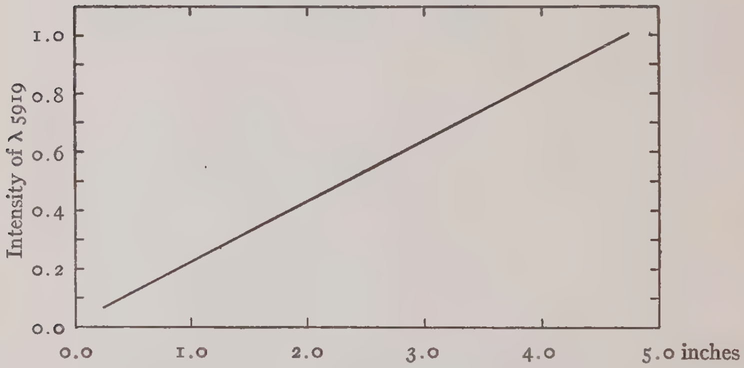

Fig. 2.—Intensity at the zenith of λ 5919 (wv) in terms of λ 5930 (Fe) for various amounts of precipitable water in the atmosphere expressed in inches.

Two spectrograms of Venus showing the B band, March 24 and March 27, 1921, were taken when the relative velocity was −10.68 km, the equivalent Doppler effect being −0.245 A. A similar spectrogram was taken August 14, when the relative velocity was +12.44 km, the Doppler displacement being +0.286 A. With the scale of 3 A per millimeter, the doublets of the B group are widely separated, but in the interspaces no lines are visible, where lines due to oxygen absorption in the atmosphere of Venus should appear, though solar lines of intensity 0 are present. Whether lines originating in the planet would be completely separated from the terrestrial lines by shifts of 0.264 A and 0.286 A depends on the widths of the lines. It is evident that at most only a small amount of oxygen is traversed in the atmosphere of Venus, and lines produced by it would be faint and narrow. On a plate of the B band taken by King with an air path of 39.4m, the mean width of the single lines is 0.19 A. The mean width of these lines on spectrogram V 359 is 0.27 A, and the Doppler shift +0.29 A, so that the edges of the lines would be separated by 0.06 A. Spectrograms V 301 and V 303 are not so suitable for this purpose, as the continuous background is fainter and the lines somewhat wider and the Doppler shift smaller than for V 359. When, however, the positions of the oxygen lines in these spectrograms are compared with their positions in the sky spectrograms, the measures show a displacement of 0.003 A to the red, whereas the Doppler shift would be 0.245 A to the violet. On V 359, the measured displacement is 0.002 A to the violet, with a possible Doppler shift of 0.286 A to the red. If, therefore, for any cause the lines of the B band produced by small amounts of oxygen on Venus are somewhat wider than those produced in the laboratory, the results show that there is no measurable influence of overlapping of the edges of the terrestrial lines by undetected Venus components.

The length of the path traversed through Venus' atmosphere in a layer of a given radial depth depends upon the phase angle of the planet and the position on the disk of the point from which the light is observed. For a point on the line perpendicular to the terminator and limb, whose distance from the limb in units of the length of that line is d, the zenith distances of the earth, z_e, and of the sun, z_s, are given by

$$\sin z_e = 1 - d - d\cos i,$$

$$z_s = i - z_e$$

where *i* is the phase angle. Table III gives the total length of the path traversed by the solar beam for different phase angles and different distances from the limb in units of the radial depth. The secant equation used here is of course not applicable just at the limb and terminator.

TABLE III

$\sec z_e + \sec z_s$

d		*i*		
		70°	100°	130°
(Limb)	0.0	∞	∞	∞
	0.1	3.0	3.7	5.5
	0.2	2.6	3.2	4.8
	0.3	2.4	3.1	4.8
	0.4	2.5	3.2	5.0
	0.5	2.6	3.5	5.6
	0.6	3.0	4.0	6.6
	0.7	3.5	5.0	8.2
	0.8	4.7	6.9	11.6
	0.9	8.1	12.9	22.9
(Terminator)	1.0	∞	∞	∞

At the middle point of the visible disk, corresponding to the center of the spectral band, the path for plates V 301 and V 303 was 5.2 times the radial depth of the layer penetrated, and for V 359 it was 2.5 times the depth. On the basis that lines of intensity 1 would be produced by 9.2 m of oxygen, it follows for V 301 and V 303 that the quantity of oxygen traversed did not exceed the equivalent of a column 2 m long under standard conditions. For light from near the terminator the path traversed in Venus' atmosphere is much longer. With the slit normal to the terminator, as in these observations, one edge of the spectrum corresponds to this longer path. For spectrograms V 301 and V 303 the path for the light at the point halfway between the center and edge of the spectrum was 7.5 times the radial depth of the layer. The edge of the spectrum shows no trace of oxygen lines due to absorption in the planet's atmosphere. Absorption capable of producing lines of intensity 1 would be expected if an oxygen layer equivalent to 1 m under normal pressure had been traversed in the passage through the atmosphere of Venus. As the oxygen in the earth's atmosphere is equivalent to a column 1500 m long, it follows that the oxygen in the path through Venus' atmosphere was less than one-thousandth of that in the terrestrial atmosphere.

WATER VAPOR

Five spectrograms of Venus taken when the relative velocity of Venus and the earth was −12.8 km, the corresponding Doppler shift being −0.252 A, form the basis of the investigation on water vapor. The relative velocity was sufficient to separate completely lines produced by absorbing gases common to both atmospheres. No traces of lines due to the planet's atmosphere are discernible on the spectrograms.

An upper limit for the amount of water vapor in the atmospheric layer on Venus penetrated by the solar beam may be found by the following considerations. Spectrogram V 282 was taken at mean zenith distance 76°. The average quantity of precipitable water above Mount Wilson is 0.69 cm[1] (the mean for the days of observation was 0.72 cm). The water-vapor line λ 5919.860 was of intensity about 5 on the Rowland scale, and telluric water-vapor lines of intensity 000 and 00 can be identified on the spectrum of Venus. Had a like quantity of water vapor been present in the planet's atmosphere above the reflecting surface, the intensity of the component of λ 5919.860 due to Venus should have been about 4 as against 5 for the terrestrial line, since the water-vapor masses traversed would have been 2.5 cm for Venus and 2.9 cm for the earth, the two respective paths being 3.6 and 4.1 times that for zenith distances 0. For the point half-way between the center of the disk and the terminator the water mass traversed would have been 4.2 cm, corresponding to solar intensity 7 for the water-vapor line λ 5919.860. These results are deduced from the graphs of Jewell's data. Terrestrial water-vapor lines of 00 intensity are easily seen on the plate, but no line is visible 0.25 A to the violet of the terrestrial line λ 5919.860, in which position 0.7 cm of water above the apparent surface of Venus would have produced a line of intensity 7. As the water vapor traversed in the atmosphere of Venus was not sufficient to produce the line λ 5919.860 with intensity 00, there must have been

[1] *Annals of the Astrophysical Observatory*, 3, 189, 1913.

less than 1 mm of water in the layer of the planet's atmosphere traversed by the solar beam, for a line of intensity 00 is produced by 16 per cent of the water vapor necessary for a line of intensity 7.

Measurements of the wave-lengths of eight water-vapor lines were made on the five spectrograms of Venus and on four of the sky. The wave-lengths in Table I were obtained from solar spectrograms with a dispersion four times that used in this investigation. For these closely crowded lines the mean excess of 0.008 A shown by the Venus measures in Table II, when they are compared with the values given in Table I, represents probably the systematic errors associated with the measurement of spectral lines not well separated and varying in intensity from time to time as is characteristic of atmospheric lines. The difference is positive, whereas it should be negative if there were a measurable effect due to partial superposition of lines produced by water vapor in Venus' atmosphere.

DISCUSSION

These observations indicate that the previous spectroscopic evidence for oxygen and water vapor in the atmosphere of Venus, depending upon visual observations of a change in line intensity, is not reliable, that in fact there is no acceptable spectroscopic evidence of the presence of either. On the other hand, they do not show the complete absence of water vapor and oxygen from the planet's atmosphere, but that, to the depth penetrated by the solar beam, they are not present beyond a definite low limit.

Previous to Russell's[1] investigation in 1898 the accepted view as to the extent of Venus' atmosphere made it much denser than our own.[2] Russell showed that the prolongation of the cusps, formerly attributed to refraction, was mainly due to diffuse reflection of light by the planet's atmosphere. He concluded that the horizontal refraction at the apparent surface cannot exceed 12′ as against 34′ for the earth, and that there is no satisfactory evidence that the atmosphere of Venus at the apparent surface is more than one-third as dense or extensive as the earth's at sea-level. The entire height above the apparent surface he thinks may be thirty miles as compared with the earth's forty, thus implying a pressure at this surface of perhaps one-tenth that of the earth's atmosphere at sea-level. He attributes the prolongation of the cusps visible in daylight to a hazy layer of fog or dust lying below the 4100-foot level, a haze-bank whose upper boundary presents a more or less abrupt decrease in haziness, and whose lower portions may at times be obscured by low mountains, evidenced by irregularities in the thin circle of illumination on the side opposite the sun when Venus is at inferior conjunction.

---

[1] *Astrophysical Journal*, **9**, 284, 1899.

[2] Young, *Manual of Astronomy*, p. 356, 1912.

A. W. Clayden[1] makes a strong presentation of the view that Venus has a moisture-laden atmosphere as dense and extensive as that of the earth. He decides on a long period of rotation, but one less than 225 days. He assumes that a high and heavy layer of pillared cumuli covers the cyclonic areas of low pressure and rising vapor, that over the regions of greater pressure the anticyclonic circulation results in lower detached masses of cumuli between which we see perhaps the shaded surface of the planet, and that a filmy veil of cirrus produces the prolongation of the cusps.

If, as suggested by Russell, the pressure at the visible surface is only one-tenth of an atmosphere, then the atmosphere of Venus is much poorer in oxygen than the earth's atmosphere, as the quantity of oxygen in Venus' atmosphere above the visible surface is less than the equivalent of 1 m, while in our atmosphere above the level of similar pressure there are 104 m of oxygen. If the reflection takes place at the upper surface of a 4100-foot haze-bank, which Russell suggests may be partially cut off at times by low mountains and therefore may not be far above the actual surface of the planet, then the oxygen above this low level is less than one-thousandth of that in the earth's atmosphere above Mount Wilson, elevation 1739 m.

If, on the other hand, it be assumed, as by Clayden, that the atmosphere of Venus is similar in composition and extent to ours, it follows that the reflected sunlight has not penetrated to a point less than 43 km from the real surface of the planet and has traversed but an insignificant path through its atmosphere, since in the earth's atmosphere there is above the 43 km level the equivalent of a meter of oxygen under normal pressure, an amount capable of registering on our spectrograms. The question of the depth to which the solar beam penetrates the planet's atmosphere and the probability that it reaches a point much nearer the real surface than 43 km are considered in detail in the discussion of water vapor.

---

[1] *Monthly Notices*, 69, 195, 1909.

TABLE IV

Amount of Oxygen above a Given Elevation

Elevation	Pressure	Oxygen
km	mm	m
0	760	1490
5	405	722
10	201	324
15	90	135
20	41	54
25	19	23
30	8.6	10.0
35	3.8	4.2
40	1.6	1.76
45	0.85	0.73
50	0.40	0.30

Any conclusion as to water vapor must rest upon the nature and temperature as well as the elevation of the apparent surface at which diffuse reflection takes place. The high albedo has been considered evidence of a cloudy surface, but the equally high reflecting power of Vesta indicates that this evidence is not definitive, since for Vesta there is no question of a cloudy surface. Russell[1] gives a Bond albedo of 0.59 for Venus. Using 65 per cent as the reflecting power of a cloudy surface, Abbot and Fowle[2] found 0.60 as the corresponding albedo for a cloud-covered earth. Aldrich,[3] under more favorable conditions of observation, obtained 78 per cent as the reflecting power of clouds, from which the albedo calculated in the same manner is 0.75 for a cloud-covered earth. Russell says that the Bond albedo A should not be used for comparison with the observed reflecting power of terrestrial substances, but a quantity p, which he defines in an article on the albedo of planets and satellites.[1] For Venus p is 0.49 while for clouds it is 0.78. Both the reflecting power and the Bond albedo are considerably less than would be expected if Venus is completely cloud covered.

---

[1] *Loc. cit.*, p. 190.

[2] *Annals of the Astrophysical Observatory*, **2**, 161–163, 1908.

[3] *Smithsonian Misc. Collections*, **69**, 10, 1919.

The conditions of Venus' atmosphere depend in large measure upon the period of rotation, the temperature, and the temperature gradients, all undetermined quantities. The period of rotation is quite probably not less than fifteen days, the limit shown by Slipher's observations with which our own agree. With a period of rotation equal to that of the orbital revolution, it is reasonable to assume, as Arrhenius suggests,[2] that water vapor and all other constituents of an atmosphere would collect and be congealed on the side of the planet turned away from the sun where a temperature near absolute zero would prevail. But the illumination of the whole circumference of the disk when Venus is at inferior conjunction, attributed to scattering and refraction, shows the presence of an atmosphere of considerable extent. These considerations give grounds for assuming that the period of rotation is shorter than that of the orbital revolution and hence is between the extremes of 15 and 225 days. For an intermediate period of rotation, an atmosphere would be present over the region of insolation, subject probably to violent disturbances near the terminator. This would be in harmony with Quenisset's[3] observations, both photographic and visual, of extensive and rapid changes in the obscuring envelope, indicating a shallow atmosphere.

The region of maximum cloudiness in the terrestrial atmosphere is mainly below 4000 m,[4] coinciding roughly with the average altitude of the zero isotherm, which is 3000 m.[5] The corresponding region of cloudiness in the atmosphere of Venus would be where the temperature and humidity conditions are similar. According to Abbot and Fowle,[6] the mean temperature of the earth's surface is

---

[1] *Astrophysical Journal*, 43, 191, 1916.

[2] *Worlds in the Making*, p. 61, 1908.

[3] *Comptes Rendus*, 172, 1645, 1921.

[4] Humphreys, *Physics of the Air*, p. 309, 1920.

[5] Hann, *Handbook of Climatology*, p. 250, 1903.

[6] *Annals of Astrophysical Observatory*, 2, 173–175, 1908.

287°.2 A, but the temperature of the true radiating surface of the earth as a planet is 263° A, this surface being chiefly the water-vapor layer at an elevation of 4000 m or more above sea-level. The elevation of a water-vapor radiating surface on Venus, however, would probably be greater owing to higher temperature. Using 2.5 calories as the solar constant, Poynting[1] gives the average temperature of an ideal planet at Venus' distance from the sun as 342° A, and at the earth's distance as 290° A. With 287°.2 A for the temperature of the earth the temperature of Venus becomes 337° A.

If the surface temperature of Venus be taken as 337° A and a temperature gradient of 6° per kilometer be assumed in Venus' atmosphere, such as obtains on the earth, the elevation of the zero isotherm would be 11 km, that of a water-vapor radiation surface 12 km, and that of the isothermal layer 19 km, which are to be compared with 3, 4, and 11 km for the earth.

The conditions at Mount Wilson offer favorable opportunities to study the increase in the relative humidity of the air above a cloudy surface. The velo cloud,[2] as the Spanish called the "high fog" of southern California, often covers the valleys to a height of 1200–3000 feet, especially during the months of May and June. For nine clear days in May and eight in June, 1921, the mean vapor pressure on Mount Wilson was 3.25 and 4.05 mm, respectively, while for nine days in May and twenty-one in June, with clear sky above and the velo cloud 4000 feet below and two to five miles distant, the respective vapor pressures were 4.65 and 5.28 mm, about 35 per cent greater. In the case of Venus' atmosphere with a water-vapor content sufficient to form a continuous layer of cumulus clouds exposed to nearly twice the intensity of the solar radiation at the earth, the water vapor above the dense cloud layer would probably exceed the increase at Mount Wilson when velo clouds are 4000 feet below and several miles away. This increment is two or three times the quantity our spectrograms should record. Granting the probable circulation in the planet's atmosphere suggested by Clayden, it seems also probable, especially over the anticyclonic areas, that the solar beam would penetrate a region of the atmosphere where water vapor would be encountered in detectable quantity. The spaces not only above, but especially between the columnar cloud masses, must be more or less moisture laden, since, under the powerful solar radiation, evaporation and convection into the neighboring drier regions would take place as over the velo clouds, and under the downward anticyclonic flow, the clouds would be carried into regions of higher temperatures and more or less dissipated. The results would be an atmosphere of high humidity over extensive areas more or less open to observation, as the high cirrus assumed by Clayden would offer little obstruction.

---

[1] *Collected Scientific Papers*, p. 315, 1920.

[2] Carpenter, *The Climate and Weather of San Diego*, 1913.

If the dusky markings upon which investigators have based the observations interpreted as showing short rotation periods are actual surface features of the planet, or if they are a transient thinning of a cloudy envelope, it is probable that we there see down to levels at which the humidity would be high in an atmosphere so heavily moisture laden that the planet is enveloped in a blanket of clouds. Spectrogram V 274 was taken eight hours later than Quenisset's photographs showing extensive dusky areas, but no traces of water-vapor lines are discernible on any part of the spectral band.

If the brilliant white spots from which the long rotation period has been deduced really belong to the planet's surface, and, as suggested, are snow-covered mountain peaks extending into the upper atmosphere, it seems probable that water vapor would be spectroscopically detectable by its absorption lines were they to stand free from the corresponding terrestrial lines, as they would in our spectrograms. It is to be considered also that the spectrograms were taken in light of long wave-length, for which scattering is relatively small and the consequent penetration into a hazy atmosphere great. In the case of the oxygen lines, near λ 6900, the depth from which the light is reflected is probably well below the apparent visual surface.

If, however, the reflecting surface consists of a permanent layer of cirro-stratus, the quantity of water vapor traversed by the reflected beam would be small, as cirro-strati are formed in the upper troposphere where the temperatures are very low. These low temperatures practically insure that cirro-strati consist of ice crystals, but as at such low temperatures there is little water to condense, their structure is necessarily more or less tenuous and fibrous and consequently the reflected light will have penetrated the layer to a great depth. Above such a cloud-surface there would be the thinner cirrus to which the prolongation of the cusps is due, and the still higher atmosphere which produces by refraction the illumination around the planet's circumference observed at inferior conjunction.

Reflection from a layer of cirri gives the shortest possible path for the light in the planet's atmosphere. The water vapor above the cirrus level may be insufficient for detection by observations on the lines in the rain-band. The spectrographic test for oxygen by observations on the B band is, however, much more sensitive. In the earth's atmosphere above the cirrus level there is the equivalent of 274 m of oxygen at sea-level; above 19 km, the elevation assumed for the cirrus level on Venus, there is still the equivalent of 65 m, but our observations show that oxygen on Venus above the reflecting surface is less than 2 per cent of this amount.

It is of interest to consider some alternatives to water-vapor clouds. It is possible that a very small quantity of water vapor would produce an impenetrable haze-bank if the atmosphere of Venus contained minute hygroscopic centers of condensation capable of producing cloud particles in an atmosphere where the humidity is much below that which otherwise would be essential to cloud formation.[1] With such a hazy atmosphere on Venus, analogous to but denser than the dry-weather haze that sometimes obscures the valley or lies along the lower reaches of the distant mountains viewed from Mount Wilson, the surface of the planet might appear much as we see it. To an observer on the planet's surface transmitted light would be rich in long wave-lengths, as to us when the earth's atmosphere is laden with volcanic dust. To an outside observer the color would depend upon the proportion of the light scattered in its atmosphere to that reflected from its surface.

Under the probable extremes of temperature on the opposite hemispheres of Venus it is conceivable that the violent atmospheric circulation would cause clouds of dust to be permanent features of the planet's atmosphere, dust composed of highly reflecting material such as that to which the high reflecting power of Vesta is due. Wilsing and Scheiner[1] give for liparitic pumice a reflecting power of 0.56, for rock salt 0.44, and for granular limestone 0.42. These are comparable with 0.49 for Venus and 0.48 for Vesta. It is to be observed, however, that the presence of two of these substances would imply the action of water at the time of their production or segregation. The dust storms that sometimes prevail for days over the deserts and occasionally sweep through the mountain passes suggest vividly the possibilities on a dry and wind-swept planet.

---

[1] Humphreys, *Physics of the Air*, p. 92, 1920.

Whether or not light reflected from the continually evaporating surfaces of clouds produces sufficient water vapor to give its absorption lines with observable intensity is a question whose answer would aid greatly in determining the character of the apparent surface of Venus and in solving the puzzling problems of its atmosphere. We hope later to obtain more observational data as to the humidity around and above clouds, and to extend the spectrographic observations to the water-vapor band near λ 7200, as the lines of this band are producible by smaller amounts of vapor and would furnish a more sensitive test of its presence. Other and quite as important information would be obtained from the relative color indices of Venus and terrestrial clouds and from direct photographs through violet and infra-red filters[2] as used by R. W. Wood for Jupiter and Saturn. These would show the apparent surfaces at widely different levels and offer the possibility of reaching the actual surface through the thinner portions of the atmospheric veil.

It has been too easily assumed, perhaps, that the atmospheric conditions on our nearest planetary neighbors are similar to those on the earth, and that on Venus development has followed along similar lines and by like stages as on the earth. It was long ago suggested by Koene,[3] of Brussels, that all free oxygen may have been formed from carbonic acid in the air. Arrhenius says that we may take it as established that the masses of free oxygen in the air and of free carbon in the sedimentary strata approximately correspond to each other, and that probably all the oxygen of the air owes its existence to plant life.[1] That a similar production of oxygen has apparently not taken place on Venus suggests that some condition is wanting. Possibly a deficiency of water has prevented or hindered the freeing of oxygen through vegetation, or it may be that the exacting conditions for the origin of life have not been satisfied so that the existing atmosphere may consist of other permanent or semipermanent gases such as nitrogen or carbon dioxide.

---

[1] *Potsdam Publications*, **20**, Part IV, 1909.

[2] *Mt. Wilson Contr.*, No. 113; *Astrophysical Journal*, **43**, 310, 1916.

[3] *Mémoires de Chimie*, 1856.

MOUNT WILSON OBSERVATORY
July 1922

---

[1] *Worlds in the Making*, pp. 58, 59.

Contributions from the Mount Wilson Observatory, No. 250
Reprinted from the *Astrophysical Journal*, Vol. LVI, pp. 400–438, 1922

THE SOURCE OF LUMINOSITY IN GALACTIC NEBULAE

By EDWIN HUBBLE

ABSTRACT

Relation of the luminosity of galactic nebulae to the magnitudes of associated stars. (1) *Diffuse nebulae.* If, as has been suggested, these nebulae owe their luminosity to radiations from associated stars, then the angular extent of nebulosity should increase with the apparent brightness of the stars. More precisely, if we assume that the clouds of nebulosity are illuminated by stellar light whose intensity varies inversely as the square of the distance from the stars; that each part of a nebula reflects or re-emits, without change in actinic value, all the starlight intercepted by it; and that the light from the stars themselves reaches us undimmed by absorption, then the square of the maximum angular extent of nebulosity a, for an exposure E, should be proportional to E times the apparent luminosity of the star I, or $a^2/E=a_1^2/60=I\times$ const., or $m+5\log a_1=B$, where a_1 is the angular distance reduced to a uniform exposure of $60^{\rm m}$. For a Seed 30 plate and a focal ratio of 5 to 1, B is equal to 11.6 or 10.6, according as the line joining the star to the faint nebulosity is perpendicular to the line of sight or has the mean inclination corresponding to random direction. To test this equation, data for eighty-two nebulae were plotted, $\log a_1$ against m. The points lie near the line: $m+4.9\log a_1=11.0$, thus showing that the inverse-square law holds closely and that the other assumptions are approximately correct. The mean deviation of the points from the line, over an interval of 14 magnitudes, is only $\pm 0^{\rm m}.8$; but thirteen points lie above the limiting theoretical curve. The probable explanation is that in these cases the apparent brightness of the stars is diminished through absorption by nebulosity between the star and the observer, that is, the third assumption is not wholly justified. This is borne out by the fact that these stars show a color excess which is usually greater than the residual magnitude. While most of the nebulae have continuous spectra, in eighteen cases the spectra are emission, and thus differ widely from the spectra of the associated stars. Since the corresponding points show no systematic deviation from the theoretical curve, the luminosity must be due to re-emission of light of the same total actinic value, rather than to reflection, and this suggests the possibility that the light producing the continuous spectrum is also re-emitted. The great loop in Cygnus is a conspicuous exception, since no sufficiently bright star is in evidence. The star, perhaps, is hidden or dimmed by nebulosity. Reduced to absolute magnitudes, the foregoing equation becomes $M+5\log l=2.5\log E-5.52$, where l is the linear distance in parsecs from star to nebulosity and E is in minutes. For Rigel, $M=-5.6$, an equivalent exposure of thirteen hours shows nebulosity, presumably made luminous by it, extending to $12^\circ.5$, or ninety-three light-years. (2) *Planetary nebulae.* When certain systematic corrections suggested by observations made at Mount Wilson are applied to data given by Curtis for the limiting exposure times and the apparent magnitudes of the nuclei for fifty-six objects, the angular distance A_1 of the brightest details of luminosity from the central stars, reduced to uniform exposure time on the assumption of an inverse-square law of luminosity with respect to the central stars as sources, varies with the photographic magnitude of the central stars according to the equations: $m+(5.3\pm0.4)\log A_1=17.9$, or $m+5\log A_1=17.6\pm0.2$. The first of these is the correlation curve derived from the data; the second, the curve having the theoretical slope which best represents the plotted points. The correlation between m and $\log A_1$, however, is not nearly as close as in the case of the diffuse nebulae. The residuals, for instance, seem to be related to the type of planetary, averaging $+1.8$ for the ring type, and -1.5 for globular

objects. The corresponding theoretical equation, based on the assumption stated above for diffuse nebulae, but for an exposure time of six seconds, is: $m+5 \log A=13.6\pm 0.3$. Hence, the observed luminosity per unit area is about four magnitudes brighter than the theoretical. The discrepancy for these nebulae may be due to a difference between the spectra of the nebulosity and of the nuclei, the latter having relatively much more energy in the ultra-violet; or it may indicate that the radiations which excite the luminosity are chiefly corpuscular.

Revised photographic magnitudes of the nuclei of planetary nebulae.—The values given by Curtis for fifty-six objects seem to require a systematic correction of

$$+0.173m-3.37 .$$

New cometary nebula at $\alpha=6^{h}3^{m}$, $\delta=+18^{\circ}42'$ (1920) shows striking similarity to the variable nebula N.G.C. 2261, although variability has not yet been established.

I. DIFFUSE GALACTIC NEBULAE

This paper gives the results of an attempt to test the theory that stellar radiations are the source of luminosity of galactic nebulae. V. M. Slipher[1] found that in the case of Merope, Maia, ρ Ophiuchi, N.G.C. 2068, and N.G.C. 7023 the absorption spectrum of the nebulosity agreed, approximately at least, with the spectra of the brightest involved stars. On this ground he suggested that these nebulosities at least are shining by reflected light from the involved stars. Hertzsprung[2] made a quantitative test of this suggestion in the case of the Pleiades nebulosity by determining the surface brightness at several points in the nebulosity and comparing the results with those derived by spreading the light of the stars over spherical shells of radii equal to the distances from the stars to the points of nebulosity whose surface brightness he had measured. He found the nebulosity to be from 4 to 5 magnitudes fainter than would be expected on a theory of total reflection, and concluded that, if a suitable albedo were assumed, the reflection of star light could account for the nebular luminosity. H. N. Russell[3] has accepted the idea of reflection for diffuse nebulae with continuous spectra, and has advanced the theory that galactic nebulae with emission spectra, diffuse as well as planetaries, are excited to luminosity by radiations from involved or neighboring stars.

The writer has found that particular stars can be selected which are obviously involved in or conspicuously associated with practically every known diffuse nebulosity. The spectra of these stars bear a definite relation to the spectrum of the associated nebulosity, such that if the stellar spectra are earlier than B1, the nebular spectrum is emission, and, if the stellar spectra are later than B1, the nebular spectrum is continuous. Nebulosity associated with stars of the critical type B1 usually possesses a spectrum of mixed characteristics. The transition in nebular spectra from emission to continuous, although rapid, is quite smooth. It is not abrupt. The only pronounced exception to the rule of spectral relation is the possibility that stars with highly enhanced spectra of the α Cygni type may be associated with nebulosity whose spectrum is predominantly emission. α Cygni itself and B.D. $-22^\circ 4510$, of the same type, appear to be associated with N.G.C. 7000 and N.G.C. 6514, respectively. Bright-line stars associated with emission nebulae are the exception and not the rule. Wolf-Rayet stars associated with diffuse nebulosity are rare. In the northern skies only two cases are known—N.G.C. 2359 and 6888. Both show some affinity with planetaries or with nova phenomena.

---

[1] *Lowell Observatory Bulletin* No. 55, 1912; 75, 1916; *Astronomical Society of the Pacific*, **30**, 63, 1918; **31**, 212, 1919.

[2] *Astronomische Nachrichten*, **195**, 449, 1913.

[3] *Proceedings of the National Academy of Sciences*, **8**, 115, 1922; *Observatory*, **44**, 72, 1921.

This definite spectral relation suggests that nebular luminosity depends to a certain degree at least on stellar radiations, and an attempt has been made to test this quantitatively. The method employed was to determine the surface brightness of diffuse nebulosities giving continuous spectra, by means of the limiting exposure times necessary just to register the nebulosity under standard conditions. Preliminary results from a small number of objects demonstrated that the brightness and extent of the nebulosity are definitely related to the magnitude of the associated stars, and that existing photographs could be used to establish the relationship. Accordingly Table I was constructed from an examination of the plates already available. In the first column is given the catalogue designation of the nebulae; in the second column, the spectral type of the nebulae, E and C for observed emission and continuous spectra, e and c for the same characteristics, not observed, but inferred from the spectral types of associated stars, according to the rules given in the preceding paragraph; in the third column the apparent photographic magnitudes, m, of the associated stars, combined, if a group of stars appears; in the fourth, the spectral type of the associated stars; in the fifth, the color excess[1] of these stars; in the sixth, the exposure time, E, in minutes, of the plates examined; in the seventh, the greatest angular distances, from the stars, in minutes of arc, at which nebulosity could be detected. For a group of stars involved in nebulosity, a was measured from the mean position of the stars. In most cases of this sort the extent of the groups of stars is small compared to the extent of nebulosity. In the eighth and ninth columns are given the quantities log E and log a; in the tenth, the corrected quantity log a_1, representing log a reduced to a uniform exposure time of 60 minutes; in the eleventh, the designations of the stars whose magnitudes are given in the third column; in the twelfth column the instruments employed in obtaining the photographs examined.

The data are fairly homogeneous, as the plates used were all Seed 30's, most of them taken with the 60-inch and 100-inch reflectors, both of focal ratio 1 to 5. Several were taken with a Tessar Ic lens, called "Kodax" in the eleventh column, and with a 10-inch Cooke astrographic lens, both of which have focal ratios 1 to 4.5. In these cases the values of log E were corrected by the quantity $+0.12$ in order to reduce them to the Newtonian reflector system. A few measures are from photographs by Barnard, made with the 10-inch Bruce lens of focal ratio 1 to 5, and designated "Barnard" in the twelfth column. A small correction should be applied to log E in these cases in order to allow for the light cut off by the Newtonian flat, but the amounts and the numbers are so small that they have been disregarded.

The photographic magnitudes for stars brighter than 6.0 are from visual magnitudes found in the *Harvard Annals*, to which have been applied both color indices and color excess. Magnitudes of the fainter stars are from polar comparisons made by the writer, and are on the Mount Wilson scale.

The quantities used in the following discussion, m, a, and E, are quite independently determined, and there is no reason to suspect

---

[1] The color excesses are taken from *Mt. Wilson Contr.* No. 187; *Astrophysical Journal*, 52, 8, 1920; and from further unpublished measures by Seares and Hubble. The latter values are provisional. Final values will appear in a joint paper to be published shortly.

TABLE I

Object	Spec. Nebula	*m*	Spec. Star	*CE*	*E* min	*a*	Log *E*	Log *a*	Log a_1	Star	Instrument
B.D. +64°13	c	10.4	B2	0.65	100	1′.5	2.000	0.176	0.065	. . . .	60-inch
N.G.C. 281	E	7.3	Oe5	0.10	210	14	2.322	1.146	0.874	B.D. +55°191	60-inch
I.C. 59, 63	E	2.2	Bop	0.00	60	33	1.898	1.518	1.458	γ Cassiopeiae	10-inch
B.D. +60°596	c	9.7	B2	0.40	120	3	2.079	0.477	0.326	. . . .	60-inch
N.G.C. 1333	C	10.9	B9p	0.30	180	4	2.255	0.602	0.364	. . . .	60-inch
B.D. +31°597	c	8.6	K2g	0.00	60	2	1.778	0.301	0.301	. . . .	100-inch
+29°565	c	9.6	A5	0.33	120	4.3	2.079	0.634	0.483	. . . .	60-inch
Merope	C	4.0	B5	0.00	120	25	2.079	1.398	1.247	. . . .	60-inch
Pleiades	c	1.2	. . . .	0.00	615	270	2.789	2.431	1.926	Entire cluster	Barnard
I.C. 348	C	9.0	B6-A1	0.80	180	2.3	2.255	0.362	0.124	B.D. +31°643	100-inch
N.G.C. 1491	E	11.3	Bo	1.00	120	1.8	2.079	0.255	0.104	. . . .	60-inch
1499	E	3.7	Oe5	0.00	120	70	2.199	1.845	1.634	ξ Persei	10-inch
1514	E	9.7	Odp	0.70	90	1.8	1.954	0.255	0.167	B.D. +30°623	100-inch
I.C. 359?	C	13.5	K8d	0.00	240	0.4	2.380	−0.398	−0.699	. . . .	100-inch
N.G.C. 1624	E	12.0	Oe5	. . . . . .	120	1.5	2.079	0.176	0.025	. . . .	60-inch
1788	C	10.2	B8	0.22	90	3	1.954	0.477	0.389	B.D. −3°1013	60-inch
I.C. 405	E	5.8	Bop	0.30	90	11.5	1.954	1.061	0.973	Boss 1249	60-inch
2118*a*	C	0.2	B8p	0.00	60	180	1.898	2.255	2.195	Rigel	10-inch
2118*b*	c	0.2	B8p	0.00	600	750	2.898	2.875	2.315	Rigel	Kodax
N.G.C. 1976	E	4.8	Oe5, Bo	. . . . . .	90	35	2.074	1.544	1.396	Trapezium	10-inch
1977	C+E	4.6	B1	. . . . . .	120	20	2.079	1.301	1.150	c′ Orionis	100-inch
I.C. 431	c	7.6	B2	0.17	120	3	2.079	0.477	0.326	B.D. −1°1001	100-inch
432	c	6.9	B2	0.05	120	4	2.079	0.602	0.451	−1°1005	100-inch
N.G.C. 2023	C	7.9	B2	0.30	90	6.8	1.954	0.832	0.744	−2°1345	60-inch
2024	E	1.4	Bo	0.00	90	33	1.954	1.518	1.430	ζ Orionis	100-inch
I.C. 435	C	8.2	B3	0.20	90	4	1.954	0.602	0.514	B.D. −2°1350	60-inch
N.G.C. 2068	C	10.8	B5	1.00	120	4.5	2.079	0.653	0.502	+0°1177	60-inch
2071	C	10.8	B9	0.80	120	2	2.079	0.301	0.150	+0°1181	60-inch
Orion	c	1.4	Bo	0.00	600	240	2.898	2.380	1.820	ζ Orionis	Kodax
Cometary Neb.	C	13.2	B1	. . . . . .	60	1.5	1.778	0.176	0.176	. . . .	100-inch
N.G.C. 2170	c	11.0	B1	1.02	90	1.5	1.954	0.176	0.088	B.D. −6°1415	60-inch

B.D. −6°1417	c	10.2	B5	0.55	90	3.1	1.954	0.491	0.403	......	60-inch
−6°1418	c	9.9	B5	0.65	90	1.5	1.954	0.176	0.088	......	60-inch
N.G.C. 2182	c	9.0	B3	......	120	2.0	2.079	0.301	0.150	B.D. −6°1431	60-inch
2183	C	14.0	B3	......	120	0.5	2.079	−0.301	−0.452	......	60-inch
2185	C	12.9	B3	......	120	1.3	2.079	0.114	−0.037	......	60-inch
B.D. −6°1444	c	10.8	B3	......	120	0.5	2.079	−0.301	−0.452	......	60-inch
N.G.C. 2175	E	7.3	Oe5	0.20	240	14	2.380	1.146	0.845	B.D. +20°1284	60-inch
2237	E	5.3	Oe5	0.00	180	35	2.375	1.544	1.246	*m* for group	10-inch
I.C. 446	C	11.8	B1	0.80	120	1.8	2.079	0.255	0.104	......	60-inch
447	C	7.7	......	......	120	7.5	2.199	0.875	0.664	*m* for group	10-inch
N.G.C. 2245	C	11.2	B1p	0.88	45	1.3	1.653	0.114	0.177	......	60-inch
2247	C	9.2	B2p	0.68	60	2.5	1.778	0.398	0.398	B.D. +10°1772	100-inch
2282	c	10.1	B2	0.35	90	2	1.954	0.301	0.213	+ 1°1503	60-inch
I.C. 2177	E	7.3	Bop	0.70	120	9	2.079	0.954	0.803	−10°1848	60-inch
B.D. −12°1771	C	8.1	B1	0.20	40	1.8	1.602	0.255	0.343	......	60-inch
−23°5277	c	9.2	B9	......	90	2.5	1.954	0.398	0.310	Triple star	60-inch
−23°5296	c	9.0	B1	......	90	2.5	1.954	0.398	0.310	......	60-inch
π Scorpii	C	2.8	B2	......	400	113	2.602	2.053	1.641	......	Barnard
I.C. 4592	C	3.9	B2	......	180	80	2.255	1.903	1.665	ν Scorpii	Barnard
4601*a*	C	7.1	B9, Aop	0.20	300	13	2.477	1.114	0.765	B.D. −19°4358, 9	100-inch
4601*b*	C	7.1	B8, Ao	0.32	300	13	2.477	1.114	0.765	−19°4361	100-inch
σ Scorpii	c	3.2	B1	0.48	270	140	2.431	2.146	1.819	......	Barnard
I.C. 4604	C	5.1	B2, B3	0.50	270	60	2.431	1.778	1.451	ρ Ophiuchi	Barnard
4605	C	4.7	B3	0.12	270	50	2.431	1.699	1.372	22 Scorpii	Barnard
N.G.C. 6514	E	7.0	Oe5	......	90	10	1.954	1.000	0.912	B.D. −23°13804	60-inch
6523	E	5.4	Oe5, Bo	......	90	12	2.074	1.079	0.931	*m* for group	10-inch
I.C. 4678	c	10.4	B3	0.50	60	2.3	1.778	0.362	0.362	B.D. −23°13906	100-inch
1274*a*	c	8.7	B1	0.35	60	2.7	1.778	0.431	0.431	−23°13997	100-inch
1274*b*	c	9.2	B1	0.35	60	2.5	1.778	0.398	0.398	−23°13998	100-inch
N.G.C. 6589	c	9.8	B2	0.42	90	1.9	1.954	0.279	0.191	−19°4940	100-inch
6590	c	10.5	B3, B5	0.40	90	2.1	1.954	0.322	0.234	−19°4946	100-inch
I.C. 1284	c	7.7	B2	0.50	90	5	1.954	0.699	0.611	−19°4953	100-inch
N.G.C. 6611	E	7.3	Oe5	......	90	6	1.954	0.778	0.690	*m* for group	60-inch
I.C. 1287	c	6.1	B2	0.62	270	25	2.551	1.398	1.011	Boss 4687	10-inch

TABLE I—*Continued*

Object	Spec. Nebula	m	Spec. Star	CE	E	a	Log E	Log a	Log a_1	Star	Instrument
N.G.C. 6726, 7	C	7.1	B9	0.10	60	3.8	1.778	0.580	0.580	B.D.−37°13023,4	100-inch
6729	C	10.0	Gp	......	60	1	1.778	0.000	0.000	R Cor. Aust.	100-inch
6888	E	6.7	Ob	......	180	8	2.255	0.903	0.665	B.D. +37°3821	60-inch
I.C. 4954, 5*a*	c	13.7	B3	1.10	60	0.4	1.778	−0.398	−0.398	....	60-inch
4954, 5*b*	c	12.2	B3	0.90	60	0.6	1.778	−0.222	−0.222	....	60-inch
4954, 5*c*	c	14.4	A3	0.55	60	0.2	1.778	−0.699	−0.699	....	60-inch
N.G.C. 6914*a*	C	8.9	B3	0.00	180	3.0	2.255	0.477	0.239	B.D. +41°3737	60-inch
6914*b*	C	9.2	B4	0.00	180	2.5	2.255	0.398	0.160	+41°3731	60-inch
γ Cygni, *a*	......	3.0	F8p	0.00	180	115	2.375	2.061	1.763	....	10-inch
γ Cygni, *b*	......	3.0	F8p	0.00	180	75	2.375	1.875	1.577	....	10-inch
N.G.C. 7000	C+E	1.8	A3p	0.00	180	220	2.375	2.342	2.044	α Cygni	10-inch
7023	C	7.4	B2p	0.55	120	6	2.079	0.778	0.627	B.D. +67°1283	60-inch
B.D. +57°2309	c	6.5	B2p	......	120	9	2.079	0.954	0.803	....	60-inch
+67°1332	c	8.2	B4	0.05	90	4	1.954	0.602	0.514	....	60-inch
N.G.C. 7129	C	10.5	B3	0.60	60	1	1.778	0.000	0.000	....	60-inch
I.C. 5146	c	10.4	B1	0.97	120	5	2.079	0.699	0.548	B.D. +46°3474	60-inch
N.G.C. 7635	E	8.5	Odp	0.20	90	6	1.954	0.788	0.690	+60°2522	100-inch

The actual E is given for 10-inch and Kodax plates, but 0.12 is added to the value of log E in these cases to reduce to the Newtonian reflector system.

Pleiades. Trumpler's value of m for the entire cluster is used, and a color index of −0.10 is applied. E and a are taken from Barnard's photograph of the exterior nebulosity. *Publications Lick Observatory*, **11**, Plate 15, 1913.

I.C. 359? A nebulous star north following the nebula at $\alpha = 4^h 14^m$, $\delta = +28°5'$ (1920), described by Barnard in *Astrophysical Journal*, **25**, 223, 1907, and which may be I.C. 359.

I.C. 2118. "a" refers to the brighter portion north preceding Rigel. "b" is the extreme limit of the faint extensions that trail off south preceding for several degrees into Eridanus.

Orion. Refers to the great exterior loop around the belt and sword of Orion. The following side of the loop was used and was referred to ζ Orionis as the nearest of the extremely bright stars. This procedure is questionable in detail but probably permissible in determining orders of magnitude.

Cometary Nebula. A bright uncatalogued cometary nebula at $\alpha = 6^h 3^m$, $\delta = +18°42'$ (1920).

π Scorpii. E and a are from Barnard's photographs reproduced in *Astrophysical Journal*, **23**, 144, 1906.

I.C. 4592, 4604, 4605. E and a are from Barnard's photographs reproduced in *Astrophysical Journal*, **31**, 8, 1910.

N.G.C. 6729. This is the variable nebula about R Coronae Australis. The star is also variable and the measures refer to a particular date.

large systematic errors. The range in m is from 0.2 to 14.4; in a from $0'.2$ to $750'$; in E from 40 min. to 790 min. The mean errors in m are estimated as about 0.1, and in a about 5 per cent. The actual observed E, is, of course, exact to the minute, but differences in sky conditions, state of mirrors, plates, and development, suggest a mean error in the equivalent exposure time of the order of 5 per cent.

The nebulosity fades more or less smoothly with increasing distance from the stars, and the points for which a was measured represent in general the limiting surface brightness which registers on the particular plate examined. If the exposures were all of the same duration, under uniform conditions, a comparison of m with a should then indicate the relation existing between nebular and stellar luminosity. If this relation were due to a reflection of star light, and the albedo of the nebulosity were constant, the relation would be expressed by $m+5 \log a=K$ where K is a constant depending on the albedo, the limiting surface brightness shown on the photographs, and the distribution of angles which the directions, stars to points, measured for a, make with planes perpendicular to the lines of sight.

As a first step in the investigation, m was plotted against log a, disregarding the differences in exposure times. This plot is shown in Figure 1. The extent of nebular illumination is clearly a function of the stellar luminosity, and the relation is approximately linear. A curve with a slope, or coefficient of log a, equal to 5 can be fitted to the plot in the form

$$m+5 \log a=11.9 \tag{1}$$

so as to represent the points fairly well. Considering the great differences in exposure times, and the fact that measures on the brighter stars are as a rule from longer exposures than those for the fainter stars, Figure 1 is pretty fair evidence that nebular luminosity obeys the inverse-square law with the associated stars as sources of illumination.

This assumption affords a simple method of referring the data to a homogeneous system by reducing log a to log a_1, corresponding to a uniform exposure E_0, or inversely, reducing log E to log E_1, corresponding to a uniform angular distance a_0. Let I and I_0 be the minimum intensities registered in exposure times E and E_0, p Schwarzschild's exponent in the reciprocity law. Then, assuming the inverse-square law to hold rigorously for nebular illumination,

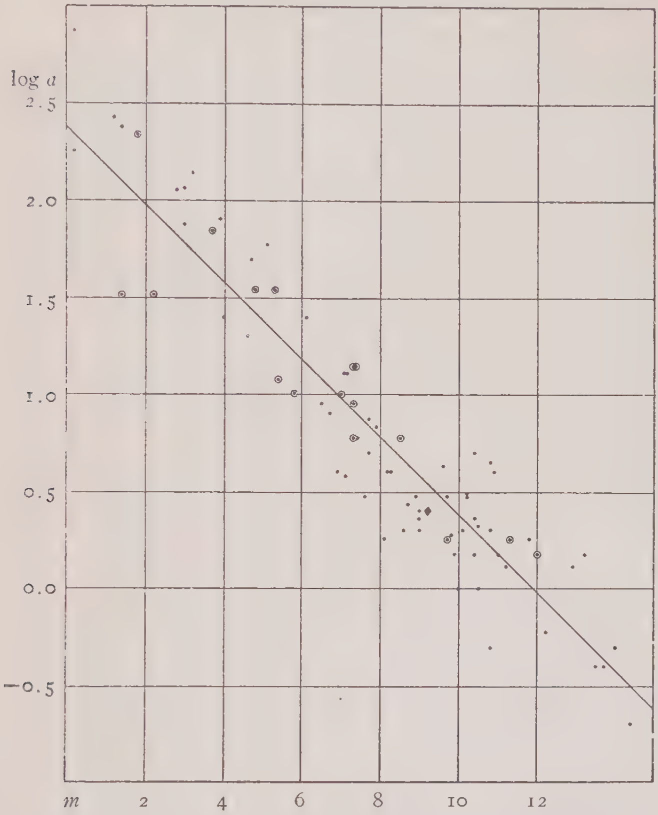

FIG. 1.—Photographic magnitudes of stars associated with diffuse nebulae (abscissae), plotted against the logarithm of the greatest angular extent of nebulosity from these stars (ordinates). The data are from Table I. Differences in exposure times of the plates examined are disregarded. The line represents the equation $m+5\log a=11.9$. The coefficient of $\log a$ indicates that the nebular luminosity obeys the inverse-square law with respect to the stars as sources.

$$\left(\frac{a}{a_1}\right)^2=\frac{I_0}{I}=\left(\frac{E}{E_0}\right)^p \tag{2}$$

$$\log a_1=\log a+\frac{p}{2}(\log E_0-\log E) \tag{3}$$

likewise

$$\log E_1 = \log E + \frac{2}{p}(\log a_0 - \log a) \qquad (4)$$

The magnitudes m can be plotted either against $\log a_1$, angular distances corresponding to a uniform exposure time, or against $\log E$, the brightness corresponding to a uniform distance; but with the scale properly chosen, the two figures would be identical, because of the relation derived from (3) and (4):

$$\log E_1 + \frac{2}{p}\log a_1 = \log E_0 + \frac{2}{p}\log a_0 = \text{Constant}$$

Log E_0 has been chosen as 60 minutes of time and log a_0 as one minute of arc, and p has been assumed as unity. Thus,

$$\log a_1 = \log a + \tfrac{1}{2}(1.778 - \log E) \qquad (5)$$

$$\log E_1 = \log E - 2 \log a \qquad (6)$$

$$\log E_1 = 2 \log a_1 = 1.778 \qquad (7)$$

Log a_1 was chosen as the quantity to be plotted against m in order that the result might be compared with Figure 1. The question of the proper value of p raises a serious theoretical difficulty which is minimized in the actual plotting by the use of a value for E_0 near the mean E, so that $\log E_0 - \log E$ in equation (5) is small. The various values of p used in discussions on stellar photometry range from about 0.75 to 1.00. No values have been directly determined for long exposures on nebular surfaces under actual observing conditions and there is very little basis on which to select the most probable value. However, the greatest difference in any particular $\log a_1$ as determined by equation (5) for the extreme values of p, is about 0.12. The mean difference is less than 0.04, which is of the same order of accuracy as the original data. These considerations seemed to justify the selection of $p = 1.00$ as the simplest procedure. The effect of using other values can be determined later, should the matter prove important.

Figure 2 shows the plot of $\log a_1$ against m. A least-squares solution gave for the adjusted curve

$$m+(4.90\pm 0.13)\log a_1=11.02\pm 0.10 \tag{8}$$

The simple mean of $m+5\log a$ is 11.10, and the corresponding curve differs from that of (8) by less than a tenth of a magnitude over the entire range of 14.2 magnitudes. The average deviation in m for both curves is about 0.8 magnitudes. The deviation of the coefficient of $\log a_1$ in (8) from the expected value of 5.0 is within the errors of observation.

A theoretical value can be computed for the constant on the right side of equation (8), by assuming the inverse-square law to hold rigorously and by assuming further that all the starlight intercepted by the nebulosity is re-emitted. Consider a point of nebulosity at distance a in minutes of arc from the star. The surface brightness of this nebulosity is determined on the above assumption by spreading the luminosity of the star over a spherical shell of radius a. Expressed in magnitudes per square second of arc, this surface brightness will be $m+2.5\log 4\pi(60a)^2$ or $m+11.64+5\log a$. Seares has determined the limiting surface brightness of an exposure of one minute on a Seed 30 plate, using a reflector of focal ratio 1 to 5.[1] This quantity, expressed in magnitudes per square second of arc, is 18.8 ± 0.3. It applies approximately to all photographic instruments of an equivalent focal ratio. For an exposure of sixty minutes corresponding to the values of $\log a_1$, the limiting surface brightness is $18.8+2.5\,p\times 1.778$ or $18.8+4.45\,p$. Equating these two expressions,

$$\left.\begin{aligned} m+5\log a_1&=7.16+4.45\,p\\ &=11.61 \text{ for } p=1.00\end{aligned}\right\} \tag{9}$$

Assuming a random distribution of directions from star to nebulosity, the mean a observed, projected on a plane perpendicular to the line of sight, should be less than the true a by the factor $\pi/2$. This difference can be corrected by increasing m by $5\log\pi/2=0.98$. Equation (9) then becomes

$$\left.\begin{aligned} m+5\log a_1&=6.18+4.45\,p\\ &=10.63 \text{ for } p=1.00\end{aligned}\right\} \tag{10}$$

---

[1] *Mt. Wilson Contr.* No. 191; *Astrophysical Journal*, 52, 162, 1920.

If the assumption that the light emitted by the nebulosity exactly equals the starlight intercepted is correct, then equation (10) should represent the points in Figure 2, and equation (9) should play the rôle of an upper limit to the points. The agreement between (10) and (8) is close enough to raise a strong presumption that the assumption just mentioned is justified by the facts. Thus

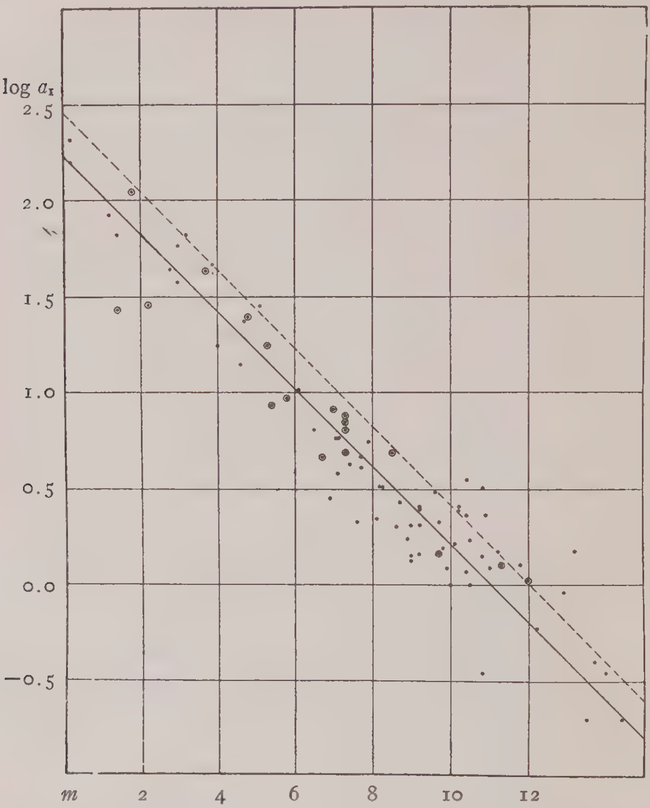

FIG. 2.—The same as Fig. 1, except that log a has been reduced to log a_1, corresponding to a uniform exposure time of one hour on Seed 30 plates with a reflector of focal ratio 1 to 5. The full line represents the curve $m+4.90 \log a_1=11.02$ derived from a least-squares solution. The broken line represents a limiting curve parallel to the full line, displaced 0.98 to the right.

(8) Observed. . . . . $m+4.90 \log a_1=11.02 \pm 0.10$

(10) Theoretical. . . . . $m+5.00 \log a_1=10.63 \pm 0.3$

The difference in slopes can scarcely be shown on the plot, and the difference in the constants on the right side of the equations is just the sum of the probable errors. It should be noted further that the constant in (8) falls nearly half-way between those for equations (9) and (10), the theoretical limiting curve and the mean curve on the assumption of random distribution of the directions from star to points measured for a. Any deviation from random distribution in the observed data would fall in this direction, for in each case the maximum a was consciously sought.

Observations and theory can also be compared by using log a and log E directly in a generalized form of equation (10). Assuming again that the total amount of starlight intercepted is re-emitted by the nebulosity

$$\left.\begin{aligned} 18.8\pm0.3+2.5\log E&=m+11.64+5\log a\\ m+5\log a-2.5\log E&=7.16\pm0.3\ \text{(limit)}\\ &=6.18\pm0.3\ \text{(mean)} \end{aligned}\right\} \qquad (11)$$

The left side can be computed from the original data and proves to be 6.65±0.07 with an average residual of about 0.82. This lies almost exactly half-way between the theoretical limiting and mean values, and supports the suggestion that the data deviate from a random distribution in the direction of large angles to the line of sight. If the coefficient of log a in equation (11) be replaced by 4.90, as indicated in equation (8), the constant becomes 6.57.

This is not an independent method, for equations (9) and (10) reduce to equation (11) when the value of log a_1 given in equation (5) is substituted into (9) and (10). The difference in the constant, $11.02-6.57=11.10-6.65=4.45$, is the quantity $2.5\,pE_0$ when p is taken as unity.

Equation (11) expresses a direct relation between the original data and should be the nicest method of procedure in the investigation. It is not well suited to least-squares solutions, however, because log a and log E are not independent. This difficulty is obviated by the transformation into equations (9) and (10).

Within the limits of error, equation (8) agrees with the theoretical mean curve expressed by equation (10). Disregarding for the moment possible deviations from random distribution in the data, a limiting curve should appear on the plot parallel to the mean curve and displaced 0.98 magnitudes toward the side of increasing *m*. Any points falling to the right of this limit require explanation, for they indicate that the nebulosity is too bright or the stars too faint for a strict agreement with the theory that diffuse nebulosity re-emits exactly the light it receives from associated stars. Such a limiting curve has been sketched as a broken line on the plot in Figure 2, and several points do fall beyond. The general evidence is very strong against the nebulosity being too bright, i.e., that it emits more light than it intercepts from the star, and such an explanation should be appealed to only as a last resource.

The most probable solution appears to be the diminution of the stars' apparent brightness by nebulosity intervening between them and the earth. This is a well-known phenomenon among stars involved in nebulosity and makes itself felt in the abnormally large color indices which such stars as a general rule possess. The color excess, measured color index *minus* that normal to the spectral type of the star observed, is probably due to scattering of starlight by intervening nebulosity. If scattering is responsible for the color excess, then the true photographic magnitude of the star, as seen free from its screen of nebulosity, would be brighter than the observed value by about twice the color excess.

The nebulosity responsible for the observed scattering is obviously between the star and the earth. If the path from star to point of nebulosity measured for *a* were reasonably free from intervening nebulosity, such a correction should certainly be applied to the observed *m*. If, on the other hand, the nebulosity responsible for the scattering is distributed symmetrically about the stars, then the observed *m* is just that which is effective in illuminating the exterior points of nebulosity which were measured.

An examination of the points falling beyond the limiting curve indicates that as a rule they are measured from stars with large color excesses, and that a correction figured on this basis will throw them on the safe side of the curve. The stars from which these 13 points were measured, with *D* their distance in magnitudes beyond the limiting curve and *CE* their measured color excesses, are listed below:

Star	*D*	*CE*
σ Scorpii	0.10	0.48
ρ Ophiuchi	0.15	0.50
B.D. +46°3474	1.05	0.97
B.D. +01177	1.20	1.00
B.D. −31013	0.10	0.22
B.D. −61417	0.20	0.55
B.D. −2312906	0.15	0.50
N.G.C. 1333	0.65	0.30
N.G.C. 2245	0.05	0.88
I.C. 446	0.30	0.80
N.G.C. 1624	0.10	....
N.G.C. 2185	0.70	....
Cometary Nebula	2.05	....

Color excesses are not available for the last three objects. N.G.C. 1624 is a small group of Oe5 stars involved in emission nebulosity. The combined magnitude is from estimated individual magnitudes and may be a few tenths in error. The stars in the last two nebulae show considerable color visually, and analogy with other objects of a similar nature suggests large values for the color excess. The cometary nebula is an uncatalogued object in a region of pronounced obscuration at $\alpha = 6^{h}3^{m}$, $\delta = +18^{\circ}42'$ (1920) which shows a striking similarity to the variable nebula N.G.C. 2261. It is being followed for variability, but thus far without positive results. The color excess may not be large enough to account for the large *D*, but a small amount of general absorption could be postulated to make up the balance.

It is reasonable to suppose that in these 13 cases, the nebulosity responsible for the color excess is for the most part between the star and the observer, and that relatively little is between the star and point of nebulosity measured for a. An idea of how general is this dissymmetry of distribution about the stars of nebulosity responsible for the scattering can be derived from a study of relations between the residuals in Figure 2 and the color excesses. Measures of this last quantity are available for 63 points. There is no systematic difference in distribution between these and the points for which color excesses have not been measured. The residuals may therefore be taken directly from Figure 2. A least-squares solution of the observational equations $x+y\ CE=$ Residual in m, gives

$$R \pm 0.08 = 0.90\ CE - 0.32 \tag{12}$$

If the scattering nebulosity were always symmetrically distributed about the stars, the coefficient of CE should be zero; if it were always between the star and observer and never between star and points measured for a, the coefficient should be approximately 2. An excess in scattering nebulosity between stars and points measured for a, over that between star and observer, would reduce the measured a and this effect could not be distinguished from that due to inclinations of the directions from star to measured points. The observed value of the coefficient of CE, namely 0.90, seems to indicate that the scattering nebulosity is distributed, not symmetrically, but rather at random about the stars. Corrections computed from equation (12) would provide only for the scattering nebulosity between star and observer in excess of that symmetrically distributed. It would reduce the constant in equation (8) by the quantity 0.32 and the resulting value, 10.70, would be in excellent agreement with that expected from theory, namely 10.63. Similar nebulosity not in the line of sight would reduce the true values of a, and a correction would in the mean tend to compensate the correction suggested by equation (12). The scattering effect probably will not seriously affect the mean values in Figure 2, although it offers a ready explanation for individual residuals.

A supplementary table of data was constructed from a homogeneous series of exposures made for the purpose of determining surface brightness of nebulosity from minimum exposure times necessary to show the nebulosity. The number of objects was small, but the results agree satisfactorily with those from Table I. The summation of $m+5\log a-2.5\log E$ is 6.50 ± 0.18, in good agreement with the theoretical value of 6.18 ± 0.30. The curve adjusted for the slope corresponding to the inverse-square law of luminosity is $m+5\log a_1=10.95\pm0.18$. The correlation curve is $m+4.38\log a_1=10.54\pm0.20$; but the points are not well distributed for a good determination of the slope, and the small value of the coefficient of log a_1 cannot seriously affect the general conclusions. The plot of log a_1 against m is shown in Figure 3.

The data in Table II are entirely independent of those in Table I except the values for m. Different points were measured for a, and the exposure times average about one-sixth of those in Table I. The range in E for the two tables is especially significant, running in the first from 40 minutes to over 10 hours and in the second from 7 seconds to 50 minutes. Individual comparisons of log a_1 have no meaning, for inclinations of the directions from star to measured points cannot be determined independently. The systematic difference in log a_1 is 0.015, or about $3\frac{1}{2}$ per cent, which is satisfactorily small and indicates that the distribution of directions and of scattering nebulosity is comparable in the two systems of data.

TABLE II

Object	m	CE	Spec. Star	E	a	Log E	Log a	Log a_1	Instrument
				min.					
N.G.C. 1333	10.9	0.30	B9p	3.0	0'.15	0.477	−0.824	−0.174	60-inch
Merope *a*	4.0	0.00	B5	1.0	1.67	0.000	0.222	1.111	60-inch
Merope *b*	4.0	0.00	B5	0.25	0.40	−0.602	−0.398	0.792	60-inch
I.C. 348	9.0	0.80	B6–B9	4.0	0.32	0.602	−0.495	0.093	60-inch
359	13.5	0.00	K8d	50	0.17	1.699	−0.778	−0.738	100-inch
N.G.C. 1788	10.2	0.22	B8	1.0	0.17	0.000	−0.778	0.112	60-inch
I.C. 2118	0.2	0.00	B8p	30	135	1.597	2.130	2.220	10-inch
N.G.C. 2023	7.9	0.30	B2	0.33	0.33	−0.477	−0.477	0.651	60-inch
I.C. 435	8.2	0.20	B3	3.0	0.40	0.477	−0.398	0.252	60-inch
N.G.C. 2068	10.8	1.00	B5	0.50	0.40	−0.301	−0.398	0.641	60-inch
2071	10.8	0.80	B9	1.0	0.30	0.000	−0.523	0.376	60-inch
Orion	1.4	0.00	B0	30	210	1.597	2.322	2.412	10-inch
N.G.C. 2245	11.2	0.88	B1p	0.25	0.17	−0.602	−0.778	0.412	60-inch
2247	9.2	0.68	B2p	0.13	0.083	−0.875	−1.079	0.247	100-inch
I.C. 4592	3.9	......	B2	40	45	1.722	1.653	1.681	10-inch
4603	8.4	0.85	B2	30	10	1.597	1.000	1.090	10-inch
4604	5.1	0.50	B2–B3	20	25	1.421	1.398	1.577	10-inch
4605	4.7	0.12	B2	10	4.5	1.120	0.653	0.982	10-inch
N.G.C. 6726	7.2	0.10	B9	0.33	0.13	−0.477	−0.875	0.252	100-inch
6727	9.1	0.80	B9	0.60	0.13	−0.222	−0.875	0.125	100-inch
6729	10.0	0.50	Gp	0.25	0.10	−0.602	−1.000	0.190	100-inch
N.G.C. 7023	7.4	0.55	B2p	0.17	0.20	−0.778	−0.699	0.569	60-inch
7129	10.5	0.60	B3	0.33	0.072	−0.477	−1.176	−0.048	60-inch

The actual E is given for 10-inch plates, but 0.12 has been added to the value of log E to reduce to the Newtonian reflector system.

Merope *a* refers to the well-known wispy nebulosity, while *b* refers to the small bright cometary nebulosity about 30″ south of the star.

I.C. 359. The catalogue designation is uncertain. The position is given in the notes to Table I.

Orion refers to the brightest portion of the great exterior loop at about $\alpha = 5^h45^m.5$, $\delta = +1°$ (1920).

The general conclusion from this investigation is that, within the errors of observation, the data can be represented on the hypothesis that diffuse nebulae derive their luminosity from involved or neighboring stars, and that they re-emit at each point exactly the amount of light radiation which they receive from the stars. Where stars of sufficient brightness are lacking in the neighborhood, or, if present, are not properly situated to illuminate the nebula as seen from the earth, the clouds of material present themselves as dark nebulosity.

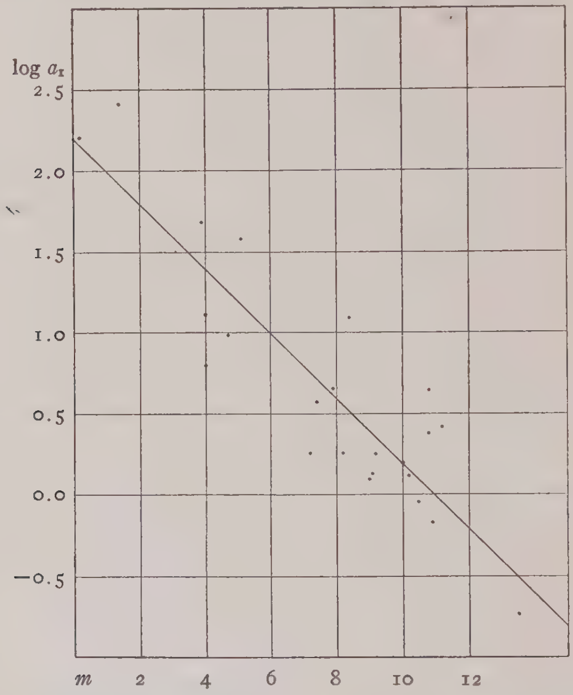

FIG. 3.—Photographic magnitudes of stars associated with diffuse nebulae (abscissae), plotted against the logarithm of the greatest angular extent of nebulosity from these stars (ordinates). The data are from Table II, derived from minimum exposures necessary just to register the brightest portions of the nebulae. Log a has been reduced to log a_1 corresponding to a uniform exposure of one hour on Seed 30 plates with a reflector of focal ratio 1 to 5. The straight line represents the equation $m+5 \log a_1=10.95$.

Eighteen of the objects listed in Table I show spectra which are predominantly emission. The points corresponding to these objects are mingled among the others in a thoroughly homogeneous manner and show no systematic characteristics whatsoever. Such a result was unexpected. The associated stars in these cases, with the exception of the Ob star B.D.+37°3821 in N.G.C. 6888, are of the usual Oe5 and B0 types,[1] hence the nebular luminosity cannot be a phenomenon of simple reflection, but must result from some process of absorption and re-emission of stellar radiation. The data indicate that within the spectral limits to which Seed 30 plates are sensitive the continuous radiations from the stars are absorbed by the nebulosity and completely re-emitted as discontinuous radiations within the same range of wave-lengths. This may be a mere coincidence, but the idea is suggestive and should be investigated in detail.[2]

The fact that the emission nebulae do not shine by simple reflected starlight raises a question as to the process of illumination in the nebulae which show continuous or absorption spectra. The evidence given by V. M. Slipher as to the agreement between spectra of nebulae and of associated stars in the cases of Merope and Maia, ρ Ophiuchi, N.G.C. 2068, and N.G.C. 7023, is in favor of the reflection theory.

Analogy with emission nebulae, however, suggests the possibility that the process may be one of absorption and re-emission. This view is supported by the manner in which emission nebulae with no perceptible continuous spectrum merge smoothly into "continuous" with no emission as the spectral types of the dominating stars pass from Oe5 to the middle B's. It is extremely difficult, in the reflection theory, to account for the absence of strong continuous spectrum from purely emission nebulae. One must suppose that the physical state of this type of nebulosity is quite different from that of "continuous" nebulosity, being such that reflection is not possible. Further, it would lead to the logical conclusion that the physical state of nebulosity depends upon and is determined by the spectral type of the associated stars. Such a relation is not impossible, for the intensity of stellar radiation, closely associated with spectral type, must play a large rôle in determining the distribution of nebulous particles of various sizes, and thus indirectly bear upon the distribution of spectral characteristics throughout a given nebula. It seems impossible at present to strike a balance between the two views concerning the mechanism of illumination, but it is worth mentioning that the analogy of emission nebulae is quite as strong an argument against, as the agreement of spectra is in favor of, the theory of pure reflection.

---

[1] γ Cassiopeiae and B.D. $-10°1848$ in I.C. 59, 63, and I.C. 2177 respectively show weak hydrogen emission lines.

[2] Plots similar to Fig. 2 were constructed for each of the various stellar spectral types in Table I; no systematic differences were found to exist.

Another striking characteristic of Figure 2 is the relatively small spread in the points and especially the complete absence of points falling far below the mean curve. The average deviation is about 0.8 in m or 0.16 in log a_1. The greatest single deviation to the left is 2.6 magnitudes or 0.53 in log a_1. A simple inspection of photographs shows at once that nebulosity as a rule is not symmetrically distributed about stars. Nevertheless Figure 2 indicates that as a rule nebulosity is found at the extreme limits to which a star will illuminate it sufficiently to be photographed with exposures of several hours duration. The explanation is probably to be found in relations between pressure and illumination effects of the stellar radiations on nebulous material of the sizes responsible for the nebular luminosity.

Several of the objects in Table I are of considerable interest individually. γ Cygni for instance is a pseudo-Cepheid with a spectral type F8p. The radiative symmetry of the several neighboring patches of nebulosity raises a strong presumption that they are associated with the star, and this is supported by the positions of the corresponding points in Figure 2. The same can be said concerning α Cygni and the North America nebula, N.G.C. 7000, as well as β Orionis and the nebula I.C. 2118 with its long extension into Eridanus. N.G.C. 1514 is really a giant planetary, conspicuous for the exceptionally bright central star.

One well-known galactic diffuse nebula is a conspicuous exception. The only object investigated for which no obviously dominating star could be located and for which no pronounced obscuration was conveniently situated to hide such a star, is the great loop in Cygnus of which N.G.C. 6960 and 6992 are brighter portions. These portions give emission spectra as could be expected from their filamentary structure. They are opposite one another at the ends of the longer diameter of the loop. Barnard's photograph reproduced on Plate 80 of the *Lick Publications*, Volume XI, shows the configuration. The major axis is roughly 2°5. One would expect to find a star of spectral type B0 or earlier approximately central, and hence about a degree and a quarter from the outer edges of the nebula. From Figure 2, the apparent photographic magnitude should be around 2.0, with a probable error of less than a magnitude. In the immediate vicinity no early-type stars can be found as bright as 9.0, the limit to which the search was pushed. The evidence from the other diffuse nebulae is too strong to admit the Cygnus loop as a real exception, shining by its own intrinsic luminosity, and explanation must be sought wherever possible. The obvious assumption is that there is a small cloud of dark nebulosity immediately in front of a central star, sufficiently opaque to dim the star by several magnitudes but inconspicuous on small-scale photographs.

Photographs of the central region made with the 100-inch reflector show no certain traces of such dark areas, and general obscuration cannot be present for at least one spiral nebula is shown on the plates. There is considerable filamentous nebulosity in this region, of much the same structural characteristics as the bordering patches of nebulosity known as N.G.C. 6960 and 6992. This suggests that the nebula as a whole may be an ellipsoidal shell rather than a simple loop. B.D. $+30^\circ 4199$, the brightest star within the loop, which is not far from the center, has enough nebulosity immediately around it to be called a nebulous star. Its visual magnitude is given in the B.D. as 7.0, and its spectrum is of highly enhanced type similar to that of α Cygni. It is just possible that this star, dimmed several magnitudes by general absorption of intervening nebulosity, is the source of illumination of the loop. This would be analogous to the association of α Cygni itself and the similar star B.D. $-22^\circ 4510$ with emission nebulosity.

Another point worth mentioning is that, using the observed magnitude for B.D. $+30^\circ 4199$, the relation between m and a for the loop would be of the same order as those for the Crab nebula (N.G.C. 1952), the Dumbbell nebula (N.G.C. 6853), and the Helical nebula in Aquarius (N.G.C. 7293). These objects appear to form a separate group, and speculation concerning their exceptional nature may well be deferred until the luminosity of planetaries has been investigated in a quantitative manner.

An interesting application of the conclusions arrived at in this paper can be made in the case of the spiral M 33. The bright knot in the spiral known as N.G.C. 604 has an emission spectrum of the galactic diffuse nebular type. That is to say, hydrogen is so strong as compared to nebulium that $H\beta$ is of about the same intensity as N_1. This is a general rule among diffuse emission nebulae, but is exceptional among the planetaries. Three of four stars involved in N.G.C. 604 strengthen the analogy with galactic diffuse nebulae. If we assume the same conditions to hold in N.G.C. 604 as in the galactic nebulae, these stars must be considered as probably Bo or Oe5, and Kapteyn's value of -2.5 for the mean absolute magnitude of Bo stars can be used with some degree of justification to estimate the parallax. The apparent magnitudes of these stars have not been measured, but a casual inspection of plates made with various instruments and exposures suggests that the order of magnitude of the brightest is about 15. An exposure of two hours shows nebulosity extending to about 10″ from the brightest star, so the corresponding point in Figure 2 would fall very close to the mean curve, and the analogy with galactic nebulae is still further strengthened. Since the brightest star alone is used, Kapteyn's value for the mean absolute magnitude can scarcely be considered too bright. The resulting modulus, $m-M$, of 17.5 corresponds to a parallax of $0\rlap{.}''000032$ or a distance of about 30,000 parsecs. If absorption were present, dimming the apparent brightness of the star, the distance would be correspondingly decreased. Measures of the color index would probably determine this point.

The general equations (11) expressing the relations between m, a, and E can be transformed into corresponding relations between M, the absolute magnitude (photographic in this case) and l, the greatest linear distance in parsecs to which luminous nebulosity extends, by means of

$$m=M-5-5\log\pi$$
$$a=3438\,\pi\,l$$

The expression for a is approximate, the exact relation being $l=2/\pi\sin a/2$, but the difference within the range covered by a is practically negligible. Substituting into the limiting general equation (11),

$$M+5\log l=2.5\log E-5.52 \tag{12}$$

It follows that for exposures of about 160 minutes on Seed 30 plates with reflectors of focal ratios 1 to 5, representing therefore a limiting surface brightness of $18.8+2.5\log 160=24.32$ magnitudes per square second of arc, the simple relation holds,

$$M+5\log l=0 \tag{13}$$

This will represent average conditions of direct nebular photography. A short table of corresponding values will emphasize the enormous distances involved.

	Parsecs		Light Years
For $M=-5$	$l=10$	or	32
-2.5	3.2		10
0	1.0		3
$+2.5$	0.31		1
5	0.1		0.3
10	0.01		0.03

The sun, with a photographic absolute magnitude around 5.65, would be capable of illuminating a surface to a brightness of 24.32 magnitudes per square second of arc at a distance of 0.074 parsecs = 0.24 light years = 1.5×10^4 astronomical units, or 470 times the mean distance of Neptune.

The greatest value of l encountered among the nebulae is for the nebulosity preceding Rigel. The absolute photographic magnitude of the star is about -5.58.[1] An exposure of ten hours with a 1.5-inch Tessar Ic lens of focal ratio 1 to 4.5 corresponds roughly to an exposure of thirteen hours with the reflectors, and from equation (13) the value of l should be about 29 parsecs or 93 light years. On the plate, nebulosity can be traced south preceding Rigel to a distance of nearly 12°.5. Using Kapteyn's value of 0″.0069 for the parallax of Rigel, this corresponds to a distance of nearly 31 parsecs or a hundred light years.

---

[1] Kapteyn's value of -5.5 for the visual absolute magnitude is corrected for the normal color index of a B8 star.

II. PLANETARIES

The fidelity with which the luminosity of diffuse nebulae having emission spectra obeys the laws derived from data obtained mainly from nebulae with continuous spectra, suggests the possibility of applying the methods developed in the preceding discussion to an investigation of luminosity relations in the planetaries. Spectra of the nuclei or central stars of these objects are predominantly continuous. Emission bands are frequently present, but, except for three or four objects, the energy in these bands is a negligible fraction of the energy in the complete spectrum. The law is definitely established that the spectra of nucleus and of nebulosity are dissimilar. In these respects the spectral relations between nebulosity and central stars are analogous to those in the case of the diffuse nebulae having emission spectra.

In other respects, however, the analogy fails to hold. The emission lines N_1 and N_2 are as a rule much stronger in the planetaries than in the diffuse nebulae. Since they are situated very near the red limit of sensitivity of Seed 30 plates, the tendency is to destroy the similarity of intensity distribution between stellar and nebular spectra which appears to hold for diffuse emission nebulae and which permits these objects to obey the same luminosity laws as diffuse nebulae with continuous spectra. Moreover, the extraordinary intensity in the ultra-violet region of the spectra of planetary nuclei introduces a new element into the luminosity relations which may differentiate them from those found among diffuse nebulae.

Difficulties are to be expected in an investigation of luminosity relations between stars with predominantly continuous spectra and nebulosity with complicated emission spectra, and, in the absence of definite theories of the mechanism of nebular illumination, the results will be in the nature of general tendencies rather than precise laws. Provisional results, however, should at least indicate some of the special features to be considered in a later and more thorough investigation.

Curtis'[1] descriptive catalogue of planetaries visible in the northern skies furnishes fairly homogeneous data for 78 objects. For each nebula he gives an illustration, an estimate of the photographic magnitude of the central star, the measured dimensions of the nebulosity, and estimates of its brightness expressed by the relative exposure necessary to register the brightest nebular feature on Seed 27 plates at the primary focus of the Crossley reflector.

---

[1] *Lick Observatory Publications*, 13, Part III, 1918.

In Table III are collected the data for the 56 objects in Curtis' catalogue which have more or less conspicuous central stars. The first column gives the designation; the second, the estimated magnitude m of the central star; the third, the angular distance, A, in seconds of arc measured from the central star to the brightest details of the nebulosity, which, as well as could be determined, are those details for which the relative exposure times are given by Curtis; the fourth, the relative exposures, e; the fifth and sixth columns, the logarithms of A and e, respectively; the seventh, the quantity log A_1, the significance of which will be explained later. The values of m and e are those given by Curtis. When A is given by Curtis, his value is listed in Table III; otherwise it is estimated from the illustrations accompanying the catalogue.

An inspection of the table indicates no trace of correlation between m and log A, but considerable, though vague, evidence of a relation between m and log e. The most conspicuous feature, however, is a rather definite relation between m and a combination of log A and log e, in the sense that bright central stars are usually associated either with bright and small or with faint and very large nebulae. Furthermore, a study of the illustrations establishes the fact that, where multiple rings are present in a nebula, the order of brightness is usually inversely that of the radii or distances from the central star, and that, in the structureless disks, there is a tendency for the brightness to diminish outward from the central star. These facts, together with the conclusions derived from the discussion of diffuse nebulae, suggest a reduction of log A to log A_1 corresponding to a uniform relative exposure, on the assumption that the central stars are the sources of luminosity and that, for a homogeneous distribution of nebulosity, the inverse-square law is rigorously obeyed.

TABLE III

PLANETARY NEBULAE

Object	m	A	e	$\log A$	$\log e$	$\log A_1$
N.G.C. 40	10	17″	4	1.23	0.60	0.93
246	9.5	100	100	2.00	2.00	1.00
650, 1	16	40	20	1.60	1.30	0.95
I.C. 1747	14	6	15	0.78	1.18	0.19
351	14	4	2	0.60	0.30	0.45
N.G.C. 1501	12	24	25	1.38	1.40	0.68
1514	8.8	60	80	1.78	1.90	0.83
1535	10	10	2	1.00	0.30	0.85
J 320	12	3.5	0.8	0.54	−0.10	0.59
I.C. 418	9	7	0.2	0.85	−0.70	1.20
N.G.C. 1952	15.2	50	60	1.70	1.78	0.81
2022	13	11	5	1.04	0.70	0.69
I.C. 2149	12	3	0.3	0.48	−0.52	0.74
N.G.C. 2371, 2	12	17	15	1.23	1.18	0.64
2392	9	9	5	0.95	0.70	0.60
2438	16	30	50	1.48	1.70	0.63
2452	19	8	20	0.90	1.30	0.25
2610	15	18	60	1.26	1.78	0.37
3242	9	13	3	1.11	0.48	0.87
3587	12	100	100	2.00	2.00	1.00
4361	10	20	30	1.30	1.48	0.56
I.C. 3568	11	5	0.2	0.70	−0.70	1.05
N.G.C. 6058	12	10	30	1.00	1.48	0.26
I.C. 4593	10	5	2	0.70	0.30	0.55
N.G.C. 6210	11	4	0.3	0.60	−0.52	0.86
6309	13	5	4	0.70	0.60	0.40
6369	16	14	70	1.15	1.85	0.23
6439	18	2	8	0.30	0.90	−0.15
6445	19	18	20	1.26	1.30	0.61
6543	9.2	8	0.2	0.90	−0.70	1.25
6563	18	18	60	1.26	1.78	0.37
6572	9	3	0.1	0.48	−1.00	0.98
6567	14	3	0.6	0.48	−0.22	0.59
6578	15	4	8	0.60	0.90	0.15
6620	15	2.5	4	0.40	0.60	0.10
6629	13	7	10	0.85	1.00	0.35
6720	13	30	6	1.48	0.78	1.09
6751	12	10	20	1.00	1.30	0.35
6772	18	26	250	1.41	2.40	0.21
6778	14	9	15	0.95	1.18	0.36
6781	14	50	80	1.70	1.90	0.75
6803	13	2.7	0.3	0.43	−0.52	0.69
6804	12	20	25	1.30	1.40	0.60
6818	14	10	0.7	1.00	−0.15	1.07
6826	9	11	1	1.04	0.00	1.04
6853	12	90	20	1.95	1.30	1.30
6891	10	3.5	2	0.54	0.30	0.39
6894	16	22	70	1.34	1.85	0.42
6905	13	18	20	1.26	1.30	0.61

TABLE III—*Continued*

Object	m	A	e	log A	log e	log A_1
N.G.C. 7008	12	40	20	1.60	1.30	0.95
7009	11	12	0.2	1.08	−0.70	1.43
7026	14	3	0.8	0.48	−0.10	0.53
7139	18	35	300	1.54	2.48	0.30
7293	11	300	150	2.48	2.18	1.39
7354	16	8	15	0.90	1.18	0.31
7662	11.5	8	0.2	0.90	−0.70	1.25

These assumptions lead to a reduction formula analogous to equation (3). Let the uniform relative exposure be unity and let the exponent p also be taken as unity. Then

$$\log A_1 = \log A - \tfrac{1}{2} \log e \tag{14}$$

Log A_1 is listed in the seventh column of Table III.

Figure 4 shows the plot of m against log A_1 for the 56 planetaries in Table III. Some degree of correlation is obvious, but the coefficient is so small that a least-squares solution in the form used in the investigation of diffuse nebulae does not give satisfactory results. Accordingly the data were treated by the method of correlations. The two regression curves are

$$RC \text{ of } m \text{ on } \log A_1 \quad . \quad . \quad . \quad . \quad m + 4.63 \log A_1 = 16.03 \tag{15}$$

$$RC \text{ of } \log A_1 \text{ on } m \quad . \quad . \quad . \quad . \quad m + 13.35 \log A_1 = 21.84 \tag{16}$$

Coefficient of correlation 0.59

$$\sigma_m = 2.80 \qquad \sigma_{\log A_1} = 0.356$$

The correlation ratio of equation (15) is 0.61, and of (16), 0.64. Attention should be called to the fact that the regression curve of m on log A_1, determined by plotting the mean m for groups of log A_1, is not a straight line but a rather well-defined curve convex to the origin of co-ordinates and hyperbolic in form. The correlation ratio is computed from this curve. The reason for such a curve is to be found in the distribution of errors, especially the systematic errors in m and e, which will be discussed later. Equation (15) is the straight line which best fits the points of the regression curve. The regression curve of log A_1 on m is a straight line.

The best simple expression for the relation between m and log A_1 is probably the curve of symmetry, or the bisector of the acute angle between the lines represented by equations (15) and (16). This reduces the sum of the perpendicular distances from the points to the line to a minimum. The bisector is

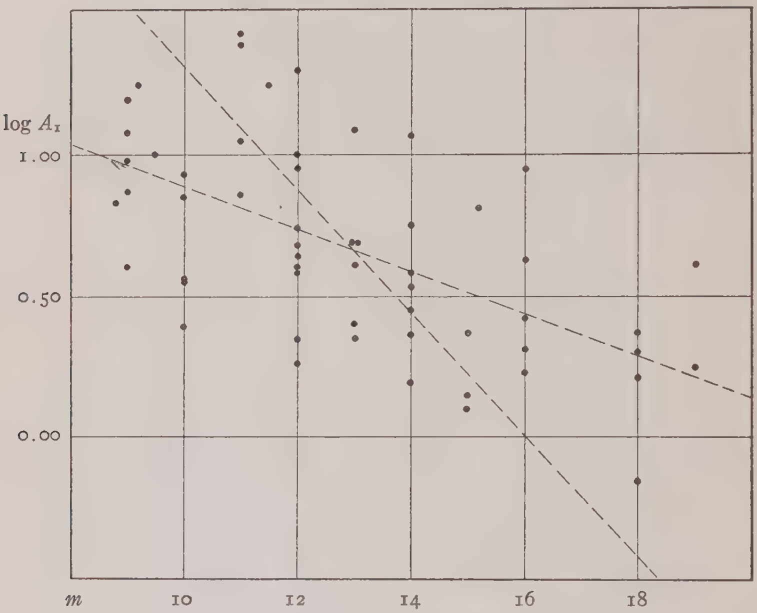

FIG. 4.—Plots of m, the photographic magnitude of central stars in planetary nebulae, against log A_1, where A_1 is the angular extent of nebulosity from the central stars reduced to a uniform exposure time. The data are taken from Table III. The broken lines are the regression curves.

$$m+(6.91\pm 0.6)\log A_1=17.55\pm 0.22 \tag{17}$$

The data are not of a high order of accuracy but the mean values should be significant. The distances A must be essentially free from serious systematic errors, although the accidental errors are probably large as compared to the values of A, especially in the many very small nebulae.

The relative exposure, *e*, seems to be fairly reliable for large and faint nebulae, but is probably too large for the small and bright objects as compared with larger-scale photographs made with the 60-inch and 100-inch reflectors. This may be due to the known dependency of minimum visibility on surface area, and to the difficulty on small-scale photographs of distinguishing the star image from bright nebulosity in its immediate neighborhood. Such errors would be especially serious in the case of stars involved in very small dense nebulae.

TABLE IV

Comparison of Mount Wilson Limiting Exposure Times with Curtis' Relative Exposures

Object	E	e	$R=\frac{E}{e}$
	a) Large and Faint Nebulae		
	sec.		
N.G.C. 246	600	100	6.00
1514	300	80	3.75
3587	600	100	6.00
6445	150	20	7.50
6853	120	20	6.00
6894	480	70	6.86
7293	900	150	6.00
Mean			6.02 ± 0.28
	b) Small and Bright Nebulae		
	sec.		
N.G.C. 3242	1	0.3	3.33
I.C. 3568	4	2.0	2.00
4593	6	2.0	3.00
N.G.C. 6210	1.5	0.3	5.00
6572	0.4	0.1	4.00
6720	10	6	1.67
7009	0.8	0.2	4.00
7662	0.8	0.2	4.00
Mean			3.38 ± 0.33

Minimum exposures in seconds of time required just to register the brightest details of nebulosity on Seed 30 plates at the primary focus of the 60-inch reflector have been derived by the writer for 15 planetaries. These are compared with Curtis' values of *e* in Table IV. The first column designates the nebulae, the second gives the minimum exposures E in seconds of time derived from the Mount Wilson plates, the third gives Curtis' values of e, and the fourth contains the ratios $R=E/e$ which represents the minimum exposure, expressed in seconds, made on Seed 30 plates with the 60-inch reflector, corresponding to Curtis' unit of relative exposure.

The values of e for N.G.C. 3242 and I.C. 3568 have been arbitrarily changed by shifting the decimal points one place to the left and to the right, respectively. Curtis' value of 3 for N.G.C. 3242 is unquestionably a misprint for 0.3, since he remarks that the inner ring shows in 10 seconds on a Seed 23 plate. His description of I.C. 3568 places its brightness about equal to that of I.C. 4593. The value $e=6$ for N.G.C. 6720, the ring nebula in Lyra, is surprisingly high. The nebula may be photographed in 10 seconds with the 60-inch, and a rather strong image registers in 15 seconds.

The unit of relative exposure corresponds to an exposure of 10 seconds on a Seed 27 plate with the Crossley reflector. A standard region in the Orion nebula near the trapezium shows well under these conditions.[1] When one considers the more favorable focal ratio of the 60-inch reflector, and the difference in intensities between that "just perceptible" and that "well shown," the ratio $E/e=6.0$ found for the large faint nebulae seems to be a reasonable value. The relative speed of the two instruments, allowing for the fact that the Crossley plates are made at the direct focus without the use of a Newtonian flat, is about 1.18 in favor of the 60-inch. The factor due to the different standards of intensities used in the two series is a matter of conjecture and can be variously estimated at from 1.25 to 1.50, in the sense that the smaller intensities, and hence shorter exposures, are employed by the writer. Using a mean value of 1.38 for this factor, and considering the difference in speed between Seed 27 and Seed 30 plates to be negligible, the computed ratio E/e should be about $10\div1.18\times1.38=6.14$. This agrees with the observed value, 6.0, for the large faint nebulae and indicates that the discrepancy between the ratios of the two lists in the preceding table is due to errors in the small bright objects.

The evidence seems rather definitely in favor of a systematic error in e for the very bright nebulae, but the data are not sufficient to determine the limitations of the error. A correction would decrease e for these objects and hence increase log A_1. Since the bright nebulae as a rule have bright central stars, the effect would be to raise the upper ends of the correlation curves compared to the lower ends, and to decrease the value of the coefficient of log A_1 in equation (17). It is probable that the systematic error in e is not serious for values of e greater than 2.0. The effect on equation (17) can be estimated by applying to each e a uniform correction equal to 2 or less and considering any errors in the larger e's as accidental. As there are only four objects with e greater than 2 and less than 5, beyond which the systematic error is almost certainly negligible, this course seems justifiable. The correction to be applied is computed from the mean of the values for the bright nebulae in Table IV, disregarding N.G.C. 6720, the discrepancy in which may be considered as an accidental error. Each e equal to 2 or less must then be divided by $6.2 \div 3.62 = 1.72$. Log e is accordingly decreased by 0.24, and log A_1 increased by 0.12. This correction is applied to eighteen objects. The mean log A_1 of Table III, 0.667, will be increased by $0.12 \times 18/56 = 0.039$. The corrected mean value will be 0.706. The mean m will remain the same, hence the corrected curve must pass through the point $m = 12.95$, log $A_1 = 0.706$. For the objects in which e has been corrected, the mean m is low, 11.3, and no m is greater than 14. Likewise the mean log A_1 is high, 0.86, and only two are less than 0.50. The result is that the intersection of the curve with the m-axis at $m = 17.55$ will be very little disturbed. The corrected curve will pass close to this point and through the point $m = 12.95$, log $A_1 = 0.706$. The equation of the corrected curve will therefore be approximately

---

[1] Curtis, *op. cit.*, p. 59.

$$m + 6.52 \log A = 17.55 \tag{18}$$

Curtis' magnitudes are estimates and therefore subject to rather large accidental errors. In addition, there is a pronounced systematic error for the brighter stars, in the sense that they are estimated too bright.

Van Maanen has given photographic magnitudes of the central stars of the planetaries which he has measured for parallax.[1] The method he employs is to count the numbers of stars equal to or brighter than the ones in question on his parallax plates and to extract the corresponding magnitude from van Rhijn's[1] tables of average stellar densities for given galactic latitudes. This procedure is subject to considerable accidental error in individual cases, especially of the brighter stars, for the field used is small enough to be seriously affected by local irregularities in stellar distribution. In the mean, however, they should be reliable within the limits of Curtis' accidental errors.

---

[1] *Mt. Wilson Contr.* No. 237, 1922.

The writer has derived provisional photographic magnitudes for several central stars, using the method of polar comparisons, with exposures timed to show a minimum of nebulosity. In general each of the values depends upon a single plate and they are not, therefore, very reliable. They should, however, be of the same order of accuracy as van Maanen's determination, and both series can be used to reduce Curtis' measures to the scale of the polar sequence. The data are given in Table V. Van Maanen's value of 8.0 for the central star in N.G.C. 1514 is omitted for the reason that the star is too bright for a good determination of the magnitude by the method of star counts.

The mean difference, van Maanen$-$Curtis, is 1.3, corresponding to a mean magnitude (Curtis) of 11.5. The mean, Hubble$-$Curtis, is 1.4 for a mean magnitude (Curtis) of 12.0. Between Curtis' magnitudes and the differences vM$-$C and H$-$C, called Δ, the combined data give a coefficient of correlation of 0.44, which has very little significance. The mean point of the material is at m (Curtis)$=11.7$, $\Delta=+1.35$. This probably represents a systematic error in Curtis' values amounting to -1.35 at his magnitude 11.7. It is improbable that the error should be uniform over the range of m covered by Table III. A more reasonable assumption is that the error vanishes near the limiting magnitude obtainable with the Crossley in an exposure of moderate length. This supposition is supported by the two faint central stars in Table V for which Δ is negligible. If this is the case, the correction to Curtis should be represented approximately by a straight line drawn through the mean point of the data of Table V, rejecting the two faint stars in N.G.C. 6445 and 6772, and cutting the axis of m at an arbitrarily chosen point, say m equals 19.5. The formula expressing Δ, the correction to be added to Curtis' m, is then

---

[1] *Groningen Publications*, No. 27, Table IV, 1917.

$$\Delta = -0.173\, m + 3.37 \tag{19}$$

The effect of this assumed correction would be in the nature of a rotation of the correlation curves of Figure 4 in a clockwise direction around the points where they cross the abscissa $m = 19.5$. Equation (18) corrected in this manner becomes

$$m + 5.40 \log A_1 = 17.88 \tag{20}$$

This curve is probably a fair representation of the data, disregarding the probable misprints in the decimal points for e in the cases of N.G.C. 3242 and I.C. 3568. Taking these into account

TABLE V

PHOTOGRAPHIC MAGNITUDES OF PLANETARY NUCLEI

Object	Curtis	van Maanen	Hubble	vM−C	H−C	H−vM
N.G.C. 40	10	11.6	....	1.6	....	....
1501	12	13.0	....	1.0	....	....
1514	8.8	....	9.7	....	0.9	....
2022	13	14.2	....	1.2	....	....
2371, 2	12	13.5	....	1.5	....	....
2392	9	10.0	....	1.0	....	....
3242	9	....	11.7	....	2.7	....
3587	12	....	14.3	....	2.3	....
I.C. 3568	11	....	12.0	....	1.0	....
4593	10	....	10.2	....	0.2	....
N.G.C. 4361	10	....	12.8	....	2.8	....
6210	11	11.7	....	0.7	....	....
6445	19	....	19	....	0.0	....
6543	9.2	11.3	....	2.1	....	....
6572	9	10.8	10.2	1.8	1.2	−0.6
6720	13	14.7	14.7	1.7	1.7	0.0
6772	18	....	18.1	....	0.1	....
6804	12	13.4	....	1.4	....	....
6853	12	....	13.6	....	1.6	....
6905	13	14.5	....	1.5	....	....
7008	12	12.8	....	0.8	....	....
7009	11	....	11.7	....	0.7	....
7026	14	15.1	....	1.1	....	....
7293	11	....	13.3	....	2.3	....
7662	11.5	12.9	12.5	1.4	1.0	−0.4
Mean	11.7	....	....	1.34	1.36	....

and correcting Curtis' values of m and e for the systematic errors suggested by the Mount Wilson observations, the recomputed correlation curves are:

RC of m on log A_1 .... $m+3.71 \log A_1=16.73$

RC of log A_1 on m .... $m+9.21 \log A_1=20.70$

Correlation curve .... $m+(5.33\pm0.4) \log A_1=17.88\pm0.18$ (21)

Coefficient of correlation 0.64

$$\sigma_m=2.28 \qquad \sigma_{\log A_1}=0.389$$

The plot corresponding to the corrected data is shown in Figure 5.

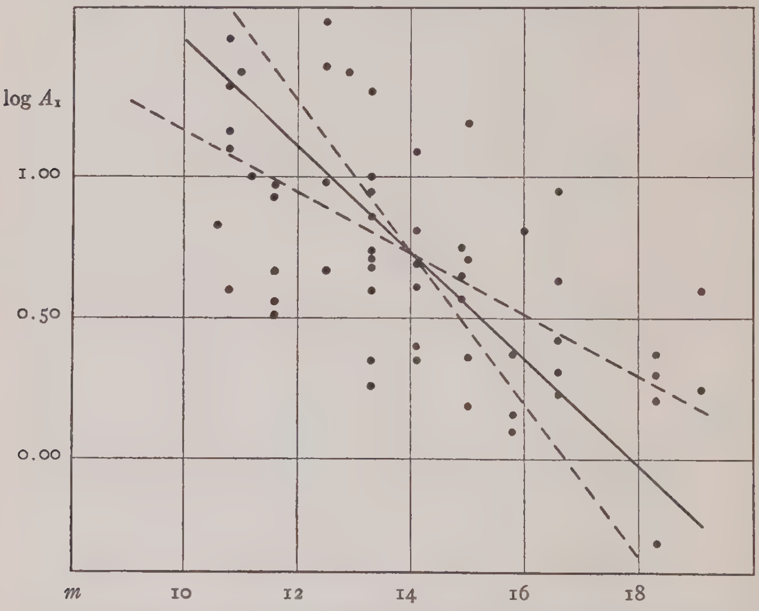

FIG. 5.—The same as Fig. 4, the data having been corrected for probable systematic errors. The full line represents the correlation curve for an equal weighting of the regression curves.

A curve passing through the mean m and log A_1 and having the slope to be expected on the assumption of an inverse-square law of luminosity can be represented by the equation

$$m+5 \log A_1=17.64\pm0.17 \qquad (22)$$

The two equations (21) and (22) agree within the limits of errors over the range covered by the data.

The general conclusion is in favor of the theory that the planetaries as well as the diffuse nebulae derive their luminosity from radiations of associated stars, and that the inverse-square law is at least one important factor in determining the distribution of luminosity throughout the nebulae. The complicated discontinuous nebular spectra of the planetaries, the great intensity in the ultra-violet of the continuous nuclear spectra, and the obvious concentration of luminous nebulosity in restricted zones, probably disturb the simple application of the inverse-square law sufficiently to account for the large residuals found in the present investigation.

There are some indications that the residuals computed from equations (21) and (22) may be related to the various types of planetaries. The four ring nebulae, N.G.C. 2438, 6720, 6894, and 7293, all show large positive residuals, averaging $+1.80$, while the globular objects I.C. 3568, 4593 and N.G.C. 6439, 6572, 6578, 6620, and 6629 all show large negative residuals, averaging -1.50. It is possible that when more precise data are available, a complete sequence can be established involving relations between residuals, on the one hand, and, on the other, spectral characteristics of nuclei and of nebulosity, color indices of nuclei, and structure of nebulosity.

It is worth mentioning at this point that when referred to B.D. +30°4199 as the central star, the loop in Cygnus discussed in the first part of this paper takes its place among the ring nebulae. The maximum distance A, measured to the following edge of N.G.C. 6992, which registers in an exposure of forty minutes, is $90'$. $m+5\log A_1=7.2+12.0=19.2$. The residual, $19.2-17.6=+1.6$, is of the order of that for the other ring nebulae.

Assuming the inverse-square law to hold rigorously with respect to the central stars as sources in the case of the planetaries, and assuming further that, within the range of wave-lengths to which the fast Seed plates are sensitive, the light emitted by the nebulosity is exactly that which it intercepts from the stars, a theoretical relation can be derived analogous to that in equation (9). Assumptions of random distribution in direction from stars to points of nebulosity measured for A are not necessary, for the symmetrical forms of the planetaries indicate that in general the directions of greatest extent of nebulosity from the central stars lie close to the plane perpendicular to the line of sight. The surface brightness of nebulosity on the above assumptions, expressed in magnitudes per square second of arc, is found by distributing the light of the star over a spherical shell with a radius equal to the distance to the point of nebulosity considered. Let this distance, A, be expressed in seconds of arc. Then

$$S.\,B. = m + 2.5 \log 4\pi A^2 = m + 5 \log A + 2.75 \tag{23}$$

The unit of relative exposure corresponds to an exposure of six seconds with the 60-inch reflector, or, if Seares's value for the limiting surface brightness just registered in an exposure of one minute is used, to a limiting surface brightness of $18.8 \pm 0.3 + 2.5 \log 0.1 = 16.3 \pm 0.3$. Substituting this value for $S.B.$ into equation (23),

$$m = 5 \log A = 13.55 \pm 0.30 \tag{24}$$

which expresses the relation between m and $\log A$, where A is measured from the star to the most distant nebulosity which just shows in an exposure of six seconds.

A comparison between this equation and the observational equations (21) and (22) shows a discrepancy in the constants amounting to from 4.1 to 4.3±0.6 magnitudes, in the sense that in general the observed nebulosity extends to a greater distance from stars of a given magnitude than the assumptions permit. Expressed in another way, the nebulosity at a given distance from the star is about 4.1 to 4.3±0.6 magnitudes per square second of arc brighter than can be accounted for on the assumption that, within the range of the fast Seed plates, the light emitted by the nebulosity is exactly the starlight intercepted. This may well account for the apparent absence of central stars or nuclei from some of the planetaries.

No adequate explanation of this discrepancy can be made without a knowledge of the mechanism by which the nebular illumination is excited, but a few suggestions may aid in formulating the problem. The source of illumination is rather definitely established as located in the central stars. The diffuse nebulae with emission spectra fail to show this discrepancy although it seems reasonable to suppose that the mechanism of illumination is much the same. The most striking difference between the nebular spectra of the planetaries and the emission spectra of diffuse nebulae is found in the much greater strength of the nebulium lines N_1 and N_2 in the planetaries. These lines are situated very close to the limits of sensitivity toward the red of the Seed 30 plates, and thus tend to destroy that equivalence of intensity distribution which the spectra of emission diffuse nebulae appear to share with the spectra of their associated stars, and by virtue of which they actually follow the same luminosity laws as do the diffuse nebulae with continuous spectra. The strengthening of the nebulium lines in the planetaries is accompanied by no corresponding strengthening of the continuous spectrum of the nuclei in this region. The maximum intensity of the continuous nuclear spectrum is shifted to the violet as compared with that of the stars associated with diffuse nebulae, and this in effect decreases the relative intensity in the region of the nebulium lines. If the nebular emission lines were considered as integrated from the continuous spectrum in their immediate vicinity, then the strong nebulium lines would represent a considerable part of the green region to which the Seed 30 plate is relatively insensitive. Such a supposition, if it were physically possible, could account for only a small part of the discrepancy, for these two lines seldom furnish more than a third of the nebular luminosity, as is shown by Wright's measures of relative intensities of nebular images made on spectrograms obtained with a slitless quartz spectrograph and a reflecting telescope, which are comparable with the direct photographs used in deriving the data of the present discussion.[1]

Another difference between planetaries and diffuse nebulae is found in the greater intensity of the ultra-violet continuous spectrum of the planetary nuclei as compared to that of the stars associated with diffuse nebulosity. The nuclear spectra are in general predominantly continuous. When corrected for atmospheric absorption, the energy curve of the continuous spectrum rises more and more steeply with decreasing wave-length up to the limits of reflectivity of silvered mirrors. Wright remarks, "Where the maximum is cannot be conjectured." It is certainly at a wave-length less than 3300 A. Thus the nebulosity receives a vast amount of energy in stellar radiations in a region of the spectrum which plays but a minor rôle in the determination of photographic magnitudes. It is entirely conceivable that the energy in these continuous radiations may be absorbed by the nebulosity and, by some mechanism analogous to that of fluorescence, be re-emitted as discontinuous radiations of longer wave-lengths. If this were the case, the m in equation (20) would be replaced by one of smaller numerical value representing a sort of ultra-violet magnitude, and the discrepancy in the constants would be materially reduced, if not entirely eliminated. Following this line of thought, the suggestion arises that the nebulium lines may possibly reveal themselves as fluorescent spectra of hydrogen or helium or a mixture of the two.

---

[1] *Lick Observatory Publications*, **13**, Part VI, 1918.

There exist in the solar system itself possible analogies to the mechanism by which emission luminosity may be excited in nebulosity by radiations emanating from a continuous source. Chief among these are the terrestrial aurorae, the solar corona, and the comets. In each of these cases, radiations of some sort emanating from the sun excite matter in a gaseous state to luminosity of a discontinuous nature. The prevailing opinion concerning the aurora is that the phenomenon is due to the ionization of atmospheric gases by high-speed charged particles.

H. N. Russell[1] has made suggestions of a similar nature to account for the spectrum of emission nebulae. Such a mechanism would account for the inverse-square law quite as well as a mechanism based on ethereal radiations, and would probably find no serious obstacle in the excessive luminosity of the planetaries. Furthermore, this explanation was also formulated from independent considerations, namely, the relations which Russell found to exist between relative sizes of monochromatic images of individual planetaries and ionization potentials of the radiations forming the images.

---

[1] *Observatory*, 44, 72, 1921. Russell states that the luminosity of gaseous nebulae is probably due to ionization of the gases by radiations from associated stars, and that the radiations may be either ethereal or corpuscular.

Relations of a similar nature are suspected in the monochromatic images of diffuse nebulae with emission spectra. In these cases, however, the quantitative agreement between nebular and stellar luminosity, both for purely emission nebulae and for those with mixed spectra, appears to favor the notion of ethereal radiations. This agreement may of course be due to the nature of the relations between intensities of corpuscular radiations and spectral types or temperatures of the stars.

MOUNT WILSON OBSERVATORY
August 1922

NOTE ADDED DECEMBER 21, 1922

The stars within the great loop of nebulosity around the belt and sword of Orion sum up to an integrated apparent photographic magnitude of about 0.0. The loop extends to about $5^\circ\!.7$ or $342'$ from the estimated center of gravity of the stars considered, and registers very nearly to this limit in exposures of about three hours. Therefore $m+5 \log a_1 = 11.5$, a value more representative than that derived from considering ζ Orionis alone.

New material on about 40 per cent of the objects in Curtis' list of planetary nebulae confirms the suggested systematic corrections for m and e as being of the right order of magnitude.

Contributions from the Mount Wilson Observatory, No. 251
Reprinted from the *Astrophysical Journal*, Vol. LVI, pp. 446–456, 1922

ORBITS OF THE SPECTROSCOPIC BINARIES LALANDE 13792 AND AOe 12584

By R. F. SANFORD

ABSTRACT

Orbits of the spectroscopic binaries Lalande 13792 and AOe 12584.—Both binaries are dwarfs, with absolute magnitudes of about +5. The elements of each, determined from more than twenty spectrograms, are respectively: P, 32.8092 and 5.4145 days; e, 0.080 and 0.000; K, 27.5 and 64.9 km/sec; γ, +19.7 and −97.4 km/sec. In the case of AOe 12584, the lines of the secondary show faintly and give for K, +74.0 km/sec, and for the functions $m \sin^3 i$ and $m_1 \sin^3 i$ the values 0.803 and $0.704\odot$. The large space velocity of AOe 12584, like that of Lalande 29330, is directed away from the quadrant which the apices of other stars of large space motion in general avoid.

Differences between dwarf and giant binaries.—The six spectroscopic binaries of the dwarf division whose orbits have been determined by the writer display smaller eccentricities for a given period group than do giant binaries, as has been shown by R. E. Wilson from data relating to both visual and spectroscopic binaries. Furthermore, they have a mean period much shorter than that of the majority of giants of the same spectral division.

The orbits of nine spectroscopic binaries determined by the writer at the Mount Wilson Observatory have appeared in two previous papers.[1] In the introduction to the first of these may be found explanations of the tables of observations, methods of obtaining and correcting the preliminary elements, and the formation of the velocity curves. In general these statements apply to the two spectroscopic binaries whose orbits are presented in the present contribution. All of the data in Table I are taken from the list of spectroscopic parallaxes of 1646[2] stars. The last column shows

TABLE I

Name	Mag.	α(1900)	δ(1900)	Spectral Class	Vis. Abs. Mag.	μ	π Sp.	No. Rev.
Lal. 13792 = H.D. 54371...	7.0	$7^h\ 3^m.5$	+25°54′	G5	4.8	0″.225	0″.036	26
AOe 12584 = H.D. 107760..	8.2	12 17.9	+73 48	G6	5.4	0.49	0.028	340

H.D. = Henry Draper Memorial Catalog.

---

[1] *Mt. Wilson Contr.*, Nos. 201, 221; *Astrophysical Journal*, **53**, 201, 1921; **55**, 30, 1922.

[2] *Mt. Wilson Contr.*, No. 199; *Astrophysical Journal*, **53**, 13, 1921.

the number of revolutions of each star in its orbit between the first and last observation of velocity recorded in the tables of observations.

LALANDE 13792 (B.D.+25°1594)

This star was placed on the spectroscopic observing list to increase the data for the curves used for the determination of absolute magnitudes, since the parallax, 0″031, derived at the Allegheny Observatory, together with the apparent magnitude, showed it to be a star of low absolute magnitude. The annual proper motion, 0″225, is in keeping with this conclusion. The parallax derived by the spectroscopic method is 0″036, in good agreement with the trigonometric value. The variability in radial velocity was strongly suspected from the measures of the third plate, and definitely confirmed by that of the fourth. Twenty-two spectrograms have been secured. (Table II.)

TABLE II

OBSERVATIONS OF LALANDE 13792

Plate No.	Date	G.M.T.	Phase	Velocity	O−C
				km/sec	km/sec
γ 8947	1920, Jan. 6	22^h02^m	13^d588	+ 1.4	−3.0
9070	Mar. 11	18 32	12.825	+ 5.2	+3.5
9600	Sept. 29	0 07	17.202	+19.2	−0.6
9715	Nov. 3	0 35	19.411	+32.6	+3.0
9733	Nov. 21	0 55	4.616	+ 1.8	+3.0
9836	Dec. 27	23 50	8.762	− 5.8	+1.5
9941	1921, Feb. 23	20 14	0.994	+13.4	−4.3
10007	Mar. 17	17 50	22.894	+33.3	−9.2
C 955	Mar. 20	17 10	25.866	+51.2	+3.8
γ 10102*	Apr. 19	16 23	23.025	+47.7	+4.9
10111*	Apr. 21	17 42	25.080	+37.7	−9.2
10681	Dec. 8	1 00	25.719	+53.6	+6.2
10754*	1922, Jan. 12	22 26	28.803	+47.4	+3.9
C 1527	Jan. 13	23 43	29.956	+39.5	−0.2
γ 10766	Jan. 15	17 13	31.586	+31.9	+0.9
10825	Feb. 14	18 32	28.831	+38.1	−5.3
C 1567	Feb. 15	19 00	29.851	+41.6	+1.9
γ 10846	Feb. 18	15 24	32.701	+26.0	+1.5
10861	Mar. 6	18 26	16.018	+12.0	−2.5
C 1596	Mar. 8	19 25	18.060	+27.6	+4.0
γ 10918	Mar. 17	17 35	26.982	+47.2	+0.1
11004	May 4	16 14	9.308	−10.6	−3.8

* Given weight ½ in least-squares solution.

The estimated spectrum is G5, with lines of satisfactory quality. There is no certain evidence of the spectrum of the secondary star. It was found possible to assemble all the velocities upon a satisfactory preliminary curve with 32.8092 days as the period. The twenty-six orbital revolutions which separate the first and last observations make an interval so long that only very small changes in the period could be made without seriously disturbing the velocity-curve. Hence this period has been considered final.

Preliminary elements derived by Russell's method and by the graphical method of Lehmann-Filhés were in substantial agreement, the latter giving

PRELIMINARY ELEMENTS

P	32.8092 days
e	0.052
ω	$99\overset{\circ}{.}7$
K	+28.3 km/sec
T	J.D. 2423073.7
γ	+21.2 km/sec

An ephemeris computed with these elements gave the residuals for the velocities. Three plates as indicated in Table II were assigned weight one-half on account of their poor quality. All others were given weight unity.

The final elements result from the correction of the preliminary values by two least-squares solutions, the second being undertaken because of rather large differences between the residuals derived from the elements as first corrected and those derived by substitution of the unknowns in the conditional equations. Although the

FINAL ELEMENTS AND PROBABLE ERRORS

P	32.8092 days
e	0.080 ± 0.039
ω	$82\overset{\circ}{.}1 \pm 26\overset{\circ}{.}1$
K	27.5 ± 1.0 km/sec
T	J.D. $2423071.941 \pm 2\overset{d}{.}334$
γ	+19.7 km/sec
$a \sin i$	12,383,000 km
$\frac{m_1^3 \sin^3 i}{(m+m_1)^2}$	0.0705 ⊙

quantity Σpv^2 for the final elements, which is seventy-two per cent of its value for the preliminary elements, scarcely differs from that for the elements as first corrected, the ephemeris and conditional equations give residuals that are in satisfactory agreement; moreover, the probable errors for ω and T have been materially reduced, although those for K and e remain as before. The probable error for a velocity of unit weight is ±3.0 km/sec.

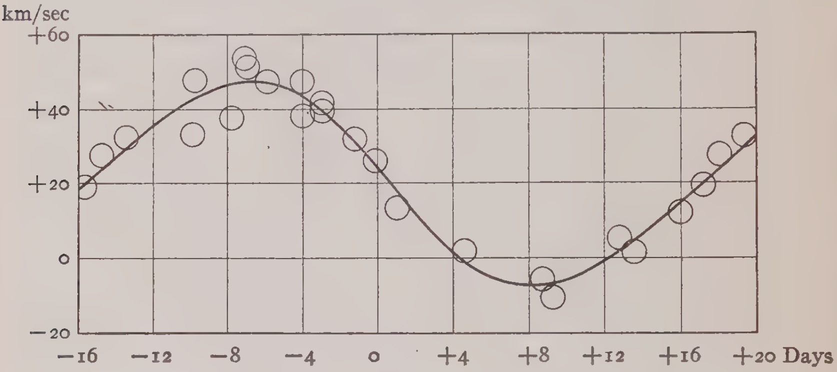

FIG. 1.—Velocity-curve of Lalande 13792

In the radial-velocity diagram (Fig. 1) the velocity of the system has not been represented in the usual way, since its value, +19.7 km/sec, is so nearly that of the line whose ordinate is +20 km/sec that, with the scale used, no distinction could be made between the two.

AOe 12584 (B.D.+74°493)

This star was placed on the Mount Wilson observing list for the determination of absolute magnitudes by the spectroscopic method because of its large annual proper motion (0″.49) and its apparent magnitude (8.2), which suggested low luminosity. The observations gave an absolute magnitude of +5.4, spectral class G6, and the second spectrogram revealed the variation in its radial velocity. Twenty-four plates (Table III) have been secured with the 60-inch reflector, using a one-prism spectrograph provided with a camera of 18-inches focus, except that for the second, third, and fourth plates a camera of 7-inches focus was used. These have been assigned half weight. The northerly declination of this object puts it beyond the reach of the Hooker telescope, the use of which would have been advantageous, for with the 60-inch reflector, even under fair conditions, it has been necessary to use exposures of about three hours. Under poor conditions, which are likely to occur at the season when the star is best placed for observation, longer exposures have been necessary and some plates are rather underexposed. Weights have been assigned accordingly. The spectrum shows a satisfactory set of lines for measurement when the velocity is near that of center of mass. But the secondary spectrum is bright enough to render the spectral lines of the primary less distinct by the superposition of the continuous spectrum when the radial velocities of the two components differ. Measures of the radial velocity of the secondary have been made on several plates, as Table III shows, but are not considered suitable to the

TABLE III

OBSERVATIONS OF AOE 12584

PLATE NO.	DATE	G.M.T.	PHASE	VELOCITY		O−C PRIM.	WT. PRIM.
				Prim.	Second		
				km/sec	km/sec	km/sec	
γ 5704	1917, Apr. 4	$20^{h}20^{m}$	$2\overset{d}{.}042$	−152.9	....	− 9.0	0.5
6929*	1918, May 24	17 25	1.001	− 70.3	....	+ 1.2	0.5
8170*	1919, May 13	19 25	3.139	−170.6	....	−16.2	0.5
8292*	June 13	17 23	1.567	−106.1	....	+ 7.2	0.5
9056	1920, Mar 8	20 30	5.385	− 33.1	−163.2	− 0.5	1.0
10000	1921, Mar. 16	21 02	4.803	− 44.1	−149.1	+ 4.0	1.0
10008	Mar. 17	20 23	0.362	− 37.7	−168.0	+ 0.4	1.0
10100	Apr. 18	19 49	5.267	− 38.6	−156.6	− 5.2	0.5
10113	Apr. 21	21 00	2.901	−151.8	− 28.0	+ 8.9	1.0
10125	Apr. 25	20 18	1.457	−102.1	....	+ 3.1	1.0
10148	May 14	18 45	4.148	− 96.4	....	− 5.6	1.0
10152	May 15	19 22	5.174	− 37.2	−167.8	− 2.3	1.0
10200	June 14	18 10	2.637	−169.4	....	− 7.3	0.5
10202	June 15	18 00	3.630	−123.8	− 33.6	+ 4.7	0.5
10206	June 16	17 58	4.629	− 59.1	....	− 1.5	0.5
10210	June 18	17 39	1.200	− 87.6	....	− 1.7	1.0
10220	June 20	17 36	3.199	−158.5	− 31.0	− 6.4	1.0
10251	July 11	17 23	2.532	−158.0	− 33.6	+ 2.9	1.0
10255	July 12	17 10	3.523	−119.3	....	+16.1	1.0
10262	July 13	17 07	4.521	− 59.1	−135.4	+ 5.2	1.0
10277	July 16	17 06	2.105	−148.8	− 27.7	− 1.7	1.0
10862	1922, Mar. 6	21 45	2.474	−158.6	− 27.2	+ 1.3	0.5
10963	Apr. 7	19 26	1.891	−137.4	....	− 2.1	0.5
11000	Apr. 18	18 29	2.021	−143.7	− 20.2	− 0.8	1.0

* Taken with 7-inch camera.

determination of any element except the amplitude and the relative masses of the two components, to be referred to later.

A set of preliminary elements, derived after twenty spectrograms had been secured, has already been published.[1] One branch of the velocity-curve was later strengthened by four additional plates, after which a second set of elements was derived.

PRELIMINARY ELEMENTS

	(1)	(2)
P	$5^d.414$	$5^d.41454$
e	0.000	0.025
ω		204°
K	64 km/sec	67 km/sec
K_1	70 km/sec	
T	J.D. 2422798.875	2422856.162
γ	−97.5 km/sec	−97.8 km/sec

The differences are slight, when it is considered that for circular elements the epoch is arbitrary and that K_1 has been left for determination in a more accurate way.

The second set indicated a slight eccentricity, the reality of which it seemed more satisfactory to leave to the outcome of a least-squares solution. Since 340 revolutions separate the first and last observations, the period has been taken as definitive. If K_1 is derived independently, and ω_1 for the secondary is taken as $\omega+180°$, there remain only five elements to be corrected by the method of least-squares.

As often happens when the eccentricity is small, two of the resulting normal equations were practically identical. Hence only four, instead of five unknowns, could be determined satisfactorily. In this case, instead of corrections to ω and T, a correction to u, the argument of latitude, results. As a matter of fact, three sets of corrections have been derived, (*a*) one which corrects all five elements, (*b*) another set which corrects three elements and the argument of latitude, u, and (*c*), a set like the second, except that it is based upon the twenty-two spectrograms that remain after the rejection of two (γ 8170 and γ 10255) with large residuals. The value of Σpv^2 for the elements thus corrected becomes less and less, both for all the observations and for the twenty-two considered in the last set. In other words, the rejection of the two observations showing large residuals leads to corrections which do not materially affect the size of these residuals and does improve the representation of the remaining observations.

---

[1] *Publications American Astronomical Society*, 4, 283, 1921.

A comparison of the residuals derived from an ephemeris based upon set (*c*) with those derived from substitution into the conditional equations showed that the elements might be further improved. Since these corrections had reduced the eccentricity to 0.005, this element was assumed to be zero and another least-squares solution for corrections to γ, K, and T was made, T now being referred to the time of the smallest negative velocity of the primary. After these corrections had been applied, ephemeris and conditional equations gave practically identical values for the residuals. Hence these elements are considered definitive.

K_1 has been determined from the relation $K_1 = K\left(\frac{V_1-\gamma}{V-\gamma}\right)$ in which V is the computed velocity for the primary, V_1 is the observed velocity of the secondary, and γ and K are elements of the primary. The weights assigned depend on the number of lines measured in determining V_1.

Final Elements and Probable Errors

P	$5^{\mathrm{d}}.41454$
K	64.9 ± 1.3 km/sec
K_1	74.0 km/sec
T	J.D. $2422853.120 \pm 0^{\mathrm{d}}.020$
γ	-97.4 km/sec
$a \sin i$	4,833,000 km
$a_1 \sin i$	5,510,000 km
$m \sin^3 i$	0.803 ⊙
$m_1 \sin^3 i$	0.704 ⊙

Reference to set (1) of the preliminary elements will show how closely they agree with the final elements, and that the choice of set (2) was not a happy one, although for this case the eccentricity was not arbitrarily assumed to be zero.

If all twenty-four plates are considered, the probable error of a single determination of radial velocity of unit weight is ±4.0 km/sec, and ±2.9 km/sec if based upon the twenty-two plates finally used. The probable errors for the elements are based on the larger of these two values, which is also used as radius for the circles representing the individual velocities in the diagram in Figure 2. The barred circles refer to velocities derived from the three spectrograms taken with low dispersion to which reference has already been made. The larger circles represent the velocities for the secondary star as far as they were measured. Their evident inaccuracy did not seem to warrant the inclusion of a velocity-curve for them.

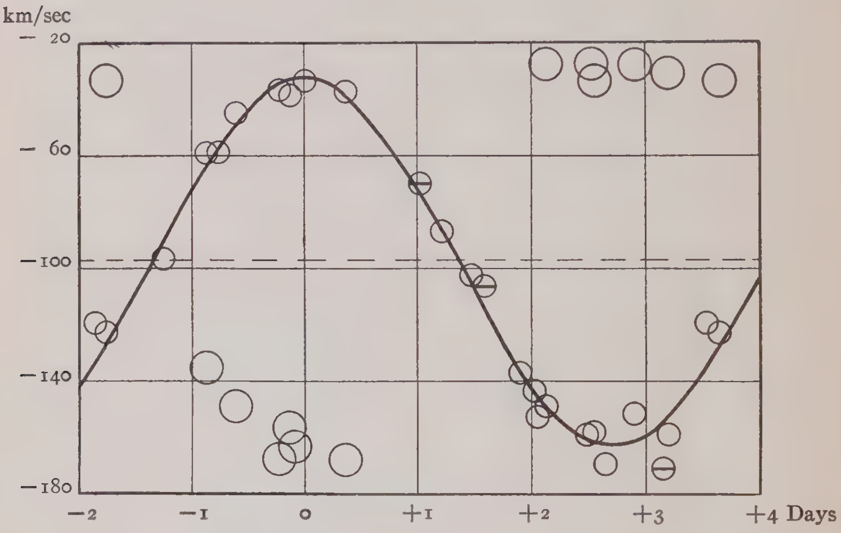

Fig. 2.—Velocity-curve of AOe 12584

Including the two binaries discussed in this paper, six of a total of eleven whose orbits have been derived by the writer at Mount Wilson have absolute magnitudes that place them in the dwarf division. Since binary stars of low luminosity are relatively few in number, it is of interest to collect certain elements for these six stars, as has been done in Table IV.

Attention has already been called to the fact that the dwarf binary Lalande 29330[1] has a period and an eccentricity both of which are small for a star of its spectral class when compared with mean values based upon hitherto existing material, relating, for the most part, to giant stars. Forming mean values of spectral class, period, eccentricity and absolute magnitude for the six binaries, we find the data of the first line of Table V. This is followed by the similar data for class G stars taken from a table by Aitken.[2]

TABLE IV

Name	App. Mag.	Sp. Class	Abs. Mag.	P	e	K	γ	$a \sin i$	$\frac{m_1^3 \sin^3 i}{(m+m_1)^2}$
						km/sec	km/sec	km	⊙
OΣ 82.....	7.0	F9	4.1	$4\overset{d}{.}0000$	0.060	36.1	+37.4	1.98×10^6	0.0193
Lal. 29330..	8.5	K0	6.0	4.2850	0.089	38.1	−60.6	2.24×10^6	0.0244
Lal. 49867..	7.3	K2	6.0	6.7217	0.059	38.5	−19.8	3.55×10^6	0.0396*
AOe 12584..	8.2	G6	5.4	5.4145	0.000	64.9	−97.4	4.83×10^6	....
75 Cancri...	6.0	G2	4.1	19.4589	0.206	20.2	+12.3	5.26×10^6	0.0157
Lal. 13792..	7.0	G5	4.8	32.8092	0.080	27.5	+19.7	12.38×10^6	0.0705

* Given erroneously as 0.0125 ⊙ in *Mt. Wilson Contr.*, No. 201.

TABLE V

Spectral Class	Period	Eccentricity	Abs. Mag.
G4..............	12 days	0.082	+5.1
G...............	267 days	0.129	Mostly giants

When it is considered that the first line shows mean values for stars whose spectral classes range from F9 to K2, and that in the table from which the second line is taken the value of e is larger for the spectral divisions which precede and follow G, it appears that in Table V we again have evidence that dwarf binaries have shorter periods and smaller eccentricities than do giant stars of approximately the same spectral class.

Dr. R. E. Wilson has also discussed the period-eccentricity relation[3] for binary stars, and as far as his data go, finds that for the same average period dwarf stars have an average eccentricity smaller than that of the giants. In order to display this feature, the material in Table I of his paper corresponding to that in Table IV above is reproduced in Table VI. The first column gives his number of the period group, the range in each of which is given in the second column. Then follow pairs of columns which show the mean eccentricity and the number of stars for giants and for dwarfs, and, finally a pair which give the same data derived from the six binaries in Table IV.

---

[1] *Mt. Wilson Contr.*, No. 201; *Astrophysical Journal*, **53**, 212, 1921.

[2] *The Binary Stars*, p. 199, 1918.

[3] *Astronomical Journal*, **33**, 147, 1921.

TABLE VI

Group	Period	Giants		Dwarfs		Dwarfs (Sanford)	
		e	No.	*e*	No.	*e*	No.
2........	4– 8 days	0.114	19	0.020	3	0.052	4
3........	8– 25 days	0.250	22	0.132	4	0.206	1
4........	25–100 days	0.468	15	0.010	1	0.080	1

It is readily seen that the eccentricities for the first column of dwarfs are systematically smaller than those for giants, which is borne out rather well by the spectroscopic binaries whose eccentricities are displayed in the next to the last column.

Both Aitken[1] and Wilson[2] have called attention to an apparently abrupt change in the mean eccentricity for the stars with periods between 25–100 days.

Although the data for such a conclusion are meager indeed, the same phenomenon is shown in the last column of eccentricities, but it is by no means certain from either the fifth or seventh columns that there is a minimum in the eccentricity-period relation for group 4 or a maximum for group 3. Two more dwarf binaries for which I have nearly enough material for orbits will add one star each to groups 2 and 3 and will have eccentricities consistent with the values given in this seventh column. Orbital elements of dwarf spectroscopic binaries falling in groups 3 and 4 are therefore especially to be desired in order to settle (*a*) the reality of this departure from a smooth curve in the period-eccentricity relation, and (*b*) whether the departure means a maximum for group 3 or a minimum for group 4.

---

[1] *The Binary Stars*, p. 197, 1921.

[2] *Astronomical Journal*, 33, 147, 1921.

It is of interest to note that two of the binaries of Table IV, Lalande 29330 and AOe 12584, have large velocities of the center of mass (γ). Their space motions place them in that group of stars of large space-velocity whose motions have been discussed by Adams and Joy[1] and later more completely by Strömberg,[2] and whose apices are directly away from the quadrant of avoidance shown to exist by these investigators.

Mount Wilson Observatory
September 1922

---

[1] *Mt. Wilson Contr.*, No. 163; *Astrophysical Journal*, **49**, 179, 1919.

[2] *Proceedings of the National Academy of Sciences*, **8**, 141, 1922.

Contributions from the Mount Wilson Observatory, No. 252
Reprinted from the *Astrophysical Journal*, Vol. LVI, pp. 457–474, 1922

STELLAR SPECTRA OF CLASS S

I. GENERAL DESCRIPTION

By PAUL W. MERRILL

ABSTRACT

Class S stars.—A number of red stars have spectra similar to that of R Geminorum, which differs from the recognized types of the Harvard classification. It is proposed to group them into an additional class with the symbol S. *A provisional list* of 22 S stars is given, including the following *long-period variables: X and R Androm., R and T Camelop., V Cancri, R Can. Min., U and S Cassiop., R Cygni, R and T Gemin., RW Librae, R Lyncis, R Orionis, T Sagittarii, and S Urs. Maj. Characteristic spectral features* are shown by typical spectrograms and by a table of forty-three lines from λ 4500 to λ 4860, particularly a complicated structure between λ 4630 and λ 4660. The absorption lines λ 4554 (Ba) and λ 4607 (Sr) are unusually strong, and there is an absorption band in the red extending from λ 6470 to longer wave-lengths. A remarkable feature is the presence of enhanced lines of iron, λλ 4584, 4924, and 5018, as emission lines. As in the case of class M stars, the variables alone show strong bright hydrogen lines (type Se); Hβ is more intense than Hγ, and the lines are narrow. A list of the plates obtained at Mount Wilson, including the dates, phases, and notes as to the individual spectra, is given. *The relationship to other classes* is discussed. While the S stars appear to be more closely related to giant Ma stars than to any other type, they probably do not belong in either the G-R-N or the G-K-M branch, but form a third branch. The recognition of these stars as a distinct group should aid in the general study of long-period variables.

In Secchi's classification of stellar spectra, made nearly sixty years ago, there are two great groups of orange and red stars, namely, types III and IV. Both types are marked by characteristic absorption bands which face in opposite directions in the two types. Those of type III are now known to be due to titanium oxide, and those of type IV to carbon. In the more detailed system of classification developed at the Harvard College Observatory, these groups, called classes M and N respectively, have been subdivided, but stars with intermediate spectra have not been found. No object is known to show both carbon and titanium bands; these spectral features seem to be mutually exclusive. Accordingly there is no place for the carbon stars in the spectral progression which runs without a break through the sequence of classes B, A, F, G, K, and M, since the latter end of this chain is characterized by increasing strength of the titanium bands. The alternative arrangement for class N is a side branch paralleling the main sequence in the K-M region. The discovery of the class R stars, which in color and spectroscopic details are intermediate between classes G and N, strongly supports this view.[1]

Among the long-period variables there are a number which are not clearly of either class M or class N, and which have been variously classified by the Harvard observers. The following statement in regard to these stars is found in the introduction to the *Henry Draper Catalogue:*

> Several spectra which have hitherto been called Md1 or Md2, in which Hβ is the strongest bright line, are found to be peculiar and are designated Pec. in Table I. The variable stars R Andromedae, U Cassiopeiae, S Cassiopeiae, R Lyncis, R Canis Minoris, T Geminorum, and R Cygni may be given as examples. These spectra do not show the titanium bands having bright edges at 4762, 4954, and 5168 as in all divisions of Class M, but more nearly resemble the spectrum of π^1 Gruis, which may be placed in a subdivision of Class R, assuming some peculiarities.

Few observations of any of these stars have been made with slit spectrographs until recently. Spectrograms of R Cygni were secured by Wright[2] in December, 1911. They showed a complicated spectrum most of whose details could not be identified. Several stars of this type were included in the radial velocity observations of long-period variables[3] made by the writer at Ann Arbor from 1913 to 1915, but in only one case was the exposure sufficient to show the absorption spectrum; R Lyncis, photographed in February, 1915, was found to have a spectrum resembling that of R Cygni as observed by Wright.

Since resuming the investigation of long-period variables at Mount Wilson, I have photographed a number of objects which have spectra of the same type as R Cygni and R Lyncis. They have been recognized as forming a special group distinct from either class M, N, or R. The designation class "S" has been suggested for them by the action of the International Astronomical Union at the Rome meeting in May, 1922.

---

[1] The relationships between classes G, R, and N have been thoroughly discussed by Rufus, *Publications of the Observatory, University of Michigan*, **2**, 103, 1916.

[2] *Monthly Notices*, **72**, 548, 1912. The preceding article gives an account of visual observations by Espin.

[3] *Publications of the Observatory, University of Michigan*, **2**, 45, 1916.

It is the purpose of this article to furnish a description of spectra of class S together with some remarks on the relationship to other classes. The general conclusion may be anticipated here by stating that the S stars probably form a third branch of the spectral sequence in addition to the G-K-M and the G-R-N branches. (See page 17.)

In Table I is given a first list of stars of class S. The observations upon which the inclusion of each star depends may be inferred from Table II, which gives a record of the Mount Wilson spectrograms, and from the Harvard notes and the brief discussions of each star which follow. It is highly probable that future observations will disclose additional stars of class S, especially among the long-period variables. It is less likely, though not impossible, that one or two stars of Table I will be shown by improved observations to belong to some other spectral class.

TABLE I

PROVISIONAL LIST OF STARS OF CLASS S

Name	H.D.	R.A. 1900	Dec. 1900	Mag.	Spect.	Period
						days
X Androm.	1167	$0^{h}10^{m}.9$	+46° 27′	8.1–14.2	Se	346.5
R Androm.	1967	0 18.8	+38 1	5.6–14.0	Se	410.7
U Cassiop.	4350	0 40.8	+47 43	8.0–16.	Se	276.0
S Cassiop.	7769	1 12.3	+72 5	7.6–14.5	Se	609.5
T Camelop.	29147	4 30.3	+65 57	7.0–13.5	Se	370
R Orionis	31798	4 53.6	+ 7 59	8.7–13.5	Se?	378.5
	35155	5 17.6	− 8 45	7.0	S	....
R Lyncis	51610	6 53.0	+55 27	7.0–13.8	Se	379.2
R Gemin.	53791	7 1.3	+22 52	6.4–13.8	Se	370
R Can. Min.	54300	7 3.2	+10 11	7.2–10.0	Se	337.7
	58881	7 22.4	−11 31	9.0	S	....
T Gemin.	63334	7 43.3	+23 59	8.0–13.5	Se	288.1
	63733	7 45.3	−18 45	8.5	S	....
V Cancri	70276	8 16.0	+17 36	7.5–13.0	Se	272.1
S Urs. Maj.	110813	12 39.6	+61 38	7.3–12.5	Se	226.5
	121447	13 50.3	−17 45	8.1	S	....
R Camelop	127226	14 25.1	+84 17	7.9–13.7	Se	269.5
RW Librae	136734	15 17.2	−23 42	8.6–11.7	Se	490 (about)
	172804	18 37.1	+ 6 43	9.1	S	....
T Sagittarii	....	19 10.5	−17 9	7.2–12.0	Se	381.3
R Cygni	....	19 34.1	+49 58	6.6–13.9	Se	426
π^1 Gruis	....	22 16.6	−46 27	6.6	S	....

Table II contains a record of most of the Mount Wilson spectrograms of stars of class S. They were secured with one-prism slit

TABLE II

Journal of Observations

Star	Plate	Date	Mag.	Phase	Intensities			Remarks
				days	Hβ	Hγ	Hδ	
X Androm.	C 1454	1921, Nov. 13	9.5	−16	12	2	.....	
	C 1462	Nov. 14	9.5	−15	4	0.5	.....	
R Androm.	γ 8725	1919, Oct. 3	7.5	−25	5	2	1	
	C 130	Oct. 15	7.5	−13	4	2	2	
	C 137	Oct. 16	7.5	−12	6	3	3	
	C 1499	1921, Dec. 15	7.5	−16	12	5	5	
U Cassiop.	C 1449	1921, Nov. 12	8.2	− 4	8	4	4	
	C 1455	Nov. 13	8.2	− 3	9	4	3	
S Cassiop.	γ 10755	1922, Jan. 13	8.9	+22	7	2	.....	
T Camelop.	γ 11245	1922, Aug. 9	8.8	−36	5	2	.....	Obs. by Hoge
H.D. 35155	C 672	1920, Sept. 26	7.0	.....	.....	.....	.....	
R Gemin.	γ 8727	1919, Oct. 3	7.4	−27	8	3	0.5	
	C 127	Oct. 14	7.0	−16	10	5	2	
	C 133	Oct. 15	7.0	−15	12	6	2	
	C 144	Oct. 17	7.0	−13	12	6	2	
	C 681	1920, Sept. 28	7.2	−30	8	3	.....	
	C 821	Dec. 27	8.3	+60	10	4	0.5	
	C 1339	1921, Sept. 21	8.1	−50	4	0.5	.....	
	γ 10524	Oct. 10	7.2	−31	12	5	1	
	C 1402	Oct. 13	7.1	−28	.....	.....	.....	Red region
	C 1408	Oct. 14	7.1	−27	.....	.....	.....	Red region
	C 1456	Nov. 13	7.2	+ 3	15	7	2	
	C 1501	Dec. 15	7.3	+35	12	7	2	
	C 1502	Dec. 15	7.3	+35	.....	.....	.....	Green region
R Can. Min.	C 294	1920, Mar. 3	8.0	−10	15	5	0.5	
	C 299	Mar. 4	8.0	− 9	15	5	0.5	
	γ 9047	Mar. 7	8.0	− 6	8	3	.....	
	C 909	1921, Feb. 25	8.3	+20	15	7	2	
	γ 9990	Feb. 28	8.3	+23	.....	.....	.....	Red region
	C 1522	1922, Jan. 12	8.5	−33	6	3	.....	
T Gemin.	C 968	1921, Mar. 28	9.1	−23	2	0.5	0.5	
	C 1009	Apr. 29	8.6	+ 9	10	5	3	
H.D. 63733	C 1464	1921, Nov. 14	8.5	.....	.....	.....	.....	
V Cancri	C 194	1919, Nov. 9	8.0	+10	15	7	2	
	γ 8875	Nov. 13	8.0	+14	7	3	1	
	γ 8883	Nov. 14	8.0	+15	6	3	0.7	
	γ 10132	1921, Apr. 27	7.9	− 3	10	5	0.7	
	γ 10757	1922, Jan. 13	7.9	−12	9	5	0.7	
	C 1552	Feb. 11	7.8	+17	15	8	3	
S Urs. Maj.	C 369	1920, Apr. 8	8.5	−31	7	3	.....	
	C 373	Apr. 10	8.5	−29	11	5	.....	
	γ 9252	June 3	8.2	+25	6	3	.....	
	γ 9848	Dec. 29	8.4	+25	6	4	1	
	C 866	1921, Jan. 28	8.8	−52	4	2	.....	
	C 1553	1922, Feb. 11	8.5	−28	7	3	.....	
	C 1626	Mar. 19	7.6	+ 8	9	6	1	
H.D. 121447	C 1706	1922, May 16	8.1	.....	.....	.....	.....	
R Camelop.	γ 8266	1919, June 9	8.2	+ 7	4	2	.....	
	γ 8272	June 10	8.2	+ 8	2−	1	.....	
	γ 8345	July 8	8.9	+36	2	1	.....	
	γ 11077	1922, May 17	8.2	−18	4	2	0.4	
H.D. 172804	C 472	1920, June 6	9.1	.....	.....	.....	.....	Obs. by Sanford

TABLE II—*Continued*

Star	Plate	Date	Mag.	Phase	Intensities			Remarks
				days	Hβ	Hγ	Hδ	
T Sagittarii	C 1059	1921, June 20	8.5±	+39	7	3	1	
		1922, July 13	9.1	+65	6	2	.....	
R Cygni	C 965	1921, Mar. 27	7.3	+31	15	6	2	
	C 966	Mar. 27	7.3	+31	.....	.....	.....	Red region
	C 1007	Apr. 28	8.9	+63	15	5	2	
	C 1038	May 26	9.2	+91	15	5	2	
	γ 11079	1922, May 17	6.8	+ 4	10	4	1	
	γ 11117	June 14	8.0	+32	15	5	2	
	C 1784	July 11	8.9	+59	15	6	2	

spectrographs with 18-inch camera-lens foci, and are of the usual photographic region unless otherwise noted in the remarks. The γ plates were secured with the 60-inch reflector; the C plates with the 100-inch Hooker reflector. The column headed "Phase" gives the number of days before (−), or after (+), the nearest maximum. The intensities of the bright hydrogen lines are estimates of the strength of the lines on the negatives, no allowance having been made for instrumental or other observational effects. Hβ is usually overexposed and the estimates of this line are doubtless only rough approximations.

X ANDROMEDAE, H.D. 1167

Remark in *H.D.:*

> On a photograph taken November 8, 1904, the spectrum was estimated Mb, having Hγ and Hδ bright, and equal in intensity.

The Mount Wilson plate taken on November 13, 1921, shows a spectrum similar to that of R Andromedae (C 137), but resembling still more closely R Geminorum (C 133) and S Ursae Majoris (C 373). The M bands are not recognizable and must be very weak, if present at all. Of the bright hydrogen lines, Hδ is not seen, Hγ is a fairly strong narrow line, and Hβ is overexposed. The intensities of Hβ and Hγ are perhaps as six or eight to one. This estimate is best made from the plate taken on the following night, which has much less exposure, and on which the strong bright Hβ line is the only outstanding feature; Hγ is clearly seen but is very weak.

It is evident that at the 1921 maximum the spectrum differed very greatly from that at the date of the Harvard observations which was less than a month after the 1904 maximum. Changes of this character are of the highest interest as bearing on the relationships between classes M and S. It is hoped to discuss them in a subsequent contribution, after more observational data have been secured.

R ANDROMEDAE, H.D. 1967

Remark in *H.D.:*

> The spectrum is very peculiar, and does not appear to be of any division of Class M. In the continuous portion between Hβ and Hγ it resembles the spectrum of π^{1} Gruis, R.A. $22^{h}16^{m}.6$, Dec. $-46^{\circ}27'$, and should probably be placed in some division of Class R. The continuous portion of the spectrum is very faint in the region having shorter wave-length than Hγ. The hydrogen lines Hβ, Hγ, Hδ, and Hζ are bright. Hβ is about 0.3 as bright as Hγ and Hδ which are nearly equal.

If we applied to S-type stars the criteria of absolute magnitude developed by Adams and Joy for K and M stars, R Andromedae would appear to be of high luminosity (perhaps comparable with K and M giants), since λ 4215 is strong and λ 4455 weak. The bright hydrogen lines are very conspicuous. The Harvard and the Mount Wilson observations agree in making bright Hζ stronger than Hϵ. This circumstance is discussed on page 15. Several narrow maxima are present in the continuous spectrum, some of which, at least, are doubtless true emission lines. Among these are the enhanced iron lines $\lambda\lambda$ 4584, 4924, 5018. (See page 16.)

U CASSIOPEIAE, H.D. 4350

Remark in *H.D.:*

> The spectrum resembles that of R Andromedae, H.D. 1967, and does not appear to be of Class M. Hγ and Hδ are bright. On a photograph taken July 10, 1894, these two lines are of equal brightness, but on photographs of October 8, 1896, and December 1, 1905, Hδ is from 3 to 6 times as bright as Hγ.

The spectrum shows considerable difference from that of R Andromedae (C 137) and more nearly resembles that of R Geminorum (C 133). There is a definite indication of the titanium band at λ 4954, and possibly a trace of the one at λ 4761.

S CASSIOPEIAE, H.D. 7769

Remark in *H.D.:*

The spectrum is peculiar, and does not appear to be of Class M, but to resemble in characteristics that of R Andromedae, H.D. 1967. On several photographs examined the brightness of Hβ varies from 2 to 10 times that of Hγ.

On the Mount Wilson spectrogram, γ 10755, bright Hβ is several times as strong as Hγ. The continuous spectrum is very weak but traces of the principal S features are seen.

T CAMELOPARDALIS, H.D. 29147

Remark in *H.D.:*

The spectrum resembles Class R, in having the strong absorption band 4640–4750, and other dark bands between Hβ and Hγ. It is very faint in the region of shorter wave-length than Hγ.

The only Mount Wilson plate is underexposed but several of the chief S features can be identified.

R ORIONIS, H.D. 31798

Remark in *H.D.:*

The line Hβ is bright. The spectrum shows strong dark bands and may belong to Class R.

H.D. 35155

Remark in *H.D.:*

The spectrum resembles that of π^1 Gruis in the region from Hβ to Hγ.

Omitting the bright hydrogen lines, this spectrum is on the whole a very good match for that of R Geminorum (C 133), although a few of the less conspicuous absorption lines are weaker than in R Geminorum and there are slight differences in the characteristic S structure near λ 4650. The titanium bands are more prominent, that at λ 4954 being fairly strong, with indications of others.

R LYNCIS, H.D. 51610

Remark in *H.D.:*

The spectrum does not appear to be of Class M, but to resemble that of R Andromedae, H.D. 1967. The lines Hβ, Hγ, and Hδ are bright. On photographs taken November 27, 1905, and December 12, 1907, the line Hγ was the strongest bright line. Hβ and Hδ were respectively 0.4 and 0.1 as strong as Hγ.

The Ann Arbor observations indicated that this spectrum is similar to that of R Cygni as observed by Wright. See *Publications of the Observatory, University of Michigan*, **2**, 52, 65, 1916.

R GEMINORUM, H.D. 53791

Remark in *H.D.:*

> The spectrum is peculiar and resembles that of Class R rather than Class M. Two dark bands are present between Hβ and Hγ. On photographs taken October 25, 1906, and October 12, 1910, Hγ is bright. The spectrum is not seen in regions of shorter wave-length than 4300.

As compared with R Andromedae there is a general similarity but many differences are obvious. Bright Hδ is much weaker relatively to Hγ than in R Andromedae. The continuous spectrum does not extend as far toward the violet. The absorption line λ 4554 is much stronger and broader. There are numerous differences in the relative intensities of lines and in the details of band structure. The spectrograms of the red region record Hα as a bright line, and show the strong absorption band at about λ 6470, which was photographed by Wright in the spectrum of R Cygni (*Monthly Notices*, **72**, 548, 1912).

R CANIS MINORIS, H.D. 54300

Remark in *H.D.:*

> The spectrum is peculiar and resembles that of R Andromedae, H.D. 1967. On photographs taken February 3, 1897, February 1, 1910, and January 24, 1911, the line Hγ is bright.

The spectrum differs somewhat from that of R Geminorum, and decidedly from that of R Andromedae. As compared with R Geminorum (C 133) there are some dissimilarities in the details of the band absorption near λ 4645, and a feature at λ 4736 is quite different. The plate of the red region is badly underexposed but shows the Hα line to be bright.

H.D. 58881

Remark in *H.D.:*

> The spectrum is not seen in the region of shorter wave-length than 4200. It resembles that of π^1 Gruis. Bright and dark bands are situated between Hβ and Hγ.

T GEMINORUM, H.D. 63334

Remark in *H.D.:*

On a photograph taken February 8, 1893, the spectrum is peculiar and probably resembles that of R Andromedae, H.D. 1967. It is very faint except in the region between Hβ and Hγ. The lines Hγ and Hδ are bright.

The spectrum is much like that of R Geminorum, though not an exact duplicate.

H.D. 63733

Remark in *H.D.:*

In the region of 4700, the spectrum resembles that of π^1 Gruis, R.A. $22^h16^m.6$, Dec. $-46°27'$. It is very faint from Hγ to the end of shorter wave-length.

Except for the bright hydrogen lines, which are missing, this spectrum is a rather close match for that of R Geminorum (C 133).

V CANCRI, H.D. 70276

Remark in *H.D.:*

On a photograph taken March 30, 1892, the lines Hβ and Hγ are nearly equally bright, and the spectrum is very faint from Hγ to the end of shorter wave-length. The spectrum may resemble that of R Andromedae, H.D. 1967.

This spectrum is much like that of R Geminorum, but the band absorption is slightly weaker.

S URSAE MAJORIS, H.D. 110813

Remark in *H.D.:*

On photographs taken February 22, 1906, and April 26, 1909, the spectrum is of a peculiar class, and resembles that of R Andromedae, H.D. 1967. The line Hγ is bright. A bright band is situated at about 4645.

This spectrum is much like that of R Geminorum. Certain changes dependent on the light phase have been observed and will be described in another contribution.

H.D. 121447

Remark in *H.D.:*

The spectrum is not seen in the region having shorter wave-length than 4200. It bears some resemblance to the spectrum of π^1 Gruis between Hβ and Hγ.

With the exception of the bright hydrogen lines, which are missing, this spectrum is a fair match for that of R Geminorum

(C 133), although there are some differences in the relative intensities of certain features. The band absorption is weaker.

R CAMELOPARDALIS, H.D. 127226

Remark in *H.D.:*

> On a photograph taken May 20, 1890, the spectrum is peculiar with bright and dark bands between Hβ and Hγ, and resembles that of R Andromedae, H.D. 1967. The lines Hβ, Hγ, and Hδ are bright. The relative intensities are 2, 10, and 2.

All of the Mount Wilson plates are underexposed. The continuous spectrum is too faint to classify with certainty, but it is probably of class S.

RW LIBRAE, H.D. 136734

Remark in *H.D.:*

> On a photograph taken June 3, 1907, the spectrum has the lines Hβ, Hγ, and Hδ bright. The intensities are 8, 10, and 3, respectively. The continuous spectrum is much stronger between Hβ and Hγ than in other portions. It is not well defined but probably resembles that of R Andromedae, H.D. 1967.

H.D. 172804

Remark in *H.D.:*

> The spectrum is faint. It may resemble that of the variable star 043065, T Camelopardalis, H.D. 29147.

With the exception of the bright hydrogen lines, which are missing, this spectrum closely resembles that of R Geminorum, but there is more contrast in certain features. The band absorption is probably stronger than in any other non-variable S-type star observed at Mount Wilson. Parts of the spectrum are much like that of π^1 Gruis, but a band-head near λ 4736 is lacking. The plate of H.D. 172804 was secured by Mr. Sanford in connection with his program for class R stars. I am indebted to him for permission to make use of it.

T SAGITTARII *191017*

Remark in *H.A.*, **56**, page 211:

> The spectrum changes from Md0 to Md4, on 8 plates. Hδ apparently changes from 30 to 70. On two plates the spectrum is peculiar, and on one plate it is Class Md peculiar.

On the Mount Wilson plates the continuous spectrum is too faint to classify with certainty but is probably of class S.

R CYGNI 193449

Remark in *H.A.*, **56**, p. 211:

> The spectrum of this star is peculiar, and shows changes on the various photographs.

This spectrum resembles that of R Geminorum (C 133) more than that of R Andromedae (C 137), but has the band absorption somewhat stronger than in R Geminorum. Photographs of the spectrum of R Cygni were secured by Wright in December, 1911, and are described in the *Monthly Notices*, **72**, 548, 1912. The Mount Wilson plate of the red region is underexposed, but shows a strong bright Hα line and the prominent band at about λ 6470 as observed by Wright. Visual observations by Espin, recorded in the *Monthly Notices*, **72**, 546, 1912, indicate that during the latter part of 1911 the spectrum varied as the brightness increased. The recent Mount Wilson photographs, including some not listed in Table II, also show very considerable changes in some features of the spectrum. They are briefly described in the *Publications of the Astronomical Society of the Pacific*, **33**, 206, 1921. A more complete discussion of the changes is reserved for another paper.

π^1 GRUIS

Remark in H.A., **56**, page 219:

> The spectra of T Camelopardalis and π^1 Gruis resemble each other and are very peculiar. The absorption band between 4640 and 4750, is present, and almost all of the continuous spectrum between this band and Hγ is cut out by other strong absorption bands.

This star is too far south for the Mount Wilson telescopes, but slit spectrograms taken at the Lick Observatory station at Santiago, Chile, in July and September, 1915, have been made available to me through the kindness of Dr. Campbell and Dr. Moore. This spectrum is the only one thus far observed with slit spectrographs which resembles R Andromedae more than R Geminorum. Several bright lines or maxima are weaker in π^1 Gruis than in R Andromedae, but on the whole the similarity is very close, with, of course, the exception of the bright hydrogen lines which are seen only in R Andromedae. The general similarity of the absorption-band spectra of these two stars was clearly brought out by Miss Cannon through a comparison of the Harvard objective-prism plates. See *Publications of the American Astronomical Society*, Twenty-third Meeting, Ann Arbor, 1919.

GENERAL DISCUSSION

The resemblance between classes R and S which appears from objective prism observations, is seen by means of slit spectra to be of the most general character only. The band in the blue is of decidedly shorter wave-length in class S, and there is throughout this region a marked lack of correspondence in the spectral details. On the other hand some of the characteristic S features are recognizable in the spectra of many giant stars of classes K and M, being more strongly developed in some stars than in others. From the comparisons which have thus far been made it appears that in general S stars are more closely related to giant Ma stars than to those of other types.

The most characteristic feature of the S spectrum is perhaps a complicated structure in the region λ 4630 to λ 4660. This apparently consists of both absorption and emission lines and probably also contains one or more band-heads in absorption. A fairly definite idea of this portion of the spectrum may perhaps be gained by comparing the illustrations with the data in Table III. An absorption band in the red with its head near λ 6470 and extending toward longer wave-lengths is probably characteristic of class S, and may prove a useful criterion for classification.

The wave-lengths in Table III depend upon measurements of one-prism spectrograms of several variables of class Se. In the second column, *a* denotes absorption line, *e*, emission line or maximum, *bh*, band-head. The values given in the table were computed upon the assumption that the *e* features have the same velocity displacement as the bright hydrogen lines, and that they are systematically 0.2 A toward the violet from the absorption lines. Thus the emission lines and maxima were corrected for the apparent velocities obtained from the bright hydrogen lines, while

PLATE XII

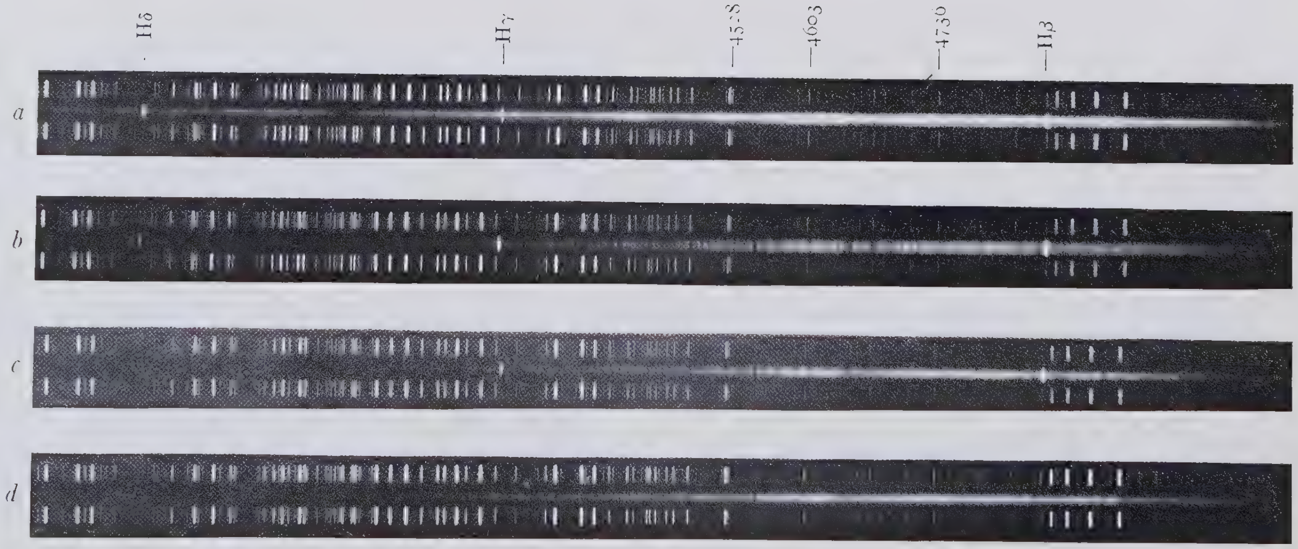

One-prism Spectrograms of Stars of Class S

(*a*) R Andromedae, October 16, 1919.
(*b*) R Geminorum, October 15, 1919.
(*c*) S Ursae Majoris, April 10, 1920.
(*d*) H. D. 35155, September 26, 1920.

TABLE III

Chief Features in Class S Spectra λ 4500–λ 4860

I.A.	Character	Intensity	Identification
4506.6	*a*	3	....
11.4	*e*	var.	....
12.8	*a*	2	Ti?
21.4	*e*	var.	....
23.1	*a*	2	Ba?
27.4	*a*	2−	Ti?
35.5	*a*	3	Ti+?
40.3	*a*	1−	....
54.0	*a*	5	Ba
62.9	*a*	1	....
68.9	*e*	....	....
71.3	*a*	2	Mg+?
80.6	*a*	1	V
83.6	*e*	var.	Fe Enh.
86.2	*a*	2	V
88.3±	*e*	....	....
94.3	*a*	2	V
4606.8	*a*	3	Sr+?
08.7	*e*	....	....
13.1	*a*	1	....
14.9	*e*	....	....
16.1	*a*	2−	Cr?
18.2	*e*	....	....
19.2	*bh*	....	....
20.2	*a*	2	....
31.5	*e*	....	....
34.1	*a*	2	....
36.6	*e*	....	....
37.5	*bh*	....	....
44.3	note	....	....
52.4±	*e*	....	....
75.1	*a*	1	Ti?
88.0	*a*	2	....
4707.1	*a*	1	....
09.9	*a*	1	....
58.6	*a*	1	....
84.1	*a*	1	....
99.8	*a*	2	Ti?
4811.7	*a*	1−	....
15.6	*a*	1	....
23.6	*a*	1−	Mn?
28.0	*a*	2	....
32.0	*a*	2	....

NOTES TO TABLE III

4511.4 *e*. This has been observed as a bright line in the spectra of four Md variables.

4521.4 *e*. This has been observed as a bright line in the spectrum of one Md variable.

4644.3. Center of broad absorption space.

4652.4 *e*. Broad or double.

4828.0 *a*, 4832.0 *a*. These lines are very persistent although of moderate strength.

4448.2. A maximum, possibly a bright line, has been measured in this position on twelve plates.

an additional correction of -0.2 A was given to the absorption lines. The need of this correction was indicated by measurements of a few plates in the region λ 4100–λ 4500. The relative displacement of bright and dark lines is analogous to that well known in Md spectra. The proper amount of the correction for the S spectra is possibly somewhat greater than 0.2 A but the data are too meager to yield a precise value. In one N variable Moore[1] found a corresponding displacement of 0.2 A. In Md variables it appears to be a function of the light period, being 0.25 to 0.3 A for the average period of the Se stars.

Continuous spectrum.—These stars are red, the color-indices of the variables probably being as great as that of the Md variables, namely, 1.8 magnitudes. As compared with Ma stars, the continuous spectrum falls off toward the violet from about λ 4500, and with greater rapidity after λ 4430.

Absorption lines.—Table III shows the chief absorption lines in the region λ 4500–λ 4860. The strength of the barium line λ 4554 makes it an outstanding feature. This line and λ 4607 (Sr) are much stronger than in classes K and M. The strength of λ 4496, compared to the neighboring line, λ 4494, is also notable. Only two or three spectrograms are available for the study of the region from λ 4450 toward the violet. Judged from these, the absorption spectrum in this region is more like that of class M than at the longer wave-lengths. In several portions of the spectrum there is, in fact, a considerable degree of correspondence between absorption lines in classes S, M, and N, in spite of their notable differences.

Bright lines.—The wave-lengths marked *e* in Table III refer to rather broad[2] maxima which vary in prominence in different spectra (especially λλ 4511.4, 4521.4, and 4583.6). In some spectra they are scarcely distinguishable from portions of continuous spectrum lying between absorption lines or spaces; in other spectra they appear to be outstanding bright features, decidedly above the general intensity of the neighboring continuous spectrum. Thus, while the designation *e* in the table may be considered merely as describing the more conspicuous maxima, it is believed by the writer that they probably correspond to actual emission. This is borne out for λ 4583.6, which is identified with the enhanced iron line λ 4583.8, by the presence of similar lines at λλ 4924, 5018, corresponding to other well-known enhanced iron lines.

---

[1] *Lick Observatory Bulletin*, **10**, 160, 1921.

[2] Exception should be made for λ 4511.4 and λ 4521.4, as these wave-lengths correspond to fairly narrow lines, the former appearing nearly monochromatic.

As in class M[1], stars showing bright hydrogen lines are long period variables. The bright hydrogen lines have quite different properties, however, in the two classes. In class S the less refrangible lines are stronger, but they rapidly decrease in intensity in passing toward the ultra-violet.[2] The relative intensities of $H\beta$, $H\gamma$, and $H\delta$ are shown in Table II.[3] The lines to the violet of $H\delta$ are usually too weak to be observed, even when $H\beta$ is strongly overexposed. In fact, $H\epsilon$ has never been seen on the Mount Wilson plates of S spectra. In one or two stars, however, the bright $H\zeta$ line has been recorded here and also at Harvard. Thus, in these cases at least, $H\zeta$ is stronger than $H\epsilon$. As is well known, this is also true in Md stars. It is particularly interesting to find it so in S spectra, where the Balmer series has widely different characteristics, as this circumstance lends support to the not wholly acceptable conclusion that $H\epsilon$ is actually emitted, but subsequently weakened through the absorption of overlying calcium vapor. $H\alpha$ is bright on the few plates of the red region thus far secured.

---

[1] Certain M stars recently found to have bright lines either do not vary in magnitude, or vary irregularly through a small range. Some of these stars are dwarfs (Adams and Joy, *Publications of the Astronomical Society of the Pacific*, **32**, 158, 1920, and **34**, 174, 1922), and others (*ibid.*, **34**, 175, 1922), while evidently giants, have spectra differing markedly from that of *o* Ceti and other well-known Md variables. Considering only stars whose underlying spectrum is similar to that of the typical M giants, we find what seems to be a perfect correspondence between variability and the presence of bright hydrogen lines.

[2] This is also true of the hydrogen lines in the peculiar M stars referred to in the preceding footnote, but, as these lines are reversed or somewhat widened, their appearance is different from the narrow hydrogen lines in S stars. See *Publications of the Astronomical Society of the Pacific*, **34**, 175, 1922. As observed with one-prism dispersion, the $H\gamma$ and $H\delta$ lines of S spectra appear monochromatic. On most of my negatives $H\beta$ is too strong to judge of its real character. It may be slightly widened.

[3] Comparable estimates of the intensities of the bright hydrogen lines in Md spectra may be found in Table III, *Mt. Wilson Contr.*, No. 200; *Astrophysical Journal*, **53**, 191, 1921.

In comparing the relative intensities of the bright hydrogen lines as given by remarks in the Harvard publications with those of the Mount Wilson plates as shown in Table II, there seem to be many striking differences, but allowance must be made for the fact that in many cases the Harvard observations were made with emulsions much less sensitive to the $H\beta$ region (relatively to $H\gamma$ and $H\delta$) than those now in use. I do not know whether or not a difference in focus between these lines on the Harvard plates could have affected the apparent relative intensities.

An unexpected feature is the presence of the enhanced lines of iron, λλ 4584, 4924, 5018. We have been accustomed to think of enhanced lines as being prominent in classes A to G, especially in the intrinsically brighter stars, and becoming inconspicuous in the later (redder) spectral classes. The presence of the above-mentioned lines in these red S variables, as well as the observations by Adams, Joy, and Humason of enhanced lines in certain peculiar M stars,[1] represents, in our present limited knowledge of stellar conditions, an anomalous circumstance which invites investigation.

The mean period of sixteen class S variables is 364 days. This is about the same as that of the Md stars having the more advanced spectra. The data for the Md stars in the following small table are taken from *Harvard Annals*, **76**, Table IX.

Class	Number	Period
Md 3, 4, 5	90	260
Md 6, 7	70	302
Md 8, 9, 10	67	355
Se	16	364

The recognition of the S stars as a distinct group may remove part of the difficulty in studying the relationship between spectral type and period among the long period variables.

The evolutionary relationship of class S stars to those of other classes, as well as the dependence of spectral modifications upon absolute luminosity, present highly interesting problems for future investigation.

[1] *Publications of the Astronomical Society of the Pacific*, **34**, 175, 1922.

It seems probable that the S stars form a third division of the giant sequence, and that they are related more closely to M than to N stars. Whether or not stars exist having spectra intermediate between Mb, Mc, and the advanced S type remains to be determined, but it is suspected that it may be possible at least to fill the gap between Ma and the early S spectra. A tentative notion of the spectral relationships among red stars is represented by the diagram in Figure 1.

Many questions are suggested which cannot profitably be discussed here. One noteworthy circumstance, however, may be pointed out, namely, that along each of the three branches, M, N, and S, there is an increasing tendency toward variability in light, and toward the presence of bright lines in the spectra. Certain facts[1] might be interpreted as indicating that the general cause of the light variations is essentially the same in both Md and Se stars, with the possibility that the differences in spectrum are due either to differences in conditions which are not important in controlling the amount of light radiated, or to differences in chemical composition. Dr. Shane, who made a special study of N-type variables,[2] is of the opinion that the main causes underlying the light variations are probably common to both Md and N stars. It is not easy to say, however, just what generalizations may properly be drawn from the analogies between the M, N, and S branches. The effective temperatures are probably not the same,

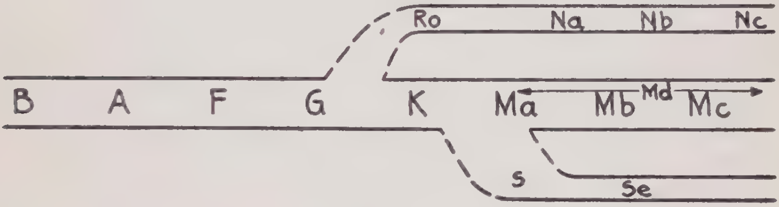

FIG. 1.—Hypothetical relationships of red stars

as several lines of evidence, especially the measurements of heat indices[1] by Nicholson and Pettit, indicate that the effective radiating temperature of the variables similar to *o* Ceti is decidedly lower than that of other red stars.

---

[1] Observations of R Cygni bearing on this matter are briefly discussed in the *Publications of the Astronomical Society of the Pacific*, **33**, 206, 1921.

[2] *Lick Observatory Bulletin*, **10**, 79, 1920.

It is hoped to treat the radial velocities of Se stars, the red portions of the S spectrum, the variable spectra of certain S stars, and the general relationship between classes M and S in future contributions.

MOUNT WILSON OBSERVATORY
August 17, 1922

NOTE ADDED APRIL, 1923

H.D. 58881 was provisionally included in the list of S-type stars, Table I, from the brief description in the *Henry Draper Catalogue*. A spectrogram of this star was secured here with the 7-inch camera on April 3, 1923. The spectrum is undoubtedly of class S. With the exception of the bright hydrogen lines, which are missing, it closely resembles S Ursae Majoris as observed with the same dispersion on July 23, 1921.

---

[1] *Publications of the Astronomical Society of the Pacific*, **34**, 181, 1922.

Contributions from the Mount Wilson Solar Observatory, No. 253
Reprinted from the *Astrophysical Journal*, Vol. LVI, pp. 475–482, 1922

THE BEHAVIOR OF SPECTRAL LINES AT THE POSITIVE POLE OF THE METALLIC ARC

By PAUL W. MERRILL

ABSTRACT

Classification of arc lines by relative strengthening at the positive pole.—In the Pfund type of arc there is a small well-defined region of luminous vapor just above the point where the core of the arc enters the molten bead which forms the positive electrode, and at the boundary of this region many spectral lines change suddenly in intensity to a greater or less degree. By keeping the core of the arc steady and focusing it on the slit of a 30-foot Littrow spectrograph, plates were obtained from which it was possible to group about 500 *iron lines* from λ 3849 to λ 5763 into six classes: change imperceptible (0), slight (1), small (2), sufficient to double the intensity (3), great (4), or very great (5). The *relationship to the furnace classification* of King was studied for each group. In general the strengthening at the pole is greater for the high-temperature lines, the average class for King's classes I, II, and III being, respectively, 0.2, 1.0, and 1.9. But the average for classes IV and V is only 1.8, and for the diffuse lines of these classes, only 1.3. Lines of each temperature class are also found in each of the positive-pole classes 0, 1, and 2; hence the correlation is only fair, although probably as close as can be expected with such different modes of excitation. The strengthening of the enhanced lines is very marked (average class being 4), so that positive pole observations may be useful in distinguishing these lines. The classifications of 180 *cobalt lines* and of some *nickel lines* show the same general relationships as were found for the iron lines.

An interesting recent development in spectroscopy has been the increasing importance attached to the classification of spectral lines according to their behavior under various conditions of excitation. This has been due in part to the desire to provide an improved basis for the interpretation of spectroscopic observations of various light sources, particularly of celestial objects, and in part to the wide discussion of the quantum and ionization theories of the emission of spectral lines.

It has long been recognized that the relative intensities of lines in light from different portions of the electric arc afford a means by which the lines may be grouped. Most of the spectroscopic investigations of the structure of the arc have been concerned with the carbon arc, but a number have dealt with arcs between metallic electrodes. Among the phenomena observed in metallic arcs, one of the most interesting and important is, that near the poles, especially the positive pole, lines appear which are absent or very weak in the center of the arc or in integrated arc light, but which are characteristic of the disruptive spark. Photographs made by the writer in 1919 exhibited this property of enhanced lines very clearly, and also showed systematic effects for other types of lines. The general results of a study of these photographs[1] are described in the present paper.

Iron was the element most extensively observed in this investigation. The arc used was of the Pfund type, the upper, negative electrode consisting of an iron rod, the lower, positive electrode of a drop of molten iron oxide. A copper rod hollowed out at the upper end served as a holder for the iron oxide and made possible an arc with a spheroid of oxide slightly smaller than usual. With currents of about two amperes the arc burned steadily with a small, sharply-defined, circular, bright area on the molten surface, from which the core of the arc proceeded. It proved important for the present purpose to have this positive "bead" localized and steady, for the vapors immediately surrounding it were the source of the special phenomena described in the following paragraphs. The general appearance of this portion of the arc is well shown in the illustrations accompanying papers on the iron arc by St. John and Babcock.[2]

An image of the arc was projected in such a way that the line joining the electrodes coincided with the slit of the 30-foot Littrow spectrograph. In the photographs thus obtained each spectral line represents the emission of that radiation along the axis of the arc. The actual arc length was about 5 mm, the magnification of the image three times. Currents ranging from 1.5 to 3.2 amperes at 250 volts were employed.

The particular subject dealt with in the present paper is the increase in the intensity of spectral lines at the bright end of the arc core just off the positive pole. The effects at the positive pole are more sharply localized than those at the negative pole. Most lines show a continuous increase in intensity on passing from the

---

[1] Reported upon at the Pasadena Meeting of the Pacific Coast Section of the American Physical Society, June, 1919; *Physical Review*, **14**, 271, 1919.

[2] *Mt. Wilson Contr.*, Nos. 106, 137; *Astrophysical Journal*, **42**, 231, 1915; **46**, 138, 1917.

PLATE XIII

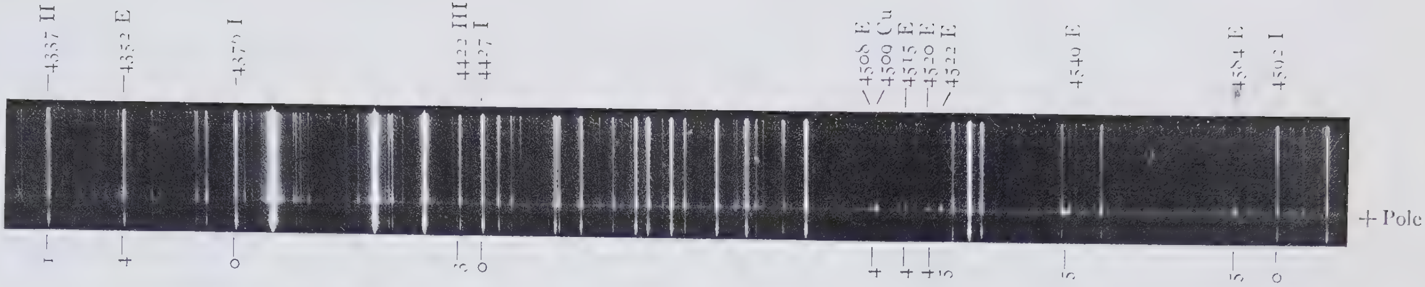

Spectrum of the Iron Arc

Showing behavior of the lines at the positive pole. The figures above the spectrum indicate the wave length and temperature class; those below the degree of strengthening at the positive pole. The extensions of the lines below the narrow strip of continuous spectrum marking the positive pole are due largely to reflection of the main portion of the arc from the molten spheroid of oxide forming the positive terminal.

center to the negative pole, but on approaching the positive pole, there is, for an affected line, a sudden increase in intensity at a point corresponding to the boundary of a small bright volume contiguous to the pole.

Nearly 550 iron lines between wave-lengths 3849 A and 5763 A were classified according to the increase of intensity at the positive pole on the following basis:

0 no increase
1 slightest observable increase
2 small increase
3 considerable increase (intensity about doubled)
4 great increase
5 very great increase

The relationship of this classification to other classifications of the same lines is exhibited in Table I, which gives for each class the number of lines of each degree of pole strengthening. Thus the numbers in the first row indicate that out of sixty-three class I lines fifty-one were not strengthened, ten were very slightly strengthened, and two showed a somewhat greater increase at the positive pole. The Roman numerals I–V refer to the temperature classes determined by King[1] from data obtained by use of the electric furnace; *E* indicates enhanced lines, and *e*, lines with a negative pole effect.[2] In compiling the numbers for this table it was noticed

TABLE I

POSITIVE POLE STRENGTHENING OF IRON LINES

Class	0	1	2	3	4	5	Total	Average
I	51	10	2	......	......	......	63	0.2
II	18	15	10	3	......	......	46	1.0
III	3	24	50	14	......	......	91	1.9
IV	4	29	65	21	3	......	122	2.0
IV*n*	3	16	15	......	......	......	34	1.4
V	......	15	24	2	......	......	41	1.8
V*n*	1	19	6	......	......	......	26	1.2
e	......	1	4	8	1	......	14	2.6
E	......	....	1	8	12	7	28	3.9

---

[1] *Mt. Wilson Contr.*, Nos. 66, 247; *Astrophysical Journal*, **37**, 239, 1913; **56**, 318 1922.

[2] St. John and Babcock, *Mt. Wilson Contr.*, No. 202; *Astrophysical Journal*, **53**, 260, 1921.

that many of the lines which fell in columns 0–2 of rows IV and V were broad or nebulous. Accordingly all lines of these classes that are so marked, either by King[1] or Burns,[2] were separated and placed in rows IV*n* and V*n*.

The chief facts brought out by this study may be seen by inspection of Table I. To facilitate comparison of the various types of lines, the average value of the pole strengthening for each has been placed in the last column. The progression in these average values is shown by the following grouping:

Class	I	II	IV*n*, V*n*	III, IV, V	*e*	*E*
Number	63	46	60	254	14	28
Average strengthening	0.2	1.0	1.3	1.9	2.6	3.9

The *e* lines in the green, λ 5364–λ 5598, are of special interest. They are in furnace class V and are greatly strengthened at the positive pole. In confirmation of the observations of St. John and Babcock it was noted that at the positive pole these lines are distended toward shorter wave-lengths. The *d* lines in the regions λ 5232–λ 5624 are in class IV and in group 2 as regards pole strengthening.

The enhanced lines, designated by *E*, are from Lockyer's table, with a few additions from other sources. The degree of strengthening at the positive pole seems to be approximately proportional to the amount of enhancement in passing from arc to spark, but the data at hand do not allow any precise determination of this relationship. They suggest that there is a sequence of types of lines from I at one end to enhanced lines at the other; that classes I, II, and III follow in regular order, but that classes IV and V contain two types of lines, one type continuing the sequence I–III and connecting it with the enhanced lines, the other type similar to the nebulous lines in regard to furnace behavior and pole strengthening but not separated from the others by the present treatment of the data. If these remaining lines, which really belong to the subgroup represented by "*n*," were removed, it is possible that the pole values for the remainder of the group would rise, and perhaps take an appropriate position between classes III and *E*. To make a complete separation of the classes IV and V into two subgroups would be rather difficult, because the characteristics of the two apparently overlap. That is to say, while subdivisions are indicated with definite differences between them, lines intermediate in their characteristics may not be lacking. It would appear rather arbitrary to attempt a division on the basis of the pole data alone. Probably the division based on the sharpness of the lines could be carried farther. The results would be of value when correlated with pole data. The *e* lines are peculiar in that, although lacking in sharpness, they have high pole strengthening.

---

[1] *Loc. cit.*

[2] *Lick Observatory Bulletin*, **8**, 27, 1913.

TABLE II

Pole Strengthening of Individual Iron Lines

λ Rowland	Furnace	Positive Pole	λ Rowland	Furnace	Positive Pole
3950.102........	III	1	4260.640.......	III	2
3951.311........	IV	2	4308.081.......	II	0
3966.212........	III	2−	4291.630.......	IA	0
3966.778*n*.......	IV	2	4294.301.......	II	1
4100.901........	IIA	0	4415.293.......	II	0+
4107.649........	III	3−	4427.482.......	I	0
4177.698........	IIA	0	4459.301.......	III	3
4181.919........	III	3	4461.818.......	I	0
4199.267........	III	2	4489.911.......	IA	0
4202.198........	I	0	4494.738.......	III	1
4206.862........	IA	0	4528.798.......	II	2
4210.494........	III	2	4531.327.......	II	0
4216.351........	I	0	4919.174.......	III	2
4219.516........	IV	4	4939.868.......	I	0
4232.887........	IA	0	5050.008.......	III	2
4233.772........	III	1+	5051.825.......	I	0
4250.287........	III	1	5166.454.......	IA	0
4250.945........	II	0+	5171.778.......	II	1
4271.325........	III	1+	5341.213.......	II	1
4271.934........	II	1	5371.734.......	I	0

It may be of interest to cite several examples of individual lines showing different behavior at the positive pole. For this purpose I have chosen pairs of lines in King's list of "Neighboring Lines Which Are Differently Affected in the Furnace."[1] This will be sufficient to exhibit typical behavior of the various classes, and also some of the common variations. Comparison with Table I will show which lines represent average values and which deviations. λ 4219.516 is included by Gale and Adams in the list of enhanced lines.

Cobalt.—Estimates of the strengthening of cobalt lines at the positive pole of the arc were made in the same manner as for iron. For the summary in Table III 180 lines between the wave-lengths 3845 and 4629 A were used.

The bright volume of vapor immediately above the spot on the positive pole in the cobalt arc is not so sharply localized as with iron, and more lines show a gradual strengthening toward the positive pole, so that the appearance of the photographs is slightly different and in some cases the estimates less definite than for iron. The main features of the phenomena are the same, however, and the mean values of pole strengthening for the different furnace classes are nearly the same as for iron.

TABLE III

Positive Pole Strengthening of Cobalt Lines

Class	0	1	2	3	4	Total	Average
I	25	12	2	....	....	39	0.4
II	2	15	8	4	....	29	1.5
III	....	11	45	9	....	65	2.0
IV	....	2	9	2	....	13	2.0
V	1	5	7	1	....	14	1.6
E	2	1	9	5	3	20	2.3

The enhanced lines in the last row are all of Lockyer's list which have been observed. Some of these lines which give small pole strengthening do not seem to be characteristic enhanced lines. If this row were restricted to well-marked cases of enhancement, a value of 3 or 4 would be found instead of 2.3.

Not many lines in the cobalt spectrum have been noted as hazy. Four class V lines of this character give a mean value of pole strengthening less than that of the whole class. Thus the meager data available agree with iron in this particular also.

---

[1] *Mt. Wilson Contr.*, No. 66; *Astrophysical Journal*, **37**, 239, 1913.

A smaller amount of data for *nickel* indicates that the same general relationships exist for this element also.

The fact that grouping the spectral lines of three elements according to their behavior at the positive pole of the arc gives a classification which runs parallel to the temperature classification is of interest in showing that the inherent differences of the various classes of lines are such as to allow them to be distinguished in sources other than those upon which the classification was based. The chief factor which differentiates the various classes of lines is, presumably, the degree of excitation required for their production. To what extent the physical conditions at the center and at the positive pole of the arc are identical with those in the furnace at low and at high temperatures is difficult to judge, but we may at least say that the relative effects upon the atom, as regards radiation, are comparable.

That the unsharp lines are subject to a smaller increase of intensity at the positive pole than are sharp lines of corresponding temperature classes is an outstanding fact for which a certain explanation is not now available. It may be that the unsharp lines represent vibrations lacking in stability, being easily perturbed, as shown by the lack of homogeneity, and that under the more intense conditions at the pole these vibrations can be executed by relatively few electrons.

The ease and definiteness with which enhanced lines can be distinguished at the positive pole suggest that arc observations should be given consideration in the formation of lists of enhanced lines. A particular advantage is that the criterion is not the strength at the pole, but the increase in intensity (amounting practically to a discontinuity) at a definite point in passing from the center to the positive pole. This can be shown by a single photograph, and the selection of enhanced lines should be less arbitrary than when based upon a comparison of the relative strength of lines in separate arc and spark exposures.

The type of observations described in the present paper is possible only on a steady arc, such as the Pfund form of iron arc. Several of the metals can be made to burn in this fashion, and perhaps methods can be developed by which the arcs of numerous elements can be sufficiently controlled to permit the gathering of similar data. With proper precautions, valuable results can probably be obtained for certain elements by using iron electrodes containing small amounts of the elements in question.

At present, positive pole phenomena would seem to be most useful in their bearing on problems connected with the classification of spectral lines, but they may also prove valuable in studying the temperature and electrical conditions at different points in the arc.

MOUNT WILSON OBSERVATORY
August 1922

Contributions from the Mount Wilson Observatory, No. 254
Reprinted from the *Astrophysical Journal*, Vol. LVI, pp. 439–445, 1922

ORBIT OF THE ECLIPSING BINARY TW ANDROMEDAE

By MARTHA BETZ SHAPLEY

ABSTRACT

Uniform and darkened orbits of the eclipsing binary TW Andromedae.—Orbits were calculated from 86 photographic observations made at Mount Wilson from 1914 to 1916. The adopted elements of light variation are

$$\text{Min.} = \text{J. D. } 2420051.618 + 4^{\mathrm{d}}.122745\,E$$

The principal eclipse is total and there is some evidence of variation of the large, faint component. The *color index* at maximum is +0.57 mag., at minimum +1.36 mag. When reduced to the photographic scale by proper allowance for color, 74 photovisual observations, as well as the photographic measures, are well represented by the curves shown in Figs. 1 and 2, corresponding to the orbits whose elements are given in Table VI.

Photographic and photovisual observations of the eclipsing variable star TW Andromedae were made by Mr. Shapley with the 60-inch reflector at Mount Wilson during the years 1914 to 1916.

TABLE I

Comparison Stars for TW Andromedae

Star	Photographic Magnitude	Photovisual Magnitude	Color Index
B.D.$+31^{\circ}5023$	10.70	9.99	$+0^{m}.71$
$23^{h}57^{m}, +32^{\circ}13'$ (1900)	11.69	10.93	+0.76
B.D.$+32^{\circ}4755$	9.27	8.81	+0.46

Miss Davis assisted in measuring and reducing the 160 multiple-exposure photographs, which contain a total of 540 images of the variable.

The magnitudes of the comparison stars, Table I, were standardized by means of the North Polar Standards.[1] Tables II and III contain the photographic and photovisual observations. The apertures employed range from nine inches to sixty inches; the exposure times from thirty seconds to two minutes.

---

[1] Seares, *Mt. Wilson Contr.*, No. 97; *Astrophysical Journal*, 41, 206, 1915.

TABLE II

PHOTOGRAPHIC OBSERVATIONS OF TW ANDROMEDAE

J.D. and Gr. H.M.T.	No. Exp.	Phase	Mag.	J.D. and Gr. H.M.T.	No. Exp.	Phase	Mag.
2420393.646....	5	−0^{d}.160	10.26	2420455.651....	4	+0^{d}.005	12.22
393.653....	5	−0.153	10.34	455.662....	4	+0.016	12.24
393.660....	5	−0.146	10.51	455.671....	4	+0.025	12.33
393.667....	5	−0.139	10.59	456.611....	5	+0.965	9.62
393.678....	5	−0.128	10.81	456.618....	4	+0.972	9.58
396.703....	4	+2.897	9.73	456.623....	4	+0.977	9.48
397.756....	5	−0.173	10.32	456.629....	4	+0.983	9.46
397.770....	5	−0.159	10.26	458.617....	4	+2.970	9.84
397.786....	5	−0.143	10.53	458.626....	4	+2.979	9.76
397.797....	5	−0.132	10.51	459.578....	4	−0.192	9.82
397.812....	5	−0.117	10.70	459.584....	4	−0.186	10.13
397.837....	5	−0.092	11.26	459.590....	4	−0.180	10.02
397.863....	5	−0.066	11.66	459.597....	4	−0.173	10.18
397.876....	5	−0.053	11.88	459.602....	4	−0.168	10.23
397.889....	5	−0.040	12.09	459.607....	4	−0.163	10.17
397.903....	5	−0.026	11.98	459.615....	4	−0.155	10.31
397.916....	5	−0.013	12.00	459.624....	4	−0.146	10.24
397.929....	5	0.000	12.06	459.637....	4	−0.133	10.51
397.944....	5	+0.015	12.29	459.647....	4	−0.123	10.67
397.958....	5	+0.029	12.16	459.656....	4	−0.114	10.68
397.973....	5	+0.044	12.12	459.667....	4	−0.103	10.88
397.986....	5	+0.057	11.77	459.679....	4	−0.091	11.04
398.003....	5	+0.074	11.53	459.689....	4	−0.081	11.35
398.017....	5	+0.088	11.32	459.698....	4	−0.072	11.52
398.031....	5	+0.102	11.03	459.727....	4	−0.043	11.98
398.035....	5	+0.107	10.88	459.736....	4	−0.034	12.04
422.707....	3	+0.042	12.29	459.745....	4	−0.025	12.12
422.734....	3	+0.069	11.56	517.669....	4	+0.181	10.01
422.746....	4	+0.081	11.38	517.676....	4	+0.188	9.91
422.757....	4	+0.092	11.21	517.687....	4	+0.199	9.71
422.777....	4	+0.112	10.81	517.694....	4	+0.206	9.65
422.787....	4	+0.122	10.53	517.704....	4	+0.216	9.64
422.797....	4	+0.132	10.36	517.712....	4	+0.224	9.73
422.811....	4	+0.146	10.52	2421050.911....	3	+1.589	9.86
425.622....	4	+2.957	10.07	050.924....	3	+1.602	9.88
425.631....	4	+2.966	10.00	051.864....	3	+2.542	9.68
425.675....	4	+3.010	9.68	051.889....	3	+2.567	9.84
425.683....	4	+3.018	9.55	052.863....	3	+3.541	9.78
425.692....	4	+3.027	9.56	052.891....	3	+3.569	9.78
425.699....	4	+3.034	9.59	053.867....	3	+0.422	9.78
425.707....	4	+3.042	9.57	053.876....	3	+0.431	9.80
425.716....	4	+3.051	9.56				
455.623....	4	−0.023	12.25				
455.632....	4	−0.014	12.16				
455.642....	4	−0.004	11.99				

TABLE III

PHOTOVISUAL OBSERVATIONS OF TW ANDROMEDAE

J.D. and Gr.H.M.T.	No. Exp.	Phase	Mag.	J.D. and Gr. H.M.T.	No. Exp.	Phase	Mag.
2420396.687....	3	+2^{d}871	9.06	2420458.622....	3	+2^{d}975	9.23
397.749....	3	−0.180	9.71	458.631....	3	+2.984	9.31
397.762....	3	−0.167	9.67	459.582....	3	−0.188	9.34
397.776....	3	−0.153	9.64	459.587....	3	−0.183	9.36
397.790....	3	−0.139	9.78	459.594....	3	−0.176	9.45
397.803....	3	−0.126	9.76	459.599....	3	−0.171	9.54
397.819....	3	−0.110	10.02	459.605....	3	−0.165	9.44
397.858....	3	−0.071	10.45	459.610....	3	−0.160	9.54
397.870....	3	−0.059	10.40	459.619....	3	−0.151	9.51
397.883....	3	−0.046	10.57	459.628....	3	−0.142	9.49
397.897....	3	−0.032	10.85	459.642....	3	−0.128	9.63
397.910....	3	−0.019	10.78	459.651....	3	−0.119	9.87
397.923....	3	−0.006	11.19*	459.660....	3	−0.110	10.03
397.936....	3	+0.007	10.77	459.674....	3	−0.096	10.23
397.952....	3	+0.023	10.87	459.685....	3	−0.085	10.25
397.966....	3	+0.037	10.68	459.694....	3	−0.076	10.42
397.979....	3	+0.050	10.64	459.702....	3	−0.068	10.63
397.995....	3	+0.066	10.60	459.731....	3	−0.039	10.90
398.009....	3	+0.080	10.40	459.740....	3	−0.030	10.77
398.024....	3	+0.095	10.15	459.749....	3	−0.021	10.88
422.728....	3	+0.063	10.82	517.673....	3	+0.185	9.47
422.740....	3	+0.075	10.64	517.681....	3	+0.193	9.23
422.752....	3	+0.087	10.35	517.691....	3	+0.203	9.31
422.769....	3	+0.104	10.08	517.698....	3	+0.210	9.13
422.783....	3	+0.118	9.81	517.708....	3	+0.220	9.19
422.792....	3	+0.127	9.71	517.715....	3	+0.227	9.38
422.801....	3	+0.136	9.72	2421050.906....	2	+1.584	9.08
425.626....	3	+2.961	8.85:	050.919....	2	+1.597	9.18
425.635....	3	+2.970	9.13	051.857....	2	+2.535	9.27
425.679....	3	+3.014	9.07	051.885....	2	+2.563	9.13
425.686....	3	+3.021	9.08	052.858....	2	+3.536	9.13
425.696....	3	+3.031	9.02	052.886....	2	+3.564	9.28
425.703....	3	+3.038	9.20	053.872....	2	+0.427	9.16
425.712....	3	+3.047	9.08	053.881....	2	+0.436	9.23
425.721....	3	+3.056	9.16				
425.799....	4	+3.134	9.16				
456.615....	3	+0.969	9.02				
456.621....	3	+0.975	9.10				
456.626....	3	+0.980	9.11				
456.632....	3	+0.986	9.02				

* Rejected observation, abnormality unexplained.

The period used for the reduction is that derived by van der Bilt.[1] To satisfy the Mount Wilson observations, a correction of $-0^{\mathrm{d}}.004$ has been made to the initial epoch, giving the adopted elements:

$$\text{Min.} = \text{J.D. } 2420051.618 + 4^{\mathrm{d}}.122745\,\text{E}.$$

The individual photographic observations are plotted in Figure 1 with the curve computed from orbital elements, based on the assumption of disks of uniform brightness. The scattering of the observations at the bottom of the minimum is believed to be due, in part at least, to actual fluctuations in the light of the presumably very red faint component, which alone is visible at the time of principal eclipse.

TABLE IV

PHOTOGRAPHIC NORMAL POINTS FOR TW ANDROMEDAE

Number	No. Obs.	Mean Phase	Mean Mag.	O–C, Darkened
1	13	$0^{\mathrm{d}}.018$	12.14	$0^{\mathrm{m}}.00$
2	5	.044	12.07	+0.05
3	5	.068	11.61	0.00
4	5	.087	11.27	+0.01
5	5	.103	10.96	−0.01
6	5	.121	10.68	−0.01
7	5	.136	10.50	0.00
8	5	.149	10.38	+0.02
9	5	.165	10.25	+0.05
10	5	.182	10.05	−0.01
11	5	0.207	9.71	−0.19
12	23	....	9.70	0.00

Tables IV and V contain the mean magnitudes, photographic and photovisual, after reflecting all observations on to one branch of the curve. The first normal group of each table contains the observations during the phase of totality; the last includes all observations outside the minimum.

The orbits are based on the photographic light curve.[2] Uniform and darkened elements were computed, and, together with other data concerning the system, are arranged in Table VI. The mean densities are not corrected for probable unequal distribution of mass.

The photographic normals are plotted as dots in Figure 2, where the co-ordinates are, respectively, light intensity, corresponding to

---

[1] *Astronomische Nachrichten*, **196**, 396 (No. 4703), 1913.

[2] A provisional orbit has been published by Stewart in *Astrophysical Journal*, **42**, 315, 1915.

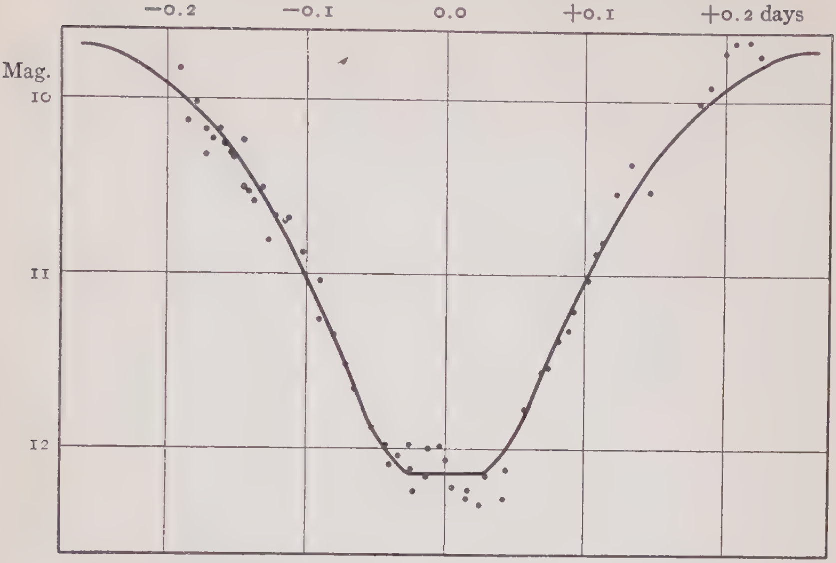

FIG. 1.—Photographic observations and computed uniform light-curve for TW Andromedae.

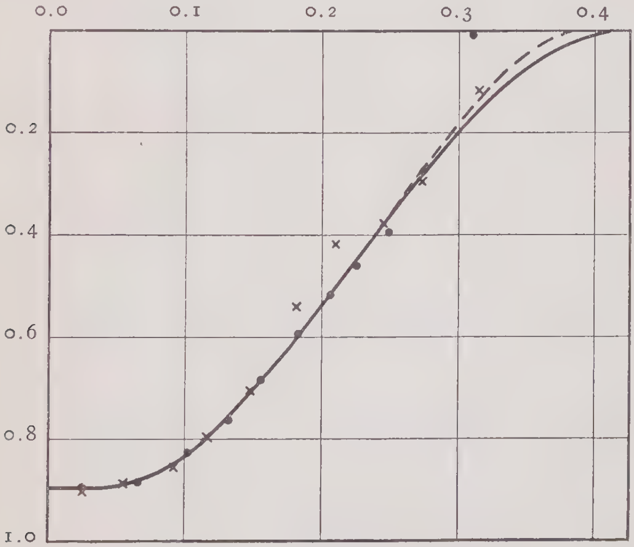

FIG. 2.—Computed intensity-curves for TW Andromedae. Ordinates are losses of light-intensity, 1−*l*; abscissae are sines of phase angles.

TABLE V

Photovisual Normal Points for TW Andromedae

Number	No. Obs.	Mean Phase	Mean Mag.	O–C, Darkened
1	4	$0^{d}.018$	10.82	$+0^{m}.04$
2	5	.037	10.75	−0.01
3	5	.061	10.62	+0.03
4	5	.077	10.43	0.00
5	5	.098	10.17	−0.02
6	5	.120	9.83	−0.11
7	5	.139	9.63	−0.13
8	5	.163	9.57	0.00
9	5	.182	9.47	+0.02
10	5	0.211	9.25	−0.04
11	24	....	9.13	0.00

TABLE VI

Orbital Elements and Other Data for TW Andromedae

Right Ascension	$23^{h}58^{m}10^{s}$ 1900	
Declination	$+32°17'.3$ 1900	
Period	$4^{d}.122745$	
Nature of eclipse	Total	
	Pg.	Pv.
Magnitude at maximum	9.70	9.13
Magnitude at minimum	12.14	10.78
Range at primary minimum	$2^{m}.44$	$1^{m}.65$
Light of brighter star	0.894	0.781
Light of fainter star	0.106	0.219
Color index at maximum	$+0^{m}.57$	
Color index at minimum	+1.36	
	Uniform	Darkened
Inclination of orbit	81°40′	86°2′
Least distance of centers	0.145	0.069
Semi-duration of primary eclipse	$0^{d}.256$	$0^{d}.285$
Semi-duration of totality	$0^{d}.026$	$0^{d}.023$
Computed range at secondary minimum	$0^{m}.02$	$0^{m}.06$
Radius of brighter star	0.127	0.174
Radius of fainter star	0.275	0.252
Ratio of radii	0.46	0.69
Most probable density of brighter star	0.193	0.075
Most probable density of fainter star	0.019	0.025
Radius of brighter star in terms of sun's radius	1.73	2.36
Radius of fainter star in terms of sun's radius	3.74	3.42
Distance of centers in terms of sun's radius	13.6	13.6
Ratio of surface brightness in photographic light	40.	17.7
Photovisual absolute magnitude of brighter star	1.4	0.7
Photovisual absolute magnitude of fainter star	2.9	2.2
Hypothetical parallax	0″.003	0″.002

the mean magnitude, and the sine of the orbital longitude, corresponding to the mean phase. The full-line curve is computed from the darkened elements; the broken curve, representing the uniform orbit, coincides with it throughout more than half the eclipse.

The photovisual normals have been reduced to the photographic light-curve by applying as a factor the ratio of photographic to photovisual range at primary minimum; they are represented by crosses in Figure 2. It is clear from the plot that the orbit derived from photographic observations satisfactorily represents both the photographic and photovisual data, when allowance is thus made for the difference in the color of the two components.

CAMBRIDGE, MASSACHUSETTS
March 1922

END OF VOL. XI

INDEX TO VOLUME XI

Nos. 228 to 254

AUTHORS

PAGE

Adams, Walter S., and Alfred H. Joy—
A Spectroscopic Method of Determining the Absolute Magnitudes of A-Type Stars and the Parallaxes of 544 Stars 273

Duncan, John C.—
Changes in the Spectrographic Elements of Y Sagittarii 373

Gingrich, C. H.—
Parallaxes of Stars in the Region of B.D.+31°643 197
The Variable Double Star X Ophiuchi 189

Hertzsprung, Ejnar—
Effective Wave-Lengths of 129 Stars within 0°5 of the North Pole and of the Σ Companion of Polaris 93

Hubble, Edwin—
A General Study of Diffuse Galactic Nebulae 217
The Source of Luminosity in Galactic Nebulae 397

Humason, Milton L. *See* Seares, Frederick H.

Joy, Alfred H. *See* Adams, Walter S.

Kapteyn, J. C.—
First Attempt at a Theory of the Arrangement and Motion of the Sidereal System. 65

Kapteyn, J. C., and P. J. van Rhijn—
On the Upper Limit of Distance to Which the Arrangement of Stars in Space Can at Present Be Determined with Some Confidence 35

King, Arthur S.—
Electric Furnace Experiments Involving Ionization Phenomena . 105
The Electric Furnace Spectrum of Iron in the Ultra-Violet, with Supplementary Data for the Blue and Violet 351
Note on the Thickness of Air Required to Produce the Atmospheric Absorption Bands, A, *a*, and B 103

Lindblad, Bertil—
Spectrophotometric Methods for Determining Stellar Luminosity . 1

PAGE

MERRILL, PAUL W.—
  The Behavior of Spectral Lines at the Positive Pole of the Metallic Arc 467
  Interferometer Observations of Double Stars 203
  Stellar Spectra of Class S. I. General Description 449

NICHOLSON, SETH B. *See* Pettit, Edison; St. John, Charles E.

PETTIT, EDISON, AND SETH B. NICHOLSON—
  The Application of Vacuum Thermocouples to Problems in Astrophysics 327

RUSSELL, HENRY NORRIS—
  Notes on Ionization in the Solar Atmosphere 155

ST. JOHN, CHARLES E., AND SETH B. NICHOLSON—
  The Absence of Oxygen and Water-Vapor Lines from the Spectrum of Venus 377

SANFORD, R. F.—
  Orbits of the Spectroscopic Binaries Lalande 13792 and AOe 12584 . 437

SEARES, FREDERICK H.—
  Revised Magnitudes for Stars near the North Pole 131

SEARES, FREDERICK H., AND MILTON L. HUMASON—
  Further Evidence on the Brightness of the Stars of the North Polar Sequence 117

SHAPLEY, MARTHA BETZ—
  Orbit of the Eclipsing Binary TW Andromedae 475

STRÖMBERG, GUSTAF—
  The Distribution of the Velocities of Stars of Spectral Types F to M 297

VAN MAANEN, ADRIAAN—
  Investigations on Proper Motion.
    Seventh Paper: Internal Motion in the Spiral Nebula N.G.C. 2403 255
    Eighth Paper: Internal Motion in the Spiral Nebula M 94 = N.G.C. 4736 263
    The Photographic Determination of Stellar Parallaxes with the 60-Inch Reflector. Sixth Series 161

VAN RHIJN, P. J. *See* Kapteyn, J. C.

SUBJECTS

Absolute magnitudes, of A-type stars, spectroscopically determined, 273
Absorption bands, A, *a*, B, 103
Air, thickness required to produce absorption bands, A, *a*, and B, 103
Arc, metallic, behavior of spectral lines at positive pole, 467
Atmosphere, solar, ionization, 155
Binaries, eclipsing, orbit of TW Andromedae, 475
———, spectroscopic, Lalande 13792 and AOe 12584; 437
Cepheid variables, Y Sagittarii, changes in spectrographic elements, 373
Electric furnace experiments involving ionization phenomena, 105
Electric furnace spectrum of iron in ultra-violet, blue, and violet, 351
Double stars, interferometer observations, 203
———, variable, X Ophiuchi, 189
Furnace. *See* Electric furnace
Interferometer observations of double stars, 203
Ionization, in solar atmosphere, 155
Ionization phenomena, in electric furnace experiments, 105
Iron spectrum, electric furnace, in ultra-violet, blue, and violet, 351
Luminosity, in galactic nebulae, 397
———, stellar, spectrophotometric methods of determination, 1
Magnitudes, evidence on brightness of stars of North Polar Sequence, 117
———, revised, for stars near North Pole, 131
Messier 94, internal motion, 263
Nebulae, diffuse galactic, 217
———, galactic, source of luminosity, 397
———, spiral, internal motion in N.G.C. 2403, M 94=N.G.C. 4736; 255, 263
N.G.C. 2403, 4736; 255, 263
Oxygen and water-vapor lines, absence from spectrum of Venus, 377
Parallaxes, of 544 stars, spectroscopically determined, 273
———, of stars in region of B.D.+31°643; 197
———, stellar, determination with 60-inch reflector, 161
Polar Sequence, magnitudes of stars, 117, 131
Proper motion, internal, in the spiral nebulae N.G.C. 2403, M 94=N.G.C. 4736; 255, 263
Sidereal system, first attempt at theory of arrangement and motion, 65
Spectra, behavior of lines at positive pole of metallic arc, 467
———, of stars of class S, 449
Spectrophotometric methods for determining stellar luminosity, 1
Spectroscopic binaries, Lalande 13792 and AOe 12584, orbits, 437
Spectroscopic method of determining absolute magnitudes, 273

Spectrum, iron, in ultra-violet, blue, and violet, 351
———, of Venus, absence of oxygen and water-vapor lines, 377
Stars, arrangement in space, upper limit of distance, 35
———, A-type, absolute magnitudes spectroscopically determined, 273
———, double, interferometer observations, 203
———, class S, spectra, 449
———, effective wave-lengths within 0°5 of the North Pole and of the Σ Companion of Polaris, 93
———, evidence on brightness of North Polar Sequence, 117
———, parallaxes, determination with 60-inch reflector, 161
———, parallaxes, in region of B.D.+31°643, 197
———, parallaxes, of 544 stars, spectroscopically determined, 273
———, revised magnitudes for stars near North Pole, 131
———, spectral types F to M, distribution of velocities, 297
———, system, first attempt at theory of arrangement and motion, 65
———, variable double, X Ophiuchi, 189
Stellar luminosity, spectrophotometric methods of determination, 1
Sun, ionization in atmosphere, 155
Thermocouples, vacuum, application to astrophysical problems, 327
Variable stars, X Ophiuchi, 189
Variables, Cepheid, Y Sagittarii, changes in spectrographic elements, 373
Velocities, of stars, distribution, 297
Venus, absence of oxygen and water-vapor lines from spectrum, 377
Water-vapor lines, absence from spectrum of Venus, 377
Wave-lengths, effective, of 129 stars within 0°5 of North Pole and Σ Companion of Polaris, 93

522.19 C28 V11

a39001 006937232b

72-1